UNIVERSITY OF COPENHAGEN
DEPARTMENT OF DRUG DESIGN AND PHARMACOLOGY

Ph.D. Thesis

Elina Tampio L'Estrade

Development and Evaluation of Potential 5-HT$_7$ Receptor PET Tracer Candidates

Supervisor: Assoc. Prof. Matthias M. Herth

This thesis has been submitted to the Graduate School of Health and Medical Sciences, University of Copenhagen on March 8th 2019.

Ph.D. Thesis

"Development and Evaluation of Potential 5-HT_7 Receptor PET Tracer Candidates"

Elina Tampio L'Estrade

Department of Drug Design and Pharmacology
University of Copenhagen

Neurobiology Research Unit

Radiation Physics, Nuclear Medicine Physics Unit
Skånes University Hospital

Thesis submission: March 8th 2019
Ph.D. defence: May 6th 2019

Academic supervisors:

Principal supervisor:

Associate Professor Matthias M. Herth

Department of Drug Design and Pharmacology, University of Copenhagen

Co-supervisors:

Professor Gitte M. Knudsen

Neurobiology Research Unit, Rigshospitalet and University of Copenhagen

Tomas Ohlsson, Ph.D.

Radiation Physics, Nuclear Medicine Physics Unit, Skånes University Hospital, Sweden

Maria Erlandsson, Ph.D.

Radiation Physics, Nuclear Medicine Physics Unit, Skånes University Hospital, Sweden

Assessment Committee:

Associate Professor Anne-Marie Heegaard (chairperson)

Department of Drug Design and Pharmacology

University of Copenhagen, Denmark

Associate Professor Stina Syvänen

Department of Public Health and Caring Sciences

Uppsala University, Sweden

Professor Tobias L. Ross

Department of Nuclear Medicine

Hannover Medical School, Germany

PREFACE

The research presented in this thesis was part of Ph.D. studies at the Graduate School of Health and Medical Sciences, University of Copenhagen during the period of January 2016 to March 2019. The project entitled ”Development and Evaluation of Potential 5-HT_7 Receptor PET Tracer Candidates” was performed under the principle supervision of Associate Professor Matthias M. Herth and co-supervision from Professor Gitte M. Knudsen, Tomas Ohlsson, Ph.D. and Maria Erlandsson, Ph.D. Funding for the PhD project was received from the Department of Drug Design and Pharmacology, University of Copenhagen (1/3), The Neurobiology Research Unit, Rigshospitalet, Copenhagen, Denmark (1/3) and Radiation Physics and Nuclear Medicine Physics Unit, Skånes University Hospital, Lund, Sweden (1/3). The experimental work described was carried out at four different research facilities. Organic chemistry was performed at the Department of Drug Design and Pharmacology and radiochemistry at Radiation Physics, Nuclear Medicine Physics Unit. Radiochemistry together with the *in vivo* evaluation and metabolism studies were also performed at the Department of Clinical Physiology, Nuclear Medicine & PET and *in vitro* autoradiography at the Neurobiology Research Unit. The thesis consists of 11 chapters, objectives and outline is provided in chapter 2. References appear in superscript and a full reference list is given at the end of each chapter. All articles and papers included in the thesis are reprinted with permission from the publisher.

LIST OF PUBLICATIONS

The Ph.D. thesis is based on the following publications and manuscripts, which are referred to by roman numerals I–VI. The publications are reprinted with permission from the publishers.

I. Towards selective PET Imaging of the 5-HT$_7$ Receptor System: Past, Present and Future

Elina T. L'Estrade[a,b,c], Maria Erlandsson[c], Tomas Ohlsson[c], Gitte M. Knudsen[a,d], Matthias M. Herth[a,b,e]

[a] *Neurobiology Research Unit, Rigshospitalet, Blegdamsvej 9, 2100 Copenhagen, Denmark*

[b] *Department for Drug Design and Pharmacology, Faculty of Health and Medical Sciences, University of Copenhagen, Universitetesparken 2, 2100 Copenhagen, Denmark*

[c] *Radiation Physics, Nuclear Medicine Physics Unit, Skånes University Hospital, Barngatan 3, 222 42 Lund, Sweden.*

[d] *Institute of Clinical Medicine, Faculty of Health and Medical Sciences, University of Copenhagen, Denmark.*

[e] *Department of Clinical Physiology, Nuclear Medicine and PET, University Hospital Copenhagen, Rigshospitalet Blegdamsvej 9, 2100 Copenhagen, Denmark*

Manuscript in preparation. Planned and invited to submit to Neuropharm.before June 30th 2019, for the special Issue: Advances in Serotonin Research: Crossing scales and boundaries.

II. Radiolabeling and *in vivo* evaluation of [^{11}C]AGH-44 - a potential lead structure to develop a positron emission tomography radioligand for the 5-HT$_7$ receptor

Elina T. L'Estrade[a,b,c], Ida N. Petersen[d,e], Mengfei Xiong[a,b], Adam S. Hogendorf[f], Agata Hogendorf[f], Jesper L. Kristensen[b], Andreas Kjær[d,e], Andrzej J. Bojarski[f], Maria Erlandsson[c], Tomas Ohlsson[c], Gitte M. Knudsen[a], Matthias M. Herth[a,b,d]

[a] *Neurobiology Research Unit, Rigshospitalet, Blegdamsvej 9, 2100 Copenhagen, Denmark*

[b] *Department for Drug Design and Pharmacology, Faculty of Health and Medical Sciences, University of Copenhagen, Universitetesparken 2, 2100 Copenhagen, Denmark*

[c] *Radiation Physics, Nuclear Medicine Physics Unit, Skånes University Hospital, Barngatan 3, 222 42 Lund, Sweden.*

[d] *Department of Clinical Physiology, Nuclear Medicine and PET, University Hospital Copenhagen, Rigshospitalet Blegdamsvej 9, 2100 Copenhagen, Denmark*

[e] *Cluster for Molecular Imaging, Faculty of Health Science, University of Copenhagen, Blegdamsvej 3, 2200 Copenhagen, Denmark*

[f] *Institute of Pharmacology, Polish Academy of Sciences, 12 Smętna,31-343 Kraków, Poland.*

Manuscript submitted to Bioorg. Med. Chem. Lett.

III. Fragment-based Labelling Using Condensation Reactions – A Possibility to Increase Throughput in Preclinical PET

Elina T. L'Estrade[a,b,c], Szabolcs Lehel[d], Ida N. Petersen[d], Fraser G. Edgar[b], Balázs Volk[e], Maria Erlandsson[c], Tomas Ohlsson[c], Gitte M. Knudsen[a,f] and Matthias M. Herth[a,b,d]

[a] *Neurobiology Research Unit, Rigshospitalet, Blegdamsvej 9, 2100 Copenhagen, Denmark*

[b] *Department for Drug Design and Pharmacology, Faculty of Health and Medical Sciences, University of Copenhagen, Universitetesparken 2, 2100 Copenhagen, Denmark*

[c] *Radiation Physics, Nuclear Medicine Physics Unit, Skånes University Hospital, Barngatan 3, 222 42 Lund, Sweden.*

[d] *Department of Clinical Physiology, Nuclear Medicine and PET, University Hospital Copenhagen, Rigshospitalet Blegdamsvej 9, 2100 Copenhagen, Denmark*

[e] *Directorate of Drug Substance Development, Egis Pharmaceuticals Plc., P.O. Box 100, H-1475 Budapest, Hungary*

[f] *Institute of Clinical Medicine, Faculty of Health and Medical Sciences, University of Copenhagen, Denmark*

Manuscript submitted to RCS Advances

IV. Development and Evaluation of Two Potential 5-HT_7 Receptor PET Tracers: [^{18}F]ENL09 and [^{18}F]ENL10

Elina Tampio L'Estrade[a,b,c], Mengfei Xiong[a,b], Vladimir Shalgunov[b], Fraser G. Edgar[b], Balázs Volk[d], Simone L. Baerentzen[a], Mikael Palner[a,e], Maria Erlandsson[c], Tomas Ohlsson[c], Gitte M. Knudsen[a,f] and Matthias M. Herth[a,b,g]

[a] *Neurobiology Research Unit, Rigshospitalet, Blegdamsvej 9, 2100 Copenhagen, Denmark*

[b] *Department for Drug Design and Pharmacology, Faculty of Health and Medical Sciences, University of Copenhagen, Universitetesparken 2, 2100 Copenhagen, Denmark*

[c] *Radiation Physics, Nuclear Medicine Physics Unit, Skånes University Hospital, Barngatan 3, 222 42 Lund, Sweden.*

[d] *Directorate of Drug Substance Development, Egis Pharmaceuticals Plc., P.O. Box 100, H-1475 Budapest, Hungary*

[e] *Center of Translational Neuroscience, Faculty of Health and Medical Sciences, University of Copenhagen, Denmark*

[f] *Institute of Clinical Medicine, Faculty of Health and Medical Sciences, University of Copenhagen, Denmark*

[g] *Department of Clinical Physiology, Nuclear Medicine and PET, University Hospital Copenhagen, Rigshospitalet Blegdamsvej 9, 2100 Copenhagen, Denmark*

Manuscript submitted to ACS Chemistry Neuroscience

V. Radiosynthesis and preclinical evaluation of [^{11}C]Cimbi-701 – Towards the imaging of cerebral 5-HT$_7$ receptors

Elina T. L'Estrade[a,b,c], Vladimir Shalgunov[b], Fraser Edgar[b], Martin G. Strebl-Bantillo[d], Mengfei Xiong[a,b], François Crestey[b], Ramesh Neelamegam[d], Agnete Dyssegaard[a], Szabolcs Lehel[e], Maria Erlandsson[c], Tomas Ohlsson[c], Jacob M. Hooker[d], Gitte M. Knudsen[a,f], Matthias M. Herth[b,e], Hanne D. Hansen[a]

[a] *Neurobiology Research Unit, Rigshospitalet, Blegdamsvej 9, 2100 Copenhagen, Denmark*

[b] *Department for Drug Design and Pharmacology, Faculty of Health and Medical Sciences, University of Copenhagen, Universitetesparken 2, 2100 Copenhagen, Denmark*

[c] *Radiation Physics, Nuclear Medicine Physics Unit, Skånes University Hospital, Barngatan 3, 222 42 Lund, Sweden.*

[d] *Athinoula A. Martinos Center for Biomedical Imaging, Department of Radiology, Massachusetts General Hospital, Harvard Medical School, 73 High Street, Charlestown, Massachusetts 02129, United States*

[e] *Department of Clinical Physiology, Nuclear Medicine and PET, University Hospital Copenhagen, Rigshospitalet Blegdamsvej 9, 2100 Copenhagen, Denmark*

[f] *Faculty of Health and Medical Sciences, University of Copenhagen, Denmark.*

Manuscript in preparation, target journal is Nuclear medicine and biology.

VI. Synthesis, Radiolabeling, *In vitro* and *In vivo* Evaluation of [^{18}F]ENL30 – A Potential PET Radiotracer for the 5-HT$_7$ Receptor

Elina T. L'Estrade[a,b,c], Fraser G. Edgar[b], Mengfei Xiong[a,b], Vladimir Shalgunov[b], Simone L. Baerentzen[a], Maria Erlandsson[c], Tomas G. Ohlsson[c], Mikael Palner[a,d], Gitte M. Knudsen [a,e], Matthias M. Herth [b,f]

[a] *Neurobiology Research Unit, Rigshospitalet, Blegdamsvej 9, 2100 Copenhagen, Denmark*

[b] *Department for Drug Design and Pharmacology, Faculty of Health and Medical Sciences, University of Copenhagen, Universitetesparken 2, 2100 Copenhagen, Denmark*

[c] *Radiation Physics, Nuclear Medicine Physics Unit, Skånes University Hospital, Barngatan 3, 222 42 Lund, Sweden.*

[d] *Center for Translational Neuromedicine, University of Copenhagen, Blegdamsvej 3B, 2200 Copenhagen N, Denmark*

[e] *Faculty of Health and Medical Sciences, University of Copenhagen, Denmark.*

[f] *Department of Clinical Physiology, Nuclear Medicine and PET, University Hospital Copenhagen, Rigshospitalet Blegdamsvej 9, 2100 Copenhagen, Denmark*

Manuscript submitted to ACS Omega

Publications not discussed in the thesis (Appendices)

Classics in Neuroimaging: The Serotonergic 2A Receptor System—from Discovery to Modern Molecular Imaging.

Elina T. L'Estrade[a,b,c], Hanne D. Hansen[a], Maria Erlandsson[c], Tomas G. Ohlsson[c], Gitte M. Knudsen[a], Matthias M. Herth[b,d]

[a]*Neurobiology Research Unit and CIMBI, Copenhagen University Hospital, Rigshospitalet, Blegdamsvej 9, 2100 Copenhagen, Denmark*

[b]*Department of Drug Design and Pharmacology, Faculty of Health and Medical Sciences, University of Copenhagen, Jagtvej 160, 2100 Copenhagen, Denmark*

[c]*Radiation Physics, Nuclear Medicine Physics Unit, Skånes University Hospital, Barngatan 3, Lund 222 42, Sweden*

[d]*Department of Clinical Physiology, Nuclear Medicine and PET, University Hospital Copenhagen, Rigshospitalet Blegdamsvej 9, 2100 Copenhagen, Denmark*

Reprinted with permission from ACS Chemical Neuroscience, **2018**, *9* (6), 1226-1229. DOI: 10.1021/acschemneuro.8b00176.

Synthesis and Pharmacological Evaluation of [^{11}C]4-Methoxy-N-[2-(thiophene-2-yl)imidazo[1,2-a]pyridine-3-yl]benzamide as a Brain Penetrant PET Ligand selective for the δ-Containing γ-Aminobutyric Acid Type A Receptors

Elina T. L'Estrade,[a,b,c,d] ‡ Hanne D. Hansen,[b] ‡ Christina Falk-Petersen,[a] Anne Haugaard, [a] Nane Griem-Krey [a] Sascha Jung,[f] Hartmut Lüddens,[e] Tanja Schirmeister,[f] Maria Erlandsson,[c] Tomas Ohlsson,[c] Gitte M. Knudsen,[b] Matthias M. Herth,[a,b,d] Petrine Wellendorph,[a] Bente Frølund[a*]

[a]*Department of Drug Design and Pharmacology, Faculty of Health and Medical Sciences, University of Copenhagen, 2100 Copenhagen, Denmark*

[b]*Neurobiology Research Unit and CIMBI, Copenhagen University Hospital, Rigshospitalet, Blegdamsvej 9, 2100 Copenhagen, Denmark*

[c]*Radiation Physics, Nuclear Medicine Physics Unit, Skånes University Hospital, Barngatan 3, Lund 222 42, Sweden*

[d]*Department of Clinical Physiology, Nuclear Medicine and PET, University Hospital Copenhagen, Rigshospitalet Blegdamsvej 9, 2100 Copenhagen, Denmark*

[e]*Department of Psychiatry and Psychotherapy, Falculty of Health and Medical Sciences, University of Medical Center Mainz, D-55131, Germany*

[f]*Institute of Pharmacy & Biochemistry, Johannes Gutenberg University Mainz, D-55128, Germany*

Manuscript submitted to ACS Omega

The Author's Contribution to Publications I–VI

I. Towards selective PET Imaging of the 5-HT_7 Receptor System: Past, Present and Future

Elina T. L'Estrade, Maria Erlandsson, Tomas Ohlsson, Gitte M. Knudsen, Matthias M. Herth

Formulated the outline, performed the literature research and contributed considerably to writing the manuscript

II. Radiolabeling and *in vivo* evaluation of [^{11}C]AGH-44 - a potential lead structure to develop a positron emission tomography radioligand for the 5-HT_7 receptor

Elina T. L'Estrade, Ida N. Petersen, Mengfei Xiong, Adam S. Hogendorf, Agata Hogendorf, Jesper L. Kristensen, Andreas Kjær, Andrzej J. Bojarski, Maria Erlandsson, Tomas Ohlsson, Gitte M. Knudsen, Matthias M. Herth

The reference and precursor synthesis was performed by A.S.H, A.H and A.B. The author established the radiosynthesis and the quality control of [^{11}C]AGH-44. The author also planned the *in vivo* evaluation and metabolism in rats. The animal experiments were performed as collaboration between the author, I.N.P, M.X and V.S. Biodistribution studies, image analysis and data interpretation was performed by the author, which also contributed considerably with writing the manuscript.

III. Fragment-based Labelling Using Condensation Reactions – A Possibility to Increase Throughput in Preclinical PET

Elina T. L'Estrade, Szabolcs Lehel, Ida N. Petersen, Fraser G. Edgar, Balázs Volk, Maria Erlandsson, Tomas Ohlsson, Gitte M. Knudsen and Matthias M. Herth

The author contributed to the designed PET tracer library. Planned and executed the organic synthesis (F.G.E was involved in the synthesis of some compounds and precursor under the supervision of the author) of the compounds. The establishment of the radiolabelling strategy for the carbon-11 fragment-based condensation strategy was done in collaboration with S.L and I.N.P. Extension to fluorine-18 labelling and optimization experiments were done by the author, as well as the establishment of the dual-condensation. The author thereafter planned and performed the fragment-based approach

on one additional labelling strategy. The author also formulated the outline and contributed considerably to writing the manuscript together with M.M.H.

IV. Development and Evaluation of Two Potential 5-HT_7 Receptor PET Tracers: [^{18}F]ENL09 and [^{18}F]ENL10

Elina Tampio L'Estrade, Mengfei Xiong, Vladimir Shalgunov, Fraser G. Edgar, Balázs Volk, Simone L. Baerentzen, Mikael Palner, Maria Erlandsson, Tomas Ohlsson, Gitte M. Knudsen and Matthias M. Herth

The author performed the reference syntheses and elaborated on the most promising candidates after *in vitro* evaluation by the PDSP, as well as scaled up the experiments and produced PET tracer for the evaluation in rats. The author also considerably contributed to the planning of the evaluation in rodents, which was performed in collaboration with M.X, F.G.E and V.S. The analysis of the PET images was done by the author. The author also formulated the outline and contributed considerably to writing the manuscript together with M.M.H.

V. Radiosynthesis and preclinical evaluation of [^{11}C]Cimbi-701 – Towards the imaging of cerebral 5-HT_7 receptors

Elina T. L'Estrade, Vladimir Shalgunov, Fraser Edgar, Martin G. Strebl-Bantillo, Mengfei Xiong, François Crestey, Ramesh Neelamegam, Agnete Dyssegaard, Szabolcs Lehel, Maria Erlandsson, Tomas Ohlsson, Jacob M. Hooker, Gitte M. Knudsen, Matthias M. Herth, Hanne D. Hansen

The reference compound was synthesized by F.G.E and F.C. The radiolabelling was established by S.L. The planning of the *in vivo* evaluation [^{11}C]Cimbi-701 in rats was performed by the author, the experiment was done by the author and M.X. while V.S produced the tracer. The author thereafter performed the PET image analysis. The pig evaluation and metabolism study was performed by H.D.H and A.D. The non-human primate *in vivo* evaluation was performed by the group of J.M.H. The author and H.D.H. formulated the outline and wrote the manuscript in collaboration with M.M.H.

VI. Synthesis, Radiolabeling, *In vitro* and *In vivo* Evaluation of [^{18}F]ENL30 – A Potential PET Radiotracer for the 5-HT$_7$ Receptor

Elina T. L'Estrade, Fraser G. Edgar, Mengfei Xiong, Vladimir Shalgunov, Simone L. Baerentzen, Maria Erlandsson, Tomas G. Ohlsson, Mikael Palner, Gitte M. Knudsen, Matthias M. Herth

Reference synthesis was made by F.G.E. The radiosynthesis and quality control was established by the author, together with F.G.E. The planning of the *in vivo* evaluation of [^{18}F]ENL30 in rats was performed by the author. The author both produced the tracer and in collaboration performed the evaluation with M.X., S.L.B and V.S. Image analysis was done by the author. *In vitro* autoradiography was established and accomplished by the author and M.X. The interpretation of the results was performed by the author (with supervision from M.P). The author also formulated the outline and contributed considerably with writing of the manuscript.

TABLE OF CONTENTS

PREFACE **5**

LIST OF PUBLICATIONS **6**

THE AUTHOR'S CONTRIBUTION TO PUBLICATIONS I–VI **10**

ABBREVIATIONS **15**

ABSTRACT **17**

ABSTRACT IN DANISH (RESUMÉ) **17**

CHAPTER 1 ..... **19**

Introduction

CHAPTER 2 ..... **45**

Objectives and outline

CHAPTER 3 ..... **49**

Towards selective PET Imaging of the 5-HT_7 Receptor System: Past, Present and Future

CHAPTER 4 ..... **97**

Radiolabelling and *in vivo* evaluation of [^{11}C]AGH-44 - a potential lead structure to develop a positron emission tomography radioligand for the 5-HT_7 receptor

CHAPTER 5 ..... **113**

Fragment-based Labelling Using Condensation Reactions – A Possibility to Increase Throughput in Preclinical PET

CHAPTER 6 ..... **193**

Development and Evaluation of Two Potential 5-HT_7 Receptor PET Tracers: [^{18}F]ENL09 and [^{18}F]ENL10

CHAPTER 7 ..... **233**

Radiosynthesis and preclinical evaluation of [^{11}C]Cimbi-701 – Towards the imaging of cerebral 5-HT_7 receptors

CHAPTER 8 265

Synthesis, Radiolabeling, *In vitro* and *In vivo* Evaluation of [^{18}F]ENL30 – A Potential PET Radiotracer for the 5-HT_7 Receptor

CHAPTER 9 319

Summary

CHAPTER 10 335

Conclusions and future perspectives

ACKNOWLEDGEMENTS 338

CHAPTER 11 339

Appendices

ABBREVIATIONS

$5\text{-}HT_7$	-	5-hydroxytryptamine (serotonin) subtype 7
$5\text{-}HT_7R$	-	5-hydroxytryptamine subtype 7 receptor
A_m	-	Molar activity
AUC	-	Area under the curve
BBB	-	Blood-brain barrier
Boc	-	*tert*-Butyloxylcarbonyl
BP	-	Binding potential
B_{max}	-	Total density (concentration) of receptors
Bq	-	Becquerel
CNS	-	Central nervous system
d.c	-	Decay corrected
cAMP	-	Cyclic adenosine monophosphate
DMF	-	*N*,*N*-Dimethylformamide
DMSO	-	Dimethyl sulfoxide
EOS	-	End of synthesis
HPLC	-	High-pressure liquid chromatography
HRRT	-	High Resolution Research Tomograph
i.v.	-	Intravenous
K_{222}	-	4,7,13,16,21,24-Hexaoxa-1,10-diazabicyclo[8.8.8]hexacosane
K_D	-	Dissociation constant
K_i	-	Inhibition constant
LC-MS	-	Liquid chromatography mass spectrometry
LogD	-	Log of distribution coefficient
LogP	-	Log of partition coefficient
LSD	-	D-lysergsyrediethylamid
MeCN	-	Acetonitrile
NMR		Nuclear magnetic resonance
PET	-	Positron emission tomography
P-gp	-	P-glycoprotein
RCC	-	Radiochemical conversion
RCY	-	Radiochemical yield
REM	-	Rapid eye movement
SPE	-	Solid-phase extraction
SUV	-	Standard uptake value
$t_{½}$	-	Half-life
tBR	-	Theoretical binding ratio
TAC	-	Time activity curve
TOI	-	Time of injection
TFA	-	Trifluoroacetic acid
THF	-	Tetrahydrofuran

TLC	-	Thin layer chromatography
UV	-	Ultraviolet
VOI	-	Volume of interest
β^+	-	Positron
e^-	-	Electron
γ	-	Gamma

ABSTRACT

Purpose: The Serotonin 7 receptor (5-HT_7R) is the most recently discovered subfamily of the serotonergic receptor system. Extensive research has resulted in evidence of its involvement in a broad variety of physiological functions and central nervous system (CNS) disorders. Molecular imaging of this receptor with Positron Emission Tomography (PET) would permit deeper insights into its *in vivo* pharmacology and function. So far, no clinical PET radiotracer exists for this interesting target. Consequently, the aim of this PhD thesis was to develop a 5-HT_7R selective PET tracer.

Strategy/Procedures: Several scaffolds were selected as a starting point to develop a 5-HT_7R PET tracer. This strategy was used to increase the likelihood to identify a suitable imaging agent. Precursors and reference compounds were either gained from cooperation partners or synthesized. Radiolabelling was carried out using carbon-11 and fluorine-18. Compounds were usually characterized based on affinity and selectivity determinations, metabolism investigations and autoradiography. Promising ligands were after-wards translated to *in vivo* PET imaging, in which blood-brain barrier (BBB) permeability, regional brain distribution and specific binding to the target was tested. To accelerate the *in vivo* throughput, a custom-made rat holder was designed and built for our high-resolution PET scanner. This set-up enabled us to scan 4 rats simultaneously. In line with these efforts, a fragment-based labelling strategy was also developed to increase tracer availability.

Results: Fifteen potential 5-HT_7R PET tracer candidates were designed, synthesized and characterized. Five structures showed suitable characteristics to be translated to *in vivo* PET studies. The selection of these structures was based on 5-HT_7R affinity, selectivity and sufficient yield during radiolabelling. Subsequent PET studies revealed that all tracers displayed poor rat brain uptake. After inhibition of the P-gp efflux transporter, high and specific 5-HT_7R uptake could be identified for [^{18}F]ENL10, [^{11}C]Cimbi-701 and [^{18}F]ENL30. Additional and undesired off-target binding was determined for [^{18}F]ENL09, [^{11}C]Cimbi-701 and [^{18}F]ENL30.

Conclusions: In this thesis, were [^{18}F]ENL10, [^{11}C]Cimbi-701 and [^{18}F]ENL30 identified to be the best tracer candidates to image the 5-HT_7R *in vivo*. Even though, all tracers are P-gp substrates in rats, we believe that translation to higher species should be carried out. This is because P-gp dependency is expected to be less of a problem in higher species. Compared to higher species, rodents display increased P-gp activity. Observed off-target binding could be addressed by dual or triple blocking regimes of these targets. Ultimately, this approach could enable selective 5-HT_7R PET imaging in higher species, maybe even in humans.

ABSTRACT IN DANISH (Resumé)

Formål: Serotonin subtype 7 receptoren (5-HT_7R) er det nyeste medlem af det serotonerge receptor system. Forskning i funktionen af 5-HT_7R har vist at den er involveret i en lang række fysiologiske funktioner og lidelser i centralnervesystemet (CNS). Molekylær billeddiagnostik af denne receptor ved brug af Positron-Emissions-Tomografi (PET) vil muliggøre flere studier og viden om receptorens *in vivo* farmakologi. På nuværende tidspunkt findes der ikke et klinisk godkendt radioaktivt sporstof til 5-HT_7R at bruge til PET. Derfor var formålet med dette Ph.d. projekt at udvikle et selektivt PET sporstof til billeddannelse af 5-HT_7R.

Strategi/metoder: Flere lovende skabeloner blev brugt til at udvikle og syntetisere 5-HT_7R PET sporstoffer. Denne strategi blev valgt for at forhøje chancen for at identificere et sporstof til 5-HT_7R. Udgangsstoffer og referencestoffer blev enten givet af samarbejdspartnere eller syntetiseret. Radiomærkning, med carbon-11 eller fluor-18, efterfulgt af *in vivo* evaluering gav viden omkring de potentielle PET sporstoffers blodhjernebarriere (BBB) permeabilitet, distribution i hjernen og specifik binding til 5-HT_7R. For at fremskynde *in vivo* evalueringen blev der konstrueret en holder til vores PET-skanner for at muliggøre skanning af 4 rotter på en gang. Derudover blev der udviklet en fragmentbaseret strategi for at accelerere sporstofsyntesen.

Resultater: 15 potentielle 5-HT_7R PET sporstoffer blev designet, syntetiseret og karateriseret. Fem af de syntetiserede PET sporstoffer viste passende karakteristika til *in vivo* billeddannelse. Udvælgelsen af disse sporstoffer var baseret på 5-HT_7R affinitet og selektivitet, samt tilstrækkeligt radiokemisk udbytte. Indledende PET studier viste et lavt optag i rottehjerne for alle sporstofferne. Blokering af P-gp efflux transporteren gav et højt, og specifikt optag for [^{18}F]ENL10, [^{11}C]Cimbi-701 og [^{18}F]ENL30. Uønsket off-target binding blev vist for [^{18}F]ENL09, [^{11}C]Cimbi-701 and [^{18}F]ENL30.

Konklusion: [^{18}F]ENL10, [^{11}C]Cimbi-701 og [^{18}F]ENL30 var i denne afhandling de bedste sporstoffer til 5-HT_7R *in vivo*. Selvom et lavt optag i rottehjernen grundet P-gp transporteren blev observeret for alle sporstofferne, forventes det at være et mindre problem i højerestående arter. Den observerede off-target binding kan undgås ved at bruge dobbel – eller trippelblokering. Endeligt kan denne fremgangsmåde muliggøre selektiv 5-HT_7R billeddannelse i højerestående arter, måske endda i mennesker.

Chapter 1

Introduction

Summary:

This chapter contains an introduction of the 5-HT_7 receptor, with emphasis on what makes this biological target so interesting, but initially will the serotonergic system be described. Further will this chapter also contain important methods and techniques used within this thesis together with important characteristics for potential PET tracer candidates.

CHAPTER 1 - Introduction

1.1 The Serotonin Transmitter System

Within the central nervous system (CNS), serotonin (5-hydroxytryptamine, 5-HT) and its receptors are involved in the regulation of physiological homeostasis. However, in instances of dysfunction, the serotonergic system can be implicated in a number of disorders. Appetite, sleep, thermoregulation, depression, migraine and schizophrenia are some motivating examples, illustrating what makes this system an interesting target for research.[1-2] The serotonergic system is comprised of a diverse family of 5-HT receptors and their neurotransmitter, 5-HT.[3]

In the brain 5-HT is biosynthesized from the essential amino acid tryptophan within neurons originating in the raphe nuclei.[3-4] Thus, 5-HT is present, synthesized and have functions elsewhere throughout the body as well.[3]

To date, 14 different serotonergic receptor subtypes have been identified. The subtypes are divided into seven families of 5-HT receptors based on pharmacology, transduction and structure. The receptor subtypes are G-protein coupled receptors (guanine-nucleotide binding protein coupled receptors, GPCR), except for the 5-HT_3 receptor which is a ligand-gated ion channel.[3, 5] Figure 1 presents a schematic overview of the major 5-HT receptors.

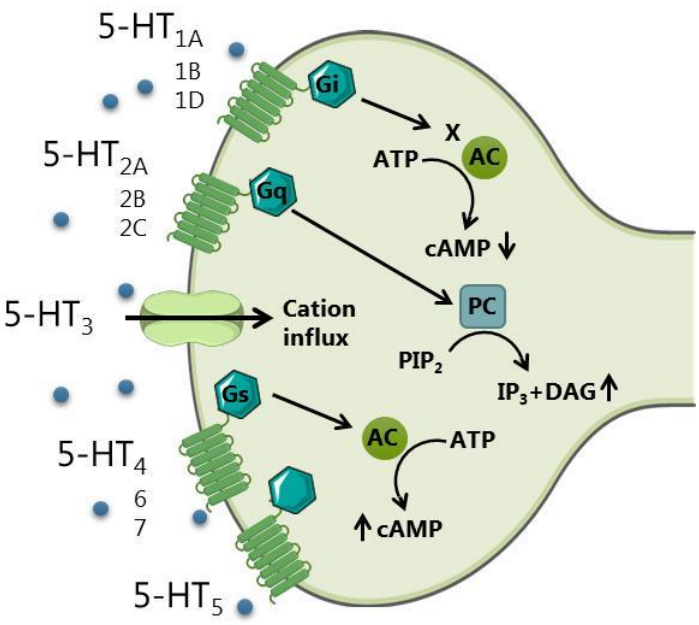

Figure 1: A schematic overview of the majority of 5-HT receptors and to which g-proteins they are coupled. The 5-HT_5 is not well studied, but it is believed to couple to the $G_{i/o}$ g-protein which decrees the production of cAMP.[3] Abbreviations: AC, adenylate cyclase; DAG, diacylglycerol; IP_3, inositol-1,4,5-trisphosphate; PIP_2, phosphatidylinositol-4,5-bisphosphate. Illustration inspired by Wong *et al* 2005.[3-4] http://smart.servier.com.

The most recently identified 5-HT receptor is the subtype 7, which was successfully cloned in 1993.[6-8] The 5-HT_7R is coupled to the stimulatory G_s protein, and activation through the binding

of serotonin (5-HT) increases the production of cyclic adenosine monophosphate (cAMP) (Figure 1).[3] This receptor will be further explained in the ensuing section.

1.2 The 5-HT$_7$ Receptor (5-HT$_7$R)

Since the discovery of the 5-HT$_7$R, a number of methods have been employed in order to investigate its biological role. Results presented in the upcoming section were mainly performed using either 5-HT$_7$R genetic knock-out mice and/or with the systemic or local administration of an antagonist - primarily the highly selective SB-269970.[9]

The 5-HT$_7$R has been found to influence a range of important normal physiological functions.[10-11] The 5-HT$_7$R was first implicated in normal sleep regulation. Results from inhibition studies of the 5-HT$_7$R led to less frequent and shorter rapid eye movement (REM) episodes. REM is a sleep phase in which there are physiological similarities to being awake. Furthermore, the effect observed by 5-HT$_7$R inhibition is opposite to what is seen in depressed patients.[12-13] Thermoregulation is another example. Hypothermia induced by the 5-HT$_{1A/7}$ receptor agonist 8-OH-DPAT could be inhibited by SB-269970.[10, 14-16] Finally, the 5-HT$_7$R system is involved in pain. For example, the flinching effect seen after formalin injection as a model for injury-produced pain could be reduced by local administration of SB-269970 prior to formalin injection.[17] In addition, systemic administration of 5-HT$_7$R agonists, such as E-55888, clearly show an analgesic effect in animal model of nociception. This hints to the possibility that 5-HT$_7$R agonists may be therapeutically useful in relieving pain.[18]

The 5-HT$_7$R has also been shown to be involved in psychiatric disorders. For example, a clear relationship has been found between 5-HT$_7$R inhibition and antidepressant effects in two commonly used models for depression; the forced swim test and the tail suspension test. The antidepressant outcome measure achieved in these two models is an increased anti-immobility, which reflects a decrease in a considered behavioural despair of the animals. These results were further supported by genetic knock-out experiments.[13, 19-23] More recently, it has been discovered that the anti-depressant effect of the well-established anti-psychotic drug amisulpride is induced by inhibiting the 5-HT$_7$R.[24] Interestingly, many other anti-psychotic drugs also display high affinity for the 5-HT$_7$R. This indicates that this receptor may, to a certain degree, be involved in the pathogenesis of schizophrenia.[25] This hypothesis is further strengthened by the fact that in post-mortem studies decreased mRNA levels for the 5-HT$_7$R has been observed in the

dorsolateral prefrontal cortex of schizophrenic patients, which is a region strongly associated to this disorder.[26]

The tissue distribution of the 5-HT$_7$R within the brain is of great value to gain a deeper understanding of the different receptor mediated functions described above. The receptor distribution is measured by *in vitro* autoradiography, B_{max} determinations or tissue homogenate measurements.[27-28] With the discovery of the high-affinity 5-HT$_7$R antagonist SB-269970, a tritiated analogue revealed the brain tissue distribution of the 5-HT$_7$R using autoradiography[29]. The results of the autoradiography on rat[30], pig[31] and human[32] brain tissue showed good agreement between the species with high binding regions found in thalamus, hypothalamus and hippocampus. Figure 2 displays a schematic overview of the highest density brain regions in the rat brain as well as their associated receptor-mediated functions.[10]

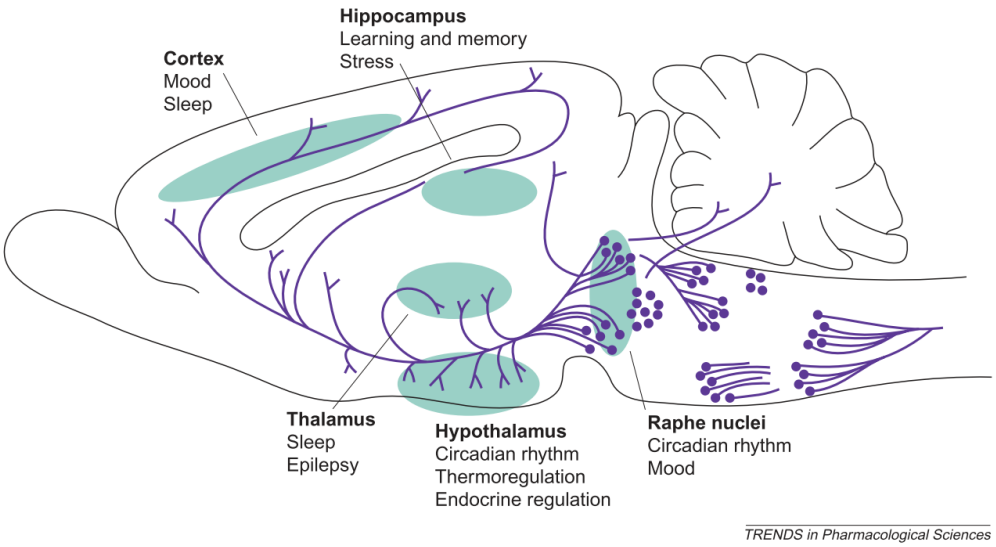

Figure 2: A schematic presentation of; regions rich in 5-HT$_7$ receptor expression, shown in green, and the projections of 5-HT-producing neurons in purple. The assumed correlation with 5-HT$_7$ receptor-mediated functions is also indicated. Reprinted from Trends in Pharmacological Sciences, 25. Peter B. Hedlund and J. Gregor Sutcliffe, Functional, molecular and pharmacological advances in 5-HT$_7$ receptor research, 481-486., Copyright (2004), with permission from Elsevier.[10]

Currently, there is no *in vivo* clinical imaging tool available to study the 5-HT$_7$R in depth.[11, 33] As mentioned, the 5-HT$_7$R is closely involved in the pathogenesis of a range of CNS disorders. The development of a selective PET tracer would allow *in vivo* visualization and quantification, in both healthy and diseased subjects, and elucidating of its biological involvement. A PET tracer could also act as a tool in the development of potential new drugs targeting the 5-HT$_7$R. Furthermore, the 5-HT$_7$R displays the highest affinity towards serotonin of all serotonergic receptors. Thus, it could be a valuable tool to determine the concentration of serotonin in the

synaptic cleft[34]. This could significantly improve our understanding of the involvement of endogenous serotonin in brain disorders[35] and potentially pave the way for new treatment options.

There have been many attempts to develop a selective PET tracer for the 5-HT_7R during the last two decades, and previous progress in the field of this on-going exploration is reviewed in **Paper I** (chapter 3). In the next section the molecular imaging technique, PET, will be further elaborated upon.

1.3 Positron Emission Tomography (PET)

PET is a molecular imaging method in which a radiotracer is administered – most commonly intravenously (i.v). It is frequently used in the clinic to monitor *in vivo* processes with high sensitivity and selectivity. Processes imaged can be enzymatic reactions, rates of metabolism or e.g. receptor−ligand interactions[36]. In contrast to structural imaging methods like X-ray that receives anatomical information, PET can visualize the physiology of a living organism. In the clinic today, PET is most frequently used in oncology, where it serves as a tool for diagnosis and treatment monitoring. In drug development, PET can be used as an *in vivo* pharmacological imaging tool to evaluate the *in vivo* behaviour of drug candidates. Thus, PET aids in the identification of the most likely to succeed drug candidate. Additionally, PET can be used in early trial phases, thereby reducing associated costs of drug development.[36-38]

Useful approaches can be structured into direct and indirect methods with different end point parameters. Pharmacokinetic properties of the new drug can be measured by PET via the direct method, if it is possible to synthesize a PET tracer with the same structure as the drug candidate. Pharmacodynamic properties are on the other hand examined using indirect methods and relative to effects on established radiotracers for the biological target. Outcome measures of these experiments are e.g., density of target receptors (B_{max}), the effect of the drug on apparent affinity (K_D) and the ligand binding potential (BP), which are calculated as the B_{max}/ K_D.[36, 39-40] The indirect methods also allow determination of the dose dependent receptor occupancy, which provides insight into the maximum dose or the dosing interval of the drug candidates. The occupancy is determined by Eq. 1; comparing the relative changes of binding potential at tracer baseline scans and after pretreatment with the drug candidate.[36]

$$Receptor\ Occupancy = \frac{BP_{baseline} - BP_{treated}}{BP_{baseline}}\ x\ 100 \qquad \text{(Eq. 1)}$$

PET relies on the use of radioactive tracers labelled with positron emitting isotopes; Table 1 presents an overview of commonly used non-metal isotopes. Due to the selective detection of the 511 keV gamma-ray photons emitted, PET is highly sensitive. The sensitivity enables administration of tracer amounts (pmol-µmol), which has the advantage of not disturbing the biological system. In the case of an input function derived from a reference region, PET is also non-invasive, except for the initial injection of the radiotracer.[37, 41]

Table 1: An overview of characteristics for commonly used non-metal PET isotopes within CNS imaging.[37, 42-44]

Isotopes	**Half-life ($t_{½}$)**	**Production**	**Mean $E_{\beta+}$ (keV)**	**Decay mode**	**R_{max} (mm)**	**R_{mean} (mm)**
^{18}F	110 min	^{18}O(p,n), ^{20}Ne(d,a)	252	β^+ (97%) EC (3%)	2.4	0.6
^{11}C	20.4 min	^{12}C(g,n), ^{14}N(p,a), ^{11}B(p,n)	390	β^+ (99.79%) EC (0.21%)	3.9	1.1
^{13}N	9.97 min	^{16}O(p,a), ^{12}C(d,n)	488	β^+ (99.8%) EC (0.2%)	5.1	1.5
^{15}O	122.24 s	^{16}N(g,n), ^{14}N(d,n), ^{15}N(p,n)	730	β^+ (99.9%) EC (0.1%)	8.0	2.5
^{68}Ga	68 min	^{68}Ge/^{68}Ga generator	844	β^+ (90%) EC (10%)	8.9	2.9

Positron-emitting isotopes are often produced by proton bombardment in a cyclotron. During decay a proton is transformed into a neutron while a positron and a neutrino are emitted (Figure 3). After injection of the radiotracer into a biological system, the radionuclide will decay, and the emitted positron will subsequently collide with an electron in the surrounding tissue after travelling a short distance. The distance is dependent on the kinetic energy of the positron. The collision results in a direct annihilation or the opposing particles may combine to form a short-lived system known as a positronium, which then annihilates itself. Both circumstances produce two gamma-ray photons that are being emitted at approximately 180° from one another. After coincidence detection of the two gamma ray photons by a circular PET scanner, a line of response (LORs) correlates the two relevant detectors. Reconstruction of the coincidence data gives an approximate location of the positron-emitting isotope and hence the radiotracer can be visualized as a 3D PET image. This image is quantifiable.[36-37]

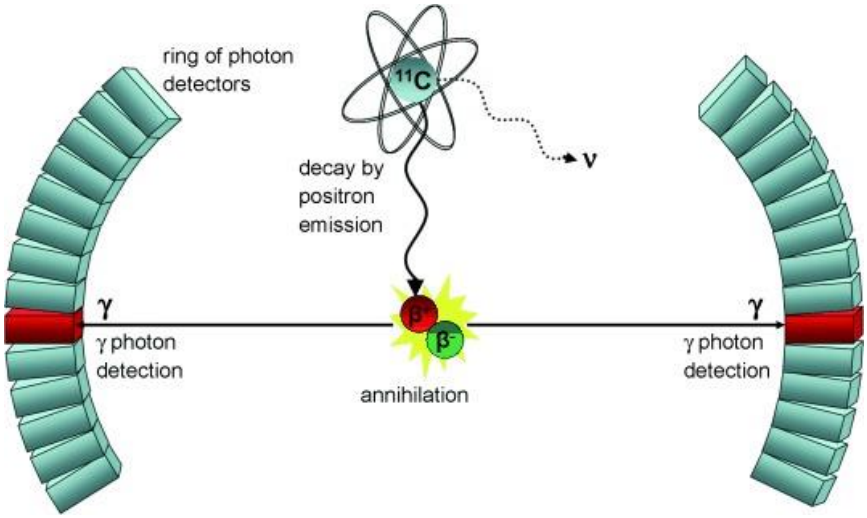

Figure 3: Illustration of the mechanism behind positron emission tomography (PET) [37] Permission for the reuse of this work has been given by John Wiley and Sons. The work was originally published by Miller, P. W.; Long, N. J.; Vilar, R.; Gee, A. D., Synthesis of ^{11}C, ^{18}F, ^{15}O, and ^{13}N radiolabels for positron emission tomography. *Angew Chem Int Ed Engl* 2008, *47* (47), 8998-9033. Copyright © 2008 WILEY-VCH Verlag GmbH & Co. KGaA, Weinheim.

1.4 Development of CNS Radiotracers

Current development strategies are largely dependent on a "trial-and-error game" as e.g., computational and *in vitro* approaches predicting the *in vivo* behaviour of CNS tracers are still unreliable.[45-47] However, some general requirements have been recognized for the development of a CNS radiotracer. This will be discussed thoroughly in **Paper I** (chapter 3), with the following Table 2, summarizing the most important characteristics and how they are determined (direct copied from **Paper I**).

Table 2: Overview of the most important characteristics within the development of a PET tracer for the CNS and how they are determined.

Contrast				**Additional**			
1	*Specific binding*		**Determined**	**1**	*BBB permeability*		**Determined**
		K_D (nM to sub-nM)	*In vitro* assay potency *In vivo* BP			**Low P-gp dependency**	*In vivo* inhibition with elacridar
		B_{max}	*In vitro* on brain slice or homogenate tissue binding studies *In vivo* quantitative kinetic modeling			**Lipophilicity** (LogP of 1.5 - 3.5)[48]	Tracer brain uptake during *in vivo* evaluation (qualitative TAC analysis)
2	*Unspecific binding*			**2**	*Metabolism*		
		High Selectivity	*In vitro* screening (PDSP) *In vivo* blocking or gene knock-out			**No brain permeable radiometabolites**	Radio-HPLC Plasma analysis of arterial blood samples during *in vivo* evaluation
3	*Non-specific binding*			**3**	*Quantification*		
		Lipophilicity (LogP of 1.5 -3.5)[48]	*"No wash"* autoradiography or *in silico* prediction *In vivo* blocking or gene knock-out			**Reversible tracer kinetics**	Qualitative TAC analysis Quantitative kinetic modeling

Many values can only be determined *in vivo*, as seen from Table 2. Moreover, *in vivo* B_{max} values and affinities may differ from those seen *in vitro*. This could for example be due to target internalization or receptor deactivation.[49] Consequently, efficient *in vivo* screening methods can accelerate the development process. Very often, the limited step in this process is to get access to a tracer library within the same or structurally diverse class. As such, it might be beneficial to simultaneously start the development process on different chemical scaffolds as well as

developing a more versatile labelling strategy that could increase the number of tracers and/or reduce the time needed to get access to more PET tracers. One method to simply increase the numbers of tracers has recently been used by Herth *et al.* in 2014 (Figure 4).[47] Instead of a late-stage labelling approach, a fragment-based method has been applied. In this case, a small fragment of the final radiotracer is first labelled and then further reacted with different building block analogues. Indeed, the strategy will inevitably reduce the achievable radiochemical yield in comparison to conventional late-stage labelling. However, the fragment-based method is expected to be more time efficient, due to the reduction of time needed for precursor synthesis. This would be achieved since it aligns the tracer syntheses with the medicinal chemistry efforts, where similar strategies are typically applied.[45-47] The fragment-based labelling strategy will be elucidated as a tool for accelerating my efforts to identify a radiotracer for the 5-HT_7R in **Paper III** (chapter 5).

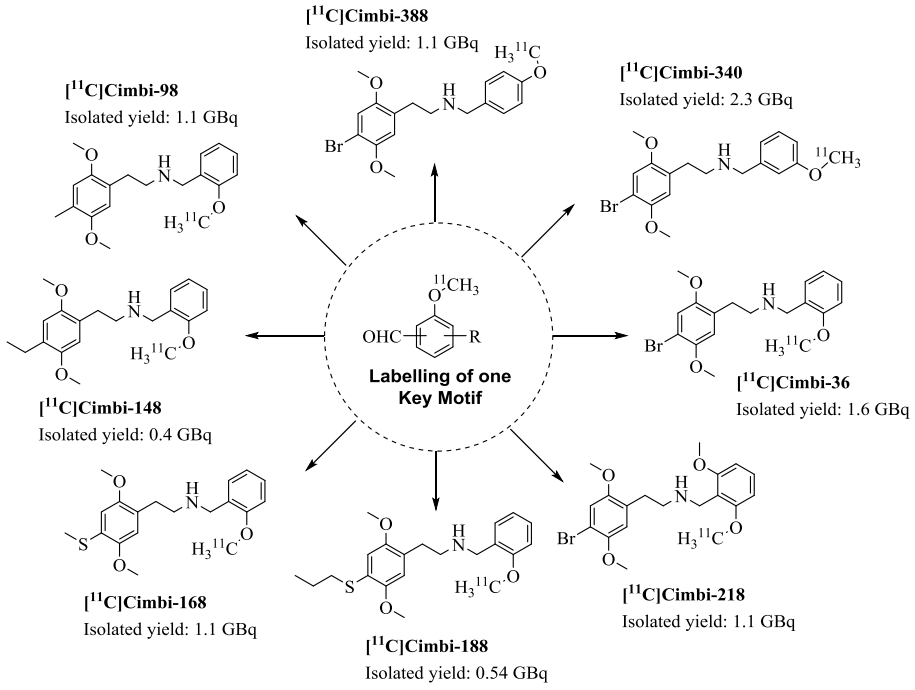

Figure 4: Schematic overview of the combinatorial-like strategy using reductive amination to make a PET tracer library for the 5-HT_{2A} receptor [47]

In the following two sections, I will elaborate on the radionuclides used within this thesis. Special attention will be drawn on advantages and disadvantages of applying them.

1.5 Fluorine-18

Fluorine-18 is the by far the most clinically applied PET radionuclide. This is because of its unique decay characteristic that is beneficial in the clinic. Fluorine-18 has a half-life of 109.77

min. It is long enough to ship the formulated radiotracer to other facilities and use the same batch of tracer for several scans during the same day.[37] Another valuable characteristic of fluorine-18 is its high branching ratio of 97% of positron (β^+) - emission (Eq. 2). The positron of fluorine-18 has also a relatively low mean kinetic energy, which results in a short positron linear range. In tissue, the mean traveling distance is 0.6 mm. This result in a relatively high spatial resolution compared to other positron emitters (Table 1).[43]

$$^{18}F \rightarrow {}^{18}O + \beta^+ + \nu_e \qquad \text{(Eq. 2)}$$

Over the years, many labelling approaches have been explored.[41] Generally, these can be divided into direct fluorination and indirect fluorination strategies.

1.5.1 Direct ^{18}F-fluorination

Direct fluorination strategies are divided into two main approaches; electrophilic and nucleophilic fluorination. Electrophilic fluorination suffers from low molar activity since standard production routes are dependent on addition of F_2 [37, 50]. Nucleophilic fluorine-18 is usually carried out in a non-carrier added (n.c.a) manner. As such, it is the preferred method for CNS application. In the following sections I will focus on nucleophilic procedures.

1.5.1.1 Nucleophilic ^{18}F-fluorination

The production of fluorine-18 as nucleophilic fluoride-18 ($[^{18}F]F^-$) is commonly performed in a cyclotron by proton bombardment of a target containing enriched $[^{18}O]H_2O$ (Eq. 3).

$$^{18}O(p,\mathrm{n})^{18}F \qquad \text{(Eq. 3)}$$

$[^{18}F]F^-$ is subsequently delivered in an aqueous solution, thus inactivated by hydrogen bonding. To increase the nucleophilicity of the ion, the water is commonly removed by concentrating the $[^{18}F]F^-$on an anion exchange cartridge. Using a basic eluting solution (e.g. K_2CO_3 dissolved in a small volume of H_2O and diluted either in MeCN or MeOH) the $[^{18}F]F^-$ is released from the anion exchange cartridge into the preferred reaction vial. The basic conditions also prevent the formation of $[^{18}F]HF$ and stabilizes the $[^{18}F]F^-$ anion. Before further reaction with the precursor, the water used to solubilize the base needs to be removed by azeotropic drying with dry MeCN.[41]

To further increase the nucleophilicity and the solubility of $[^{18}F]F^-$ in the polar, aprotic solvents used within nucleophilic ^{18}F-fluorination reactions, a phase transfer catalyst (e.g. 4,7,13,16,21,24-Hexaoxa-1,10-diazabicyclo[8.8.8]hexacosan (Kryptofix$_{222}$)) is added to the eluting solution.[41]

Nucleophilic ^{18}F-fluorination methods include classical nucleophilic substitution reactions such as S_N2 and nucleophilic aromatic substitution (S_NAr) etc. Common leaving groups for the S_N2 nucleophilic ^{18}F-substitution reactions are e.g. tosylate (p-toluenesulphonate), mesylate (methanesulphonate), halogens and nitro groups. Usually, the reactions are performed under heat, in aprotic solvents and in the presence of base (Scheme 1).[41]

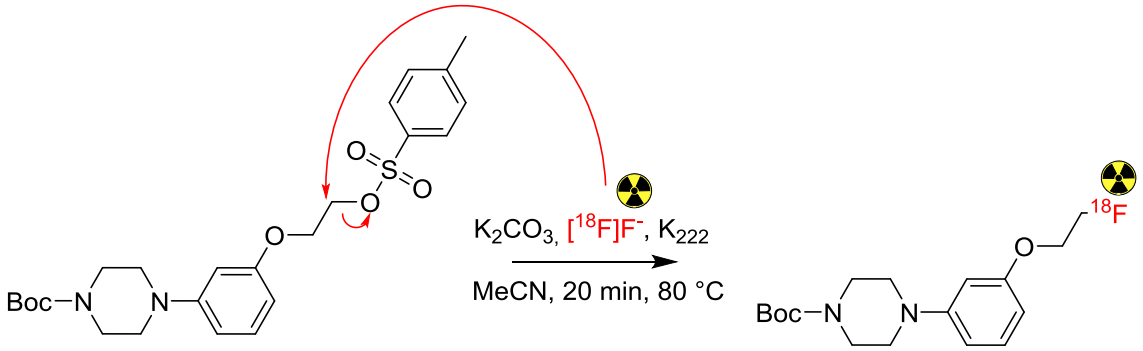

Scheme 1: Reaction mechanism of a S_N2 nucleophilic ^{18}F-substitution.

1.5.1.2 Nucleophilic aromatic substitution (S_NAr)

A highly motivating feature of fluorinated aromatic compounds is that they are less prominent to be defluorinated *in vivo* compared with aliphatic labelled compounds. Nucleophilic aromatic ^{18}F-substitution (S_NAr) requires the aromatic system to be activated towards nucleophiles by an electron withdrawing group. Thus, nucleophilic ^{18}F-substitution of electron-rich aromatic systems is challenging if not impossible using standard conditions. Thus, much effort has recently been carried out to be able to label both neutral and electron-rich aromatic structures; the following section will present some of these promising strategies.[51-58]

Diaryliodonium salts

An attempt to solve this issue was presented by Pike *et al.* in 1995, where they reported successful use of diaryliodonium salts as a precursor for nucleophilic ^{18}F-substitution of electron-rich aromatic systems.[59] Limitations like regioselectivity which depends on both electronic properties of the arenes and environmental influences, led to the development of a modified version of the abovementioned reaction using heteroaromatic iodonium salts by Ross *et al*. in 2007. In this approach, the regioselectivity could be influenced by introducing an electron-rich leaving group.[57] Harsh labelling conditions and tedious precursor synthesis led to the development of a Cu-mediated approach, where the more stable aryl(mesityl)iodonium salts are used as precursors. This strategy requires lower temperatures due to the Cu-mediated

acceleration of the reaction and a regioselectivity that only depends on steric influence of the mesityl group.[55] But due to the sensitivity of the Cu-species, reduced yields were gained during the more basic conditions applied in up-scaled reactions.[60] The latter remains a major drawback of this strategy.

Iodonium ylides

In 2010, Satyamurthy *et al*. developed a new approach for ^{18}F-fluorination of both electron-rich and electron-deficient substrates using iodonium ylides as precursors broadening the scope of substrates. In comparison to the diarylidonium salts, the ylides were more stable and easier to handle.[61] This strategy was further improved in 2014 when Liang *et al.* reported the use of spirocyclic ylides. These precursor moieties turned out to be even more stable and had excellent regioselectivity.[54]

Cu-mediated approaches

In 2014, Gouverneur and co-workers published a radically different approach using a Cu-mediated oxidative ^{18}F-fluorination strategy of boronic esters.[53, 62-64] The strategy was inspired from oxidative fluorination reactions using fluorine and arylstannanes with Cu(II) or Ag(I).[65-66] A suggested reaction mechanism for this labelling strategy is presented in Scheme 2. The proposed mechanism starts with an anion exchange, which is followed by air oxidation of the Cu-species (stabilized by pyridine ligands) and subsequent transmetalation that achieves ^{18}F-fluorinated aryl(III)cuprates. Finally, a reductive elimination releases the wanted ^{18}F-radiolabelled product.[67] This radiolabelling method is used within **Paper III** (chapter 5).The substrate scope of this strategy has been further investigated. Aryl boronic acids, trifluoroborate precursors and tin species are additional suitable starting materials.[52, 68-69]

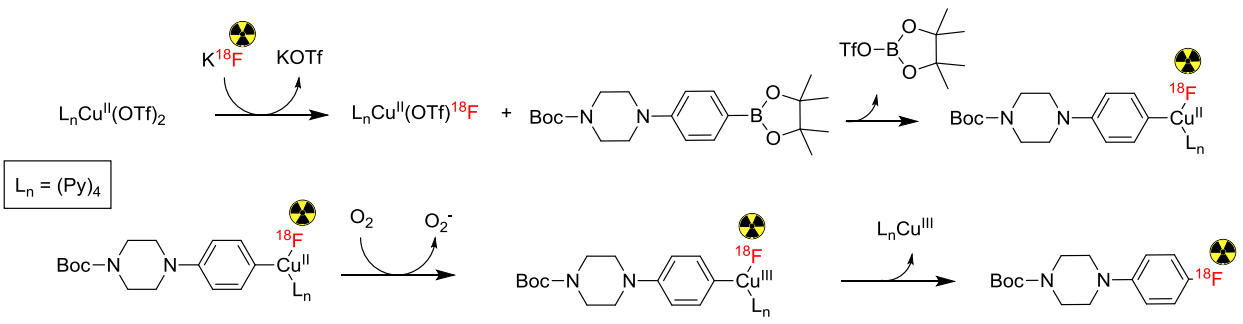

Scheme 2: A proposed reaction mechanism for Cu-mediated ^{18}F-fluorination of boronic pinacole ester precursors.[67]

1.5.2 Indirect ^{18}F-fluorination

Indirect fluorination strategies use a small fluorine-18 labelled molecule containing a reactive group, a so-called synthon or prosthetic group. This synthon is thereafter used to further react with the molecule of interest in a multi-step manner. Reasons for using an indirect strategy could be that a molecule or biomolecule cannot withstand the harsh conditions necessary for the direct fluorination or that they contain functional groups (e.g. hydroxyl and amine) which are incompatible, such as hydrogen donors that deactivate the fluoride-18. Some commonly used synthons for indirect ^{18}F-fluorination are; 2-[^{18}F]fluoroethyl-1-tosylate ([^{18}F]FETos),[70] and the 'click'-reagent [^{18}F]fluoroethyl azide.[71]

1.6 Carbon-11

Carbon-11 labelled tracers also have a key role within the clinic, but even more so within drug development processes. This is due to the half-life of 20.3 min that enables test-retests scans during the same day within the same patient. Carbon-11 results in a lower radiation burden than fluorine-18 and furthermore, and most importantly, the abundance of carbon atoms within organic and drug molecules makes it possible to create a radiotracer with the exact same chemical structure as the original compound. As such, the biological behaviour of the original structure can be imaged and not that of a close analogue which is often the case for ^{18}F-labeled ligands. Even small changes can alter the *in vivo* behaviour of the target molecule.[37] From a radiochemical point of view, carbon-11 has a branching ratio of close to 100% (99.79%) for β^+-emission (Eq. 4). Carbon-11 can readily be produced in a cyclotron by proton bombardment on nitrogen-14 (Eq. 5).

$$^{11}C \rightarrow {}^{11}B + \beta^+ + \nu_e \qquad \text{(Eq. 4)}$$

$$^{14}N(p,\alpha)^{11}C \qquad \text{(Eq. 5)}$$

The most common ^{11}C-labeling strategy are methylation reactions using [^{11}C]CH_3I or [^{11}C]CH_3OTf, which are produced starting from either [^{11}C]CH_4 or [^{11}C]CO_2.[37] However, work with carbon-11 is challenged by its short half-life, which makes multi-step syntheses demanding. In addition, the mean traveling distance of the positron of carbon-11 is a bit longer of that of fluorine-18. This could lead to a lower spatial resolution.[37] However, in many scanners the limiting factor in respect to spatial resolution is in fact the detector size.[72]

1.7 Molar Activity (A_m)

The molar activity of a radiotracer is a measure of its activity per µmol of total moles of molecule, presented with the units GBq/µmol. For all radionuclides used in PET the maximal molar activity can be calculated with Eq. 6, however, contamination of the corresponding stable nuclide is inescapable leading to a lower molar activity.[37]

$$A_m = \frac{\ln(2) * N}{t_{½}} \qquad \text{(Eq. 6)}$$

High molar activity is essential within CNS tracer development, as it reduces the risk of receptor binding site saturation with non-radiolabelled product (Figure 5, reused from **Paper I,** chapter 3). For the 5-HT_7R in rodents, a high molar activity is of extra importance, as only a very low amount of target exists within the rat brain.

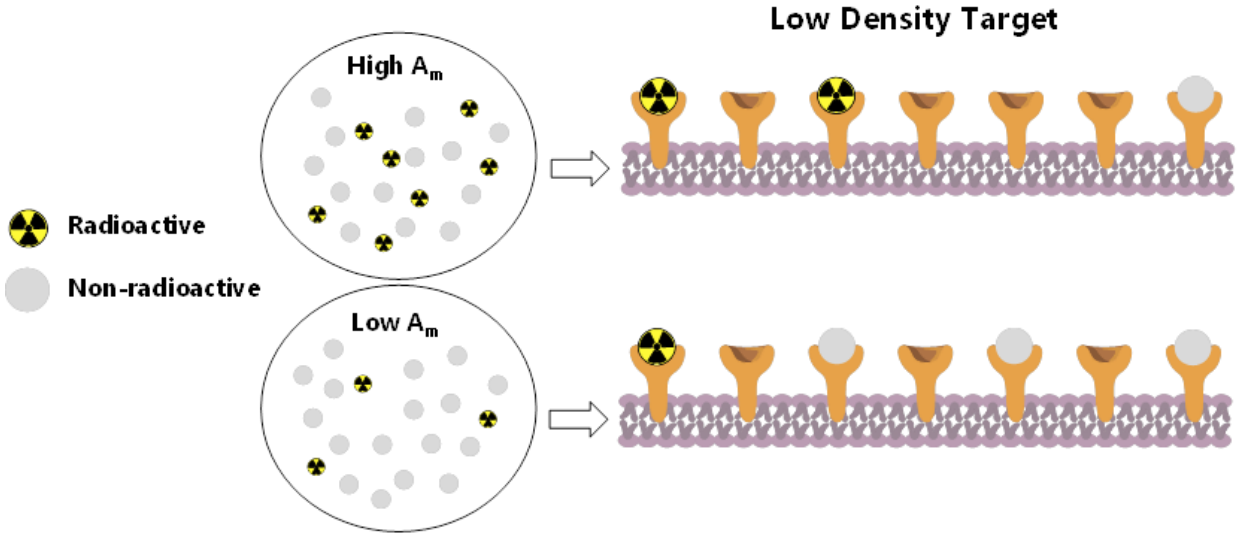

Figure 5: Molar activity (A_m) is the quantity of radioactivity per mol of labelled compound. This Figure shows a schematic presentation of high and low molar activities (A_m) (left) and it consequence for a low-density target (right). High A_m are needed to prevent or reduce the possibility to block the target with non-labelled drug. This is of special importance for low density targets.

1.8 Rats as an Experimental Animal for PET Tracer Development

Throughout this thesis, rats were the main choice of experimental animal. This is because of its accessibility, the reduction of costs and fewer ethical considerations compared to using pigs or baboons.[73] Compared to mice, another often applied species, rats are advantageous in neuroimaging due to the bigger brain size and consequently the better imaging quality of different brain regions. Even though the brain size is bigger than in mice, partial-volume effect (PVE) can still occur and degrade the image quality. The partial-volume effect refers to two effects that cause the intensity values in images to differ from what they actually are. The first phenomenon is the 3-dimensional (3D) image blurring introduced by the restricted spatial resolution of the imaging system. The 3D blurring can cause spill-over between regions; this makes the image of a small source into a larger but blurrier source. The reason for this is that part of the signal from the source "spills out" and hence is seen outside the actual source. The other phenomenon causing PVE is called the tissue fraction effect, which has to do with the fact that PET images are sampled as voxels on a grid. The voxels are often not co-occurring with the exact shape of the tracer distribution; hence different tissues often get sampled within the same voxel. Signal intensities inside each voxel get calculated as a mean, which gives a biased final image (Figure 6).[74]

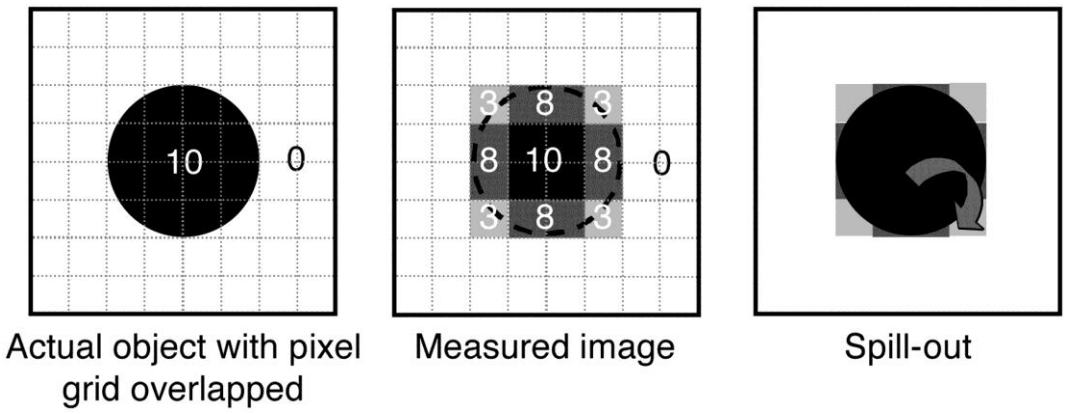

Figure 6: Influences of Partial-volume effect (PVE) of PET image quality. Schematic presentations of the tissue fraction effect by voxel image sampling and 3D image blurring by spill-out. This research was originally published in JNM. Soret, M.; Bacharach, S. L.; Buvat, I., Partial-volume effect in PET tumor imaging. *Journal of Nuclear Medicine* 2007, *48* (6), 932-945© SNMMI.

Working with PET scanners with a higher spatial resolution decreases the risk of the 3D image blurring, but problems associated with the tissue fraction effect still remain and are even more difficult to prevent.[74] Another challenge of applying rats as an experimental model for CNS targets is that due to the small total blood volume of rats, blood sampling during the PET scan

can be very difficult. Moreover, arterial blood sampling is even more complicated, which in turn is required to perform quantifying kinetic modelling.

1.9 Tracer Kinetic Modelling

PET enables the visualization and quantification of biological processes when studying the interaction of a radiotracer and its target. The measured outcome is usually the binding potential (BP). This BP is defined as the ratio between B_{max} over K_D (see section 1.4). For kinetic analysis, it is advantageous that this measure can also be derived from the Michaelis-Menten equilibrium equation (Eq. 7). Within this equation, K_{on} is defined as the association rate constant, [L] as the concentration of free radiotracer, [R] as the number of available receptors, K_{off} as the dissociation constant and [LR] as the concentration of ligand receptor complex (can also be described as bound [B]).

$$K_{on} * [L] * [R] = K_{off} * [LR] \quad \text{(Eq. 7)}$$

At equilibrium, K_{on} and K_{off} can be replaced by the equilibrium dissociation constant K_D. If the available receptors are substituted with B_{max}-[B], Eq. 7 can be rewritten into Eq. 8.

$$[B] = ([B_{max}] * [L]) / (K_D + [L]) \quad \text{(Eq. 8)}$$

Further simplifications of Eq. 8 can be done due to the tracer doses used in PET, thus [L] is much smaller than K_D and can therefore be neglected and gives Eq. 9.

$$[B] = ([B_{max}] * [L]) / K_D \text{ or } [BP] = [B_{max}]/K_D = [B]/[L] \quad \text{(Eq. 9)}$$

Different kinetic mathematical models exist, which simplify the real biological situation to a set of linear equations and can be used to estimate the constants needed to calculate the BP for the respective PET tracer. The most commonly used models are the compartment models. A compartment is defined as one possible state of the tracer, like its physical location and its chemical state. The frequently used one-tissue and the simplified reference tissue model are illustrated in Figure 7.

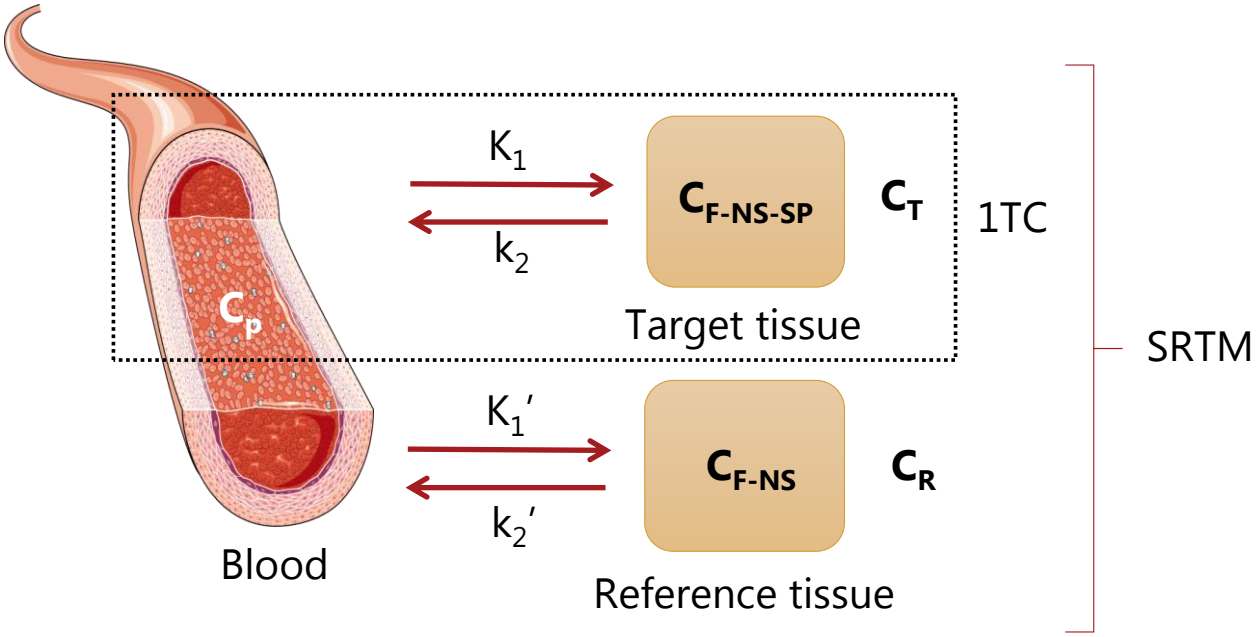

Figure 7: Illustrative presentation of two commonly used compartment models within kinetic modelling, the one-tissue compartment model (1TC) and the simplified reference tissue model (SRTM). Abbreviations: C_P = concentration of tracer in plasma, C_F = concentration of free tracer, C_{NS} = concentration non-specifically bound tracer C_{SP} = concentration specifically bound tracer, C_T = concentration of tracer in target tissue and C_R = concentration of tracer in reference tissue.[75] http://smart.servier.com

The one-tissue compartment model (1TC) uses arterial blood sampling and subsequent metabolite and plasma protein binding analyses to estimate the amount free tracer in the plasma (C_p). The first and only compartment within this simplified model represents the concentration of tracer in the target tissue (C_T) and is derived from the dynamic PET image. C_T contains the sum of the concentration of free- (C_F), non-specifically (C_{NS}) and specifically (C_S) bound tracer, which are not distinguishable from each other in this model. Using the one-tissue compartment model, the specific radiotracer binding can be determined at equilibrium relative to plasma radiotracer with the outcome BP_P. In order to avoid arterial blood sampling as necessary in the one-tissue compartment model, using a non-specific binding region in the brain are often preferred. One such model is the simplified reference tissue model (SRTM), were a reference region does not contain any specific binding to the biological target. The outcome measure achieved from reference tissue methods is $BP_{ND,}$ as it compares the concentration of radiotracer in receptor-rich to receptor-free regions.[75-76]

References

1. Berger, M.; Gray, J. A.; Roth, B. L., The Expanded Biology of Serotonin. *Annual Review of Medicine* **2009,** *60* (1), 355-366.

2. Muller, C. P.; Jacobs, B., *Handbook of the behavioral neurobiology of serotonin*. Academic Press: **2009**; Vol. 21.

3. Nichols, D. E.; Nichols, C. D., Serotonin Receptors. *Chemical Reviews* **2008,** *108* (5), 1614-1641.

4. Wong, D. T.; Perry, K. W.; Bymaster, F. P., The discovery of fluoxetine hydrochloride (Prozac). *Nature reviews Drug discovery* **2005,** *4* (9), 764.

5. Hoyer, D.; Hannon, J. P.; Martin, G. R., Molecular, pharmacological and functional diversity of 5-HT receptors. *Pharmacology Biochemistry and Behavior* **2002,** *71* (4), 533-554.

6. Bard, J. A.; Zgombick, J.; Adham, N.; Vaysse, P.; Branchek, T. A.; Weinshank, R. L., Cloning of a novel human serotonin receptor (5-HT_7) positively linked to adenylate cyclase. *Journal of Biological Chemistry* **1993,** *268* (31), 23422-23426.

7. Plassat, J. L.; Amlaiky, N.; Hen, R., Molecular cloning of a mammalian serotonin receptor that activates adenylate cyclase. *Molecular Pharmacology* **1993,** *44* (2), 229-236.

8. Ruat, M.; Traiffort, E.; Leurs, R.; Tardivel-Lacombe, J.; Diaz, J.; Arrang, J.-M.; Schwartz, J.-C., Molecular cloning, characterization, and localization of a high-affinity serotonin receptor (5-HT_7) activating cAMP formation. *Proceedings of the National Academy of Sciences* **1993,** *90* (18), 8547-8551.

9. Lovell, P. J.; Bromidge, S. M.; Dabbs, S.; Duckworth, D. M.; Forbes, I. T.; Jennings, A. J.; King, F. D.; Middlemiss, D. N.; Rahman, S. K.; Saunders, D. V., A novel, potent, and selective 5-HT_7 antagonist:(R)-3-(2-(2-(4-methylpiperidin-1-yl) ethyl) pyrrolidine-1-sulfonyl) phenol (SB-269970). *Journal of medicinal chemistry* **2000,** *43* (3), 342-345.

10. Hedlund, P. B.; Sutcliffe, J. G., Functional, molecular and pharmacological advances in 5-HT_7 receptor research. *Trends in Pharmacological Sciences* **2004,** *25* (9), 481-486.

11. Matthys, A.; Haegeman, G.; Van Craenenbroeck, K.; Vanhoenacker, P., Role of the 5-HT_7 receptor in the central nervous system: from current status to future perspectives. *Molecular Neurobiology* **2011,** *43* (3), 228-53.

12. Hagan, J. J.; Price, G. W.; Jeffrey, P.; Deeks, N. J.; Stean, T.; Piper, D.; Smith, M. I.; Upton, N.; Medhurst, A. D.; Middlemiss, D. N.; Riley, G. J.; Lovell, P. J.; Bromidge, S. M.;

Thomas, D. R., Characterization of SB-269970-A, a selective 5-HT_7 receptor antagonist. *British Journal of Pharmacology* **2000,** *130* (3), 539-548.

13. Hedlund, P. B.; Huitron-Resendiz, S.; Henriksen, S. J.; Sutcliffe, J. G., 5-HT_7 Receptor Inhibition and Inactivation Induce Antidepressantlike Behavior and Sleep Pattern. *Biological Psychiatry* **2005,** *58* (10), 831-837.

14. Hedlund, P. B.; Kelly, L.; Mazur, C.; Lovenberg, T.; Sutcliffe, J. G.; Bonaventure, P., 8-OH-DPAT acts on both 5-HT1A and 5-HT_7 receptors to induce hypothermia in rodents. *European journal of pharmacology* **2004,** *487* (1-3), 125-132.

15. Faure, C.; Mnie-Filali, O.; Scarna, H.; Debonnel, G.; Haddjeri, N., Effects of the 5-HT_7 receptor antagonist SB-269970 on rat hormonal and temperature responses to the 5-HT1A/7 receptor agonist 8-OH-DPAT. *Neuroscience letters* **2006,** *404* (1-2), 122-126.

16. Guscott, M.; Egan, E.; Cook, G.; Stanton, J.; Beer, M.; Rosahl, T.; Hartmann, S.; Kulagowski, J.; McAllister, G.; Fone, K., The hypothermic effect of 5-CT in mice is mediated through the 5-HT_7 receptor. *Neuropharmacology* **2003,** *44* (8), 1031-1037.

17. Rocha-González, H. I.; Meneses, A.; Carlton, S. M.; Granados-Soto, V., Pronociceptive role of peripheral and spinal 5-HT_7 receptors in the formalin test. *Pain* **2005,** *117* (1-2), 182-192.

18. Brenchat, A.; Romero, L.; García, M.; Pujol, M.; Burgueño, J.; Torrens, A.; Hamon, M.; Baeyens, J. M.; Buschmann, H.; Zamanillo, D., 5-HT_7 receptor activation inhibits mechanical hypersensitivity secondary to capsaicin sensitization in mice. *Pain* **2009,** *141* (3), 239-247.

19. Wesołowska, A.; Nikiforuk, A.; Stachowicz, K., Potential anxiolytic and antidepressant effects of the selective 5-HT_7 receptor antagonist SB 269970 after intrahippocampal administration to rats. *European journal of pharmacology* **2006,** *553* (1-3), 185-190.

20. Wesołowska, A.; Nikiforuk, A.; Stachowicz, K.; Tatarczyńska, E., Effect of the selective 5-HT_7 receptor antagonist SB 269970 in animal models of anxiety and depression. *Neuropharmacology* **2006,** *51* (3), 578-586.

21. Mnie-Filali, O.; Lambas-Señas, L.; Scarna, H.; Haddjeri, N., Therapeutic potential of 5-HT_7 receptors in mood disorders. *Current drug targets* **2009,** *10* (11), 1109-1117.

22. Mnie-Filali, O.; Lambás-Señas, L.; Zimmer, L.; Haddjeri, N., 5-HT_7 receptor antagonists as a new class of antidepressants. *Drug News Perspect* **2007,** *20* (10), 613-618.

23. Guscott, M.; Bristow, L. J.; Hadingham, K.; Rosahl, T. W.; Beer, M. S.; Stanton, J. A.; Bromidge, F.; Owens, A. P.; Huscroft, I.; Myers, J.; Rupniak, N. M.; Patel, S.; Whiting, P. J.; Hutson, P. H.; Fone, K. C.; Biello, S. M.; Kulagowski, J. J.; McAllister, G., Genetic knockout and pharmacological blockade studies of the 5-HT_7 receptor suggest therapeutic potential in depression. *Neuropharmacology* **2005,** *48* (4), 492-502.

24. Abbas, A. I.; Hedlund, P. B.; Huang, X.-P.; Tran, T. B.; Meltzer, H. Y.; Roth, B. L., Amisulpride is a potent 5-HT_7 antagonist: relevance for antidepressant actions *in vivo*. *Psychopharmacology* **2009,** *205* (1), 119-128.

25. Roth, B. L.; Craigo, S. C.; Choudhary, M. S.; Uluer, A.; Monsma, F.; Shen, Y.; Meltzer, H. Y.; Sibley, D. R., Binding of typical and atypical antipsychotic agents to 5-hydroxytryptamine-6 and 5-hydroxytryptamine-7 receptors. *Journal of Pharmacology and Experimental Therapeutics* **1994,** *268* (3), 1403-1410.

26. East, S.; Burnet, P.; Kerwin, R.; Harrison, P., An RT-PCR study of 5-HT_6 and 5-HT_7 receptor mRNAs in the hippocampal formation and prefrontal cortex in schizophrenia. *Schizophrenia research* **2002,** *57* (1), 15-26.

27. Yamamura, H. I.; Snyder, S. H., Muscarinic cholinergic binding in rat brain. *Proceedings of the National Academy of Sciences* **1974,** *71* (5), 1725-1729.

28. Young III, W. S.; Kuhar, M. J., A new method for receptor autoradiography:[^{3}H] opioid receptors in rat brain. *Brain research* **1979,** *179* (2), 255-270.

29. Thomas, D. R.; Atkinson, P. J.; Ho, M.; Bromidge, S. M.; Lovell, P. J.; Villani, A. J.; Hagan, J. J.; Middlemiss, D. N.; Price, G. W., [^{3}H]-SB-269970 – A selective antagonist radioligand for 5-HT_7 receptors. *British Journal of Pharmacology* **2000,** *130* (2), 409-417.

30. Horisawa, T.; Ishiyama, T.; Ono, M.; Ishibashi, T.; Taiji, M., Binding of lurasidone, a novel antipsychotic, to rat 5-HT_7 receptor: analysis by [^{3}H]SB-269970 autoradiography. *Progress in Neuro-Psychopharmacology and Biological Psychiatry* **2013,** *40*, 132-137.

31. Hansen, H. D.; Herth, M. M.; Ettrup, A.; Andersen, V. L.; Lehel, S.; Dyssegaard, A.; Kristensen, J. L.; Knudsen, G. M., Radiosynthesis and *in vivo* evaluation of novel radioligands for PET imaging of cerebral 5-HT_7 receptors. *Journal of Nuclear Medicine* **2014,** *55* (4), 640-6.

32. Varnäs, K.; Thomas, D. R.; Tupala, E.; Tiihonen, J.; Hall, H., Distribution of 5-HT_7 receptors in the human brain: a preliminary autoradiographic study using [^{3}H]SB-269970. *Neuroscience letters* **2004,** *367* (3), 313-316.

33. Zimmer, L.; Billard, T., Molecular imaging of the serotonin 5-HT_7 receptors: from autoradiography to positron emission tomography. *Reviews in the Neurosciences* **2014,** *25* (3), 357-365.

34. Thomas, D. R.; Atkinson, P. J.; Hastie, P. G.; Roberts, J. C.; Middlemiss, D. N.; Price, G. W., [^{3}H]-SB-269970 radiolabels 5-HT_7 receptors in rodent, pig and primate brain tissues. *Neuropharmacology* **2002,** *42* (1), 74-81.

35. Paterson, L. M.; Tyacke, R. J.; Nutt, D. J.; Knudsen, G. M., Measuring endogenous 5-HT release by emission tomography: promises and pitfalls. *Journal of Cerebral Blood Flow & Metabolism* **2010,** *30* (10), 1682-1706.

36. Piel, M.; Vernaleken, I.; Rösch, F., Positron Emission Tomography in CNS Drug Discovery and Drug Monitoring. *Journal of Medicinal Chemistry* **2014,** *57* (22), 9232-9258.

37. Miller, P. W.; Long, N. J.; Vilar, R.; Gee, A. D., Synthesis of ^{11}C, ^{18}F, ^{15}O, and ^{13}N radiolabels for positron emission tomography. *Angewandte Chemie International Edition* **2008,** *47* (47), 8998-9033.

38. Kristensen, J. L.; Herth, M. M., Textbook of Drug Design and Discovery: *In vivo* imaging in drug discovery. In *Textbook of Drug Design and Discovery*, CRC Press: 2017.

39. Herth M. M., K. G. M., PET Imaging of the 5-$HT2_A$ Receptor System: A Tool to Study the Receptor's *In Vivo* Brain Function. 5-$HT2_A$ Receptors in the Central Nervous System. In *5-$HT2_A$ Receptors in the Central Nervous System*, Guiard B., D. G. G., Ed. Humana Press, Cham: **2018**, 32, 85-134.

40. Innis, R. B.; Cunningham, V. J.; Delforge, J.; Fujita, M.; Gjedde, A.; Gunn, R. N.; Holden, J.; Houle, S.; Huang, S.-C.; Ichise, M., Consensus nomenclature for *in vivo* imaging of reversibly binding radioligands. *Journal of Cerebral Blood Flow & Metabolism* **2007,** *27* (9), 1533-1539.

41. Edem, P. E.; Steen, E. J. L.; Kjær, A.; Herth, M. M., Chapter 2 - Fluorine-18 Radiolabeling Strategies—Advantages and Disadvantages of Currently Applied Labeling Methods. In *Late-Stage Fluorination of Bioactive Molecules and Biologically-Relevant Substrates*, Postigo, A., Ed. Elsevier: **2019**; pp 29-103.

42. Sanchez-Crespo, A., Comparison of Gallium-68 and Fluorine-18 imaging characteristics in positron emission tomography. *Applied Radiation and Isotopes* **2013,** *76*, 55-62.

43. Ross, T.; Wester, H., 18 F: Labeling Chemistry and Labeled Compounds. In *Handbook of nuclear chemistry*, Springer: **2011**; pp 2021-2071.

44. Atkins, H.; Christman, D.; Fowler, J. and others., *ORGANIC RADIOPHARMACEUTICALS LABELED WITH ISOTOPES OF SHORT HALF-LIFE. V. ^{18}F-LABELED 5-AND 6-FLUOROTRYPTOPHAN*., Brookhaven National Lab., Upton, NY;: **1972**.

45. Guo, Q.; Brady, M.; Gunn, R. N., A biomathematical modeling approach to central nervous system radioligand discovery and development. *The Journal of Nuclear Medicine* **2009,** *50* (10), 1715.

46. Zhang, L.; Villalobos, A.; Beck, E. M.; Bocan, T.; Chappie, T. A.; Chen, L.; Grimwood, S.; Heck, S. D.; Helal, C. J.; Hou, X., Design and selection parameters to accelerate the discovery of novel central nervous system positron emission tomography (PET) ligands and their application in the development of a novel phosphodiesterase 2A PET ligand. *Journal of medicinal chemistry* **2013,** *56* (11), 4568-4579.

47. Herth, M. M.; Leth-Petersen, S.; Lehel, S.; Hansen, M.; Knudsen, G. M.; Gillings, N.; Madsen, J.; Kristensen, J. L., Accelerating preclinical PET-screening: reductive amination with [^{11}C] methoxybenzaldehydes. *RSC Advances* **2014,** *4* (41), 21347-21350.

48. Waterhouse, R. N., Determination of lipophilicity and its use as a predictor of blood–brain barrier penetration of molecular imaging agents. *Molecular Imaging & Biology* **2003,** *5* (6), 376-389.

49. Koenig, J. A.; Edwardson, J. M., Endocytosis and recycling of G protein-coupled receptors. *Trends in pharmacological sciences* **1997,** *18* (4), 276-287.

50. Lee, E.; Kamlet, A. S.; Powers, D. C.; Neumann, C. N.; Boursalian, G. B.; Furuya, T.; Choi, D. C.; Hooker, J. M.; Ritter, T., A fluorine-derived electrophilic late-stage fluorination reagent for PET imaging. *Science* **2011,** *334* (6056), 639-642.

51. Rotstein, B. H.; Wang, L.; Liu, R. Y.; Patteson, J.; Kwan, E. E.; Vasdev, N.; Liang, S. H., Mechanistic studies and radiofluorination of structurally diverse pharmaceuticals with spirocyclic iodonium (III) ylides. *Chemical science* **2016,** *7* (7), 4407-4417.

52. Mossine, A. V.; Brooks, A. F.; Makaravage, K. J.; Miller, J. M.; Ichiishi, N.; Sanford, M. S.; Scott, P. J., Synthesis of [^{18}F] arenes via the copper-mediated [^{18}F] fluorination of boronic acids. *Organic letters* **2015,** *17* (23), 5780-5783.

53. Tredwell, M.; Preshlock, S. M.; Taylor, N. J.; Gruber, S.; Huiban, M.; Passchier, J.; Mercier, J.; Génicot, C.; Gouverneur, V., A general copper-mediated nucleophilic ^{18}F fluorination of arenes. *Angewandte Chemie* **2014,** *126* (30), 7885-7889.

54. Rotstein, B. H.; Stephenson, N. A.; Vasdev, N.; Liang, S. H., Spirocyclic hypervalent iodine (III)-mediated radiofluorination of non-activated and hindered aromatics. *Nature communications* **2014,** *5*, 4365.

55. Ichiishi, N.; Brooks, A. F.; Topczewski, J. J.; Rodnick, M. E.; Sanford, M. S.; Scott, P. J., Copper-catalyzed [^{18}F] fluorination of (mesityl)(aryl) iodonium salts. *Organic letters* **2014,** *16* (12), 3224-3227.

56. Ross, T. L.; Ermert, J.; Coenen, H. H., Synthesis of No-Carrier-Added 4-[18F] Fluorophenol from 4-Benzyloxyphenyl-(2-thienyl) iodonium Bromide. *Molecules* **2011,** *16* (9), 7621-7626.

57. Ross, T. L.; Ermert, J.; Hocke, C.; Coenen, H. H., Nucleophilic 18F-fluorination of heteroaromatic iodonium salts with no-carrier-added [^{18}F] fluoride. *Journal of the American Chemical Society* **2007,** *129* (25), 8018-8025.

58. Ross, T.; Ermert, J.; Coenen, H. NCA ^{18}F-Fluorination of various arenes via aryl (2-thienyl) iodonium salts, *Journal of labelled compounds and radiopharmacueticals*, **2005**; pp S153-S153.

59. Pike, V. W.; Aigbirhio, F. I., Reactions of cyclotron-produced [^{18}F] fluoride with diaryliodonium salts—a novel single-step route to no-carrier-added [^{18}]F fluoroarenes. *Journal of the Chemical Society, Chemical Communications* **1995,** (21), 2215-2216.

60. Zlatopolskiy, B. D.; Zischler, J.; Krapf, P.; Zarrad, F.; Urusova, E. A.; Kordys, E.; Endepols, H.; Neumaier, B., Copper-mediated aromatic radiofluorination revisited: efficient production of PET tracers on a preparative scale. *Chemistry–A European Journal* **2015,** *21* (15), 5972-5979.

61. Satyamurthy, N. B., J. R. No-carrier-added nucleophilic [F-18] fluorination of aromatic compounds. **2010**.

62. Preshlock, S.; Calderwood, S.; Verhoog, S.; Tredwell, M.; Huiban, M.; Hienzsch, A.; Gruber, S.; Wilson, T. C.; Taylor, N. J.; Cailly, T., Enhanced copper-mediated ^{18} F-fluorination of aryl boronic esters provides eight radiotracers for PET applications. *Chemical Communications* **2016,** *52* (54), 8361-8364.

63. Preshlock, S.; Tredwell, M.; Gouverneur, V., 18F-Labeling of arenes and heteroarenes for applications in positron emission tomography. *Chemical reviews* **2016,** *116* (2), 719-766.

64. Taylor, N.; Emer, E.; Preshlock, S.; Schedler, M.; Tredwell, M.; Verhoog, S.; Mercier, J.; Genicot, C.; Gouverneur, V. E., De-Risking the Cu-Mediated ^{18}F-Fluorination of

Heterocyclic PET Radioligands. *Journal of American Chemical Society*, **2017**.*139*(24), 8267-8276.

65. Tang, P.; Furuya, T.; Ritter, T., Silver-catalyzed late-stage fluorination. *Journal of the American Chemical Society* **2010,** *132* (34), 12150-12154.

66. Gamache, R. F.; Waldmann, C.; Murphy, J. M., Copper-mediated oxidative fluorination of aryl stannanes with fluoride. *Organic letters* **2016,** *18* (18), 4522-4525.

67. Zarrad, F.; Zlatopolskiy, B.; Krapf, P.; Zischler, J.; Neumaier, B., A Practical Method for the Preparation of ^{18}F-Labeled Aromatic Amino Acids from Nucleophilic [^{18}F]Fluoride and Stannyl Precursors for Electrophilic Radiohalogenation. *Molecules* **2017,** *22* (12), 2231.

68. Ye, Y.; Schimler, S. D.; Hanley, P. S.; Sanford, M. S., Cu (OTf) 2-mediated fluorination of aryltrifluoroborates with potassium fluoride. *Journal of the American Chemical Society* **2013,** *135* (44), 16292-16295.

69. Makaravage, K. J.; Brooks, A. F.; Mossine, A. V.; Sanford, M. S.; Scott, P. J., Copper-Mediated Radiofluorination of Arylstannanes with [^{18}F] KF. *Organic letters* **2016,** *18* (20), 5440-5443.

70. Kniess, T.; Laube, M.; Brust, P.; Steinbach, J., 2-[^{18}F] Fluoroethyl tosylate–a versatile tool for building ^{18}F-based radiotracers for positron emission tomography. *Medicinal chemical communications* **2015,** *6* (10), 1714-1754.

71. Van Der Born, D.; Pees, A.; Poot, A. J.; Orru, R. V.; Windhorst, A. D.; Vugts, D. J., Fluorine-18 labelled building blocks for PET tracer synthesis. *Chemical Society Reviews* **2017,** *46* (15), 4709-4773.

72. Moses, W. W., Fundamental limits of spatial resolution in PET. *Nuclear Instruments and Methods in Physics Research Section A: Accelerators, Spectrometers, Detectors and Associated Equipment* **2011,** *648*, S236-S240.

73. Sherwin, C. M.; Christiansen, S. B.; Duncan, I. J.; Erhard, H. W.; Lay Jr, D. C.; Mench, J. A.; O'Connor, C. E.; Petherick, J. C., Guidelines for the ethical use of animals in applied ethology studies. *Applied Animal Behaviour Science* **2003,** *81* (3), 291-305.

74. Soret, M.; Bacharach, S. L.; Buvat, I., Partial-volume effect in PET tumor imaging. *Journal of Nuclear Medicine* **2007,** *48* (6), 932.

75. Gunn, R. N.; Gunn, S. R.; Cunningham, V. J., Positron emission tomography compartmental models. *Journal of Cerebral Blood Flow & Metabolism* **2001,** *21* (6), 635-652.

76. Innis, R. B.; Cunningham, V. J.; Delforge, J.; Fujita, M.; Giedde, A.; Gunn, R. N.; Holden, J.; Houle, S.; Huang, S. C.; Ichise, M.; Lida, H.; Ito, H.; Kimura, Y.; Koeppe, R. A.; Knudsen, G. M.; Knuuti, J.; Lammertsma, A. A.; Laruelle, M.; Logan, J.; Maguire, R. P.; Mintun, M. A.; Morris, E. D.; Parsey, R.; Price, J. C.; Slifstein, M.; Sossi, V.; Suhara, T.; Votaw, J. R.; Wong, D. F.; Carson, R. E., Consensus nomenclature for *in vivo* imaging of reversibly binding radioligands. *Journal of Cerebral Blood Flow & Metabolism* **2007,** *27* (9), 1533-1539.

Chapter 2

Objectives and Outline

Summary:

This chapter contains a description of the objectives for this Ph.D project, combined with how this thesis is outlined.

CHAPTER 2 – Objectives and Outline

The objective of this Ph.D. thesis was to develop a 5-HT_7R selective positron emission tomography (PET) tracer for molecular imaging. Novel strategies were also developed to increase synthesis through-put and accelerate the preclinical evaluation process. Approaches were chosen to increase the likelihood to identify a promising tracer candidate more efficiently.

Paper I (chapter 3) is a review on previous efforts on developing a 5-HT_7R PET tracer. It also highlights the main obstacles within this endeavour and discusses the future perspectives. **Paper I** can be seen as an extension to the introductory chapter (chapter 1). In the following **Papers II-VI** (chapter 4-8), we aimed to develop a potential PET tracer for the 5-HT_7R. Our efforts were based on the three distinct scaffolds shown in Figure 1. Promising selectivity and lipophilicity profiles were the key parameters for this selection.[1-3] The decision to use distinct scaffolds was mainly driven by risk mitigation considerations. If one scaffold would be insufficient to image the 5-HT_7R, another scaffold could counteract.

In **Paper II** (chapter 4), based on a new scaffold of low-basicity 5-HT_7R agonists, [^{11}C]AGH-44 was explored for its potential to be used as a selective PET tracer. **Paper III and IV** (chapter 5 and 6) made use of (arylpiperazinyl-butyl)oxindole derivatives that have recently been shown as a promising starting point for the development of a 5-HT_7R selective PET tracer.[4-7] In **Paper V and VI** (chapter 7 and 8), derivatives of the highly 5-HT_7R selective antagonist SB-269970[3] were synthesized and evaluated. The syntheses of precursors, reference compounds and labelling procedures as well as the according *in vitro* and *in vivo* evaluation are described in each paper.

Current PET tracer development strategies suffer from time-consuming and lengthy lead identification. This is among other factors due to commonly applied late-stage labelling approaches which result in the need to synthesize a distinct precursor for every tracer. Furthermore, brain tracer evaluation in rats is usually limited by the amount of test animals that can be used. We aimed to accelerate this process by applying a fragment-based labelling strategy as well as to use a through-put screening set-up applying our high resolution research tomography (HRRT) scanner. Figure 2 displays the applied methods. Strategies to achieve these goals are shown in **Paper II-VI** (chapter 4-8).

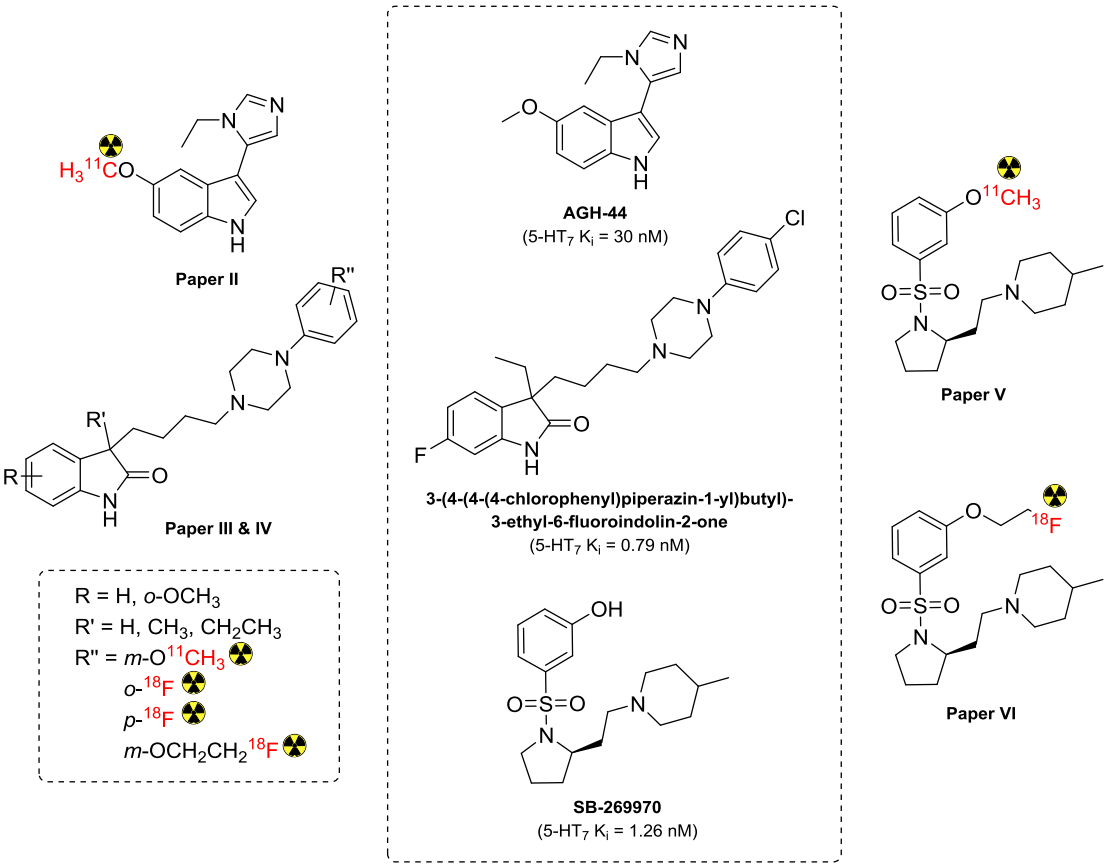

Figure 1: Within this thesis will the following promising scaffolds be investigated as potential PET tracers for the 5-HT_7R.[1-3]

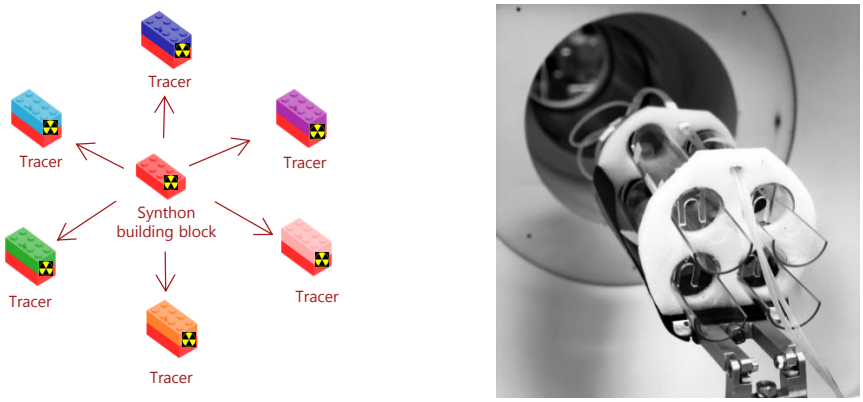

Figure 2: A schematic overview of the combinatorial-like approach (left) and an image of the 2x2 custom-made holder for increased throughput in preclinical PET screening (right).

Finally, will this thesis end with a discussion and reflection of results obtained in **Paper II-VI**, chapter 9 is dedicated for this purpose. Chapter 10 will focus on the conclusions drawn while doing this work. The overall future perspective of the research topic will also be elaborated on in chapter 10.

References:

1. Hogendorf, A. S.; Hogendorf, A.; Kurczab, R.; Satala, G.; Lenda, T.; Walczak, M.; Latacz, G.; Handzlik, J.; Kiec-Kononowicz, K.; Wieronska, J. M.; Wozniak, M.; Cieslik, P.; Bugno, R.; Staron, J.; Bojarski, A. J., Low-basicity 5-HT_7 Receptor Agonists Synthesized Using the van Leusen Multicomponent Protocol. *Scientific Reports* **2017,** *7* (1), 1444.

2. Volk, B.; Barkóczy, J.; Hegedus, E.; Udvari, S.; Gacsályi, I.; Mezei, T.; Pallagi, K.; Kompagne, H.; Lévay, G.; Egyed, A., (Phenylpiperazinyl-butyl) oxindoles as selective 5-HT_7 receptor antagonists. *Journal of medicinal chemistry* **2008,** *51* (8), 2522-2532.

3. Lovell, P. J.; Bromidge, S. M.; Dabbs, S.; Duckworth, D. M.; Forbes, I. T.; Jennings, A. J.; King, F. D.; Middlemiss, D. N.; Rahman, S. K.; Saunders, D. V.; Collin, L. L.; Hagan, J. J.; Riley, G. J.; Thomas, D. R., A novel, potent, and selective 5-HT(7) antagonist: (R)-3-(2-(2-(4-methylpiperidin-1-yl)ethyl)pyrrolidine-1-sulfonyl) phen ol (SB-269970). *Journal of medicinal chemistry* **2000,** *43* (3), 342-345.

4. Herth, M. M.; Andersen, V. L.; Hansen, H. D.; Stroth, N.; Volk, B.; Lehel, S.; Dyssegaard, A.; Ettrup, A.; Svenningsson, P.; Knudsen, G. M.; Kristensen, J. L., Evaluation of 3-Ethyl-3-(phenylpiperazinylbutyl)oxindoles as PET Ligands for the Serotonin 5-HT(7) Receptor: Synthesis, Pharmacology, Radiolabeling, and *in Vivo* Brain Imaging in Pigs. *Journal of medicinal chemistry* **2015,** *58* (8), 3631-3636.

5. Hansen, H. D.; Herth, M. M.; Ettrup, A.; Andersen, V. L.; Lehel, S.; Dyssegaard, A.; Kristensen, J. L.; Knudsen, G. M., Radiosynthesis and *in vivo* evaluation of novel radioligands for PET imaging of cerebral 5-HT_7 receptors. *Journal of medicinal chemistry* **2014,** *55* (4), 640-646.

6. Herth, M. M.; Volk, B.; Pallagi, K.; Kofoed Bech, L.; Antoni, F. A.; Knudsen, G. M.; Kristensen, J. L., Synthesis and *in vitro* evaluation of oxindole derivatives as potential radioligands for 5-HT_7 receptor imaging with PET. *ACS Chemical Neuroscience* **2012,** *3* (12), 1002-1007.

7. Andersen, V. L.; Herth, M. M.; Lehel, S.; Knudsen, G. M.; Kristensen, J. L., Palladium-mediated conversion of para-aminoarylboronic esters into para-aminoaryl-^{11}C-methanes. *Tetrahedron Letters* **2013,** *54* (3), 213-216.

Chapter 3

Paper I

Towards selective PET Imaging of the 5-HT_7 Receptor System: Past, Present and Future

---

Summary:

*This chapter contains **Paper I**, which is a review paper and can be seen as an extension of the introductory chapter 1. This paper reviews the work that has been done to develop a 5-HT_7 receptor PET tracer during the last two decades. It also presents important characteristics for successful PET imaging and critically discusses the previous efforts.*

Authors' contribution:

Formulated the outline, performed the literature research and contributed considerably to writing the manuscript

Disclaimer:

*This review article manuscript contains summarized results of **Paper IV-VI**, which will be entirely presented in the following chapters 6-8. This manuscript will be submitted after the publications of the mentioned papers.*

Towards selective PET Imaging of the 5-HT$_7$ Receptor System: Past, Present and Future

Elina T. L'Estrade[a,b,c], Maria Erlandsson[c], Tomas Ohlsson[c], Gitte M. Knudsen[a,d], Matthias M. Herth[a,b,e,*]

[a] *Neurobiology Research Unit, Rigshospitalet, Blegdamsvej 9, 2100 Copenhagen, Denmark*

[b] *Department for Drug Design and Pharmacology, Faculty of Health and Medical Sciences, University of Copenhagen, Universitetesparken 2, 2100 Copenhagen, Denmark*

[c] *Radiation Physics, Nuclear Medicine Physics Unit, Skånes University Hospital, Barngatan 3, 222 42 Lund, Sweden.*

[d] *Institute of Clinical Medicine, Faculty of Health and Medical Sciences, University of Copenhagen, Denmark.*

[e] *Department of Clinical Physiology, Nuclear Medicine and PET, University Hospital Copenhagen, Rigshospitalet Blegdamsvej 9, 2100 Copenhagen, Denmark*

Abstract

Since its discovery in 1993, the serotonin receptor subtype 7 (5-HT$_7$) has attracted attention as a drug target. Therefore, it is not surprising that relatively early efforts have been undertaken to develop a positron emission tomography (PET) imaging agent for it. PET can be used to study *in vivo*, in a clinical set-up a receptor system and investigate a drug's occupancy against this system. This review focuses on the development efforts towards a 5-HT$_7$R selective PET tracer over the last 20 years, critically reflects on applied strategies and used chemical structures and suggests future approaches that are needed to develop successfully a PET tracer for this important target.

Graphical Abstract

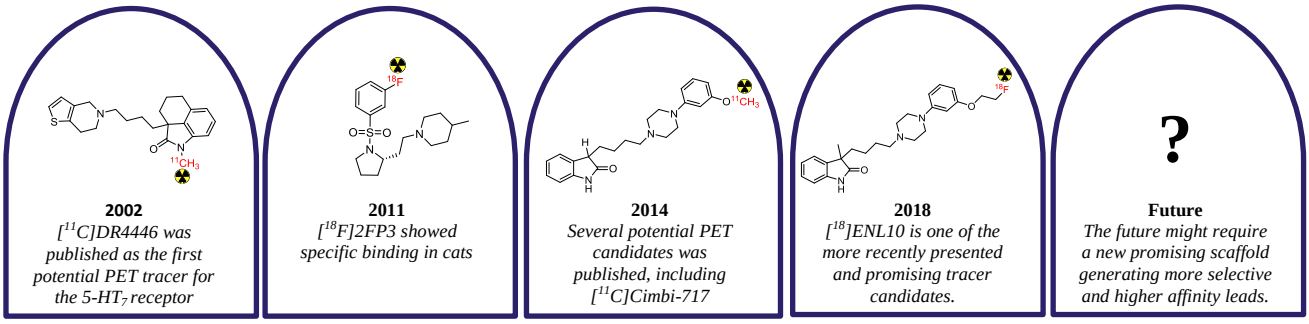

∗ Corresponding author. Tel.: +0045 93565414; fax: +0045 35 33 60 41; e-mail: matthias.herth@sund.ku.dk

1. Introduction

The 5-HT_7 receptor (5-HT_7R) is an important and somewhat underexplored receptor subtype within the serotonergic Guanidine protein-coupled receptors (GPCR) family. In this introductory section, we will briefly highlight its function and importance. This will be followed by a short discussion how PET can be used to study this receptor *in vivo*. The section will be finished describing essential criteria that have to be fulfilled to be able to develop a 5-HT_7 receptor PET imaging agent.

1.1 The 5-HT_7 receptor within the serotonergic system

The serotonergic system is spread throughout the human body and includes 7 subfamilies with 14 receptor subtypes. The amount, the widespread projections and the variety of serotonin (5-hydroxytryptamine, 5-HT) receptors within the brain let researchers early speculate about the impact of the serotonergic system in psychological processes, behavioural patterns and generally spoken in controlling the mind.[1] Already in 1984, Glennon *et al.* could show that the strong psychedelic effects of lysergic acid diethylamide (LSD) can be elucidated by serotonergic 2A receptor activation.[2-3] The neurotransmitter serotonin itself is one of the oldest structures developed in evolution and central to life. Its involvement spans from early developmental events related to neurogenesis and maturation, to apoptosis and neurodegeneration.[1] Serotonin was discovered in 1948 and its name was chosen to reflect the site where it was firstly isolated from ("ser" for serum) and the effect identified along with it ("tonin" to indicate that serotonin changes the tone in blood vessels).[4-5]

Over the years, many receptors have been identified that are activated by 5-HT. The most recent addition to this portfolio is the 5-HT_7R.[6-7] In fact, this receptor was for a long time believed to be a member of the 5-HT_1-like receptor family. Its high sequence similarity with the 5-HT_{1A} receptor leads to this misconception.[8] In 1993, this changed when more sophisticated methodologies became more available.[7] Almost simultaneously, the 5-HT_7R was cloned from human[9], mouse[10] and rat[11] tissue. Three splice variants have been identified in humans; namely the 5-HT_{7a}, 5-HT_{7b}, and 5-HT_{7d} receptor. However, even though the splice variants differ in their intracellular carboxyl terminal (C-terminal) tail, they have similar constitutive activity and effect after inverse agonist binding.[12-13] From a more receptor pharmacology point of view, the 5-HT_7R is a GPCR, positively coupled to adenylyl cyclase through the stimulatory G_s protein. Activation of the 5-HT_7R leads to a cascade which ultimately converts ATP to cyclic AMP (cAMP) and subsequently interacts with a numerous of intracellular targets. Cyclic AMP can for example

activate the cAMP response element binding protein (CREB). This protein stimulates in turns the gene expression levels.[5] In comparison to other 5-HT receptors, the 5-HT_7R has a distinguishable pharmacological profile. Among other things, it displays the highest affinity towards 5-HT (K_i = 0.3-8) of all serotonergic receptors.[6-7, 14-17]

The 5-HT_7R can be found throughout the whole body. It is expressed in the brain, heart, blood vessels and the gastrointestinal tract, with the highest abundance in the latter.[18] In 1996, Gustafson *et al*. described the 5-HT_7R rat brain tissue distribution. This became possible using an *in situ* hybridization assay.[19] Four years later, a highly selective 5-HT_7R ligand, SB-269970, was identified, subsequently tritiated and applied to autoradiographic imaging studies. The binding pattern of this compound was in good agreement with the results obtained in the *in situ* hybridization assay.[19-20,21] In addition to rat tissue, autoradiography was later performed on pig[22], non-human primate (NHP)[23] and human[24] brain slices. An overview of the autoradiography results is shown in Table 1. Highest binding was detected in thalamus, hypothalamus and hippocampus in all three species. However, interspecies differences were detected. For example, a 4-fold lower 5-HT_7R concentration was determined in human thalamus compared to rat and pig thalamic regions.[21-22, 24] Pig and NHP cerebellum did displayed specific 5-HT_7R ligand binding, whereas this region did not show any specific binding in either rat or human tissue.

Table 1: Comparison of regional 5-HT_7 R distributions determined by [^{3}H]SB-269970 specific binding to rat (fmol/mg tissue ± SE), pig (fmol/mg TE), NHP (fmol/mg TE) and human(fmol/mg tissue original wet weight) brain slices. Abbreviations: TE: tissue equivalents, ACG: anterior cingulate gyrus; AM: amygdala; ATh: anterior thalamus; Ca: caudate nucleus; PCG: posterior cingulate gyrus; Pu: putamen; PVN: paraventricular thalamic nucleus and Th: thalamus.[19, 21-24]

	Rat[I]	**Pig[II]**	**NHP[III]**	**Human[IV]**
	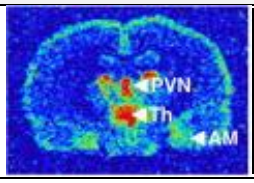	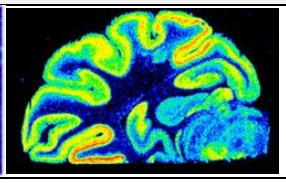	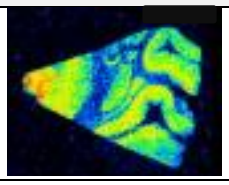	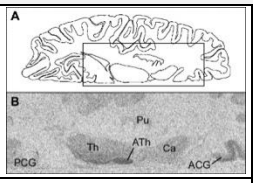
Thalamus	47 ± 5	45.6 ± 0.19	32.3 ± 3.61	11 ± 3.5
Thalamus (high binding region)		62.0 ± 5.53		
Anterior thalamus				16 ± 4.9
Paraventricular thalamic nucleus	83 ± 10			
Hypothalamus	36 ± 6	43.0 ± 6.03		5.9 ± (5.5, 6.4)
Hippocampus	14 ± 2	37.5 ± 3.35		5.7 ± 4.7
Dendate gyrus				8.7 ± 3.7
Amygdala	21 ± 2	48.3 ± 5.01		4.2 ± 1.9
Putamen	4 ± 1	21.6 ± 1.64		0.97 ± 1.0
Caudate	4 ± 1	24.4 ± 2.81		0.72 ± 0.8
Prefrontal cortex		32.7 ± 1.60		
Frontal cortex	11 ± 1	38.3 ± 2.68		
Superior frontal gyrus				2.6 ± 1.3
Inferior frontal gyrus				2.0 ± 0.67
Temporal cortex		41.0 ± 3.03	21.5 ± 4.32	2.3 ± 1.7
Cingulate cortex	12 ± 1	44.9 ± 2.60		
Occipital cortex		33.2 ± 2.40		1.2 ± 0.57
Cerebellum	0	13.4 ± 2.22	14.3 ± 0.93	< 1

[I] Reprinted from Progress in Neuro-Psychopharmacology and Biological Psychiatry, 40, Horisawa, T.; Ishiyama, T.; Ono, M.; Ishibashi, T.; Taiji, M., Binding of lurasidone, a novel antipsychotic, to rat 5-HT_7 receptor: analysis by [3H] SB-269970 autoradiography, 132-137., Copyright (**2013**), with permission from Elsevier.

[II] This work was originally published in JNM. Hansen, H. D.; Herth, M. M.; Ettrup, A.; Andersen, V. L.; Lehel, S.; Dyssegaard, A.; Kristensen, J. L.; Knudsen, G. M., Radiosynthesis and *in vivo* evaluation of novel radioligands for PET imaging of cerebral 5-HT_7 receptors. *J Nucl Med* **2014**, 55 (4), 640-646. © SNMMI.

[III] Permission for the reuse of this work has been given by John Wiley and Sons. The work was originally published by Hansen, H. D.; Constantinescu, C. C.; Barret, O.; Herth, M. M.; Magnussen, J. H.; Lehel, S.; Dyssegaard, A.; Colomb, J.; Billard, T.; Zimmer, L., Evaluation of [18F] 2FP3 in pigs and non-human primates. *Journal of Labelled Compounds and Radiopharmaceuticals* **2018,** 1-9.

[IV] Reprinted from *Neuroscience letters*, 367 (3), Varnäs, K.; Thomas, D. R.; Tupala, E.; Tiihonen, J.; Hall, H, Distribution of 5-HT_7 receptors in the human brain: a preliminary autoradiographic study using [3H] SB-269970, 313-316., Copyright (**2004**), with permission from Elsevier.

The availability of 5-HT_7R selective ligands and its corresponding tritiated counterparts have not only allowed to determine the receptor brain distribution, but also to study the receptor's involvement in physiological processes and diseases.[21-22, 24-33] The development of 5-HT_7R knock-out mice allowed further investigations in this respect[29, 34] and were together with the application of aforementioned ligands able to associate the 5-HT_7R system with thermoregulation, learning, memory, circadian rhythm, mood, depression and drug abuse.[25-33, 35-36] From a drug development perspective, especially the later make this receptor an extremely interesting drug target.[37-38] In Europe, approximately 33.3 million people suffer from mood disorders including depression and the estimated costs for medical treatment are approximately 113,405 million euro. For drug abuse, the numbers are not less prevalent. 15.5 million people suffer from addiction, which is estimated to result in annual costs of 65,684 million euro.[39] Molecular imaging techniques would help further to clarify the involvement of the 5-HT_7R in these diseases or to identify the optimal dose for 5-HT_7R dependent drugs during drug development.[40-42] In this respect, PET plays an outstanding role. It is a non-invasive molecular nuclear imaging technique, which is quantitative and can be used independently of the tissue depth in which the target is located.[40-41] The aim of this review is to discuss current challenges in the development of 5-HT_7R selective PET tracers, summarize past and current research efforts and suggest potential possibilities to target this receptor in the future.

1.2 Requirements for a CNS PET tracer to image the 5-HT_7R System

Computational approaches that predict the *in vivo* behaviour of CNS tracers are still unreliable.[43-45] Therefore, current development strategies are largely dependent on a "trial-and-error game". However, some general requirements have been identified.[41-42, 46-47] In the following, we will discuss these in respect to the development process of a 5-HT_7R selective PET tracer.

1.2.1 Imaging contrast

High contrast between the object and the background is in every imaging technique necessary to receive a clear, well-defined picture (Figure 1). In molecular imaging, the object is a biological target. This target can be visualized when an imaging probe is capable to bind selectively and in sufficient amounts to it. Consequently, it is not surprising that a higher number of targets within a certain volume help to boost the target signal. Within pharmacokinetics, the number of targets within a certain density is defined as the receptor density (B_{max}). Values in human brain tissue that are reported to display sufficient numbers for PET imaging purposes are reported to be in the broad range between 0.7 – 1407 nM.[48] Usually, B_{max} values are determined on brain slice or

homogenate tissue binding studies.[49] The affinity of the probe for its target displays another key factor. It is a measure for how good the probe binds its target. It is usually measured as the dissociation constant (K_D) and can be determined in *in vitro* cell binding assays.[46-47, 50] Values for clinically applied tracers are typically within the range of 0.02 to 33 nM.[48]

The binding potential (BP) (Eq. 1) an essential measure that combines both parameters and allows estimating how likely a receptor system can be imaged by a specific imaging agent. It is defined as the ratio of B_{max} over K_D. As a rule of thumb and only based on empirical experience, the BP of a successfully PET tracer should have a minimum value of 5.[46] However, routinely and clinically applied tracers such as [^{11}C]raclopride, [^{18}F]FE-PE2I or [^{18}F]altanserin display a BP of 12 to 684 in their high binding regions.[47-48, 51-55]

$$BP = \frac{B_{max}}{K_D} \qquad \text{(Eq. 1)}$$

These values are concerning for the development of a 5-HT$_7$R PET tracer at least in humans since a maximal B_{max} of 11 ± 3.5 fmol/mg tissue original wet weight is found for the 5-HT$_7$R even in the highest binding region (Table 1).[24] Consequently, a successful PET tracer should have a K_D of 0.015 - 0.65 nM to reach similar high BPs. On the other hand, a K_D of 2.2 nM is required to reach the minimum suggested BP. If a tracer with such a BP will succeed in the clinic has to be investigated. Within another CNS system, namely the dopaminergic $D_{2/3}$ receptor system, tracers with such a low BP were not successful in the clinic. For example, [^{11}C]raclopride, a $D_{2/3}$ receptor PET ligand, is not able to image the receptor systems in low binding areas where a BP of 0.36 is calculated. In high binding regions, [^{11}C]raclopride displays a BP of 12 and in these regions, the tracer is successfully be used in the clinic.[56-57] In contrast, [^{18}F]fallypride, a PET tracer with a 83-fold increased affinity for the $D_{2/3}$ receptor system is able to image the receptor system in low binding regions. [^{18}F]fallypride displays a BP of 30 in these regions.[57-58] Maybe, similar BPs have to be reached to be able to image the 5-HT$_7$R system in the human brain. However, these concerns are to some extent diminished in other species such as rats, pigs or NHP. The respective B_{max} values are roughly 3- to 4-fold higher (Table 1) and therefore, tracers with lower affinity could be applicable.

The BP is an important measure to validate the possibility of a compound to image a specific target. However, the image quality is not only influenced by the signal received from the target-bound imaging probe (specific binding), but also, and maybe even more importantly by the received background signal from the probe (unspecific and non-specific binding). This can be exemplified using the analogy “the stars (specific binding) are always in the sky, we can only discern them at night because daylight (unspecific and non-specific binding) overwhelms their signal”.[46] In

consequence, high specific binding and low unspecific/non-specific binding are crucial for a successful PET tracer (Figure 1).

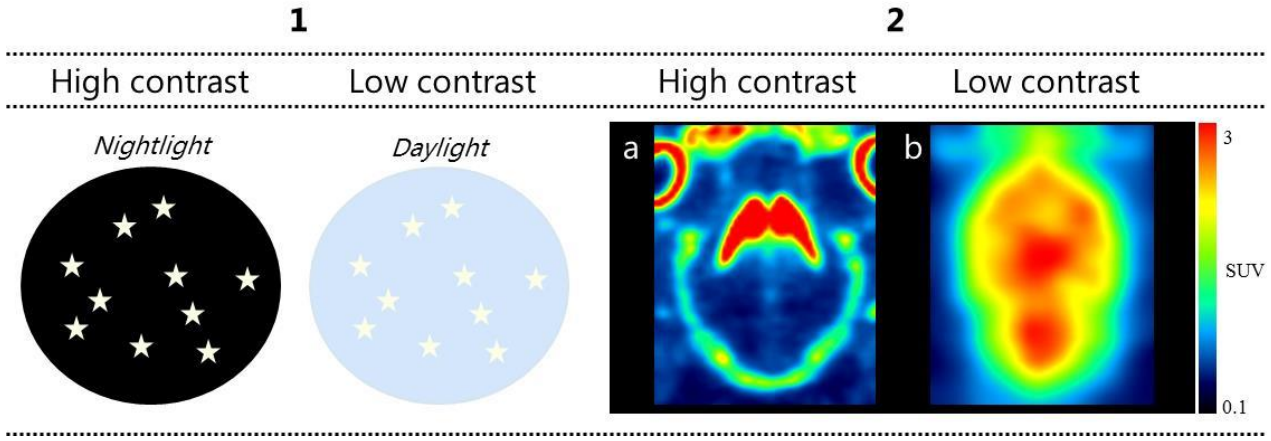

Figure 1: Schematic presentation of the importance of contrast within PET images. **1)** Is a visualization of high and low contrast by an analogy of the visibility of the stars during night and day. **2)** Demonstrated horizontal rodent brain summed PET images with high and low contrast. **a)** [^{18}F]Fallypride in baseline **b)** [^{11}C]pimavanserin after pretreatment with elacridar (P-gp inhibitor).

It is important to distinguish between unspecific and non-specific binding of a tracer because these parameters are two independent factors that indeed both influence a tracer's background signal. Binding of the imaging probe to off-targets is referred to as unspecific binding, whereas non-specific binding is defined as the non-displaceable binding of the probe to membranes, proteins, lipids or other cell components. Even though, there is a certain lipophilicity dependency of an imaging probe towards the *in vivo* non-specific binding component (a $LogD_{7.4}$ between 1.5-3.5 is considered reasonable for CNS PET tracers)[59], there is no clear trend and estimates are just a rudimentary.[60] For example, Ettrup *et al.* developed several 5-HT_{2A} receptor tracers with similar lipophilicity and selectivity. However, these tracers largely differed in their non-specific binding component.[61] *In vitro* methods to determine the *in vivo* non-specific binding component are in its infancy and cannot directly be translated.[61] For example, Patel *et al*. have suggested that no-wash *in vitro* autoradiography studies can determine the *in vivo* non-specific binding component.[62] However, the according study was only performed on a few tracers and results could be misleading based on these limited examples. Currently, the most reliable way to determine the *in vivo* non-specific binding component is estimations derived from PET studies.

Beside the non-specific binding component of a tracer, also the unspecific binding component contributes to the background signal. It can be predicted from the selectivity profile of the tracer and the according receptor B_{max} values. "The theoretical, binding ratio of the target to a specific off-target" ($tBR_{target/off\text{-}target}$) can be used for such estimations. It is based on the selectivity of the tracer

between the target and off-target as well as the respective receptor abundance (Eq. 2). A value > 5 should be observed to guarantee selective imaging.[47]

$$tBR_{target/off-target} = \left(\frac{K_{D,off-target}}{K_{D,target}}\right) x \left(\frac{B_{avail,target}}{B_{avail,off-\ target}}\right) \quad \text{(Eq. 2)}$$

In case of tracers targeting the 5-HT_7R, a potential and problematic off-target is the 5-HT_{1A}R. This as it has been shown that agonist for the 5-HT_7R, often also has high affinity for the 5-HT_{1A}R.[5, 63] Moreover, 5-HT_{1A}Rs are distributed within the same brain regions as 5-HT_7Rs. High abundance has been detected in the cortex or the hippocampus for both receptors.[24, 64]. However, concerns are too some extent mitigated since in the highest 5-HT_7R region, the thalamus,[24] low receptor densities of 5-HT_{1A}R have been determined.[64] This can be exemplified using Eq. 2, where a 4 times higher affinity for the 5-HT_7R is necessary to reach 10 times higher binding to the target compared to the 5-HT_{1A}R in human thalamus.[65]

1.2.2 Efflux transport dependency, metabolic fate and reversible tracer kinetics

Additional characteristics, that have to be considered when developing new PET tracers, are e.g. the dependency of the compound towards efflux transporters or the compound's metabolic fate. Strong efflux transporter dependency greatly reduces the concentration of the tracer within the brain and make it difficult if not impossible to determine specific binding.[41, 46]. Syvänen *et al*. have recently shown that because of the higher P-glycoprotein (P-gp) activity in rodents, several tracers performed poorly in rodent imaging studies, even though the same tracers worked satisfactorily in higher species.[66] It is important to keep that in mind evaluating PET tracers in rodents. Unfortunately, *in vitro* assays fail often to predict the *in vivo* dependency of a tracer towards P-gp[67-70] and consequently, the dependency is usually determined *in vivo* PET studies. Brain permeable radioactive metabolites should be avoided.[46, 71] This is because these metabolites greatly complicate kinetic modelling, as the PET scanner cannot distinguish between the signal derived from these radiometabolites or the intact molecular imaging probe. One possibility to achieve this is to choose the labelling position in such a way that less brain penetrant radiometabolites are formed.[46, 71] Finally, reversible tracer kinetics are desirable since common kinetic models require steady state conditions for accurate estimations.[46, 50, 72] Tracer kinetics can only be determined *in vivo*.

Table 2 summarizes the discussed issues in 1.2.1 and 1.2.2 point-by-point. Many values can only be determined *in vivo*.

Table 2: Summary of the important characteristics of a CNS PET tracer candidate and how these can be determined.

Contrast				**Additional**			
1	*Specific binding*		**Determined**	**1**	*BBB permeability*		**Determined**
		K_D (nM to sub-nM)	*In vitro* assay potency *In vivo* BP			**Low P-gp dependency**	*In vivo* inhibition with elacridar
		B_{max}	*In vitro* on brain slice or homogenate tissue binding studies *In vivo* quantitative kinetic modeling			**Lipophilicity** (LogP of 1.5 - 3.5)[59]	Tracer brain uptake during *in vivo* evaluation (qualitative TAC analysis)
2	*Unspecific binding*			**2**	*Metabolism*		
		High Selectivity	*In vitro* screening (PDSP) *In vivo* blocking or gene knock-out			**No brain permeable radiometabolites**	Radio-HPLC Plasma analysis of arterial blood samples during *in vivo* evaluation
3	*Non-specific binding*			**3**	*Quantification*		
		Lipophilicity (LogP of 1.5 -3.5)[59]	*"No wash"* autoradiography or *in silico* prediction *In vivo* blocking or gene knock-out			**Reversible tracer kinetics**	Qualitative TAC analysis Quantitative kinetic modeling

1.3 PET 5-HT_7R imaging in rodents

High molar activity (A_m) is an essential parameter for many CNS PET tracers as it defines in which amount the radiotracer is diluted with non-radioactive counterparts (Eq. 3 and Figure 2). A higher A_m ensures that a lower number of receptors or other drug targets are occupied when the same amount of radioactivity is injected. A lower number of occupied receptors allows to investigate the specific biological target without disturbing the naïve state[73] and is a premise for many kinetic PET modelling estimations.[50, 72] In general, a maximum number of 5% of all receptors are allowed to be occupied in PET studies.[41, 72-73] However, lower numbers are preferred. For PET studies in rodents, this precondition displays a bigger challenge than in bigger species. The brain is simply smaller and thus, a lower number of drug targets exist.[41] Higher molar activities are therefore needed to occupy the same percentage of drug targets.

$$A_m = \frac{\ln(2) * N}{t_{½}} \qquad \text{(Eq. 3)}$$

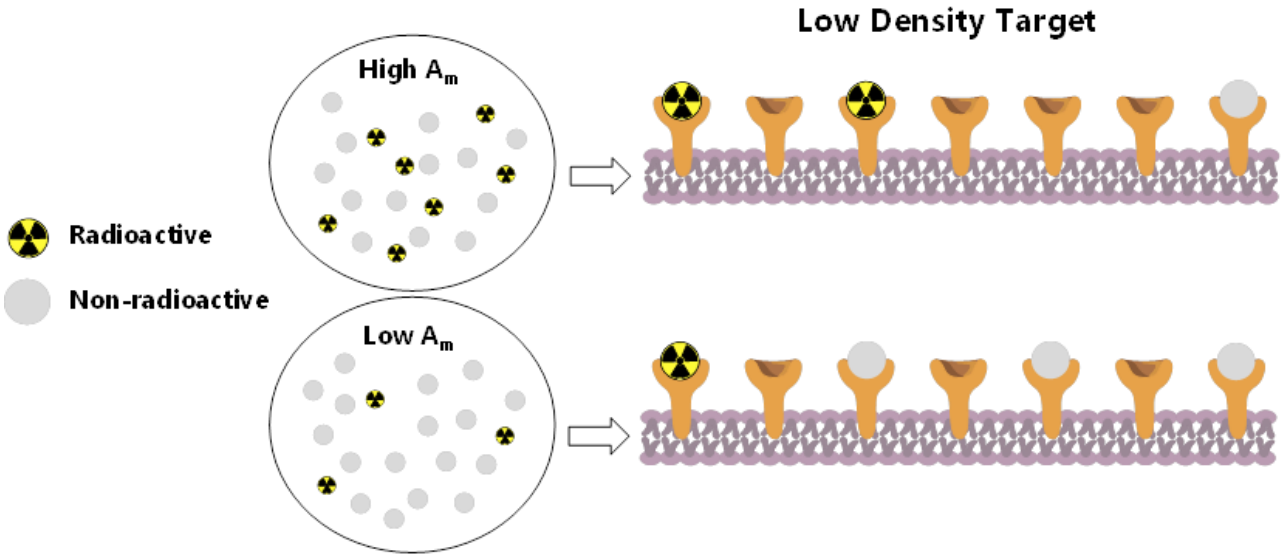

Figure 2: Molar activity (A_m) is the quantity of radioactivity per mol of labelled compound. This Figure shows a schematic presentation of high and low molar activities (A_m) (left) and it consequence for a low-density target (right). High A_m are needed to prevent or reduce the possibility to block the target with non-labelled drug. This is of special importance for low density targets.

In the following, we want to exemplify what consequence these considerations result in when conducting PET studies of the 5-HT_7R in rats. The total amount of 5-HT_7R in the rat thalamus is approximately 2100 fmol. Five percentages thereof is 105 fmol. This is the amount that is allowed to be occupied in PET studies in rats. For a tracer with a K_D of 1 nM, approximately 4.5 pmol are required to occupy this number when the tracer only accumulates in the target region. Usually, around 0.3% of the initial injected dose reaches the target area in PET studies. Consequently, approximately 1500 pmol of tracer can be injected. 20 MBq of a radiotracer is a typical injected activity amount in small PET imaging studies using rats. Therefore, an A_m of 13.5 GBq/µmol is required to fulfil the 5% occupancy criterion. In contrast, in higher species like pigs or humans the injected dose per bodyweight is usually around 1000 times smaller compared to rodents. This together with a larger mass of the respective brain region and hence a higher amount of target receptors, results in the fact that lower A_m are acceptable.

2. Past and Present Development efforts: Towards a 5-HT_7R selective PET tracer

Development of a PET tracer is in general a fairly time-consuming, costly and complex process that suffers from high failure rates. Compared to medicinal chemistry drug development, the success rate within PET tracer development is even lower. This can be explained by the empirical nature within current approaches.[43-44, 74] In chapter 1, we have discussed numerous and sometimes conflicting characteristics (see 1.2)[43] that have to be fulfilled for a ligand to become a successful PET imaging agent. In general, poor blood-brain barrier permeability and high non-specific binding are very often the main reasons for a CNS PET tracer to fail.[44, 75] Other reasons could be that the tracer candidate cannot reliable and in sufficient high radiochemical yields be labelled or that the tracer is even at tracer dose toxic. In the following, past and present efforts will be presented which aimed to develop a 5-HT_7R selective PET tracer. These efforts will be critically reflected in respect to identified requirements (see 1.2) and gained results. Figure 3 displays all PET tracer candidates that will be discussed within this review. Table 3 displays their according selectivity profiles and lipophilicities.

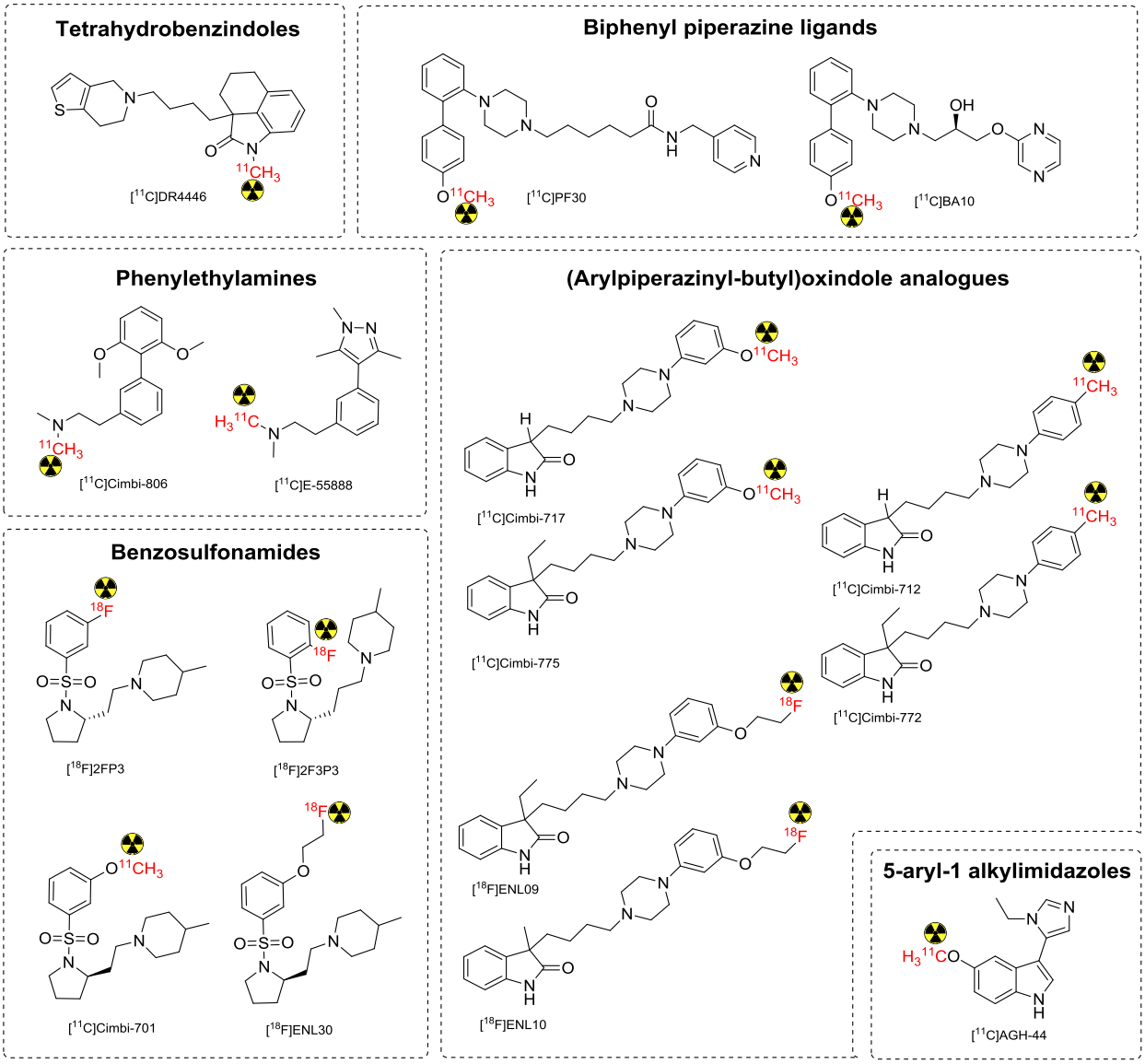

Figure 3: Structural overview of the presented 5-HT$_7$R PET candidates within this review article.

Table 3: An overview of the discussed tracer within this review and their affinities for some selected receptors. The *in vitro* affinities were measured on human receptors if not otherwise stated. a) Determined by Lovell *et al*. in 2000. b) Submitted manuscript. n.d = not determined.[22-23, 65, 68, 76-89]

		K_i (nM)					
	Log $D_{7.4}$	**5-HT_7**	**5-HT_{1A}**	**5-HT_{2A}**	**α_1**	**σ_1**	**σ_2**
DR4446	3.7 (logP)	9.7	770	>10.000	Negligible	n.d	n.d
PF30	3.33(clogD7.4)	11.2 ± 0.3	239 ± 20	n.d	30.5 ± 5.1	n.d	n.d
BA10	3.72(clogD7.4)	1.1	242 ± 10	n.d	n.d	n.d	n.d
Cimbi-806	4.4	8.6	4826	n.d	n.d	n.d	n.d
E-55888	1.4	2.5	700	>10.000	>10.000	>10.000	>10.000
Cimbi-712	5.19	1.1	2410	113	53	45	24
Cimbi-717	4.37	2.6	261	132	47	59	49
(±)-Cimbi-772	6.17	6.5	469	39	431	37	40
(+)-Cimbi-772	6.17	5.6	787	94	951	33	347
(-)-Cimbi-772	6.17	82	633	110	487	390	61
(±)-Cimbi-775	5.75	7.8	83	92	434	42	22
(+)-Cimbi-775	5.75	11	192	352	>10.000	46	152
(-)-Cimbi-775	5.75	56	151	66	794	249	16
ENL09	4.01	13	107	160	>10.000	29	67
ENL10	3.57	5.6	72	53	748	18	65
2FP3	1.43	1.43	$EC_{50}>10^{-5}$	n.d	n.d	n.d	n.d
2F3P3	1.58	7.6	> 10000	n.d	n.d	n.d	n.d
Cimbi-701	1.92	10^a,18^b	633	>10.000	>10.000	9.2	1.6
ENL30	2.12	0.75 ± 0.5*	n.d	n.d	n.d	n.d	n.d
AGH-44	1.93	30	661	>10.000	n.d	n.d	n.d

*K_D determined by autoradiography on rat brain slices

2.1 Tetrahydrobenzindoles

[^{11}C]DR4446

In 2002, the first attempt was reported to develop a 5-HT$_7$R selective PET tracer.[89] The antagonist DR4446 was selected as a candidate structure because on its high affinity towards the 5-HT$_7$R (K_i = 9.7 nM), its good selectivity profile over other 5-HT receptors (Table 3) and because of its weak or negligible affinity for dopaminergic and adrenergic receptors. [^{11}C]DR4446 could easily be radiolabeled in an estimated radiochemical yield (RCY) of 28-32% (decay corrected (d.c.)) and with satisfying A_m (73–120 GBq/µmol at the end of synthesis (EOS)). Evaluation studies were carried out in monkeys (Macaca mulatta). High brain uptake could be observed with a slightly higher signal in thalamus, a brain region with the highest 5-HT$_7$R density.[19, 21, 23-24, 89] Self-block experiments showed reduction in this brain region. However, the blocking effect was not very pronounced (Figure 4). Metabolite analysis showed that [^{11}C]DR4446 was relatively stable. Only low amounts of metabolites (9% after 2 min and 30% after 30 min) were found in plasma.[89]

In general, [^{11}C]DR4446 did not appear a good candidate tracer in monkeys. Indeed, good brain uptake and reversible tracer kinetics were identified despite of the relatively high lipophilicity (logP = 3.7) of DR4446. However, the very low blocking effect within a self-block study was very discouraging. If this unsatisfying result is due the low calculated BP of 3.3 is difficult to predict, but the low number could be one explanation for the observed behaviour. In consequence, higher affinity would be desirable; presumably a 10 to 100-fold affinity increase should be obtained. Moreover, the selectivity profile of [^{11}C]DR4446 is for many receptors unknown and should be evaluated in depth before initiating a structure activity relationship (SAR) study around DR4446. Despite of the unsatisfying results so far, we believe that DR4446 can still be a good lead structure to develop a 5-HT$_7$R selective PET tracer. However, extensive medicinal chemistry efforts are needed.

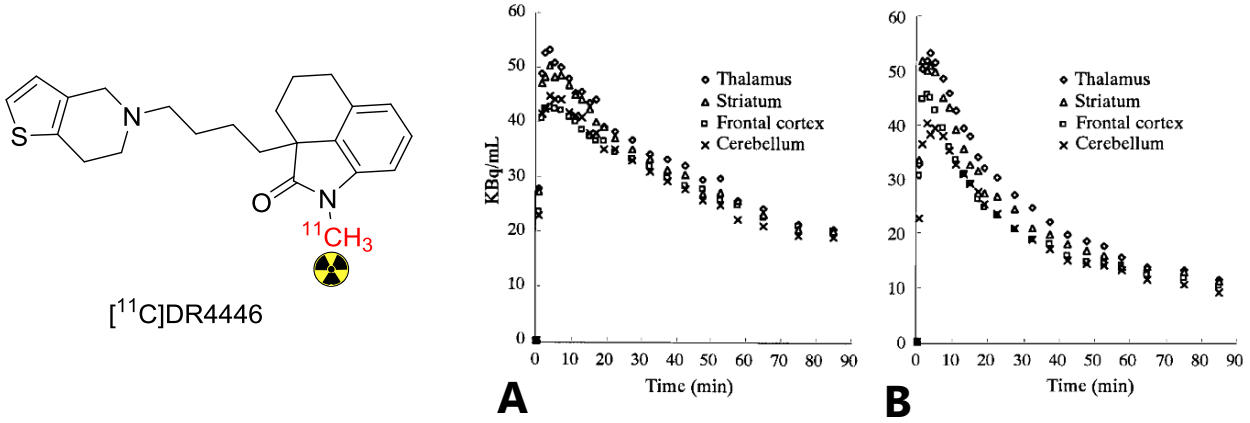

Figure 4: Molecular structure of [^{11}C]DR4446 to the left and to the right time-activity curves of [^{11}C]DR4446 in 4 regions of the monkey brain, each point normalized to an injected dose of 98 MBq. **A)** Baseline conditions. **B)** 1 mg/kg self-block (DR4446). In **A)** is a regional difference in the brain uptake displayed, with higher uptake in thalamus and striatum and lower in cerebellum. After the pre-administration of DR4446 (see **B)**), thalamus, striatum, frontal cortex and cerebellum was reduced to 71–79% of baseline signal at 15 min, to 55–60% of baseline signal at 45 min, and to 47–52% of baseline signal by the end of the PET scan.[V] These results do indicate specific binding of [^{11}C]DR4446 in the brain, but whether it is to the 5-HT$_7$R needs to be further elucidated.

2.2 Biphenyl piperazine ligands

[^{11}C]PF30 and [^{11}C]BA10

In 2014, an Italian/Danish collaboration investigated the possibility to use biphenyl piperazine based ligands to develop a 5-HT$_7$R selective PET tracer.[83,79] [^{11}C]PF30 was the first compound that was radiolabeled an evaluated within this series (Figure 5).[83] As DR4446, PF30 displayed an affinity value around 10 nM (Table 3) resulting in similar low BP values. Limited selectivity data were assessed (Table 3). A calculated $tBR_{5\text{-}HT7/\alpha1}$ of 0.12 in thalamus indicated that the detectable signal in PET stems from 5-HT$_7$R, but to a larger extent from α_1 receptors. In other brain regions the calculated $tBR_{5\text{-}HT7/\alpha1}$ was even lower and consequently, the received signal from these regions should represent to a lesser extent 5-HT$_7$R binding. Carbon-11 labelling was, nevertheless, performed. The RCY was >40% and the A_m was determined to be 196 ± 133

[V] Permission for the reuse of this work has been given by John Wiley and Sons. The work was originally published by Zhang, M. R.; Haradahira, T.; Maeda, J.; Okauchi, T.; Kida, T.; Obayashi, S.; Suzuki, K.; Suhara, T., Synthesis and preliminary PET study of the 5-HT7 receptor antagonist [^{11}C] DR4446. *Journal of Labelled Compounds and Radiopharmaceuticals: The Official Journal of the International Isotope Society* **2002,** *45* (10), 857-866. Copyright © 2002 John Wiley & Sons, Ltd.

GBq/µmol at time of injection (TOI).[83] *In vivo* evaluation studies in pigs were afterwards initiated. Poor brain uptake was observed. This low uptake could be attributed to the fact that [^{11}C]PF30 was identified as a strong P-gp efflux transporter substrate at tracer dose levels *in vivo* (Figure 5).[83] Interestingly, *in vitro* experiments conducted beforehand were not able to predict the observed behavior.[83] Because of these discouraging results and also because of the slow tracer kinetics observed (Figure 5), [^{11}C]PF30 evaluation studies were discontinued.

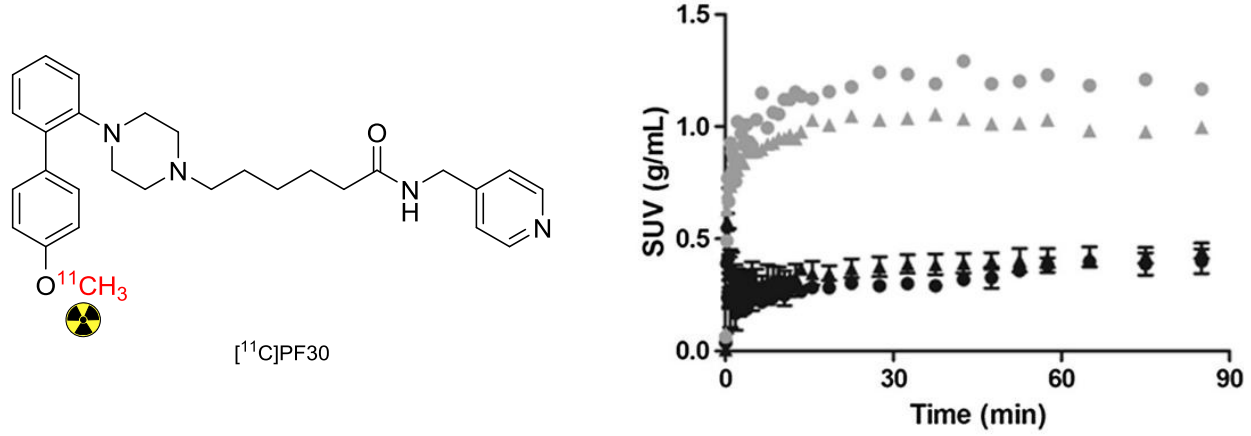

Figure 5: Molecular structure of [^{11}C]PF30 is illustrated to the left and to the right TACs from [^{11}C]PF30 evaluation in pigs. The black symbols representing baseline conditions and grey symbols indicate CsA pretreatment. The circles represent the signal thalamus and triangles represent cerebellum. SUV = standardized brain uptake.[VI] The TACs show poor brain uptake in baseline conditions but it increased after CsA pretreatment, indicating P-gp dependency. The brain uptake after P-pg inhibition match the distribution of the 5-HT$_7$R with higher uptake in thalamus and lower in cerebellum.[19, 21-24]

Small structural changes within a molecule can change dramatically the biological *in vivo* behaviour of a PET tracer[61]. Therefore, the same Italian/Danish team decided to investigate a second structure within this compound class.[79] BA10 showed a 10-fold improved affinity profile compared to PF30 (Figure 6 and Table 3). Consequently, the calculated BP is 41 in pigs and 10 in humans. These BP are well above the recommended values. [^{11}C]BA10 was successfully radiolabeled with a RCY of 56% and an A_m in the range of 60 - 150 GBq/µmol at EOS. *In vivo* evaluation of the tracer was conducted in pigs. High brain uptake and reversible tracer kinetics

[VI] Reprinted from *Bioorg Med Chem*, *22* (5), Lacivita, E.; Niso, M.; Hansen, H. D.; Di Pilato, P.; Herth, M. M.; Lehel, S.; Ettrup, A.; Montenegro, L.; Perrone, R.; Berardi, F.; Colabufo, N. A.; Leopoldo, M.; Knudsen, G. M., Design, synthesis, radiolabeling and *in vivo* evaluation of potential positron emission tomography (PET) radioligands for brain imaging of the 5-HT(7) receptor, 1736-1750., Copyright (**2014**), with permission from Elsevier.

were detected even though BA10 showed a lipophilicity of clog$D_{7.4}$ = 3.72. [^{11}C]BA10 displayed good regional distribution between high binding (thalamus) and low binding (cerebellum) regions. Specific binding was elucidated by pretreatment with the structurally different 5-HT_7R antagonist SB-269970 (Figure 6).[20, 79] Surprisingly, only an occupancy of 18% was detected.[79] If this low numbers can be explained by the unknown selectivity profile of BA10 or are in fact due to missing power in statistics should be investigated. To the authors' knowledge, no further studies have been carried out with this promising scaffold.

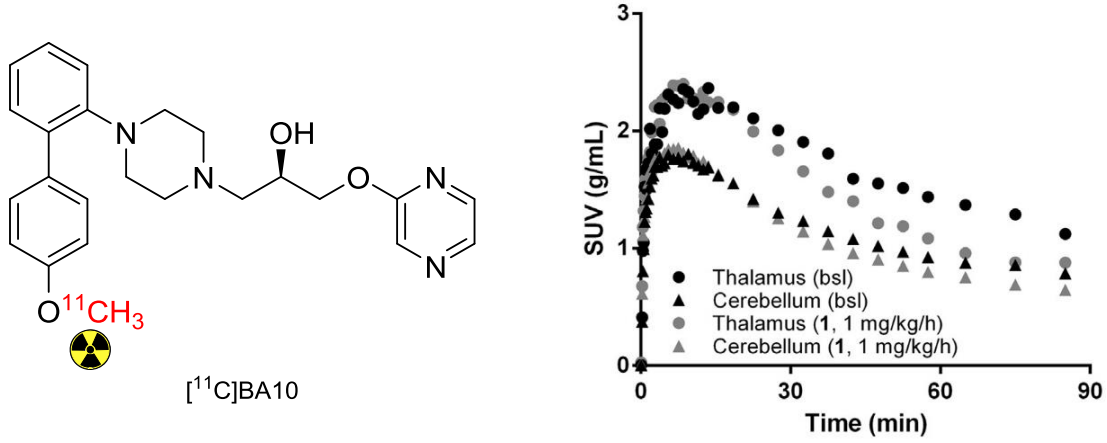

Figure 6: Molecular structure of [^{11}C]BA10 is illustrated to the left and to the right the TAC from [^{11}C]BA10 evaluation in pigs. The black symbols represent baseline conditions and grey symbols display the results of pretreatment with SB-269970 (**1**, 1 mg/kg(h). Thalamus is represented as circles and cerebellum as triangles. SUV = standardized uptake value.[VII] A mean of two experiments is presented for both baseline and pretreatment experiments. The results of the baseline conditions clearly show a difference in uptake in the two regions and the pretreatment reduce the signal in thalamus to similar SUV as in cerebellum. This indicates specific binding to the 5-HT_7R *in vivo*.

[VII] Reprinted from *Eur J Med Chem, 79.* Hansen, H. D.; Lacivita, E.; Di Pilato, P.; Herth, M. M.; Lehel, S.; Ettrup, A.; Andersen, V. L.; Dyssegaard, A.; De Giorgio, P.; Perrone, R.; Berardi, F.; Colabufo, N. A.; Niso, M.; Knudsen, G. M.; Leopoldo, M., Synthesis, radiolabeling and *in vivo* evaluation of [^{11}C](R)-1-[4-[2-(4-methoxyphenyl)phenyl]piperazin-1-yl]-3-(2-pyrazinyloxy)-2-p ropanol, a potential PET radioligand for the 5-HT(7) receptor**.,** 152-163. Copyright **(2014).** Permission after email contact with Elsevier. First email sent 25th Feb 2019, the first reminder the 1st of March and the second reminder the 6th of March.

2.3 Phenylethylamines

[^{11}C]Cimbi-806

The first phenylethylamine that has been used to develop a 5-HT$_7$R selective PET tracer was based on a biphenyl moiety.[81] Cimbi-806 displayed an *in vitro* inhibition constant (K_D) of roughly 9 nM on pig brain sections.[81, 90] Consequently, the BP was estimated to be 5.7 in pigs and 1.25 in humans and as such rather concerning for translational work. Selectivity data only exist towards the 5-HT$_{1A}$R (Table 3). The calculated $tBR_{target/off\text{-}target}$ in thalamus, frontal cortex and hippocampus were all above 40. No interference should as such occur from 5-HT$_{1A}$R binding.^{11}C-labeling was performed by N-methylation using [^{11}C]methyltriflate. [^{11}C]Cimbi-806 could be synthesized in a RCY of ~95% with an A_m ranging from 50 to 300 GBq/µmol at EOS. *In vivo* evaluation in pigs revealed good brain permeability, appropriate radiometabolism and despite of a very high lipophilicity ($logD_{7.4}$ = 4.4) reversible kinetics. A regional uptake was observed that was consistent with the known 5-HT$_7$R brain distribution.[19, 21-24] To evaluate if [^{11}C]Cimbi-806 bound specifically to 5-HT$_7$Rs *in vivo*, a blocking study with the highly selective 5-HT$_7$R antagonist SB-269970 was carried out. Surprisingly and in contrast to the *in vitro* situation, no reduction of binding was observed (Figure 7). Discouraged by these results, the work with [^{11}C]Cimbi-806 was discontinued.[81]

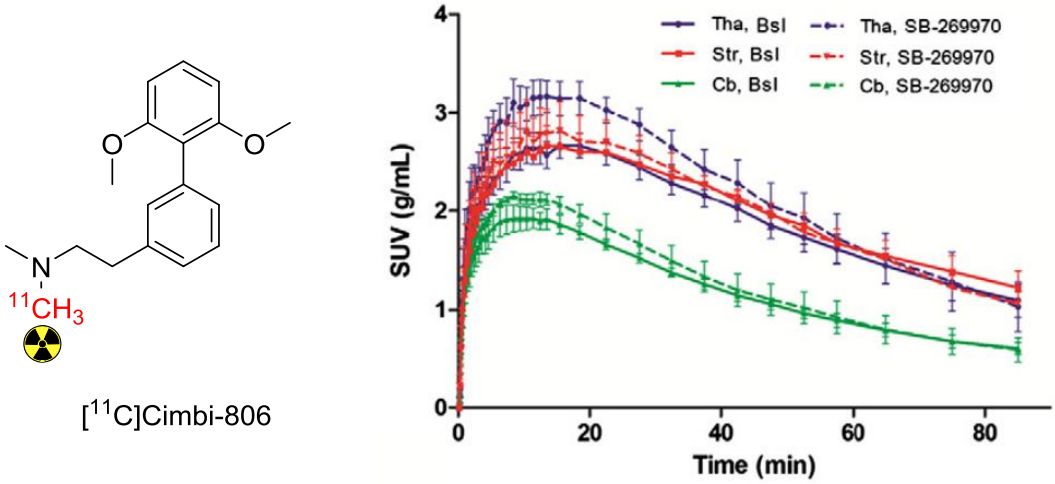

Figure 7: Molecular structure of [^{11}C]Cimbi-806 is illustrated to the left and to the right the TAC from [^{11}C]Cimbi-806 evaluation in pigs. The full lines represent baseline conditions and the dotted lines display the results of pretreatment with SB-

269970. Thalamus is represented as blue lines, striatum as red and cerebellum as green. SUV = standardized uptake value.[VIII] The results of the baseline conditions clearly show a difference in uptake in the brain regions with higher uptake in thalamus and striatum than in cerebellum. The pretreatment with SB-269970 increased the uptake all regions, with the highest change in thalamus. This could indicate specific blocking of peripheral receptors thus increasing the input of tracer to the brain.

[^{11}C]E-55888

In 2015, the second phenylethylamine structure was investigated as a potential 5-HT$_7$R PET tracer.[78] E-55888 is reported to be highly selective agonist for the 5-HT$_7$R with no significant affinity for other 5-HT receptor subtypes and 170 additional targets.[91] Table 3 displays an excerpt out of its selectivity profile.[78] All calculated $tBR_{target/off\text{-}target}$ in thalamus were >900. As such, E-55888 displayed an excellent candidate to develop a 5-HT$_7$R PET tracer. Carbon-11 N-methylation of the suitable precursor succeeded in high RCYs (80–90% non-decay corrected) with good A_m at TOI (A_m = 217 ± 65 GBq/µmol). [^{11}C]E-55888 showed high brain permeability, reversible tracer kinetics and moderate to good separation between high and low binding regions in pigs (Figure 8). Unfortunately, the PET signal could not be attributed to 5-HT$_7$R binding. Neither a self-block nor a blocking study with the 5-HT$_7$R selective antagonist SB-269970 could decrease the binding *in vivo* (Figure 8). Interestingly, pretreatment with SB-269970 massively increased the brain uptake, possibly by blocking 5-HT$_7$R within the blood pool. The same experimental setup using E-55888 did not alter the brain uptake at all. These results are not easily understandable and should be investigated further. No *in vitro* studies were performed to show if E-55888 binding could be displaced using autoradiography. It is not clear if E-55888 induces receptor internalization or similar effects that could prevent receptor bound E-55888 to be displaced. Radiometabolism was investigated but could not explain the observations.[78] Especially, the increased brain uptake after blocking with SB-269970 could for example not be attributed to radiometabolites. It would be worthwhile to test the tracer in other animal species to rule out that the observed behaviour is specific for pigs.

[VIII] Reprinted from *Bioorg Med Chem*, *20* (14), Herth, M. M.; Hansen, H. D.; Ettrup, A.; Dyssegaard, A.; Lehel, S.; Kristensen, J.; Knudsen, G. M., Synthesis and evaluation of [^{11}C]Cimbi-806 as a potential PET ligand for 5-HT(7) receptor imaging, 4574-4581., Copyright (**2012**), with permission from Elsevier**.**

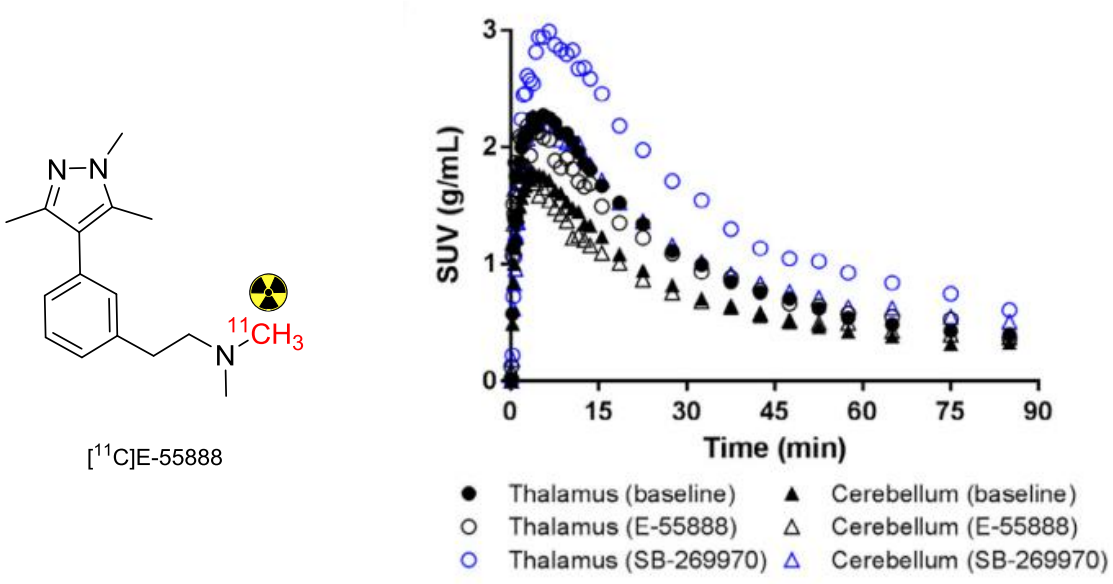

Figure 8: Molecular structure of [^{11}C]E-55888 is illustrated to the left and to the right the TAC from [^{11}C]E-55888 evaluation in pigs. The filled symbols represent baseline conditions (n=3) and the open symbols display the results of pretreatment experiment with either E-55888 (5 mg/kg (n=1)) or SB-269970 (1 mg/kg/h (n=1)). Thalamus is represented as circles and cerebellum as triangles. SUV = standardized uptake value.[IX] The results of the baseline conditions show a brain uptake matching the known distribution of the 5-HT$_7$R.[19, 21-24] But the self-block experiments with E-55888 did not decrease the signal in either of the regions of interest and pretreatment using SB-269970 even increased the uptake.

2.4 (Arylpiperazinyl-butyl)oxindole

(Arylpiperazinyl-butyl)oxindole are another interesting structural class as a starting point to develop 5-HT$_7$R selective PET tracers. These structures were described by Volk *et al*. in 2008 and displayed high affinity for 5-HT$_7$Rs accompanied by a good selectivity profile.[88]

[^{11}C]Cimbi-712 and [^{11}C]Cimbi-717

In 2014, Hansen *et al.* utilized this scaffold to develop a 5-HT$_7$R PET tracer for the first time. Cimbi-712 and Cimbi-717 were identified as suitable structures (e.g. an encouraging BP > 17 in pig thalamus was calculated) and consequently radiolabeled (Figure 9 and Table 3).[20,65,62] Both structures were radiolabelled with a RCY of approximately ~20% (d.c.) and A$_m$s were in the range of 50 to 100 GBq/µmol at EOS. [^{11}C]Cimbi-712 as well as [^{11}C]Cimbi-717 were evaluated

[IX] Reprinted from *Bioorg Med Chem Lett*, *25* (9), Author(s), Hansen, H. D.; Andersen, V. L.; Lehel, S.; Magnussen, J. H.; Dyssegaard, A.; Stroth, N.; Kristensen, J. L.; Knudsen, G. M.; Herth, M. M., Labeling and preliminary in vivo evaluation of the 5-HT(7) receptor selective agonist [(11)C]E-55888, 1901-1904., Copyright (**2015**), with permission from Elsevier.

as potential 5-HT_7R PET tracers in pigs (Figure 9). It is worthwhile to mention that only the racemic structures of [^{11}C]Cimbi-712 and [^{11}C]Cimbi-717 were evaluated as separation of the pure enantiomers failed due to re-racemization of both structure in solution[22]. Both [^{11}C]Cimbi-712 and [^{11}C]Cimbi-717 showed high brain uptake, and specific binding to the 5-HT_7R, which were displayed by blocking studies using the selective 5-HT_7R antagonist SB-269970 resulting in occupancies around 75 %.[5, 22, 28, 87] [^{11}C]Cimbi-717 did also show a reversible kinetics and a slow metabolism (50% remaining after 30 min), which led to the conclusion that it was the most promising PET tracer candidate of the two.[22] The selectivity profile for [^{11}C]Cimbi-712 and [^{11}C]Cimbi-717 has been further extended when following studies implied that both candidates show moderate affinities for the σ-receptors (Table 3).[80] For [^{11}C]Cimbi-717, the calculated $tBR_{5\text{-HT7R}/\sigma\text{-receptors}}$ for 5-HT_7R over the σ-receptors in the human thalamus is roughly 40. This indicates that of the observed binding 40 times more will be represented by binding to the 5-HT_7R than to the σ-receptors.[22, 47] As such, binding to σ-receptors is most likely neglectable.

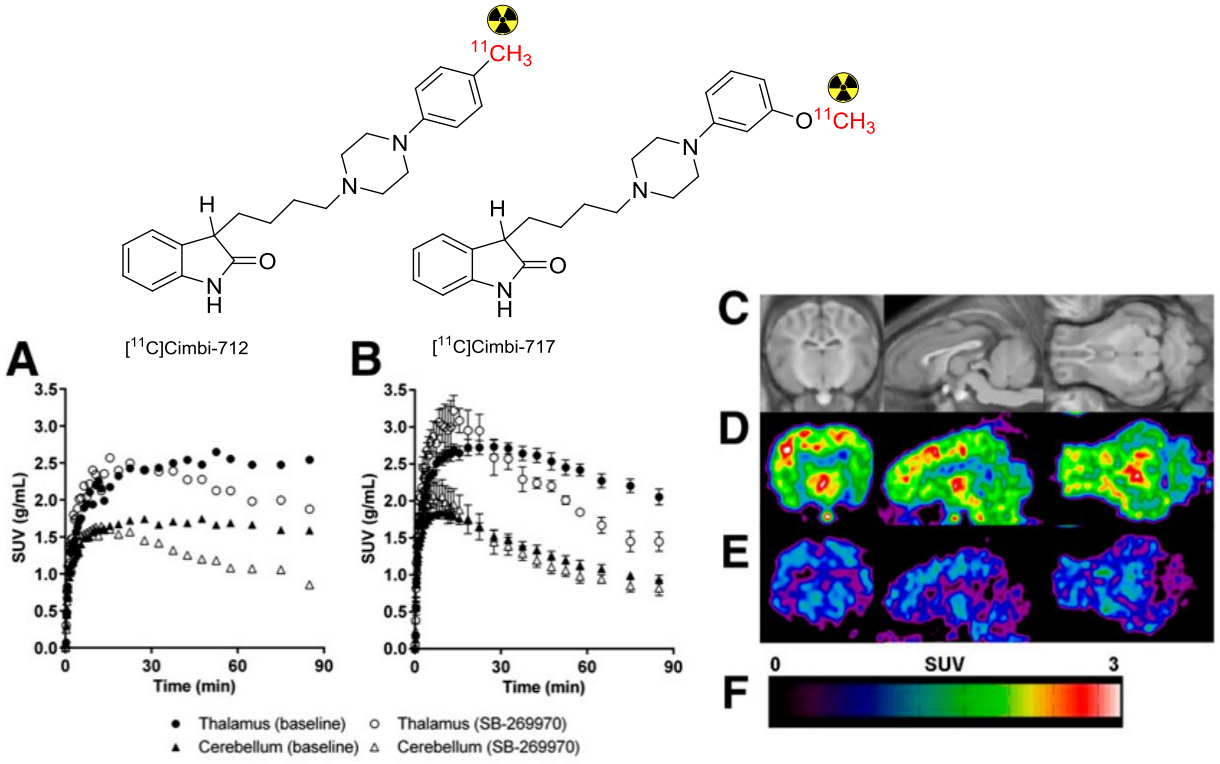

Figure 9: *In vivo* evaluation results of [^{11}C]Cimbi-712 and [^{11}C]Cimbi-717 in pigs **A)** The molecular structure (above) and TACs of [^{11}C]Cimbi-712 at baseline (filled symbols) and after blocking with 1 mg/kg/h SB-269970 (open symbols). **B)** The molecular

structure (above) and TACs of [^{11}C]Cimbi-717 at baseline (filled symbols) and after blocking with 1 mg/kg/h SB-269970 (open symbols). **C)** MR-based atlas of pig brain. **D)** Summed PET images (0-90 min) of [^{11}C]Cimbi-717 at baseline. **E)** Summed PET images (0-90 min) of [^{11}C]Cimbi-717 pretreated with SB-269970. **F)** Colour bar of standardized uptake value (SUV) (g/mL). Error bars = SEM.[X] As seen in both A and B, brain uptake displayed a difference in the two brain regions corresponding to the known distribution of the 5-HT$_7$R. [19, 21-24] After pretreatment with SB-269970 a reduction of the signal was seen in both brain regions for [^{11}C]Cimbi-712 and only for thalamus for [^{11}C]Cimbi-717. As only a small density of 5-HT$_7$R has been determined in the pig cerebellum [22], blocking of signal in this region is not desired. Comparing the TACs in A and B, the reversible tracer kinetics seen for [^{11}C]Cimbi-717 were also preferable.

[^{11}C]Cimbi-772 and [^{11}C]Cimbi-775

In 2015, derivatives alkylated on the 3-position of the butyloxindole, from the same structural class were radiolabelled and evaluated.[80] In contrast to their non-alkylated counterparts[22], respective rotamers could be isolated. In general, the rotamers with (-)-optical rotation decreased the affinity towards the 5-HT$_7$R, while the (+)-rotamers resulted in a better selectivity profile (Table 3). Cimbi-772 and Cimbi-775 were selected for their promising selectivity profiles. The calculated BP of racemic Cimbi-772 and Cimbi-775 in pig thalamus were 7 and 5.85, respectively and as such, in the order of acceptable values. Radiolabelling was performed in a similar matter as described in the previous section. Initially the racemic PET tracer candidates were synthesised to evaluate their *in vivo* potential, before eventually synthesizing the more complicated enantiomeric precursors or separating both enantiomers radiolabelled. Sufficient RCYs (estimated to around 3% at EOS (d.c)) and A_m (in average 234-343 GBq/μmol) could be isolated and justified further evaluation studies in pigs. Both tracers showed good brain permeability despite their high lipophilicity, together with reversible tracer kinetics. A clear regional distribution could also be determined between high and low density 5-HT$_7$R regions (Figure 10). Similar to results obtained from [^{11}C]E-55888 or [^{11}C]Cimbi-806, neither tracer could be displaced *in vivo* by SB-269970 pretreatment. Consequently, specific 5-HT$_7$R binding of both tracer candidates could so far not be confirmed.[80]

[X] This work was originally published in JNM. Hansen, H. D.; Herth, M. M.; Ettrup, A.; Andersen, V. L.; Lehel, S.; Dyssegaard, A.; Kristensen, J. L.; Knudsen, G. M., Radiosynthesis and in vivo evaluation of novel radioligands for PET imaging of cerebral 5-HT$_7$ receptors. *J Nucl Med* **2014**, 55 (4), 640-646. © SNMMI.

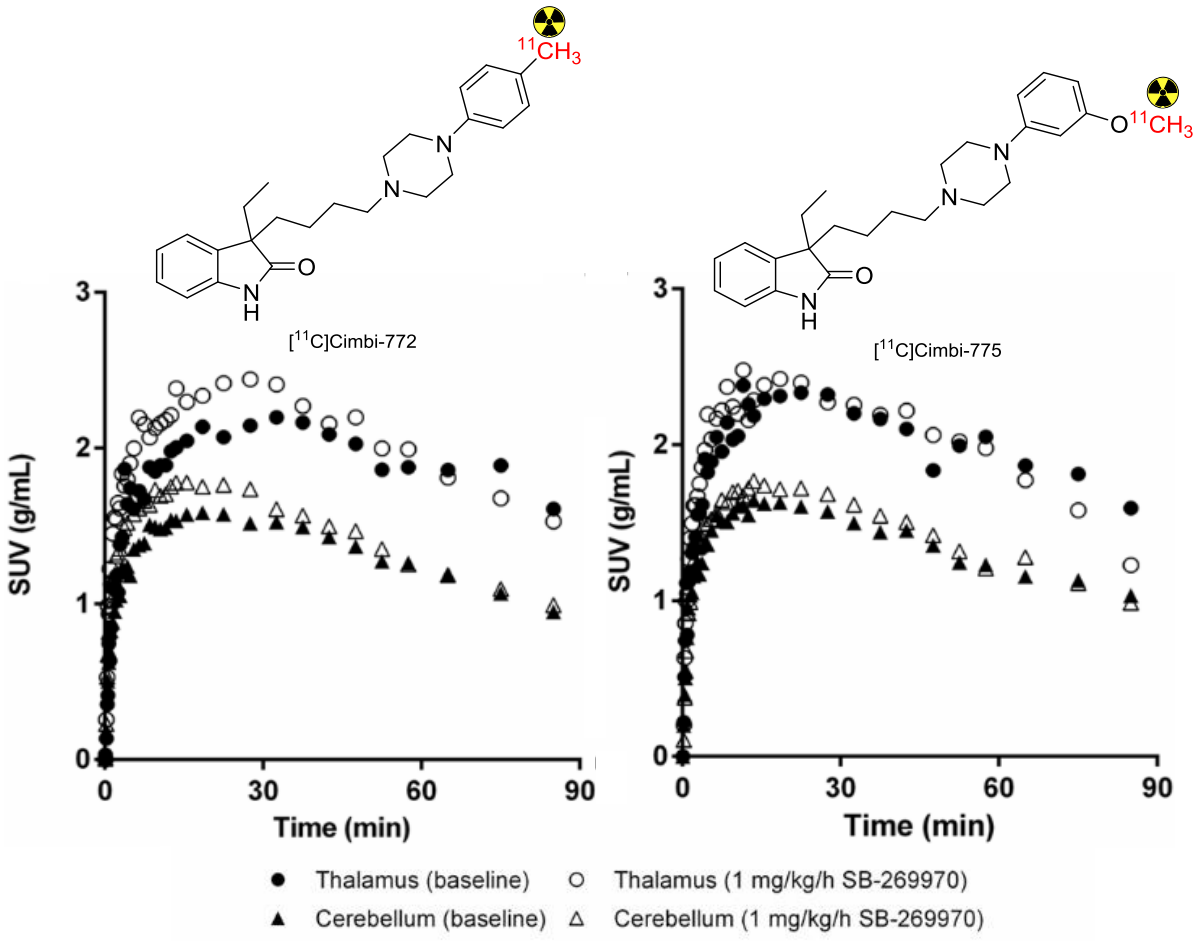

Figure 10: TACS of [^{11}C]Cimbi-772 and [^{11}C]Cimbi-775 from PET evaluation in pigs showing the respective molecular structures above. The filled symbols represent the baseline conditions and the open symbols are after pretreatment of 1 mg/kg/h SB-269970. Two regions of interest were elucidated, thalamus (circles) and cerebellum (triangles).[XI] Good brain permeability is seen for both PET tracer candidates and a regional uptake corresponding to the distribution of the 5-HT$_7$R.[19, 21-24] Neither of [^{11}C]Cimbi-772 or [^{11}C]Cimbi-775 got a reduced signal after pretreatment with SB-269970, indicating that the uptake seen in thalamus is not due to specific binding to the 5-HT$_7$R.

[^{18}F]ENL09 and [^{18}F]ENL10

In light of the promising results obtained with [^{11}C]Cimbi-717, several ^{18}F-derivatives have been developed.[92-93] ENL09 and ENL10 display the most promising characteristics (Figure 11 and Table 3). They displayed high affinity for the 5-HT$_7$R combined with a reasonable selectivity

[XI] Adapted with permission from Herth, M. M.; Andersen, V. L.; Hansen, H. D.; Stroth, N.; Volk, B.; Lehel, S.; Dyssegaard, A.; Ettrup, A.; Svenningsson, P.; Knudsen, G. M.; Kristensen, J. L., Evaluation of 3-Ethyl-3-(phenylpiperazinylbutyl)oxindoles as PET Ligands for the Serotonin 5-HT(7) Receptor: Synthesis, Pharmacology, Radiolabeling, and *in Vivo* Brain Imaging in Pigs. *J Med Chem* **2015,** *58* (8), 3631-6.). Copyright (2015) American Chemical Society.

profile. The estimated BPs for ENL09 in rat/pig thalamus was 3.5 and as such, a bit below the recommended value. ENL10 showed a higher and satisfying BP of approximately 8. In respect to selective imaging, σ-receptors were identified as a concern. The $tBR_{5\text{-}HT7R/\sigma\text{-}receptors}$ was determined to only be 2.15 in rat thalamus for ENL10 and as such should be considered a potential issue. To evaluate the binding pattern of both compounds *in vivo*, ENL09 and ENL10 were labelled using a two-step fragment-based strategy yielding in a RCY of 1.78-5.15% (d.c.). Sufficient A_m to perform PET scans in rodents were isolated (range of 10 to 136 GBq/µmol). Interestingly, [^{18}F]ENL09 and [^{18}F]ENL10 were radiolabelled in a one-pot approach in a simultaneous fashion yielding in two compounds in one synthesis (Figure 11). This strategy combined with a 2x2 rat holder increased evaluation through-put.[94-95] [^{18}F]ENL09 and [^{18}F]ENL10 were identified to be a P-gp efflux transporter substrate. P-gp inhibition with elacridar[96] massively increased the brain uptake of both substances. To evaluate if the observed binding could be attributed to 5-HT_7R binding, a double inhibition/blocking experiment was designed using first elacridar to increase brain uptake and then the high 5-HT_7R affinity antagonist SB-269970 to block specific binding. Only [^{18}F]ENL10 showed a reduced signal in 5-HT_7R high density brain region using this experimental design.[92] To investigate if σ-receptors contribute to the observed signal, a similar double inhibition/blocking experiment was used. The σ-receptor binder haloperidol was used as specific receptor blockers. No reduction of signal was seen in thalamus and only a small signal reduction in cerebellum was observed after haloperidol pretreatment. Consequently, the σ-binding component of [^{18}F]ENL10 is negligible *in vivo*. These results are encouraging for future translational work as rodents have a more efficient P-gp system compared to higher species such as pigs, NHP or humans.[66, 92]

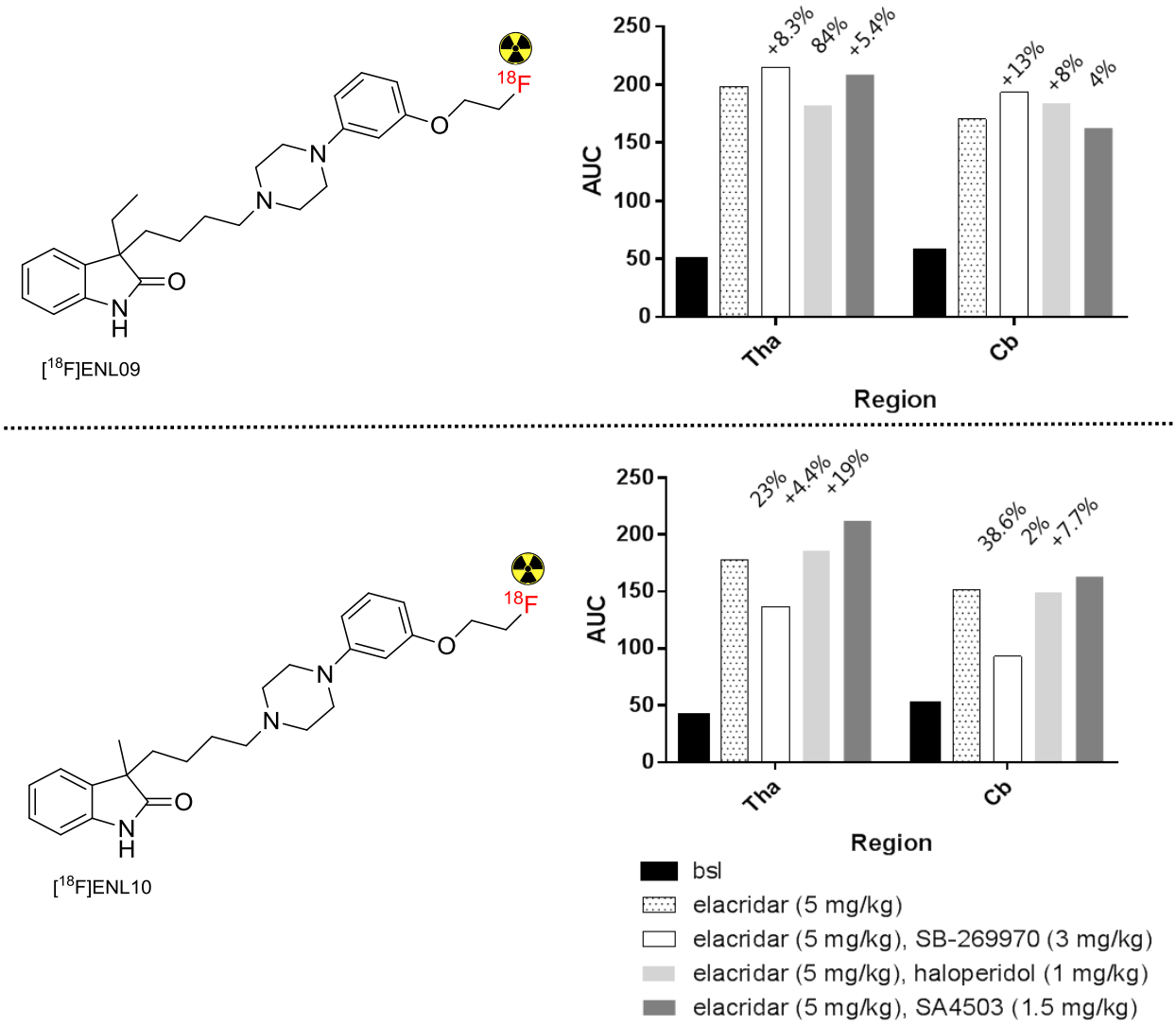

Figure 11: Molecular structures and results from the *in vivo* evaluation of [^{18}F]ENL09 (above) and [^{18}F]ENL10 (below) presented as area under the representative TACs. The results show that low brain uptake was seen for both PET tracer candidates in baseline condition. When the P-gp efflux transporter was inhibited with elacridar[96] the brain uptake were increased and displayed a distribution comparable to the 5-HT$_7$R. Out of [^{18}F]ENL09 (above) and [^{18}F]ENL10 (below), only the latter showed a decreased AUC after pretreatment of the selective 5-HT$_7$R antagonist SB-269970, indicating specific binding. [^{18}F]ENL10 (below) only displayed a 2% reduction of AUC in cerebellum and non in thalamus, when pretreating with the non-selective σ-receptor binder haloperidol.

2.5 Benzosulfonamides

The last structural class that has extensively been used to develop a 5-HT_7R selective PET ligand are benzosulfonamides.[23, 68, 76-77, 85, 87] Originally, this compound class was developed in the early 1930s by a team of researchers at Bayer laboratories in Germany.[97] In 2000, Lovell *et al*. identified 3-[[(2R)-2-[2-(4-methyl-1-piperidinyl)ethyl]-1-pyrrolidinyl]sulfonyl]-phenol (SB-269970) as a very selective 5-HT_7R compound. Its tritiated version is still used as a "Gold-standard" to visualize and quantify 5-HT_7R binding *in vitro*.[19, 21-24] It was also reported that SB-269970 showed good brain permeability.[20, 28, 87]

[^{18}F]2FP3

In 2011, Lemoine *et al.* developed SB-269970 derivatives into a 5-HT_7R PET tracer.[85] Within this series, 2FP3 displayed the most promising 5-HT_7R affinity (1.43 nM). High selectivity over the 5-HT_{1A}R and 5-HT_6R (both having K_B>>10000 nM) was observed.[76, 85] Encouraged by the calculated BP of 7.7 in humans and high $tBR_{target/off-target}$, [^{18}F]2FP3 was radiolabelled. A RCY between 39% and 48% (d.c.) and a A_m ranging from 40 - 130 GBq/µmol at EOS was reached. Radiometabolism and brain uptake of [^{18}F]2FP3 was first evaluated in *ex vivo* rat studies. No major radiometabolites were detected and minimum 95% of the activity within the rat brain was attributed to parent compound. In light of these findings, [^{18}F]2FP3 was evaluated in cats. High brain uptake was detected with accumulation differences in high and low 5-HT_7R density regions. The tracer displayed reversible binding kinetics and could be specifically blocked with SB-269970 (5 mg/kg) (signal concentrations fell to near zero in all regions) (Figure 12A).[85] These results promoted further translation of this tracer to other species such as pigs, but also to NHPs.[23] In pigs, high brain uptake and reversible tracer kinetics were detected. Kinetics were slower compared to the observation in cats. A good regional distribution between high and low 5-HT_7R density region was detected, however, the separation was less pronounced than in cats. Pretreatment with the selective 5-HT_7R antagonist SB-269970 resulted in a limited decrease of binding in the order of 20% in the highest 5-HT_7R density region. The A_m at TOI was 24 ± 23 GBq/µmol (n = 3) in pigs (Figure 12B). This number can only result in a limited self-blocking effect and can therefore not explain the low blocking. In NHP, good brain uptake and reversible tracer kinetics was observed. However, similar to the observed binding pattern of [^{11}C]DR4446 in NHP, almost no regional differences in brain distribution were detected. No specific binding could be determined, even though very high A_m values were reached (270.4 ± 44.2 GBq/µmol) (Figure 12C).[23] The estimated BP is pigs and NHP are 3.8-5.5, as such very similar and cannot

explain the observed findings. Radiometabolism in pigs and NHP were also similar and could neither explain the discrepancy between the results obtained. The acquired results are relatively difficult to interpret. Obviously, there are species differences. Estimated BPs are similar in these species and nevertheless, huge differences in binding patterns have been detected. Further studies are needed to investigate possible explanations for this. Some questions that arise immediately are: 1) Why is the non-specific binding component so different in cats and pigs? 2) Why is the regional tracer uptake in high and low 5-HT_7R affinity regions so different between cats, pigs and NHPs, even though similar B_{max} values are found? 3) Does [^{18}F]2FP3 bind to an off-target that is more abundant in cats than in pigs and more abundant in pigs than in NHPs?

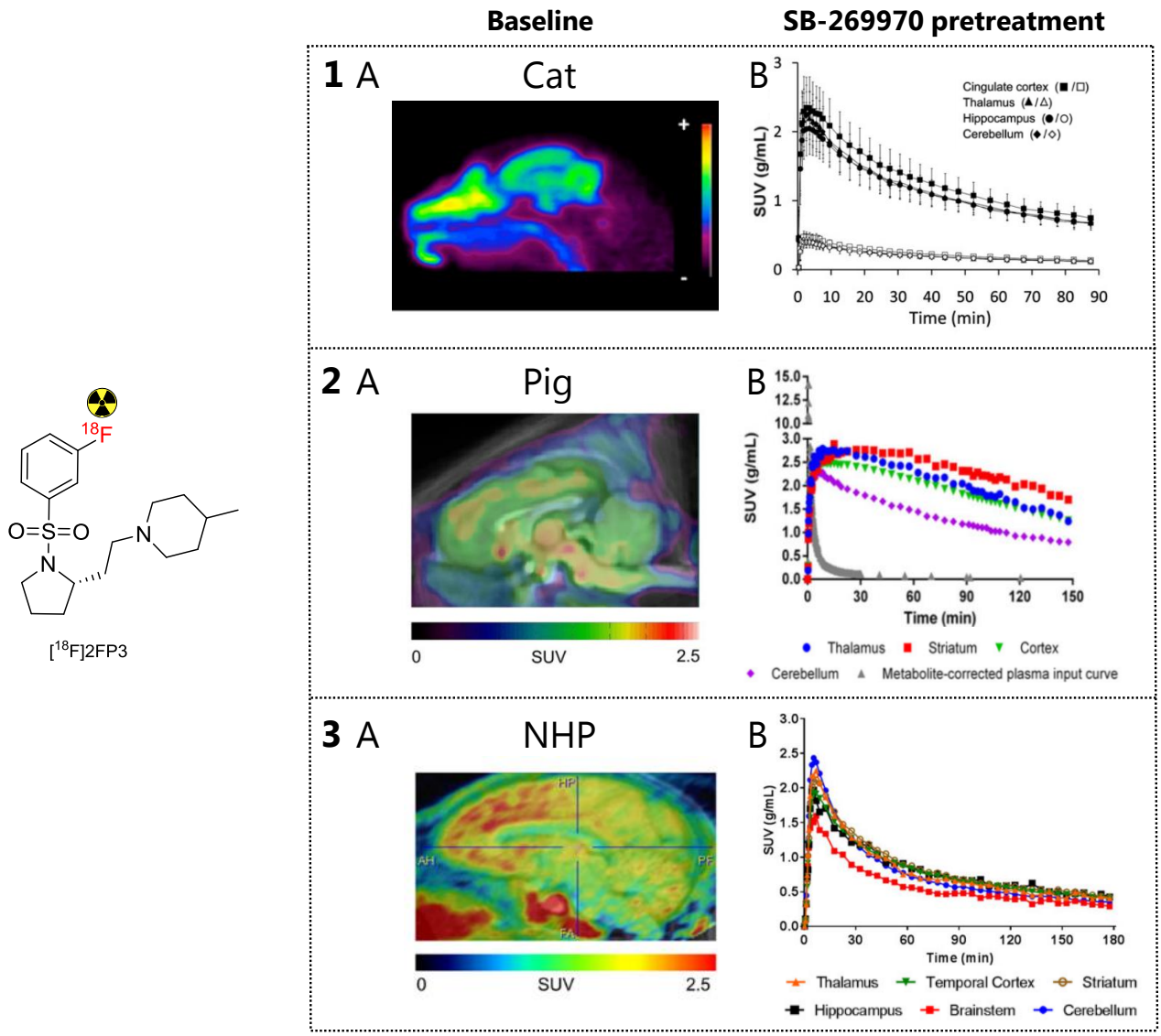

Figure 12: The molecular structure of [^{18}F]2FP3 is illustrated to the left and an overview of the *in vivo* evaluation results in cat **(1)**[XII], pig **(2)** and NHP **(3)**[XIII] is presented to the right. **1A)** Representative sagittal summed PET image (0–90 min), showing the distribution of [^{18}F]2FP3 in cat brain. **1B)** Representative TACs of [^{18}F]2FP3 at baseline (filled symbols) and after pretreatment of SB-26990 (open symbols) 5 mg/kg, 30 min before radiotracer injection (duplicated experiments). **2)** Overview of the *in vivo* evaluation results in pig **A)** Summed PET image (0-90 min) of the biodistribution of [^{18}F]2FP3 in the pig brain at baseline

[XII] This research was originally published in JNM. Lemoine, L.; Andries, J.; Le Bars, D.; Billard, T.; Zimmer, L., Comparison of 4 radiolabeled antagonists for serotonin 5-HT(7) receptor neuroimaging: toward the first PET radiotracer. *J Nucl Med* **2011,** *52* (11), 1811-8. © SNMMI.

[XIII] Permission for the reuse of this work has been given by John Wiley and Sons. The work was originally published by Hansen, H. D.; Constantinescu, C. C.; Barret, O.; Herth, M. M.; Magnussen, J. H.; Lehel, S.; Dyssegaard, A.; Colomb, J.; Billard, T.; Zimmer, L., Evaluation of [^{18}F] 2FP3 in pigs and non-human primates. *Journal of Labelled Compounds and Radiopharmaceuticals* **2018,** 1-9. © 2018 John Wiley & Sons, Ltd

conditions. **2B)** Representative TACs after administration of SB-269970 (1 mg/kg/h for 3 h) before and during the [^{18}F]2FP3 injection. **3)** Overview of the *in vivo* evaluation results in NHP. **A)** Summed PET image (0-90 min) of the biodistribution of [^{18}F]2FP3 in the NHP brain at baseline conditions. **3B)** Representative TACs for [^{18}F]2FP3 after pre-administration of SB266970 (3 mg/kg). The results show that in cat, [^{18}F]2FP3 displayed specific binding to the 5-HT$_7$R *in vivo* by a substantial decrease of the signal after pretreatment with SB-269970 and also reversible binding. In pig the uptake of [^{18}F]2FP3 was distributed accordingly to the 5-HT$_7$R distribution, but the signal could only be blocked to a low degree (20%) by SB-269970.In NHP the uptake of [^{18}F]2FP3 was more uniform throughout the whole brain and no specific binding to the 5-HT$_7$R could be determined.

[^{18}F]2F3P3

In 2014, an attempt to optimize the binding characteristics of [^{18}F]2FP3 was carried out and the distance between the two nitrogen-heterocycles increased.[98] The resulting compound, [^{18}F]2FP3, showed higher affinity for the 5-HT$_7$R, increased 5-HT$_{1A}$R selectivity and a lipophilicity of log$D_{7.4}$ =1.58 (Table 3).[68] These findings prompted further investigations. [^{18}F]2F3P3 could successfully be radiolabeled with a RCY of 20% ± 4 (n = 4) and a A_m = 98 ± 4 GBq/µmol. Low brain uptake was observed in rodent PET studies. This behaviour could be attributed to an interaction of [^{18}F]2F3P3 with the P-gp efflux transporter.[68] Similar to [^{11}C]PF30, the work with [^{18}F]2F3P3 was discontinued after revealing that it is a P-gp efflux transporter substrate.[68, 83] In light of the results published by Syvänen *et al.*, it would be interesting to determine if [^{18}F]2F3P3 is also a P-gp substrate in higher species. Results from the study by Syvänen *et al.* indicate that PET tracers being a strong substrate in rodents might not show the same behaviour in higher species such as pigs or NHPs.[66]

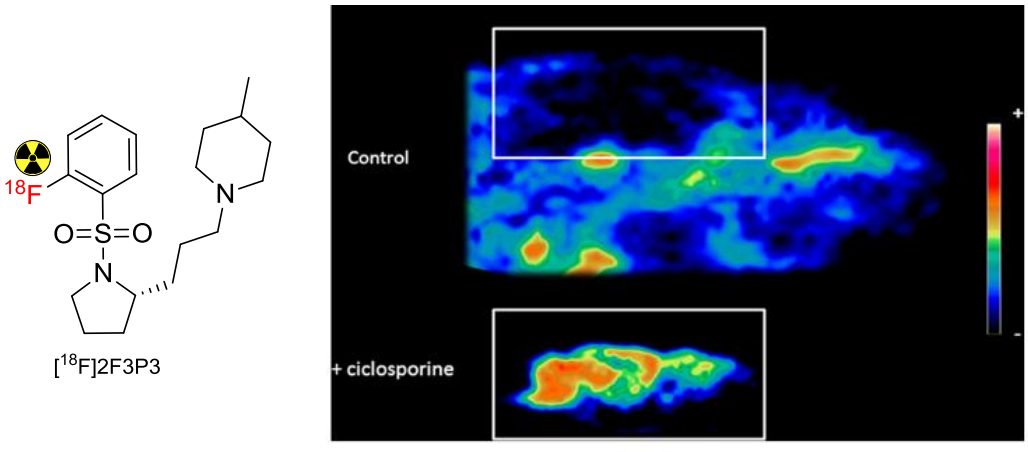

Figure 13: Molecular structure of [^{18}F]2F3P3 (left) and microPET images of rat (right). The microPET images show the brain uptake of [^{18}F]2F3P3 at baseline (above) and after pretreatment with CsA (50 mg/kg, iv)[99] 30 min before [^{18}F]2F3P3 injection (sagittal brain sections at the brain level, indicated by the white square) (below). Pseudocolor scale is from low (blue) to high

binding level (red).[XIV] The inhibition of the P-gp efflux transporters using CsA greatly increase the brain uptake of [^{18}F]2F3P3, hence indicate that this tracer is a P-gp substrate.

^{11}C- and ^{18}F-alkylated derivatives of SB-269970

In 2019, two additional analogues of SB-269970 have been reported and evaluated as 5-HT$_7$R PET tracers.[100-101] Both tracers were O-alkylated analogues of SB-269970 (Figure 14 and 15, Table 3).

[^{11}C]Cimbi-701

Cimbi-701 ($K_{i\ 5\text{-}HT7}$ = 10 nM, log$D_{7.4}$ = 1.92) is an O-methylated analogue of SB-269970. *In vitro* selectivity profiling showed that Cimbi-701 displays even higher affinity for the σ-1 (K_i = 9.2 nM) and σ-2 receptors (K_i = 1.6 nM). The representative calculated BP for Cimbi-701 in rat/pig/NHP thalamus is approximately 2.6, and thus a bit below the threshold of 5. The $tBR_{5\text{-}HT7R/\sigma\text{-receptors}}$ in rat/pig/NHP thalamus are ca. 0.2 indicating that only 1/10 of signal detected in thalamus could stem from 5-HT$_7$R binding. Keeping this in mind, [^{11}C]Cimbi-701 was radiolabeled and consequently evaluated in PET studies. Radiolabeling succeeded in a RCY of 10-22% and in a satisfying A_m of 256 ± 127 GBq/μmol at EOS. [^{11}C]Cimbi-701 was initially evaluated in rats, where it displayed poor brain uptake (Figure 14). Standard uptake values (SUVs) increased after pretreatment with the P-gp efflux transporter inhibitor elacridar.[96] Specific binding to the 5-HT$_7$R were then elucidated by the pretreatment of SB-269970 (3 mg/kg). Reduced uptake in thalamus (13.6%) was observed indicating 5-HT$_7$R specific binding. To investigate whether [^{11}C]Cimbi-701 also binds to σ-receptors *in vivo*, haloperidol (1 mg/kg) was used as blocking agents. Haloperidol pretreatment decreased both thalamus and cerebellum uptake by around 20%. This indicates that [^{11}C]Cimbi-701 consists of an addition σ-receptor binding component *in vivo*. Consequently, it will only be possible to image the 5-HT$_7$R system with [^{11}C]Cimbi-701 when σ-receptors are blocked in the same experiments. In light of that, [^{11}C]Cimbi-701 was translated into a pig animal model. Sufficient high brain uptake of [^{11}C]Cimbi-701 (Figure 14) was observed, with the highest uptake in thalamus and with the lowest uptake in cerebellum. The kinetics of [^{11}C]Cimbi-701 were very slow with minor washout

[XIV] Reprinted from Publication Colomb, J.; Becker, G.; Forcellini, E.; Meyer, S.; Buisson, L.; Zimmer, L.; Billard, T., Synthesis and pharmacological evaluation of a new series of radiolabeled ligands for 5-HT$_7$ receptor PET neuroimaging. *Nucl Med Biol* **2014,** *41* (4), 330-337. Copyright (2914), with permission from Elsevier

of the radiotracer. Investigation whether this PET tracer bound specifically to the 5-HT_7R was performed by pre-administration of SB-258719 and Cimbi-717.[65, 102] The uptake of [^{11}C]Cimbi-70 was dose-dependently decreased in all investigated brain regions using both 5-HT_7R blockers. As in rats, binding to the σ receptors was elucidated. Pre-administrating of haloperidol (0.1 mg/kg) greatly reduced the uptake of [^{11}C]Cimbi-701 (~35 % lowered SUV) and showed that [^{11}C]Cimbi-701 also binds to σ-receptors in pigs. Metabolism studies revealed that the tracer was quickly metabolized with 28% intact tracer after 30 min.

With these data in hand, [^{11}C]Cimbi-701 was translated into a baboon study.[46] The rationality behind this was to test whether a specific signal could be obtained in baboon, the animal model that resembles the human the most, before a specific σ-receptor block was carried out that would enable specific 5-HT_7R binding. Similar to rats, [^{11}C]Cimbi-701 exhibited poor BBB permeability in baboons, which could be due to a strong P-gp dependency of [^{11}C]Cimbi-701 also in this species. Because of that, further evaluation experiments were discarded. Discrepancy in brain uptake due to e.g. differences of the P-gp efflux transporter has also previously been observed in the rat, pig, monkey and human BBB.[66, 103-104]

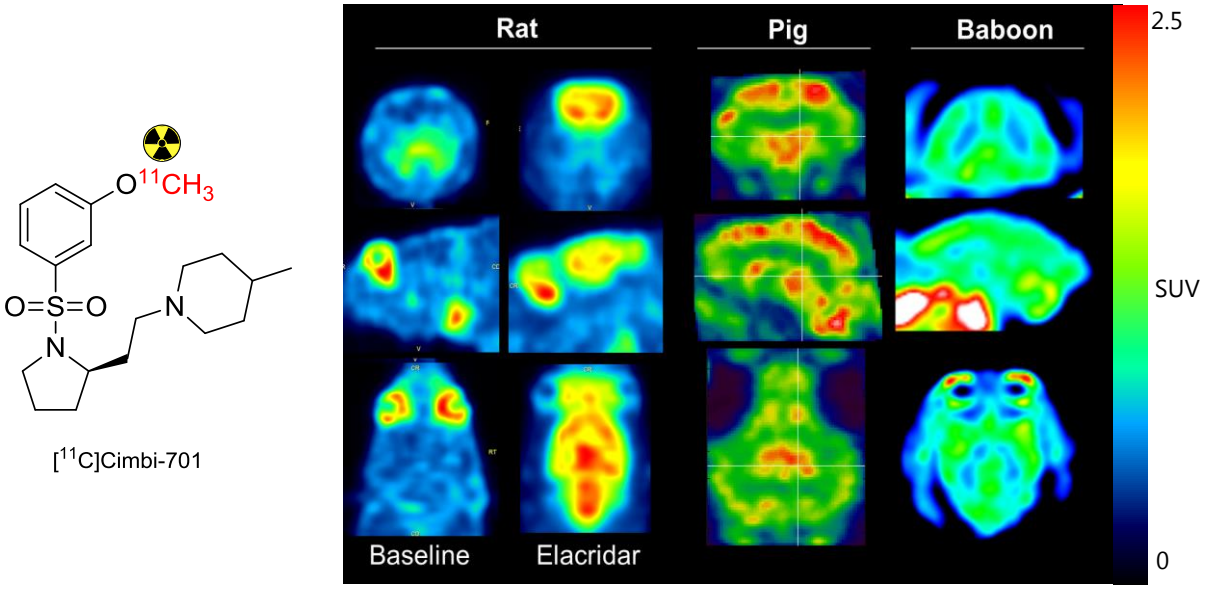

Figure 14: The molecular structure of ^{11}C]Cimbi-701 (left) and summed PET images in the rat, pig and the baboon brain. [^{11}C]Cimbi-701 in rats is shown before and after pretreatment with the P-gp efflux inhibitor elacridar (5 mg/kg, 30 min prior to injection of the radiotracer) (right). [^{11}C]Cimbi-701 was evaluated in the 3 different species; rats, pigs and baboon. The results of the evaluation displayed a species related difference in brain uptake, and a P-gp dependency was found in rats by pretreatment with elacridar[96] giving an increased BBB permeability.

[^{18}F]ENL30

[^{18}F]ENL30 was developed simultaneously to [^{11}C]Cimbi-701 and is its fluoroethoxy analogue.[105] The main idea behind this effort was to get access to a ^{18}F-derivative, which would allow to perform rodent studies over a full experimental day with only one production.[40] A similar labelling strategy was applied as recently published.[106-108] This strategy made use of [^{18}F]fluoroethyl tosylate as a synthon.[106] [^{18}F]ENL30 could be radiolabeled in a RCY ranging between 1.2 and 15% (decay corrected, n = 8%) and with a satisfactorily A_m of 108 - 197 GBq/µmol. [^{18}F]ENL30 was afterwards used to determine the affinity of ENL30 as well as to determine a limited selectivity profile. This was done using autoradiographic experiments on rat brain slices. Surprisingly, [^{18}F]ENL30 showed an approximately 10-fold affinity increase towards the 5-HT$_7$R compared to its methoxy derivative. A K_D of 0.75 ± 0.5 nM was determined. An increased and more promising BP (for rodents/pigs and NHPs) of approximately 50 was consequently calculated.

In a next step and because of the structural similarity of ENL30 to Cimbi-701 (Figure 14 and 15), the selectivity of ENL30 towards σ-receptor was determined by blocking experiments with the σ-receptor binder haloperidol on autoradiographic rat brain slices. A dose dependant reduction of the signal in thalamus with around 20% reduction was observed using the highest dose. Even though these experiments indicated that [^{18}F]ENL30 displays to some extent a σ-receptor binding component, the tracer was evaluated in rat PET studies because specific blocking of σ-receptors could enable selective 5-HT$_7$R imaging. Low rat brain uptake was observed, which increased dramatically (0.3 SUV to around 3.0 SUV) when the P-gp efflux transporter was blocked. This indicates that [^{18}F]ENL30 is a strong P-gp substrate in rats (Figure 15A). Specific binding was shown using the previously described double inhibition/blocking experiment (see [^{18}F]ENL09 and [^{18}F]ENL10 section). Results are displayed in Figure 15B. Both SB-269970 and the dissimilar 5-HT$_7$R binding compound Cimbi-717 resulted in a reduction of the area-under-curve (AUC) in both thalamus and cerebellum of >20%. Pretreatment of haloperidol and the σ-1 selective SA4503 reduced the signal in both brain regions of interest (12-24%). Consequently, [^{18}F]ENL30 displays a 5-HT$_7$R and a σ-receptors binding component *in vivo*. Future studies in higher species would be beneficial to investigate if [^{18}F]ENL30 could be used to image selectively 5-HT$_7$Rs and if a simultaneous block of σ-receptors is needed in the respect.

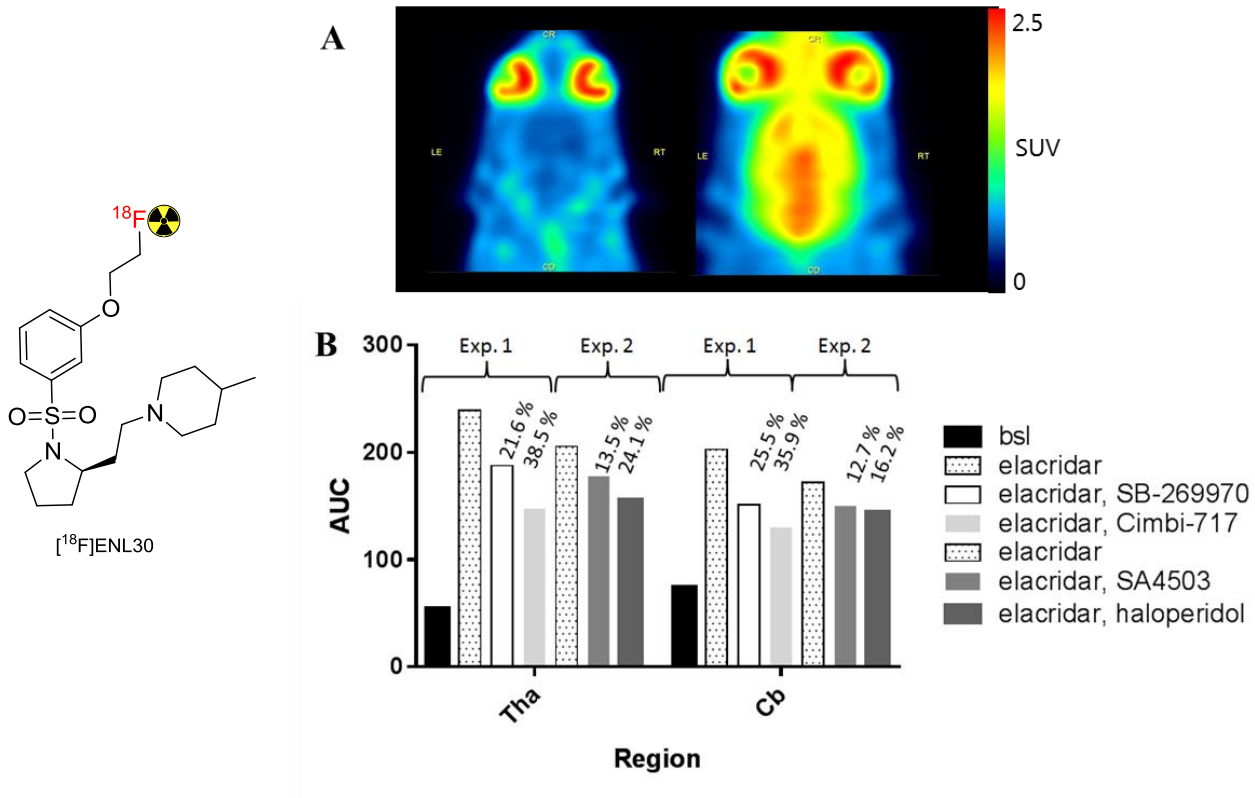

Figure 15: Summed PET brain images, molecular structure and calculated area-under-curves (AUCs) for all TACs of [^{18}F]ENL30 evaluated in rat. **A)** Horizontal summed (5-120 min) PET images of [^{18}F]ENL30 in baseline condition (right) and after inhibition of the P-gp efflux transporter using elacridar (5 mg/kg)(left). **B)** The AUCs from baseline [^{18}F]ENL30 and blocking experiments displayed as a grouped barplot, indicating percentage AUC reduction above the blocking agent bars. [^{18}F]ENL30 was determined to be a strong P-gp efflux transporter substrate after inhibition using elacridar greatly increased the brain uptake **(A)**). In the SB-269970 (3 mg/kg) blocking experiment a reduction around 21-25% of the AUC was seen in both thalamus and cerebellum, indicating specific binding to the 5-HT$_7$R. An even larger reduction of AUC was seen after pretreatment with the dissimilar 5-HT$_7$R binding compound Cimbi-717 (3 mg/kg). Haloperidol (1 mg/kg), a drug having affinity for both σ-receptors reduced the AUC in thalamus 24.1% and 16.2% in cerebellum. The σ-1 selective compound SA4503 (1.5 mg/kg) gave a lesser reduction (around 13%) in each of the brain regions of interest. These results indicate that there is a σ-receptors binding component in the seen brain uptake of [^{18}F]ENL30.

3. Reflections and future efforts

Despite many promising attempts to develop a 5-HT_7R PET tracer, thus far no 5-HT_7R PET tracer has been validated and reached the clinic. [^{11}C]Cimbi-717, [^{18}F]2FP3, [^{11}C]Cimbi-701, [^{11}C]BA10 or [^{18}F]ENL10 display promising characteristics to be translated into the clinic. However, the tracers most investigated within this set, [^{11}C]Cimbi-717, [^{18}F]2FP3 and [^{11}C]Cimbi-701, did not show promise in NHPs, the animal model closest resembling humans generally spoken. This is surprising since similar receptor densities have been determined in rodents, pigs and NHPs. As such, the question arises if the NHP model is representative for humans or if other species would translate more accurately. Within the literature, there are not many tracers described that fail in NHP but work in humans, however some examples exist. One being the PET tracer [^{11}C]clorgyline, which selectively binds to monoamine oxidase A (MAO A) in the human brain, but is not retained in either the baboon or the rhesus monkey brain.[103, 109] We speculate that the 5-HT_7R system could be another example in where such a behaviour is observed. In this respect, it would be interesting to evaluate [^{11}C]BA10 and [^{18}F]ENL10 in NHPs and determine if they behave in a similar way. From a broader perspective, all developed tracers display calculated BPs close to the lower recommended limit in humans. Further structure activity relationship studies aiming to increase affinity and selectivity of these ligands are therefore highly desired and should be carried out. In addition, new entities should be explored in this respect.

In summary, the development of a 5-HT_7R selective PET tracer has started roughly 20 years ago, progress has been made and promising PET ligands have been developed. However, there is still a long journey ahead until a successful tracer for this interesting receptor system will be available within the clinic.

5. References

1. Azmitia, E. C., Evolution of serotonin: sunlight to suicide. In *Handbook of Behavioral Neuroscience*, Elsevier: **2010**; Vol. 21, pp 3-22.

2. T. L'Estrade, E.; Hansen, H. D.; Erlandsson, M.; Ohlsson, T. G.; Knudsen, G. M.; Herth, M. M., Classics in Neuroimaging: The Serotonergic 2A Receptor System—from Discovery to Modern Molecular Imaging. ACS Publications: **2018**. 1226-1229.

3. Glennon, R. A.; Titeler, M.; McKenney, J., Evidence for 5-HT_2 involvement in the mechanism of action of hallucinogenic agents. *Life sciences* **1984,** *35* (25), 2505-2511.

4. Matthys, A.; Haegeman, G.; Van Craenenbroeck, K.; Vanhoenacker, P., Role of the 5-HT_7 receptor in the central nervous system: from current status to future perspectives. *Molecular Neurobiology* **2011,** *43* (3), 228-253.

5. Nichols, D. E.; Nichols, C. D., Serotonin Receptors. *Chemical Reviews* **2008,** *108* (5), 1614-1641.

6. Bard, J. A.; Zgombick, J.; Adham, N.; Vaysse, P.; Branchek, T. A.; Weinshank, R. L., Cloning of a novel human serotonin receptor (5-HT_7) positively linked to adenylate cyclase. *Journal of Biological Chemistry* **1993,** *268* (31), 23422-23426.

7. Ruat, M.; Traiffort, E.; Leurs, R.; Tardivel-Lacombe, J.; Diaz, J.; Arrang, J.-M.; Schwartz, J.-C., Molecular cloning, characterization, and localization of a high-affinity serotonin receptor (5-HT_7) activating cAMP formation. *Proceedings of the National Academy of Sciences* **1993,** *90* (18), 8547-8551.

8. Hoyer, D.; Hannon, J. P.; Martin, G. R., Molecular, pharmacological and functional diversity of 5-HT receptors. *Pharmacology Biochemistry and Behavior* **2002,** *71* (4), 533-554.

9. Bard, J. A.; Zgombick, J.; Adham, N.; Vaysse, P.; Branchek, T. A.; Weinshank, R. L., Cloning of a novel human serotonin receptor (5-HT_7) positively linked to adenylate cyclase. *Journal of Biological Chemistry* **1993,** *268* (31), 23422-6.

10. Plassat, J. L.; Amlaiky, N.; Hen, R., Molecular cloning of a mammalian serotonin receptor that activates adenylate cyclase. *Molecular Pharmacology* **1993,** *44* (2), 229-236.

11. Ruat, M.; Traiffort, E.; Leurs, R.; Tardivel-Lacombe, J.; Diaz, J.; Arrang, J. M.; Schwartz, J. C., Molecular cloning, characterization, and localization of a high-affinity serotonin receptor (5-HT_7) activating cAMP formation. *Proceedings of the National Academy of Sciences* **1993,** *90* (18), 8547-8551.

12. Heidmann, D. E.; Metcalf, M. A.; Kohen, R.; Hamblin, M. W., Four 5-hydroxytryptamine7 (5-HT_7) receptor isoforms in human and rat produced by alternative splicing: species differences due to altered intron-exon organization. *Journal of neurochemistry* **1997,** *68* (4), 1372-1381.

13. Krobert, K. A.; Levy, F. O., The human 5-HT_7 serotonin receptor splice variants: constitutive activity and inverse agonist effects. *British journal of pharmacology* **2002,** *135* (6), 1563-1571.

14. Eglen, R. M.; Jasper, J. R.; Chang, D. J.; Martin, G. R., The 5-HT_7 receptor: orphan found. *Trends in Pharmacological Sciences* **1997,** *18* (4), 104-107.

15. Lovenberg, T. W.; Baron, B. M.; de Lecea, L.; Miller, J. D.; Prosser, R. A.; Rea, M. A.; Foye, P. E.; Racke, M.; Slone, A. L.; Siegel, B. W., A novel adenylyl cyclase-activating serotonin receptor (5-HT_7) implicated in the regulation of mammalian circadian rhythms. *Neuron* **1993,** *11* (3), 449-458.

16. Paterson, L. M.; Tyacke, R. J.; Nutt, D. J.; Knudsen, G. M., Measuring endogenous 5-HT release by emission tomography: promises and pitfalls. *Journal of Cerebral Blood Flow & Metabolism* **2010,** *30* (10), 1682-1706.

17. Thomas, D. R.; Atkinson, P. J.; Hastie, P. G.; Roberts, J. C.; Middlemiss, D. N.; Price, G. W., [^{3}H]-SB-269970 radiolabels 5-HT_7 receptors in rodent, pig and primate brain tissues. *Neuropharmacology* **2002,** *42* (1), 74-81.

18. Kumar, J. S. D.; Mann, J. J., PET Tracers for Serotonin Receptors and Their Applications. *Central nervous system agents in medicinal chemistry* **2014,** *14* (2), 96-112.

19. Gustafson, E. L.; Durkin, M. M.; Bard, J. A.; Zgombick, J.; Branchek, T. A., A receptor autoradiographic and in situ hybridization analysis of the distribution of the 5-HT_7 receptor in rat brain. *British Journal of Pharmacology l* **1996,** *117* (4), 657-666.

20. Thomas, D. R.; Atkinson, P. J.; Ho, M.; Bromidge, S. M.; Lovell, P. J.; Villani, A. J.; Hagan, J. J.; Middlemiss, D. N.; Price, G. W., [^{3}H]-SB-269970 – A selective antagonist radioligand for 5-HT_7 receptors. *British Journal of Pharmacology* **2000,** *130* (2), 409-417.

21. Horisawa, T.; Ishiyama, T.; Ono, M.; Ishibashi, T.; Taiji, M., Binding of lurasidone, a novel antipsychotic, to rat 5-HT_7 receptor: analysis by [^{3}H] SB-269970 autoradiography. *Progress in Neuro-Psychopharmacology and Biological Psychiatry* **2013,** *40*, 132-137.

22. Hansen, H. D.; Herth, M. M.; Ettrup, A.; Andersen, V. L.; Lehel, S.; Dyssegaard, A.; Kristensen, J. L.; Knudsen, G. M., Radiosynthesis and in vivo evaluation of novel radioligands for PET imaging of cerebral 5-HT_7 receptors. *J Nucl Med* **2014,** *55* (4), 640-646.

23. Hansen, H. D.; Constantinescu, C. C.; Barret, O.; Herth, M. M.; Magnussen, J. H.; Lehel, S.; Dyssegaard, A.; Colomb, J.; Billard, T.; Zimmer, L., Evaluation of [^{18}F] 2FP3 in pigs and non-human primates. *Journal of Labelled Compounds and Radiopharmaceuticals* **2018**, 1-9.

24. Varnäs, K.; Thomas, D. R.; Tupala, E.; Tiihonen, J.; Hall, H., Distribution of 5-HT_7 receptors in the human brain: a preliminary autoradiographic study using [^{3}H] SB-269970. *Neuroscience letters* **2004,** *367* (3), 313-316.

25. Sprouse, J.; Reynolds, L.; Li, X.; Braselton, J.; Schmidt, A., 8-OH-DPAT as a 5-HT_7 agonist: phase shifts of the circadian biological clock through increases in cAMP production. *Neuropharmacology* **2004,** *46* (1), 52-62.

26. Guscott, M.; Bristow, L.; Hadingham, K.; Rosahl, T.; Beer, M.; Stanton, J.; Bromidge, F.; Owens, A.; Huscroft, I.; Myers, J., Genetic knockout and pharmacological blockade studies of the 5-HT_7 receptor suggest therapeutic potential in depression. *Neuropharmacology* **2005,** *48* (4), 492-502.

27. Gardani, M.; Biello, S., The effects of photic and nonphotic stimuli in the 5-HT_7 receptor knockout mouse. *Neuroscience* **2008,** *152* (1), 245-253.

28. Hagan, J. J.; Price, G. W.; Jeffrey, P.; Deeks, N. J.; Stean, T.; Piper, D.; Smith, M. I.; Upton, N.; Medhurst, A. D.; Middlemiss, D. N.; Riley, G. J.; Lovell, P. J.; Bromidge, S. M.; Thomas, D. R., Characterization of SB-269970-A, a selective 5-HT_7 receptor antagonist. *British Journal of Pharmacology* **2000,** *130* (3), 539-548.

29. Guscott, M.; Egan, E.; Cook, G.; Stanton, J.; Beer, M.; Rosahl, T.; Hartmann, S.; Kulagowski, J.; McAllister, G.; Fone, K., The hypothermic effect of 5-CT in mice is mediated through the 5-HT_7 receptor. *Neuropharmacology* **2003,** *44* (8), 1031-1037.

30. Hedlund, P. B.; Kelly, L.; Mazur, C.; Lovenberg, T.; Sutcliffe, J. G.; Bonaventure, P., 8-OH-DPAT acts on both 5-$HT1_A$ and 5-HT_7 receptors to induce hypothermia in rodents. *European journal of pharmacology* **2004,** *487* (1-3), 125-132.

31. Faure, C.; Mnie-Filali, O.; Scarna, H.; Debonnel, G.; Haddjeri, N., Effects of the 5-HT_7 receptor antagonist SB-269970 on rat hormonal and temperature responses to the 5-$HT_{1A/7}$ receptor agonist 8-OH-DPAT. *Neuroscience letters* **2006,** *404* (1-2), 122-126.

32. Gasbarri, A.; Cifariello, A.; Pompili, A.; Meneses, A., Effect of 5-HT_7 antagonist SB-269970 in the modulation of working and reference memory in the rat. *Behavioural brain research* **2008,** *195* (1), 164-170.

33. Wesołowska, A.; Nikiforuk, A.; Stachowicz, K.; Tatarczyńska, E., Effect of the selective 5-HT_7 receptor antagonist SB 269970 in animal models of anxiety and depression. *Neuropharmacology* **2006,** *51* (3), 578-586.

34. Hedlund, P.; Danielson, P.; Thomas, E.; Slanina, K.; Carson, M.; Sutcliffe, J., No hypothermic response to serotonin in 5-HT_7 receptor knockout mice. *Proceedings of the National Academy of Sciences* **2003,** *100* (3), 1375-1380.

35. Hedlund, P. B.; Sutcliffe, J. G., Functional, molecular and pharmacological advances in 5-HT_7 receptor research. *Trends in Pharmacological Sciences* **2004,** *25* (9), 481-486.

36. Hauser, S. R.; Hedlund, P. B.; Roberts, A. J.; Sari, Y.; Bell, R. L.; Engleman, E. A., The 5-HT_7 receptor as a potential target for treating drug and alcohol abuse. *Frontiers in neuroscience* **2015,** *8*, 448.

37. Mnie-Filali, O.; Lambas-Señas, L.; Scarna, H.; Haddjeri, N., Therapeutic potential of 5-HT_7 receptors in mood disorders. *Current drug targets* **2009,** *10* (11), 1109-1117.

38. Mnie-Filali, O.; Lambás-Señas, L.; Zimmer, L.; Haddjeri, N., 5-HT_7 receptor antagonists as a new class of antidepressants. *Drug News Perspect* **2007,** *20* (10), 613-618.

39. Gustavsson, A.; Svensson, M.; Jacobi, F.; Allgulander, C.; Alonso, J.; Beghi, E.; Dodel, R.; Ekman, M.; Faravelli, C.; Fratiglioni, L.; Gannon, B.; Jones, D. H.; Jennum, P.; Jordanova, A.; Jönsson, L.; Karampampa, K.; Knapp, M.; Kobelt, G.; Kurth, T.; Lieb, R.; Linde, M.; Ljungcrantz, C.; Maercker, A.; Melin, B.; Moscarelli, M.; Musayev, A.; Norwood, F.; Preisig, M.; Pugliatti, M.; Rehm, J.; Salvador-Carulla, L.; Schlehofer, B.; Simon, R.; Steinhausen, H.-C.; Stovner, L. J.; Vallat, J.-M.; den Bergh, P. V.; van Os, J.; Vos, P.; Xu, W.; Wittchen, H.-U.; Jönsson, B.; Olesen, J., Cost of disorders of the brain in Europe 2010. *European Neuropsychopharmacology* **2011,** *21* (10), 718-779.

40. Miller, P. W.; Long, N. J.; Vilar, R.; Gee, A. D., Synthesis of ^{11}C, ^{18}F, ^{15}O, and ^{13}N radiolabels for positron emission tomography. *Angewandte Chemie International Edition* **2008,** *47* (47), 8998-9033.

41. Piel, M.; Vernaleken, I.; Rösch, F., Positron Emission Tomography in CNS Drug Discovery and Drug Monitoring. *Journal of Medicinal Chemistry* **2014,** *57* (22), 9232-9258.

42. Kristensen, J. L.; Herth, M. M., Textbook of Drug Design and Discovery: In vivo imaging in drug discovery. In *Textbook of Drug Design and Discovery*, CRC Press: 2017.

43. Guo, Q.; Brady, M.; Gunn, R. N., A biomathematical modeling approach to central nervous system radioligand discovery and development. *The Journal of Nuclear Medicine* **2009,** *50* (10), 1715.

44. Zhang, L.; Villalobos, A.; Beck, E. M.; Bocan, T.; Chappie, T. A.; Chen, L.; Grimwood, S.; Heck, S. D.; Helal, C. J.; Hou, X., Design and selection parameters to accelerate the discovery of novel central nervous system positron emission tomography (PET) ligands and their application in the development of a novel phosphodiesterase 2A PET ligand. *Journal of medicinal chemistry* **2013,** *56* (11), 4568-4579.

45. Herth, M. M.; Leth-Petersen, S.; Lehel, S.; Hansen, M.; Knudsen, G. M.; Gillings, N.; Madsen, J.; Kristensen, J. L., Accelerating preclinical PET-screening: reductive amination with [^{11}C] methoxybenzaldehydes. *RSC Advances* **2014,** *4* (41), 21347-21350.

46. Van de Bittner, G. C.; Ricq, E. L.; Hooker, J. M., A philosophy for CNS radiotracer design. *Accounts of chemical research* **2014,** *47* (10), 3127-3134.

47. Herth M. M., K. G. M., PET Imaging of the 5-HT2$_A$ Receptor System: A Tool to Study the Receptor's In Vivo Brain Function. 5-HT$_{2A}$ Receptors in the Central Nervous System. In *5-HT2$_A$ Receptors in the Central Nervous System*, Guiard B., D. G. G., Ed. Humana Press, Cham: **2018**; 32, 85-134.

48. Fridén, M.; Wennerberg, M.; Antonsson, M.; Sandberg-Ställ, M.; Farde, L.; Schou, M., Identification of positron emission tomography (PET) tracer candidates by prediction of the target-bound fraction in the brain. *EJNMMI research* **2014,** *4* (1), 50.

49. Devane, W. A.; Dysarz, F. r.; Johnson, M. R.; Melvin, L. S.; Howlett, A. C., Determination and characterization of a cannabinoid receptor in rat brain. *Molecular pharmacology* **1988,** *34* (5), 605-613.

50. Wernick, M. N.; Aarsvold, J. N., *Emission tomography: the fundamentals of PET and SPECT*. Elsevier: 2004.

51. López-Giménez, J. F.; Vilaró, M. T.; Palacios, J. M.; Mengod, G., [^{3}H] MDL 100,907 labels 5-HT2A serotonin receptors selectively in primate brain. *Neuropharmacology* **1998,** *37* (9), 1147-1158.

52. Madras, B. K.; Gracz, L. M.; Fahey, M. A.; Elmaleh, D.; Meltzer, P. C.; Liang, A. Y.; Stopa, E. G.; Babich, J.; Fischman, A. J., Altropane, a SPECT or PET imaging probe for

dopamine neurons: III. Human dopamine transporter in postmortem normal and Parkinson's diseased brain. *Synapse* **1998,** *29* (2), 116-127.

53. Kristiansen, H.; Elfving, B.; Plenge, P.; Pinborg, L. H.; Gillings, N.; Knudsen, G. M., Binding characteristics of the 5-$HT2_A$ receptor antagonists altanserin and MDL 100907. *Synapse* **2005,** *58* (4), 249-257.

54. Schou, M.; Steiger, C.; Varrone, A.; Guilloteau, D.; Halldin, C., Synthesis, radiolabeling and preliminary in vivo evaluation of [^{18}F] FE-PE2I, a new probe for the dopamine transporter. *Bioorganic & medicinal chemistry letters* **2009,** *19* (16), 4843-4845.

55. Hall, H.; Farde, L.; Halldin, C.; Lundkvist, C.; Sedvall, G., Autoradiographic localization of 5-HT2A receptors in the human brain using [^{3}H] M100907 and [^{11}C] M100907. *Synapse* **2000,** *38* (4), 421-431.

56. Tang, S. W.; Helmeste, D. M.; Fang, H.; Li, M.; Vu, R.; Bunney Jr, W.; Potkin, S.; Jones, E. G., Differential labeling of dopamine and sigma sites by [^{3}H] nemonapride and [^{3}H] raclopride in postmortem human brains. *Brain research* **1997,** *765* (1), 7-12.

57. Rieck, R. W.; Ansari, M.; Whetsell Jr, W. O.; Deutch, A. Y.; Kessler, R. M., Distribution of dopamine D 2-like receptors in the human thalamus: autoradiographic and PET studies. *Neuropsychopharmacology* **2004,** *29* (2), 362.

58. Siessmeier, T.; Zhou, Y.; Buchholz, H.-G.; Landvogt, C.; Vernaleken, I.; Piel, M.; Schirrmacher, R.; Rösch, F.; Schreckenberger, M.; Wong, D. F., Parametric mapping of binding in human brain of D2 receptor ligands of different affinities. *Journal of Nuclear Medicine* **2005,** *46* (6), 964-972.

59. Waterhouse, R. N., Determination of lipophilicity and its use as a predictor of blood–brain barrier penetration of molecular imaging agents. *Molecular Imaging & Biology* **2003,** *5* (6), 376-389.

60. Vraka, C.; Nics, L.; Wagner, K.-H.; Hacker, M.; Wadsak, W.; Mitterhauser, M., LogP, a yesterday's value? *Nuclear Medicine and Biology* **2017,** *50*, 1-10.

61. Ettrup, A.; Hansen, M.; Santini, M. A.; Paine, J.; Gillings, N.; Palner, M.; Lehel, S.; Herth, M. M.; Madsen, J.; Kristensen, J.; Begtrup, M.; Knudsen, G. M., Radiosynthesis and in vivo evaluation of a series of substituted ^{11}C-phenethylamines as 5-HT_{2A} agonist PET tracers. *Eur J Nucl Med Mol Imaging* **2011,** *38* (4), 681-693.

62. Patel, S.; Hamill, T.; Hostetler, E.; Burns, H. D.; Gibson, R. E., An *In Vitro* Assay for Predicting Successful Imaging Radiotracers. *Molecular Imaging & Biology* **2003,** *5* (2), 65-71.

63. Bonaventure, P.; Nepomuceno, D.; Hein, L.; Sutcliffe, J.; Lovenberg, T.; Hedlund, P., Radioligand binding analysis of knockout mice reveals 5-hydroxytryptamine7 receptor distribution and uncovers 8-hydroxy-2-(di-n-propylamino) tetralin interaction with α2 adrenergic receptors. *Neuroscience* **2004,** *124* (4), 901-911.

64. Hall, H.; Lundkvist, C.; Halldin, C.; Farde, L.; Pike, V.; McCarron, J.; Fletcher, A.; Cliffe, I.; Barf, T.; Wikström, H., Autoradiographic localization of 5-HT_{1A} receptors in the post-mortem human brain using [^{3}H] WAY-100635 and [^{11}C] way-100635. *Brain research* **1997,** *745* (1-2), 96-108.

65. Herth, M. M.; Volk, B.; Pallagi, K.; Kofoed Bech, L.; Antoni, F. A.; Knudsen, G. M.; Kristensen, J. L., Synthesis and *in vitro* evaluation of oxindole derivatives as potential radioligands for 5-HT_7 receptor imaging with PET. *ACS Chemical Neuroscience* **2012,** *3* (12), 1002-7.

66. Syvänen, S.; Lindhe, Ö.; Palner, M.; Kornum, B. R.; Rahman, O.; Långström, B.; Knudsen, G. M.; Hammarlund-Udenaes, M., Species differences in blood-brain barrier transport of three positron emission tomography radioligands with emphasis on P-glycoprotein transport. *Drug metabolism and disposition* **2009,** *37* (3), 635-643.

67. Clark, D. E., In silico prediction of blood–brain barrier permeation. *Drug discovery today* **2003,** *8* (20), 927-933.

68. Colomb, J.; Becker, G.; Forcellini, E.; Meyer, S.; Buisson, L.; Zimmer, L.; Billard, T., Synthesis and pharmacological evaluation of a new series of radiolabeled ligands for 5-HT_7 receptor PET neuroimaging. *Nuclear Medicine and Biology* **2014,** *41* (4), 330-337.

69. Kelder, J.; Grootenhuis, P. D.; Bayada, D. M.; Delbressine, L. P.; Ploemen, J.-P., Polar molecular surface as a dominating determinant for oral absorption and brain penetration of drugs. *Pharmaceutical research* **1999,** *16* (10), 1514-1519.

70. Norinder, U.; Haeberlein, M., Computational approaches to the prediction of the blood–brain distribution. *Advanced drug delivery reviews* **2002,** *54* (3), 291-313.

71. Herth, M. M.; Knudsen, G. M., Current radiosynthesis strategies for 5-HT2A receptor PET tracers. *Journal of Labelled Compounds and Radiopharmaceuticals* **2015,** *58* (7), 265-273.

72. Innis, R. B.; Cunningham, V. J.; Delforge, J.; Fujita, M.; Gjedde, A.; Gunn, R. N.; Holden, J.; Houle, S.; Huang, S.-C.; Ichise, M., Consensus nomenclature for in vivo imaging of reversibly binding radioligands. *Journal of Cerebral Blood Flow & Metabolism* **2007,** *27* (9), 1533-1539.

73. Hume, S. P.; Gunn, R. N.; Jones, T., Pharmacological constraints associated with positron emission tomographic scanning of small laboratory animals. *European journal of nuclear medicine* **1998,** *25* (2), 173-176.

74. Laruelle, M.; Slifstein, M.; Huang, Y., Relationships between radiotracer properties and image quality in molecular imaging of the brain with positron emission tomography. *Molecular Imaging & Biology* **2003,** *5* (6), 363-375.

75. Pike, V. W., PET radiotracers: crossing the blood–brain barrier and surviving metabolism. *Trends in pharmacological sciences* **2009,** *30* (8), 431-440.

76. Andries, J.; Lemoine, L.; Le Bars, D.; Zimmer, L.; Billard, T., Synthesis and biological evaluation of potential 5-HT_7 receptor PET radiotracers. *European Journal of Medicinal Chemistry* **2011,** *46* (8), 3455-3461.

77. Andries, J.; Lemoine, L.; Mouchel-Blaisot, A.; Tang, S.; Verdurand, M.; Le Bars, D.; Zimmer, L.; Billard, T., Looking for a 5-HT_7 radiotracer for positron emission tomography. *Bioorg Med Chem Lett* **2010,** *20* (12), 3730-3.

78. Hansen, H. D.; Andersen, V. L.; Lehel, S.; Magnussen, J. H.; Dyssegaard, A.; Stroth, N.; Kristensen, J. L.; Knudsen, G. M.; Herth, M. M., Labeling and preliminary in vivo evaluation of the 5-HT_7 receptor selective agonist [(^{11})C]E-55888. *Bioorg Med Chem Lett* **2015,** *25* (9), 1901-4.

79. Hansen, H. D.; Lacivita, E.; Di Pilato, P.; Herth, M. M.; Lehel, S.; Ettrup, A.; Andersen, V. L.; Dyssegaard, A.; De Giorgio, P.; Perrone, R.; Berardi, F.; Colabufo, N. A.; Niso, M.; Knudsen, G. M.; Leopoldo, M., Synthesis, radiolabeling and in vivo evaluation of [^{11}C](R)-1-[4-[2-(4-methoxyphenyl)phenyl]piperazin-1-yl]-3-(2-pyrazinyloxy)-2-p ropanol, a potential PET radioligand for the 5-HT(7) receptor. *Eur J Med Chem* **2014,** *79*, 152-63.

80. Herth, M. M.; Andersen, V. L.; Hansen, H. D.; Stroth, N.; Volk, B.; Lehel, S.; Dyssegaard, A.; Ettrup, A.; Svenningsson, P.; Knudsen, G. M.; Kristensen, J. L., Evaluation of 3-Ethyl-3-(phenylpiperazinylbutyl)oxindoles as PET Ligands for the Serotonin 5-HT(7) Receptor: Synthesis, Pharmacology, Radiolabeling, and in Vivo Brain Imaging in Pigs. *Journal of medicinal chemistry* **2015,** *58* (8), 3631-6.

81. Herth, M. M.; Hansen, H. D.; Ettrup, A.; Dyssegaard, A.; Lehel, S.; Kristensen, J.; Knudsen, G. M., Synthesis and evaluation of [^{11}C]Cimbi-806 as a potential PET ligand for 5-HT_7 receptor imaging. *Bioorganic & medicinal chemistry* **2012,** *20* (14), 4574-81.

82. Hogendorf, A. S.; Hogendorf, A.; Kurczab, R.; Satala, G.; Lenda, T.; Walczak, M.; Latacz, G.; Handzlik, J.; Kiec-Kononowicz, K.; Wieronska, J. M.; Wozniak, M.; Cieslik, P.;

Bugno, R.; Staron, J.; Bojarski, A. J., Low-basicity 5-HT_7 Receptor Agonists Synthesized Using the van Leusen Multicomponent Protocol. *Scientific Reports* **2017,** *7* (1), 1444.

83. Lacivita, E.; Niso, M.; Hansen, H. D.; Di Pilato, P.; Herth, M. M.; Lehel, S.; Ettrup, A.; Montenegro, L.; Perrone, R.; Berardi, F.; Colabufo, N. A.; Leopoldo, M.; Knudsen, G. M., Design, synthesis, radiolabeling and in vivo evaluation of potential positron emission tomography (PET) radioligands for brain imaging of the 5-HT_7receptor. *Bioorganic & Medicinal Chemistry* **2014,** *22* (5), 1736-50.

84. Lacivita, E.; Patarnello, D.; Stroth, N.; Caroli, A.; Niso, M.; Contino, M.; De Giorgio, P.; Di Pilato, P.; Colabufo, N. A.; Berardi, F., Investigations on the 1-(2-biphenyl) piperazine motif: identification of new potent and selective ligands for the serotonin 7 (5-HT_7) receptor with agonist or antagonist action *in vitro* or ex vivo. *Journal of medicinal chemistry* **2012,** *55* (14), 6375-6380.

85. Lemoine, L.; Andries, J.; Le Bars, D.; Billard, T.; Zimmer, L., Comparison of 4 radiolabeled antagonists for serotonin 5-HT_7 receptor neuroimaging: toward the first PET radiotracer. *Journal of NuclearMedicine* **2011,** *52* (11), 1811-1818.

86. Leopoldo, M.; Lacivita, E.; De Giorgio, P.; Fracasso, C.; Guzzetti, S.; Caccia, S.; Contino, M.; Colabufo, N. A.; Berardi, F.; Perrone, R., Structural Modifications of N-(1,2,3,4-Tetrahydronaphthalen-1-yl)-4-Aryl-1-piperazinehexanamides: Influence on Lipophilicity and 5-HT_7 Receptor Activity. Part III. *Journal of Medicinal Chemistry* **2008,** *51* (18), 5813-5822.

87. Lovell, P. J.; Bromidge, S. M.; Dabbs, S.; Duckworth, D. M.; Forbes, I. T.; Jennings, A. J.; King, F. D.; Middlemiss, D. N.; Rahman, S. K.; Saunders, D. V., A novel, potent, and selective 5-HT_7 antagonist:(R)-3-(2-(2-(4-methylpiperidin-1-yl) ethyl) pyrrolidine-1-sulfonyl) phenol (SB-269970). *Journal of medicinal chemistry* **2000,** *43* (3), 342-345.

88. Volk, B.; Barkóczy, J.; Hegedus, E.; Udvari, S.; Gacsályi, I.; Mezei, T.; Pallagi, K.; Kompagne, H.; Lévay, G.; Egyed, A., (Phenylpiperazinyl-butyl) oxindoles as selective 5-HT_7 receptor antagonists. *Journal of medicinal chemistry* **2008,** *51* (8), 2522-2532.

89. Zhang, M. R.; Haradahira, T.; Maeda, J.; Okauchi, T.; Kida, T.; Obayashi, S.; Suzuki, K.; Suhara, T., Synthesis and preliminary PET study of the 5-HT_7 receptor antagonist [^{11}C] DR4446. *Journal of Labelled Compounds and Radiopharmaceuticals: The Official Journal of the International Isotope Society* **2002,** *45* (10), 857-866.

90. Paillet-Loilier, M.; Fabis, F.; Lepailleur, A.; Bureau, R.; Butt-Gueulle, S.; Dauphin, F.; Lesnard, A.; Delarue, C.; Vaudry, H.; Rault, S., Novel aminoethylbiphenyls as 5-HT 7 receptor ligands. *Bioorganic & medicinal chemistry letters* **2007,** *17* (11), 3018-3022.

91. Brenchat, A.; Romero, L.; García, M.; Pujol, M.; Burgueño, J.; Torrens, A.; Hamon, M.; Baeyens, J. M.; Buschmann, H.; Zamanillo, D., 5-HT_7 receptor activation inhibits mechanical hypersensitivity secondary to capsaicin sensitization in mice. *Pain* **2009,** *141* (3), 239-247.

92. Elina Tampio L'Estrade, Mengfei. Xiong., Vladimir Shalgunov, Fraser G. Edgar, Balázs Volk, Simone L. Baerentzen, Mikael Palner, Maria Erlandsson, Tomas Ohlsson, Gitte M. Knudsen and Matthias M. Herth, Development and Evaluation of the Two Potential 5-HT_7 Receptor PET Tracers: [^{18}F]ENL09 and [^{18}F]ENL10 *Submitted Manuscript* **2019**.

93. Elina Tampio L'Estrade, S. L., Ida Nymann Petersen, Fraser G. Edgar, Balázs Volk, Maria Erlandsson, Tomas Ohlsson, Gitte M. Knudsen and Matthias M. Herth, Fragment-based Labelling Using Condensation Reactions – A Possibility to Increase Throughput in Preclinical PET. *Submitted Manuscript* **2019**.

94. Keller, S. H.; L'Estrade, E. N.; Dall, B.; Palner, M.; Herth, M. In *Quantification accuracy of a new HRRT high throughput rat hotel using transmission-based attenuation correction: A phantom study*, Nuclear Science Symposium, Medical Imaging Conference and Room-Temperature Semiconductor Detector Workshop (NSS/MIC/RTSD), 2016, IEEE: **2016**; pp 1-3.

95. L'Estrade, E. N.; Palner, M.; Petersen, I. N.; Keller, S. H.; Lehel, S.; Dall, B.; Kristensen, J. L.; Erlandsson, M.; Olsson, T.; Knudsen, G. M.; Herth, M. M., Accelerating PET tracer development: Establishment of a combinatorial-like, high-throughput development approach using condensation reactions and high-throughput screening. *European Journal of Nuclear Medicine and Molecular Imaging* **2016,** *43*, 455-456.

96. Kallem, R.; P Kulkarni, C.; Patel, D.; Thakur, M.; Sinz, M.; P Singh, S.; Shahe Mahammad, S.; Mandlekar, S., A simplified protocol employing elacridar in rodents: a screening model in drug discovery to assess P-gp mediated efflux at the blood brain barrier. *Drug metabolism letters* **2012,** *6* (2), 134-144.

97. Domagk, G., Ein beitrag zur chemotherapie der bakteriellen infektionen. *DMW-Deutsche Medizinische Wochenschrift* **1935,** *61* (07), 250-253.

98. Badarau, E.; Suzenet, F.; Bojarski, A. J.; Fînaru, A.-L.; Guillaumet, G., Benzimidazolone-based serotonin 5-HT 1A or 5-HT 7 R ligands: synthesis and biological evaluation. *Bioorganic & medicinal chemistry letters* **2009,** *19* (6), 1600-1603.

99. Laćan, G.; Plenevaux, A.; Rubins, D. J.; Way, B. M.; Defraiteur, C.; Lemaire, C.; Aerts, J.; Luxen, A.; Cherry, S. R.; Melega, W. P., Cyclosporine, a P-glycoprotein modulator,

increases [^{18} F] MPPF uptake in rat brain and peripheral tissues: microPET and ex vivo studies. *European Journal of Nuclear Medicine and Molecular Imaging* **2008,** *35* (12), 2256-2266.

100. Elina T. L'Estrade, V. S., Fraser G. Edgar, Martin G. Strebl-Bantillo, Mengfei Xiong, François Crestey, Ramesh Neelamegam, Agnete Dyssegaard, Szabolcs Lehel, Maria Erlandsson, Tomas Ohlsson, Jacob M. Hooker, Gitte M. Knudsen, Matthias M. Herth, Hanne D. Hansen, Radiosynthesis and preclinical evaluation of [^{11}C]Cimbi-701 – Towards the imaging of cerebral 5-HT$_7$ receptors. *Manuscript in preparation.* **2019**.

101. Elina T. L'Estrade, F. G. E., Mengfei Xiong, Vladimir Shalgunov, Simone L. Baerentzen, Maria Erlandsson, Tomas G. Ohlsson, Mikael Palner, Gitte M. Knudsen, Matthias M. Herth, Synthesis, Radiolabeling, *In vitro* and *In vivo* Evaluation of [^{18}F]ENL30 – A Potential PET Radiotracer for the 5-HT$_7$ Receptor *Submitted Manuscript* **2019**.

102. Thomas, D. R.; Gittins, S. A.; Collin, L. L.; Middlemiss, D. N.; Riley, G.; Hagan, J.; Gloger, I.; Ellis, C. E.; Forbes, I. T.; Brown, A. M., Functional characterisation of the human cloned 5-HT$_7$ receptor (long form); antagonist profile of SB-258719. *British journal of pharmacology* **1998,** *124* (6), 1300-1306.

103. Fowler, J. S.; Ding, Y.-S.; Logan, J.; MacGregor, R. R.; Shea, C.; Garza, V.; Gimi, R.; Volkow, N. D.; Wang, G.-J.; Schlyer, D., Species differences in [^{11}C] clorgyline binding in brain. *Nuclear medicine and biology* **2001,** *28* (7), 779-785.

104. Kubo, Y.; Ohtsuki, S.; Uchida, Y.; Terasaki, T., Quantitative determination of luminal and abluminal membrane distributions of transporters in porcine brain capillaries by plasma membrane fractionation and quantitative targeted proteomics. *Journal of Pharmaceutical Sciences* **2015,** *104* (9), 3060-3068.

105. Herth, M.; Hansen, H.; Anders, E.; Lehel, S.; Kristensen, J.; Billard, T.; Zimmer, L.; Knudsen, G., Development of a novel ^{11}C-labelled SB-269970 derivative for imaging the cerebral 5-HT$_7$ receptors. *Journal of Nuclear Medicine* **2014,** *55* (supplement 1), 1814-1814.

106. Herth, M. M.; Debus, F.; Piel, M.; Palner, M.; Knudsen, G. M.; Luddens, H.; Rosch, F., Total synthesis and evaluation of [^{18}F]MHMZ. *Bioorganic & medicinal chemistry letters* **2008,** *18* (4), 1515-1519.

107. Edem, P. E.; Steen, E. J. L.; Kjær, A.; Herth, M. M., Chapter 2 - Fluorine-18 Radiolabeling Strategies—Advantages and Disadvantages of Currently Applied Labeling Methods. *Late-Stage Fluorination of Bioactive Molecules and Biologically-Relevant Substrates*, Postigo, A., Ed. Elsevier: **2019**; pp 29-103.

108. Van Der Born, D.; Pees, A.; Poot, A. J.; Orru, R. V.; Windhorst, A. D.; Vugts, D. J., Fluorine-18 labelled building blocks for PET tracer synthesis. *Chemical Society Reviews* **2017,** *46* (15), 4709-4773.

109. Bergström, M.; Westerberg, G.; Kihlberg, T.; Långström, B., Synthesis of some ^{11}C-labelled MAO-A inhibitors and their in vivo uptake kinetics in rhesus monkey brain. *Nuclear medicine and biology* **1997,** *24* (5), 381-388.

Chapter 4

Paper II

Radiolabeling and *in vivo* evaluation of [^{11}C]AGH-44 - a potential lead structure to develop a positron emission tomography radioligand for the 5-HT$_7$ receptor

---

Summary:

*Chapter 4 contains **Paper II**, in this paper we elucidate the potential of a new structure class of 5-HT$_7$ receptor agonists as potential PET tracer candidates. AGH-44 was successfully ^{11}C-labelled and evaluated in vivo in rats.*

Authors' contribution:

The reference and precursor synthesis was performed by A.S.H, A.H and A.B. The author established the radiosynthesis and the quality control of [^{11}C]AGH-44. The author also planned the in vivo evaluation and metabolism in rats. The animal experiments were performed as collaboration between the author, I.N.P, M.X and V.S. Biodistribution studies, image analysis and data interpretation was performed by the author, which also contributed considerably with writing the manuscript

.

Graphical Abstract

Radiolabeling and *in vivo* evaluation of [^{11}C]AGH-44 - a potential lead structure to develop a positron emission tomography radioligand for the 5-HT$_7$ receptor

Elina T. L'Estrade, Ida N. Petersen, Mengfei Xiong, Adam S. Hogendorf, Agata Hogendorf, Jesper L. Kristensen, Andreas Kjær, Andrzej J. Bojarski, Tomas Ohlsson, Maria Erlandsson, Gitte M. Knudsen, Matthias M. Herth.

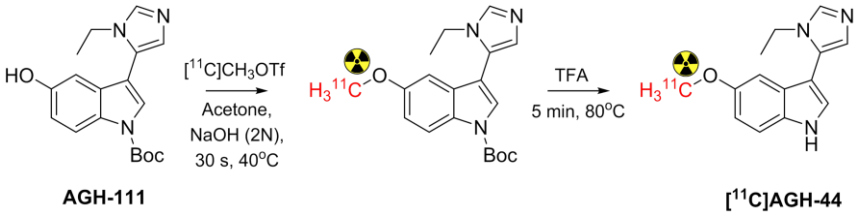

Radiolabeling and *in vivo* evaluation of [^{11}C]AGH-44 - a potential lead structure to develop a positron emission tomography radioligand for the 5-HT$_7$ receptor

Elina T. L'Estrade[a,b,c], Ida N. Petersen[d,e], Mengfei Xiong[a,b], Adam S. Hogendorf[f], Agata Hogendorf[f], Jesper L. Kristensen[b], Andreas Kjær[d,e], Andrzej J. Bojarski[f], Maria Erlandsson[c], Tomas Ohlsson[c], Gitte M. Knudsen[a], Matthias M. Herth[a,b,d,*]

[a] *Neurobiology Research Unit, Rigshospitalet, Blegdamsvej 9, 2100 Copenhagen, Denmark*

[b] *Department for Drug Design and Pharmacology, Faculty of Health and Medical Sciences, University of Copenhagen, Universitetesparken 2, 2100 Copenhagen, Denmark*

[c] *Radiation Physics, Nuclear Medicine Physics Unit, Skånes University Hospital, Barngatan 3, 222 42 Lund, Sweden.*

[d] *Department of Clinical Physiology, Nuclear Medicine and PET, University Hospital Copenhagen, Rigshospitalet Blegdamsvej 9, 2100 Copenhagen, Denmark*

[e] *Cluster for Molecular Imaging, Faculty of Health Science, University of Copenhagen, Blegdamsvej 3, 2200 Copenhagen, Denmark*

[f] *Institute of Pharmacology, Polish Academy of Sciences, 12 Smętna,31-343 Kraków, Poland.*

Keywords: AGH-44, 5-HT$_7$, PET, Carbon-11.

Abstract

AGH-44 has been described as a selective low-basicity serotonin 7 receptor (5-HT$_7$R) agonist. In this paper, we evaluate if AGH-44 can act as a lead structure to develop a 5-HT$_7$R selective positron emission tomography (PET) tracer. ^{11}C-labeling of AGH-44 succeeded in a two-step, one-pot procedure in good yields. Subsequent PET studies showed that [^{11}C]AGH-44 displays low blood-brain-barrier passage in Long-Evans rats. Moreover, [^{11}C]AGH-44 brain accumulation showed to be independent on permeability glycoprotein (P-gp) efflux inhibition. The results from the following biodistribution and metabolism studies could neither explain the observed low brain uptake. As such, we believe that this scaffold is not an optimal starting point to develop a 5-HT$_7$R selective PET tracer development.

Corresponding author. Tel.: +0045 93565414; fax: +0045 35 33 60 41; e-mail: matthias.herth@sund.ku.dk

The 5-HT_7 receptor (5-HT_7R) is the latest addition to the serotonin receptor family. It belongs to the Guanidine protein–coupled receptors (GPCR) and is involved in numerous central nervous system (CNS) disorders such as depression and schizophrenia.[1-2] For example, treatment with 5-HT_7R selective antagonists evokes antidepressant-like activity in commonly used depression models and similar effects could be observed in 5-HT_7R knock-out mice.[3-4]

Positron emission tomography (PET) is a routinely used non-invasive nuclear imaging modality that can be applied to study the physiology of CNS receptors *in vivo*. PET allows to accurately determine binding characteristics and parameters such as receptor specificity, binding kinetics and receptor occupancy.[5-6] Currently, there are no validated 5-HT_7R selective PET tracer available. In light of that, several attempts have been directed to develop such a tracer.[7-12] In this study, we complement these efforts. AGH-44 (3-(1-ethyl-1H-imidazol-5-yl)-5-(methoxy-^{11}C)-1H-indole) is a 5-HT_7R selective agonist that was identified and synthesized using a multicomponent reaction approach.[13] AGH-44 is metabolically stable in human liver microsomes, exhibits very low toxicity in HEK-293 and HepG2 cells and is water soluble. The affinity (30 nM) and selectivity profile of AGH-44 is inferior to evaluated 5-HT_7R PET tracers such as [^{11}C]Cimbi-717 or [^{18}F]2FP3 [Table 1].[8, 11] However, AGH-44 displays an interesting starting point from where one can develop structurally diverse PET ligands. Current applied tracers have not been validated in depth or tested in different animal models.[14]

Table 1: This table shows affinity (K_i in nM) and selectivity profile of AGH-44 compared to that of other evaluated 5-HT_7R PET tracers, including Cimbi-717 and 2FP3. n.d. = not determined

Name	Structure	5-HT_7	5-HT_{1A}	5-HT_{2A}
AGH-44	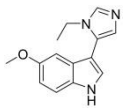	30	660	>10000
Cimbi-717	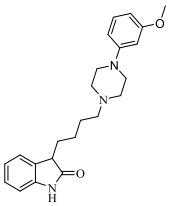	5.1	59	65
2FP3	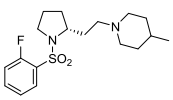	1.43 *(K_B)*	>10000	n.d.

An important feature to consider for a CNS tracer is the ability of the ligand to cross the blood-brain barrier (BBB) and AGH-44 has so far not been tested in this respect. However, its iodine analogue 3-(1-ethyl-1H-imidazol-5-yl)-5-iodo-1H-indole showed high BBB permeability and rapid brain uptake *in vivo*.[13] These characteristics encouraged us to radiolabel AGH-44 with carbon-11 (Scheme 1) and subsequently evaluate its *in vivo* behaviour. Our primary aim was to investigate if AGH-44 has sufficient blood-brain barrier permeability at tracer levels and thereby the molecule shows promise for modifications into derivatives with an improved selectivity profile.

Precursor and reference compound were synthesized as previously described.[13] In short, the synthesis succeeded applying the van Leusen reaction as a key step and using a multicomponent protocol (Scheme 2).

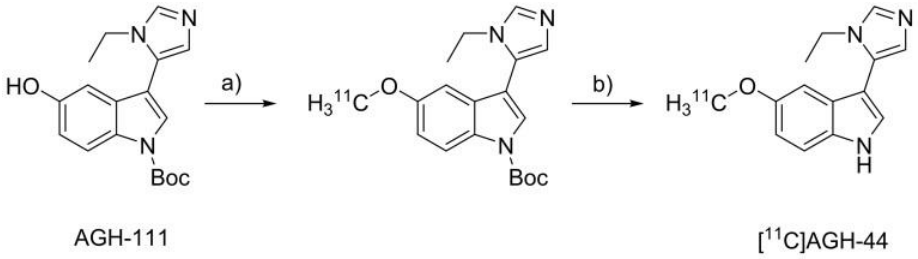

Scheme 1: Radiolabeling of [^{11}C]AGH-44. a) [^{11}C]CH_3OTf, Acetone, NaOH (2N), 40°C for 30 s. b) TFA, 80°C for 5 min.

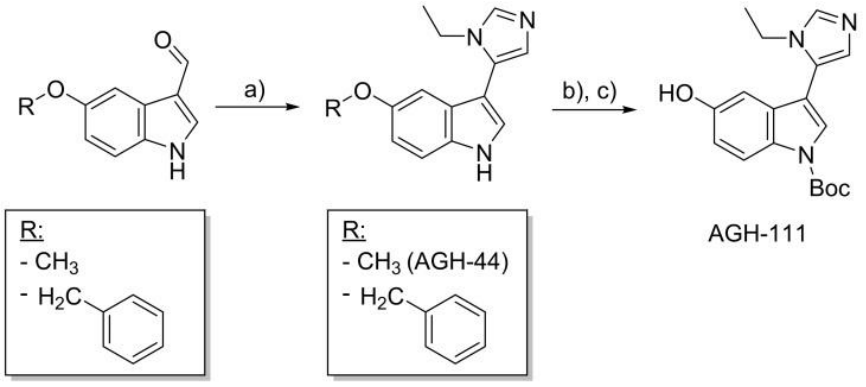

Scheme 2: Precursor (AGH-111) and reference (AGH-44) synthesis scheme. a) $EtNH_2$, TosMIC, K_2CO_3, MeOH; b) Boc_2O, DMAP, THF c) Pd/C, H_2, MeOH.

Radiolabelling of [^{11}C]AGH-44 succeeded using a 2-step, one-pot labelling procedure. In the first step, [^{11}C]MeOTf was reacted with the precursor (AGH-111) and in the second step, the protecting group was removed using acidic conditions.[15]

[^{11}C]AGH-44 could be isolated via semi-preparative HPLC-purification (1.6 ± 0.1 GBq of [^{11}C]AGH-44 in a >96% radiochemical purity, in a radiochemical non-decay corrected yield of 80–90% at the end of synthesis (comparing the detected radioactivity amounts on three consecutive

analytical HPLC runs) (Figure 1). Typical molar activities were in a range of 637 ± 50 GBq/μmol (time of injection) and the overall synthesis, purification, and formulation time was approximately 60 minutes. [15]

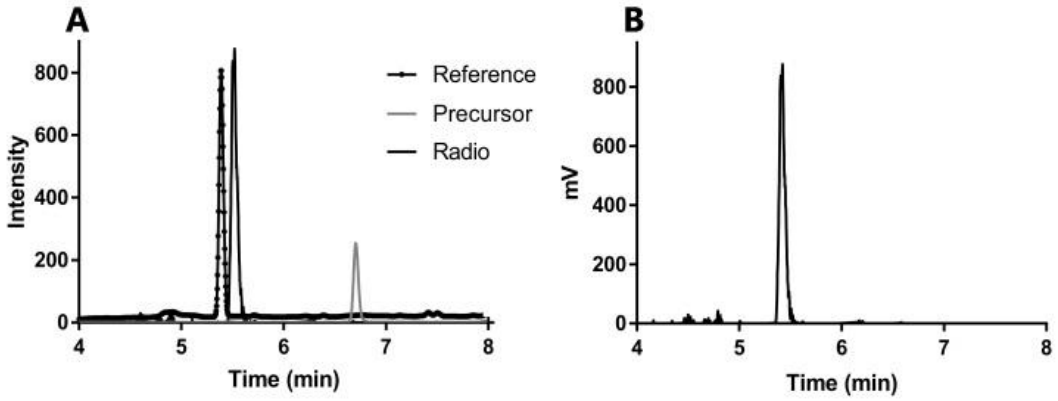

Figure 1: Analytical HPLC diagram. **A**) Combined chromatogram showing that AGH-44 (black line with dots) can be separated from the precursor AGH-111 (gray line). The radiotracer [^{11}C]AGH-44 (black line) is also shown. (**B**) Chromatogram of [^{11}C]AGH-44 showing > 95 % radiochemical purity.

Encouraged by these results, [^{11}C]AGH-44 was evaluated with respect to its *in vivo* binding characteristics.[16,17] PET studies were performed in a high-resolution research tomography (HRRT) scanner (Siemens AG, Munich, Germany) and female Long-Evans rats were used as research animals. A costume made 2x2 rat insert was applied to increase research through-put (Figure 2).

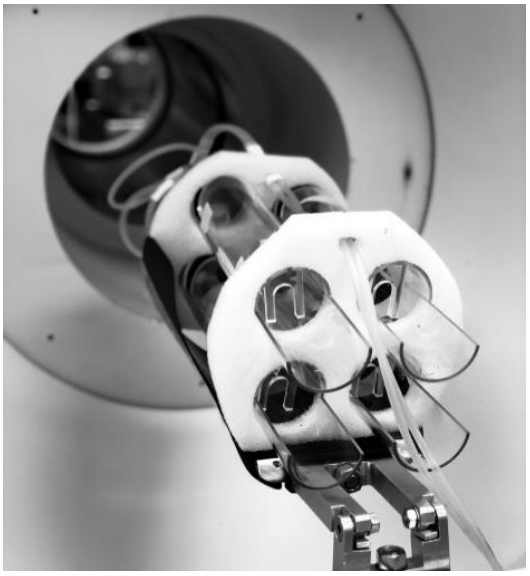

Figure 2: Costume made 2x2 rat insert to increase scanning through-put

Since no significant brain uptake was observed of [^{11}C]AGH-44 (Figure 3), it was questioned if [^{11}C]AGH-44 is a P-glycoprotein (P-gp) substrate. A relatively common phenomenon of PET

tracers evaluated in rodents.[18] Elacridar is a selective inhibitor of the P-gp efflux transporters at the BBB.[19] It was used to investigate if [^{11}C]AGH-44 brain uptake could be increased while inhibiting this efflux transporter.[16] We detected a small but not significant increase in brain uptake after pretreatment with Elacridar (Figure 3). We conducted biodistribution[17] and metabolism studies[20] to investigate if the observed behaviour could be attributed to these parameters. [^{11}C]AGH-44 is rapidly cleared from the blood and excreted by the urine, as seen in Table 2 (TACs can be found in the SI). The blood and plasma input function (Figure 4) show that already after 10 min the majority of the tracer is gone. Metabolism was determined. During the first 30 min, only parent compound could be detected. Only around 10% radioactive metabolites were seen on the HPLC chromatograms after 29 min (See supporting information). These results are not uncommon for CNS PET tracers and can as such not explain the observed low brain uptake.

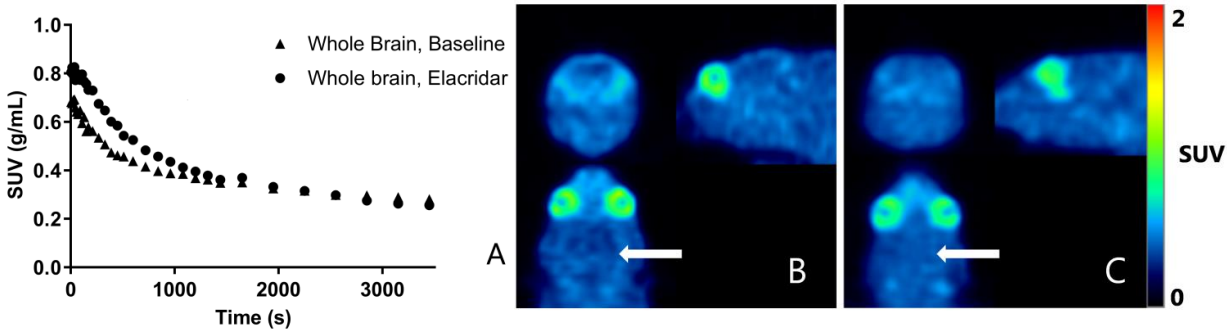

Figure 3: A) Time-activity curves for the whole rat brain with and without pretreatment with Elacridar (5 mg/kg). **B**) Coronal, sagittal (left to right up) and horizontal (down) summed PET images (baseline scan, 5–60 min) of [^{11}C]AGH-44 in the head of the rat, brain is indicated by white arrow in the horizontal image. **C**) Coronal, sagittal (left to right up) and horizontal (down) summed PET images (Elacridar (5 mg/kg) pretreatment scan, 5–60 min) of [^{11}C]AGH-44 the head of the rat, brain is indicated by white arrow in the horizontal image. **SUV**= standardized uptake value.

Table 2: The biodistribution of [^{11}C]AGH-44 in female Long Evans rats (% ID/mL)[a]

Organ	5 min	10 min	20 min	60 min
Heart and lungs	0.22 ± 0.01	0.20 ± 0.01	0.18 ± 0.01	0.13 ± 0.01
Liver	1.58 ± 0.14	1.54 ± 0.15	1.41 ± 0.18	1.24 ± 0.11
Kidneys	1.39 ± 0.19	1.35 ± 0.18	1.19 ± 0.14	0.94 ± 0.12
Bladder	0.35 ± 0.23	0.58 ± 0.40	1.04 ± 0.49	1.81 ± 0.34
Brain	0.24 ± 0.04	0.20 ± 0.03	0.16 ± 0.02	0.10 ± 0.002

[a] Data are presented as the mean ± S.D. of 3 animals at 5, 10, 20 and 60 min after intravenous injection of [^{11}C]AGH-44.

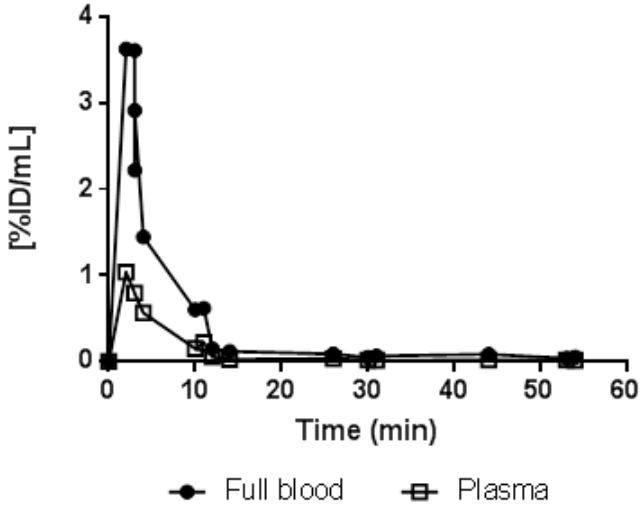

Figure 4: Whole blood and plasma functions achieved from venous blood samples, decay corrected (d.c) and calculated to percentage injected dose per mL (%ID/mL).

In conclusion, [^{11}C]AGH-44 could successfully be labelled with carbon-11. We subsequently showed by PET imaging that [^{11}C]AGH-44 does not cross the BBB to any major extent. Inhibition of P-gp did not satisfactory increase brain accumulation. As such, [^{11}C]AGH-44 is not a strong substrate of P-gp. Our findings do not provide much support for AGH-44 being an ideal starting structure for development of a PET tracer for the 5-HT$_7$R.

Acknowledgments

The authors wish to thank the staff at the PET and Cyclotron unit for expert technical assistance.

References and notes

1. Matthys, A.; Haegeman, G.; Van Craenenbroeck, K.; Vanhoenacker, P. *Mol Neurobiol* **2011,** *43* (3), 228-53.
2. Ruat, M.; Traiffort, E.; Leurs, R.; Tardivel-Lacombe, J.; Diaz, J.; Arrang, J.-M.; Schwartz, J.-C. *Proc Natl Acad Sci USA* **1993,** *90* (18), 8547-8551.
3. Guscott, M.; Bristow, L. J.; Hadingham, K.; Rosahl, T. W.; Beer, M. S.; Stanton, J. A.; Bromidge, F.; Owens, A. P.; Huscroft, I.; Myers, J.; Rupniak, N. M.; Patel, S.; Whiting, P. J.; Hutson, P. H.; Fone, K. C.; Biello, S. M.; Kulagowski, J. J.; McAllister, G. *Neuropharmacology* **2005,** *48* (4), 492-502.
4. Hedlund, P. B.; Huitron-Resendiz, S.; Henriksen, S. J.; Sutcliffe, J. G. *Biol Psychiatry* **2005,** *58* (10), 831-837.
5. Miller, P. W.; Long, N. J.; Vilar, R.; Gee, A. D. *Angew Chem Int Ed Engl* **2008,** *47* (47), 8998-9033.

6. Herth, M. M.; Knudsen, G. M., PET Imaging of the 5-HT $_{2A}$ Receptor System: A Tool to Study the Receptor's *In Vivo* Brain Function. In *5-HT$_{2A}$ Receptors in the Central Nervous System*, Springer: **2018**; pp 85-134.
7. Herth, M. M.; Volk, B.; Pallagi, K.; Kofoed Bech, L.; Antoni, F. A.; Knudsen, G. M.; Kristensen, J. L. *ACS Chem Neurosci* **2012,** *3* (12), 1002-7.
8. Hansen, H. D.; Herth, M. M.; Ettrup, A.; Andersen, V. L.; Lehel, S.; Dyssegaard, A.; Kristensen, J. L.; Knudsen, G. M. *J Nucl Med* **2014,** *55* (4), 640-6.
9. Herth, M. M.; Andersen, V. L.; Hansen, H. D.; Stroth, N.; Volk, B.; Lehel, S.; Dyssegaard, A.; Ettrup, A.; Svenningsson, P.; Knudsen, G. M.; Kristensen, J. L. *J Med Chem* **2015,** *58* (8), 3631-6.
10. Andries, J.; Lemoine, L.; Mouchel-Blaisot, A.; Tang, S.; Verdurand, M.; Le Bars, D.; Zimmer, L.; Billard, T. *Bioorg Med Chem Lett* **2010,** *20* (12), 3730-3.
11. Lemoine, L.; Andries, J.; Le Bars, D.; Billard, T.; Zimmer, L. *J Nucl Med* **2011,** *52* (11), 1811-8.
12. Hansen, H. D.; Andersen, V. L.; Lehel, S.; Magnussen, J. H.; Dyssegaard, A.; Stroth, N.; Kristensen, J. L.; Knudsen, G. M.; Herth, M. M. *Bioorg Med Chem Lett* **2015,** *25* (9), 1901-4.
13. Hogendorf, A. S.; Hogendorf, A.; Kurczab, R.; Satala, G.; Lenda, T.; Walczak, M.; Latacz, G.; Handzlik, J.; Kiec-Kononowicz, K.; Wieronska, J. M.; Wozniak, M.; Cieslik, P.; Bugno, R.; Staron, J.; Bojarski, A. J. *Sci Rep* **2017,** *7* (1), 1444.
14. Herth, M.; Hansen, H.; Anders, E.; Lehel, S.; Kristensen, J.; Billard, T.; Zimmer, L.; Knudsen, G. *J Nucl Med* **2014,** *55* (supplement 1), 1814-1814.
15. Radiosynthesis of [^{11}C]AGH-44: [^{11}C]methyl trifluoromethanesulfonate was produced in an automated system and used as methylation agent. It was trapped in a 300 µL acetone solution containing the precursor tert-butyl 3-(1-ethyl-1H-imidazol-5-yl)-5-hydroxy-1H-indole-1-carboxylate (AGH-111, 0.3 mg, 0.91 µmol) and 2N NaOH (2 µL) at -10 °C. The mixture was heated for 30 seconds at 40 °C afterwards TFA (0.25 mL) added. This solution was heated at 80 °C for 5 min. Thereafter, the crude mixture was neutralized with a mix of 2N NaOH (0.75 mL) and H_20 (3.5 mL). The final product was subsequently isolated using semi-preparative HPLC (Luna 5-µm C18(2) 100-A˚ column (Phenomenex Inc. 250 • 10 mm), EtOH/0.1% H_3PO_4 in H_2O (20:70), at a flow rate of 3 mL/min). Retention times were 780 seconds for [^{11}C]AGH-44 and 400 seconds for the precursor AGH-111. The labeled product was collected in a 20 mL vial and thereafter diluted with phosphate–buffer (1.65

mL, 100 mM, pH 7). The final product was analyzed by analytical HPLC (Luna, 5µ, C-18(2) 100-A˚ column (Phenomenex Inc. 150 • 4.6 mm); 0.1 % TFA in MeCN/H_2O (0-100 % over 15 minutes) 2 mL/min – retention time for [^{11}C]AGH-44 was 5.4 minutes and 6.7 min for the precursor AGH-111) (Figure 1). Molar activities were in the range of 637 ± 50 GBq/µmol (time of injection) and was determined as the integrated area of the UV absorbance peak corresponding to the radiolabeled product on the HPLC chromatogram. This area was converted into a molar mass by comparison with an average of integrated areas (triplet) of a known standard of the reference compound.

16. PET evaluation in rats: The PET tracers were given as intravenous (i.v.) bolus injections via tail vein catheters at the start of the scan (0 min), the injected doses were between 5-20 MBq. The rats were subsequently scanned in a high-resolution research tomography (HRRT) scanner (Siemens AG, Munich, Germany), first for a 60 min dynamic PET scan followed by a transmission scan (Tx50). The scans were performed using a homemade 2x2 rat insert which enabled the possibility of scanning 4 rats simultaneously (Figure 2).[21] The animals were scanned at baseline and after receiving pretreatment of Elacridar (5 mg/kg) 30 min before tracer injection. Anesthesia was induced at 3-3.5% isoflurane in oxygen and maintained at 1.5-2.5% during scans. The rats were housed in groups of 2-4 animals per cage in a climate controlled rodent facility with a 12h/12h light cycle. 200-300 grams Long-Evans WT female littermates were used in this study and they were transported to the scanner at least one hour before the experiment started. The animals were fed ad libitum and had free access to water. All procedures were conducted in accordance with the FELASA guidelines for animal research and with approval from The Danish Animal Experiments Inspectorate (license number: 2017-15-0201-01283) as well as the Department of Experimental Medicine, University of Copenhagen.
17. Reconstruction and pre-processing of PET data: The Sixty-minute list-mode PET data were reconstructed into 33 dynamic frames (6 × 10, 6 × 20, 6 × 60, 8 × 120, and 7 × 300 seconds). The Images consisted of 207 planes of 256 x 256 voxels of 1.22 x 1.22 x 1.22 mm. From this image the rats of interest could be extracted into separate images. Summed pictures of all counts in the time interval 5-60 min of the scans was made for each rat and used for co-registration to a standardized MRI-based VOI atlas of the rat brain.[22-23] The time activity curves (TACs) were calculated for a whole brain volume of interest (VOI), to elucidate the brain uptake. For biodistribution analysis VOIs for the organs of instrest were manually registrated. Outcome measure in the time-activity curves (TACs) was calculated as

radioactive concentration (kBq/cc) and normalized to either the injected dose corrected for animal weight, yielding standardized uptake values (SUV) or only corrected to the injected dose yielding procentage injected does per mL (%ID/mL).

18. Syvänen, S.; Lindhe, Ö.; Palner, M.; Kornum, B. R.; Rahman, O.; Långström, B.; Knudsen, G. M.; Hammarlund-Udenaes, M. *Drug Metab Dispos* **2009,** *37* (3), 635-643.
19. Kallem, R.; P Kulkarni, C.; Patel, D.; Thakur, M.; Sinz, M.; P Singh, S.; Shahe Mahammad, S.; Mandlekar, S. *Drug Metab Lett* **2012,** *6* (2), 134-144.
20. Metabolism studies in rats: the animals were kept and handled as described for the PET evaluation.[17] 9-17 MBq of the PET tracers were given as intravenous (i.v.) bolus injections via tail vein catheters at the start of the experiments (n=3). Blood samples were thereafter taken from a a second tail vein catheters at different timepoints ranging from 2 – 54 min into heparin coated vials. From the blood samples aliquots of 20 µL were measured using a well counter (Cobra 5003; PerkinElmer). The rest of the blood sample was cetrifuged (4000 rpm, 5 min at 4 °C) and 10 µL aliquots of the plasma were subsequently measured in the same manner as the full blood. The rest of the plasma was analysed for radiolabeled parent compound and metabolites using HPLC with online radioactivity detection, by direct injection of plasma in a columnswitching HPLC system.[24]
21. Keller, S. H.; L'Estrade, E. N.; Dall, B.; Palner, M.; Herth, M. *Nuclear Science Symposium, Medical Imaging Conference and Room-Temperature Semiconductor Detector Workshop (NSS/MIC/RTSD*), **2016**, IEEE: 2016; pp 1-3.
22. Schwarz, A. J.; Danckaert, A.; Reese, T.; Gozzi, A.; Paxinos, G.; Watson, C.; Merlo-Pich, E. V.; Bifone, A. *Neuroimage* **2006,** *32* (2), 538-550.
23. Garcia, D. V.; Casteels, C.; Schwarz, A. J.; Dierckx, R. A.; Koole, M.; Doorduin, J. *PLoS One* **2015,** *10* (3), e0122363.
24. Gillings, N. *Nuclear medicine and biology* **2009**, *36* (8) 961-965.

Supporting Information

Radiolabeling and *in vivo* evaluation of [^{11}C]AGH-44 - a potential lead structure to develop a positron emission tomography radioligand for the 5-HT$_7$ receptor

Elina T. L'Estrade[a,b,c], Ida N. Petersen[d,e], Mengfei Xiong[a,b], Adam S. Hogendorf[f], Agata Hogendorf[f], Jesper L. Kristensen[b], Andreas Kjær[d,e], Andrzej J. Bojarski[f], Maria Erlandsson[c], Tomas Ohlsson[c], Gitte M. Knudsen[a], Matthias M. Herth[a,b,d,*]

[a] *Neurobiology Research Unit, Rigshospitalet, Blegdamsvej 9, 2100 Copenhagen, Denmark*

[b] *Department for Drug Design and Pharmacology, Faculty of Health and Medical Sciences, University of Copenhagen, Universitetesparken 2, 2100 Copenhagen, Denmark*

[c] *Radiation Physics, Nuclear Medicine Physics Unit, Skånes University Hospital, Barngatan 3, 222 42 Lund, Sweden.*

[d] *Department of Clinical Physiology, Nuclear Medicine and PET, University Hospital Copenhagen, Rigshospitalet Blegdamsvej 9, 2100 Copenhagen, Denmark*

[e] *Cluster for Molecular Imaging, Faculty of Health Science, University of Copenhagen, Blegdamsvej 3, 2200 Copenhagen, Denmark*

[f] *Institute of Pharmacology, Polish Academy of Sciences, 12 Smętna,31-343 Kraków, Poland.*

CONTENTS

RESULTS 109

Biodistribution in rats 109

Radiometabolism in rats 110

* Corresponding author. Tel.: +0045 93565414; fax: +0045 35 33 60 41; e-mail: matthias.herth@sund.ku.dk

Results

Biodistribution in rats

Supporting Figure 1: Results from the biodistribution study. Time-activity curves for the rat liver, bladder, kidney, brain, heart and lung for **A)** Baseline conditions. **B)** Elacridar (5 mg/kg) pretreatment **C)** Elacridar (5 mg/kg) and SB-269970 (3 mg/kg) pretreatment.

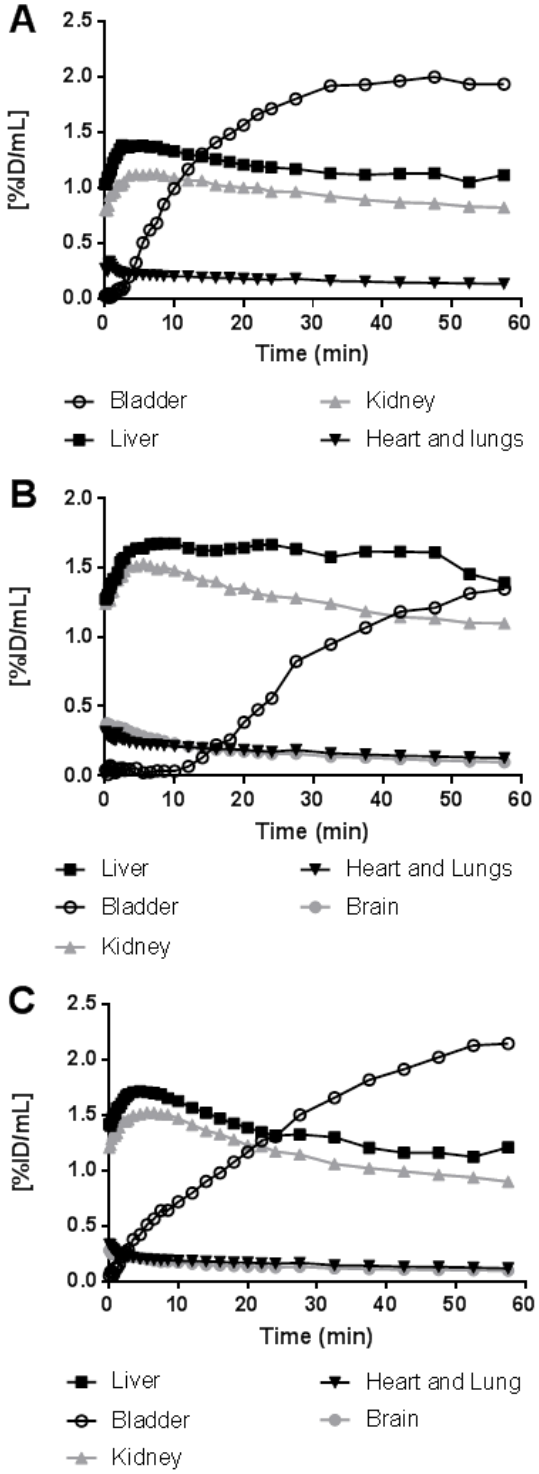

Radiometabolism in rats

Supporting table 1: Table showing the ID of the samples the time they were taken after the injection of [^{11}C]AGH-44 and the volume of plasma injected on the HPLC system.

ID:	Time:	Inj. Volume:
M6	3 min	80 µL
M7	4 min	60 µL
M8	10 min	60 µL
M12	29 min	120 µL

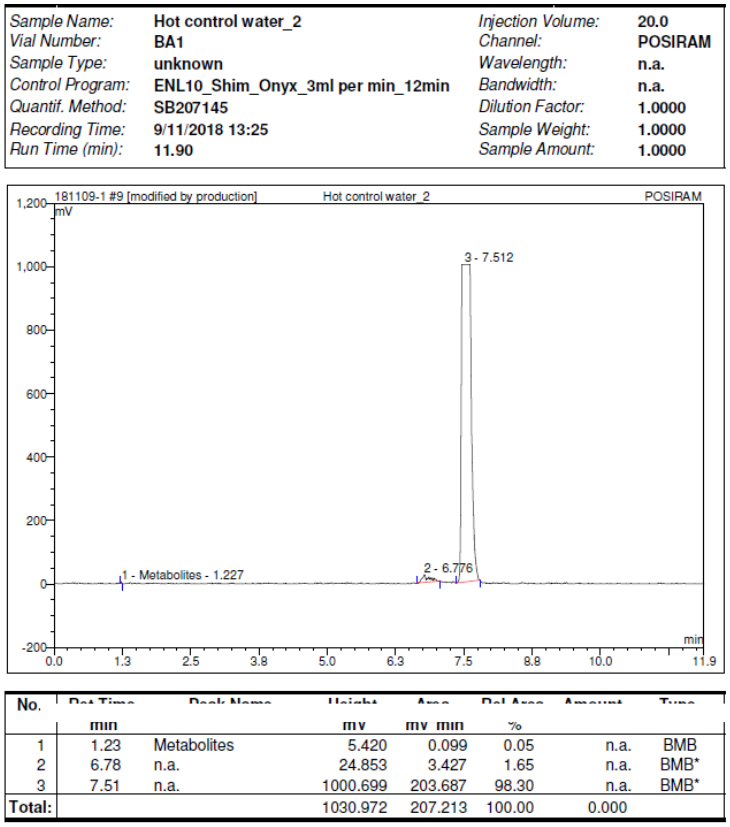

No.	Ret.Time	Peak Name	Height	Area	Rel.Area	Amount	Type
	min		mV	mV*min	%		
1	1.23	Metabolites	5.420	0.099	0.05	n.a.	BMB
2	6.78	n.a.	24.853	3.427	1.65	n.a.	BMB*
3	7.51	n.a.	1000.699	203.687	98.30	n.a.	BMB*
Total:			1030.972	207.213	100.00	0.000	

Supporting Figure 2: Representative radio-chromatogram of [^{11}C]AGH-44.

Sample Name:	**11C-AGH-44 M6**	*Injection Volume:*	**20.0**
Vial Number:	**BA2**	*Channel:*	**POSIRAM**
Sample Type:	**unknown**	*Wavelength:*	**n.a.**
Control Program:	**ENL10_Shim_Onyx_3ml per min_12min**	*Bandwidth:*	**n.a.**
Quantif. Method:	**SB207145**	*Dilution Factor:*	**1.0000**
Recording Time:	**9/11/2018 13:38**	*Sample Weight:*	**1.0000**
Run Time (min):	**11.90**	*Sample Amount:*	**1.0000**

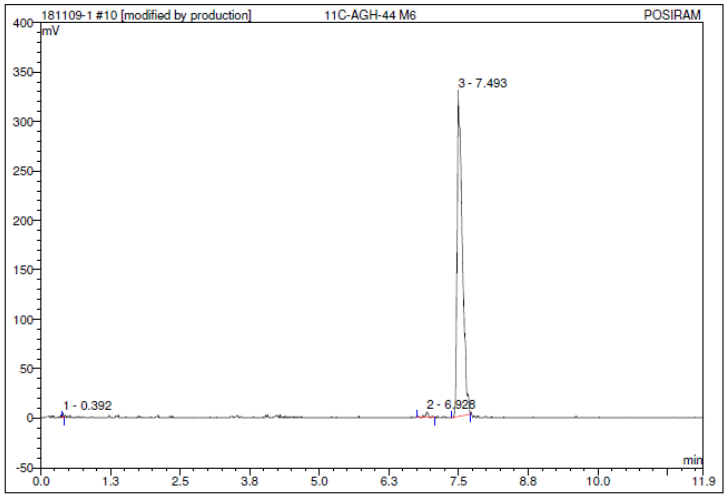

No.	Ret.Time min	Peak Name	Height mV	Area mV*min	Rel.Area %	Amount	Type
1	0.39	n.a.	5.039	0.084	0.24	n.a.	BMB
2	6.93	n.a.	5.580	0.279	0.78	n.a.	BMB*
3	7.49	n.a.	330.100	35.410	98.98	n.a.	BMB*
Total:			340.719	35.773	100.00	0.000	

Supporting Figure 3: Representative radio-chromatogram of rat plasma sample taken 3 min after injection with [^{11}C]AGH-44.

Sample Name:	**11C-AGH-44 M7**	*Injection Volume:*	**20.0**
Vial Number:	**BA3**	*Channel:*	**POSIRAM**
Sample Type:	**unknown**	*Wavelength:*	**n.a.**
Control Program:	**ENL10_Shim_Onyx_3ml per min_12min**	*Bandwidth:*	**n.a.**
Quantif. Method:	**SB207145**	*Dilution Factor:*	**1.0000**
Recording Time:	**9/11/2018 13:50**	*Sample Weight:*	**1.0000**
Run Time (min):	**11.90**	*Sample Amount:*	**1.0000**

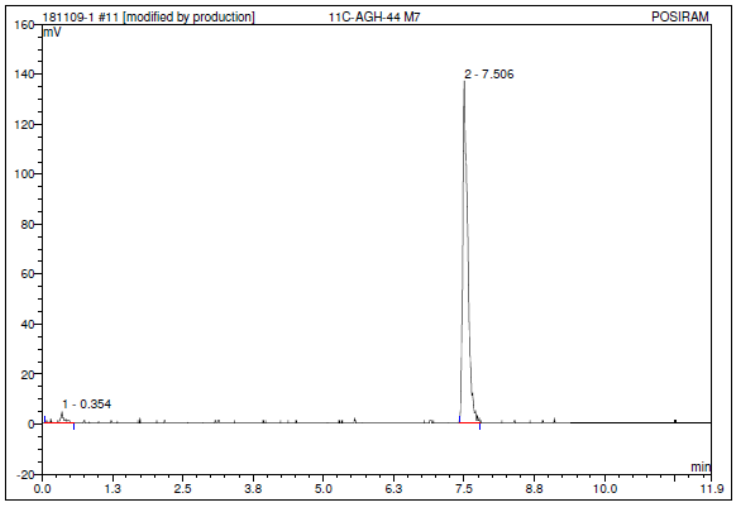

No.	Ret.Time min	Peak Name	Height mV	Area mV*min	Rel.Area %	Amount	Type
1	0.35	n.a.	4.625	0.346	2.39	n.a.	BMB*
2	7.51	n.a.	136.936	14.140	97.61	n.a.	BMB*
Total:			141.561	14.486	100.00	0.000	

Supporting Figure 4: Representative radio-chromatogram of pig plasma sample taken 4 min after injection with [^{11}C]AGH-44.

Sample Name:	**11C-AGH-44 M8**	*Injection Volume:*	**20.0**
Vial Number:	**BA4**	*Channel:*	**POSIRAM**
Sample Type:	**unknown**	*Wavelength:*	**n.a.**
Control Program:	**ENL10_Shim_Onyx_3ml per min_12min**	*Bandwidth:*	**n.a.**
Quantif. Method:	**SB207145**	*Dilution Factor:*	**1.0000**
Recording Time:	**9/11/2018 14:03**	*Sample Weight:*	**1.0000**
Run Time (min):	**11.90**	*Sample Amount:*	**1.0000**

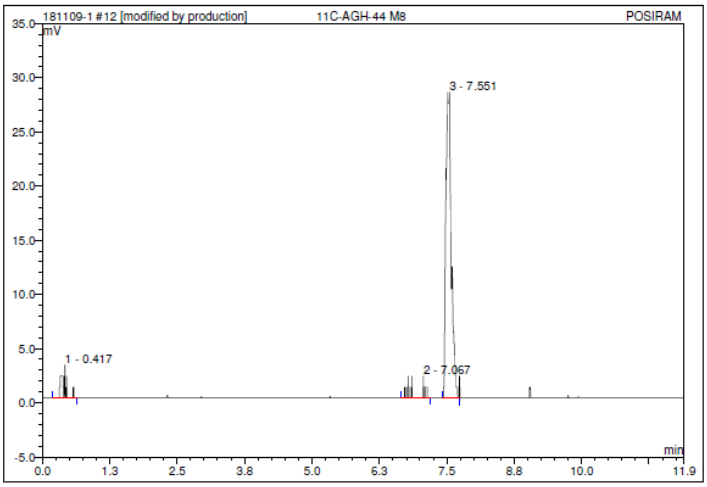

No.	Ret.Time min	Peak Name	Height mV	Area mV*min	Rel.Area %	Amount	Type
1	0.42	n.a.	3.028	0.203	5.62	n.a.	BMB*
2	7.07	n.a.	2.012	0.132	3.64	n.a.	BMB*
3	7.55	n.a.	28.206	3.277	90.74	n.a.	BMB*
Total:			33.246	3.611	100.00	0.000	

Supporting Figure 5: Representative radio-chromatogram of pig plasma sample taken 10 min after injection with [^{11}C]AGH-44.

Sample Name:	**11C-AGH-44 M12**	*Injection Volume:*	**20.0**
Vial Number:	**BA8**	*Channel:*	**POSIRAM**
Sample Type:	**unknown**	*Wavelength:*	**n.a.**
Control Program:	**ENL10_Shim_Onyx_3ml per min_12min**	*Bandwidth:*	**n.a.**
Quantif. Method:	**SB207145**	*Dilution Factor:*	**1.0000**
Recording Time:	**9/11/2018 14:53**	*Sample Weight:*	**1.0000**
Run Time (min):	**11.90**	*Sample Amount:*	**1.0000**

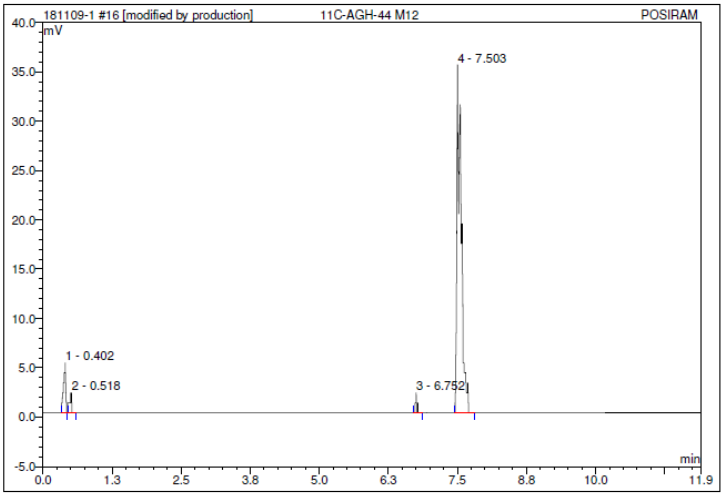

No.	Ret.Time min	Peak Name	Height mV	Area mV*min	Rel.Area %	Amount	Type
1	0.40	n.a.	5.037	0.234	6.63	n.a.	BMB
2	0.52	n.a.	2.007	0.094	2.68	n.a.	BMB*
3	6.75	n.a.	2.008	0.030	0.86	n.a.	BMB*
4	7.50	n.a.	35.258	3.170	89.83	n.a.	BMB*
Total:			44.310	3.529	100.00	0.000	

Supporting Figure 6: Representative radio-chromatogram of pig plasma sample taken 29 min after injection with [^{11}C]AGH-44.

Chapter 5

Paper III

Fragment-based Labelling Using Condensation Reactions – A Possibility to Increase Throughput in Preclinical PET

Summary:

In this chapter ***Paper III*** *presents the establishment of the fragment-based radiolabelling strategy by condensation reactions. This strategy has previously been displayed to increase the preclinical evaluation throughput. This was motivating the aim of this paper, focusing on making a PET tracer library containing radiolabelled (arylpiperazinyl-butyl)oxindole analogues.*

Authors' contribution:

The author contributed to the designed PET tracer library. Planned and executed the organic synthesis (F.G.E was involved in the synthesis of some reference compounds and precursors under the supervision of the author) of the reference compounds. The establishment of the radiolabelling strategy for the carbon-11 fragment-based condensation strategy was done in collaboration with S.L and I.N.P. Extension to the fluorine-18 labelling and optimization experiments was done by the author, as well as the establishment of the dual condensation. The author thereafter planned and performed the fragment-based approach on one additional labelling strategy. The author also formulated the outline and contributed considerably to writing the manuscript under supervision of M.M.H.

Fragment-based Labelling Using Condensation Reactions – A Possibility to Increase Throughput in Preclinical PET

Elina Tampio L'Estrade[a,b,c], Szabolcs Lehel[d], Ida Nymann Petersen[d], Fraser G. Edgar[b], Balázs Volk[e], Tomas Ohlsson[c], Maria Erlandsson[c], Gitte M. Knudsen[a,f] and Matthias M. Herth[a,b,d,†]

[a] *Neurobiology Research Unit, Rigshospitalet, Blegdamsvej 9, 2100 Copenhagen, Denmark*

[b] *Department for Drug Design and Pharmacology, Faculty of Health and Medical Sciences, University of Copenhagen, Universitetesparken 2, 2100 Copenhagen, Denmark*

[c] *Radiation Physics, Nuclear Medicine Physics Unit, Skånes University Hospital, Barngatan 3, 222 42 Lund, Sweden.*

[d] *Department of Clinical Physiology, Nuclear Medicine and PET, University Hospital Copenhagen, Rigshospitalet Blegdamsvej 9, 2100 Copenhagen, Denmark*

[e] *Directorate of Drug Substance Development, Egis Pharmaceuticals Plc., P.O. Box 100, H-1475 Budapest, Hungary*

[f] *Institute of Clinical Medicine, Faculty of Health and Medical Sciences, University of Copenhagen, Denmark*

[†] Corresponding Author: Tel.: +45 93565414; fax: +45 35 33 60 41; e-mail: matthias.herth@sund.ku.dk.

IN THIS WORK, A fragment-based labelling procedure was developed based on condensation reactions. Six ^{18}F-labelled (arylpiperazinyl-butyl)oxindole derivatives were synthesized. These structures are interesting lead compounds in respect to develop a 5-HT$_7$R PET tracer. They were radiolabelled in sufficient radiochemical yields, purities and molar activities for future *in vivo* evaluation in rodents

Positron emission tomography (PET) is a valuable, non-invasive, molecular imaging technique that can be applied to characterize biological receptor or enzyme systems.[1-3] Today PET is routinely used in the clinic to assess disease stage and progression.[4] During the development of drugs acting in the central nervous system (CNS), the most important data determined by PET is information enabling the determination of receptor occupancies.[1-2, 5] Receptor occupancies can e.g. be used to estimate the optimal dose needed to maximize treatment efficacy, while minimizing side-effects.[1, 5]

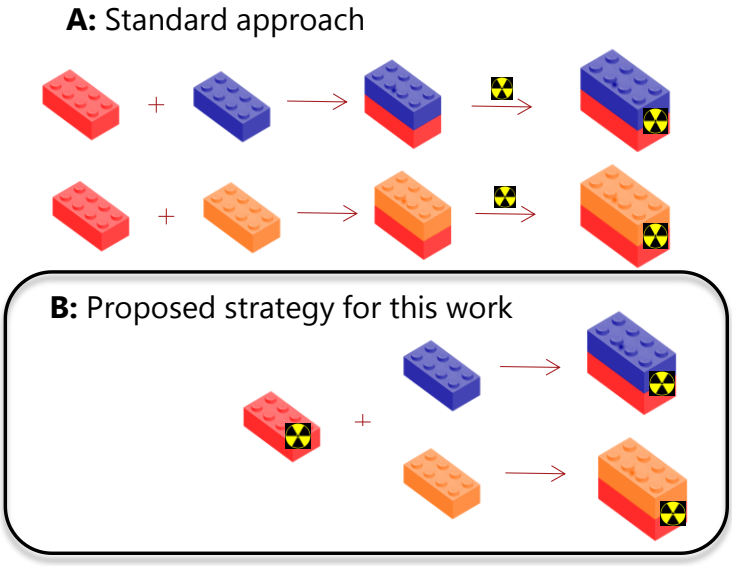

Figure 1: Illustrative presentation of standardly applied last-step labelling approaches (A) and the in this work proposed fragment-based strategy (B). The latter consists of two steps; first a synthon is radiolabelled which is then reacted with a secondary building block. This approach reduces precursor synthesis steps.

Developing a successful PET tracer is a challenging and complex process. Success rates are low, the process is time-consuming and expensive because of its multifaceted nature.[6-7] Development of a successful PET radiotracer cannot be reliably predicted from *in vitro* data and have thus far to be determined *in vivo*. For example, the blood-brain barrier permeability, the non-displaceable binding component and the respective kinetics of a tracer are parameters that are currently best estimated *in vivo*.[5, 8-9] Consequently, the development of a PET-tracer is largely a "trial-and-error task".[7] This can be exemplified by our recent effort to develop a 5-HT_{2A} receptor agonist PET tracer.[10-11] We identified 12 potential candidates with similar affinities, selectivity, metabolism and lipophilicity that were radiolabelled and evaluated *in vivo*. The *in vivo* characteristics were substantially different and this was impossible to predict beforehand, i.e. all tracers had to be developed in order to identify the most promising one. A more efficient strategy to synthesize and radiolabel a set

of PET tracers would have helped to accelerate the biological screening process. In light of this, we here adapt a fragment-based labelling strategy which was based on reductive aminations. This strategy can greatly reduce time-consuming precursor syntheses compared to the commonly applied late-stage labelling approach (Figures 1 and 2).[12-14]

By means of this strategy, we radiolabelled 8 tracers within two weeks. By contrast, last-step labelling would have taken at least three months. Although the fragment-based labelling strategy resulted in lower radiochemical yields (RCYs), we could isolate sufficient radioactivity amounts (> 300 MBq) needed for preclinical studies. From a general point of view, the fragment-based labelling approach aims to identify the best radiotracer with the least synthetic effort, whereas last-step labelling strategies aim to reach the highest possible RCY.

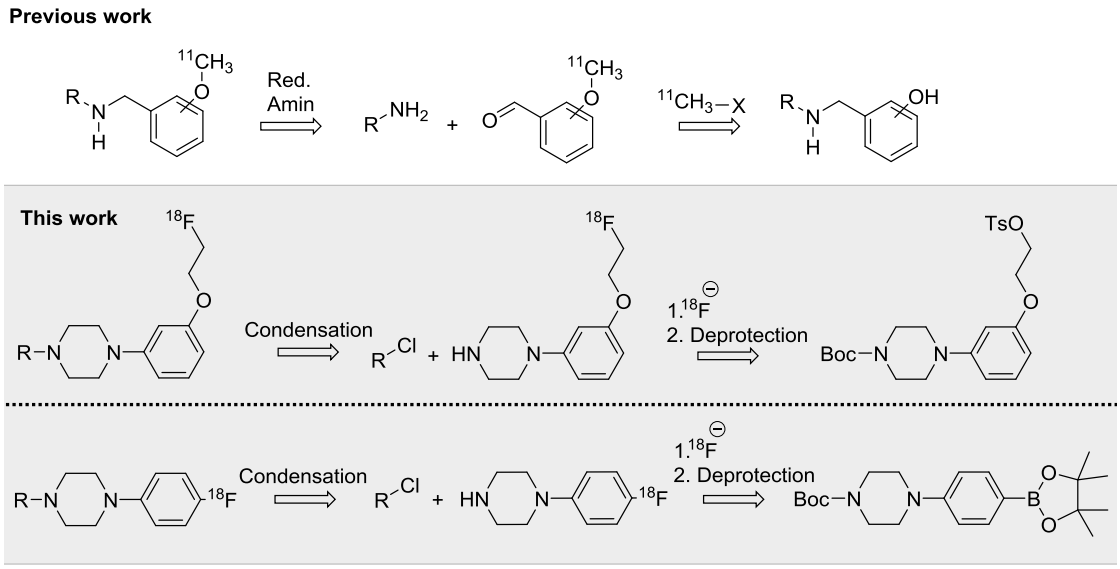

Figure 2: Overview of previous work of the fragment-based labelling with reductive animations (Red. Amin) and the extension to condensation reactions within this work.

The aim of this work was to expand the fragment-based labelling strategy from reductive aminations to condensation reactions between radiolabelled piperazines and oxindoles (Figure 2). These fragments were chosen because our group wishes to develop 5-HT_7R selective PET tracers, and (arylpiperazinyl-butyl)oxindoles are a promising scaffold in this respect.[15-19] Moreover, the piperazinyl moiety is commonly used in medicinal chemistry[20-22] and as such, the feasibility of these building blocks to be used in fragment-based PET tracer development is of interest.

As proof-of-principle, we decided to ^{11}C-label a piperazine building block and subsequently condense it with 3-(4-chlorobutyl)-3-ethylindolin-2-one (BO-1). This strategy was chosen in order to prove that fragment-based labelling using condensation reactions and a radionuclide possessing a relatively short half-life (20.4 min) is possible. The feasibility of this reaction would also prove that condensation reactions with radionuclides with less time-restrictive half-lives, for example fluorine-18 (110 min) or iodine-124 (4.18 days), are possible. Furthermore and a bit out of the direct scope of this work, we were interested if selective ^{11}C-labelling of a phenolic hydroxyl group over a secondary amine is achievable using [^{11}C]MeOTf. Ten different bases in four different solvent systems were screened in order to identify the best conditions (SI Table 1 and 2). The highest radiochemical incorporation and best reproducibility was gained using following conditions: [^{11}C]Methyl trifluoromethanesulfonate ([^{11}C]MeOTf) was bubbled through a solution of the precursor 3-(piperazin-1-yl)phenol (1 mg, 5.6 eqv.) and RbOH (2 µL, 2 M aq., 1 eqv.) in 1 mL of DMF at a flow rate of 25 mL/min at 10 ˚C. Afterwards, this solution was heated to 40 ˚C over a period of 100 seconds and further reacted at this temperature for a total of 5 min. A radiochemical incorporation of 58 ± 14 (n=7) was determined (see SI). In the next step, the yielded intermediate ([^{11}C]OMe) was further reacted with BO-1 to afford [^{11}C]Cimbi-775 in a RCY (d.c.) of approximately 2.5%, a molar activity of 4 GBq/µmol and a radiochemical purity above 98% over two steps (Scheme 1) (see SI). This proof-of-principle experiment showed the feasibility of the reaction, even though only low isolated amounts and molar activities had been achieved.

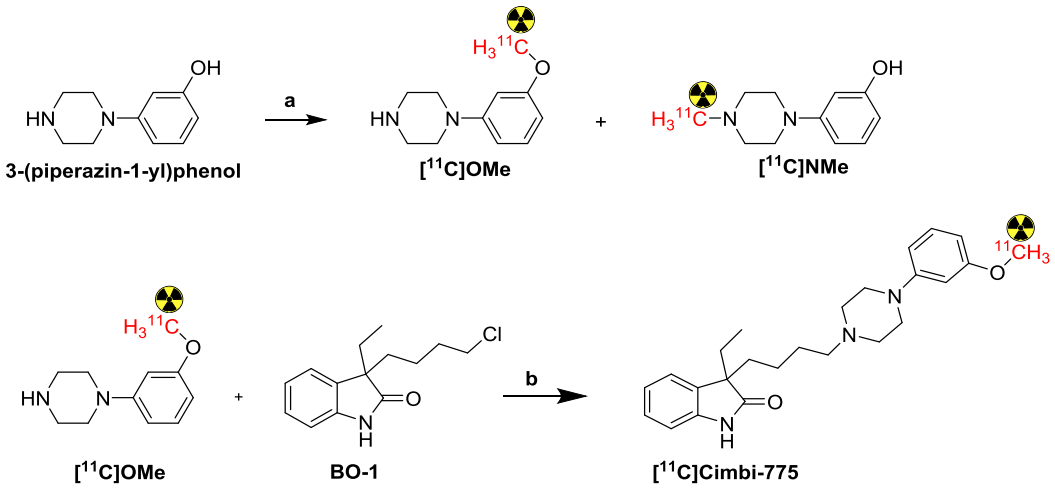

Scheme 1: Reaction scheme of the synthesis of [^{11}C]Cimbi-775 using the fragment based labelling strategy. **a)** [^{11}C]CH_3OTf, RbOH (2 M aq.), DMF, 40 ˚C for 5 min. **b)** K_2CO_3, 170 °C for 15 min.

A building block labelled with longer-lived radionuclides potentially improves the radioactivity amount and molar activities. For this reason, we applied the developed fragment-based labelling method to ^{18}F-labelled arylpiperazine building blocks (Figure 3) and aimed to radiolabel seven analogues (Figure 4). Reference compounds were synthesized using a previously described method.[15,18] In short, butyloxindoles were mixed with the corresponding arylpiperazine derivatives and Na_2CO_3, melted at 120 ˚C and reacted for 1 hour. An overview of synthesized reference compounds and respective experimental details can be found in SI.

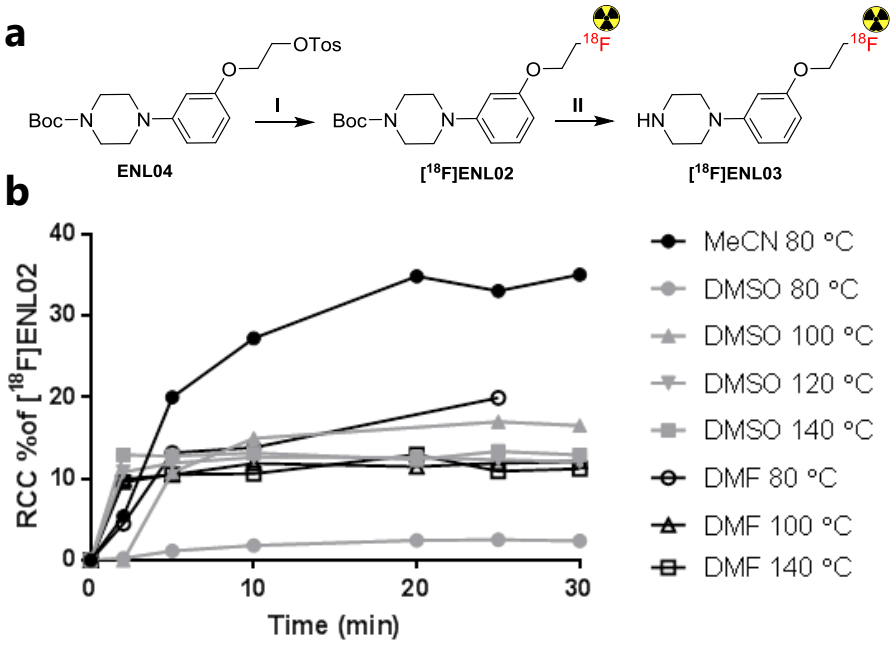

ENL04	2 mg	4 mg	6 mg	9 mg
RCC (%) of [^{18}F]ENL02	35%	51%	77%	59%

Figure 3: Optimization efforts to ^{18}F-label [^{18}F]ENL03; **a)** final reaction conditions **I)** [^{18}F]F$^-$, K_2CO_3, K_{222}, MeCN, 80 ˚C for 20 min **II)** 25% TFA in MeCN, 80 ˚C for 10 min. b) Reaction time, temperature and solvent dependency on the radiochemical incorporation (RCC) of [^{18}F]ENL02 using 2 mg of ENL04. The table shows that the optimal amount of precursor was determined to 6 mg. RCCs are determined using radio-HPLC and verified by radio-TLC. N=3 and standard deviation < ± 2.5. The deprotection to achieve the final synthon [^{18}F]ENL03 was performed with a full conversion.

In parallel to the synthesis of reference compounds, the fragment-based labelling approach was developed. Precursors were successfully synthesized (see SI) and subsequently labelled. Figure 3a displays the general labelling strategy. The labelling procedure of [^{18}F]ENL02 was optimized with respect to temperature, solvent, reaction time and precursor amount. The results from the optimization procedure are illustrated in Figure 3b. The best radiochemical incorporation were reached using the following reaction conditions: 6 mg precursor

(ENL04) dissolved in MeCN was reacted with dried [^{18}F]F^{-}/K$_{222}$/K^{+} for 20 min at 80 °C. Under these conditions the radiochemical incorporations were 77 ± 9.6% (n = 8). Synthesis of [^{18}F]ENL03 succeeded by hydrolysis of the Boc-group using acidic conditions, which led to a quantitative conversion from [^{18}F]ENL02 (n =8) (see SI).

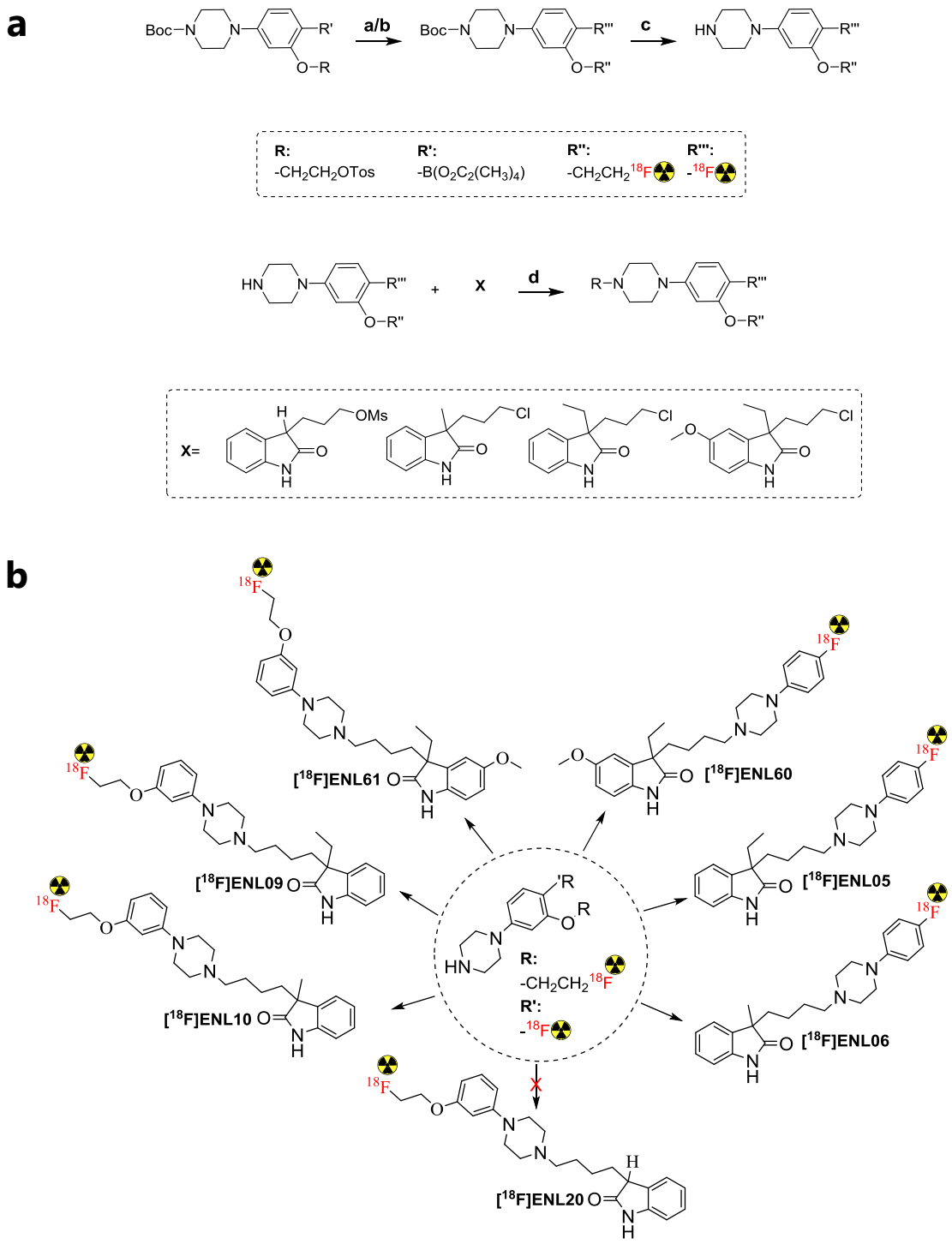

Figure 4: a) Overview of the synthetic strategy, **b)** Structures labelled within this work applying the fragment-based labelling strategy.

In a next step, the condensation between the ^{18}F-labelled arylpiperazine and the butyloxindole derivatives (Figure 4) were carried out and then optimized. In addition to the aforementioned optimisation parameters such as temperature, time or solvent, we also investigated the influence of base amount towards the RCY (see SI Figure 1). The optimisation was carried out for [^{18}F]ENL09 and the identified conditions afterwards directly applied to [^{18}F]ENL10 and [^{18}F]ENL61 without further optimization attempts. Best RCCs (as determined with radio-HPLC and verified by radio-TLC) were achieved using 18-20 mg of the respective butyloxindole building block, 28-32 mg K_2CO_3, DMSO as solvent and a reaction time of 15 min at 170 °C. Sufficient isolated radiochemical yields (RCY, isolated activity amount > 230 MBq) for preclinical evaluation studies in rodents, good molar activities and radiochemical purities were made available using this fragment-based labelling strategy (Table 1). The synthesis of [^{18}F]ENL20 failed using the aforementioned conditions. This is most likely due to tautomerization of the hydrogen in the 3-position of the butyloxindole scaffold, which results in a variety of side-reactions. Similar behaviour has recently been observed.[18] Encouraged by the successful synthesis of 3 tracers, we investigated if other ^{18}F-arylpiperazines could be used for fragment-based labelling attempts. Direct fluorination of electron-rich aromatic systems was recently reported.[23-29] As such, we wanted to investigate if 1-(4-fluorophenyl)piperazine ([^{18}F]FGE06) could be radiolabelled and used for fragment-based labelling.

Table 1: Overview of radiochemical yields (RCY), molar activities (A_m) and radiochemical purities (RCP) of the 6 isolated PET tracers. **a)** Respective tracers were labelled via nucleophilic substitution. **b)** Respective tracers were labelled via Cu-mediated fluorination

	Compound	RCY (%) (d.c)	A_m(GBq/µmol)	RCP (%)
a)	[^{18}F]ENL10	2.8 ± 2.3%	138	> 98%
	[^{18}F]ENL09	4.7 ± 0.2%	136	> 98%
	[^{18}F]ENL61	3.5 ± 0.5%	121	> 98%
b)	[^{18}F]ENL06	0.4 ± 0.1%	1	> 98%
	[^{18}F]ENL05	0.2 ± 0.05%	21	> 98%
	[^{18}F]ENL60	1.2 ± 0.5%	5	> 98%

Labelling was carried out using Cu-mediated ^{18}F-fluorination of the corresponding boronic pinacol ester precursor (Figure 4). Conditions used were recently published by Preshlock *et al*. in 2016, adapted by Petersen *et al*. in 2017 and were used with only a minor optimisation

effort.[30-31] A largely varying RCC of 39 ± 33 (n = 3) were determined for the radiofluorination of [^{18}F]FGE06. Subsequently, after hydrolysis of the Boc-group using acidic conditions, the synthon was coupled to the respective butyloxindole analogue, using the optimized condensation reaction conditions (as previously described). [^{18}F]ENL05, [^{18}F]ENL06 and [^{18}F]ENL60 could be isolated in low RCY of 0.2-1.2% (d.c, isolated activity amount only > 1.5 MBq) and with low molar activity in the range of 1-21 GBq/µmol (Table 1) (see SI). This molar activity is on the border of being too low to be used in rodent studies.[2, 32-33]

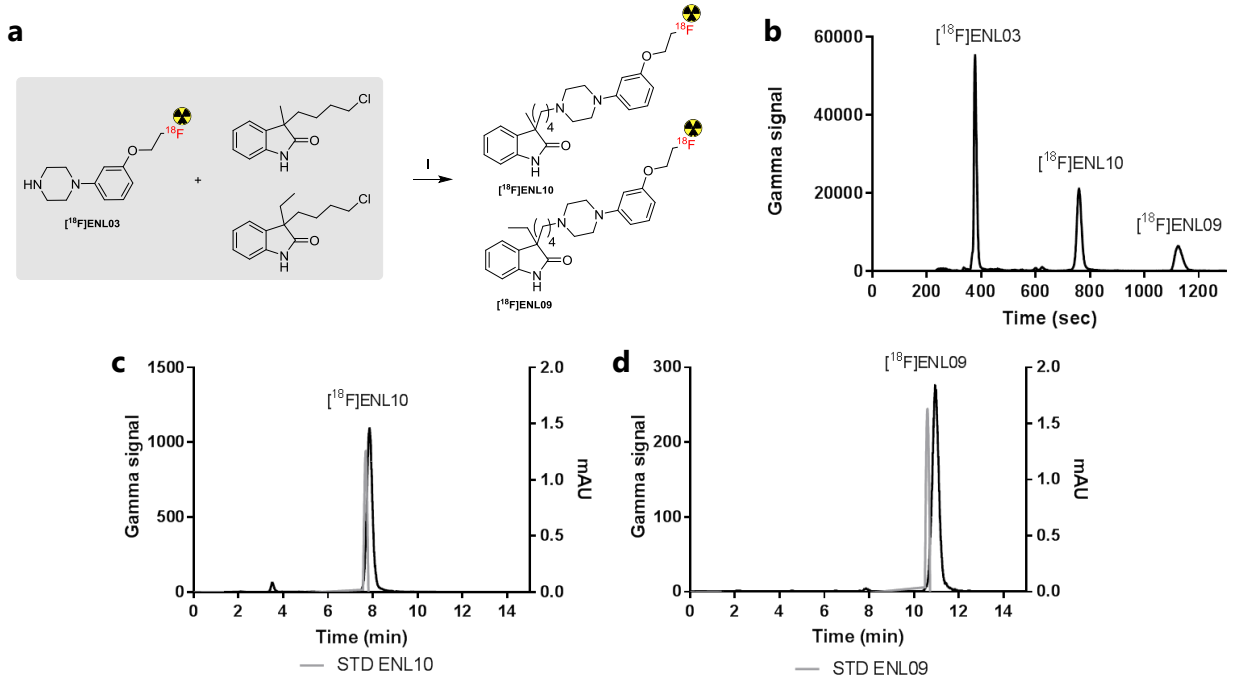

Figure 5: a) Reaction scheme of the simultanous dual-condensation. **I)** K_2CO_3, 170 °C for 15 min. **b)** Chromatogram of the semi-preparative HPLC method used to isolate [^{18}F]ENL09 and [^{18}F]ENL10.**c)** and **d)** Analytica radio- and UV absorption chromatograms after separation of [^{18}F]ENL09 and [^{18}F]ENL10. Chromatograms are spiked with their respective reference compound

We were also interested if fragment-based labelling can be used to simultaneously label and isolate two PET tracers from one batch. Figure 5 displays the applied synthesis strategy, the semi-preparative HPLC and the final product analysis. Labelling was carried out using the same conditions as described in the standard method. However, instead of one butyloxindole two analogues were added (see SI). [^{18}F]ENL09 could be isolated in a RCY of 1.8-4.1% (n =3) and [^{18}F]ENL10 in a RCY of 3.7-5.2% (n = 3). Both products could easily be separated (Figures 5b, c and d).

In conclusion, the fragment-based labelling procedure was successfully applied to synthesize six (arylpiperazinyl-butyl)oxindole analogues with RCYs and radiochemical purities sufficient for subsequent *in vivo* evaluation. As such, fragment-based labelling strategies using piperazine labelled building blocks can be applied to create rapidly a library of piperazine-based PET tracers for preclinical evaluation studies in small animals such as rodents.

Conflicts of interest

There are no conflicts to declare.

Notes and references

1. Kristensen, J. L.; Herth, M. M., Textbook of Drug Design and Discovery: *In vivo* imaging in drug discovery. In *Textbook of Drug Design and Discovery*, CRC Press: **2017**.
2. Piel, M.; Vernaleken, I.; Rösch, F., Positron Emission Tomography in CNS Drug Discovery and Drug Monitoring. *Journal of Medicinal Chemistry* **2014,** *57* (22), 9232-9258.
3. Miller, P. W.; Long, N. J.; Vilar, R.; Gee, A. D., Synthesis of ^{11}C, ^{18}F, ^{15}O, and ^{13}N radiolabels for positron emission tomography. *Angewandte Chemie International Edition***2008,** *47* (47), 8998-9033.
4. Frank, R. A.; Långström, B.; Antoni, G.; Montalto, M. C.; Agdeppa, E. D.; Mendizabal, M.; Wilson, I. A.; Vanderheyden, J. L., The imaging continuum: bench to biomarkers to diagnostics. *Journal of Labelled Compounds and Radiopharmaceuticals: The Official Journal of the International Isotope Society* **2007,** *50* (9-10), 746-769.
5. Zhang, L.; Villalobos, A.; Beck, E. M.; Bocan, T.; Chappie, T. A.; Chen, L.; Grimwood, S.; Heck, S. D.; Helal, C. J.; Hou, X., Design and selection parameters to accelerate the discovery of novel central nervous system positron emission tomography (PET) ligands and their application in the development of a novel phosphodiesterase 2A PET ligand. *Journal of medicinal chemistry* **2013,** *56* (11), 4568-4579.
6. Guo, Q.; Brady, M.; Gunn, R. N., A biomathematical modeling approach to central nervous system radioligand discovery and development. *The Journal of Nuclear Medicine* **2009,** *50* (10), 1715.
7. Herth, M. M.; Leth-Petersen, S.; Lehel, S.; Hansen, M.; Knudsen, G. M.; Gillings, N.; Madsen, J.; Kristensen, J. L., Accelerating preclinical PET-screening: reductive amination with [^{11} C] methoxybenzaldehydes. *RSC Advances* **2014,** *4* (41), 21347-21350.

8. Herth M. M., K. G. M., PET Imaging of the 5-HT2A Receptor System: A Tool to Study the Receptor's *In Vivo* Brain Function. 5-HT_{2A} Receptors in the Central Nervous System. In *5-HT2A Receptors in the Central Nervous System*, Guiard B., D. G. G., Ed. Humana Press, Cham: 2018; Vol. 32, pp 85-134.

9. Pike, V. W., PET radiotracers: crossing the blood–brain barrier and surviving metabolism. *Trends in pharmacological sciences* **2009,** *30* (8), 431-440.

10. Ettrup, A.; Hansen, M.; Santini, M. A.; Paine, J.; Gillings, N.; Palner, M.; Lehel, S.; Herth, M. M.; Madsen, J.; Kristensen, J.; Begtrup, M.; Knudsen, G. M., Radiosynthesis and *in vivo* evaluation of a series of substituted ^{11}C-phenethylamines as 5-HT_{2A} agonist PET tracers. *European Journal of Nuclear Medicine and Molecular Imaging* **2011,** *38* (4), 681-93.

11. Herth, M. M.; Petersen, I. N.; Hansen, H. D.; Hansen, M.; Ettrup, A.; Jensen, A. A.; Lehel, S.; Dyssegaard, A.; Gillings, N.; Knudsen, G. M., Synthesis and evaluation of ^{18}F-labeled 5-HT2A receptor agonists as PET ligands. *Nuclear medicine and biology* **2016,** *43* (8), 455-462.

12. Petersen, I.; Villadsen, J.; Hansen, H.; Madsen, J.; Jensen, A.; Gillings, N.; Lehel, S.; Herth, M.; Knudsen, G.; Kristensen, J., 18 F-Labelling of electron rich iodonium ylides: application to the radiosynthesis of potential 5-HT_{2A} receptor PET ligands. *Organic & biomolecular chemistry* **2017,** *15* (20), 4351-4358.

13. Petersen, I. N.; Villadsen, J.; Hansen, H. D.; Jensen, A. A.; Lehel, S.; Gillings, N.; Herth, M. M.; Knudsen, G. M.; Kristensen, J. L., Convergent ^{18}F-labeling and evaluation of N-benzyl-phenethylamines as 5-HT2A receptor PET ligands. *Bioorganic & medicinal chemistry* **2016,** *24* (21), 5353-5356.

14. Herth, M. M.; Leth-Petersen, S.; Lehel, S.; Hansen, M.; Knudsen, G. M.; Gillings, N.; Madsen, J.; Kristensen, J. L., Accelerating preclinical PET-screening: reductive amination with [^{11}C]methoxybenzaldehydes. *RSC Advances* **2014,** *4* (41), 21347-21350.

15. Volk, B.; Barkóczy, J.; Hegedus, E.; Udvari, S.; Gacsályi, I.; Mezei, T.; Pallagi, K.; Kompagne, H.; Lévay, G.; Egyed, A., (Phenylpiperazinyl-butyl) oxindoles as selective 5-HT_7 receptor antagonists. *Journal of medicinal chemistry* **2008,** *51* (8), 2522-2532.

16. Herth, M. M.; Andersen, V. L.; Hansen, H. D.; Stroth, N.; Volk, B.; Lehel, S.; Dyssegaard, A.; Ettrup, A.; Svenningsson, P.; Knudsen, G. M.; Kristensen, J. L., Evaluation of 3-Ethyl-3-(phenylpiperazinylbutyl)oxindoles as PET Ligands for the Serotonin 5-HT_7 Receptor: Synthesis, Pharmacology, Radiolabeling, and *in Vivo* Brain Imaging in Pigs. *Journal of medicinal chemistry* **2015,** *58* (8), 3631-6.

17. Herth, M. M.; Hansen, H. D.; Ettrup, A.; Dyssegaard, A.; Lehel, S.; Kristensen, J.; Knudsen, G. M., Synthesis and evaluation of [(1)(1)C]Cimbi-806 as a potential PET ligand for 5-HT_7 receptor imaging. Bioorganic & Medicinal Chemistry **2012,** *20* (14), 4574-81.

18. Herth, M. M.; Volk, B.; Pallagi, K.; Kofoed Bech, L.; Antoni, F. A.; Knudsen, G. M.; Kristensen, J. L., Synthesis and *in vitro* evaluation of oxindole derivatives as potential radioligands for 5-HT(7) receptor imaging with PET. *ACS Chemical Neuroscience* **2012,** *3* (12), 1002-7.

19. Volk, B.; Gacsályi, I.; Pallagi, K.; Poszávácz, L.; Gyönös, I.; Szabó, É.; Bakó, T.; Spedding, M.; Simig, G.; Szénási, G., Optimization of (arylpiperazinylbutyl) oxindoles exhibiting selective 5-HT_7 receptor antagonist activity. *Journal of medicinal chemistry* **2011,** *54* (19), 6657-6669.

20. Shaquiquzzaman, M.; Verma, G.; Marella, A.; Akhter, M.; Akhtar, W.; Khan, M. F.; Tasneem, S.; Alam, M. M., Piperazine scaffold: A remarkable tool in generation of diverse pharmacological agents. *European journal of medicinal chemistry* **2015,** *102*, 487-529.

21. Yonar, D.; Sünnetçioğlu, M. M., Spectroscopic and calorimetric studies on trazodone hydrochloride–phosphatidylcholine liposome interactions in the presence and absence of cholesterol. *Biochimica et Biophysica Acta (BBA)-Biomembranes* **2014,** *1838* (10), 2369-2379.

22. Zajdel, P.; Marciniec, K.; Maślankiewicz, A.; Grychowska, K.; Satała, G.; Duszyńska, B.; Lenda, T.; Siwek, A.; Nowak, G.; Partyka, A., Antidepressant and antipsychotic activity of new quinoline-and isoquinoline-sulfonamide analogs of aripiprazole targeting serotonin 5-HT_{1A}/5-HT_{2A}/5-HT_7 and dopamine D 2/D 3 receptors. *European journal of medicinal chemistry* **2013,** *60*, 42-50.

23. Pike, V. W.; Aigbirhio, F. I., Reactions of cyclotron-produced [^{18}F] fluoride with diaryliodonium salts—a novel single-step route to no-carrier-added [^{18}F] fluoroarenes. *Journal of the Chemical Society, Chemical Communications* **1995,** (21), 2215-2216.

24. Ross, T. L.; Ermert, J.; Hocke, C.; Coenen, H. H., Nucleophilic ^{18}F-fluorination of heteroaromatic iodonium salts with no-carrier-added [^{18}F] fluoride. *Journal of the American Chemical Society* **2007,** *129* (25), 8018-8025.

25. Ichiishi, N.; Brooks, A. F.; Topczewski, J. J.; Rodnick, M. E.; Sanford, M. S.; Scott, P. J., Copper-catalyzed [^{18}F] fluorination of (mesityl)(aryl) iodonium salts. *Organic letters* **2014,** *16* (12), 3224-3227.

26. Rotstein, B. H.; Stephenson, N. A.; Vasdev, N.; Liang, S. H., Spirocyclic hypervalent iodine (III)-mediated radiofluorination of non-activated and hindered aromatics. *Nature communications* **2014,** *5*, 4365.

27. Tredwell, M.; Preshlock, S. M.; Taylor, N. J.; Gruber, S.; Huiban, M.; Passchier, J.; Mercier, J.; Génicot, C.; Gouverneur, V., A general copper-mediated nucleophilic ^{18}F fluorination of arenes. *Angewandte Chemie* **2014,** *126* (30), 7885-7889.

28. Mossine, A. V.; Brooks, A. F.; Makaravage, K. J.; Miller, J. M.; Ichiishi, N.; Sanford, M. S.; Scott, P. J., Synthesis of [^{18}F] arenes via the copper-mediated [^{18}F] fluorination of boronic acids. *Organic letters* **2015,** *17* (23), 5780-5783.

29. Makaravage, K. J.; Brooks, A. F.; Mossine, A. V.; Sanford, M. S.; Scott, P. J., Copper-Mediated Radiofluorination of Arylstannanes with [^{18}F] KF. *Organic letters* **2016,** *18* (20), 5440-5443.

30. Preshlock, S.; Calderwood, S.; Verhoog, S.; Tredwell, M.; Huiban, M.; Hienzsch, A.; Gruber, S.; Wilson, T. C.; Taylor, N. J.; Cailly, T., Enhanced copper-mediated ^{18}F-fluorination of aryl boronic esters provides eight radiotracers for PET applications. *Chemical Communications* **2016,** *52* (54), 8361-8364.

31. Petersen, I. N.; Kristensen, J. L.; Herth, M. M., Nucleophilic ^{18}F-labeling of spirocyclic iodonium ylide or boronic pinacol ester precursors: advantages and disadvantages. *European Journal of Organic Chemistry* **2017,** *2017* (3), 453-458.

32. Hume, S. P.; Gunn, R. N.; Jones, T., Pharmacological constraints associated with positron emission tomographic scanning of small laboratory animals. *European journal of nuclear medicine* **1998,** *25* (2), 173-176.

33. Innis, R. B.; Cunningham, V. J.; Delforge, J.; Fujita, M.; Gjedde, A.; Gunn, R. N.; Holden, J.; Houle, S.; Huang, S.-C.; Ichise, M., Consensus nomenclature for *in vivo* imaging of reversibly binding radioligands. *Journal of Cerebral Blood Flow & Metabolism* **2007,** *27* (9), 1533-1539.

Supplementary information

Fragment-based Labelling Using Condensation Reactions – A Possibility to Increase Throughput in Preclinical PET

Elina Tampio L'Estrade[a,b,c], Szabolcs Lehel[d], Ida Nymann Petersen[d], Fraser G. Edgar[b], Balázs Volk[e], Tomas Ohlsson[c], Maria Erlandsson[c], Gitte M. Knudsen[a,f] and Matthias M. Herth[a,b,d,*]

[a] *Neurobiology Research Unit, Rigshospitalet, Blegdamsvej 9, 2100 Copenhagen, Denmark*

[b] *Department for Drug Design and Pharmacology, Faculty of Health and Medical Sciences, University of Copenhagen, Universitetesparken 2, 2100 Copenhagen, Denmark*

[c] *Radiation Physics, Nuclear Medicine Physics Unit, Skånes University Hospital, Barngatan 3, 222 42 Lund, Sweden.*

[d] *Department of Clinical Physiology, Nuclear Medicine and PET, University Hospital Copenhagen, Rigshospitalet Blegdamsvej 9, 2100 Copenhagen, Denmark*

[e] *Directorate of Drug Substance Development, Egis Pharmaceuticals Plc., P.O. Box 100, H-1475 Budapest, Hungary*

[f] *Institute of Clinical Medicine, Faculty of Health and Medical Sciences, University of Copenhagen, Denmark*

CONTENTS

EXPERIMENTAL/MATERIAL AND METHODS 127

GENERAL RADIOCHEMISTRY 134

CHROMATOGRAPHIC INFORMATION 141

REFERENCES 149

APPENDICES 150

Experimental/Material and methods

General information

Solvents and reagents were purchased from Sigma Aldrich (Merck, Darmstadt, Germany) or Thermo Fisher Scientific and used as received unless otherwise noted. Three butyloxindole analogues were received from Balázs Volk. The reference compounds **ENL20 and Cimbi-775** were aquired from Matthias Herth. NMR (^{1}H, ^{13}C) spectra were acquired on a 600 MHz Bruker Avance III HD or a 400 MHz Bruker Avance II at room temperature. Chemical shift (δ) are expressed in parts per million and referenced to residual solvent peak. The resonance multiplicity is abbreviated as follows or combinations thereof: s (singlet), d (doublet), t (triplet), q (quartet), p (quintet) and m (multiplet). The analysis of the NMR spectra was performed using the software MestReNova v12.0.0 (Mestrelab Research S.L.). Thin-layer chromatography (TLC) was run on silica plated aluminium sheets (Silica gel 60 F254) from Merck and the spots were visualized by ultraviolet light at 254 nm. Flash column chromatography was carried out manually on silica gel 60 (0.040–0.063 mm). Analytical high performance liquid chromatography (HPLC) was performed on a Dionex system consisting of a P680A pump and a UVD 170U detector. The HPLC system was controlled by Chromeleon 6.8 software. The molecular names are acquired from ChemDraw Proffesional.

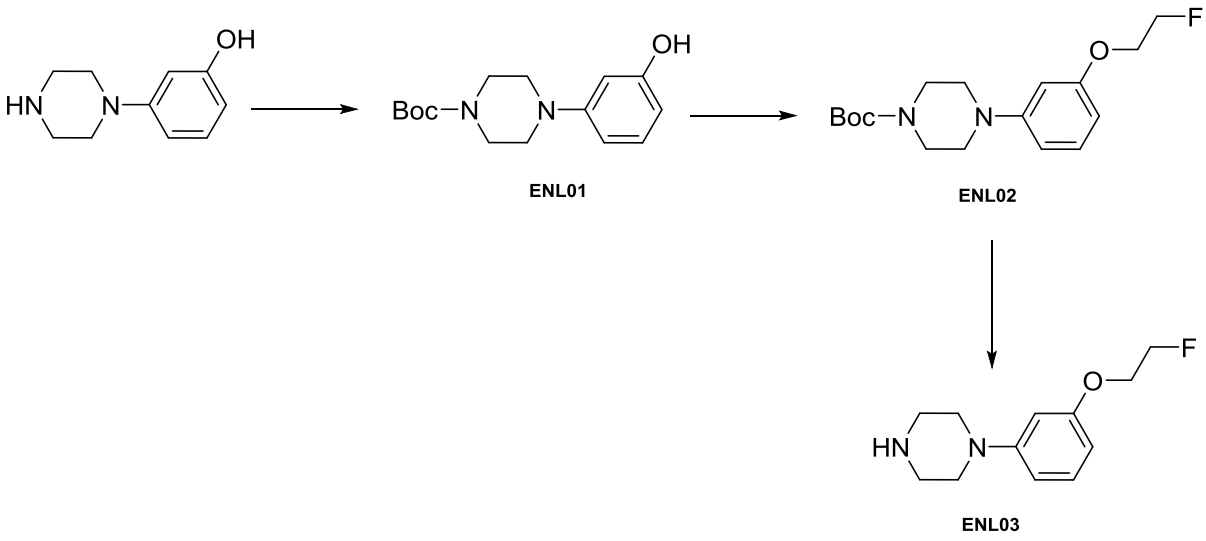

Supplementary Scheme 1: Overview of the synthetic route of the reference compound ENL03.

4-(3-Hydroxyphenyl)-piperazine-1-Boc **(ENL01)**[1]

To a solution of *N*-(3-hydroxyphenyl) piperazine (5.00 g, 28.1 mmol) and $NaHCO_3$ (4.11g, 49.3 mmol) in THF (70 mL), H_2O (70 mL) and Dioxane (70 mL); di-tert–butyl dicarbonate (7.32 g, 33.9 mmol) was added and stirred over night at room temperature. The solution was diluted with water and extracted using DCM, and thereafter dried with Na_2SO_4 and evaporated *in vacuo*; ENL01 was afforded as an orange/white solid (639.5 mg, 91.9%). ^{1}H NMR (400 MHz, chloroform-*d*) δ 7.11 (t, *J* = 8.1 Hz, 1H), 6.49 (dd, *J* = 8.3, 2.3 Hz, 1H), 6.40 (t, *J* = 2.4 Hz, 1H), 6.34 (dd, *J* = 8.0, 2.3 Hz, 1H), 3.56 (t, *J* = 5.2 Hz, 4H), 3.16–3.08 (m, 4H), 1.48 (s, 9H). ^{13}C NMR (151 MHz, chloroform-*d*) δ 156.82, 154.94, 152.88, 130.23, 109.10, 107.22, 103.62, 80.22, 49.27, 28.59. UPLC-MS (ESI): RT: 1.46 min, m/z: 279.1 $[M^+H]^+$ at 215-254 nm. R_f: 0.23 (Hep:EtOAc 7:3). **Appendices 1-3**

4-(3-(2-Flouro-ethoxy)-phenyl)-piperazine-1-Boc **(ENL02)**[1]

To a solution of **ENL01** (0.842 g, 3.00 mmol) in dry DMF (21 mL), sodium hydride (60%) (126.4 mg, 3.00 mmol) was added portion wise, under nitrogen and on cooling (ice-bath). Thereafter it was left stirring for another 30 min. When at 0 °C 1.2-Bromoflouroethane (0.22 mL, 3 mmol) was slowly added. This mixture was then stirred for an additional 20 h at 60 °C and then evaporated *in vacuo*. The residue was dissolved in ethyl acetate (EtOAc) and washed with water and brine and it was extracted using EtOAc. The organic layers were dried over $MgSO_4$. Column chromatography (CC) (Hept/EtOAc 7:3) afforded ENL02 as a yellow oil (435.7 mg, 45%). ^{1}H NMR (400 MHz, chloroform-*d*) δ 7.18 (t, *J* = 8.2 Hz, 1H), 6.61–6.55 (m, 1H), 6.52 (s, 1H), 6.48–6.42 (m, 1H), 4.87–4.59 (m, 2H), 4.20 (ddd, *J* = 27.8, 5.1, 3.2 Hz, 2H), 3.57 (t, *J* = 5.1 Hz, 4H), 3.14 (t, *J* = 5.2 Hz, 4H), 1.48 (s, 9H).^{13}C NMR (101 MHz, chloroform-*d*) δ 159.61, 154.86, 130.09, 110.06, 104.05, 100.13, 82.95, 81.25, 80.09, 67.25, 28.58. UPLC-MS (ESI): RT: 4.33 min, m/z: 325.1 $[M^+H]^+$ at 215-254 nm. R_f: 0.21 (Hept/EtOAc 7:3). **Appendices 4-6.**

1-[3-(2-Fluoro-ethoxy)-phenyl]-piperazine **(ENL03)**[1]

ENL02 was dissolved in 4M HCl in dioxane (20 mL) and left stirring for 90 min. It was then concentrated by rotary evaporation to a yellow solid (737.5 mg, >99%). ^{1}H NMR (400 MHz, chloroform-*d*) δ 7.18 (t, *J* = 8.2 Hz, 1H), 6.63–6.40 (m, 3H), 4.83–4.64 (m, 2H), 4.20 (ddd, *J* = 27.8, 5.1, 3.2 Hz, 2H), 3.57 (t, *J* = 5.1 Hz, 4H), 3.14 (t, *J* = 5.2 Hz, 4H), 1.48 (s, 9H). ^{13}C NMR (151 MHz, DMSO-d_6) δ 159.13, 151.34, 129.91, 108.76, 105.65, 102.76, 82.17, 66.90, 45.38, 42.51. UPLC-MS (ESI): RT: 2.81 min, m/z: 225.2 $[M^+H]^+$ at 215-254 nm. R_f: 0.29 ($CHCl_3$:MeOH:Et_3N 90:9:1). **Appendices 7-9.**

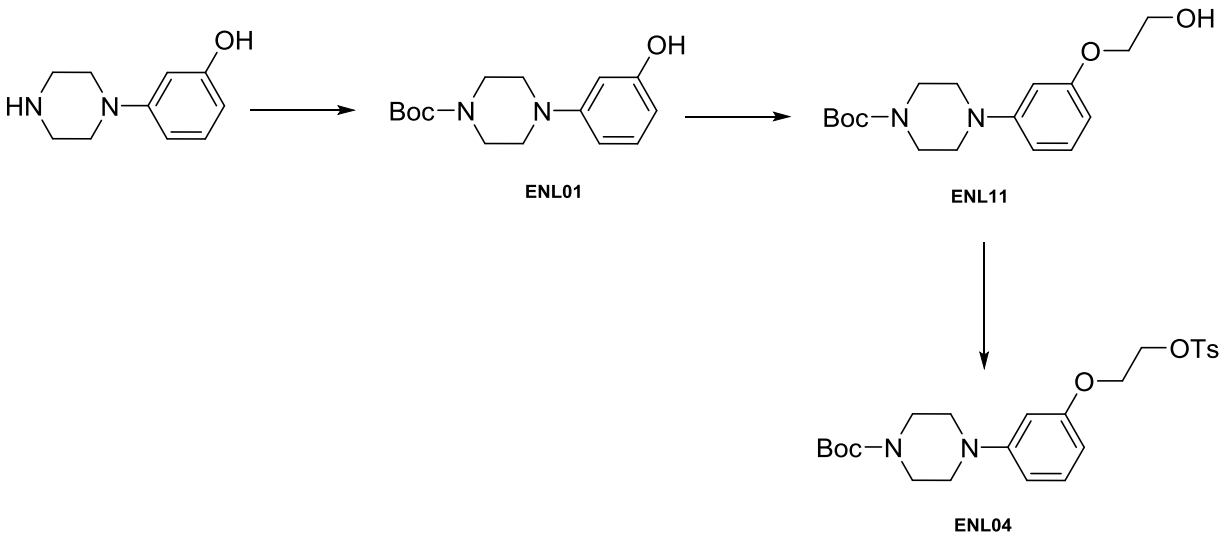

Supplementary Scheme 2: Overview of the synthetic route of the precursor ENL04.

tert-Butyl 4-(3-(2-hydroxyethoxy)phenyl)piperazine-1-carboxylate **(ENL11)**

A mixture of **ENL01** (400 mg, 1.44 mmol), 2-bromoethanol (0.15 mL, 2.16 mmol) and sodium carbonate (362.9 mg, 4.32 mmol) in DMF (15 mL) was heated for six hours at 90 °C. The mixture was then cooled to room temperature, followed by a dilution with water. The mixture was then further diluted with diethyl ether, and the organic layer was separated. The combined organic layers were washed with brine, dried over magnesium sulfate and concentrated *in vacuo*. The residue was purified using flash chromatography (EtOAc:Hept 1:1) to yield pure **ENL11** as a solid yellow oil (275 mg, 59%). ^{1}H NMR (400 MHz, chloroform-*d*) δ 7.17 (t, *J* = 8.2 Hz, 1H), 6.55 (dd, *J* = 8.3, 2.3 Hz, 1H), 6.48 (d, *J* = 2.4 Hz, 1H), 6.44 (dd, *J* = 8.2, 2.3 Hz, 1H), 4.11–4.02 (m, 2H), 3.94 (t, *J* = 4.5 Hz, 2H), 3.56 (t, *J* = 5.2 Hz, 4H), 3.12 (t, *J* = 5.1 Hz, 4H), 1.48 (s, 9H). UPLC-MS (ESI): RT: 4.23 min, m/z: 323.2 $[M^{+}H]^{+}$ at 215-254 nm. R_f: 0.3 (Hep:EtOAc 1:1). **Appendices 10-11.**

tert-Butyl 4-(3-(2-(tosyloxy)ethoxy)phenyl)piperazine-1-carboxylate **(ENL04)**.[2]

ENL11 (120.5 mg, 0.37 mmol) was dissolved in DCM (10 mL) in a round-bottom flask, to which p-TsCl (70.5 mg, 0.37 mmol) and DMAP (1 mg, 8.2 μmol) were added. A reflux condenser was attached and the resultant solution stirred for 10 minutes. Triethylamine (58.5 μL, 0.42 mmol) was then added dropwise to the reaction over 15 minutes, as a result the trimethylammonium salt precipitated, with the release of heat (visible condensation on the condenser). After 1 hour, the reflux condenser was removed and replaced by a stopper. The reactions progress was monitored by TLC to observe the consumption of starting materials. Following reaction completion, 1M HCl was added. The organic layer was separated, washed,

dried and concentrated. The product **ENL04** was yielded as a light yellow oil and did not require further purification (134.7 mg, 76.4%). ^{1}H NMR (600 MHz, chloroform-*d*) δ 7.85–7.80 (m, 2H), 7.34 (d, *J* = 8.1 Hz, 2H), 7.13 (t, *J* = 8.2 Hz, 1H), 6.54 (dd, *J* = 8.3, 2.3 Hz, 1H), 6.36 (t, *J* = 2.4 Hz, 1H), 6.31 (dd, *J* = 8.2, 2.3 Hz, 1H), 4.38–4.33 (m, 2H), 4.16–4.12 (m, 2H), 3.56 (t, *J* = 5.1 Hz, 4H), 3.11 (t, *J* = 5.2 Hz, 4H), 2.45 (s, 3H), 1.48 (s, 9H). ^{13}C NMR (151 MHz, chloroform-*d*) δ 159.01, 154.65, 152.57, 144.82, 132.92, 129.82, 127.97, 109.84, 105.36, 103.65, 79.88, 68.06, 65.39, 49.13, 46.19, 28.38, 21.61. UPLC-MS (ESI): RT: 3.06 min, m/z: 477.6 $[M^{+}H]^{+}$ at 215 - 254 nm. R_f: 0.64 (90:9:1 $CHCl_3$:MeOH:Et_3N). **Appendices 12-14**

tert-Butyl 4-(4-fluorophenyl)piperazine-1-carboxylate **(FGE06):**

To a solution of 1-(4-Fluorophenyl)piperazine (121 mg, 0.671 mmol) and sodium carbonate (128.2 mg, 1.209 mmol) in THF (1.7 mL), water (1.7 mL), dioxane (1.7 mL), di-*tert*-butyldicarbonate (175.7 mg, 0.805 mmol) was added. The solution was stirred overnight at room temperature. The solution was diluted with water and extracted with DCM. Thereafter the organic layer was dried with $MgSO_4$, and the resultant solution concentrated *in vacuo* (120 mg, 85.7%). ^{1}H NMR (400 MHz, DMSO-d_6) δ 7.06 (dd, *J* = 9.2, 8.5 Hz, 2H), 6.99–6.93 (m, 2H), 3.45 (t, *J* = 5.2 Hz, 5H), 3.02 (dd, *J* = 6.2, 4.2 Hz, 4H), 1.42 (s, 9H). ^{13}C NMR (151 MHz, DMSO-d_6) δ 157.10, 155.54, 153.87, 147.86, 117.85, 115.42, 115.28, 79.03, 49.22, 28.09. Appendices **15-16**

3-(4-Hydroxybutyl)indolin-2-one **(ENL12):**[3]

A mixture of 2-oxindole (1.99 g, 15 mmol), butan-1,4-diol (30 mL, 340 mmol) and Raney® nickel (1.62 g) was heated to 200 °C in acetone in an autoclave and stirred overnight. Following cooling the reaction, the mixture was diluted with acetone, filtered over celite and the filtrate concentrated. The excess alcohol was then removed using Kugelrohr distillation. The product was purified using column chromatography (EtOAc; 846.1 mg, 27.4%). ^{1}H NMR (600 MHz, DMSO-d_6) δ 10.31 (s, 1H), 7.23 (d, *J* = 7.3 Hz, 1H), 7.16 (tt, *J* = 7.7, 1.0 Hz, 1H), 6.94 (td, *J* = 7.5, 1.0 Hz, 1H), 6.81 (d, *J* = 7.7 Hz, 1H), 4.32 (t, *J* = 5.1 Hz, 1H), 3.41 (t, *J* = 5.9 Hz, 1H), 3.36–3.32 (m, 2H), 1.87 (ddt, *J* = 13.4, 11.0, 5.5 Hz, 1H), 1.76 (tdd, *J* = 11.3, 8.5, 5.5 Hz, 1H), 1.42–1.33 (m, 2H), 1.24 (m, *J* = 21.2, 13.2, 11.3, 5.3 Hz, 1H). ^{13}C NMR (151 MHz, DMSO-d_6) δ 178.86, 142.74, 129.73, 127.48, 123.92, 121.17, 109.06, 60.50, 45.13, 32.53, 29.78, 21.83. UPLC-MS (ESI): RT: 1.54 min, m/z: 206.1 $[M^{+}H]^{+}$ at 215-254 nm. R_f: 0.44 (EtOAc). **Appendices 17-19.**

4-(2-Oxoindolin-3-yl)butyl methanesulfonate **(ENL14):**[3]

ENL12 (358.5 mg, 1.70 mmol) was dissolved in THF (2.5 mL). Triethyl amine (0.47 mL, 3.4 mmol) was then added, and the solution cooled to -78 °C, thereafter MsCl (0.26 mL, 3.4 mmol) was added dropwise. After addition, the mixture was warmed to room temperature and stirred for a further hour. The white precipitate was filtered off, and the filtrate concentrated. The residual oil was dissolved in ethyl acetate, and extracted with 2M HCl until pH 5. The organic layer was dried over sodium sulfate, and evaporated. The product should be pure enough for direct use, alternatively product can be purified by flash chromatography (242.4 mg, 50%). ^{1}H NMR (600 MHz, chloroform-*d*) δ 7.50 (s, 1H), 7.17–7.13 (m, 2H), 6.97 (td, *J* = 7.5, 1.0 Hz, 1H), 6.81–6.78 (m, 1H), 4.15–4.11 (m, 2H), 3.42 (t, *J* = 6.0 Hz, 1H), 2.91 (s, 3H), 1.99–1.92 (m, 2H), 1.71 (dddd, *J* = 12.9, 9.0, 6.5, 2.8 Hz, 2H), 1.47–1.34 (m, 2H). ^{13}C NMR (151 MHz, chloroform-*d*) δ 179.10, 141.14, 129.14, 127.99, 124.13, 122.43, 109.44, 77.16, 76.95, 76.74, 69.40, 45.47, 37.34, 29.72, 28.98, 21.66. UPLC-MS (ESI): RT: 3.16 min, m/z: 382.2 $[M^{+}H]^{+}$ at 215-254 nm. R_f: 0.78 (EtOAc). **Appendices 20-22**

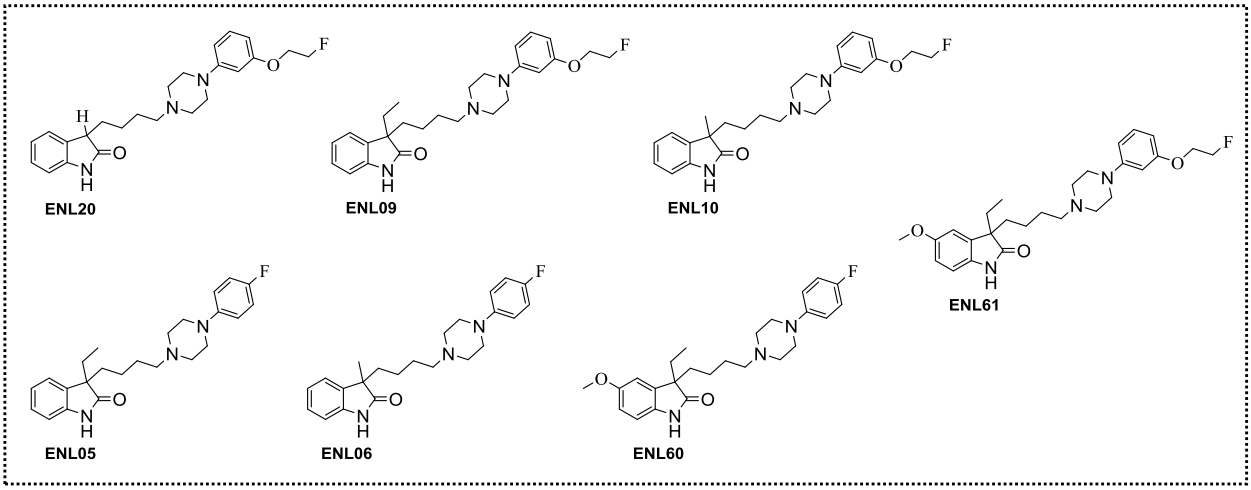

Supplementary Scheme 3: Molecular strutures of all the synthesized compounds

General synthesis of reference compounds[3-5]

The melt of the secondary amine (0.5 mmol) and sodium carbonate (0.5 mmol) was heated to 120 °C under slow stirring. Thereafter the oxindole (0.5 mmol) was added and after 1 h reaction time, the crude mixture was cooled to ambient temperature. Ethyl acetate and water were added to the residue and the layers were separated. The organic layer was dried over $MgSO_4$ and evaporated *in vacuo*. CC (EtOAc) afforded the isolated product.

3-(4-(4-(3-(2-Fluoroethoxy)phenyl)piperazin-1-yl)butyl)indolin-2-one **(ENL20):**[3]

This reference was received from Matthias Herth.

^{1}H NMR (600 MHz, DMSO-d_6) δ 10.33 (s, 1H), 7.26 (d, *J* = 7.4 Hz, 1H), 7.18 (tt, *J* = 7.7, 1.1 Hz, 1H), 7.12 (t, *J* = 8.2 Hz, 1H), 6.96 (td, *J* = 7.5, 1.0 Hz, 1H), 6.83 (d, *J* = 7.7 Hz, 1H), 6.54 (dd, *J* = 8.1, 2.3 Hz, 1H), 6.47 (t, *J* = 2.4 Hz, 1H), 6.39 (dd, *J* = 8.0, 2.3 Hz, 1H), 4.79–4.75 (m, 1H), 4.72–4.65 (m, 1H), 4.26–4.20 (m, 1H), 4.19–4.15 (m, 1H), 3.45 (t, *J* = 5.9 Hz, 1H), 3.10 (t, *J* = 5.0 Hz, 4H), 2.44 (t, *J* = 5.0 Hz, 4H), 2.27 (t, *J* = 7.1 Hz, 2H), 1.96–1.76 (m, 2H), 1.45 (h, *J* = 7.1, 6.5 Hz, 2H), 1.35–1.25 (m, 2H). ^{13}C NMR (151 MHz, DMSO-d_6) δ 178.72, 159.07, 152.88, 142.81, 129.72, 129.62, 127.49, 123.93, 121.16, 109.07, 104.48, 101.89, 99.49, 82.20, 66.86, 57.57, 52.65, 48.06, 45.04, 29.65, 26.19, 23.12. UPLC-MS (ESI): RT: 2.93 min, m/z: 412.3 $[M^+H]^+$ at 215-254 nm. **Appendices 23-25**

3-(4-(4-(3-(2-Fluoroethoxy)phenyl)piperazin-1-yl)butyl)-3-methylindolin-2-one **(ENL10):**

57.1 mg, 27%. ^{1}H NMR (600 MHz, DMSO-d_6) δ 10.30 (s, 1H), 7.22 (dd, *J* = 7.4, 1.2 Hz, 1H), 7.15 (td, *J* = 7.7, 1.2 Hz, 1H), 7.09 (t, *J* = 8.2 Hz, 1H), 6.96 (td, *J* = 7.5, 1.0 Hz, 1H), 6.83 (d, *J* = 7.7 Hz, 1H), 6.50 (dd, *J* = 8.2, 2.3 Hz, 1H), 6.43 (t, *J* = 2.3 Hz, 1H), 6.36 (dd, *J* = 8.1, 2.3 Hz, 1H), 4.75–4.72 (m, 1H), 4.67–4.64 (m, 1H), 4.22–4.18 (m, 1H), 4.17–4.13 (m, 1H), 3.04 (t, *J* = 5.0 Hz, 4H), 2.61 (p, *J* = 1.8 Hz, 1H), 2.40–2.33 (m, 4H), 2.19–2.11 (m, 2H), 1.73 (ddd, *J* = 9.7, 5.7, 3.2 Hz, 2H), 1.36–1.24 (m, 1H), 1.22 (s, 3H), 1.01–0.73 (m, 2H). ^{13}C NMR (151 MHz, DMSO-d_6) δ 181.54, 159.04, 152.43, 141.58, 134.29, 129.61, 127.43, 122.84, 121.40, 109.17, 108.26, 104.47, 101.88, 99.49, 82.75, 81.65, 66.86, 57.46, 52.57, 48.01, 47.93, 37.53, 26.29, 23.77, 22.08. UPLC-MS (ESI): RT: 3.29 min, m/z: 426.3 $[M^+H]^+$ at 215-254 nm. R_f: 0.15 (EtOAc). **Appendices 26–28.**

3-Ethyl-3-(4-(4-(3-(2-fluoroethoxy)phenyl)piperazin-1-yl)butyl)indolin-2-one **(ENL09):**

7.0 mg, 4%. ^{1}H NMR (600 MHz, chloroform-*d*) δ 7.93–7.85 (m, 1H), 7.20 (td, *J* = 7.6, 1.3 Hz, 1H), 7.15 (t, *J* = 8.2 Hz, 1H), 7.11 (d, *J* = 7.3 Hz, 1H), 7.05 (td, *J* = 7.5, 1.0 Hz, 1H), 6.87 (d, *J* = 7.7 Hz, 1H), 6.53 (dd, *J* = 8.3, 2.3 Hz, 1H), 6.47 (t, *J* = 2.3 Hz, 1H), 6.41 (dd, *J* = 8.1, 2.3 Hz, 1H), 4.77 (dd, *J* = 4.8, 3.5 Hz, 1H), 4.69 (dd, *J* = 4.8, 3.5 Hz, 1H), 4.21 (dd, *J* = 4.9, 3.5 Hz, 1H), 4.17 (dd, *J* = 4.9, 3.4 Hz, 1H), 3.19 (t, *J* = 5.0 Hz, 4H), 2.63–2.58 (m, 4H), 2.33 (d, *J* = 8.4 Hz, 2H), 1.96–1.88 (m, 2H), 1.78 (ddd, *J* = 12.7, 7.9, 5.1 Hz, 2H), 1.52–1.40 (m, 2H), 1.26 (t, *J* = 4.9 Hz, 1H), 1.11 (tdd, *J* = 18.0, 9.8, 5.4 Hz, 1H), 0.92 (tdd, *J* = 17.4, 9.9, 5.1 Hz, 1H), 0.63 (t, *J* = 7.4 Hz, 3H). ^{13}C NMR (151 MHz, chloroform-*d*) δ 181.83, 159.34, 141.02, 132.38, 129.79, 127.60, 123.05, 122.41, 109.31, 103.34, 82.47, 81.34, 66.91, 57.94, 53.98, 52.74, 48.44, 37.37,

31.06, 22.15, 8.47. UPLC-MS (ESI): RT: 3.61 min, m/z: 440.3 $[M^+H]^+$ at 215 - 254 nm. R_f: 0.15 (EtOAc). **Appendices 29–31**

3-Ethyl-3-(4-(4-(3-(2-fluoroethoxy)phenyl)piperazin-1-yl)butyl)-5-methoxyindolin-2-one **(ENL61):**

64.4 mg, 27.4%. ^{1}H NMR (600 MHz, chloroform-*d*) δ 8.50 (s, 1H), 7.14 (t, *J* = 8.2 Hz, 1H), 6.81–6.78 (m, 1H), 6.74–6.70 (m, 2H), 6.53 (dd, *J* = 8.3, 2.3 Hz, 1H), 6.47 (t, *J* = 2.4 Hz, 1H), 6.39 (dd, *J* = 8.1, 2.3 Hz, 1H), 4.78–4.74 (m, 1H), 4.70–4.67 (m, 1H), 4.22–4.19 (m, 1H), 4.17–4.14 (m, 1H), 3.80–3.77 (m, 27H), 3.14 (t, *J* = 5.0 Hz, 4H), 2.49 (t, *J* = 5.0 Hz, 4H), 2.27–2.21 (m, 2H), 1.91 (ddd, *J* = 13.5, 8.3, 6.0 Hz, 2H), 1.81–1.69 (m, 2H), 1.49–1.35 (m, 1H), 1.11 (tdt, *J* = 13.4, 10.1, 5.3 Hz, 1H), 0.95–0.86 (m, 1H), 0.63 (t, *J* = 7.4 Hz, 3H). ^{13}C NMR (151 MHz, chloroform-*d*) δ 182.46, 159.49, 155.96, 152.85, 134.91, 134.28, 129.88, 111.74, 110.65, 109.44, 104.83, 103.30, 82.67, 81.55, 67.21, 58.33, 55.85, 54.84, 53.18, 48.95, 37.77, 31.27, 27.01, 22.40, 8.70. UPLC-MS (ESI): RT: 3.22 min, m/z: 470.4 $[M^+H]^+$ at 215 - 254 nm. R_f: 0.18 (EtOAc). **Appendices 32-34.**

3-(4-(4-(4-Fluorophenyl)piperazin-1-yl)butyl)-3-methylindolin-2-one **(ENL06):**

63.2 mg, 33%. ^{1}H NMR (600 MHz, DMSO-d_6) δ 10.30 (s, 1H), 7.22 (dd, *J* = 7.1, 1.2 Hz, 1H), 7.15 (td, *J* = 7.6, 1.3 Hz, 1H), 7.09–6.99 (m, 2H), 6.96 (td, *J* = 7.5, 1.1 Hz, 1H), 6.92–6.88 (m, 2H), 6.83 (d, *J* = 7.7 Hz, 1H), 2.99 (t, *J* = 4.9 Hz, 4H), 2.61 (p, *J* = 1.9 Hz, 2H), 2.40–2.36 (m, 6H), 2.19–2.12 (m, 2H), 1.73 (ddd, *J* = 9.6, 5.7, 3.1 Hz, 2H), 1.22 (s, 3H). ^{13}C NMR (151 MHz, DMSO-d_6) δ 181.52, 159.84, 147.94, 141.58, 134.29, 127.43, 122.83, 121.40, 116.94, 115.17, 109.17, 57.43, 52.59, 48.90, 47.93, 37.53, 26.30, 23.77, 22.08. UPLC-MS (ESI): RT: 3.16 min, m/z: 382.2 $[M^+H]^+$ at 215-254 nm. R_f: 0.26 (EtOAc). **Appendices 35-37**

3-Ethyl-3-(4-(4-(4-fluorophenyl)piperazin-1-yl)butyl)indolin-2-one **(ENL05):**[4]

109.9 mg, 55%.^{1}H NMR (600 MHz, DMSO-d_6) δ 10.33 (s, 1H), 7.29–7.08 (m, 2H), 7.06–6.96 (m, 3H), 6.95–6.89 (m, 2H), 6.84 (d, *J* = 7.7 Hz, 1H), 3.00 (t, *J* = 4.9 Hz, 4H), 2.55–2.53 (m, 1H), 2.40 (tdd, *J* = 6.5, 4.3, 2.1 Hz, 4H), 2.16 (ddd, *J* = 8.1, 6.5, 3.2 Hz, 2H), 1.80–1.68 (m, 4H), 1.37–1.23 (m, 2H), 1.03–0.93 (m, 1H), 0.51 (t, *J* = 7.4 Hz, 3H). ^{13}C NMR (151 MHz, DMSO-d_6) δ 180.80, 155.10, 147.95, 142.47, 132.24, 127.44, 122.97, 121.39, 116.94, 115.17, 109.01, 57.44, 53.13, 52.58, 48.89, 36.88, 30.32, 26.36, 21.86, 8.39. UPLC-MS (ESI): RT: 3.13 min, m/z: 396.3 $[M^+H]^+$ at 215-254 nm. R_f: 0.16 (EtOAc). **Appendices 38-40.**

3-Ethyl-3-(4-(4-(4-fluorophenyl)piperazin-1-yl)butyl)-5-methoxyindolin-2-one **(ENL60):** 101.1 mg, 47%. ^{1}H NMR (600 MHz, DMSO-d_6) δ 10.13 (s, 1H), 7.02 (t, *J* = 8.9 Hz, 2H), 6.92–6.88 (m, 2H), 6.84 (t, *J* = 1.5 Hz, 1H), 6.72 (d, *J* = 1.5 Hz, 2H), 3.69 (s, 3H), 2.99 (t, *J* = 5.0 Hz, 4H), 2.61 (p, *J* = 1.9 Hz, 1H), 2.40–2.36 (m, 4H), 2.19–2.13 (m, 2H), 1.76–1.65 (m, 4H), 1.29 (dtd, *J* = 34.9, 14.2, 13.3, 6.8 Hz, 2H), 0.94 (td, *J* = 17.3, 16.6, 6.3 Hz, 1H), 0.49 (t, *J* = 7.4 Hz, 3H). ^{13}C NMR (151 MHz, DMSO-d_6) δ 181.14, 155.35, 136.22, 134.20, 117.51, 115.60, 112.24, 110.75, 109.72, 55.83, 54.18, 52.99, 37.34, 30.83, 22.27, 8.91. UPLC-MS (ESI): RT: 3.21 min, m/z: 426.3 $[M^{+}H]^{+}$ at 215-254 nm. R_f: 0.12 (EtOAc). **Appendices 41-43.**

General Radiochemistry

Precursors, solvents and reagents were purchased from Sigma Aldrich (Merck, Darmstadt, Germany) or Thermo Fisher Scientific and used as received unless otherwise noted. [^{11}C]Methane was produced via the ^{14}N(p,α)^{11}C reaction by bombardment of an [^{14}N]N_2 target containing 10% H_2 with a 17 MeV proton beam in a Scanditronix MC32NI cyclotron. [^{11}C]Carbon dioxide was produced via the ^{14}N(p,α)^{11}C reaction by bombardment of an [^{14}N]N_2 target containing 0.1-2% O_2 with a 11 MeV proton beam in a CTI/Siemens Eclipse with 2 aluminium high pressure gas targets.

[^{18}F]Fluoride was produced via the (p,n)-reaction in a cyclotron (CTI Siemens and Scanditronix, Rigshospitalet, Denmark) by irradiating [^{18}O]H_2O with a 11 MeV proton beam. Analytical high performance liquid chromatography (HPLC) was performed on a Dionex system consisting of a P680A pump, a UVD 170U detector and a Scansys radiodetector. The HPLC system was controlled by Chromeleon 6.8 software. Thin-layer chromatography (TLC) was carried out on silica plated aluminum sheets (Silica gel 60 F254, Merck). The fraction of radioactivity on the TLC-plates was measured with either an instant imager from Packard or a Bioscan Mini-scan, flow-count and UCI-100.

Radiosynthesis of [^{11}C]Cimbi-775

[^{11}C]methyl trifluoromethanesulfonate was produced in an automated system and trapped in a DMF (300 µL) solution containing the precursor 3-(piperazin-1-yl)phenol (1 mg, 5.6 µmol) and 2M RbOH (2 µL, 1 µmol) at a flow rate of 25 mL/min. For the O- over N-methylation the mixture was subsequently heated for 5 min at 40°C. During the optimization of these conditions a crude sample were taken and analysed by an analytical HPLC method (Luna 5µm C18 4.60 × 50 mm, eluent: 30% MeCN in ionpair buffert (1000 mL H_2O, 420 µL 85% H_3PO_4, 2.59 g $NaH_2PO_4 \cdot H_2O$ and 1.22 g Na-decanesulfonate) for 6 min at a flow

rate of 2 mL/min to gain the radiochemical conversion (RCC (%) of the carbon-11 O-methylated precursor ([^{11}C]OMe, RT = 4 min). Thereafter [^{11}C]OMe was transferred to a second reaction vial containing 15 mg (0.06 mmol) of 3-(4-chlorobutyl)-3-ethylindolin-2-one (BO-1) and 30 mg of K_2CO_3 (0.22 mmol) for the final condensation. After reacting at 170 °C for 15 min the crude mixture was cooled down and diluted with 30:70 EtOH: 0.1% H_3PO_4 in H_2O (3.0 mL). The final product was subsequently isolated using semi-preparative HPLC (Luna 10µm C18(2) 100-A˚ column (Phenomenex Inc. 250 × 10 mm), 25:75 EtOH: 0.1% H_3PO_4 in H_2O, at a flow rate of 6 mL/min). Retention times were 1300 s for [^{11}C]Cimbi-775 and the labelled product was collected in 20-mL vial. The final product was analysed by an analytical HPLC method (Luna, 5µ, C18(2) 100-A˚ column (Phenomenex Inc. 150 × 4.6 mm) MeCN/ 0.1% H_3PO_4 in H_2O (gradient 0-100% MeCN over 15 min) at a flow rate of 2 mL/min – retention time for [^{11}C]Cimbi-775 was 7 minutes). The overall synthesis, purification, and formulation time was approximately 70 minutes and the product had radiochemical purity above 98%.

Supplementary Table 1: Crude analysis results of the O-over N methylation optimization experiments.

Base	Solvent	RCC (%)* O-Me	RCC (%)* N-Me
TBAH (1 M aq.)			
	Acetone	46	46
	ACN	40	57
	DMF	54	29
	THF	56	29
K_2CO_3 (2 M aq.)			
	Acetone	0	100
	ACN	0	0
	DMF	30	0
	THF	0	0
Rb_2CO_3 (s)			
	Acetone	4	89
	ACN	14	66
	DMF	10	58
	THF	0	57
Cs_2CO_3 (s)			
	Acetone	64	25
	ACN	26	72
	DMF	48	21
	THF	0	82
LiOH (2 M aq.)			

	Acetone	0	100
	ACN	0	100
	DMF	57	38
	THF	0	100
NaOH (2 M aq.)			
	Acetone	45	46
	ACN	45	22
	DMF	58	23
	THF	<1	49
KOH (2 M aq.)			
	Acetone	71	27
	ACN	15	85
	DMF	70	24
	THF	0	96
RbOH (2 M aq.)			
	Acetone	19	23
	ACN	20	80
	DMF	87.5	7.5
	THF	0	100
CsOH (2 M aq.)			
	Acetone	20	13
	ACN	58	41
	DMF	55	28
	THF	0	100
Ag_2O (s)			
	Acetone	0	82
	ACN	0	77
	DMF	0	94
	THF	0	0

*Estimated using radio-HPLC

Reproducibility

Supplementary Table 2: Repeatability results for the best condition determined in supplementary Table 1.

Base	Solvent	RCC (%)* O-Me	RCC (%)* N-Me
RbOH (2 M aq.)	DMF	87.5	7.5
	DMF	48	39
	DMF	43	44
	DMF	56	34
	DMF	51	37
	DMF	60	16
	DMF	60	28

*Estimated using radio-HPLC

Radiosyntheses of [^{18}F]ENL09, [^{18}F]ENL10 and [^{18}F]ENL61

No-carrier-added ^{18}F-fluoride from the target was collected at a non-conditioned but activated (10 mL ethanol, 20 mL water and dried with air) anion-exchange cartridge (QMA). To elute the ^{18}F-fluoride off the cartridge, a solution of 1,10-diaza-4,7,13,16,21,24-hexaoxabicyclo[8.8.8]hexacosane (Kryptofix®222, 20 mg) and K_2CO_3 (3.3 mg) dissolved in a methanol-water mixture (97/3 v/v, 0.65 mL) was used. The eluted mixture was thereafter dried by evaporation at 110 °C under helium and then dried twice again after subsequently addition of 1 mL dry MeCN. To the dried Kryptofix®222/[^{18}F]fluoride complex (24-48 GBq) the precursor ENL04 (6 mg, 0.013 mmol) dissolved in MeCN (1 mL) was added and heated at 80 °C for 20 min to yield [^{18}F]ENL02. During the optimization of the ^{18}F-labelling acquiring [^{18}F]ENL02 RCC was assessed by an analytical HPLC method (Luna 5µm C18 4.60 × 50 mm, eluent: MeCN/ 0.1% H_3PO_4 in H_2O (0-100% MeCN, 25 min gradient)) at a flow rate of 1.5 mL/min;[^{18}F]ENL02 had a retention time of 12.9 min. The results were further verified by radio-TLC using Hep:EtOAc (1:1), R_f = 0.66.

The crude reaction mixture was thereafter diluted in water (20-30 mL) and transferred to a SepPak C18 plus (short) cartridge for purification from free fluoride-18, base and impurities. MeCN (1 mL) was used to elute [^{18}F]ENL02 off the cartridge, and subsequently a deprotection of the Boc group was performed by addition of TFA (0.25 mL) and reacting for 10 min at 80˚C to give the deprotected product [^{18}F]ENL03. Following so, the TFA and MeCN was evaporated off at 110 °C under vacuum and further dried twice after addition of dry MeCN (1 mL). To evaluate the conversion of the deprotection gaining [^{18}F]ENL03 the same HPLC conditions as for [^{18}F]ENL02 was used. The retention time of [^{18}F]ENL03 was 5.14 min.

To the dried [^{18}F]ENL03, DMSO (1 mL) was added and the solution was transferred to a reaction vial containing butyloxindole derivative (16 mg, 0.064-0.084 mmol) and K_2CO_3 (30 mg, 0.22 mmol) for the final condensation. The reaction mix was heated to 160 °C for 15 min and subsequently quenched with EtOH: 0.1% H_3PO_4 in H_2O (30:70, 3.5 mL) prior to HPLC purification. For dual-condensation two butyloxindole derivatives (8 mg, 0.032-0.042mmol) of each were used in the condensation step. During the optimization of the condensation reaction conditions RCC (%) were assessed by an analytical HPLC method (Luna 5µm C18 4.60 × 50 mm, eluent: MeCN/ 0.1% H_3PO_4 in H_2O (0-100% MeCN, 25 min gradient) at a flow rate of 1.5 mL/min, [^{18}F]ENL09 had a retention time = 7.39 min.

The tracer candidates were isolated by semi-preparative HPLC [Luna 5 µm C18(2) 10 × 250 mm column, flow rate 3 mL/min, eluent: EtOH: 0.1% H_3PO_4 in H_2O (30:70)]. The retention time for [^{18}F]ENL03 was around 400 s, [^{18}F]ENL09 1100 s, [^{18}F]ENL10 800 s and [^{18}F]ENL61was 1200 s.

Chemical and radiochemical purities were assessed by analytical HPLC [Luna 5µm C18 4.60 × 50 mm, eluent: MeCN/ 0.1% H_3PO_4 in H_2O (30:70) RT: [^{18}F]ENL09 = 10.5 min; [^{18}F]ENL10 7.9 min and [^{18}F]ENL61 6.8 min at a flow rate of 1.5 mL/min]. Molar activity (A_m) of the radiotracer was determined as follows: the area of the UV absorbance peak corresponding to the radiolabeled product was measured (integrated) on the HPLC chromatogram. This value was then converted into a molar mass by comparison with an average integrated area of a known standard of the reference compound.

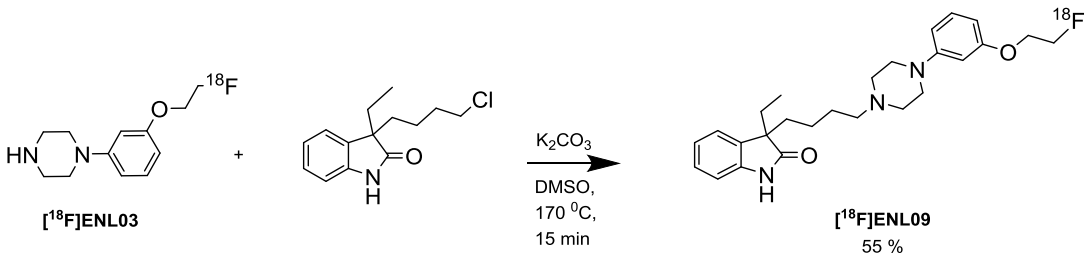

[18F]ENL03 [18F]ENL09 55 %

Oxindole mg (Equiv.)	Base	Base amount mg (Equiv.)	Solvent	Temp. (^{o}C)	Reaction time (min)	RCC (%)*
20 (2)	K_2CO_3	32 (5.5)	DMF	150	5	8
20 (2)	K_2CO_3	32 (5.5)	DMF	150	10	14
20 (2)	K_2CO_3	32 (5.5)	DMF	150	15	21
20 (2)	K_2CO_3	32 (5.5)	DMF	150	20	26
18 (2)	K_2CO_3	28 (5.5)	DMSO	170	5	34
18 (2)	K_2CO_3	28 (5.5)	DMSO	170	10	50
18 (2)	K_2CO_3	28 (5.5)	DMSO	170	15	55
18 (2)	K_2CO_3	28 (5.5)	DMSO	170	20	49
21 (2)	K_2CO_3	49 (9)	DMSO	170	15	44
9 (1)	K_2CO_3	20 (3.6)	DMSO	170	15	11
14 (1.5)	K_2CO_3	21 (3.6)	DMSO	170	15	33
9 (1)	Cs_2CO_3	26 (2)	DMSO	170	15	16

*Estimated using radio-HPLC and verified by radio-TLC

Supplementary Figure1: Synthetic route for the condensation step of [^{18}F]ENL09 (above) and an overview of the optimization of reaction conditions for the final condensation reaction (below).

Radiosyntheses [^{18}F]ENL05, [^{18}F]ENL06 and [^{18}F]ENL60

The 3-step radiosynthesis of the tracers [^{18}F]ENL05, [^{18}F]ENL06 and [^{18}F]ENL60 started out with a Cu-mediated direct fluorination using, $Cu(OTf)_2(py)_4$ and [^{18}F]fluoride on the boronic pinacole ester precursor (*tert*-butyl 4-(4-(4,4,5,5-tetramethyl-1,3,2-dioxaborolan-2-yl)phenyl)piperazine-1-carboxylate), followed by a deprotection and a condensation reaction to end up with the final tracers.

No-carrier-added ^{18}F-fluoride from the target was collected at an anion-exchange cartridge (QMA - acquired preconditioned from ABX advanced biochemical compounds, Radeberg, Germany). To elute the ^{18}F-fluoride off the cartridge, a solution of 1,10-diaza-4,7,13,16,21,24- hexaoxabicyclo[8.8.8]hexacosane (Kryptofix®222, 3.63 mg), K_2CO_3 (0.22 mg) and $K_2C_2O_4$ (2 mg) dissolved in a MeCN-H_2O mixture (80/20 v/v, 1 mL) was used. The eluted mixture was thereafter dried by evaporation at 110 °C under helium and dried twice again after subsequent addition of dry MeCN (1 mL). To the dried Kryptofix®222/[^{18}F]fluoride complex, DMF (0.4 mL) was added and an aliquot (0.2 mL) of the solution was thereafter transferred to the reaction vial containing the precursor *tert*-butyl 4-(4-(4,4,5,5-tetramethyl-1,3,2-dioxaborolan-2-yl)phenyl)piperazine-1-carboxylate (7.23 mg, 0.02 mmol) and $Cu(OTf)_2(py)_4$ (7.76 mg, 0.011 mmol) dissolved in DMF (0.2 mL), the reaction mixture was then heated at 120 °C for 25 min to synthesize [^{18}F]FGE06. During the optimization RCC was assessed by analytical HPLC [Luna 5µm C18 4.60 × 50 mm, eluent: MeCN/ 0.1% H_3PO_4 in H_2O (0-100% MeCN, 25 min gradient) RT: 13 min, and by TLC (EtOAc), R_f = 0.7.

The Boc deprotection, condensation and isolation were performed as described for the previous fluorine-18 labelling synthesis. The retention times with the semi-preparative HPLC method were for [^{18}F]1-(4-fluorophenyl)piperazine 600 s, [^{18}F]ENL05 1900 s, [^{18}F]ENL06 1450 s and [^{18}F]ENL60 2100 s (only 2.4 mL/min for [^{18}F]ENL60). Using the analytical HPLC method (Luna, 5 µm, C18(2) 100-A˚ column (Phenomenex Inc. 150 × 4.6 mm) MeCN/ 0.1% H_3PO_4 in H_2O (gradient 0-100% MeCN over 15 min) at a flow rate of 2 mL/min, the retention times were: [^{18}F]ENL05 6.8 min, [^{18}F]ENL06 5.7 min and [^{18}F]ENL60 6.8 min.

Chromatographic information

Carbon-11 O-over N methylation

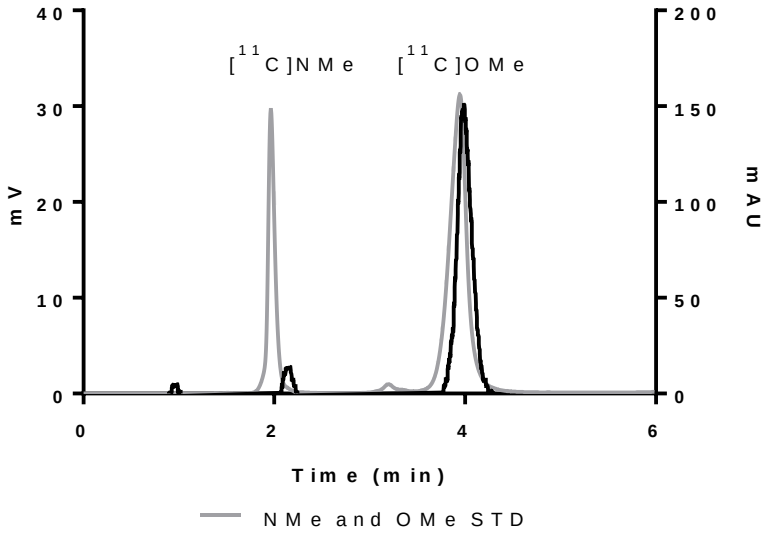

Supplementary Figure 2: Analysis of the O-over N methylation results performed with RbOH (2M a.q.) in DMF using an analytical HPLC method. Radio is presented in black and the reference UV (245 nm) in gray. The retention times for the NMe and the OMe are around 2 min and 4 min respectively.

[^{11}C]Cimbi-775

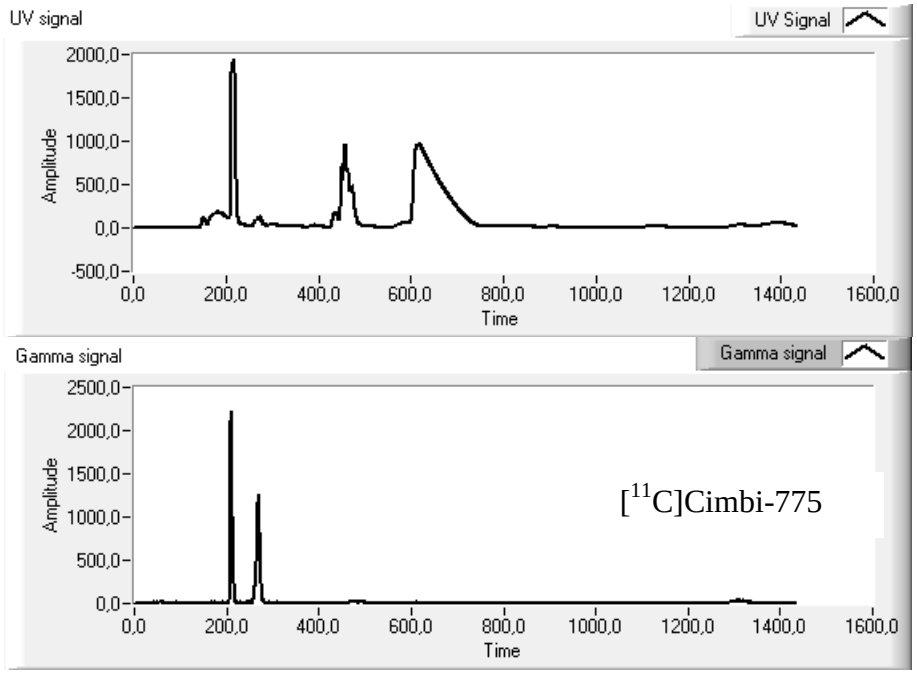

Supplementary Figure 3: UV (254 nm) and radio chromatograms of [^{11}C]Cimbi-775 using the described semi-preparative HPLC method.

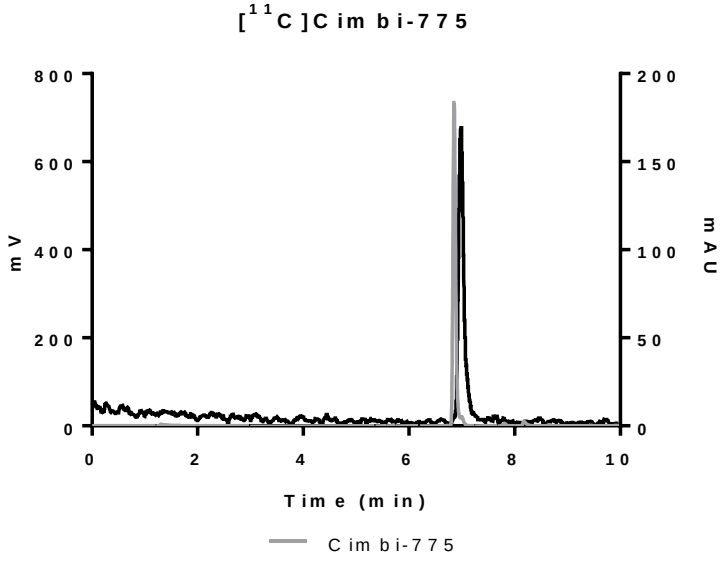

Supplementary Figure 4: UV (290 nm) and radio chromatograms of [^{11}C]Cimbi-775 using the described analytical HPLC method.

[^{18}F]ENL09

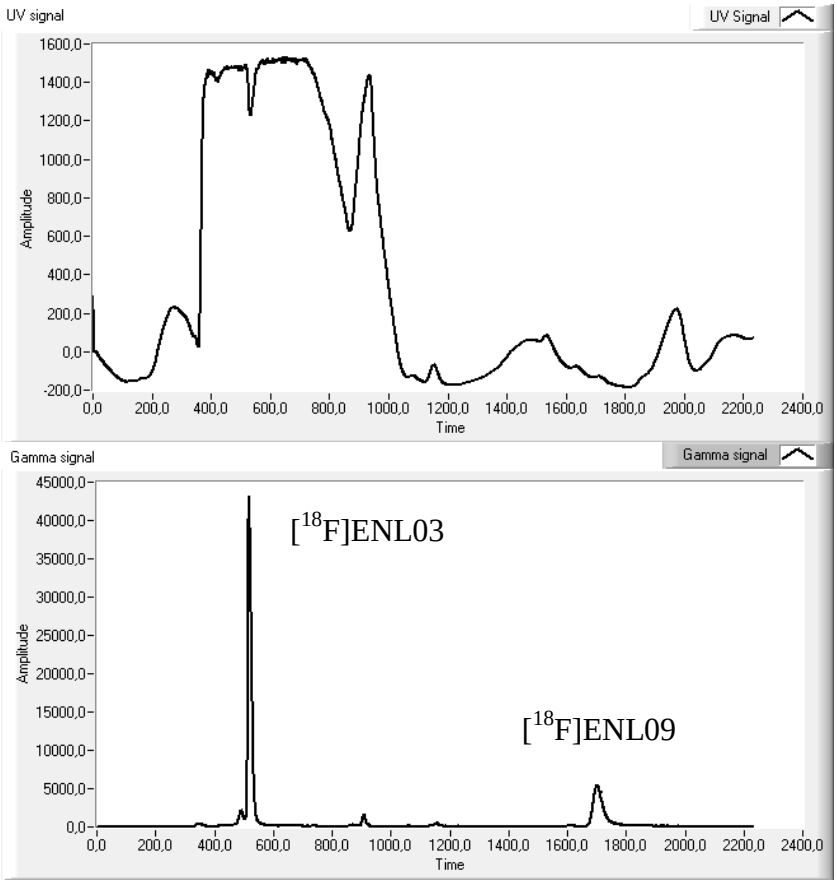

Supplementary Figure 5: UV (254 nm) and radio chromatograms of [^{18}F]ENL09 using the described semi-preparative HPLC method.

[^{18}F]ENL10

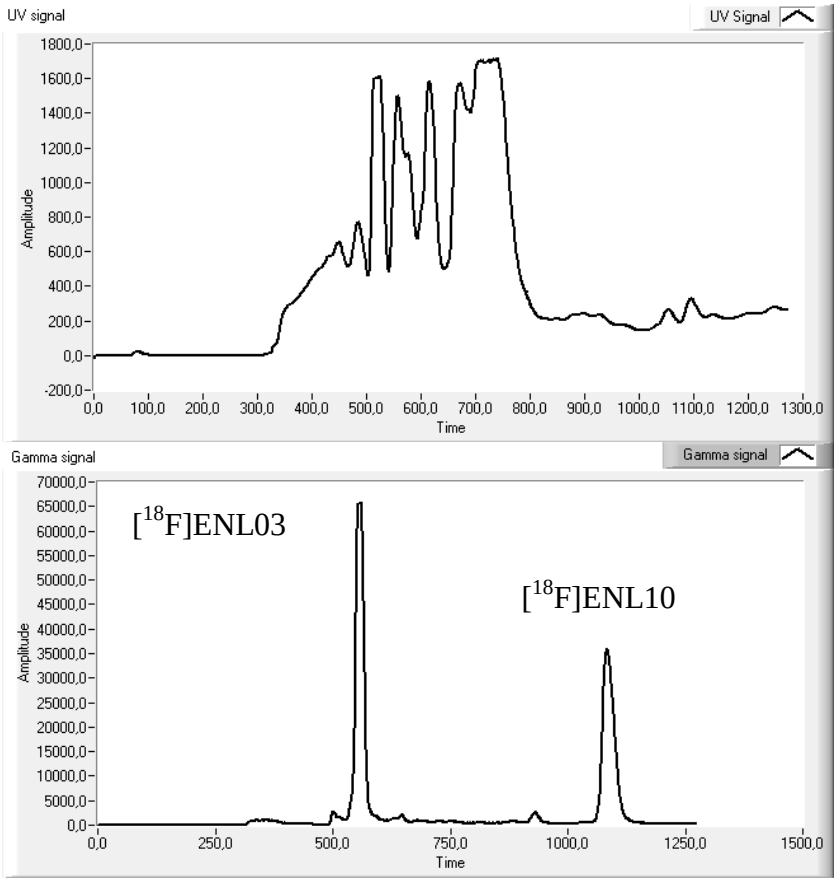

Figure 6: UV (254 nm) and radio chromatograms of [^{18}F]ENL10 using the described semi-preparative HPLC method.

[^{18}F]ENL61 (synthesized by dual-condensation)

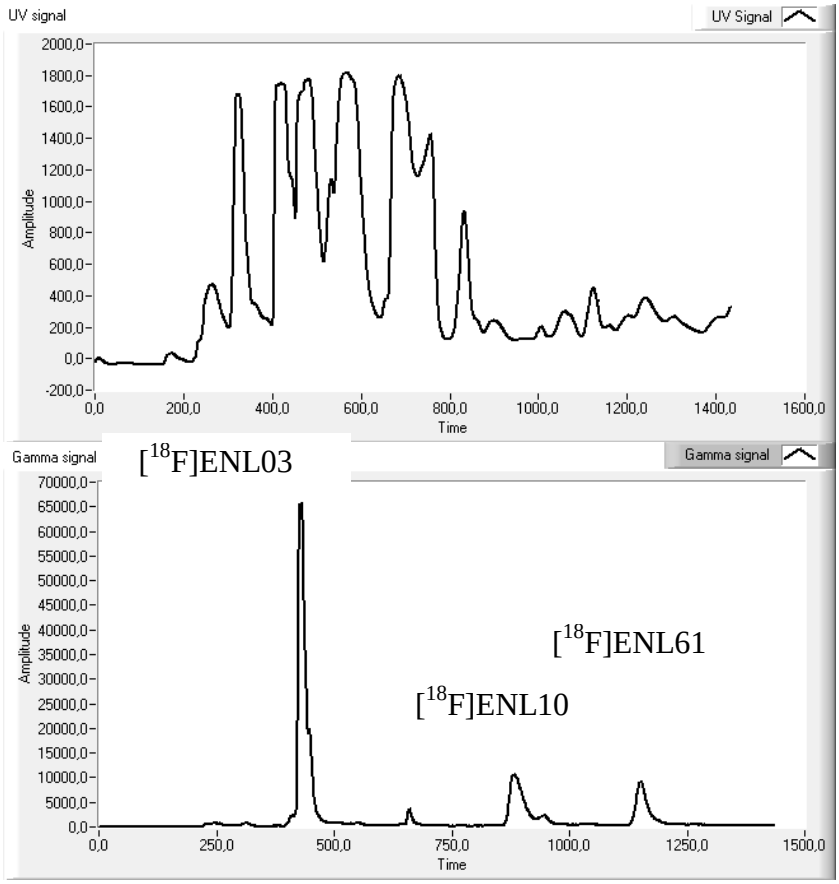

Supplementary Figure 7: UV (254 nm) and radio chromatograms of [^{18}F]ENL61 using the described semi-preparative HPLC method.

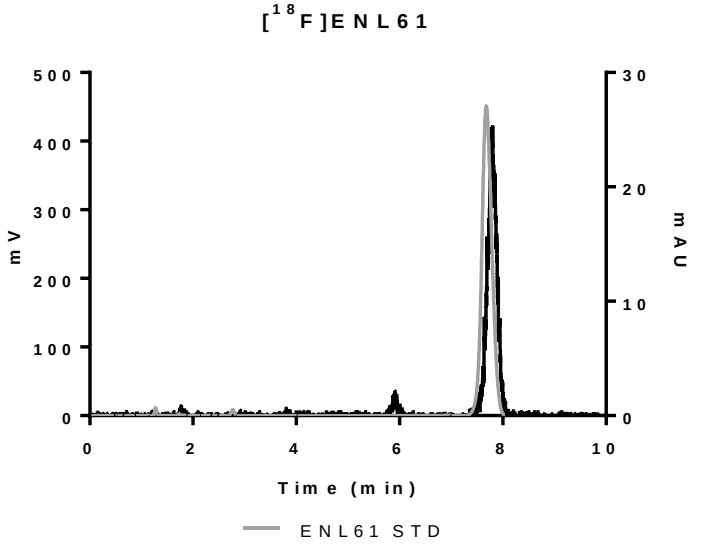

Supplementary Figure 8: UV (290 nm) and radio chromatograms of [^{18}F]ENL61 using the described analytical HPLC method.

[^{18}F]ENL05

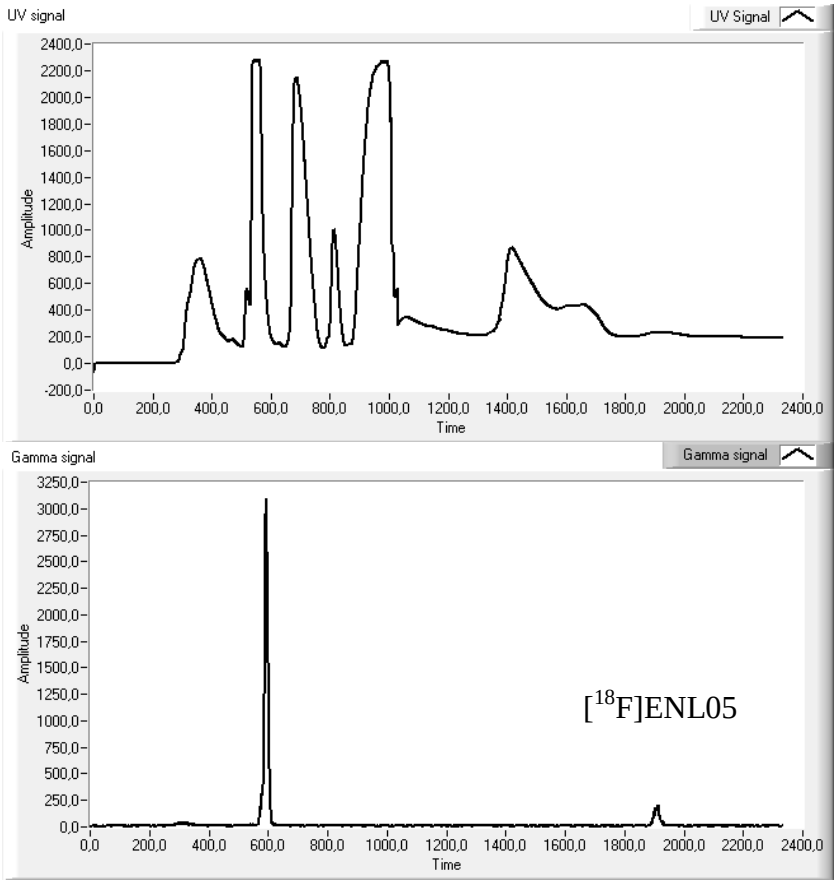

Supplementary Figure 9: UV (254 nm) and radio chromatograms of [^{18}F]ENL05 using the described semi-preparative HPLC method.

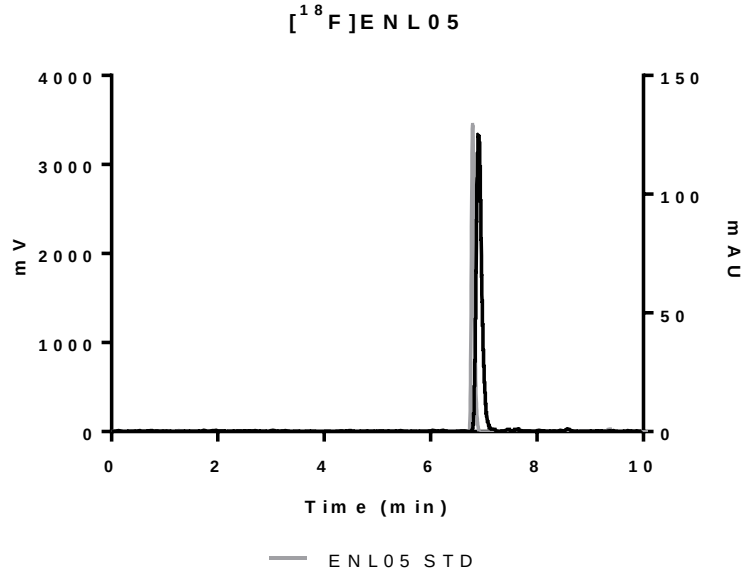

Supplementary Figure 10: UV (290 nm) and radio chromatograms of [^{18}F]ENL05 using the described analytical HPLC method.

[^{18}F]ENL06

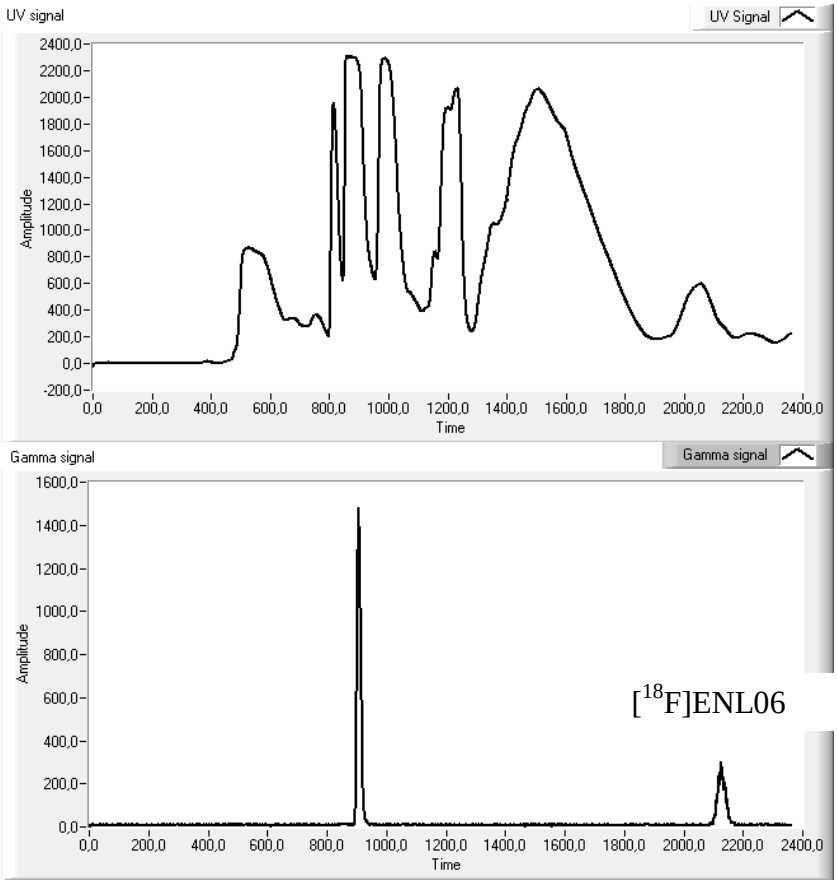

Supplementary Figure 11: UV (254 nm) and radio chromatograms of [^{18}F]ENL06 using the described semi-preparative HPLC method.

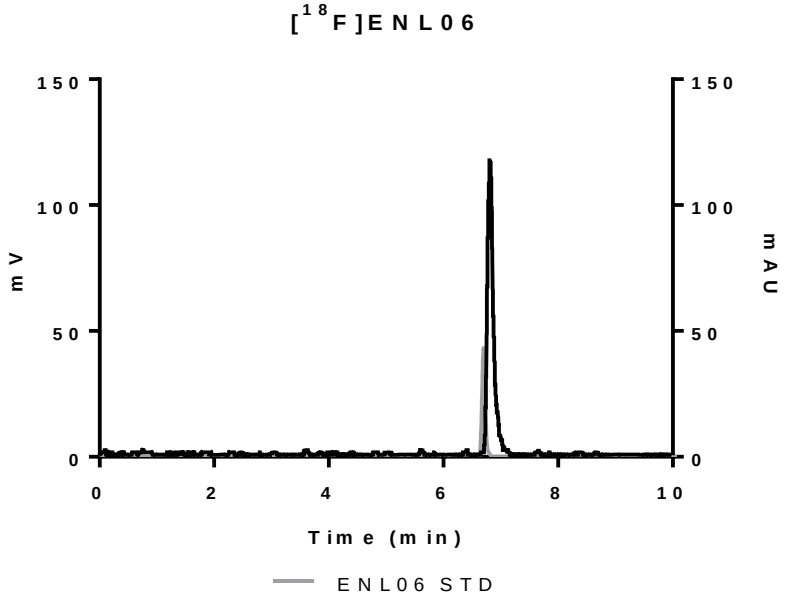

Supplementary Figure 12: UV (290 nm) and radio chromatograms of [^{18}F]ENL09 using the described analytical HPLC method.

[^{18}F]ENL60

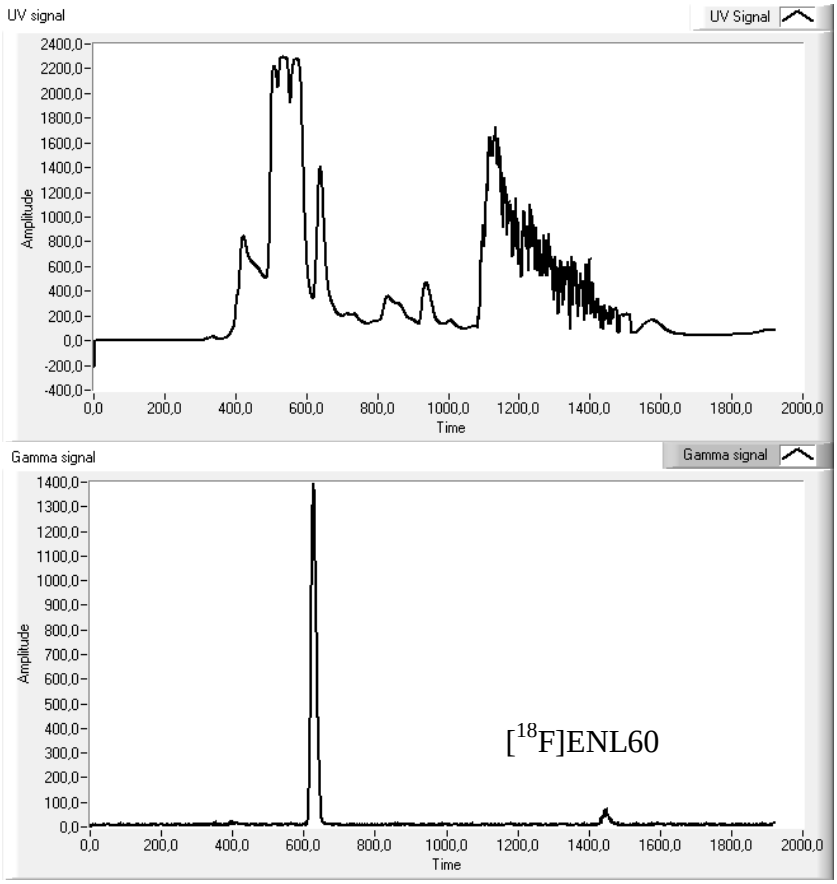

Supplementary Figure 13: UV (254 nm) and radio chromatograms of [^{18}F]ENL60 using the described semi-preparative HPLC method.

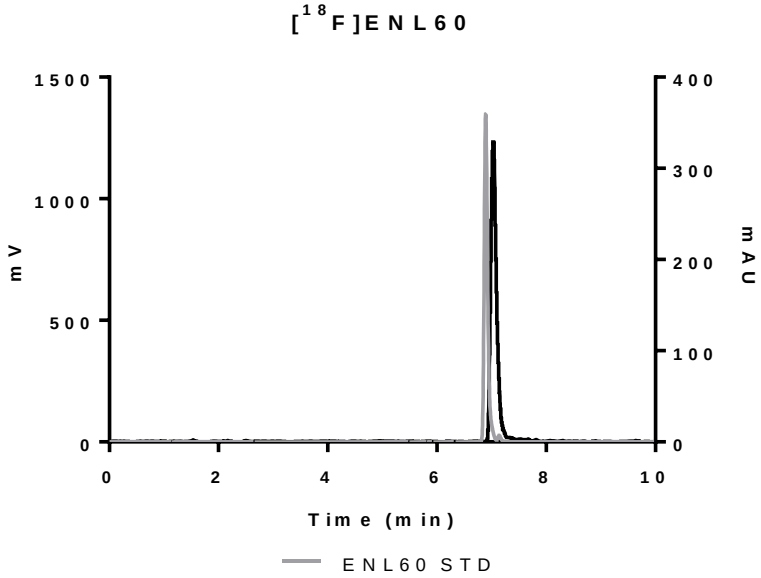

Supplementary Figure 14: UV (290 nm) and radio chromatograms of [^{18}F]ENL60 using the described analytical HPLC method.

References

1. Herth, M. M.; Kramer, V.; Rösch, F., Synthesis of novel WAY 100635 derivatives containing a norbornene group and radiofluorination of [^{18}F] AH1. MZ as a serotonin 5-HT_{1A} receptor antagonist for molecular imaging. *Journal of Labelled Compounds and Radiopharmaceuticals: The Official Journal of the International Isotope Society* **2009,** *52* (6), 201-207.

2. Prante, O.; Tietze, R.; Hocke, C.; Lober, S.; Hubner, H.; Kuwert, T.; Gmeiner, P., Synthesis, radiofluorination, and *in vitro* evaluation of pyrazolo[1,5-a]pyridine-based dopamine D4 receptor ligands: discovery of an inverse agonist radioligand for PET. *Journal of medicinal chemistry* **2008,** *51* (6), 1800-1810.

3. Herth, M. M.; Volk, B.; Pallagi, K.; Kofoed Bech, L.; Antoni, F. A.; Knudsen, G. M.; Kristensen, J. L., Synthesis and *in vitro* evaluation of oxindole derivatives as potential radioligands for 5-HT_7 receptor imaging with PET. *ACS Chemical Neuroscience* **2012,** *3* (12), 1002-1007.

4. Volk, B.; Barkóczy, J.; Hegedus, E.; Udvari, S.; Gacsályi, I.; Mezei, T.; Pallagi, K.; Kompagne, H.; Lévay, G.; Egyed, A., (Phenylpiperazinyl-butyl) oxindoles as selective 5-HT_7 receptor antagonists. *Journal of medicinal chemistry* **2008,** *51* (8), 2522-2532.

5. Volk, B.; Gacsályi, I.; Pallagi, K.; Poszávácz, L.; Gyönös, I.; Szabó, É.; Bakó, T.; Spedding, M.; Simig, G.; Szénási, G., Optimization of (arylpiperazinylbutyl) oxindoles exhibiting selective 5-HT_7 receptor antagonist activity. *Journal of medicinal chemistry* **2011,** *54* (19), 6657-6669.

Appendices

Appendix 1 – ^{1}H NMR of ENL01

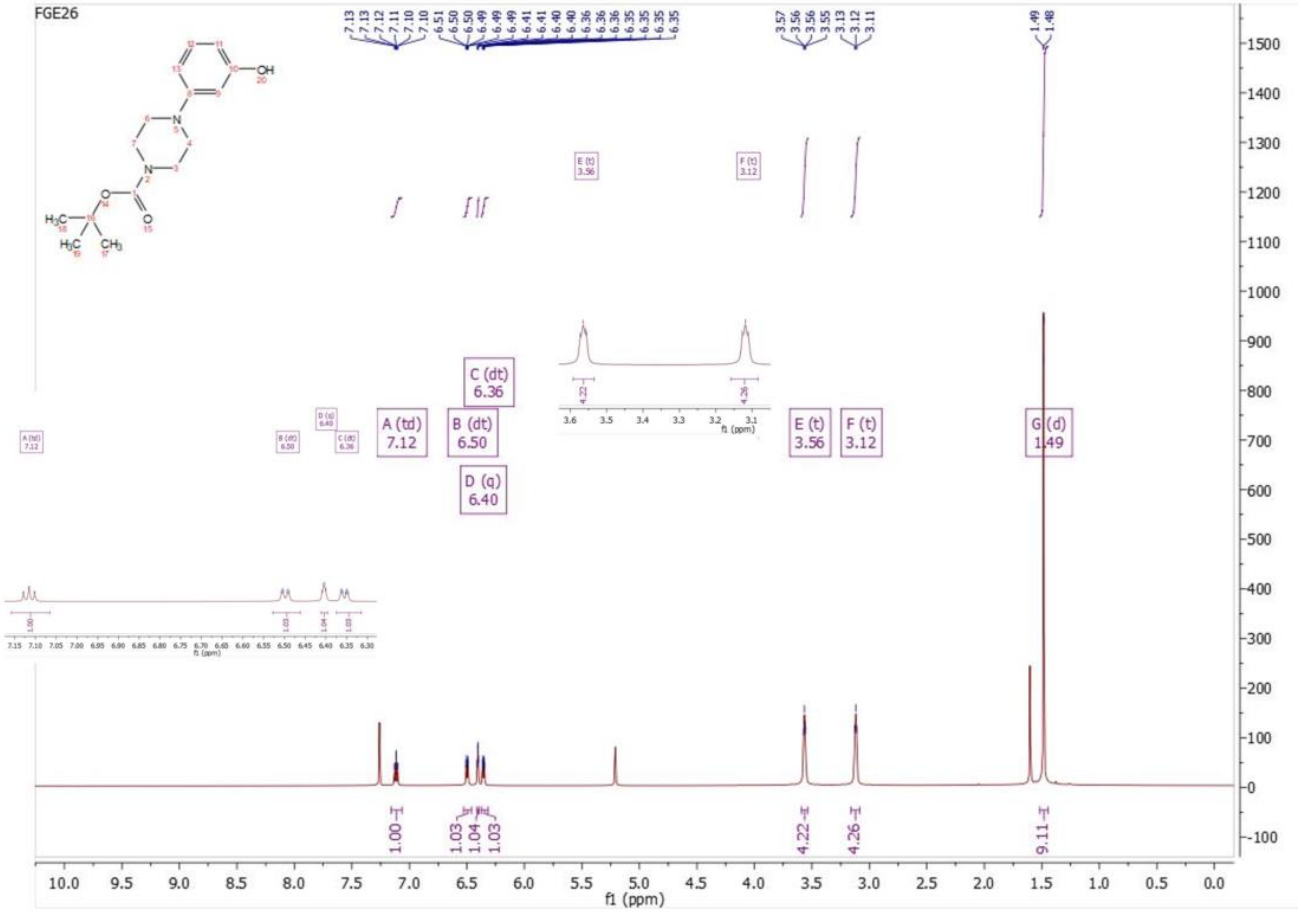

Appendix 2– ^{13}C NMR of ENL01

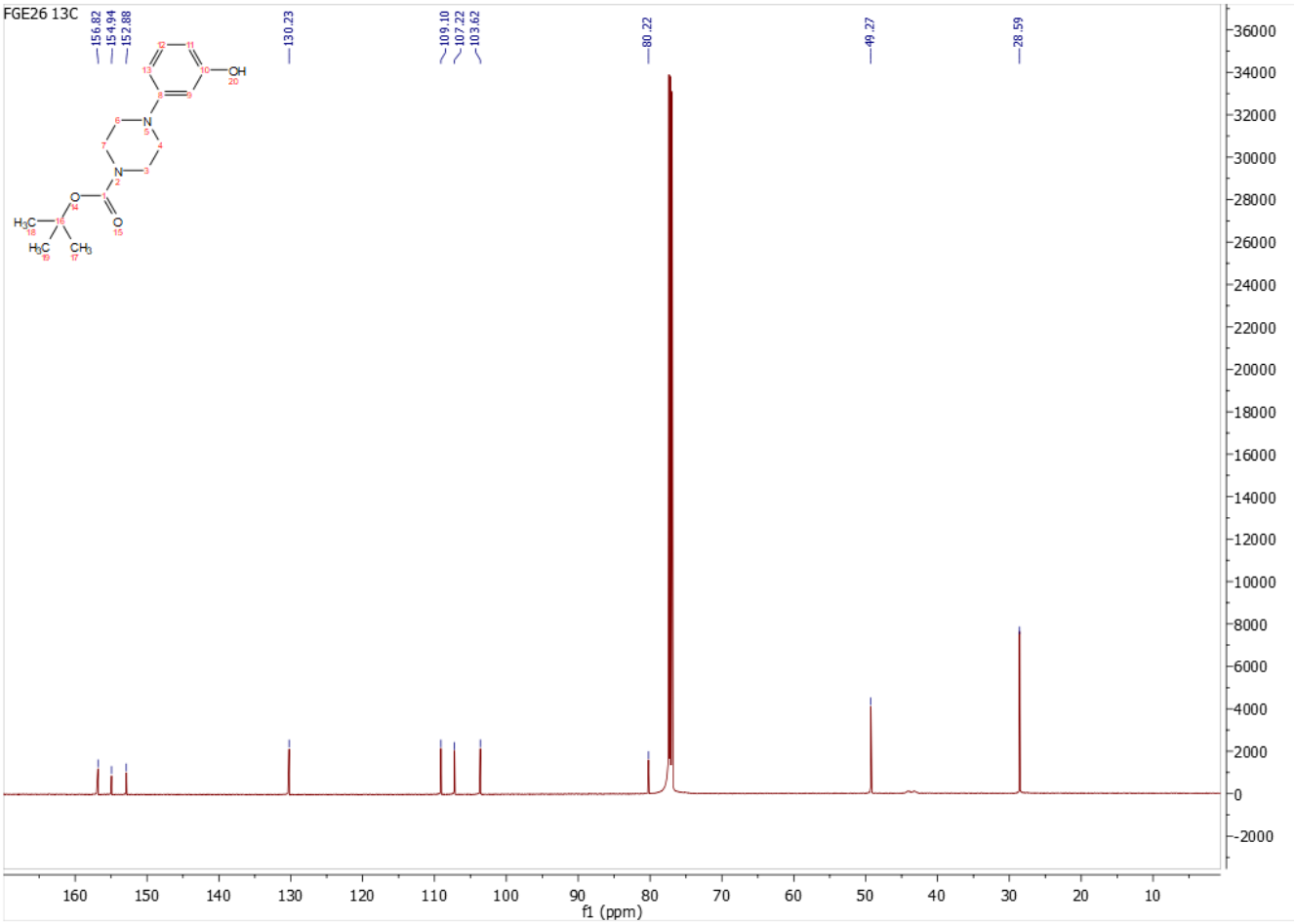

Appendix 3– UPLC-MS of ENL01

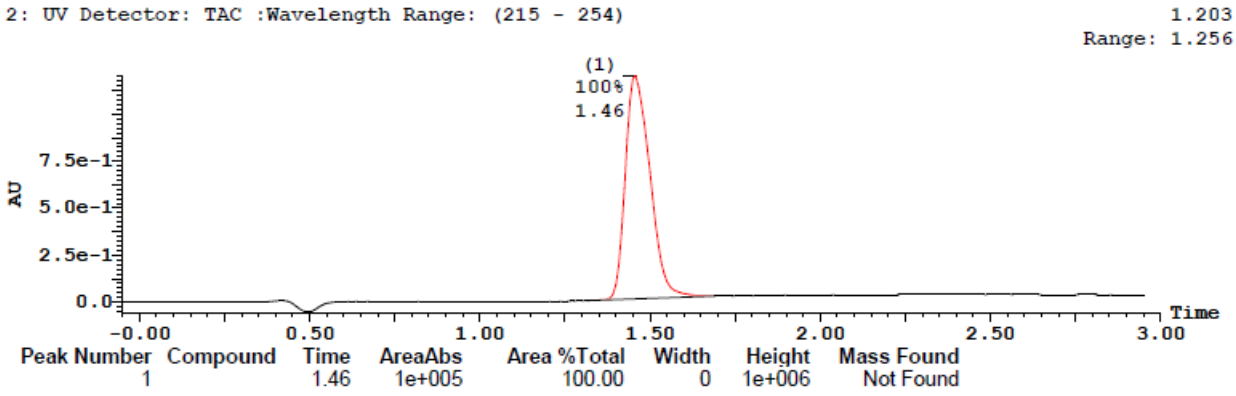

Peak Number	Compound	Time	AreaAbs	Area %Total	Width	Height	Mass Found
1		1.46	1e+005	100.00	0	1e+006	Not Found

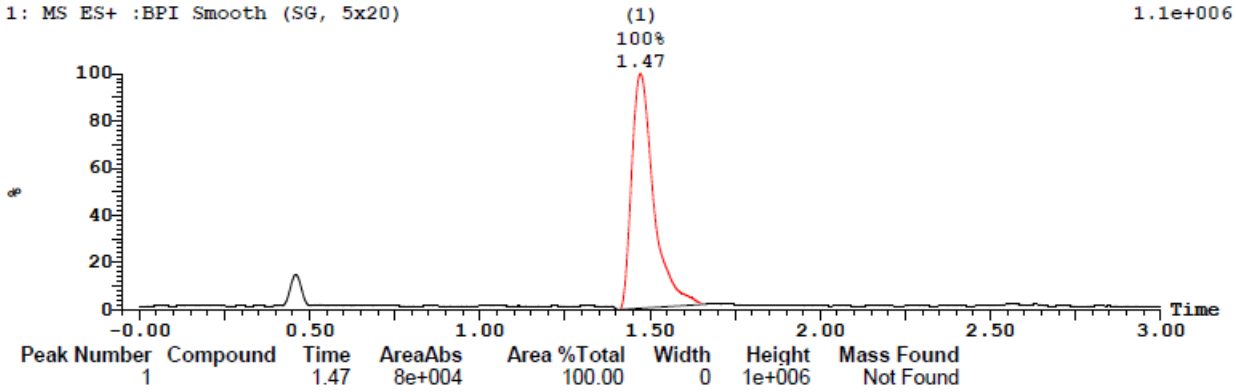

Peak Number	Compound	Time	AreaAbs	Area %Total	Width	Height	Mass Found
1		1.47	8e+004	100.00	0	1e+006	Not Found

Peak ID	Compound	Time	Mass Found
1		1.47	Not Found

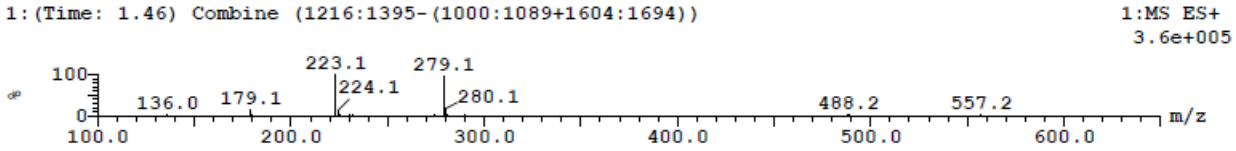

Appendix 4– ^{1}H NMR of ENL02

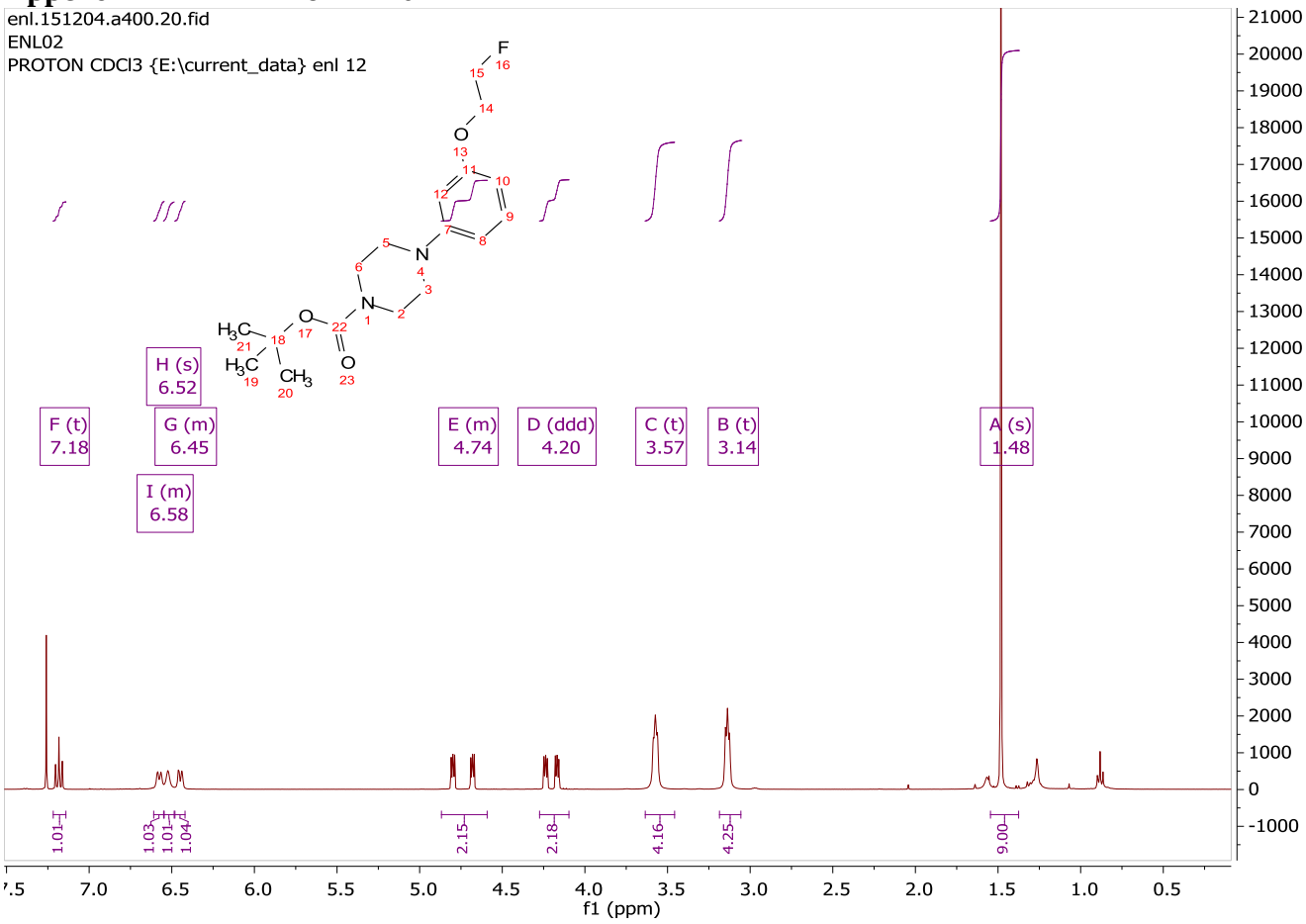

Appendix 5– ^{13}C NMR of ENL02

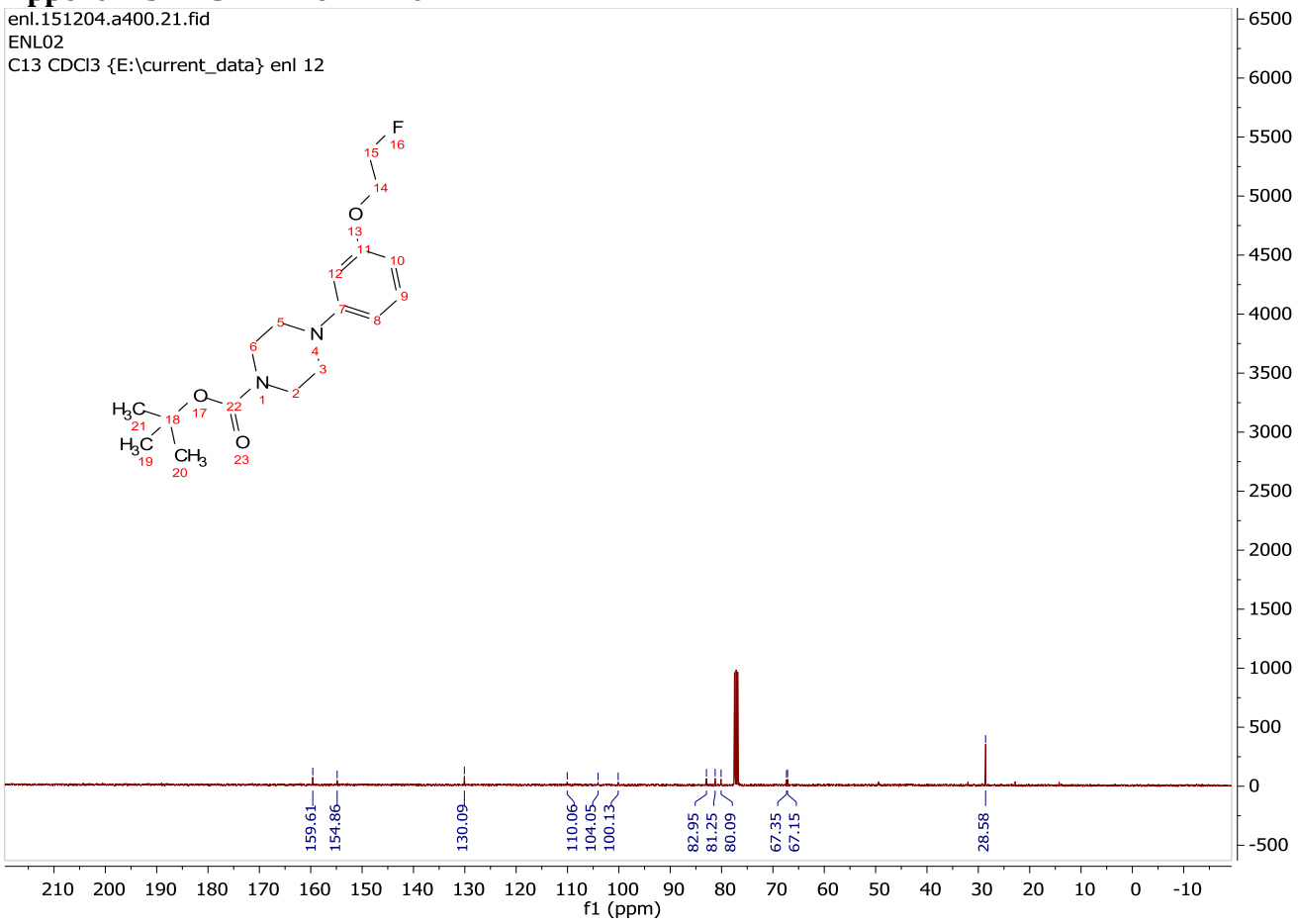

Appendix 6– UPLC-MS of ENL02

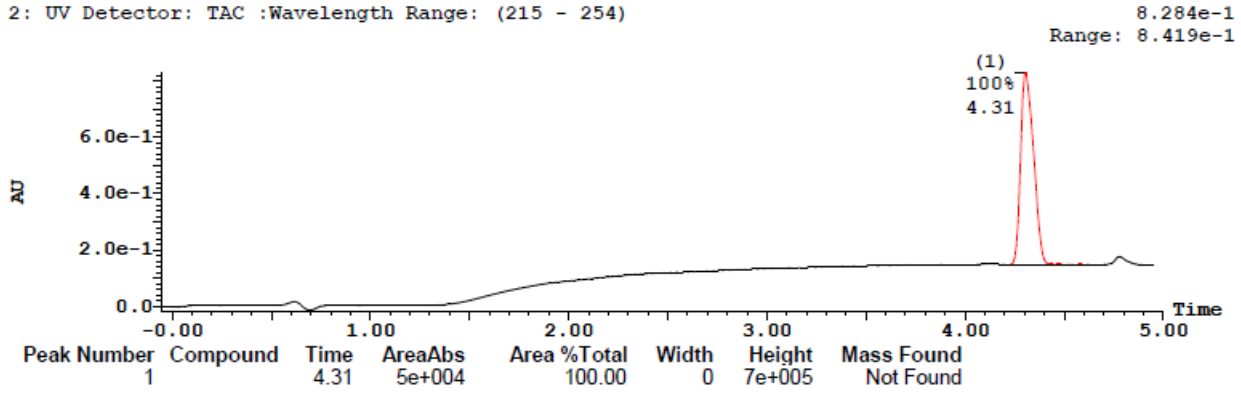

Peak Number	Compound	Time	AreaAbs	Area %Total	Width	Height	Mass Found
1		4.31	5e+004	100.00	0	7e+005	Not Found

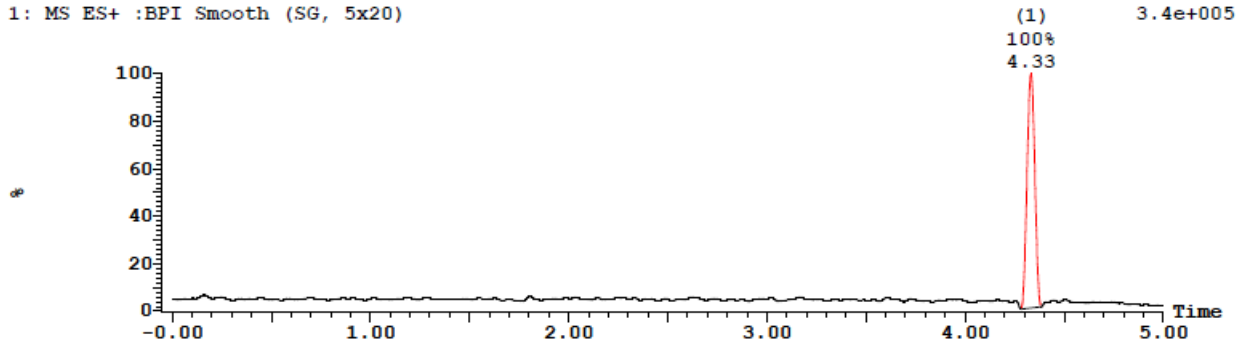

Peak ID	Compound	Time	Mass Found
1		4.33	Not Found

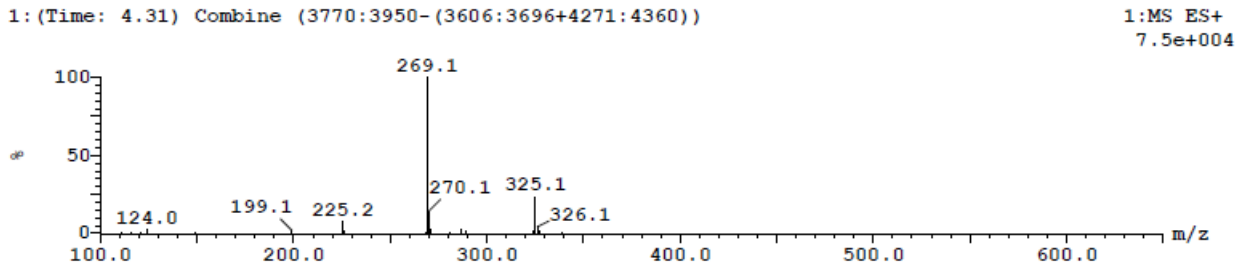

Appendix 7– ^{1}H NMR of ENL03

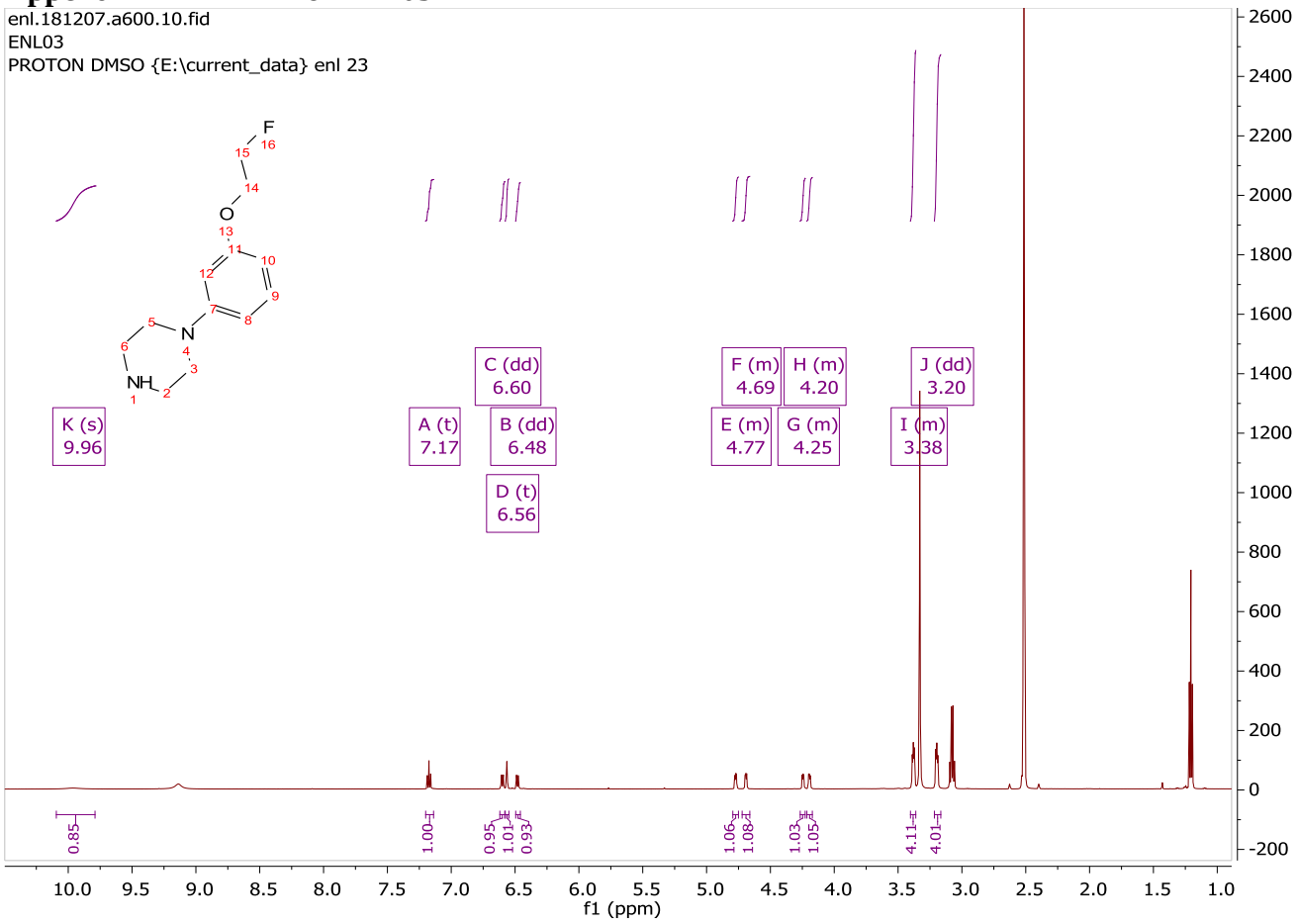

Appendix 8– ^{13}C NMR of ENL03

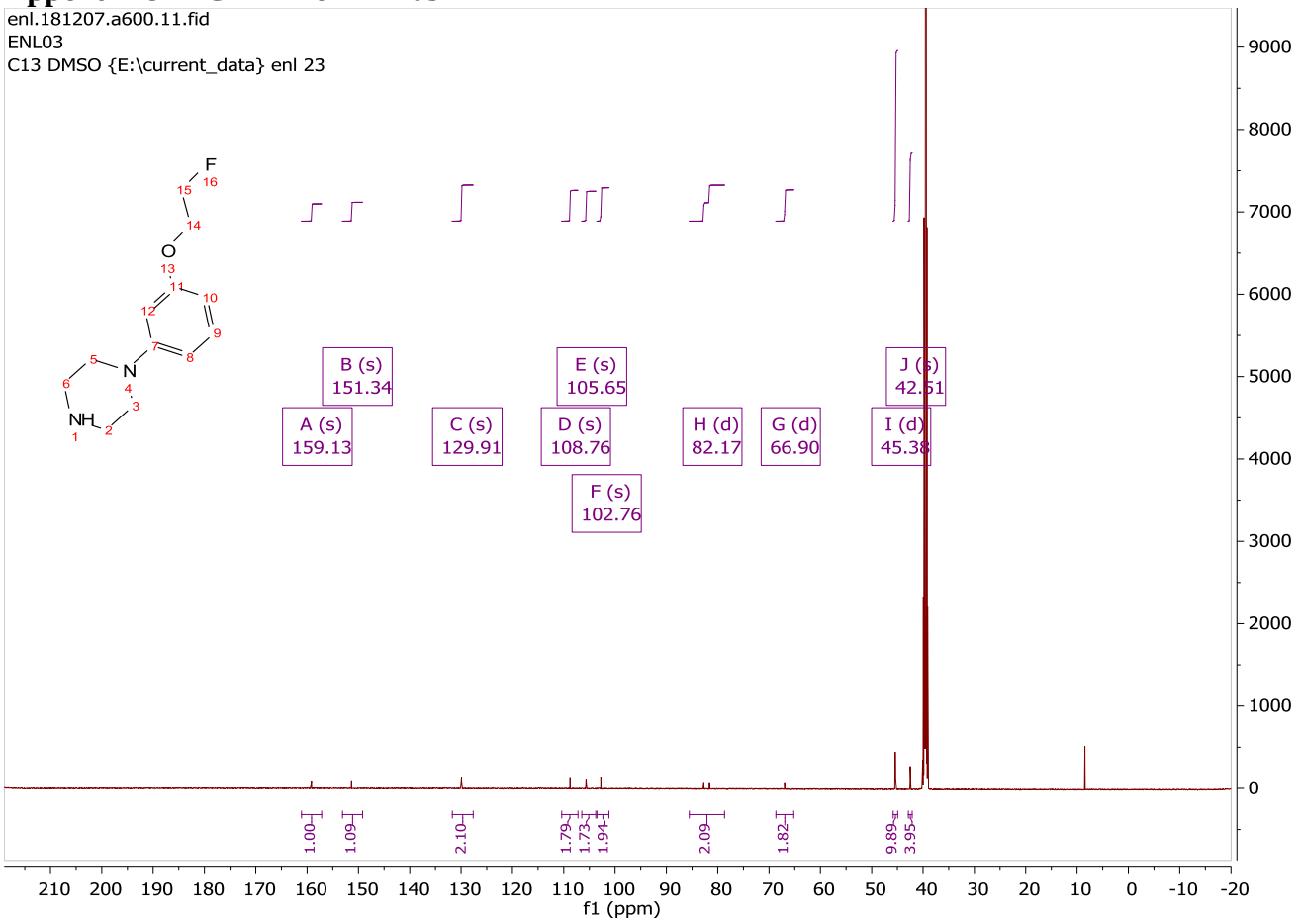

Appendix 9– UPLC-MS of ENL03

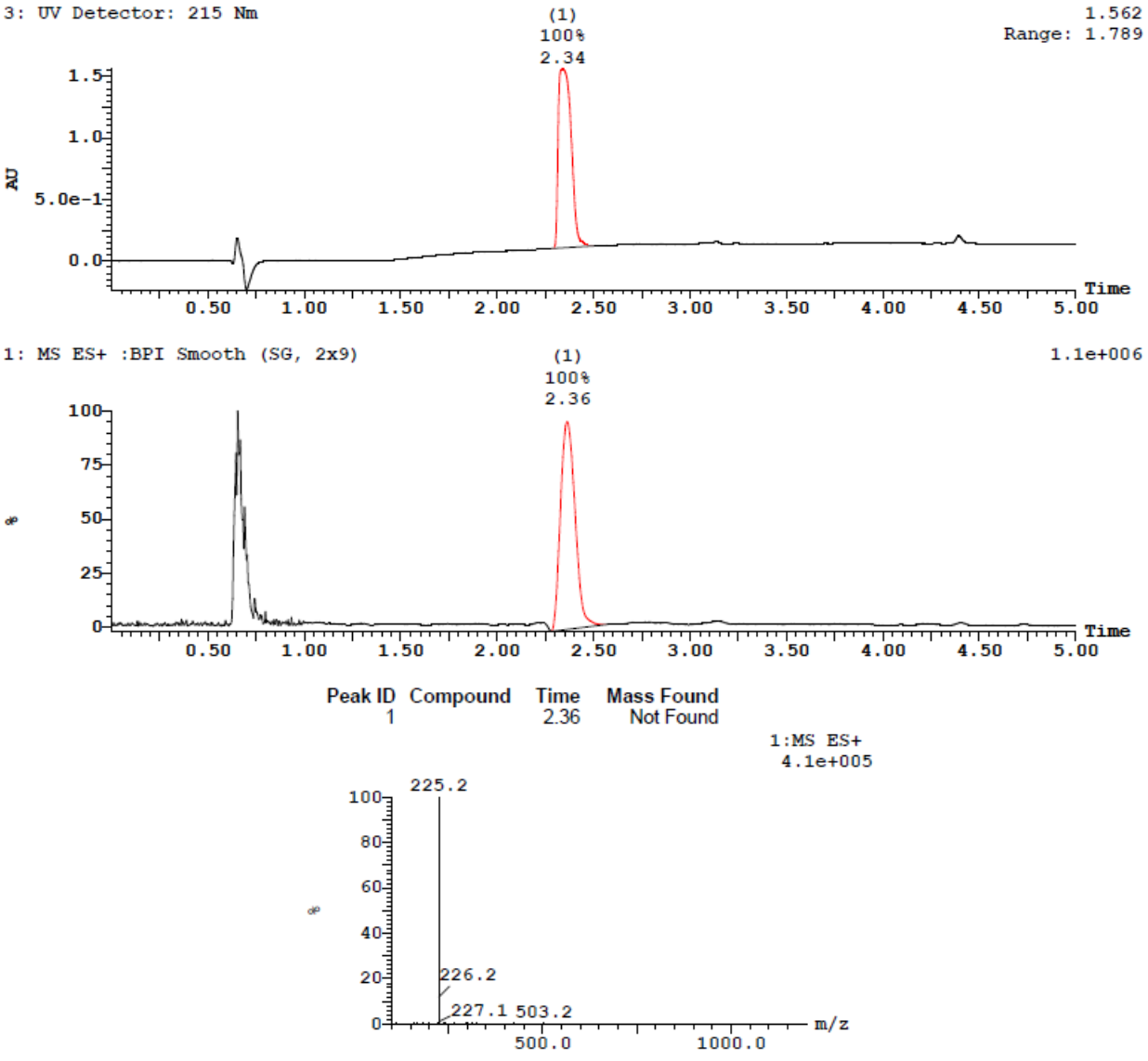

Appendix 10 – ^{1}H NMR of ENL11

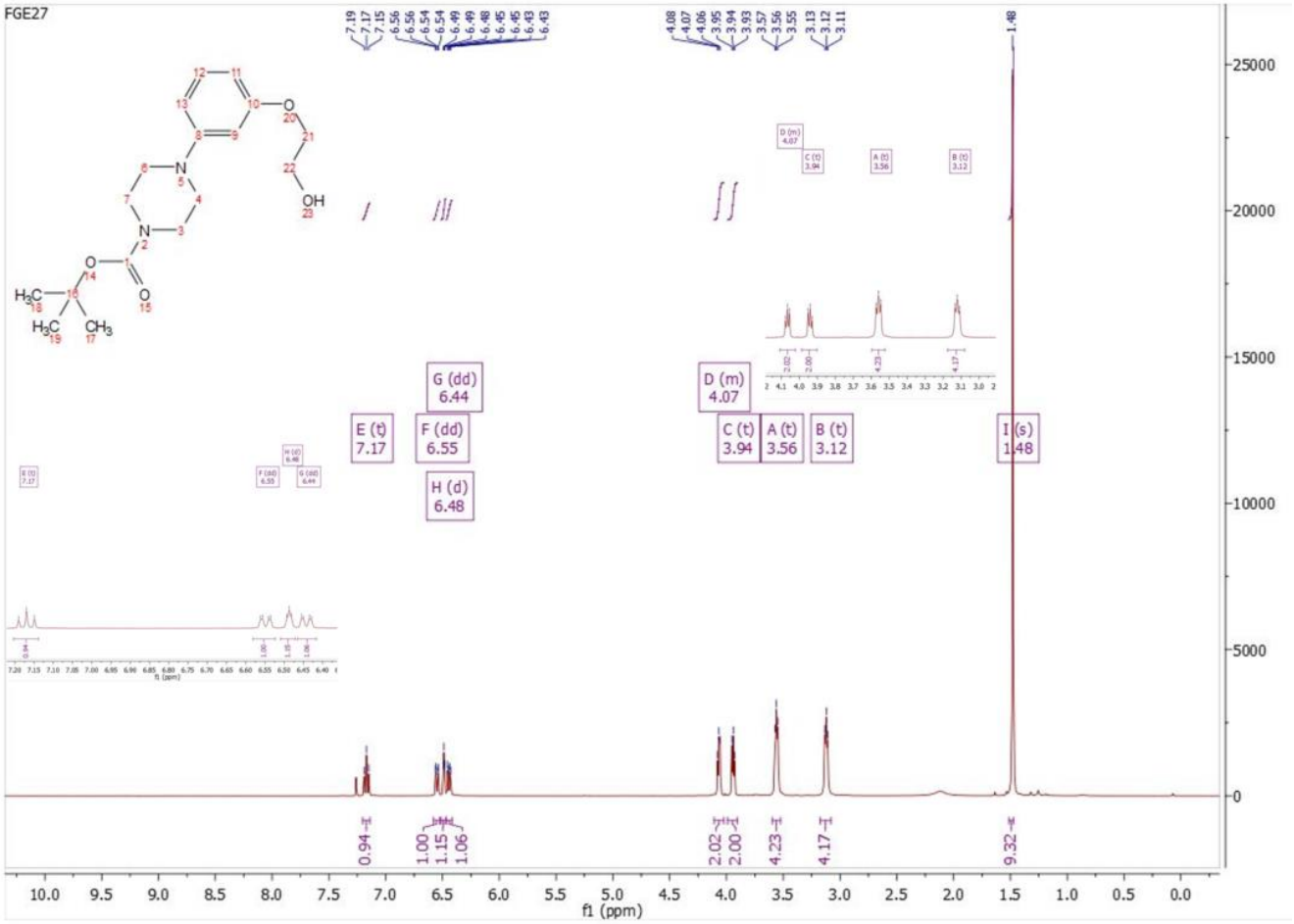

Appendix 11– UPLC-MS of ENL11

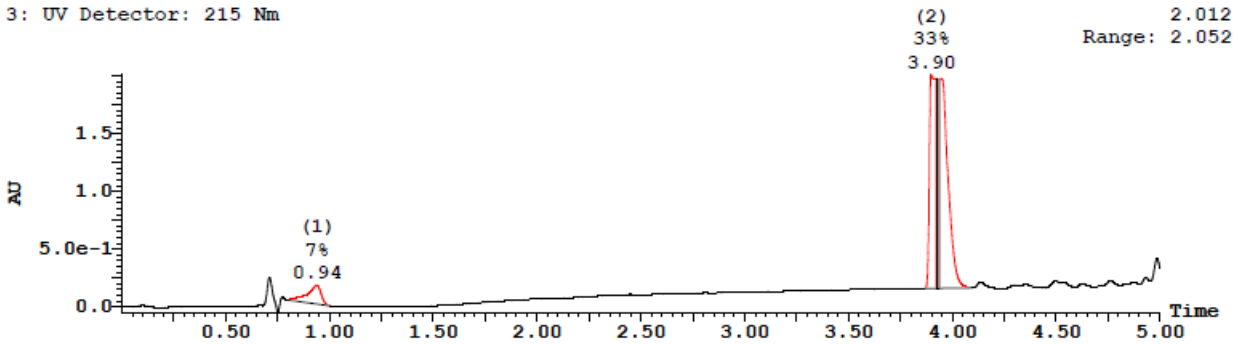

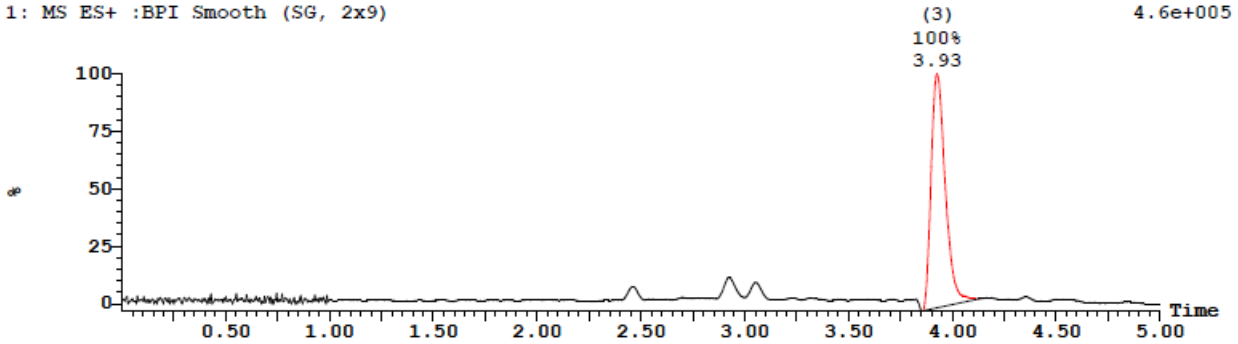

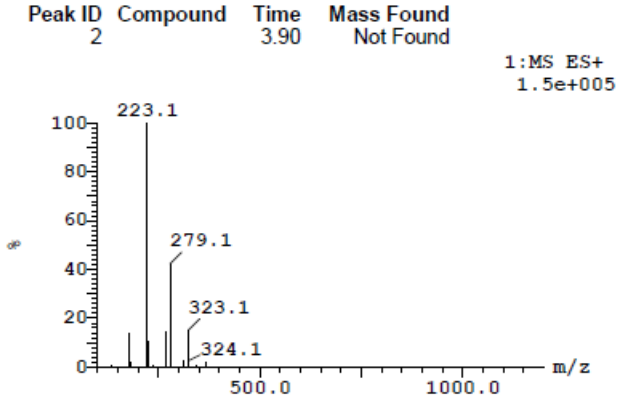

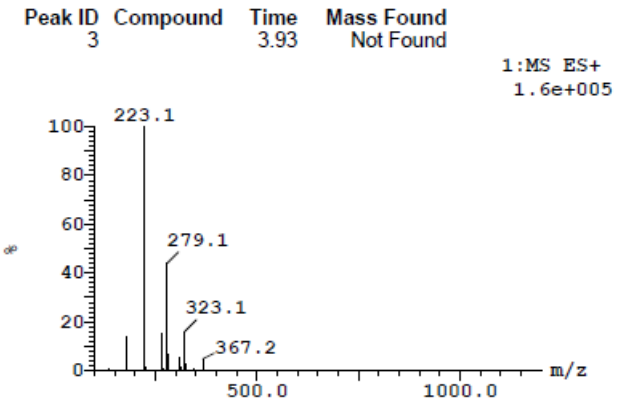

Appendix 12 – ^{1}H NMR of ENL04

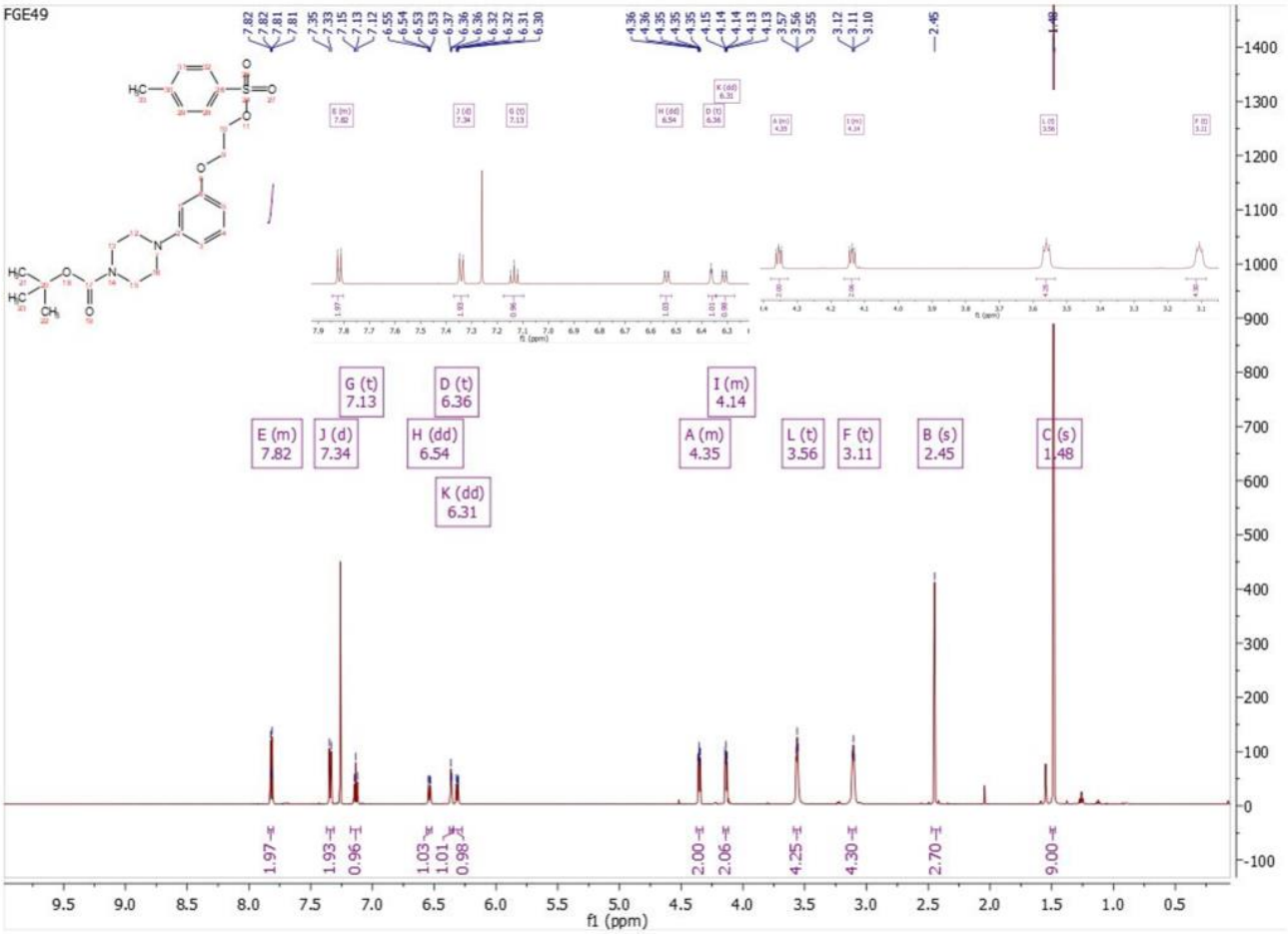

Appendix 13 – ^{13}C NMRof ENL04

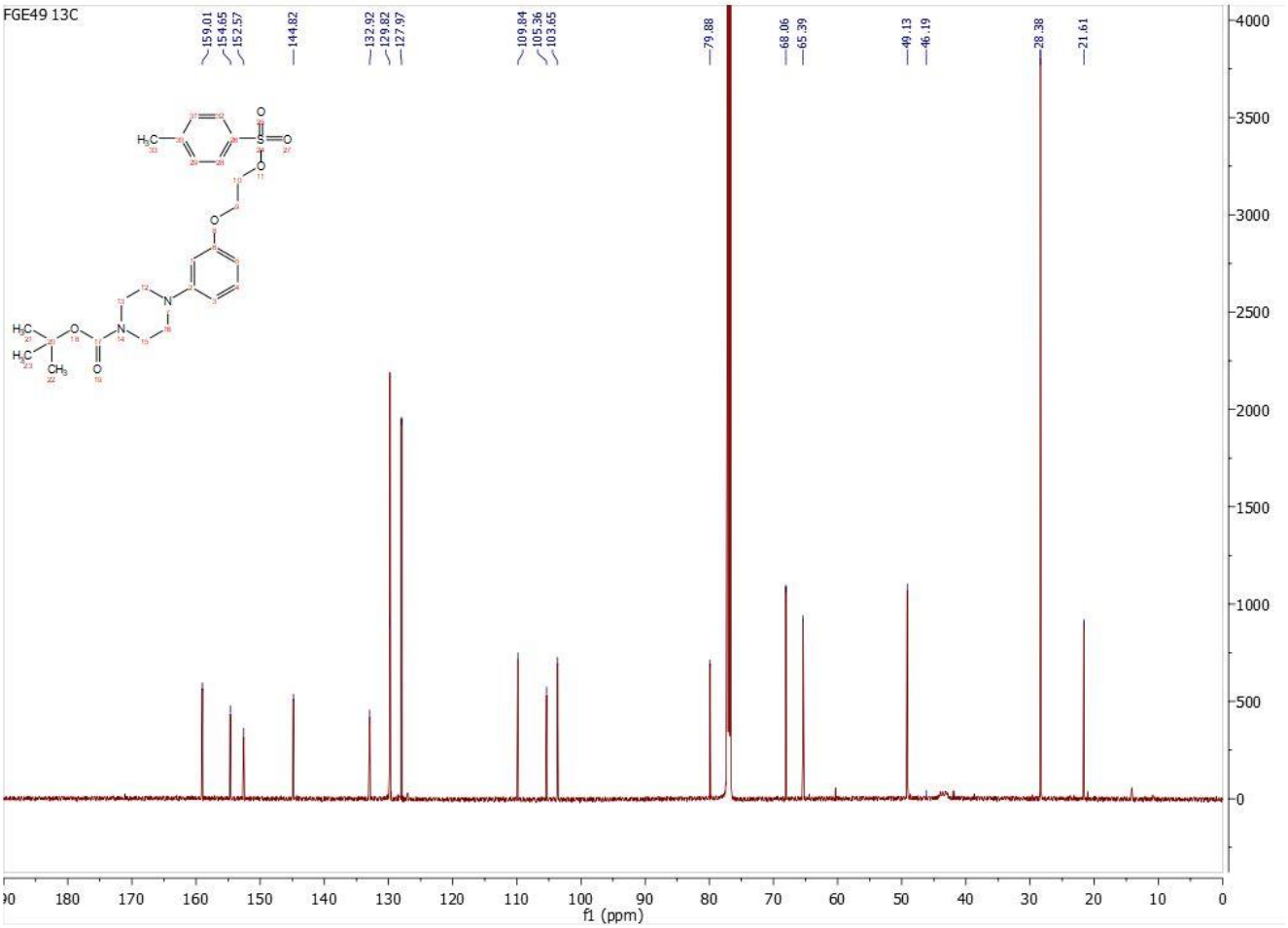

Appendix 14– UPLC-MS of ENL04

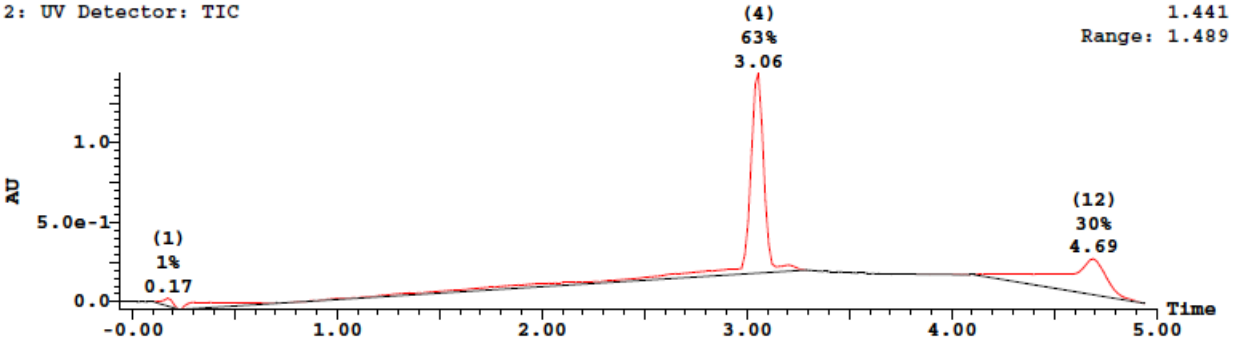

Sample 1 Vial 2:23 ID MCR_KB20-1 File MCR_KB20-1 Date 19-Jun-2018 Time 12:45:04 Description ENL04_PURE

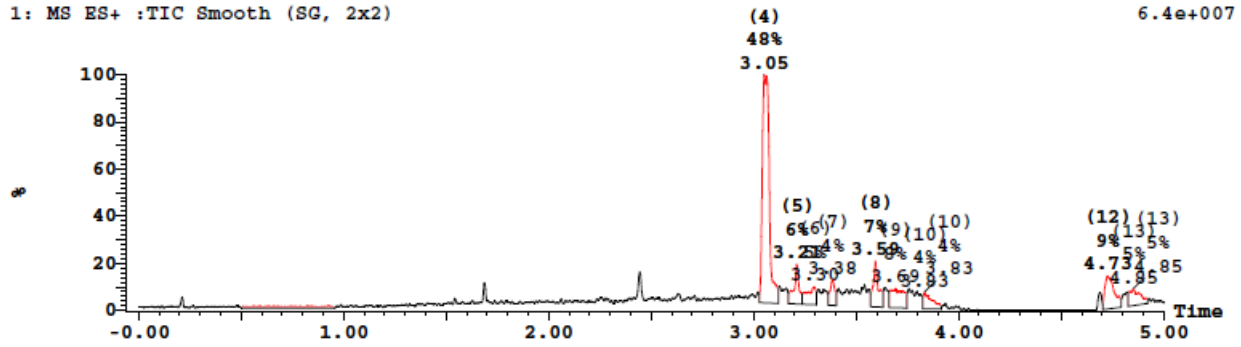

Peak ID	Compound	Time	Mass Found
4		3.05	

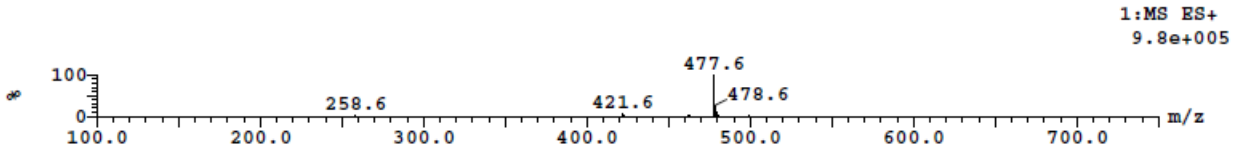

Appendix 15 – ^{1}H NMR of FGE06

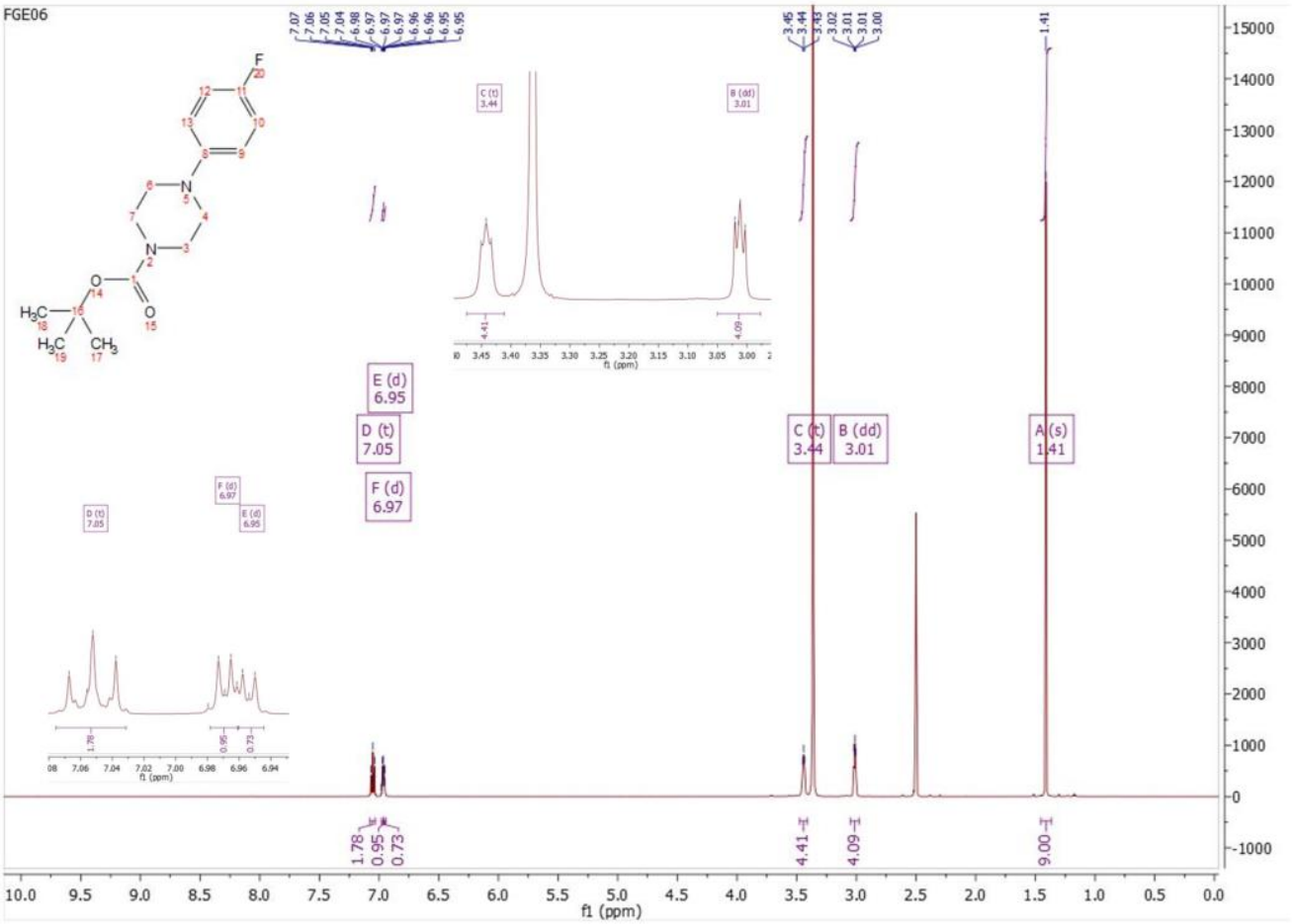

Appendix 16 – ^{13}C NMR of FGE06

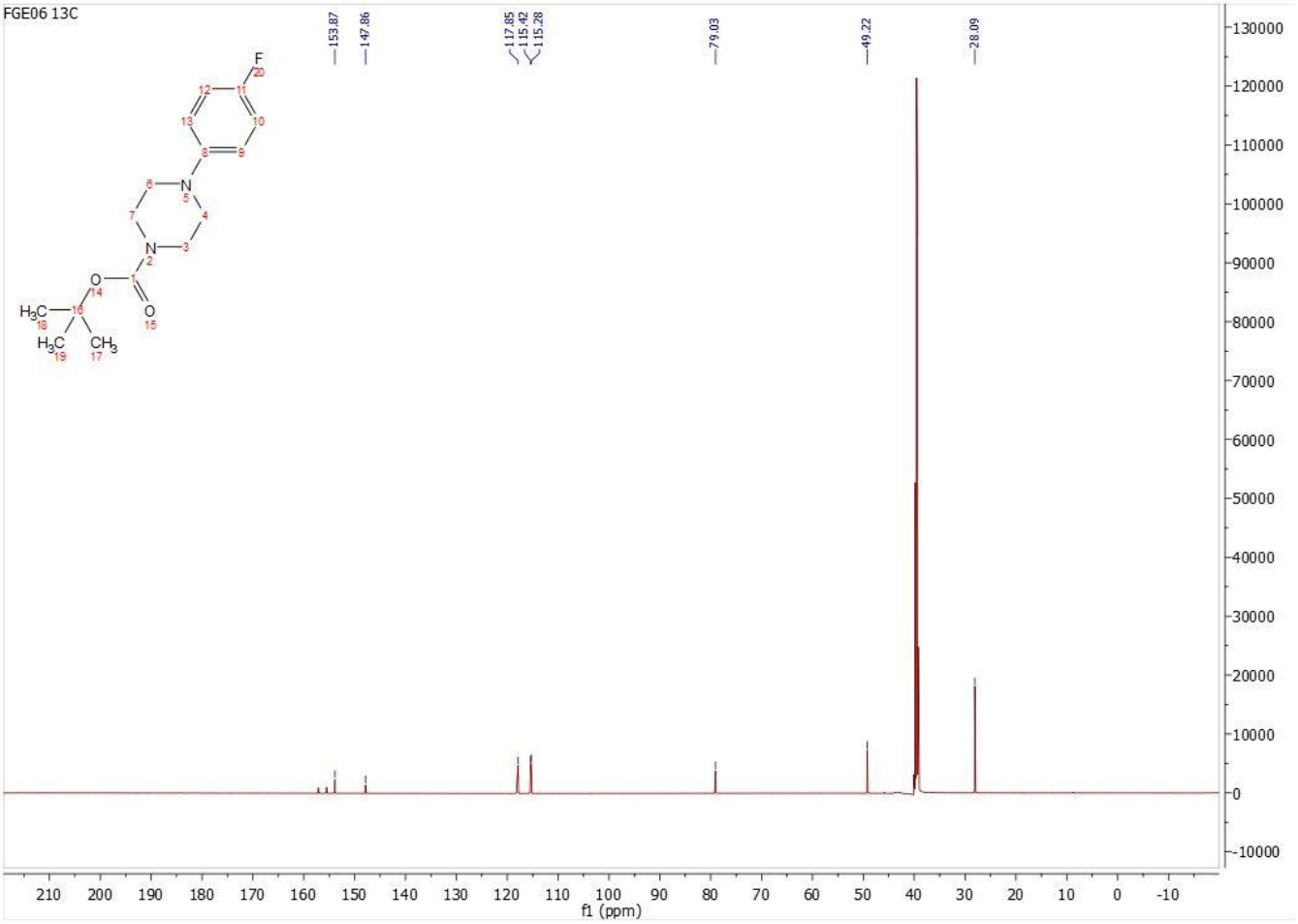

Appendix 17 – ^{1}H NMR of ENL12

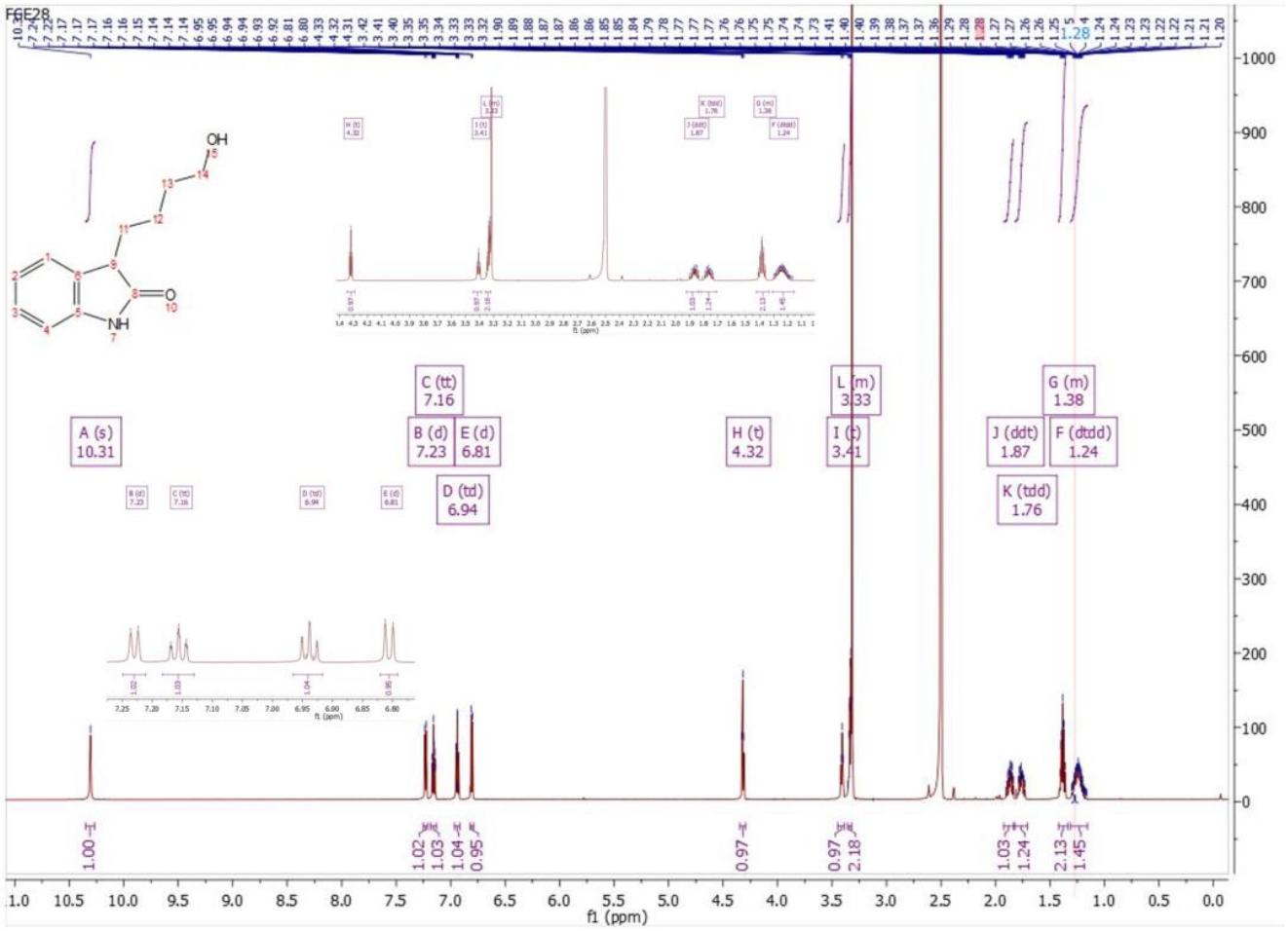

Appendix 18 – ^{13}C NMR of ENL12

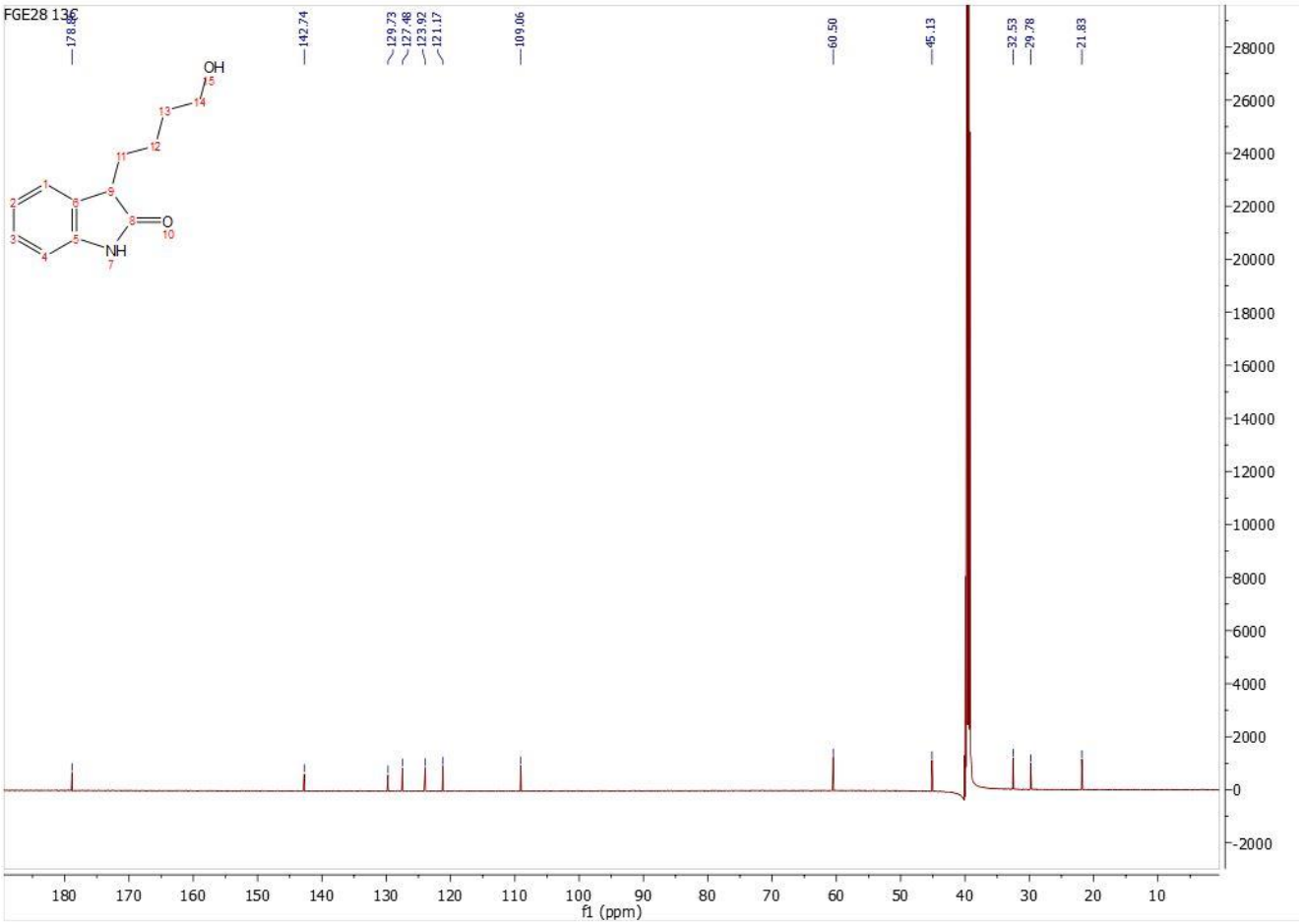

Appendix 19– UPLC-MS of ENL12

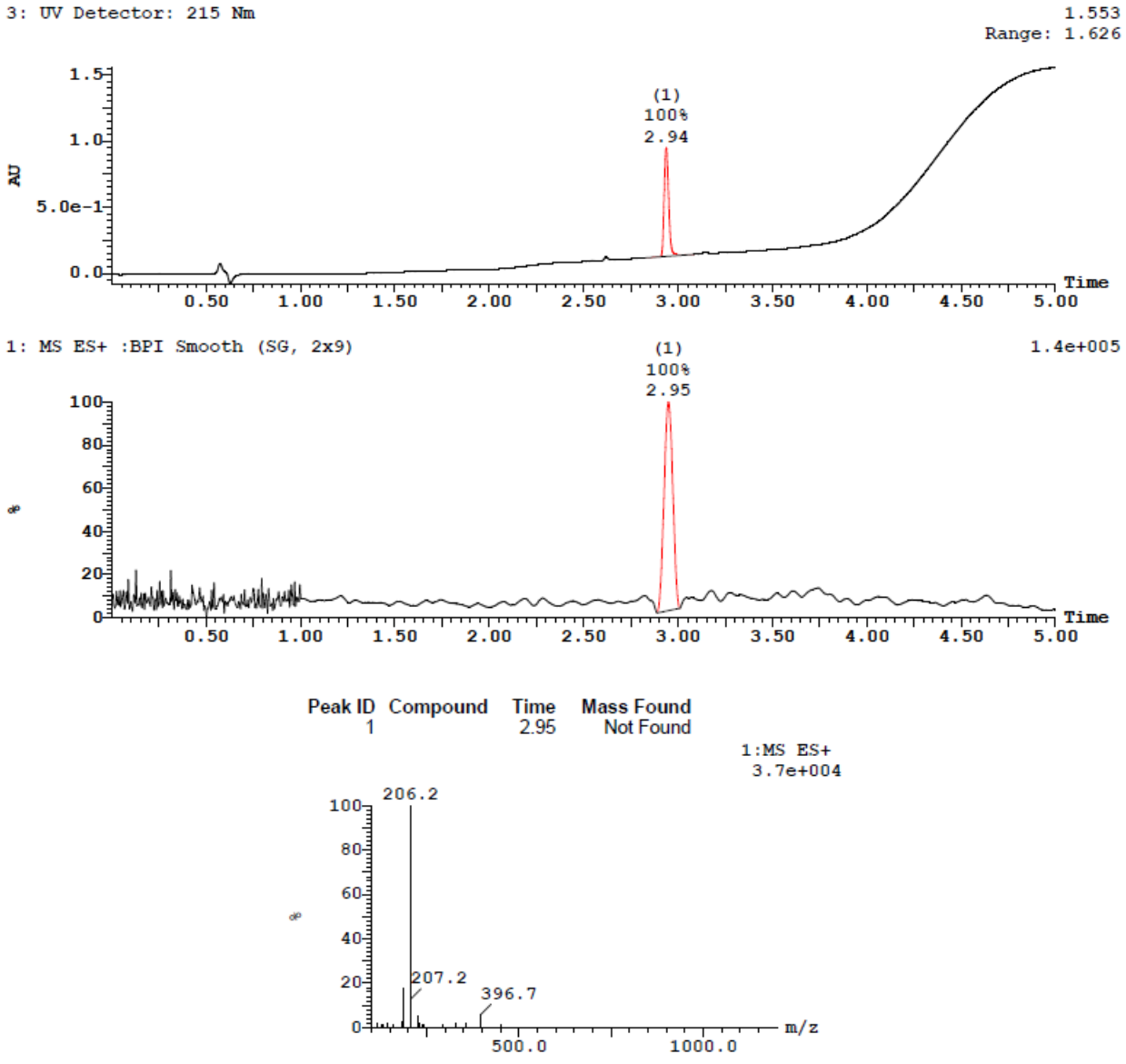

Appendix 20 – ^{1}H NMR of ENL14

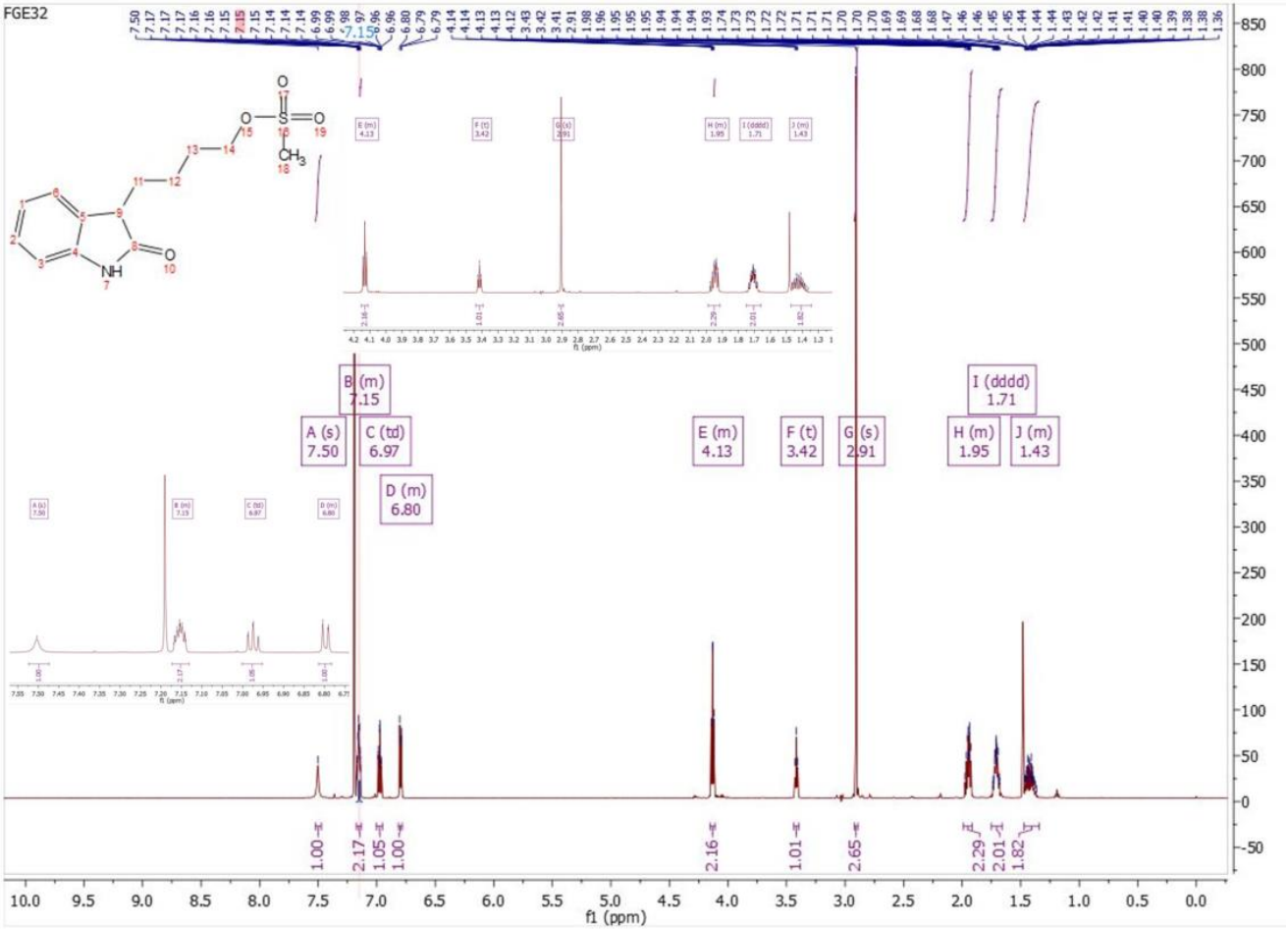

Appendix 21 – ^{13}C NMR of ENL14

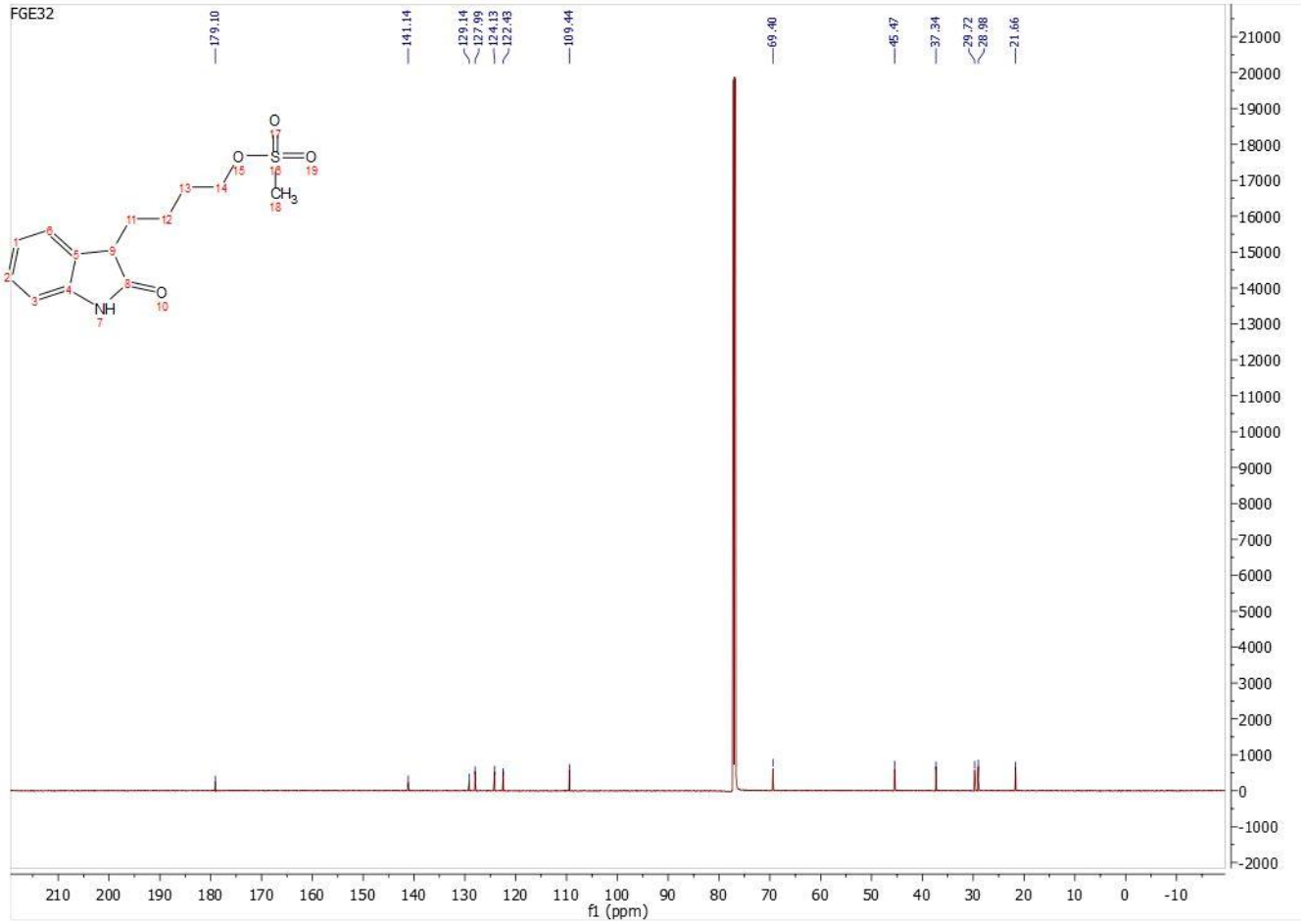

Appendix 22– UPLC-MS of ENL14

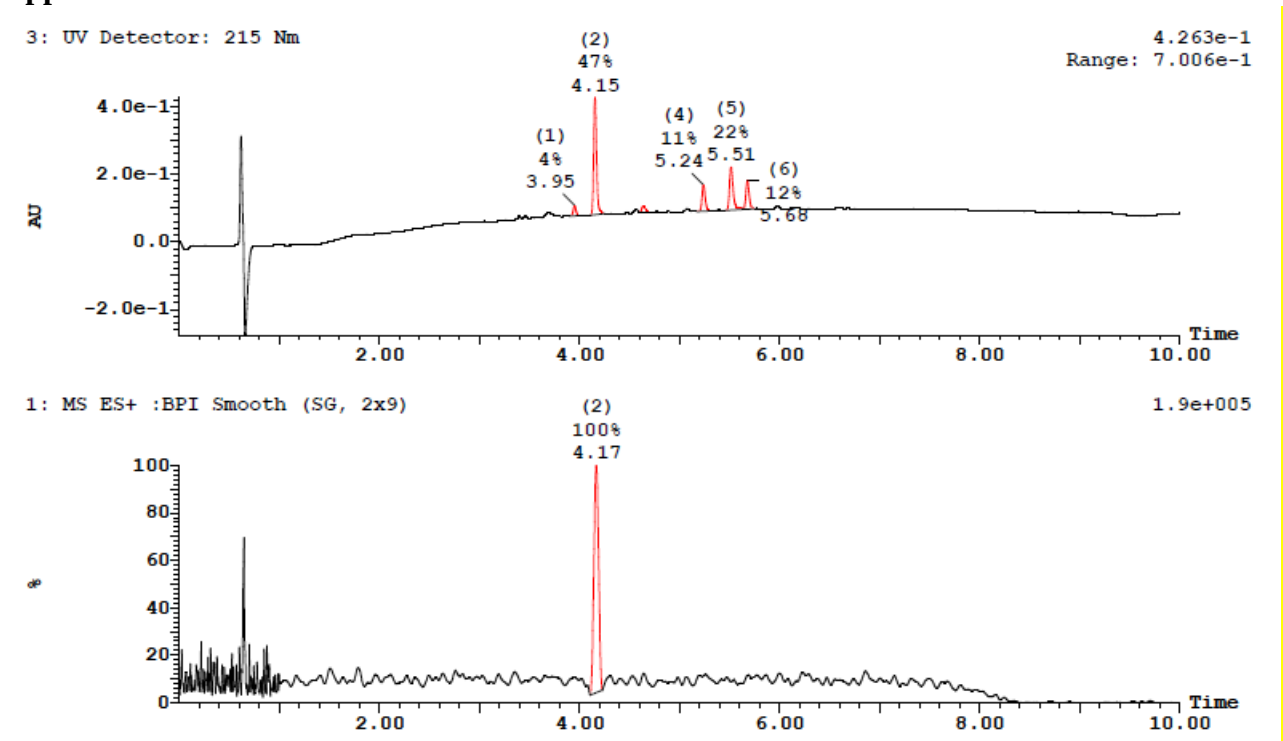

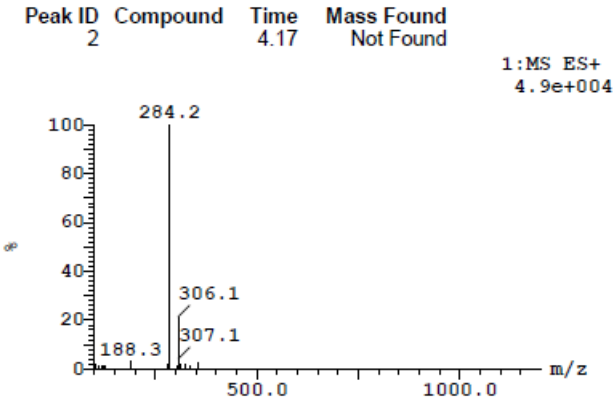

Appendix 23 – ^{1}H NMR of ENL20

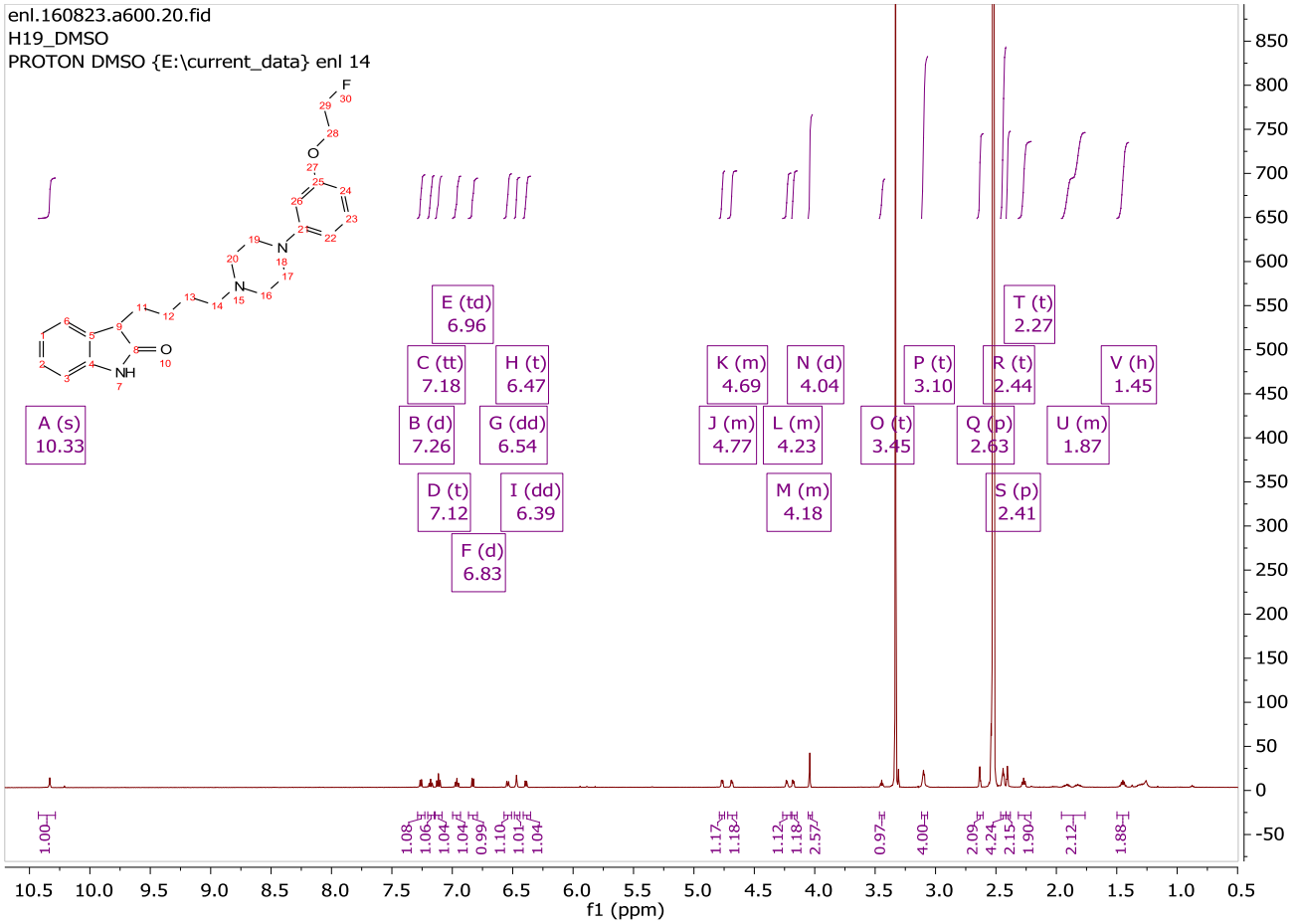

Appendix 24 – ^{13}C NMR of ENL20

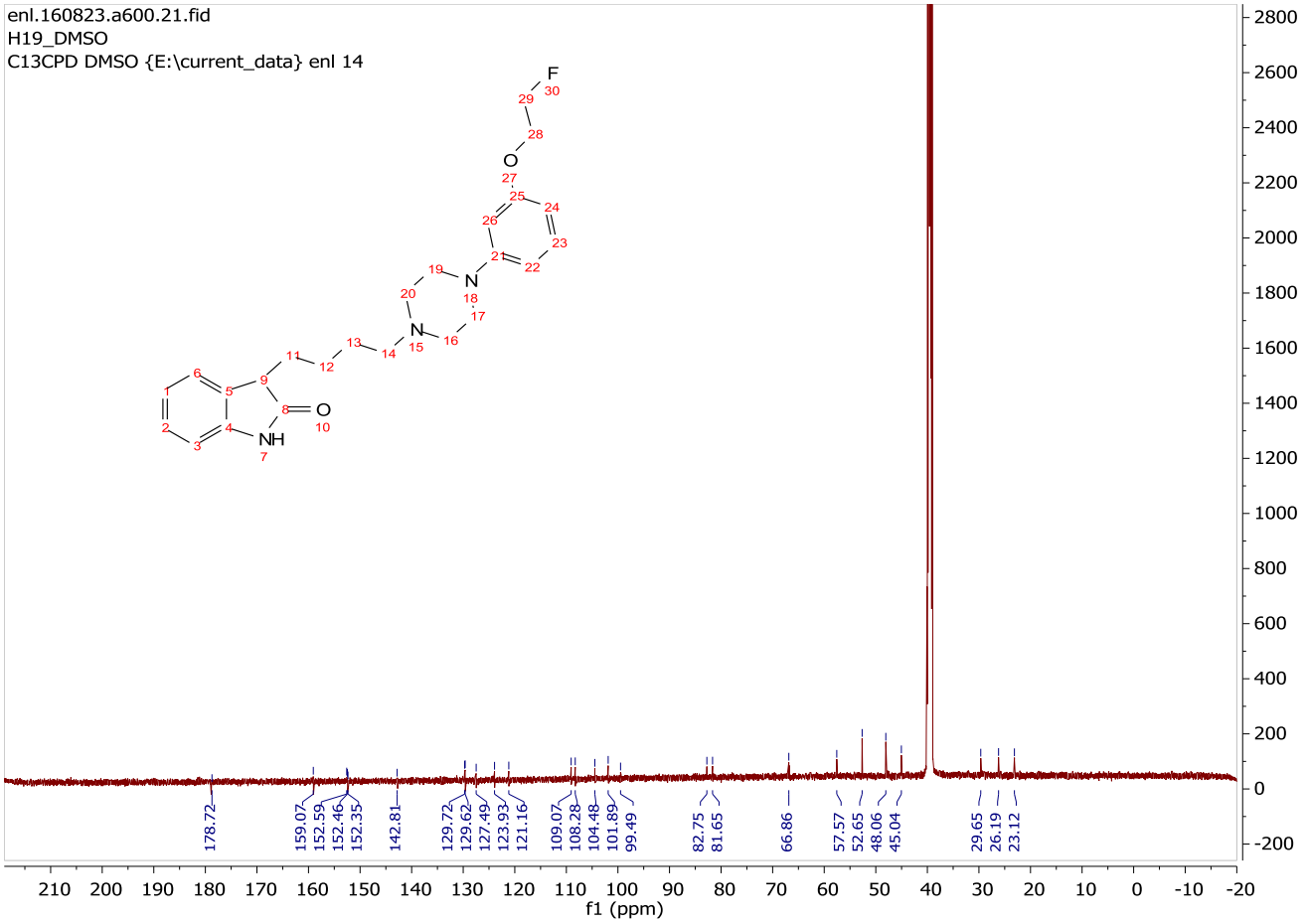

Appendix 25– UPLC-MS of ENL20

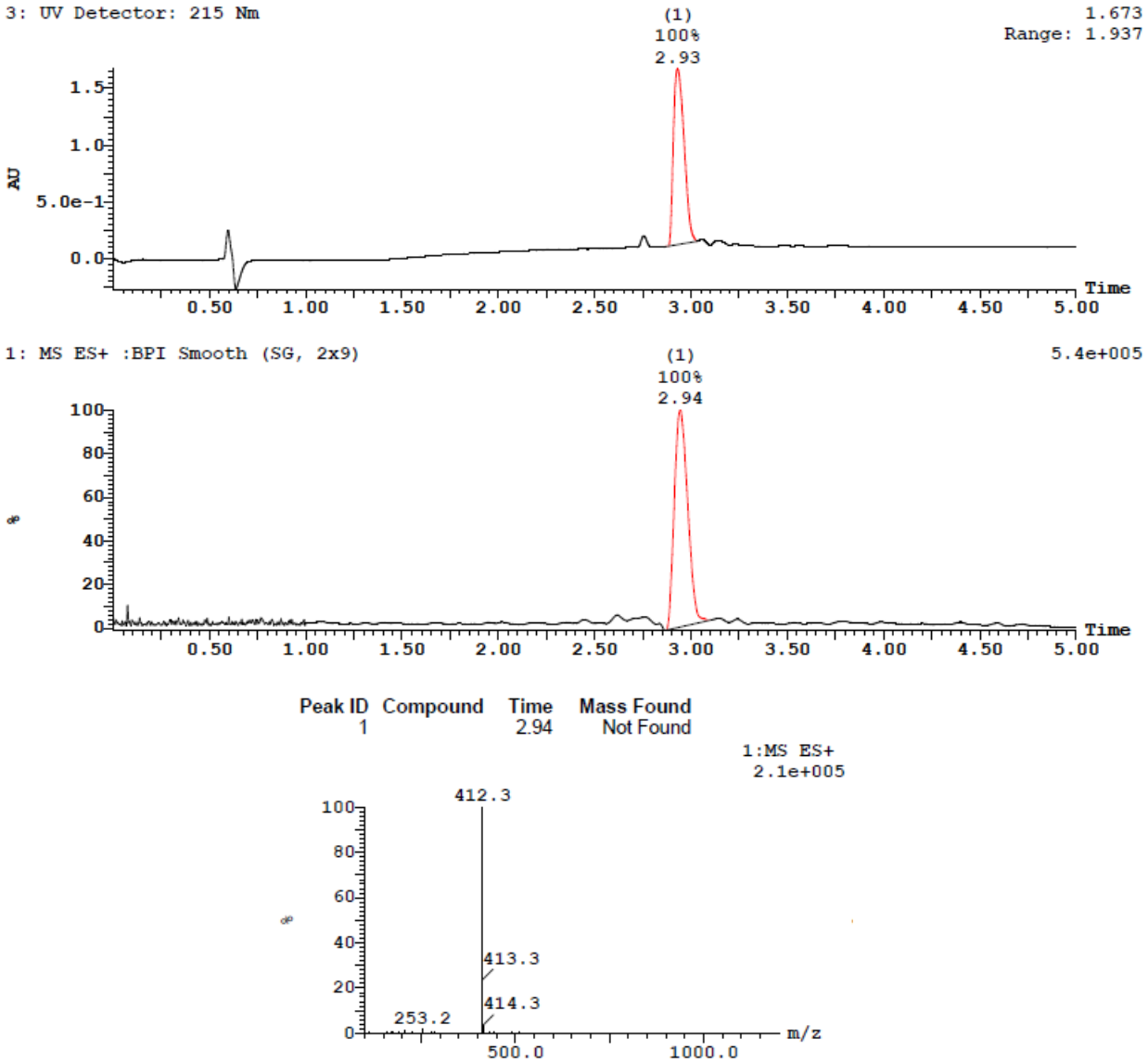

Appendix 26– ^{1}H NMR of ENL10

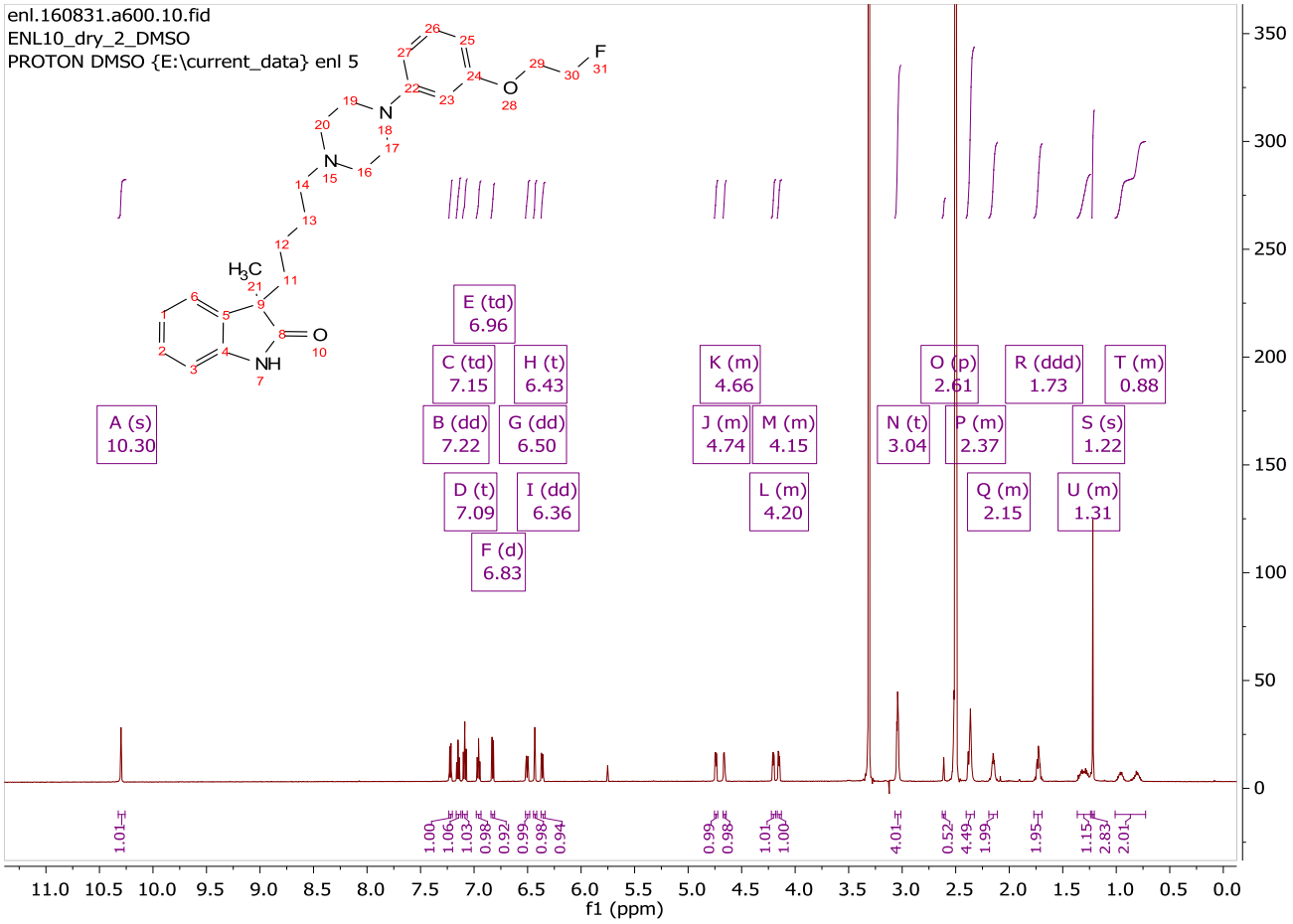

Appendix 27 – ^{13}C NMR of ENL10

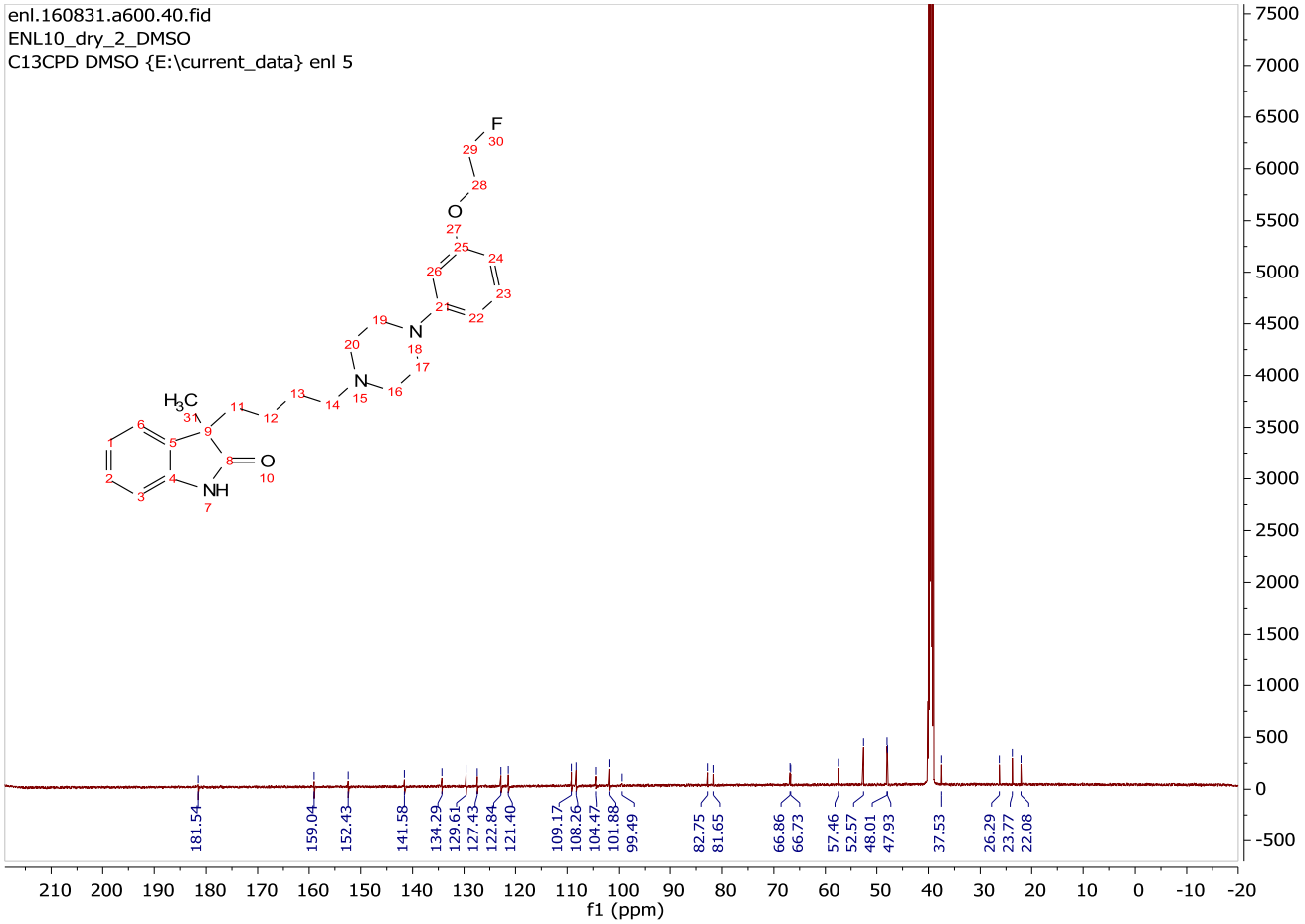

Appendix 28– UPLC-MS of ENL10

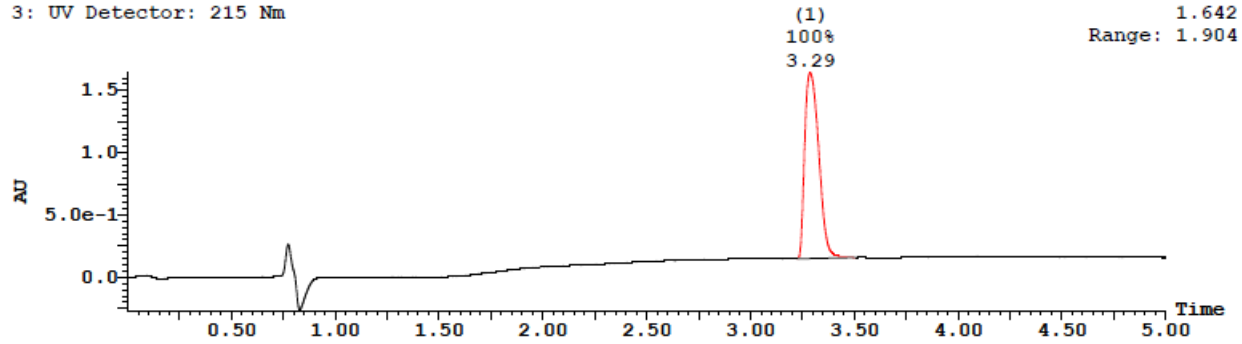

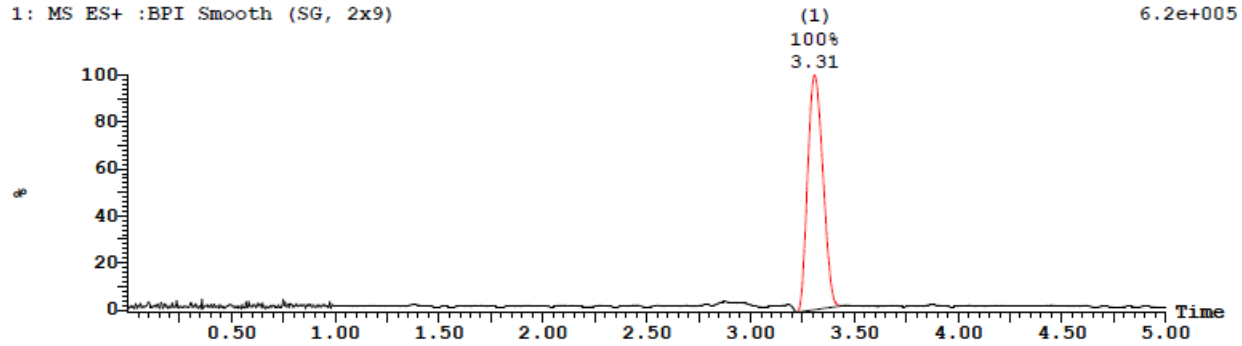

Peak ID	Compound	Time	Mass Found
1		3.31	Not Found

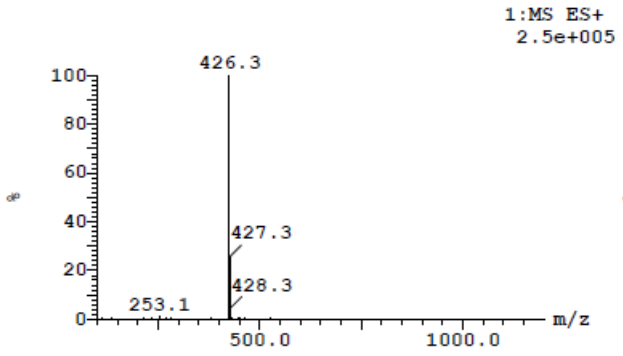

Appendix 29 – ^{1}H NMR of ENL09

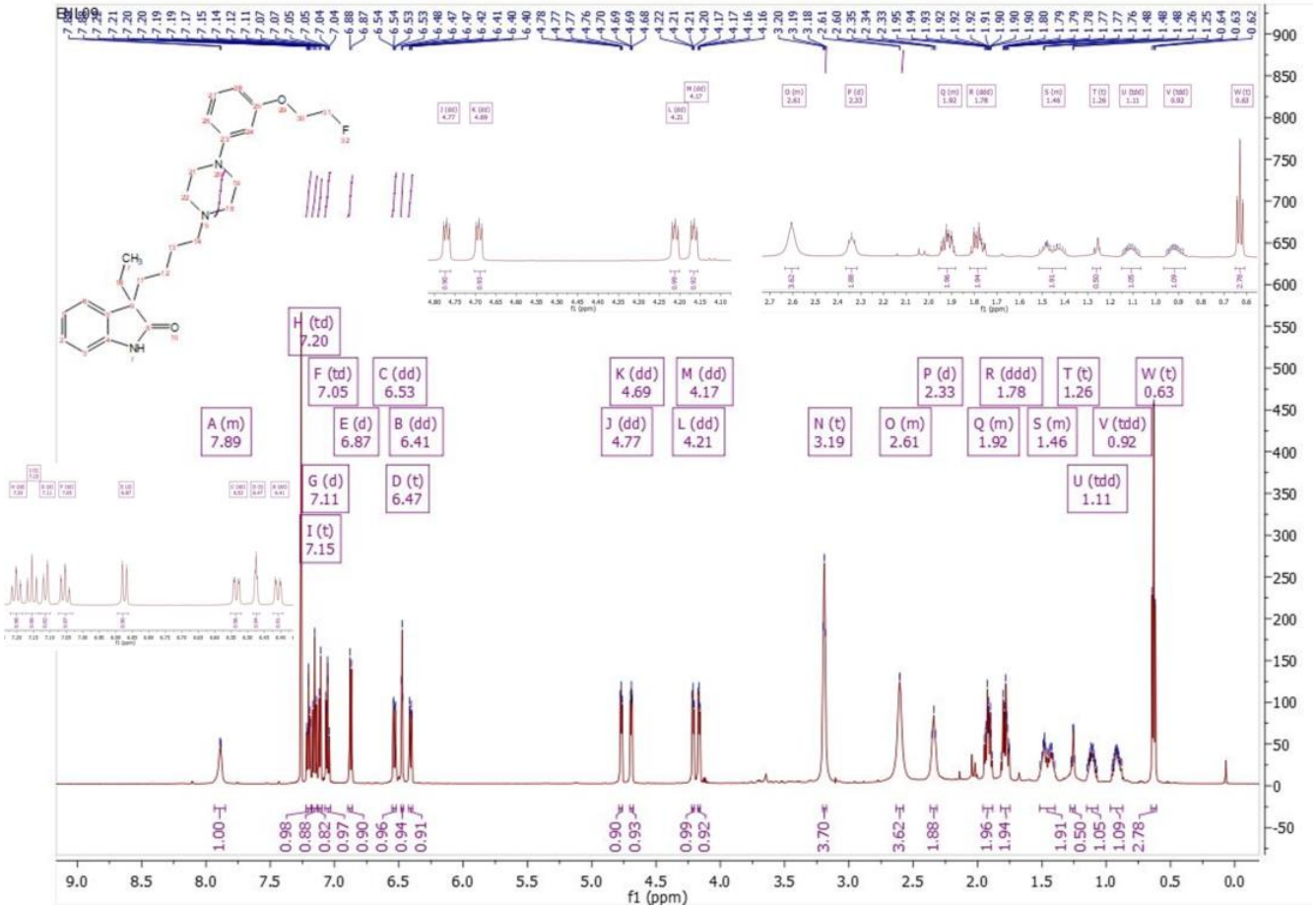

Appendix 30 – ^{13}C NMR of ENL09

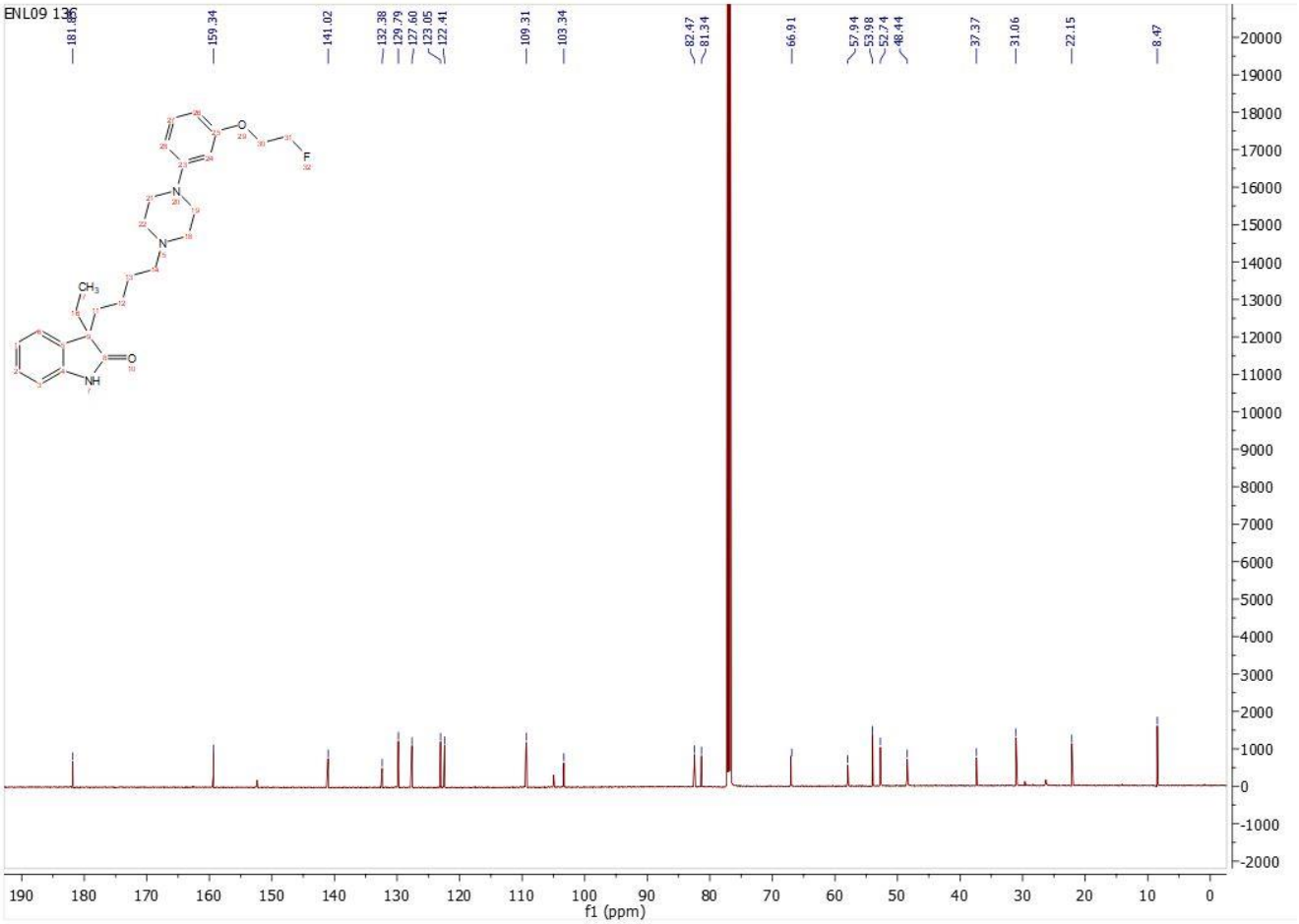

Appendix 31– UPLC-MS of ENL09

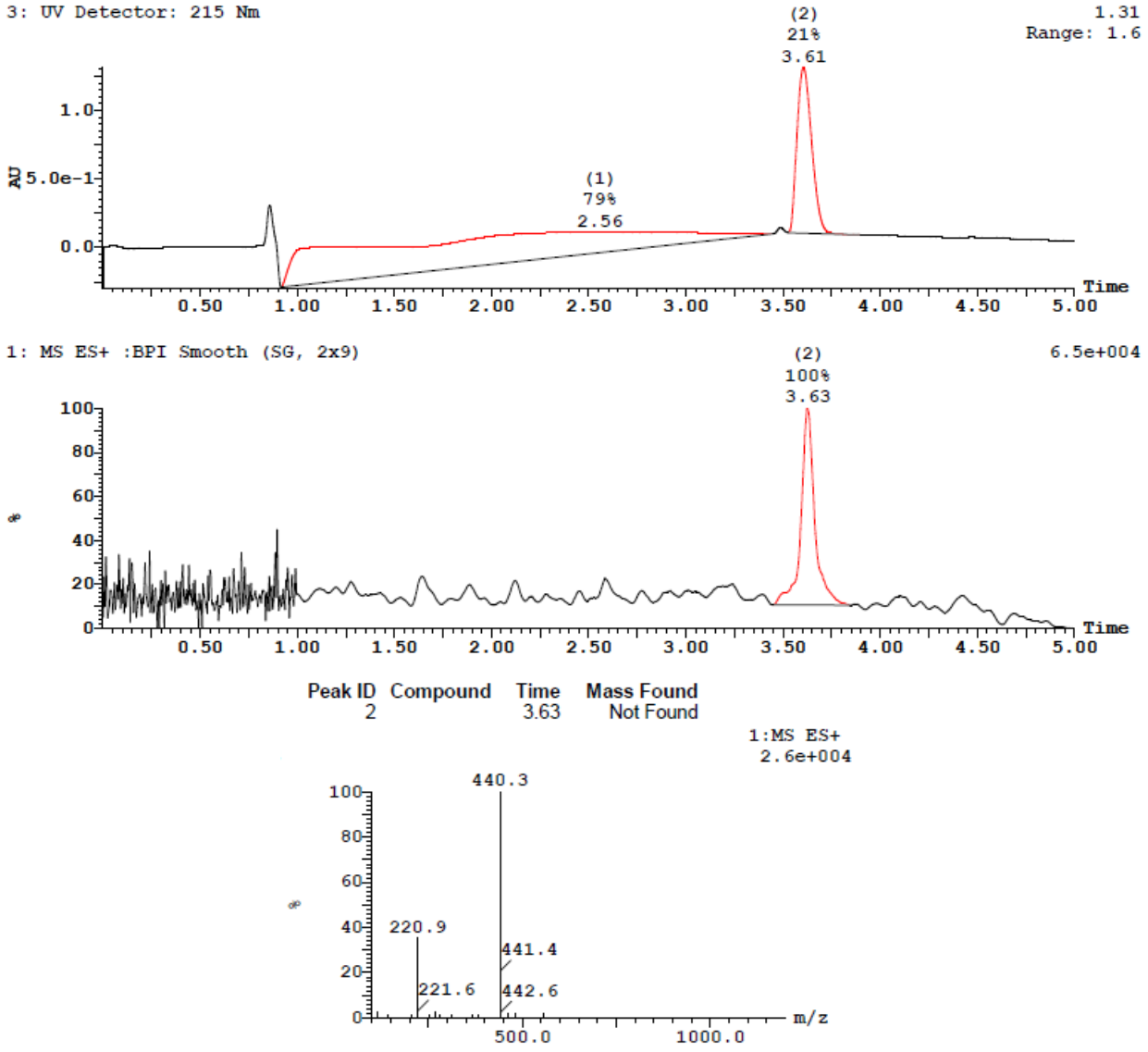

Appendix 32 – ^{13}C NMR of ENL61

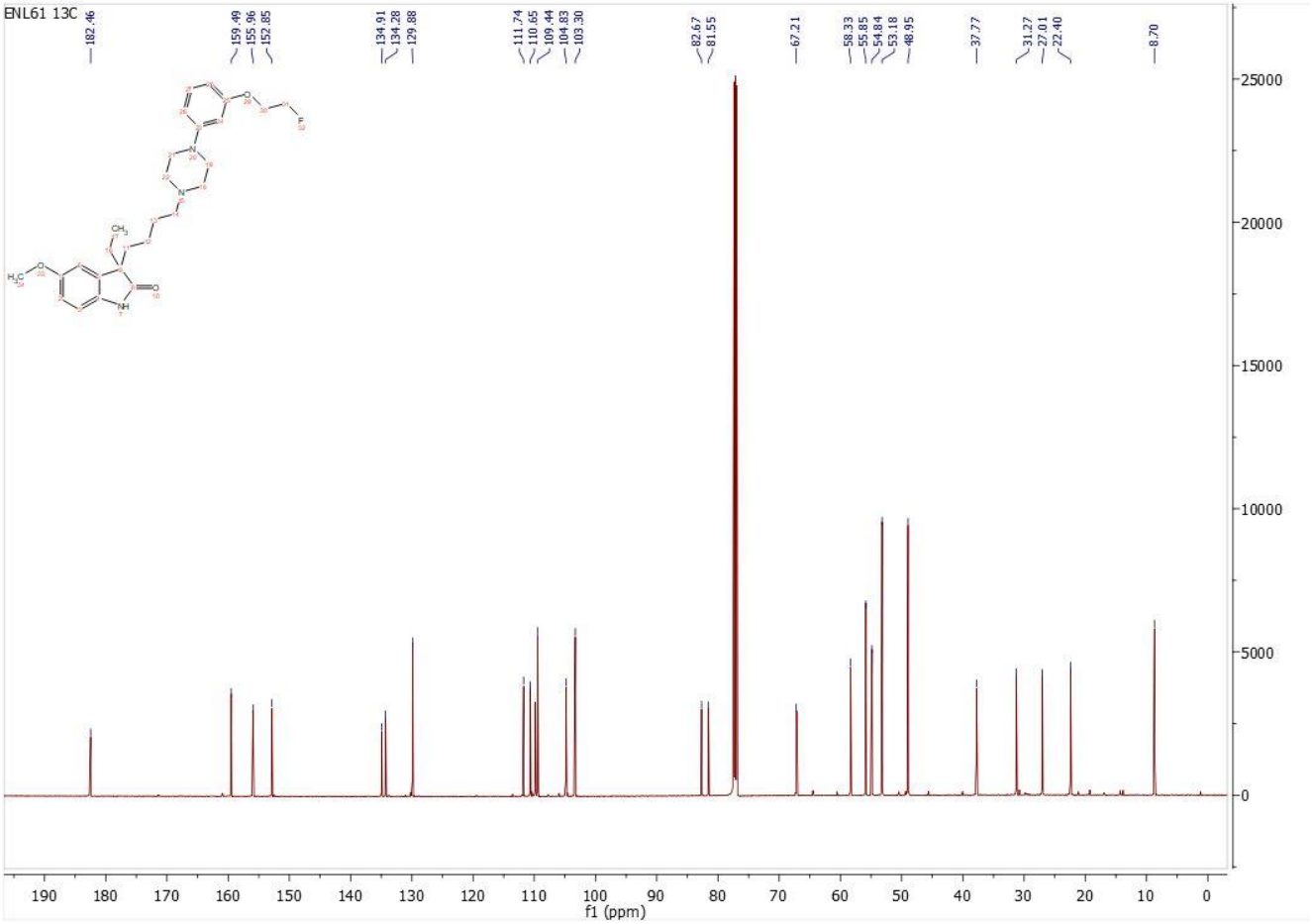

Appendix 33 – ^{1}H NMR of ENL61

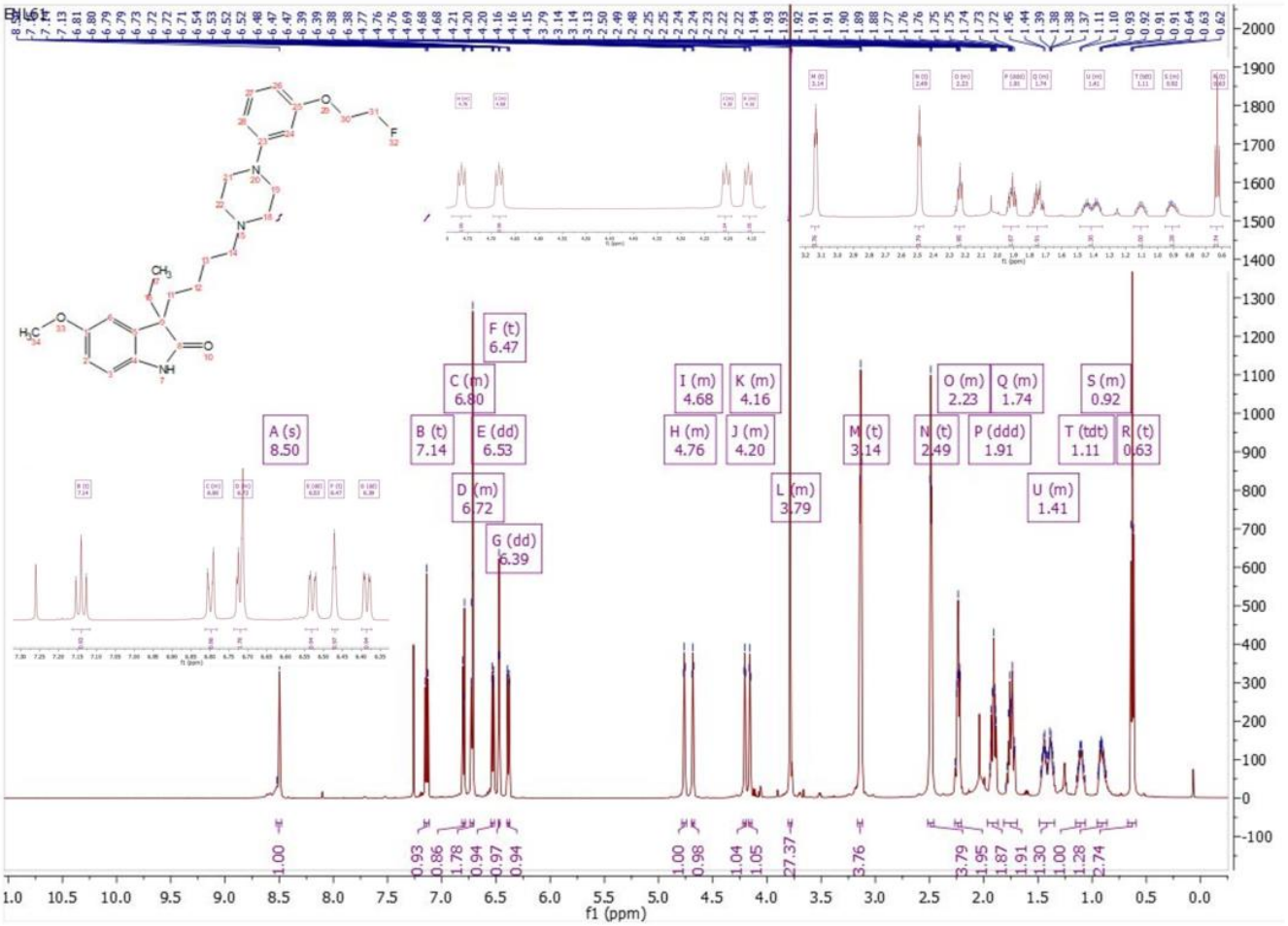

Appendix 34– UPLC-MS of ENL61

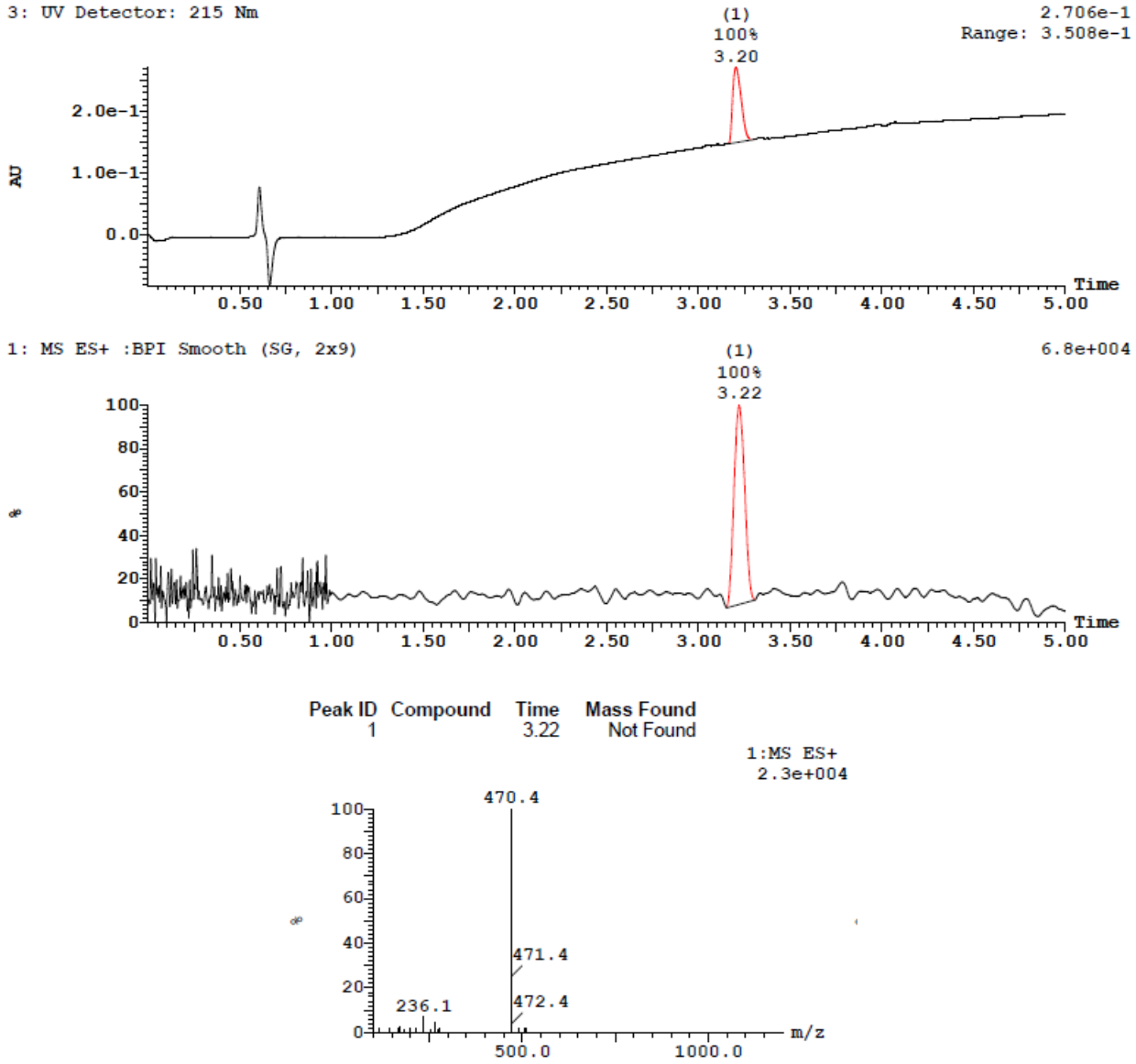

Peak ID	Compound	Time	Mass Found
1		3.22	Not Found

Appendix 35 – ^{1}H NMR of ENL06

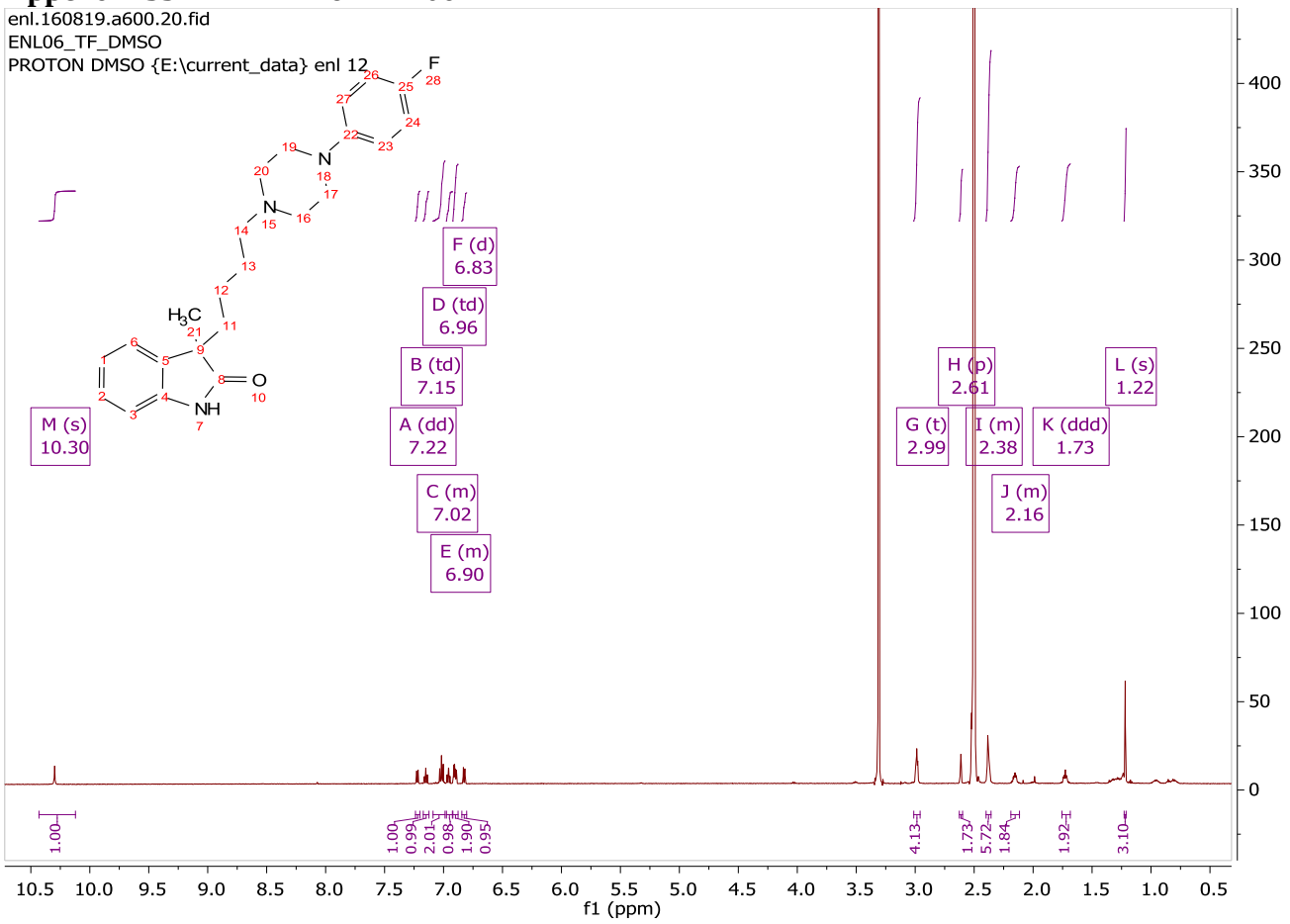

Appendix 36 – ^{13}C NMR of ENL06

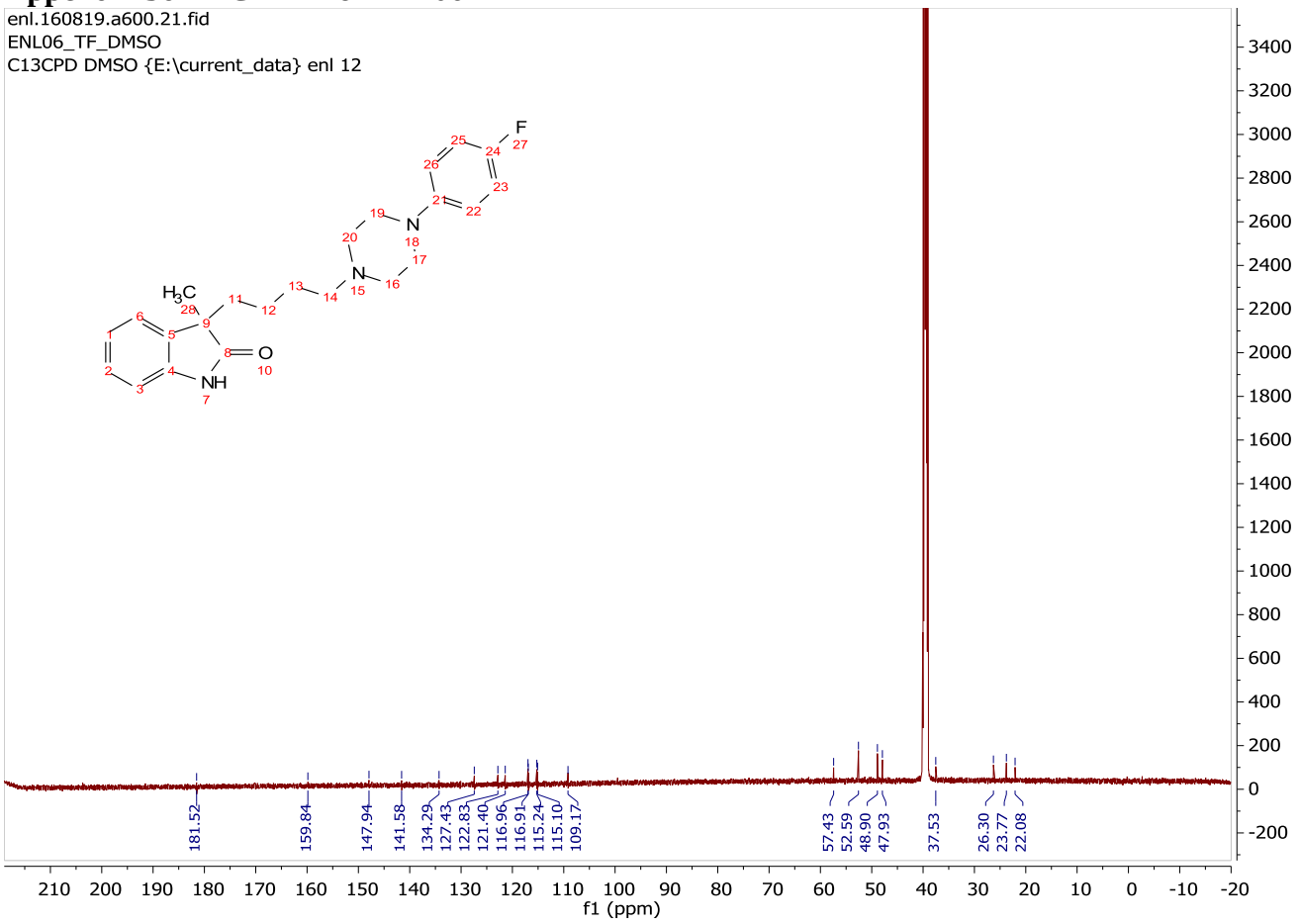

Appendix 37– UPLC-MS of ENL06

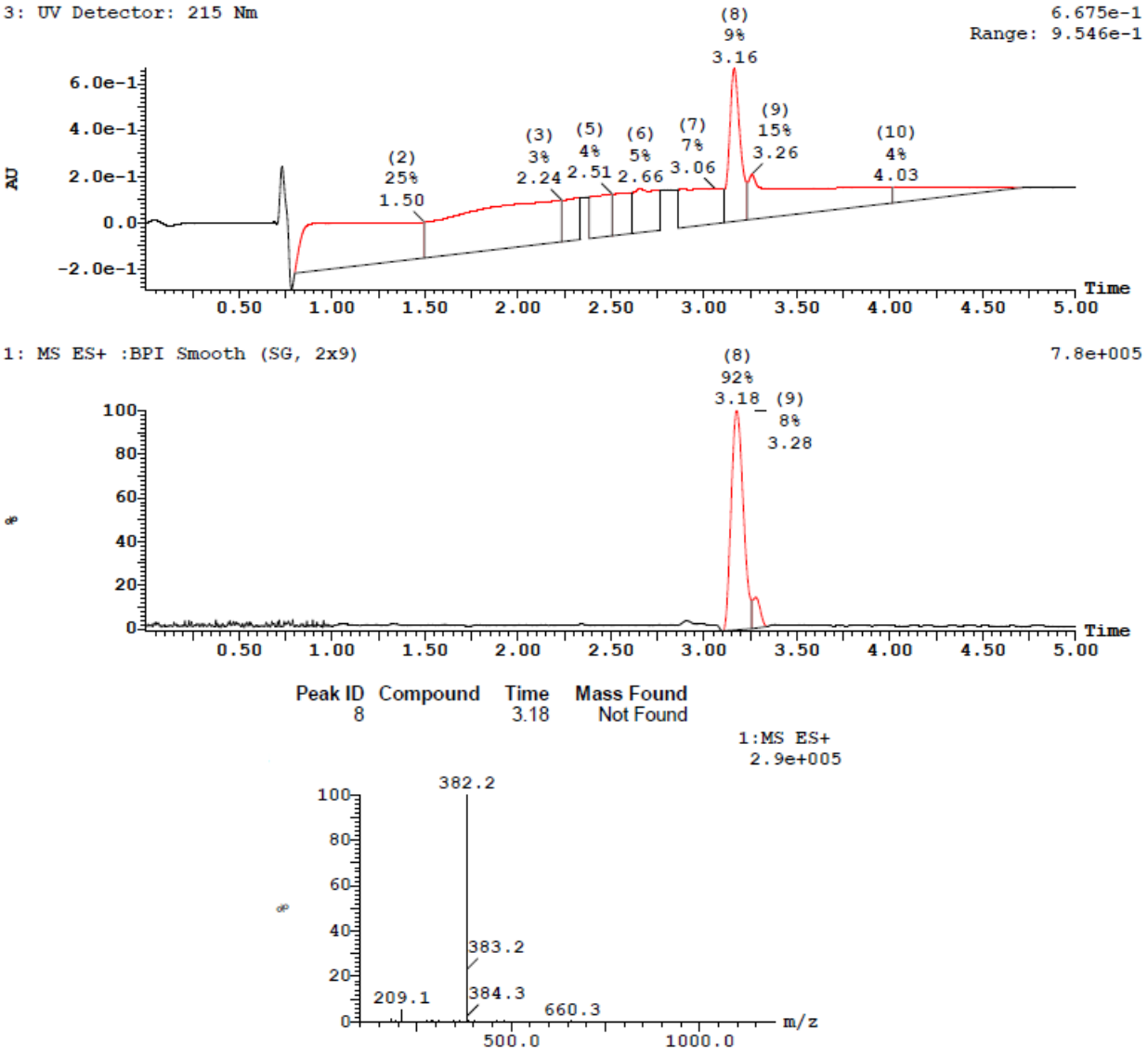

Appendix 38 – ^{1}H NMR of ENL05

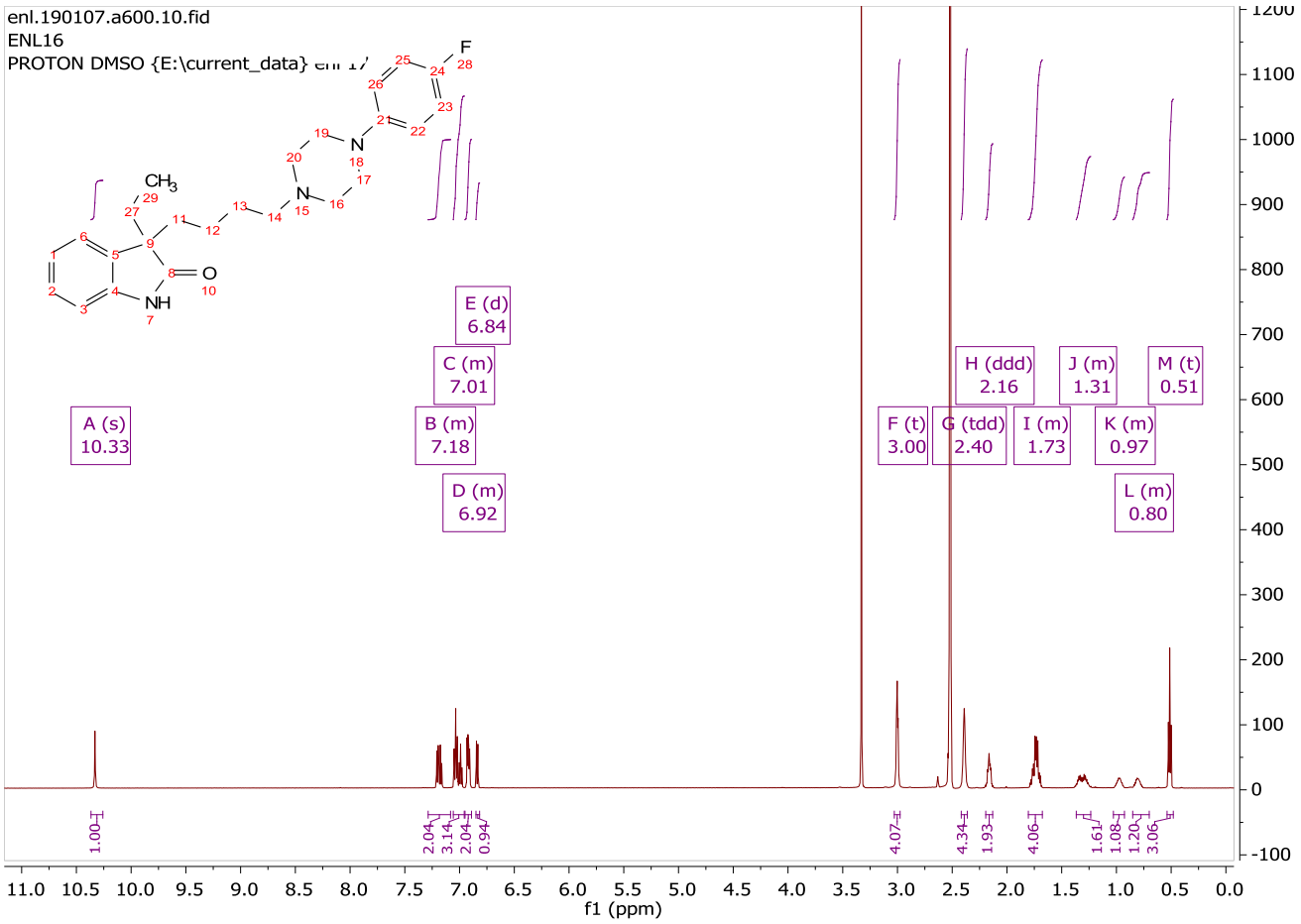

Appendix 39 – ^{13}C NMR of ENL05

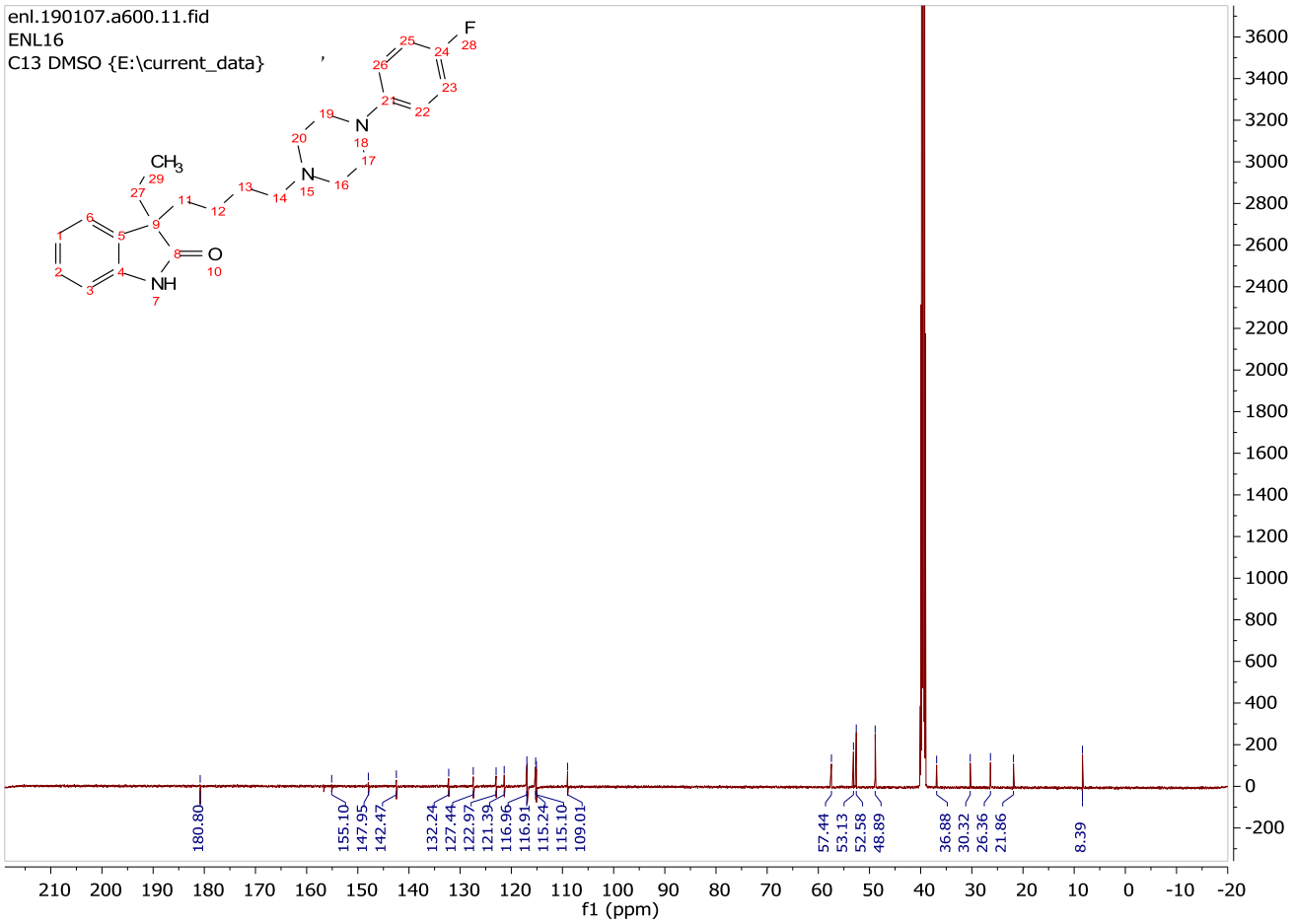

Appendix 40– UPLC-MS of ENL05

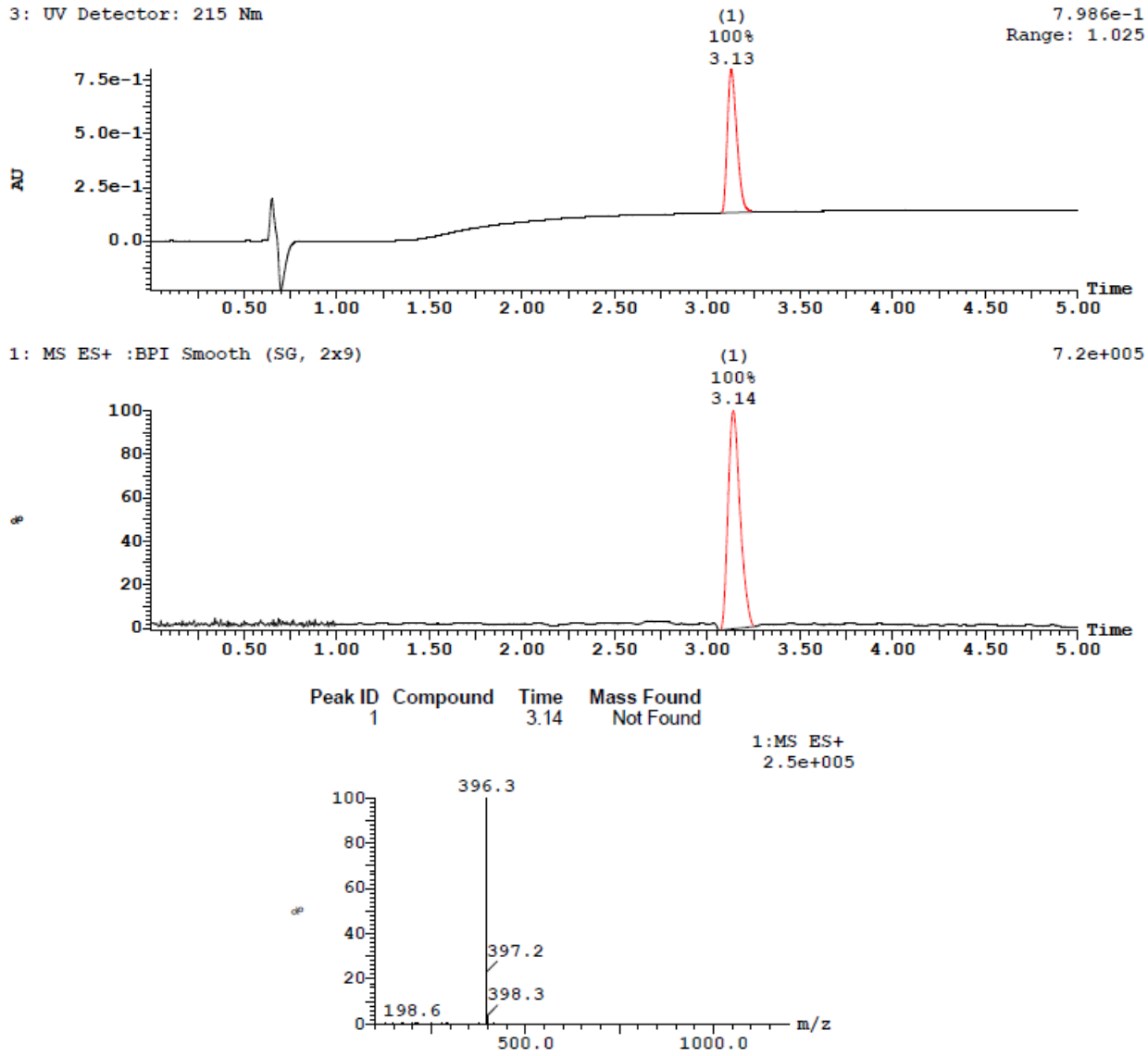

Appendix 41 – ^{1}H NMR of ENL60

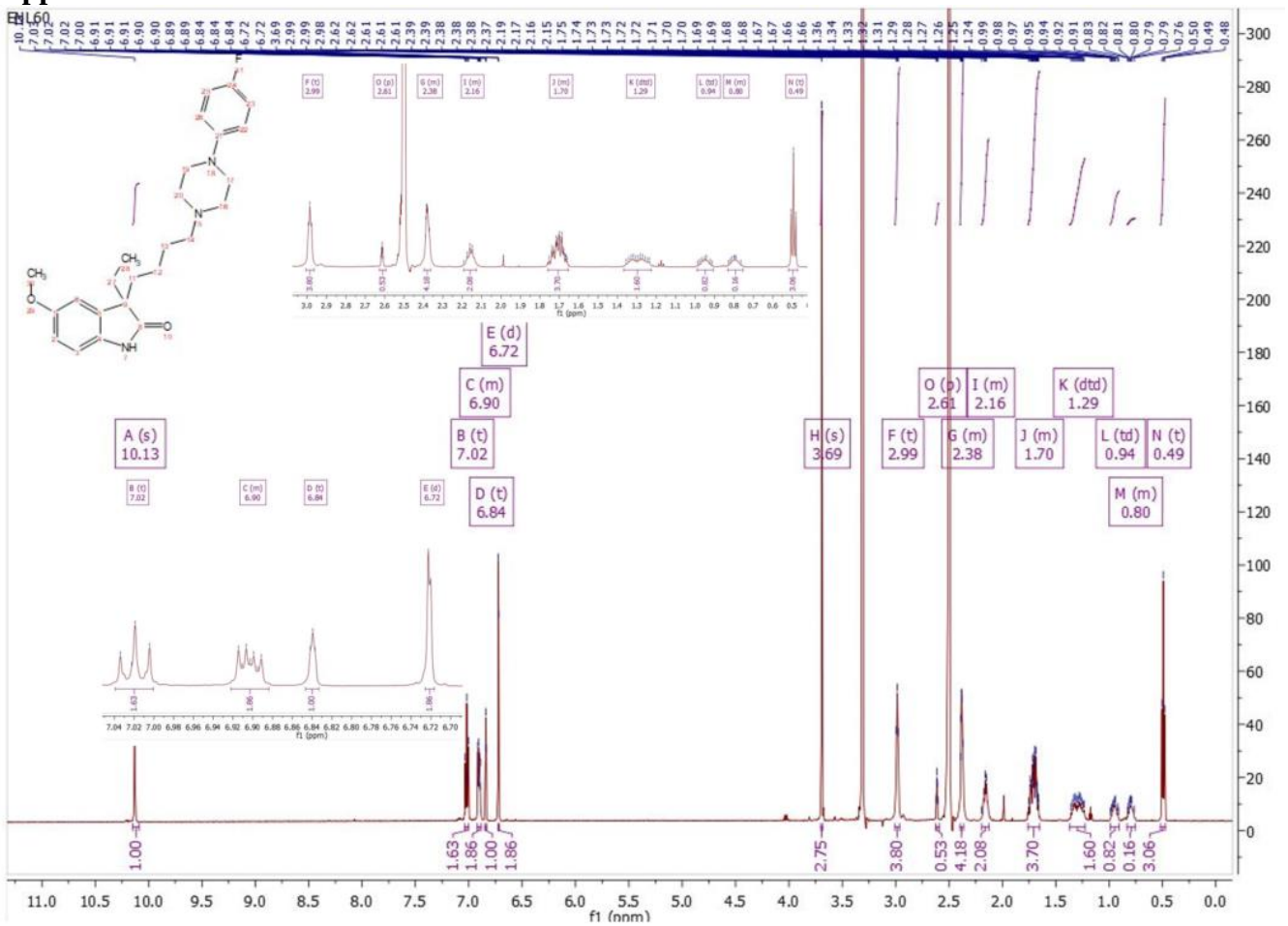

Appendix 42 – ^{13}C NMR of ENL60

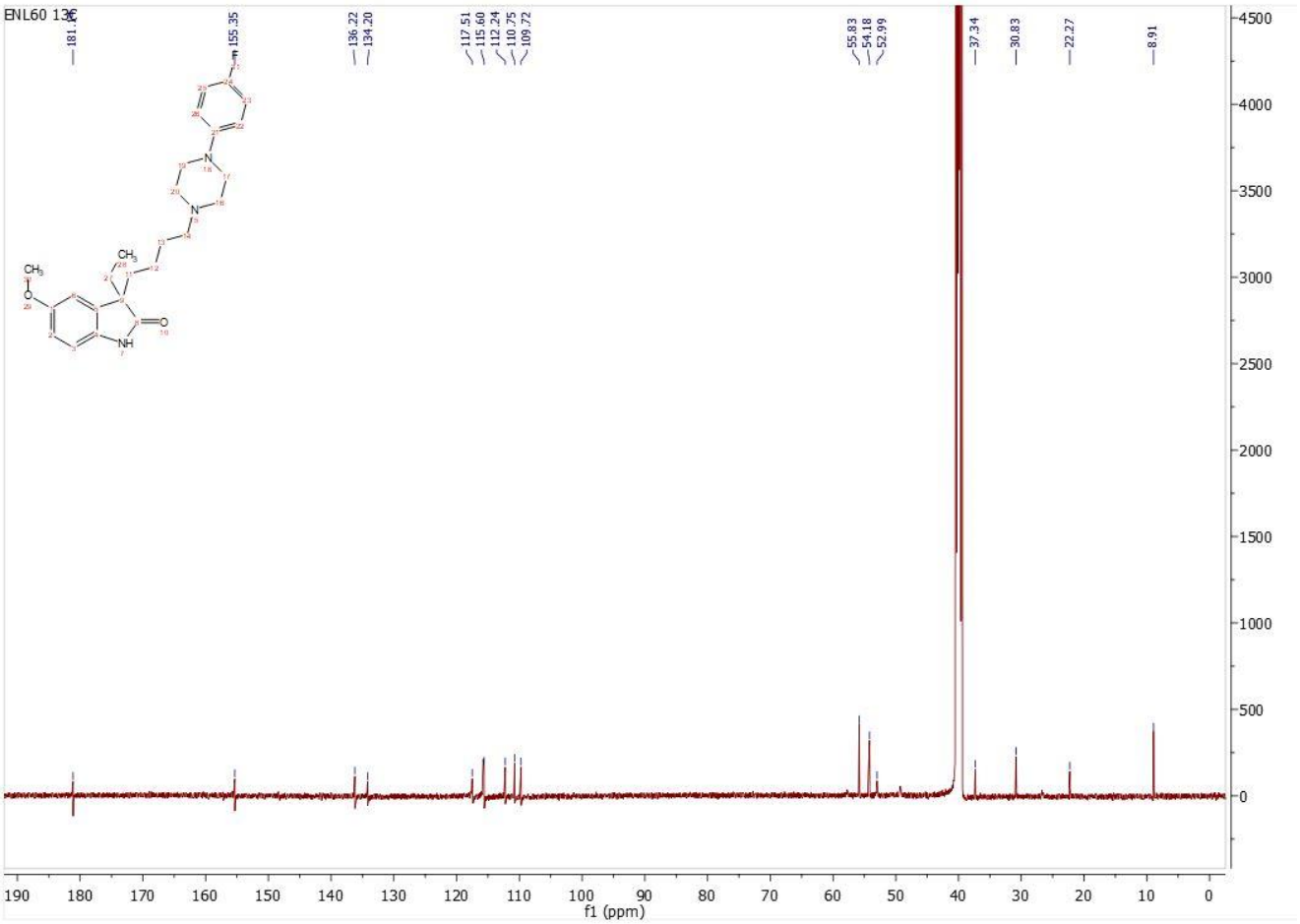

Appendix 43– UPLC-MS of ENL60

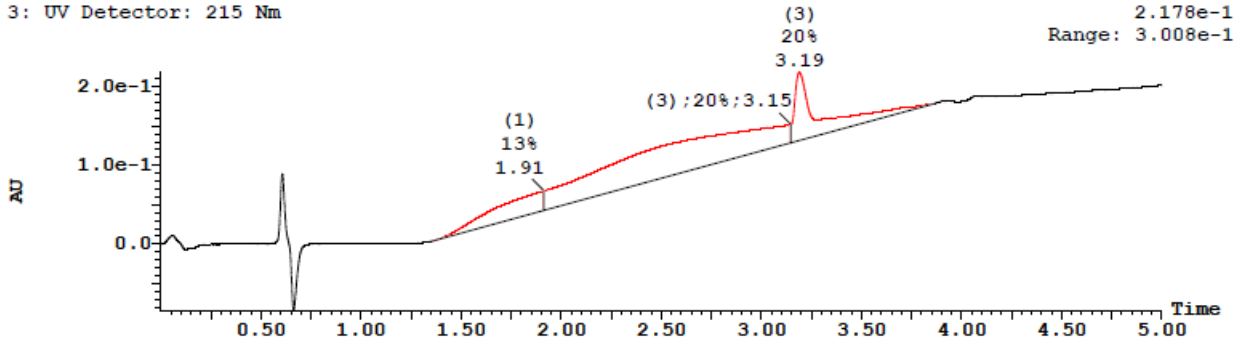

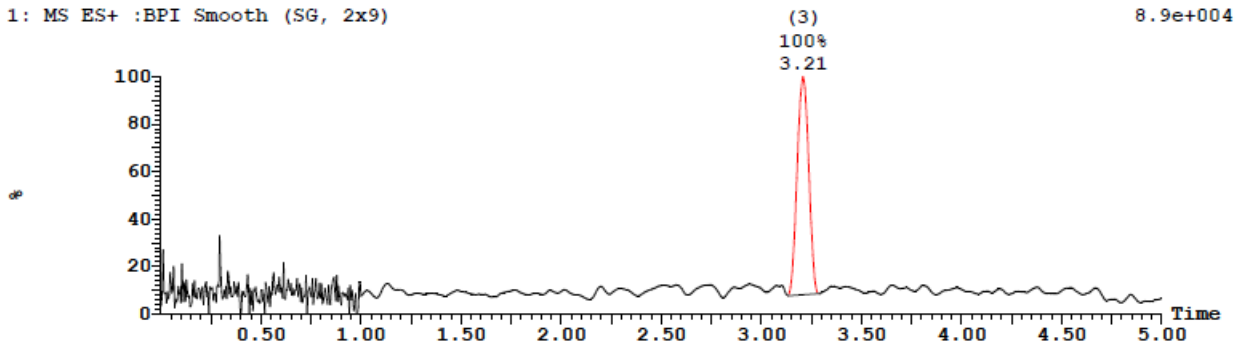

Peak ID	Compound	Time	Mass Found
3		3.21	Not Found

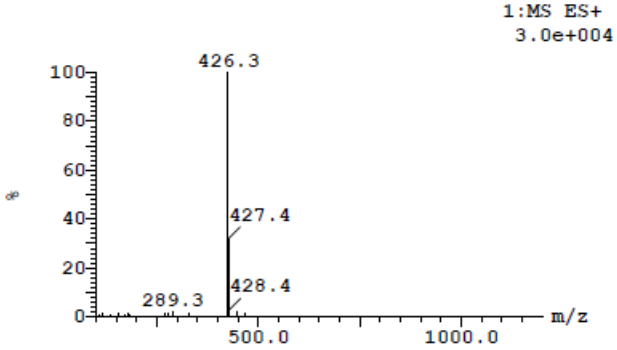

Chapter 6

Paper IV

Development and Evaluation of Two Potential 5-HT_7 Receptor PET Tracers: [^{18}F]ENL09 and [^{18}F]ENL10

Summary:

Paper IV *is here presented in chapter 6 of this thesis. In this paper the PET tracer library synthesized in chapter 5 (**Paper III**) is further extended with 4 more analogues. The reference compounds are thereafter evaluated in vitro for their potential as PET tracers for the 5-HT_7R. The results points out [^{18}F]ENL09 and [^{18}F]ENL10 as promising candidates and therefor were they further evaluated in vivo.*

Authors' contribution:

The author performed the reference syntheses and elaborated on the most promising candidates after in vitro evaluation by the PDSP, as well as scaled up the experiments and produced PET tracer for the evaluation in rats. The author also considerably contributed to the planning of the evaluation in rodents, which was performed in collaboration with M.X, F.G.E and V.S. The analysis of the PET images was done by the author. The author also formulated the outline and contributed considerably to writing the manuscript together with M.M.H.

Development and Evaluation of Two Potential 5-HT$_7$ Receptor PET Tracers: [^{18}F]ENL09 and [^{18}F]ENL10

Elina Tampio L'Estrade[a,b,c], Mengfei Xiong[a,b], Vladimir Shalgunov[b], Fraser G. Edgar[b], Balázs Volk[d], Simone L. Baerentzen[a], Mikael Palner[a,e], Maria Erlandsson[c], Tomas Ohlsson[c], Gitte M. Knudsen[a,f] and Matthias M. Herth[a,b,g,*]

[a]*Neurobiology Research Unit, Rigshospitalet, Blegdamsvej 9, 2100 Copenhagen, Denmark*

[b]*Department for Drug Design and Pharmacology, Faculty of Health and Medical Sciences, University of Copenhagen, Universitetesparken 2, 2100 Copenhagen, Denmark*

[c]*Radiation Physics, Nuclear Medicine Physics Unit, Skånes University Hospital, Barngatan 3, 222 42 Lund, Sweden.*

[d]*Directorate of Drug Substance Development, Egis Pharmaceuticals Plc., P.O. Box 100, H-1475 Budapest, Hungary*

[e]*Center of Translational Neuroscience, Faculty of Health and Medical Sciences, University of Copenhagen, Denmark*

[f]*Institute of Clinical Medicine, Faculty of Health and Medical Sciences, University of Copenhagen, Denmark*

[g]*Department of Clinical Physiology, Nuclear Medicine and PET, University Hospital Copenhagen, Rigshospitalet Blegdamsvej 9, 2100 Copenhagen, Denmark*

*Corresponding Author: Tel.: +45 93565414; fax: +45 35 33 60 41; e-mail: matthias.herth@sund.ku.dk

Abstract

The latest addition to the serotonin (5-HT) receptor family is the 5-HT$_7$ receptor (5-HT$_7$R). This receptor has gained interest as a drug target due to its involvement in various disorders such as depression or schizophrenia. There is currently no clinically validated positron emission tomography (PET) tracer for the 5-HT$_7$R available. But, the (arylpiperazinyl-butyl)oxindole scaffold provides a promising lead structure for this purpose. Here, we synthesized 12 (arylpiperazinyl-butyl)oxindole derivatives and *in vitro* affinity screening identified two structures with suitable affinity and selectivity to be radiolabelled and tested as 5-HT$_7$R selective PET tracers. Next, the radiolabelled products [^{18}F]ENL09 and [^{18}F]ENL10 were evaluated as PET tracers in rats. Both tracers were found to be P-gp substrates but after P-gp inhibition, the brain uptake showed a regional distribution in line with the known 5-HT$_7$R distribution and [^{18}F]ENL10 brain binding was displaceable with a 5-HT$_7$R selective ligand, whereas [^{18}F]ENL09 was not. We find that [^{18}F]ENL10 is a promising 5-HT$_7$R selective PET tracer candidate that should be investigated in higher species.

Keywords: PET, 5-HT$_7$R, Fluorine-18, Fragment-based Dual-labelling, PDSP, Rat

Introduction

The 5-HT_7 receptor (5-HT_7R) is the latest addition to the serotonin (5-HT) receptor family, and the 5-HT_7R has been shown to be involved in many central nervous system (CNS) disorders such as depression or schizophrenia.[1-8] For example, administration of the selective 5-HT_7R antagonist SB-269970 is associated with anti-depressive effects.[2, 9-11] The involvement of the 5-HT_7R in depression is further supported by studies in 5-HT_7R knock-out mice.[9] From a drug development perspective, it would be beneficial to determine the *in vivo* occupancy of a5-HT_7R selective drug. Receptor occupancy studies can e.g. be used to identify the optimal dose of a given drug and correlate drug binding with treatment efficacy.[12-15] Positron emission tomography (PET) is an *in vivo*, non-invasive, molecular imaging technique that can be used to determine receptor occupancies when an appropriate tracer exists.[16-17] Currently, there is no clinically validated PET tracer available to image the 5-HT_7R.

Among other scaffolds, (arylpiperazinyl-butyl)oxindole analogues have recently turned out as promising lead structures to develop a 5-HT_7R selective PET tracer.[12, 18-22], we have previously demonstrated that a ^{11}C-labeled arylpiperazine derivative, namely [^{11}C]Cimbi-717, was able to image the 5-HT_7R in pigs (Figure 1.1). High brain uptake, reversible tracer kinetics and a dose-dependent decrease in binding after pretreatment with SB-269970 (a selective 5-HT_7R antagonist) (Figure 1.1) was observed in pigs.[21]

These results inspired us to develop a ^{18}F-labeled derivative of [^{11}C]Cimbi-717. Fluorine-18 has several advantages over carbon-11 in a clinical setup. For example, does the longer half-life enable bigger batch sizes. Consequently, more patients could be scanned, or more experiments could be conducted with one batch. Also, transportation of the PET tracer to other sites is made feasible. Figure 1.2 outlines the methodology used and the chemical structures investigated within this work.

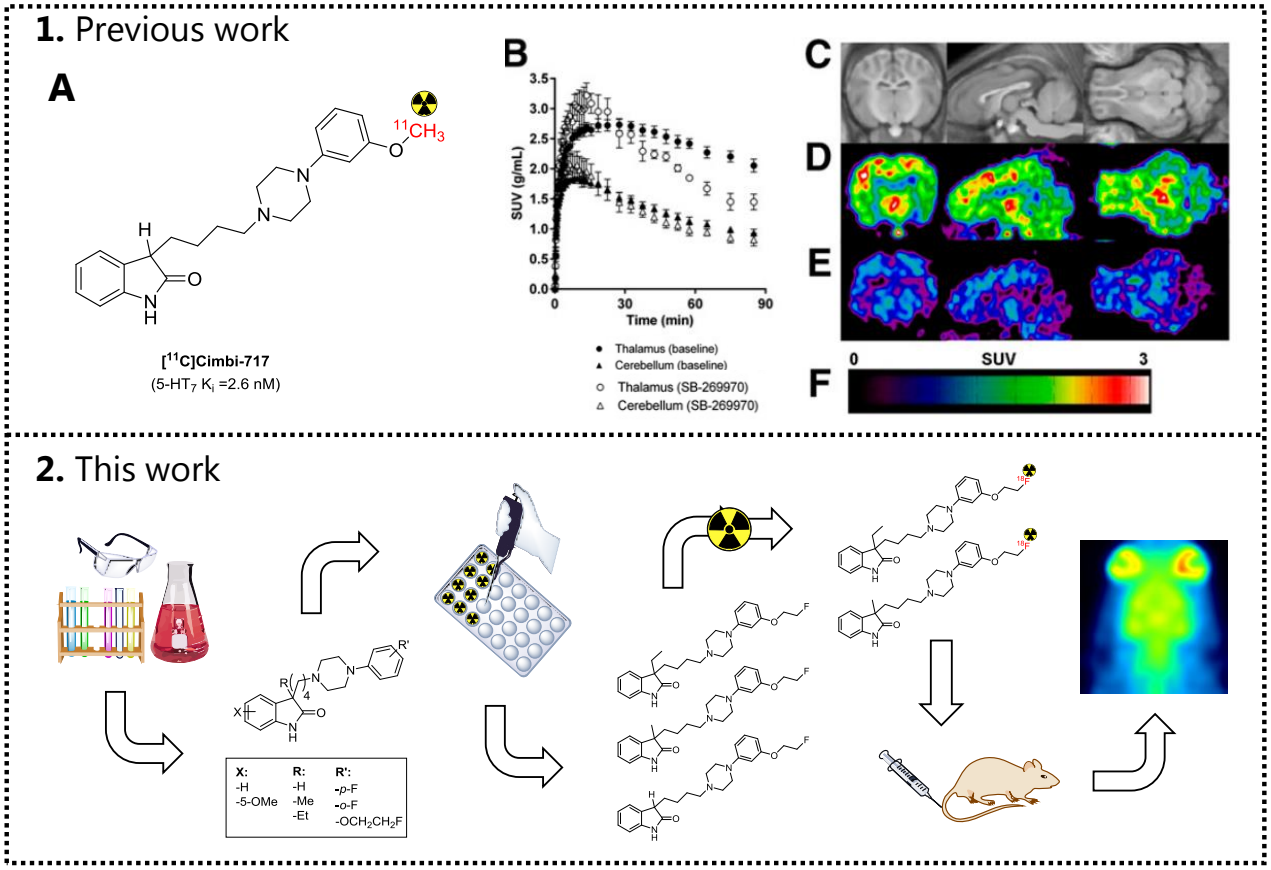

Figure 1: Panel **1** illustrates previous work on [^{11}C]Cimbi-717, which inspired the work of this study displayed in panel **2**. **1) A)** The molecular structure of [^{11}C]Cimbi-717. **B)** Representative time-activity curves (TACs) from the *in vivo* evaluation [^{11}C]Cimbi-717 in pigs at baseline (filled symbols) and after blocking with 1 mg/kg/h SB-269970 (open symbols). **C)** MR-based atlas of a pig brain. **D)** Summed PET images (0–90 min) of [^{11}C]Cimbi-717 at baseline. **E)** Summed PET images (0–90 min) of [^{11}C]Cimbi-717 pretreated with SB-269970. **F)** Colour bar of standardized uptake value (SUV) (g/mL). This research was originally published in Hansen, H. D.; Herth, M. M.; Ettrup, A.; Andersen, V. L.; Lehel, S.; Dyssegaard, A.; Kristensen, J. L. and Knudsen, G. M. Radiosynthesis and *in vivo* evaluation of novel radioligands for PET imaging of cerebral 5-HT$_7$ receptors. J. Nucl. Med. 2014, 55:640–646. © SNMMI. **2)** Shows the working flow of this work. Starting with the synthesis of the 12 compounds, followed by *in vitro* selectivity testing. From the affinities acquired only 3 compounds were selected to be further radiolabelled. During the radiolabelling only [^{18}F]ENL09 and [^{18}F]ENL10 was successfully yielded, hence could be evaluated *in vivo* in rats. [^{18}F]ENL10 was found to be a P-gp substrate and specifically bind to the 5-HT$_7$R in both thalamus and cerebellum. No contribution due to σ- receptor binding could be concluded, thus motivating for further translation to higher species.

Results and discussion

Synthesis and selectivity screening – PET lead compound selection

Compounds outlined in Table 1 were synthesized using a similar synthesis strategy as previously described.[18-19, 22] In short, the 4-chlorobutyl- or 4-mesyloxybutyloxindoles were reacted with the corresponding arylpiperazine derivatives and Na_2CO_3 in melt at 120 ˚C for 1 hour. Reactions preceded in yields of 11-70%. No solvent was used as this promoted the formation of side-products.[18-19, 22] Synthesized structures were selected based on previously reported structure-

activity relationship studies.[19,18] An overview of the synthesized compounds can be found in Table 1.

Subsequently, the 5-HT_7R binding affinity and cross-selectivity towards 11 targets was determined for all compounds via National Institute of Mental Health's Psychoactive Drug Screening Program (NIMH PDSP). Apart from ENL61 and ENL15, all compounds displayed 5-HT_7R affinities (K_i) below 15 nM. The density of 5-HT_7R (B_{max}) in rat thalamus is 47 ± 5 fmol/mg tissue ± SE[23]. Our compounds could therefore be expected to have a binding potential (BP) of approximately 5 in this region, which within the recommended range for a successful PET tracer.[24] But the selectivity of all compounds against σ-receptors, was a cause for concern. The calculated theoretical binding ratio ($tBR_{target/off\text{-}target}$, Eq.1) is a measure to estimate the image contrast in a certain region obtained from two receptors correlating the selectivity of a drug towards these receptors and the regional abundance of these. The $tBRs_{5\text{-}HT7Rt/\sigma\text{-}receptor}$ were acceptable (> 2.15 in rat thalamus) only for ENL20, ENL09 and ENL10 (see example in SI). Therefore, these three compounds were selected for radiolabelling

$$tBR_{target/off-target} = \left(\frac{K_{D,off-target}}{K_{D,target}}\right) x \left(\frac{B_{avail,target}}{B_{avail,off-\ target}}\right) \qquad \text{(Eq. 1)}$$

Table 1: The general synthetic route and the main pharmacological selectivity profile of all synthesized reference compounds.

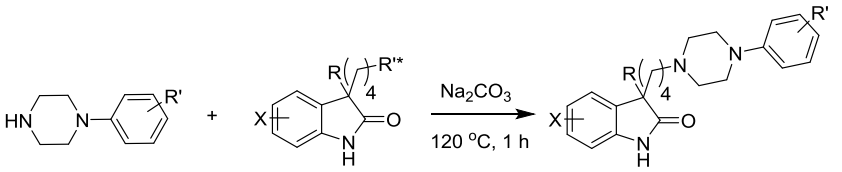

							K_i (nM)					
ID	**X**	**R**	**R'**	**R''**	**Yield (%)**	**LogD$_{7.4}$**	**5-HT$_7$**	5-HT1A	**5-HT$_{2A}$**	**α_{1A}**	**σ_1**	**σ_2**
ENL20	H	H	*m*-OCH_2CH_2F	OMs	-	2.95	9.5	145	162	339	26	51
ENL10	H	Me	*m*-OCH_2CH_2F	Cl	27	3.57	5.6	72	53	748	18	65
ENL09	H	Et	*m*-OCH_2CH_2F	Cl	11	4.01	13	107	160	-	29	67
ENL61	5-OMe	Et	*m*-OCH_2CH_2F	Cl	26	3.87	38	389	103	878	165	62
ENL21	H	H	*p*-F	OMs	-	3.09	1.5	288	28	130	8.1	2.1
ENL06	H	Me	*p*-F	Cl	33	3.71	2.8	306	21	239	11	3.5
ENL05	H	Et	*p*-F	Cl	55	4.15	2.4	190	37	280	15	1.4
ENL60	5-OMe	Et	*p*-F	Cl	47	4.00	5.6	267	29	132	39	2
ENL17	H	H	*o*-F	OMs	38	3.46	8.3	144	113	40	9.9	2.9
ENL08	H	Me	*o*-F	Cl	70	4.05	5.2	38	121	41	3.7	1.7
ENL07	H	Et	*o*-F	Cl	35	4.50	11	49	100	128	6.8	2.5
ENL15	5-OMe	Et	*o*-F	Cl	60	4.35	92	155	48	159	38	1.7

The full selectivity profiles for all compounds can be found in the supplementary information. $LogD_{7.4}$ values, displayed in Table 1, for the potential PET tracers were estimated using Chemicalize (ChemAxon Ltd.).

Radiolabelling

^{18}F-labelling of ENL20, ENL09 and ENL10 has recently been tested, resulting in that only [^{18}F]ENL09 and [^{18}F]ENL10 could be successfully radiolabelled.[25] In short, the Boc-protected arylpiperazine fragment ENL04 was first radiolabelled with fluoride-18, purified and deprotected, yielding [^{18}F]ENL03. This fragment was then coupled simultaneously to two chlorobutyl-oxindole analogues in a one-pot procedure. The resulting compounds [^{18}F]ENL09 and [^{18}F]ENL10 were subsequently isolated by semi-preparative HPLC (Figure 2.b). Both PET tracers could be obtained in sufficient amounts to conduct evaluation experiments in rodents. The radiochemical yield (RCY) was 1.78–4.10% and 3.74–5.15% for [^{18}F]ENL09 and

[^{18}F]ENL10, respectively. Radiochemical purities were > 98% and molar activities were 76 ± 60 GBq/µmol (n=3) for [^{18}F]ENL09 and 25 ± 50 GBq/µmol (n =4) [^{18}F]ENL10.

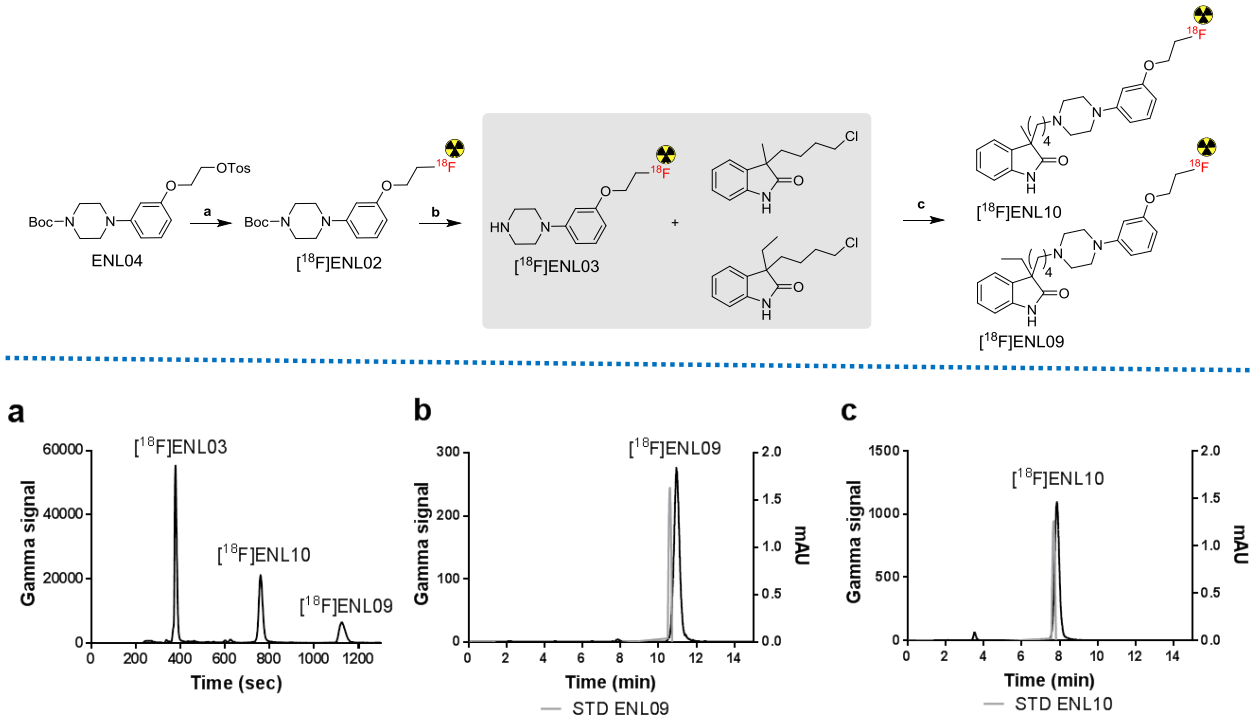

Figure 2: Radiolabelling procedure of [^{18}F]ENL09 and [^{18}F]ENL10. **Upper panel:** Radiolabelling of the synthon [^{18}F]ENL03 and subsequent condensation with two building blocks simultaneously in one-pot. **a)** [^{18}F]F^- , K_{222}, K_2CO_3, MeCN, 80 °C for 20 min. **b)** 25% TFA in MeCN at 80 °C for 10 min**. c)** K_2CO_3**,** DMSO, 170 °C for 15 min. **Lower panel:** Purification and identification control of [^{18}F]ENL09 and [^{18}F]ENL10 **a)** Semi-preparative HPLC of [^{18}F]ENL09 and [^{18}F]ENL10 [Luna 5 µm C18(2) 10×250 mm column, flow rate 4 mL/min, eluent: EtOH:0.1% H_3PO_4 in H_20 (30:70)] **b)** Analytical HPLC analysis [Luna 5 µm C18(2) 4.60×50 mm column, flow rate 1.5 mL/min, eluent: EtOH:0.1% H_3PO_4 in H_20 (30:70)] of [^{18}F]ENL09 and its respective reference ENL09 **c)** and [^{18}F]ENL10 and ENL10.

In vivo evaluation of [^{18}F]ENL09 and [^{18}F]ENL10 in rats

Both [^{18}F]ENL09 and [^{18}F]ENL10 were evaluated in rats using our high-throughput set-up, as previously described.[26-27] This set-up enabled us to image fours rats simultaneously. Since both tracers showed poor brain uptake (Figure 3), we suspected that the compounds could be substrates of the P-glycoprotein (P-gp) efflux transporter, which is especially highly expressed in rodents.[28] Thus, after inhibition of the P-gp transporter with elacridar, a known P-gp inhibitor[29], we found an increased brain uptake of both [^{18}F]ENL09 and [^{18}F]ENL10, from 1 to 2.0-2.5 SUV, confirming that both tracers were P-gp substrates in rat (Figures 3a–f). The brain uptake after elacridar was higher in the 5-HT_7R rich region (thalamus) compared to the 5-HT_7R low density region cerebellum (Figures 3b, d, e and f).

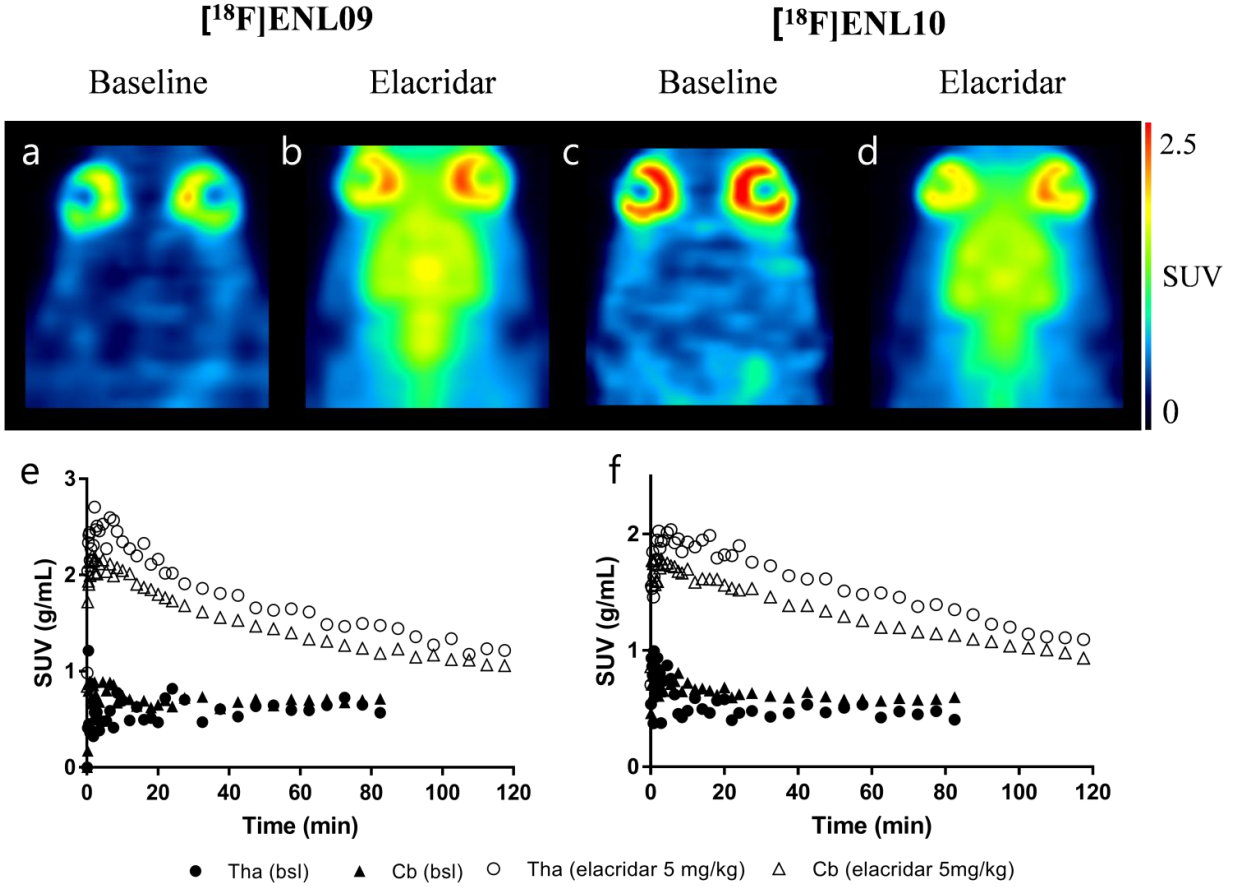

Figure 3: Horizontal rat PET images of [^{18}F]ENL09 and [^{18}F]ENL10 (**a–d**) and their representative time-activity curves (TACs) (**e–f**). Summed images are created from a 2–120 min dynamic PET. **a**) Summed PET image of [^{18}F]ENL09 at baseline **b)** Summed PET image of [^{18}F]ENL09 after pretreatment with elacridar (5 mg/kg). **c**) Summed PET image of [^{18}F]ENL10 at baseline **d)** Summed PET image of [^{18}F]ENL10 after pretreatment with elacridar (5 mg/kg). **e)** Thalamus (circles, Tha) and cerebellum (triangles, Cb) TACs for [^{18}F]ENL09 at baseline and after pretreatment with elacridar (5 mg/kg). **f)** Thalamus and cerebellum TACs for [^{18}F]ENL10 at baseline and after pretreatment with elacridar (5 mg/kg).

To evaluate if this binding is specific towards the 5-HT$_7$R, blocking with the selective 5-HT$_7$R antagonist SB-269970[10-11] was subsequently carried out, preceded by P-gp efflux transporter inhibition. With this experimental design, we found an *increased* area under the time activity curve (AUC) for [^{18}F]ENL09 in receptor rich thalamus and receptor low cerebellum (Supplementary data). In contrast, did [^{18}F]ENL10 show a reduction in both thalamus (23%) and cerebellum (38.6%) (Figures 4a and c). Consequently, specific binding of [^{18}F]ENL10 to the 5-HT$_7$R was detected.

In order elucidate that the [^{18}F]ENL10 brain binding is mainly ascribed to 5-HT$_7$R binding, we also tested σ-receptor blockade (Table 1). As blocking agents, we used the multi-affinity drug haloperidol (σ_1 K_i = 4 nM, σ_2 K_i = 14 nM)[30-31] and the selective σ_1 agonist SA4503 (IC_{50} = 17 nM)[32], still while simultaneously inhibiting the P-gp efflux transporter (Figures 4b and c).

Haloperidol (1 mg/kg) administration resulted in only negligible changes in AUC in cerebellum (-2%) and thalamus (+4.4%) (Figure 4b and c). SA4503 (1.5 mg/kg) resulted in an *increased* AUC in thalamus (19%) and cerebellum (8%) (Figure 4c), possibly because of an increased systemic availability of the parent compound. Consequently, the binding of [^{18}F]ENL10 in thalamus and cerebellum could not be attributed to σ-binding. Figure 4c displays the summarized results for all calculated AUC.

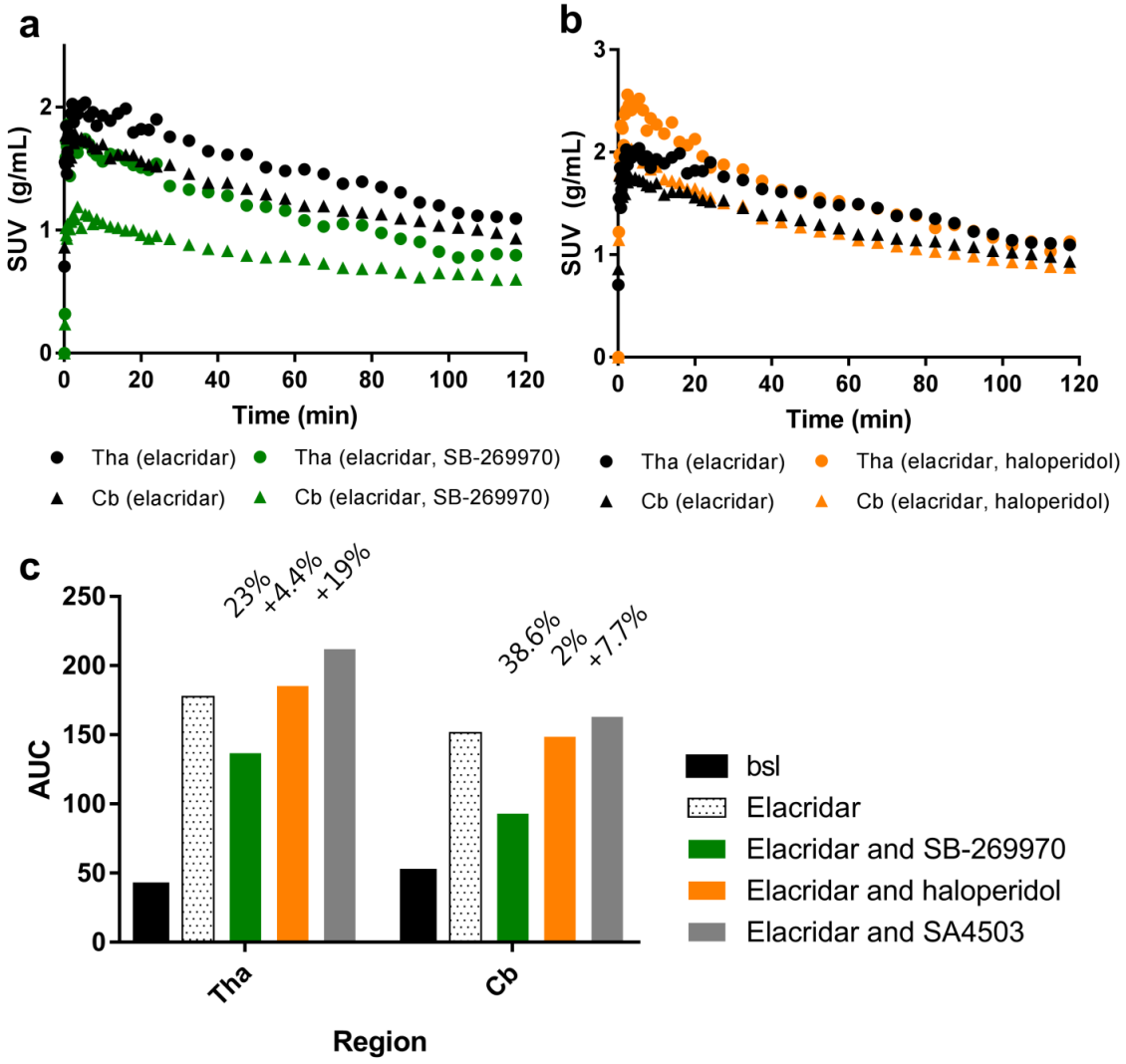

Figure 4: Representative time-activity curves (TACs) of [^{18}F]ENL10 in the thalamus (circles, Tha) and cerebellum (triangles, Cb) in the rat brain. a) Thalamus and cerebellum TACs after pretreatment with elacridar and elacridar + SB-269970 (3 mg/kg). b) Thalamus and cerebellum TACs after pretreatment with elacridar and elacridar + haloperidol (1 mg/kg). c) Calculated area-under-curve (AUC) for all TACs displayed as a grouped barplot. The reduction of AUC compared to elacridar (baseline) is displayed above the bar, the plus sign indicates an increased AUC: All TACs are normalized to injected radioactivity and animal weight resulting in the standard uptake value (SUV). Pretreatment dose of SA4503 was 1.5 mg/kg.

Conclusion

In conclusion, [^{18}F]ENL10 is a P-gp substrate and displaceable by a 5-HT$_7$R antagonist in rats, hence makes it a promising candidate for translation into higher species, such as pigs or non-human primates. This suggestion is mainly driven by the recent observation that in higher species express less P-gp activity compared to rodents[28], which suggests that blocking of the P-gp transporter may not be needed to validate its usefulness for 5-HT$_7$R PET imaging.

Methods

General information

Solvents and reagents were purchased from Sigma Aldrich (Merck, Darmstadt, Germany) or Thermo Fisher Scientific and used as received unless otherwise noted. The chlorobutyl-oxindole analogues and reference compound for the ENL21 were acquired from Balázs Volk. NMR (^{1}H, ^{13}C) spectra were acquired on a 600 MHz Bruker Avance III HD or a 400 MHz Bruker Avance II spectrometer at room temperature. Chemical shift (δ) are expressed in parts per million and referenced to residual solvent peak. The resonance multiplicity is abbreviated as follows or combinations thereof: s (singlet), d (doublet), t (triplet), q (quartet) and m (multiplet). The analysis of the NMR spectra was performed using the software MestReNova v12.0.0 (Mestrelab Research S.L.). Thin layer chromatography (TLC) was run on silica plated aluminium sheets (Silica gel 60 F254) purchased from Merck and the spots were visualized by ultraviolet light at 254 nm. Flash column chromatography (CC) was carried out manually on silica gel 60 (0.040–0.063 mm). Analytical high-performance liquid chromatography (HPLC) was performed on a Dionex system consisting of a P680A pump, a UVD 170U detector and a Scansys radiodetector. The HPLC system was controlled by Chromeleon 6.8 software. The experimental information of the previously published reference compounds and appendices can be found in the Supplementary data.

General synthesis of reference compounds

As previously described, the melt of the secondary amine (0.5 mmol) and sodium carbonate (0.5 mmol) was heated to 120 °C under slow stirring. Thereafter the chlorobutyl- or mesyloxybutyl-oxindole analogue (0.5 mmol) was added and after 1 h reaction time, the crude mixture was cooled to ambient temperature. Ethyl acetate and water were added to the residue and the layers were separated. The organic layer was dried over $MgSO_4$ and evaporated *in vacuo*. Column chromatography (EtOAc) afforded the isolated product.[18-19, 22]

3-(4-{4-[3-(2-Fluoroethoxy)phenyl]piperazin-1-yl}butyl)-3-methyl-1,3-dihydro-2H-indol-2-one **(ENL10)**[25] Experimental information is described in **Paper III**, chapter 5.

3-Ethyl-3-(4-{4-[3-(2-fluoroethoxy)phenyl]piperazin-1-yl}butyl)-1,3-dihydro-2H-indol-2-one **(ENL09)**[25] Experimental information is described in **Paper III**, chapter 5.

3-{4-[4-(2-Fluorophenyl)piperazin-1-yl]butyl}-1,3-dihydro-2H-indol-2-one **(ENL17):** 35 mg, 38%. ^{1}H NMR (400 MHz, DMSO-d_6) δ 10.33 (s, 1H), 7.27 (d, *J* = 7.3 Hz, 1H), 7.21–7.07 (m, 3H), 7.06–6.90 (m, 3H), 6.83 (d, *J* = 7.7 Hz, 1H), 3.45 (t, *J* = 5.8 Hz, 1H), 2.99 (t, *J* = 4.9 Hz, 4H), 2.48–2.43 (m, 4H), 2.29 (t, *J* = 7.2 Hz, 2H), 1.99–1.72 (m, 2H), 1.45 (p, *J* = 7.4 Hz, 2H), 1.37–1.19 (m, 2H). ^{13}C NMR (150 MHz, DMSO-d_6) δ 178.89, 155.72, 142.73, 129.71, 127.49, 124.78, 122.17, 121.17, 119.11, 115.92, 115.80, 109.07, 57.54, 52.72, (50.09, 50.07), 45.04, 29.63, 26.17, 23.10. UPLC-MS (ESI): RT: 3.07 min, m/z: 368.3 $[M^{+}H]^{+}$ at 215-254 nm. R_f: 0.3 (EtOAc). **Appendices 1–3.**

3-{4-[4-(2-Fluorophenyl)piperazin-1-yl]butyl}-3-methyl-1,3-dihydro-2H-indol-2-one **(ENL08):** 131.5 mg, 70%. ^{1}H NMR (400 MHz, DMSO-d_6) δ 10.32 (s, 1H), 7.25 (dd, *J* = 7.4, 1.2 Hz, 1H), 7.20–7.07 (m, 3H), 7.04–6.92 (m, 3H), 6.87–6.83 (m, 1H), 2.95 (t, *J* = 4.8 Hz, 4H), 2.42 (t, *J* = 4.9 Hz, 4H), 2.24–2.13 (m, 2H), 1.81–1.69 (m, 2H), 1.41–1.26 (m, 2H), 1.24 (s, 3H), 0.99 (tq, *J* = 15.8, 8.6, 7.5 Hz, 1H), 0.90–0.76 (m, 1H). ^{13}C NMR (150 MHz, $CDCl_3$) δ 182.18, 156.54, 154.91, 140.31, 133.84, 128.13, 125.07, 123.10, 122.90, 120.19, 116.73, 116.60, 109.99, 57.33, 51.87, 48.64, 47.71, 37.42, 24.24, 23.40, 22.15. UPLC-MS (ESI): RT: 3.29 min, m/z: 426.3 $[M^{+}H]^{+}$ at 215-254 nm. R_f: 0.17 (EtOAc). **Appendices 4–6.**

3-Ethyl-3-{4-[4-(2-fluorophenyl)piperazin-1-yl]butyl}-1,3-dihydro-2H-indol-2-one **(ENL07):** 66.9 mg, 35%. ^{1}H NMR (400 MHz, DMSO-d_6) δ 10.33 (s, 1H), 7.23–7.06 (m, 4H), 6.98 (m, *J* = 14.2, 7.6, 5.3, 1.7 Hz, 3H), 6.85 (d, *J* = 7.6 Hz, 1H), 2.95 (t, *J* = 4.8 Hz, 4H), 2.42 (t, *J* = 5.0 Hz, 4H), 2.24–2.10 (m, 2H), 1.74 (dt, *J* = 7.7, 3.9 Hz, 2H), 1.30 (dq, *J* = 20.3, 6.7, 6.0 Hz, 2H), 1.05–0.93 (m, 1H), 0.89–0.71 (m, 1H), 0.52 (t, *J* = 7.3 Hz, 3H). ^{13}C NMR (150 MHz, $CDCl_3$) δ 181.80, 155.93, 141.39, 137.24, 132.13, 128.31, 125.30, 123.53, 123.07, 120.45, 116.96, 116.83, 110.03, 57.54, 54.12, 52.03, 47.96, 36.89, 31.60, 23.67, 22.17, 8.82. UPLC-MS (ESI): RT: 3.12 min, m/z: 396.2 $[M^{+}H]^{+}$ at 215-254 nm. R_f: 0.17 (EtOAc). **Appendices 7–9.**

3-Ethyl-3-{4-[4-(2-fluorophenyl)piperazin-1-yl]butyl}-5-methoxy-1,3-dihydro-2H-indol-2-one **(ENL15):**

128.2 mg, 60%. ^{1}H NMR (600 MHz, CD_3OD) δ 7.12–7.09 (m, 1H), 7.05 (t, *J* = 1.9 Hz, 1H), 7.04 (d, *J* = 1.7 Hz, 1H), 7.03 (t, *J* = 1.8 Hz, 1H), 7.00–6.96 (m, 1H), 6.86 (d, *J* = 5.6 Hz, 1H), 6.86 (s, 1H), 6.82 (d, *J* = 2.2 Hz, 1H), 3.81 (s, 3H), 3.08 (t, *J* = 5.0 Hz, 4H), 2.60 (s, 4H), 2.32 (m, *J* = 9.6, 6.1 Hz, 2H), 1.91–1.82 (m, 4H), 1.46 (m, *J* = 21.4, 11.9, 5.9, 3.0 Hz, 1H), 1.17–1.04 (m, 1H), 0.99–0.86 (m, 2H), 0.62 (t, *J* = 7.4 Hz, 3H). ^{13}C NMR (150 MHz, CD_3OD) δ 184.32, 157.64, 156.32, 141.21, 136.78, 135.29, 125.72, 125.70, 123.88, 120.24, 116.97, 113.42, 111.28, 59.30, 56.26, 56.20, 54.17, 51.29, 38.58, 32.10, 27.49, 23.53, 8.79. UPLC-MS (ESI): RT: 3.47 min, m/z: 426.3 $[M^+H]^+$ at 215-254 nm. R_f: 0.16 (EtOAc). **Appendices 10–12.**

In vitro affinity screening and $LogD_{7.4}$ estimations

Receptor binding profile was generously provided by the National Institute of Mental Health's Psychoactive Drug Screening Program, Contract # HHSN-271-2018-00023-C (NIMH PDSP). The NIMH PDSP is directed by Bryan L. Roth MD, PhD at the University of North Carolina at Chapel Hill and Project Officer Jamie Driscoll at NIMH, Bethesda MD, USA. The $LogD_{7.4}$ values presented for all compounds were estimated using Chemicalize (ChemAxon Ltd.).

General Radiochemistry

Production of fluoride-18

[^{18}F]Fluoride was produced via the (p,n)-reaction in a cyclotron (CTI Siemens and Scanditronix, Rigshospitalet, Denmark) by irradiating [^{18}O]H_2O with a 11 MeV proton beam.

Dual-condensation of [^{18}F]ENL09 and [^{18}F]ENL10[25]

As described in in **Paper III**, chapter 5.

No-carrier-added ^{18}F-fluoride from the target was collected at a non-conditioned but activated (10 mL ethanol, 20 mL water and dried with air) anion-exchange cartridge (QMA). To elute the ^{18}F-fluoride off the cartridge, a solution of 1,10-diaza-4,7,13,16,21,24-hexaoxabicyclo[8.8.8]hexacosane (Kryptofix®222, 20 mg) and K_2CO_3 (3.3 mg) dissolved in a methanol–water mixture (97/3 v/v, 0.65 mL) was used. The elute was thereafter dried by evaporation at 110 °C under helium and then dried twice again after subsequent addition of dry MeCN (1 mL). To the dried Kryptofix®222/[^{18}F]fluoride complex (24–48 GBq), the precursor ENL04 (6 mg, 0.013 mmol) dissolved in MeCN (1 mL) was added and heated at 80 °C for 20 min to yield [^{18}F]ENL02.

The crude reaction mixture was thereafter diluted in water (20–30 mL) and subsequently transferred onto a SepPak C18 plus (short) cartridge for purification from free fluoride-18, base and impurities. MeCN (1 mL) was used to elute [^{18}F]ENL02 from the cartridge, and subsequently a deprotection of the Boc group was performed by addition of TFA (0.25 mL) and thereafter heating for 10 min at 80 ˚C to give the deprotected product [^{18}F]ENL03. TFA and MeCN was evaporated at 110 °C under vacuum and further dried twice after addition of dry MeCN (1 mL).

To dried [^{18}F]ENL03, DMSO (1 mL) was added and the solution was further transferred to a reaction vial containing butyloxindole derivatives (8 mg, 0.042–0.032 mmol of each) and K_2CO_3 (30 mg, 0.22 mmol) for the final dual condensation. The reaction mix was heated to 160 °C for 15 min and afterwards the crude mixture was quenched with EtOH:0.1 % H_3PO_4 in H_2O (30:70, 3.5 mL) before loaded onto the column.

[^{18}F]ENL09 and [^{18}F]ENL10 were isolated by semi-preparative HPLC [Luna 5 µm C18(2) 10 × 250 mm column, flow rate 4 mL/min, eluent: EtOH: 0.1% H_3PO_4 in H_2O (30:70)]. The retention time for [^{18}F]ENL03 was 350–400 seconds, that of [^{18}F]ENL09 was 700–750 seconds, while that of [^{18}F]ENL10 was 1100–1150 seconds. The products were separately collected into sterile 20 mL vials and thereafter diluted with PBB (100 mM, pH 7).
The product was visually inspected for clarity, absence of colour and visible particles. Chemical and radiochemical purities were assessed by analytical HPLC [Luna 5 µm C18(2) 4.60 × 50 mm, eluent: MeCN/ 0.1% H_3PO_4 in H_20 (30:70) RT: [^{18}F]ENL09 = 10 min; [^{18}F]ENL10 = 8 min and flow rate 1.5 mL/min]. Molar activities (A_m) of the radiotracers were determined as follows: the area of the UV absorbance peak corresponding to the radiolabelled product was integrated on the HPLC chromatogram.

Experimental procedures, rats

16 Long-Evans female rats (200–300 g) were used in this study. The animals were fed ad libitum and had free access to water. The rats were housed in groups of 2–4 animals per cage in a climate controlled rodent facility with 12h/12h light cycle. All procedures were conducted in accordance with the FELASA guidelines for animal research and with approval from The Danish Council for Animal Ethics (license number: 2017-15-0201-01283) as well as the Department of Experimental Medicine, University of Copenhagen. On the day of the experiment rats were transported to the scanner at least 1 h prior to experiment start.

[^{18}F]ENL09 and [^{18}F]ENL10 were given as intravenous (i.v.) bolus injections in tail vein catheters at the start of the scan (0 min), and the injected doses were 10–25 MBq. The rats were subsequently scanned in a high-resolution research tomography (HRRT) scanner (Siemens AG, Munich, Germany), first for a 120 min dynamic PET scan followed by a transmission scan (Tx50). The scans were performed using a custom-made 2×2 rat insert, which enabled the possibility of scanning 4 rats simultaneously.[26-27] The animals were scanned at baseline and after receiving pretreatment of either elacridar (5 mg/kg, Carbosynth, Compton, United Kingdom) and/or with SB-269970 (3 mg/kg, Tocris Bioscience, Abingdon, United Kingdom), haloperidol (1 mg/kg, Janssen-Cilag, Birkerød, Denmark) or SA4503 (1.5 mg/kg, Merck, Darmstadt, Germany) 15–30 min before tracer injection. Anaesthesia was induced at 3–3.5% isoflurane in oxygen and maintained at 1.5–2.5% during scans.

The one hundred and twenty-minute list-mode PET data were reconstructed into 45 dynamic frames (6×10, 6×20, 6×60, 8×120 and 19×300 seconds). The images consisted of 207 planes of 256×256 voxels of 1.22×1.22×1.22 mm. From this image each of the four rats were extracted into 4 separate images. Summed pictures of all counts in the time interval 5–120 min of the scans was made for each rat and used for co-registration to a standardized MRI-based atlas of the rat brain[33-34]. The TACs were extracted for thalamus and cerebellum volumes of interests (VOIs) for each rat. Resulting TACs were calculated as radioactive concentration (kBq/cc) over time, which were thereafter corrected for animal weight, yielding standardized uptake values (SUV). Areas under the curves (AUCs) were calculated for the TACs and visualized in grouped bar plots.

Author information

Corresponding Author: Matthias M. Herth, University of Copenhagen, Department of Drug Design and Pharmacology, Jagtvej 160, 2100 Copenhagen, Denmark, Tel.: +45 93565414, Fax: +45 35 33 60 41, e-mail: matthias.herth@sund.ku.dk

Author contributions

Experimental work and data evaluation were carried out by Elina T. L'Estrade, Fraser G. Edgar, Mengfei Xiong, Simone L. Baerentzen, Vladimir Shalgunov, Maria Erlandsson and Mikael Palner. Balázs Volk, Tomas G. Ohlsson, Gitte M. Knudsen and Matthias M. Herth designed the experiments, supervised the work, contributed to the research idea and were strongly involved in the evaluation of the experimental data. The manuscript was written through contributions of all authors. All authors have given approval to the final version of the manuscript.

Acknowledgement

The authors wish to thank the staff of the PET and Cyclotron Unit at Rigshospitalet for expert technical assistance and the John and Birthe Meyer Foundation for donation of the HRRT scanner. Receptor binding profile was generously provided by the National Institute of Mental Health's Psychoactive Drug Screening Program, Contract # HHSN-271-2018-00023-C (NIMH PDSP). The NIMH PDSP is Directed by Bryan L. Roth MD, PhD at the University of North Carolina at Chapel Hill and Project Officer Jamie Driscoll at NIMH, Bethesda MD, USA.

References

1. Roth, B. L.; Craigo, S. C.; Choudhary, M. S.; Uluer, A.; Monsma, F.; Shen, Y.; Meltzer, H. Y.; Sibley, D. R., Binding of typical and atypical antipsychotic agents to 5-hydroxytryptamine-6 and 5-hydroxytryptamine-7 receptors. *Journal of Pharmacology and Experimental Therapeutics* **1994,** *268* (3), 1403-1410.

2. Hedlund, P. B.; Huitron-Resendiz, S.; Henriksen, S. J.; Sutcliffe, J. G., 5-HT_7 Receptor Inhibition and Inactivation Induce Antidepressantlike Behavior and Sleep Pattern. *Biological Psychiatry* **2005,** *58* (10), 831-837.

3. Wesołowska, A.; Nikiforuk, A.; Stachowicz, K., Potential anxiolytic and antidepressant effects of the selective 5-HT_7 receptor antagonist SB 269970 after intrahippocampal administration to rats. *European journal of pharmacology* **2006,** *553* (1-3), 185-190.

4. Mnie-Filali, O.; Lambas-Señas, L.; Scarna, H.; Haddjeri, N., Therapeutic potential of 5-HT_7 receptors in mood disorders. *Current drug targets* **2009,** *10* (11), 1109-1117.

5. Mnie-Filali, O.; Lambás-Señas, L.; Zimmer, L.; Haddjeri, N., 5-HT_7 receptor antagonists as a new class of antidepressants. *Drug News Perspect* **2007,** *20* (10), 613-8.

6. Guscott, M.; Bristow, L. J.; Hadingham, K.; Rosahl, T. W.; Beer, M. S.; Stanton, J. A.; Bromidge, F.; Owens, A. P.; Huscroft, I.; Myers, J.; Rupniak, N. M.; Patel, S.; Whiting, P. J.; Hutson, P. H.; Fone, K. C.; Biello, S. M.; Kulagowski, J. J.; McAllister, G., Genetic knockout and pharmacological blockade studies of the 5-HT_7 receptor suggest therapeutic potential in depression. *Neuropharmacology* **2005,** *48* (4), 492-502.

7. Hedlund, P. B.; Sutcliffe, J. G., Functional, molecular and pharmacological advances in 5-HT_7 receptor research. *Trends in Pharmacological Sciences* **2004,** *25* (9), 481-486.

8. Hauser, S. R.; Hedlund, P. B.; Roberts, A. J.; Sari, Y.; Bell, R. L.; Engleman, E. A., The 5-HT_7 receptor as a potential target for treating drug and alcohol abuse. *Frontiers in neuroscience* **2015,** *8*, 448.

9. Guscott, M.; Bristow, L.; Hadingham, K.; Rosahl, T.; Beer, M.; Stanton, J.; Bromidge, F.; Owens, A.; Huscroft, I.; Myers, J., Genetic knockout and pharmacological blockade studies of the 5-HT_7 receptor suggest therapeutic potential in depression. *Neuropharmacology* **2005,** *48* (4), 492-502.

10. Hagan, J. J.; Price, G. W.; Jeffrey, P.; Deeks, N. J.; Stean, T.; Piper, D.; Smith, M. I.; Upton, N.; Medhurst, A. D.; Middlemiss, D. N.; Riley, G. J.; Lovell, P. J.; Bromidge, S. M.; Thomas, D. R., Characterization of SB-269970-A, a selective 5-HT_7 receptor antagonist. *British Journal of Pharmacology* **2000,** *130* (3), 539-548.

11. Lovell, P. J.; Bromidge, S. M.; Dabbs, S.; Duckworth, D. M.; Forbes, I. T.; Jennings, A. J.; King, F. D.; Middlemiss, D. N.; Rahman, S. K.; Saunders, D. V., A novel, potent, and selective 5-HT_7 antagonist:(R)-3-(2-(2-(4-methylpiperidin-1-yl) ethyl) pyrrolidine-1-sulfonyl) phenol (SB-269970). *Journal of medicinal chemistry* **2000,** *43* (3), 342-345.

12. Zhang, L.; Villalobos, A.; Beck, E. M.; Bocan, T.; Chappie, T. A.; Chen, L.; Grimwood, S.; Heck, S. D.; Helal, C. J.; Hou, X., Design and selection parameters to accelerate the discovery of novel central nervous system positron emission tomography (PET) ligands and their application in the development of a novel phosphodiesterase 2A PET ligand. *Journal of medicinal chemistry* **2013,** *56* (11), 4568-4579.

13. Piel, M.; Vernaleken, I.; Rösch, F., Positron Emission Tomography in CNS Drug Discovery and Drug Monitoring. *Journal of Medicinal Chemistry* **2014,** *57* (22), 9232-9258.

14. Morgan, P.; Van Der Graaf, P. H.; Arrowsmith, J.; Feltner, D. E.; Drummond, K. S.; Wegner, C. D.; Street, S. D., Can the flow of medicines be improved? Fundamental pharmacokinetic and pharmacological principles toward improving Phase II survival. *Drug discovery today* **2012,** *17* (9-10), 419-424.

15. Kristensen, J. L.; Herth, M. M., Textbook of Drug Design and Discovery: *In vivo* imaging in drug discovery. In *Textbook of Drug Design and Discovery*, CRC Press: **2017**.

16. Taylor, N.; Emer, E.; Preshlock, S.; Schedler, M.; Tredwell, M.; Verhoog, S.; Mercier, J.; Genicot, C.; Gouverneur, V. E., De-Risking the Cu-Mediated ^{18}F-Fluorination of Heterocyclic PET Radioligands. *J Am Chem Soc* **2017**.

17. Miller, P. W.; Long, N. J.; Vilar, R.; Gee, A. D., Synthesis of ^{11}C, ^{18}F, ^{15}O, and ^{13}N radiolabels for positron emission tomography. *Angew Chem Int Ed Engl* **2008,** *47* (47), 8998-9033.

18. Volk, B.; Barkóczy, J.; Hegedus, E.; Udvari, S.; Gacsályi, I.; Mezei, T.; Pallagi, K.; Kompagne, H.; Lévay, G.; Egyed, A., (Phenylpiperazinyl-butyl) oxindoles as selective 5-HT_7 receptor antagonists. *Journal of medicinal chemistry* **2008,** *51* (8), 2522-2532.

19. Herth, M. M.; Volk, B.; Pallagi, K.; Kofoed Bech, L.; Antoni, F. A.; Knudsen, G. M.; Kristensen, J. L., Synthesis and *in vitro* evaluation of oxindole derivatives as potential radioligands for 5-HT(7) receptor imaging with PET. *ACS Chemical Neuroscience* **2012,** *3* (12), 1002-7.

20. Herth, M. M.; Andersen, V. L.; Hansen, H. D.; Stroth, N.; Volk, B.; Lehel, S.; Dyssegaard, A.; Ettrup, A.; Svenningsson, P.; Knudsen, G. M.; Kristensen, J. L., Evaluation of 3-Ethyl-3-(phenylpiperazinylbutyl)oxindoles as PET Ligands for the Serotonin 5-HT(7) Receptor: Synthesis, Pharmacology, Radiolabeling, and *in Vivo* Brain Imaging in Pigs. *Journal of medicinal chemistry* **2015,** *58* (8), 3631-6.

21. Hansen, H. D.; Herth, M. M.; Ettrup, A.; Andersen, V. L.; Lehel, S.; Dyssegaard, A.; Kristensen, J. L.; Knudsen, G. M., Radiosynthesis and *in vivo* evaluation of novel radioligands for PET imaging of cerebral 5-HT_7 receptors. *Journal of Nuclear Medicine* **2014,** *55* (4), 640-6.

22. Volk, B.; Gacsályi, I.; Pallagi, K.; Poszávácz, L.; Gyönös, I.; Szabó, É.; Bakó, T.; Spedding, M.; Simig, G.; Szénási, G., Optimization of (arylpiperazinylbutyl) oxindoles exhibiting selective 5-HT_7 receptor antagonist activity. *Journal of medicinal chemistry* **2011,** *54* (19), 6657-6669.

23. Horisawa, T.; Ishiyama, T.; Ono, M.; Ishibashi, T.; Taiji, M., Binding of lurasidone, a novel antipsychotic, to rat 5-HT_7 receptor: analysis by [^{3}H] SB-269970 autoradiography. *Progress in Neuro-Psychopharmacology and Biological Psychiatry* **2013,** *40*, 132-137.

24. Van de Bittner, G. C.; Ricq, E. L.; Hooker, J. M., A philosophy for CNS radiotracer design. *Accounts of chemical research* **2014,** *47* (10), 3127-3134.

25. Elina Tampio L'Estrade, S. L., Ida Nymann Petersen, Fraser G. Edgar, Balázs Volk, Maria Erlandsson, Tomas Ohlsson, Gitte M. Knudsen and Matthias M. Herth, Fragment-based Labelling Using Condensation Reactions – A Possibility to Increase Throughput in Preclinical PET. *Submitted Manuscript* **2019**.

26. Keller, S. H.; L'Estrade, E. N.; Dall, B.; Palner, M.; Herth, M. In *Quantification accuracy of a new HRRT high throughput rat hotel using transmission-based attenuation correction: A phantom study*, Nuclear Science Symposium, Medical Imaging Conference and Room-Temperature Semiconductor Detector Workshop (NSS/MIC/RTSD), 2016, IEEE: 2016; pp 1-3.

27. L'Estrade, E. N.; Palner, M.; Petersen, I. N.; Keller, S. H.; Lehel, S.; Dall, B.; Kristensen, J. L.; Erlandsson, M.; Olsson, T.; Knudsen, G. M.; Herth, M. M., Accelerating PET tracer development: Establishment of a combinatorial-like, high-throughput development approach using condensation reactions and high-throughput screening. *European Journal of Nuclear Medicine and Molecular Imaging* **2016,** *43*, S455-S456.

28. Syvänen, S.; Lindhe, Ö.; Palner, M.; Kornum, B. R.; Rahman, O.; Långström, B.; Knudsen, G. M.; Hammarlund-Udenaes, M., Species differences in blood-brain barrier transport of three positron emission tomography radioligands with emphasis on P-glycoprotein transport. *Drug metabolism and disposition* **2009,** *37* (3), 635-643.

29. Kallem, R.; P Kulkarni, C.; Patel, D.; Thakur, M.; Sinz, M.; P Singh, S.; Shahe Mahammad, S.; Mandlekar, S., A simplified protocol employing elacridar in rodents: a screening model in drug discovery to assess P-gp mediated efflux at the blood brain barrier. *Drug metabolism letters* **2012,** *6* (2), 134-144.

30. McLeod, M. C.; Aubé, J.; Frankowski, K. J., Decahydrobenzoquinolin-5-one sigma receptor ligands: Divergent development of both sigma 1 and sigma 2 receptor selective examples. *Bioorganic & medicinal chemistry letters* **2016,** *26* (23), 5689-5694.

31. Li, P.; L Snyder, G.; E Vanover, K., Dopamine targeting drugs for the treatment of schizophrenia: past, present and future. *Current topics in medicinal chemistry* **2016,** *16* (29), 3385-3403.

32. Matsuno, K.; Nakazawa, M.; Okamoto, K.; Kawashima, Y.; Mita, S., Binding properties of SA4503, a novel and selective σ1 receptor agonist. *European journal of pharmacology* **1996,** *306* (1-3), 271-279.

33. Schwarz, A. J.; Danckaert, A.; Reese, T.; Gozzi, A.; Paxinos, G.; Watson, C.; Merlo-Pich, E. V.; Bifone, A., A stereotaxic MRI template set for the rat brain with tissue class distribution maps and co-registered anatomical atlas: application to pharmacological MRI. *Neuroimage* **2006,** *32* (2), 538-550.

34. Garcia, D. V.; Casteels, C.; Schwarz, A. J.; Dierckx, R. A.; Koole, M.; Doorduin, J., A standardized method for the construction of tracer specific PET and SPECT rat brain templates: validation and implementation of a toolbox. *PLoS One* **2015,** *10* (3), e0122363.

Table of Contents/Abstract Graphics

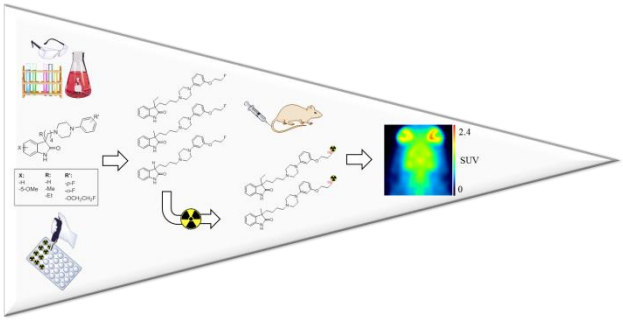

Supporting information

Development and Evaluation of Two Potential 5-HT$_7$ Receptor PET Tracers: [^{18}F]ENL09 and [^{18}F]ENL10

Elina Tampio L'Estrade[a,b,c], Mengfei Xiong[a,b], Vladimir Shalgunov[b], Fraser G. Edgar[b], Balázs Volk[d], Simone L. Baerentzen[a], Mikael Palner[a,e], Maria Erlandsson[c], Tomas Ohlsson[c], Gitte M. Knudsen[a,f] and Matthias M. Herth[a,b,g,*]

[a]*Neurobiology Research Unit, Rigshospitalet, Blegdamsvej 9, 2100 Copenhagen, Denmark*

[b]*Department for Drug Design and Pharmacology, Faculty of Health and Medical Sciences, University of Copenhagen, Universitetesparken 2, 2100 Copenhagen, Denmark*

[c]*Radiation Physics, Nuclear Medicine Physics Unit, Skånes University Hospital, Barngatan 3, 222 42 Lund, Sweden.*

[d]*Directorate of Drug Substance Development, Egis Pharmaceuticals Plc., P.O. Box 100, H-1475 Budapest, Hungary*

[e]*Center of Translational Neuroscience, Faculty of Health and Medical Sciences, University of Copenhagen, Denmark*

[f]*Institute of Clinical Medicine, Faculty of Health and Medical Sciences, University of Copenhagen, Denmark*

[g]*Department of Clinical Physiology, Nuclear Medicine and PET, University Hospital Copenhagen, Rigshospitalet Blegdamsvej 9, 2100 Copenhagen, Denmark*

Keywords: PET, 5-HT$_7$R, Fluorine-18, Fragment-based Dual-labelling, PDSP, Rat

*Corresponding Author: Tel.: +45 93565414; fax: +45 35 33 60 41; e-mail: matthias.herth@sund.ku.dk

CONTENTS

REFERENCE SYNTHESES 213

***IN VITRO* AFFINITY SCREENING 214**

CALCULATIONS OF AN THEORETICAL BINDING RATIO 214

***IN VIVO* EVALUATION IN RAT 215**

REFERENCES 217

Reference syntheses

The syntheses and experimental information of these previously presented compounds are described in **Paper III**, chapter 5.

- *4-(3-Hydroxyphenyl)-piperazine-1-Boc* **(ENL01)**[1]
- *4-(3-(2-Flouro-ethoxy)-phenyl)-piperazine-1-Boc* **(ENL02)**[1]
- *1-[3-(2-Fluoro-ethoxy)-phenyl]-piperazine* **(ENL03)**[1]
- *tert-Butyl 4-(3-(2-hydroxyethoxy)phenyl)piperazine-1-carboxylate* **(ENL11)**[2]
- *tert-Butyl 4-(3-(2-(tosyloxy)ethoxy)phenyl)piperazine-1-carboxylate* **(ENL04)**[3]
- *3-(4-Hydroxybutyl)indolin-2-one* **(ENL12)**[4]
- *4-(2-Oxoindolin-3-yl)butyl methanesulfonate* **(ENL14)**[4]
- *3-(4-(4-(3-(2-Fluoroethoxy)phenyl)piperazin-1-yl)butyl)indolin-2-one* **(ENL20)**[4] (This reference was received from Matthias Herth.)
- *3-Ethyl-3-(4-(4-(3-(2-fluoroethoxy)phenyl)piperazin-1-yl)butyl)-5-methoxyindolin-2-one* **(ENL61)**[2]
- *3-(4-(4-(4-Fluorophenyl)piperazin-1-yl)butyl)-3-methylindolin-2-one* **(ENL06)**[2]
- *3-Ethyl-3-(4-(4-(4-fluorophenyl)piperazin-1-yl)butyl)indolin-2-one* **(ENL05)**[6]
- *3-Ethyl-3-(4-(4-(4-fluorophenyl)piperazin-1-yl)butyl)-5-methoxyindolin-2-one* **(ENL60)**[2]

3-(4-(4-(4-Fluorophenyl)piperazin-1-yl)butyl)indolin-2-one **(ENL21):**[4]
This reference compound was received from Balázs Volk.
^{1}H NMR (600 MHz, CD_3OD) δ 7.30 (dt, *J* = 7.4, 0.8 Hz, 1H), 7.23 (td, *J* = 7.7, 1.2 Hz, 1H), 7.05 (td, *J* = 7.5, 1.0 Hz, 1H), 7.01–6.96 (m, 4H), 6.92 (d, *J* = 7.8 Hz, 1H), 3.15–3.10 (m, 4H), 2.65–2.60 (m, 4H), 2.40 (td, *J* = 7.1, 1.5 Hz, 2H), 2.03 (m, *J* = 36.1, 13.7, 10.7, 5.4 Hz, 2H), 1.58 (dtd, *J* = 14.8, 6.8, 3.2 Hz, 2H), 1.44 – 1.24 (m, 3H). ^{13}C NMR (151 MHz, CD_3OD) δ 182.44, 158.72 (d, *J* = 232.7 Hz), 149.41, 143.79, 131.12, 128.94, 125.16, 123.30, 119.27, 116.36, 116.21, 110.76, 59.36, 54.21, 50.96, 49.85, 31.01, 27.42, 24.48. UPLC-MS (ESI): RT: 2.89 min, m/z: 368.2 $[M^+H]^+$ at 215-254 nm. **Appendices 13-15.**

In vitro affinity screening

Supplementary Table 1: pharmacological selectivity profile of all synthesized reference compounds

ID	K_i (nM)										
	5-HT_{1A}	5-HT_{2A}	5-HT_6	5-HT_7	α_{1A}	α_{1B}	α_{1D}	H1	SERT	σ_1	σ_2
ENL20	145	162	2373	9.5	339	668	502	-	-	26	51
ENL10	72	53	422	5.6	748	825	1288	-	-	18	65
ENL09	107	160	1389	13	-	1413	-	-	2344	29	67
ENL61	389	103	-	38	878	448	1373	-	274	165	62
ENL21	288	28	-	1.5	130	228	162	-	305	8.1	2.1
ENL06	306	21	230	2.8	239	174	375	-	1712	11	3.5
ENL05	190	37	292	2.4	280	168	300	-	848	15	1.4
ENL60	267	29	389	5.6	132	208	135	-	148	39	2
ENL17	144	113	2219	8.3	40	346	33	-	1278	9.9	2.9
ENL08	38	121	685	5.2	41	263	66	-	3569	3.7	1.7
ENL07	49	100	1042	11	128	430	116	-	2477	6.8	2.5
ENL15	155	48	-	92	159	-	157	-	1280	38	1.7

Calculations of an theoretical binding ratio ($tBR_{target/off\text{-}target}$)

$$tBR_{target/off-target} = \left(\frac{K_{D,off-target}}{K_{D,target}}\right) x \left(\frac{B_{avail,target}}{B_{avail,off-\ target}}\right)$$

Example:

ENL10: $K_{i,\ 5\text{-}HT7}$ = 5.6 nM, $K_{i,\ \sigma 1}$ = 18 nM (averaged σ-receptor affinity)

B_{max} for the rat 5-HT_7R in thalamus: 47 fmol/mg tissue.[7]

B_{max} for the rat σ-receptor in thalamus: 600 fmol/mg of σ-1 and 833 fmol/mg (according to the density in an adult rat, hence 3 times lower than the measured density in 1 day old rats) of σ-2 receptors gives a (600+833)/2 ~700 fmol/mg protein of the σ-receptors in rat thalamus.[8] This can roughly be estimated to 70 fmol/mg tissue.[9]

$tBR_{target/off\text{-}target}$ = (18 nM/5.6 nM) x (47 pmol/g tissue /70 fmol/mg tissue) = 2.15

In vivo evaluation in rat

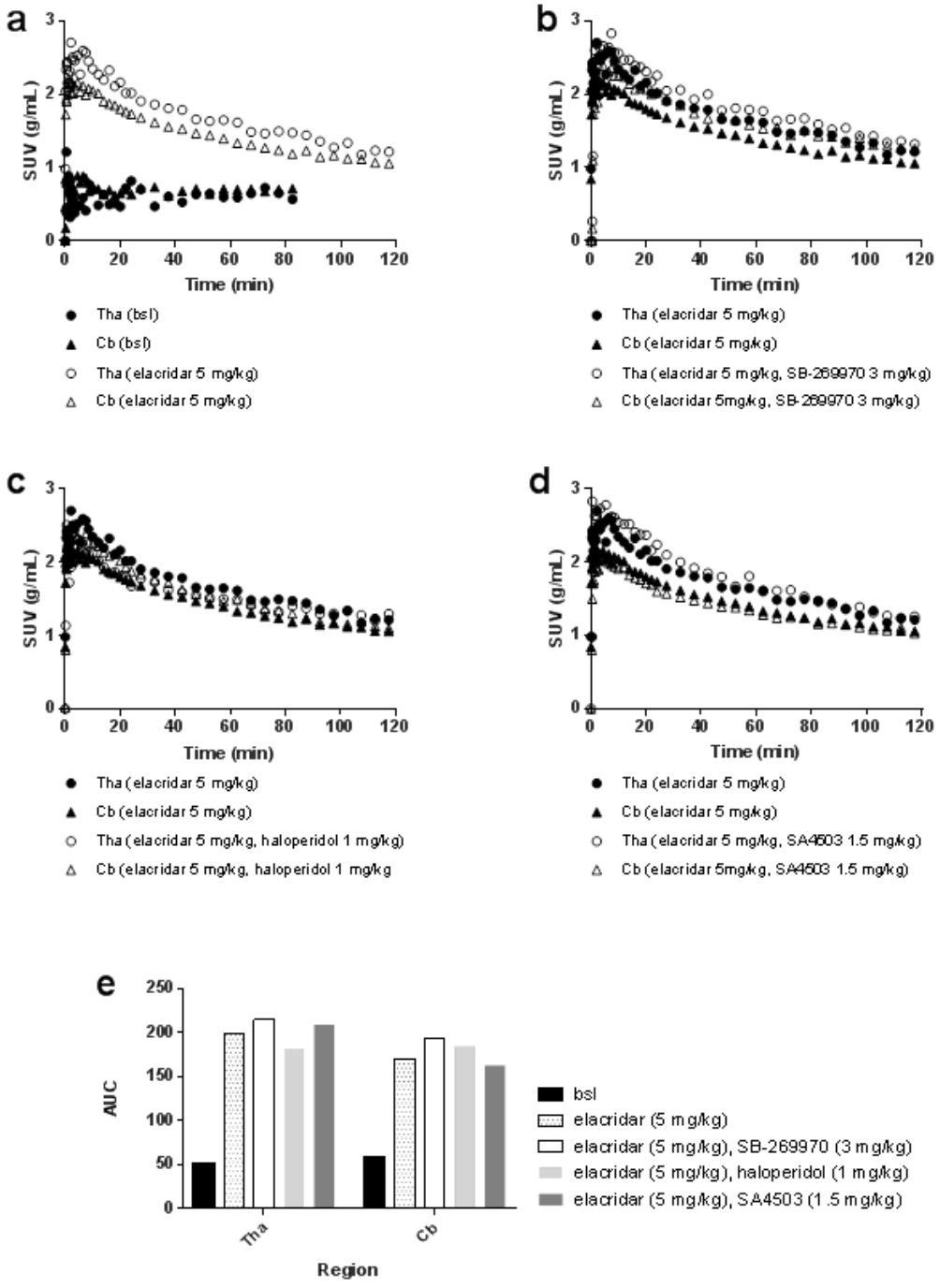

Supplementary Figure 1: Representative time-activity curves (TACs) of [^{18}F]ENL09 in the thalamus (circles, tha) and cerebellum (triangles, Cb) in the rat brain. a) TACs at baseline (bsl) and after pretreatment with elacridar (5 mg/kg). b) Thalamus and cerebellum TACs after pretreatment with elacridar and elacridar + SB-269970 (3 mg/kg). c) Thalamus and cerebellum TACs after pretreatment with elacridar and elacridar + haloperidol (1 mg/kg). d) Thalamus and cerebellum TACs after pretreatment with elacridar and elacridar + SA4503 (1.5 mg/kg). e) Calculated area-under-curve (AUC) for all TACs displayed as a grouped barplot. All TACs are normalized to injected radioactivity and animal weight resulting in the standard uptake value (SUV).

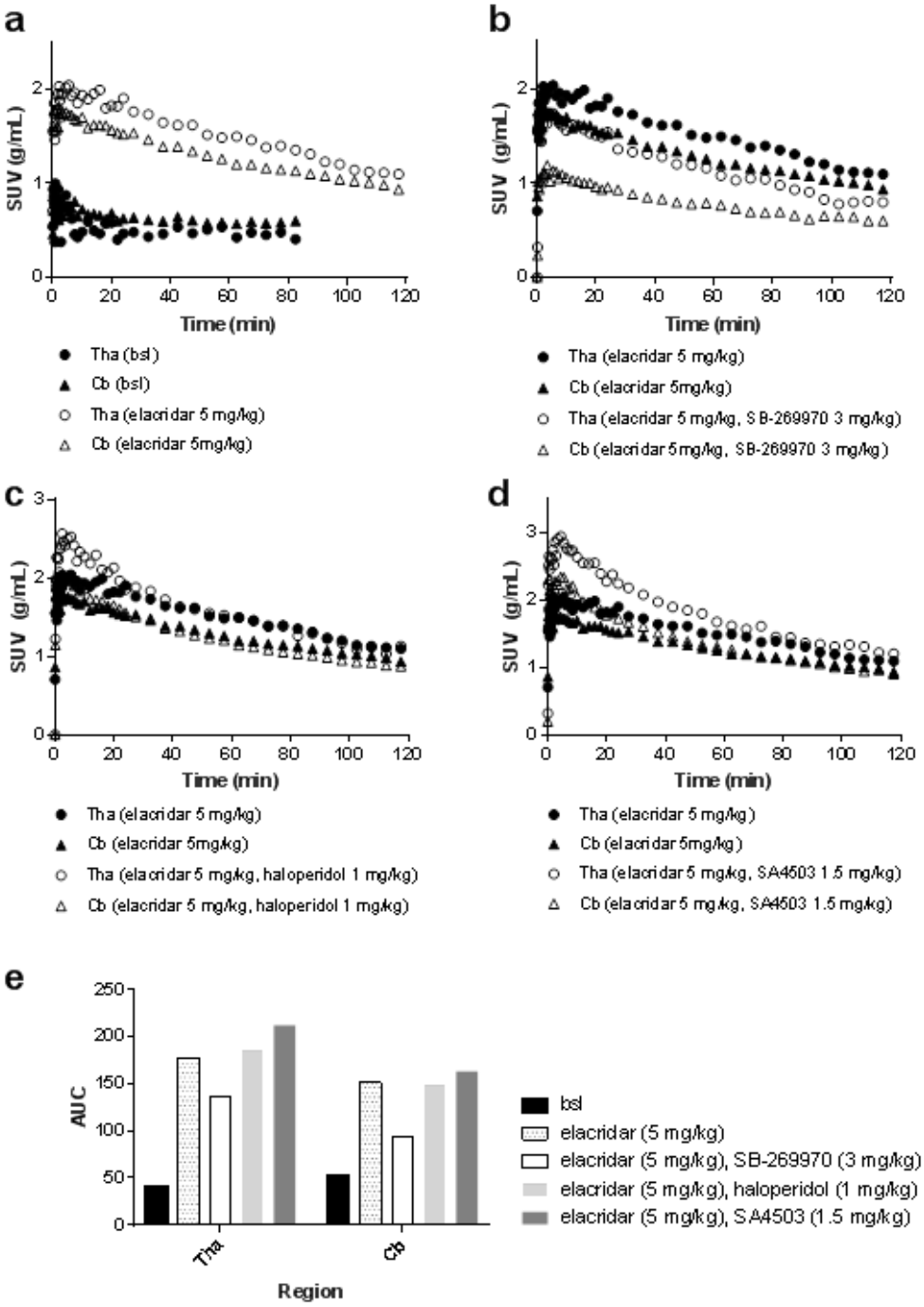

Supplementary Figure 2: Representative time-activity curves (TACs) of [^{18}F]ENL10 in the thalamus (circles, tha) and cerebellum (triangles, Cb) in the rat brain. a) TACs at baseline (bsl) and after pretreatment with elacridar (5 mg/kg). b) Thalamus and cerebellum TACs after pretreatment with elacridar and elacridar + SB-269970 (3 mg/kg). c) Thalamus and cerebellum TACs after pretreatment with elacridar and elacridar + haloperidol (1 mg/kg). d) Thalamus and cerebellum TACs after pretreatment with elacridar and elacridar + SA4503 (1.5 mg/kg). e) Calculated area-under-curve (AUC) for all TACs displayed as a grouped barplot. All TACs are normalized to injected radioactivity and animal weight resulting in the standard uptake value (SUV).

References

1. Herth, M. M.; Kramer, V.; Rösch, F., Synthesis of novel WAY 100635 derivatives containing a norbornene group and radiofluorination of [^{18}F] AH1. MZ as a serotonin 5-HT$_{1A}$ receptor antagonist for molecular imaging. *Journal of Labelled Compounds and Radiopharmaceuticals: The Official Journal of the International Isotope Society* **2009,** *52* (6), 201-207.

2. Elina Tampio L'Estrade, S. L., Ida Nymann Petersen, Fraser G. Edgar, Balázs Volk, Maria Erlandsson, Tomas Ohlsson, Gitte M. Knudsen and Matthias M. Herth, Fragment-based Labelling Using Condensation Reactions – A Possibility to Increase Throughput in Preclinical PET. *Submitted Manuscript* **2019**.

3. Prante, O.; Tietze, R.; Hocke, C.; Lober, S.; Hubner, H.; Kuwert, T.; Gmeiner, P., Synthesis, radiofluorination, and *in vitro* evaluation of pyrazolo[1,5-a]pyridine-based dopamine D4 receptor ligands: discovery of an inverse agonist radioligand for PET. *Journal of medicinal chemistry* **2008,** *51* (6), 1800-1810.

4. Herth, M. M.; Volk, B.; Pallagi, K.; Kofoed Bech, L.; Antoni, F. A.; Knudsen, G. M.; Kristensen, J. L., Synthesis and *in vitro* evaluation of oxindole derivatives as potential radioligands for 5-HT(7) receptor imaging with PET. *ACS Chemical Neuroscience* **2012,** *3* (12), 1002-7.

5. Volk, B.; Gacsályi, I.; Pallagi, K.; Poszávácz, L.; Gyönös, I.; Szabó, É.; Bakó, T.; Spedding, M.; Simig, G.; Szénási, G., Optimization of (arylpiperazinylbutyl) oxindoles exhibiting selective 5-HT$_7$ receptor antagonist activity. *Journal of medicinal chemistry* **2011,** *54* (19), 6657-6669.

6. Volk, B.; Barkóczy, J.; Hegedus, E.; Udvari, S.; Gacsályi, I.; Mezei, T.; Pallagi, K.; Kompagne, H.; Lévay, G.; Egyed, A., (Phenylpiperazinyl-butyl) oxindoles as selective 5-HT$_7$ receptor antagonists. *Journal of medicinal chemistry* **2008,** *51* (8), 2522-2532.

7. Horisawa, T.; Ishiyama, T.; Ono, M.; Ishibashi, T.; Taiji, M., Binding of lurasidone, a novel antipsychotic, to rat 5-HT$_7$ receptor: analysis by [^{3}H] SB-269970 autoradiography. *Progress in Neuro-Psychopharmacology and Biological Psychiatry* **2013,** *40*, 132-137.

8. McCann, D. J.; Weissman, A. D.; Su, T. P., Sigma-1 and Sigma-2 sites in rat brain: Comparison of regional, ontogenetic, and subcellular patterns. *Synapse* **1994,** *17* (3), 182-189.

9. Cumming, P., Absolute abundances and affinity states of dopamine receptors in mammalian brain: a review. *Synapse* **2011,** *65* (9), 892-909.

Appendices

Appendix 1 – ^{1}H NMR of ENL17

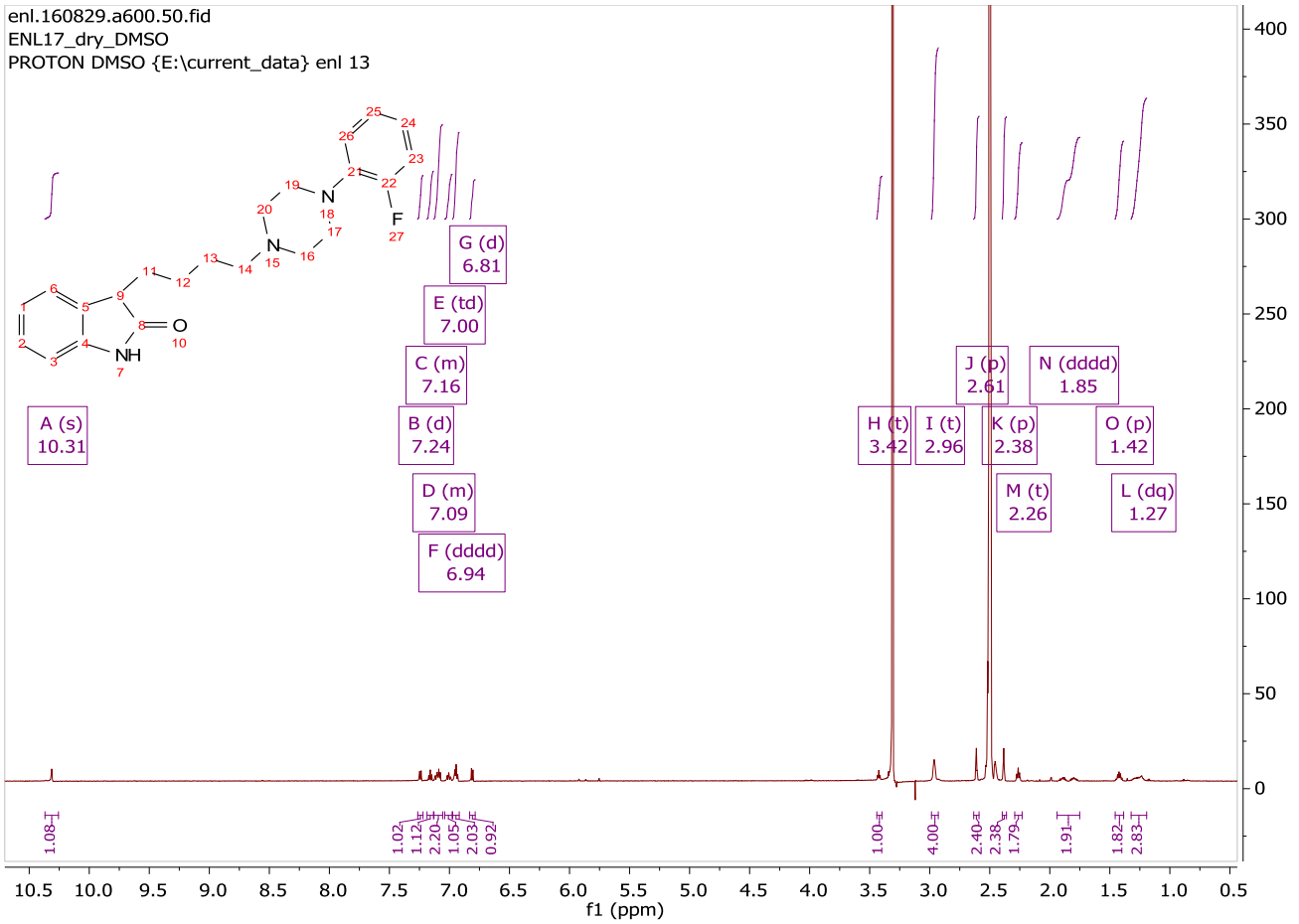

Appendix 2 – ^{13}C NMR of ENL17

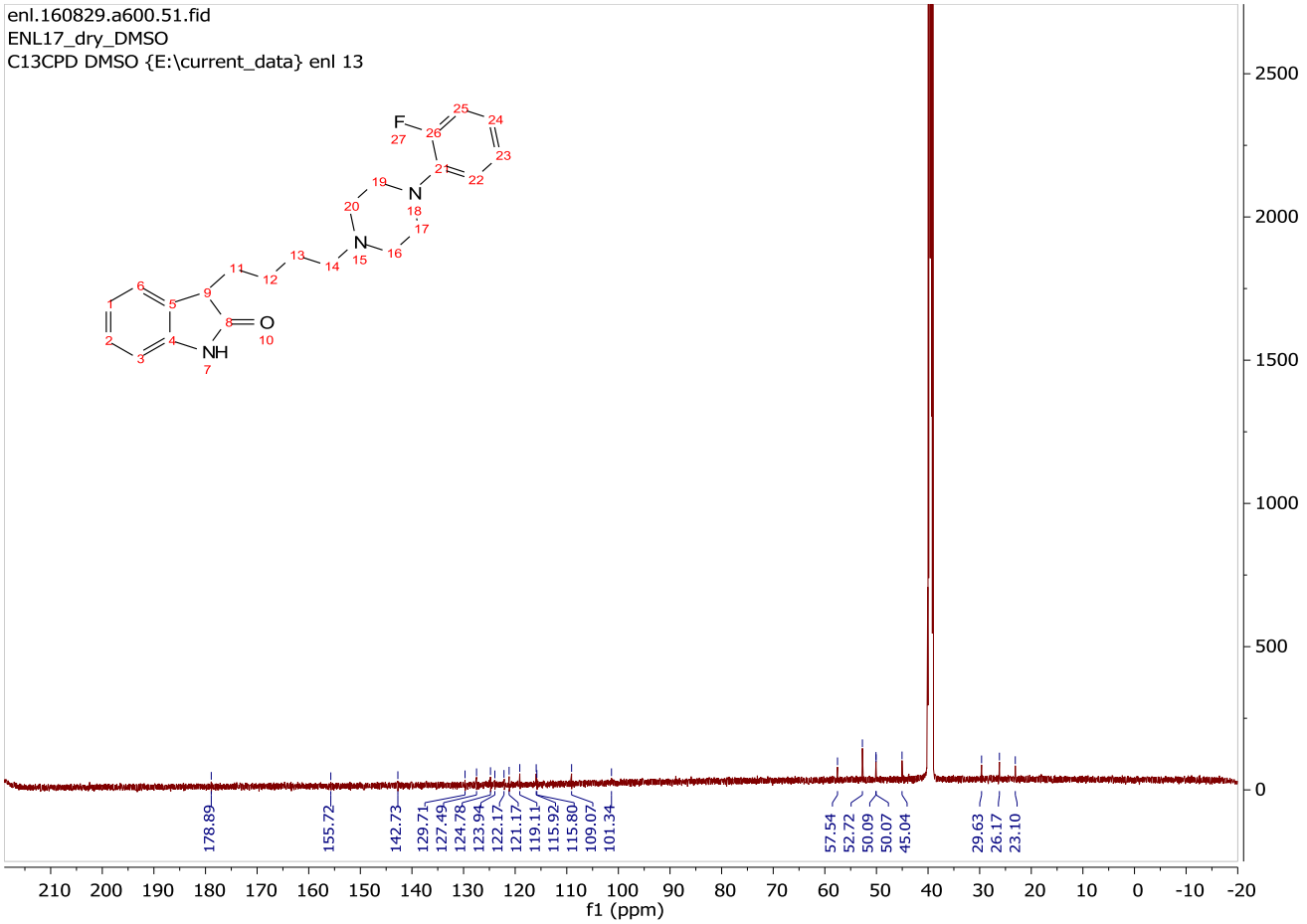

Appendix 3– UPLC-MS of ENL17

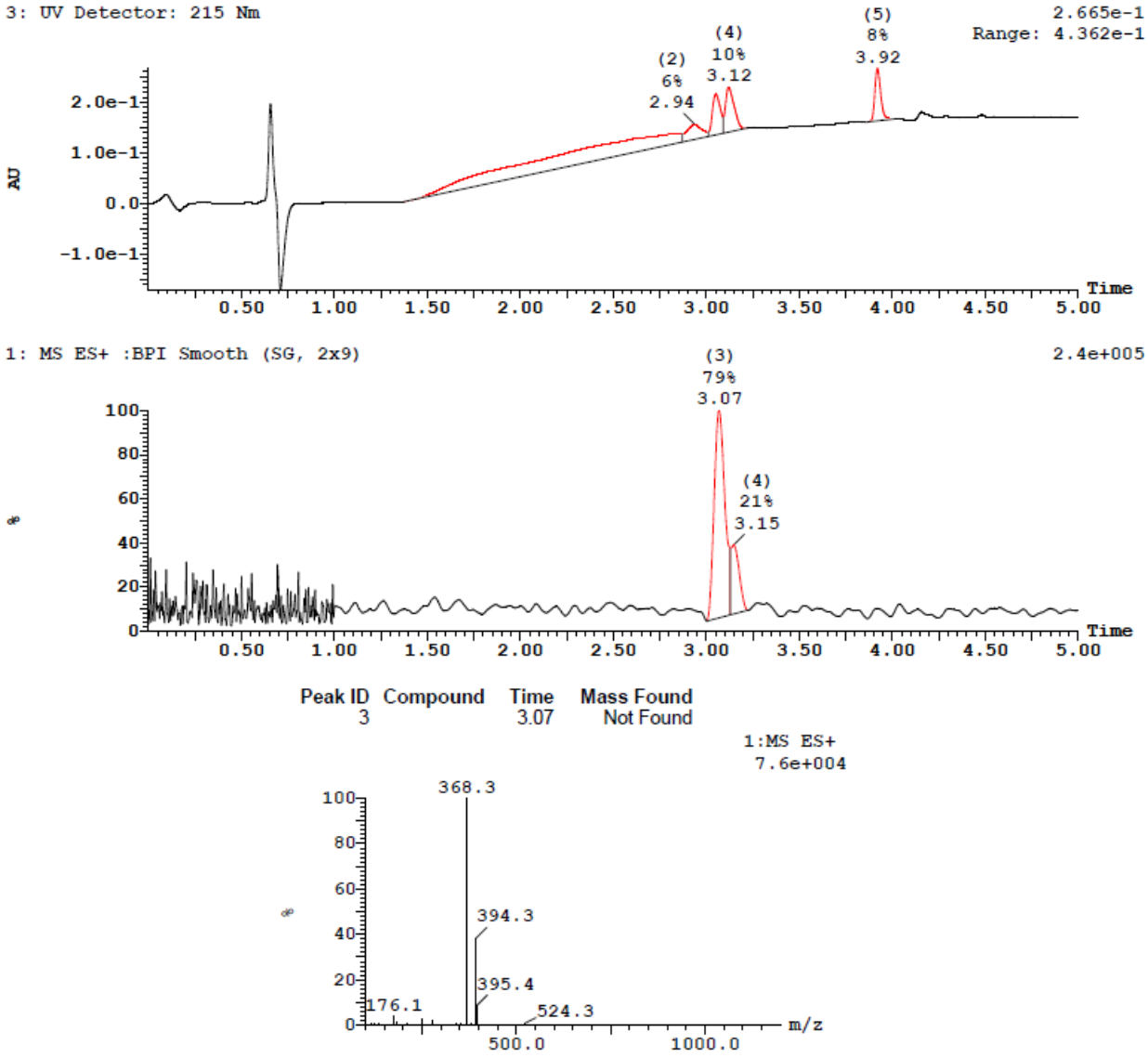

Appendix 4 – ^{1}H NMR of ENL08

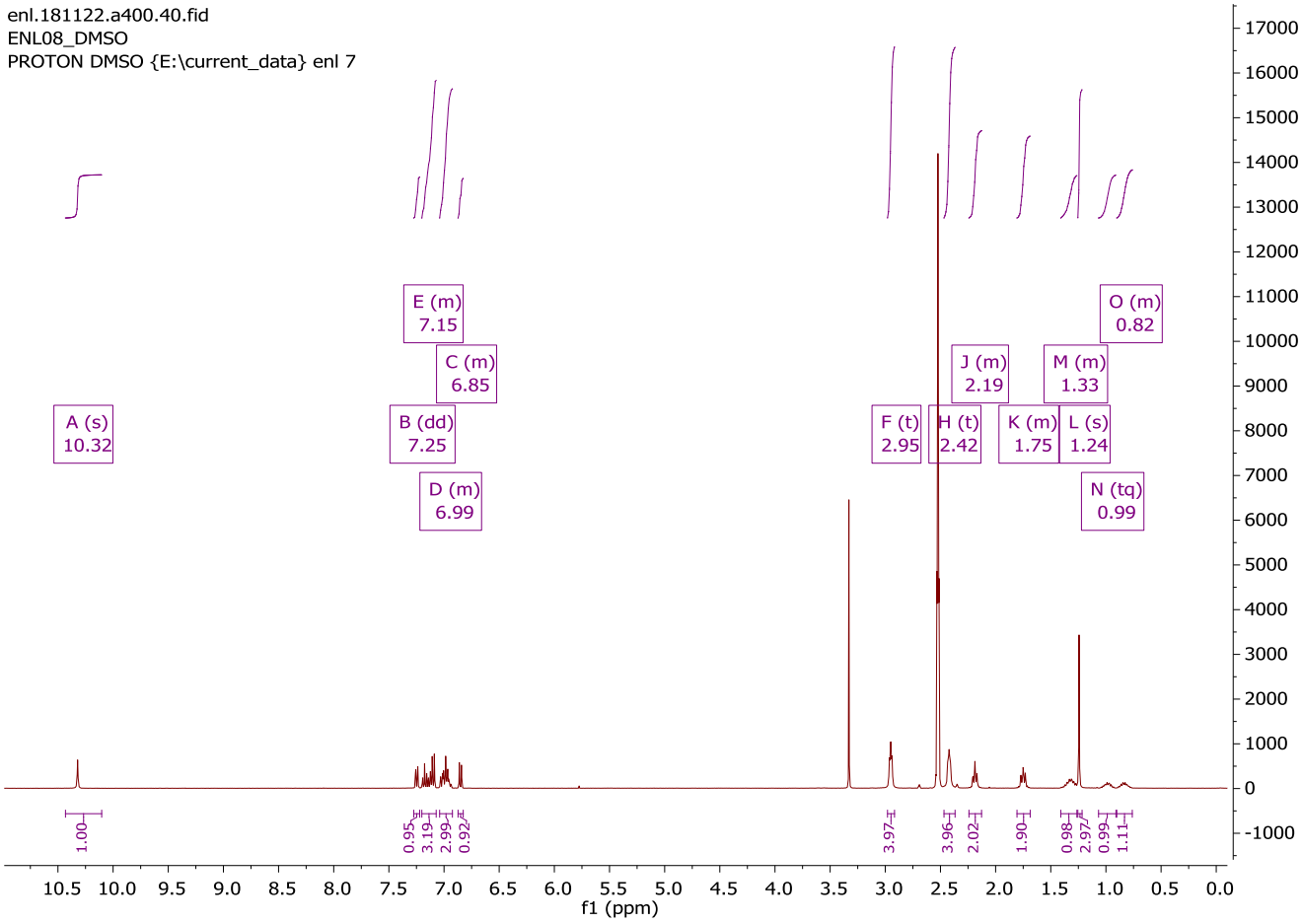

Appendix 5 – ^{13}C NMR of ENL08

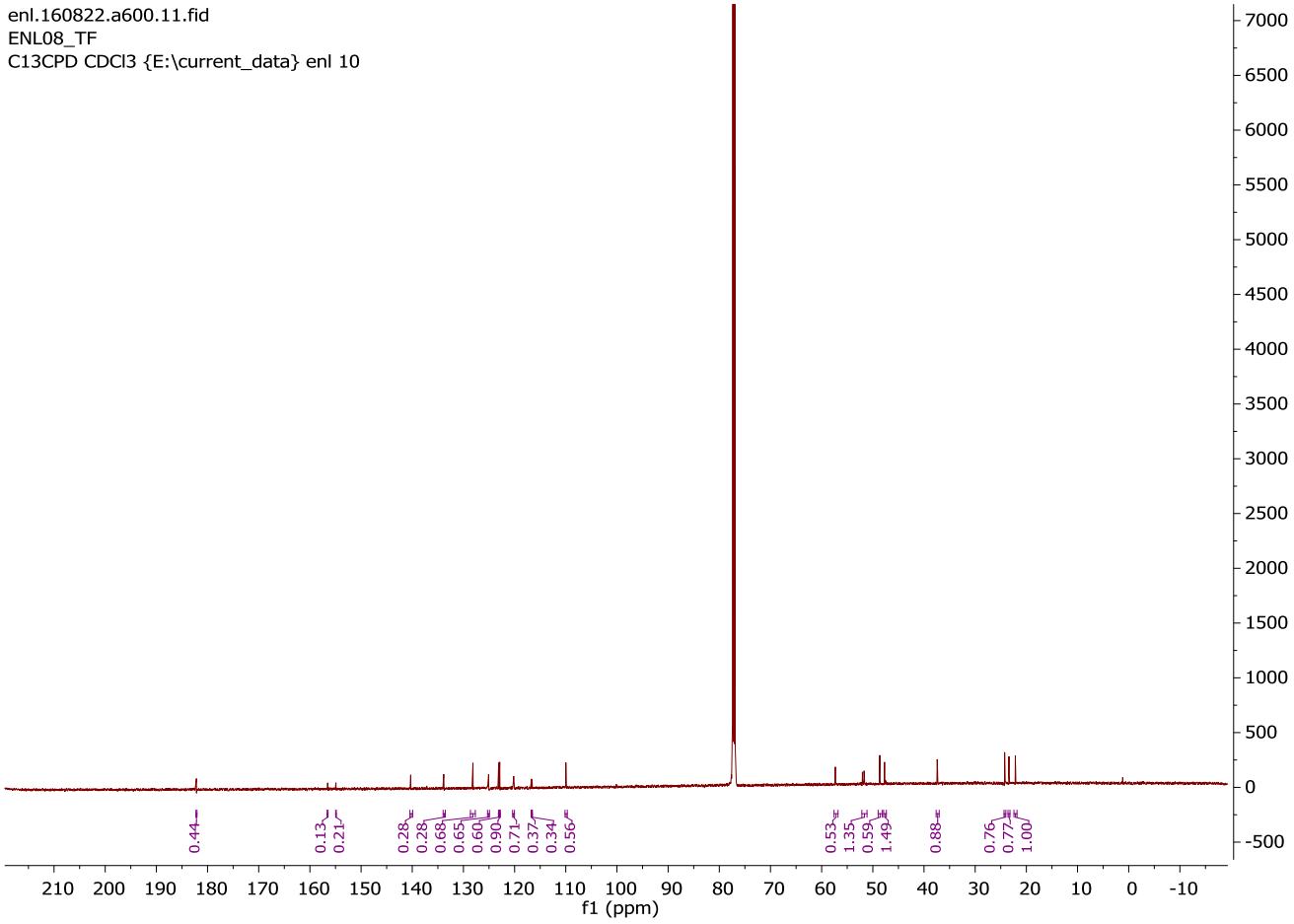

Appendix 6– UPLC-MS of ENL08

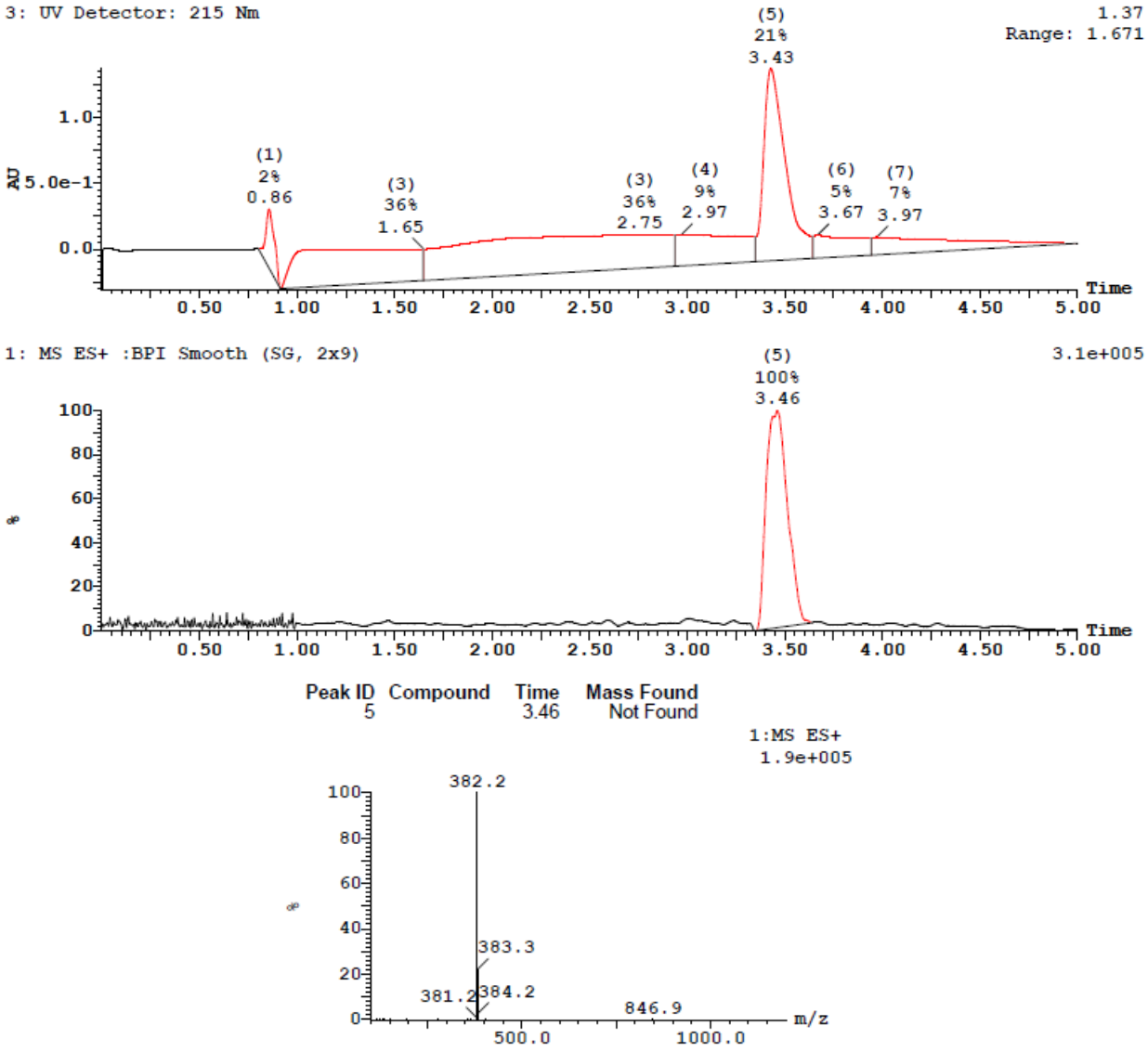

Appendix 7 – ^{1}H NMR of ENL07

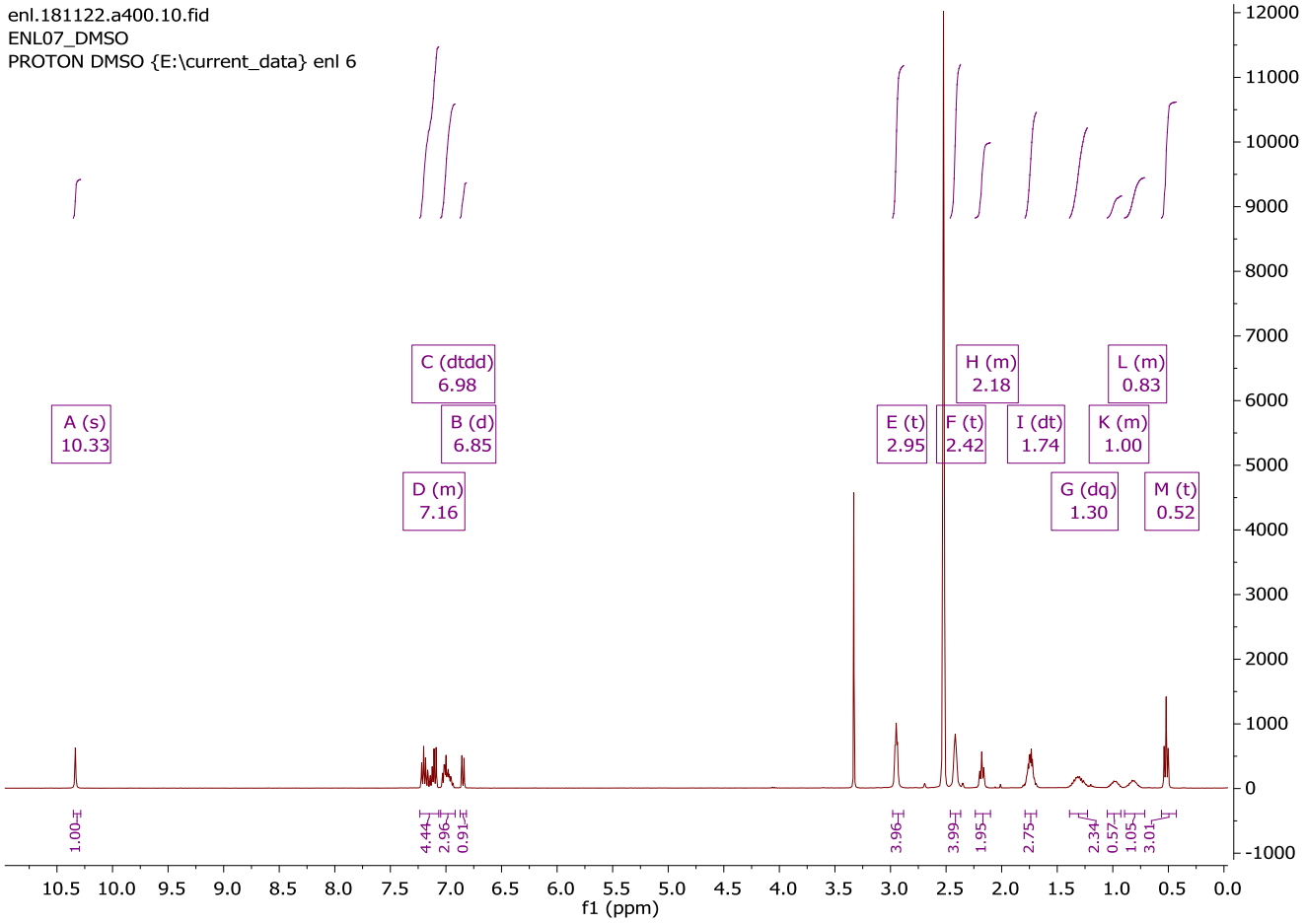

Appendix 8 – ^{13}C NMR of ENL07

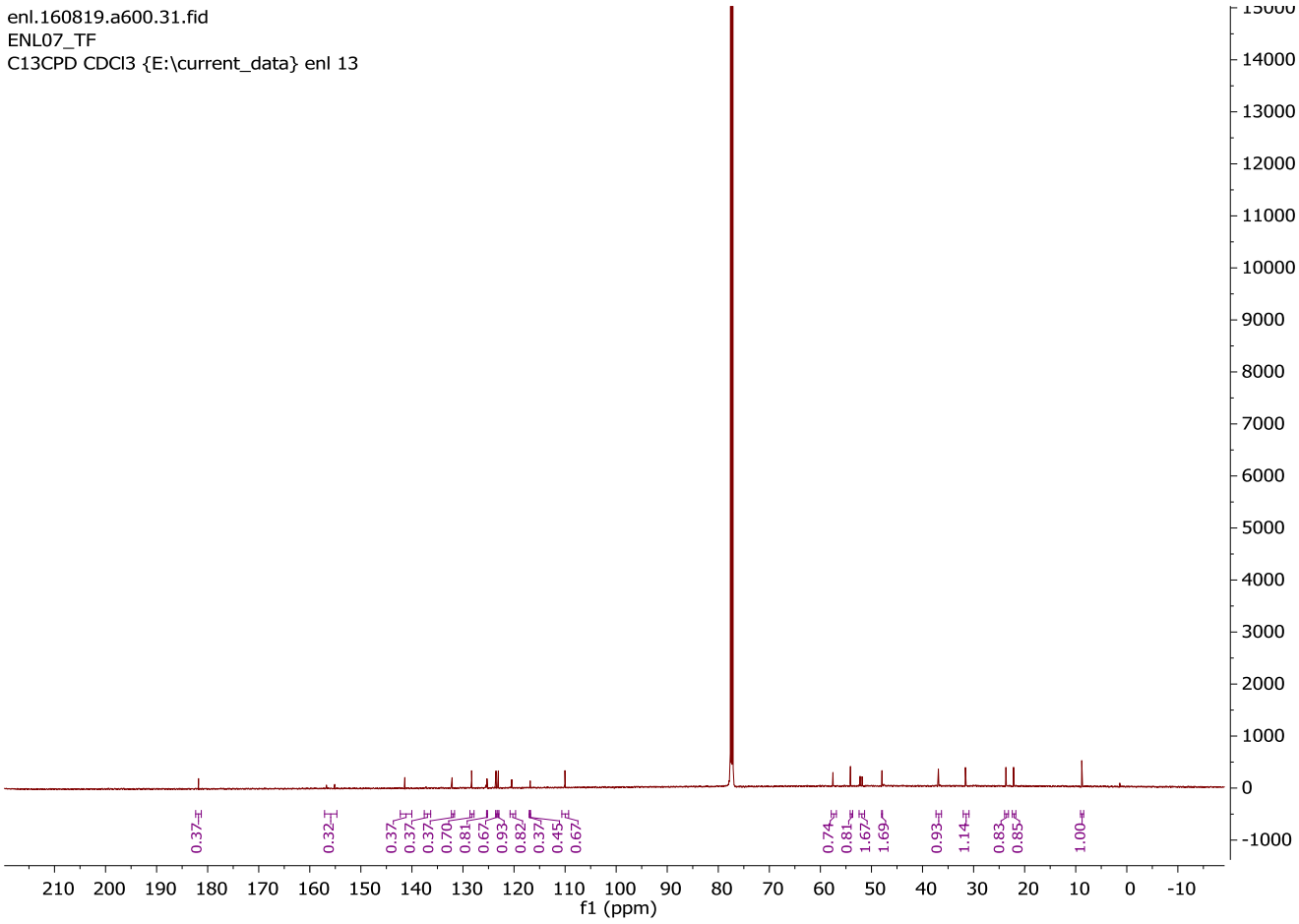

Appendix 9– UPLC-MS of ENL07

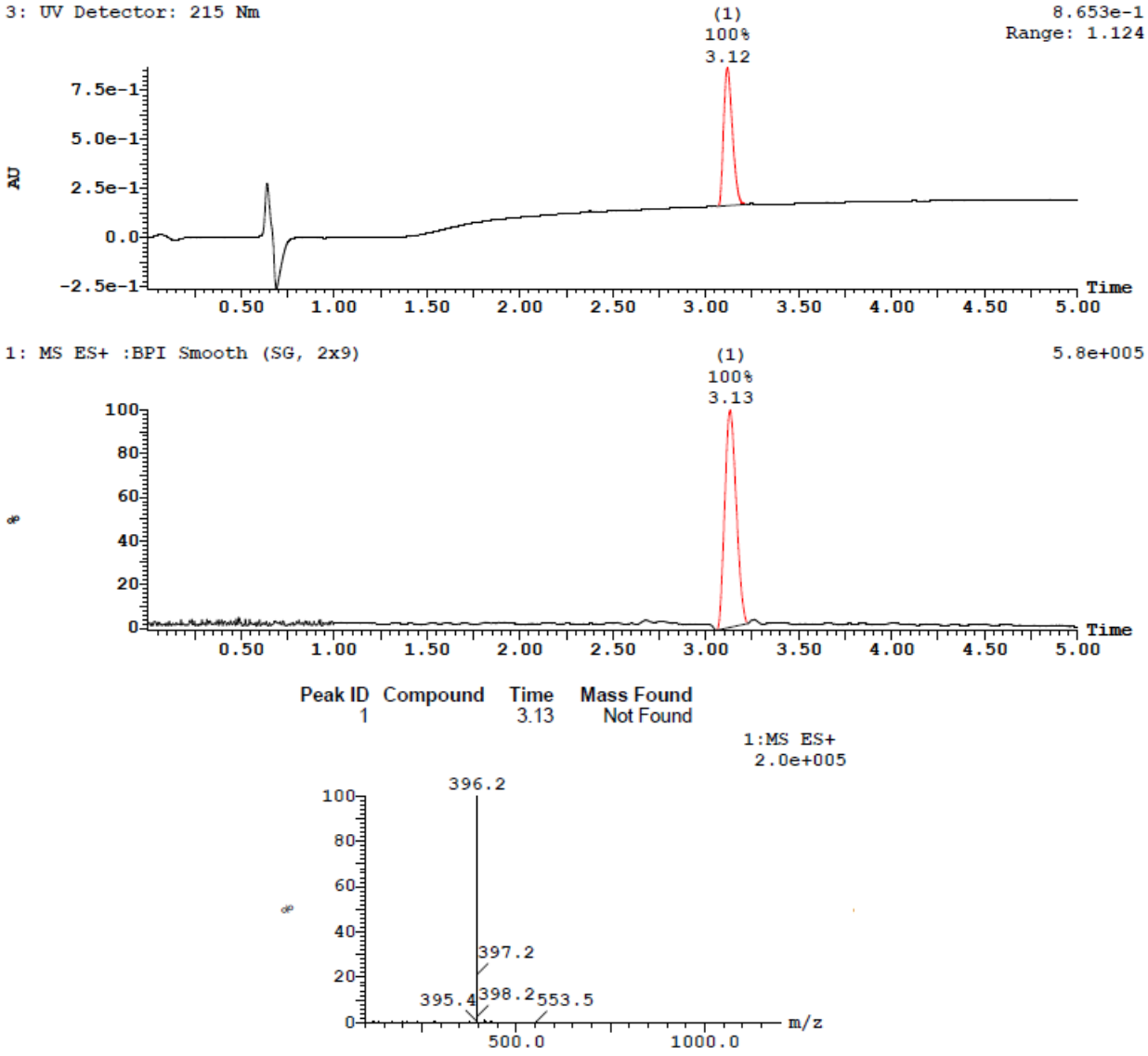

Appendix 10 – ^{1}H NMR of ENL15

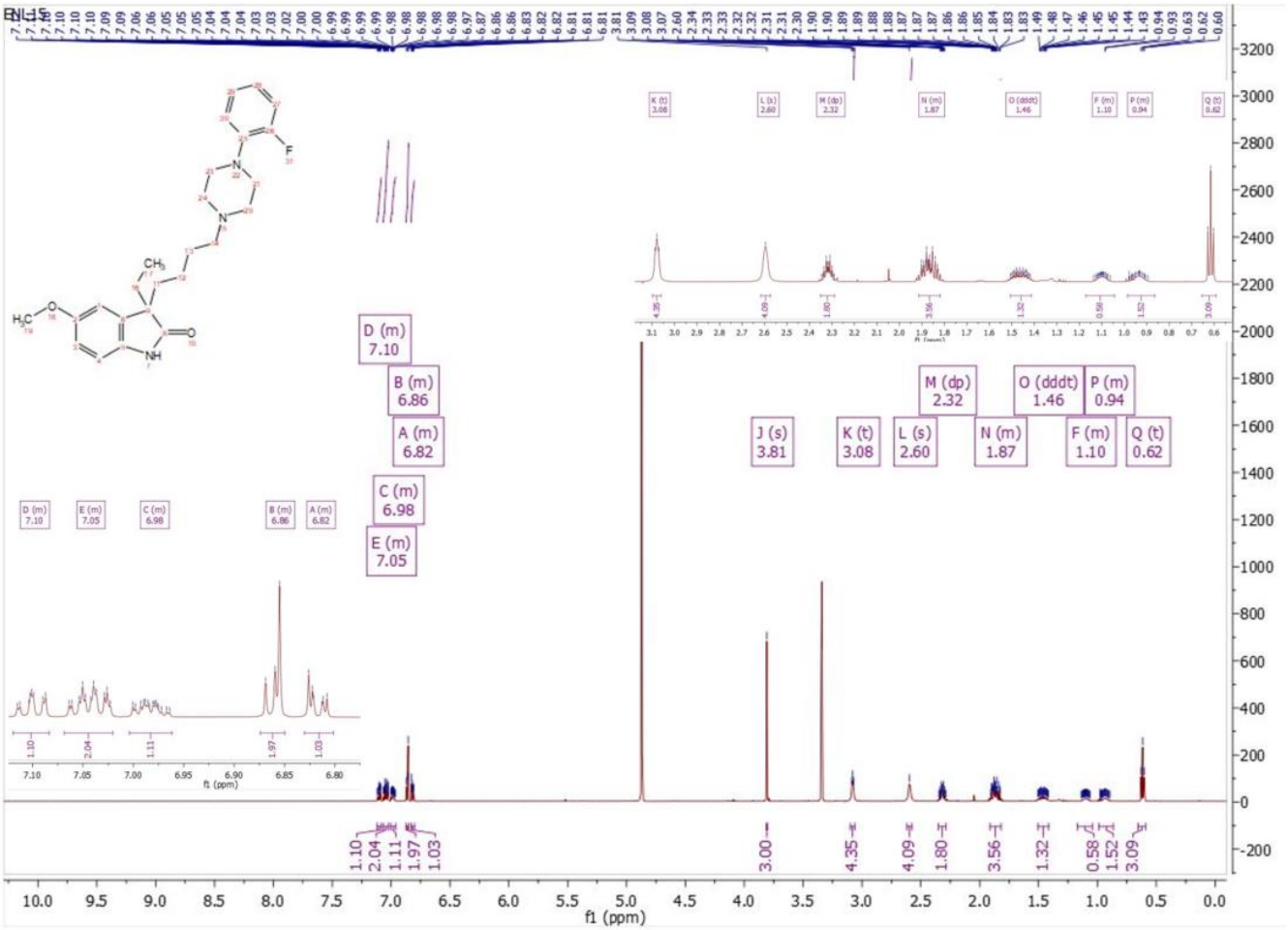

Appendix 11 – ^{13}C NMR of ENL15

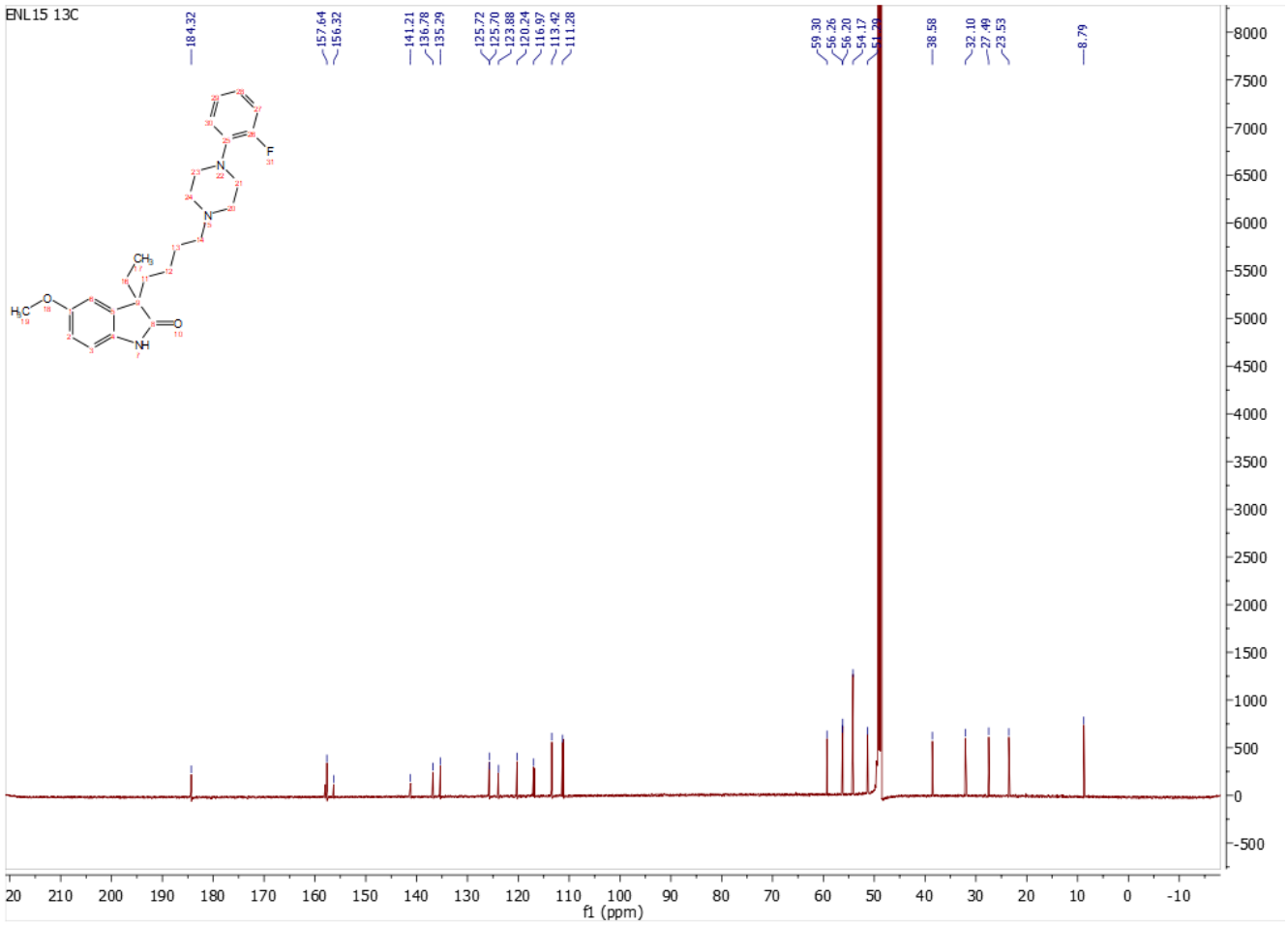

Appendix 12– UPLC-MS of ENL15

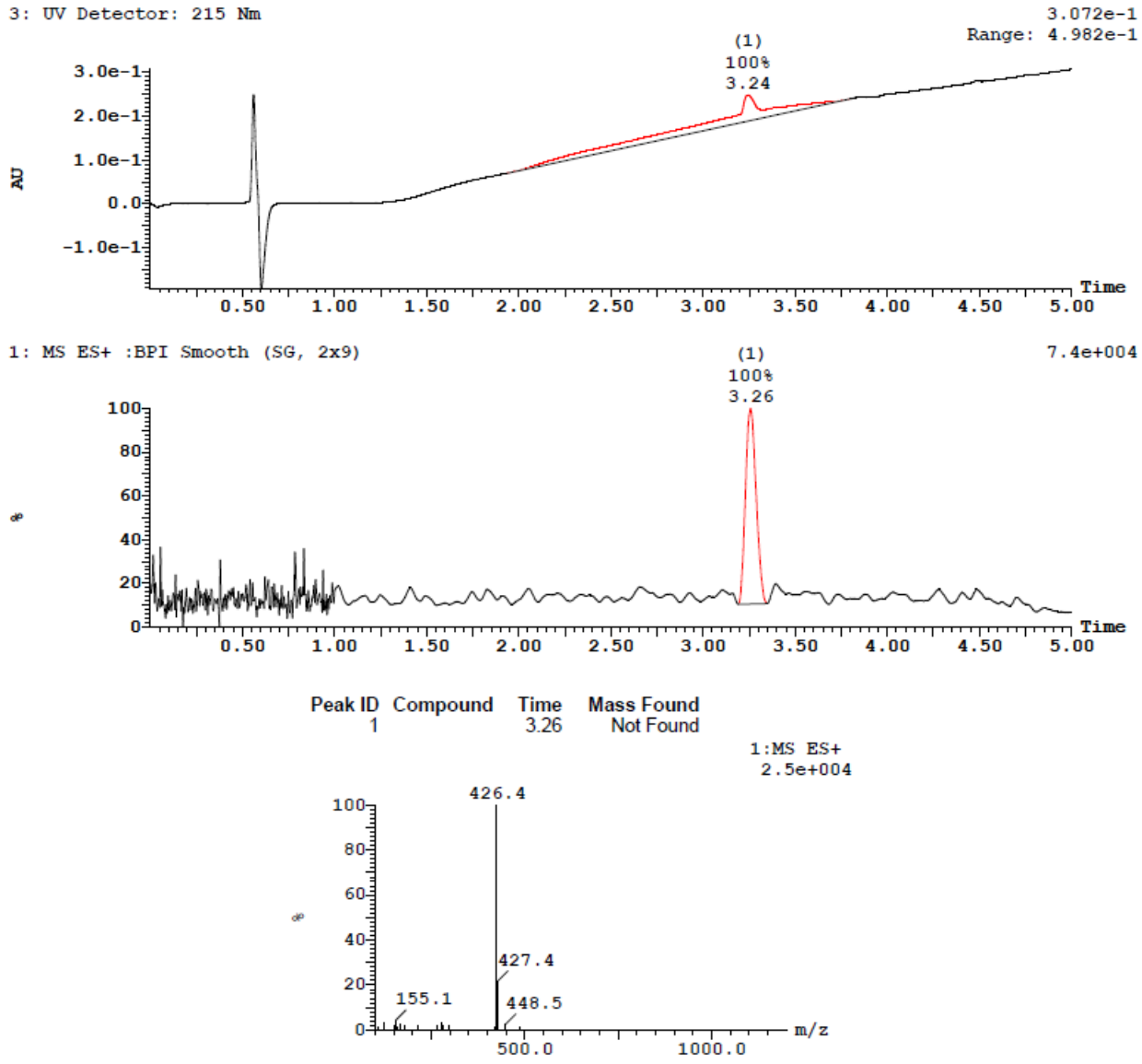

Peak ID	Compound	Time	Mass Found
1		3.26	Not Found

Appendix 13 – ^{1}H NMR of ENL21

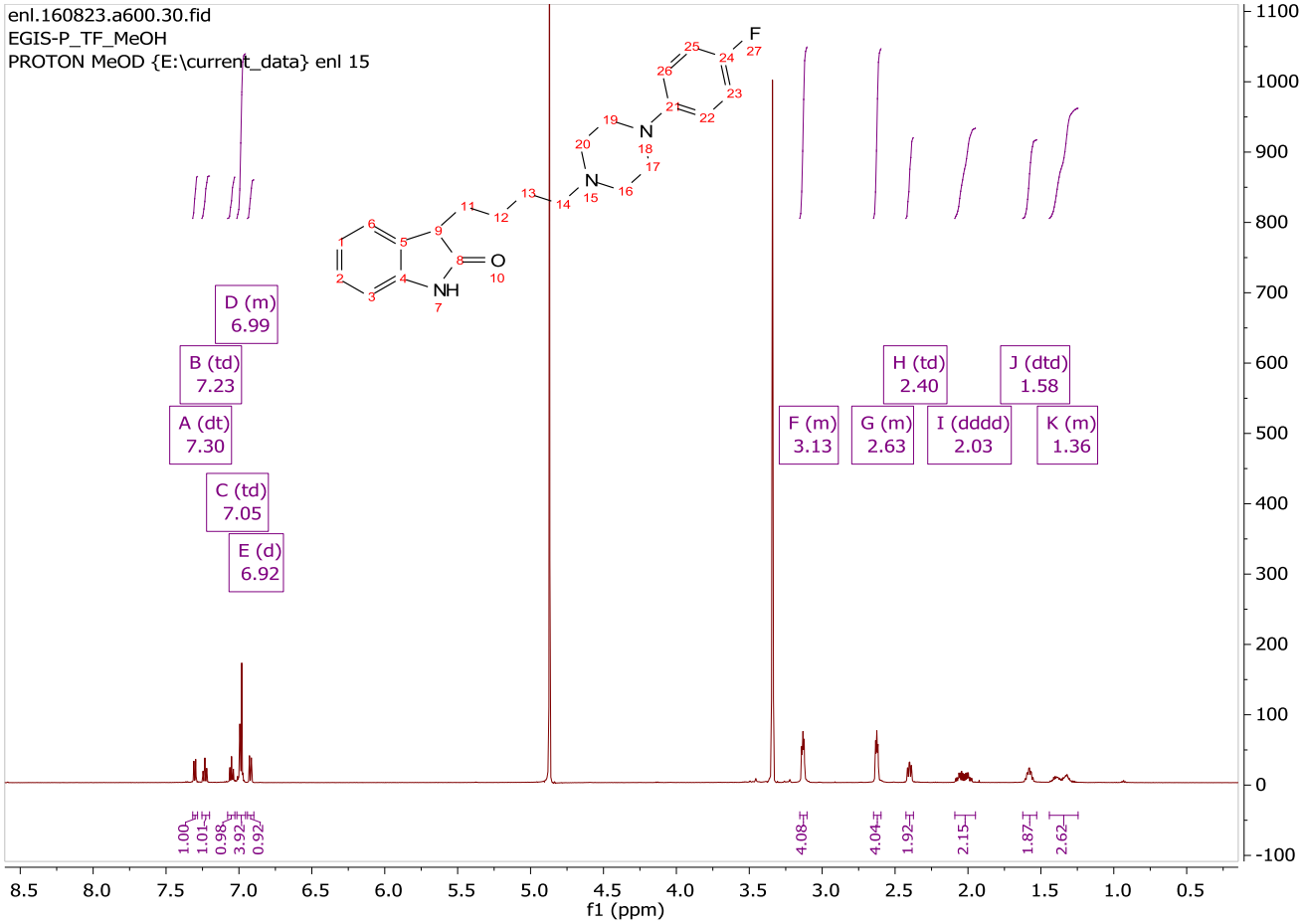

Appendix 14 – ^{13}C NMR of ENL21

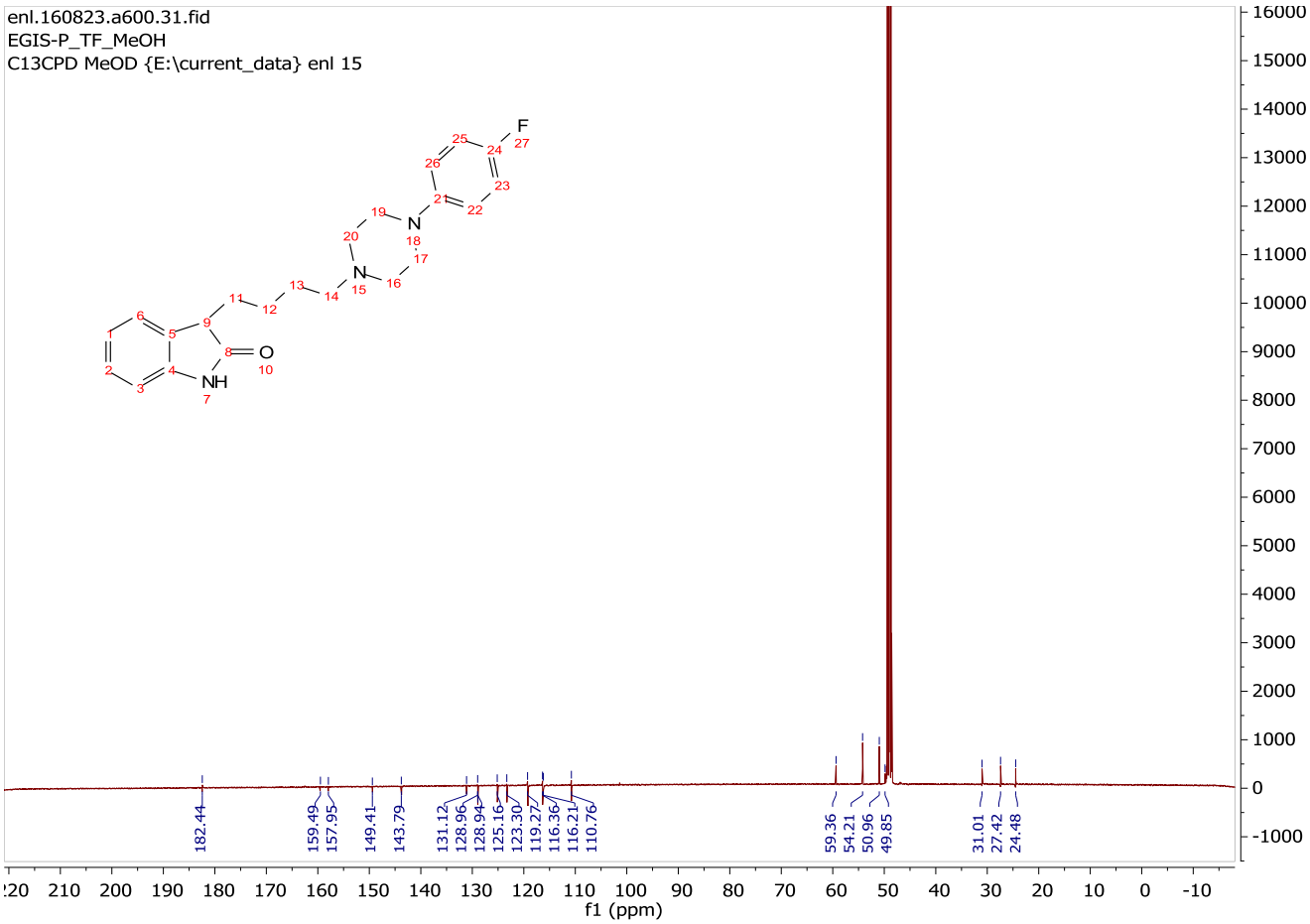

Appendix 15– UPLC-MS of ENL21

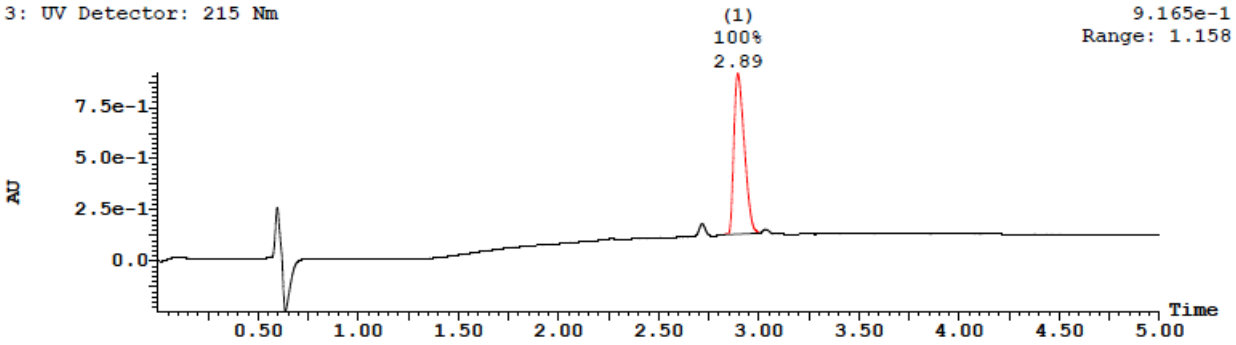

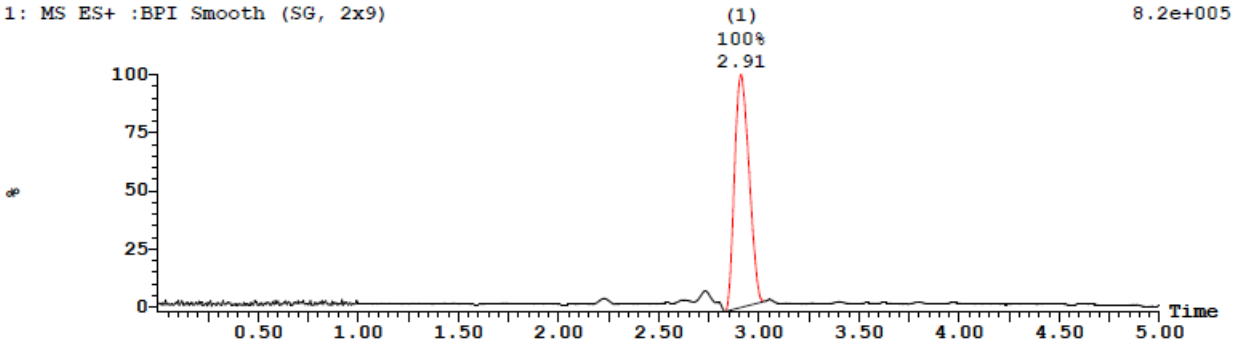

Peak ID	Compound	Time	Mass Found
1		2.91	Not Found

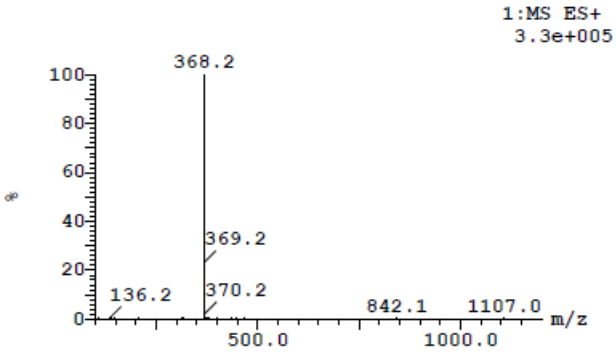

Chapter 7

Paper V

Radiosynthesis and preclinical evaluation of [^{11}C]Cimbi-701 – Towards the imaging of cerebral 5-HT$_7$ receptors

---

Summary:

*This chapter contains **Paper V**, in which [^{11}C]Cimbi-701 a benzosulfonamide and analogue of the highly selective 5-HT$_7$ receptor antagonist SB-269970 was elucidated as a potential PET tracer. [^{11}C]Cimbi-701 was in vivo evaluated in 3 species with varying results indicating species specific differences.*

Authors' contribution:

The reference compound was synthesized by F.G.E and F.C. The radiolabelling was established by S.L. The planning of the in vivo evaluation [^{11}C]Cimbi-701 in rats was performed by the author, the experiment was done by the author and M.X. while V.S produced the tracer. The author thereafter performed the PET image analysis. The pig evaluation and metabolism study was performed by H.D.H and A.D. The non-human primate in vivo evaluation was performed by the group of J.M.H. The author and H.D.H. formulated the outline and wrote the manuscript in collaboration with M.M.H.

Radiosynthesis and preclinical evaluation of [^{11}C]Cimbi-701 – Towards the imaging of cerebral 5-HT$_7$ receptors.

Elina T. L'Estrade[a,b,c], Vladimir Shalgunov[b], Fraser Edgar[b], Martin G. Strebl-Bantillo[d], Mengfei Xiong[a,b], François Crestey[b], Ramesh Neelamegam[d], Agnete Dyssegaard[a], Szabolcs Lehel[e], Maria Erlandsson[c], Tomas Ohlsson[c], Jacob M. Hooker[d], Gitte M. Knudsen[a,f], Matthias M. Herth[b,e], Hanne D. Hansen[a]

[a] *Neurobiology Research Unit, Rigshospitalet, Blegdamsvej 9, 2100 Copenhagen, Denmark*

[b] *Department for Drug Design and Pharmacology, Faculty of Health and Medical Sciences, University of Copenhagen, Universitetesparken 2, 2100 Copenhagen, Denmark*

[c] *Radiation Physics, Nuclear Medicine Physics Unit, Skånes University Hospital, Barngatan 3, 222 42 Lund, Sweden.*

[d] *Athinoula A. Martinos Center for Biomedical Imaging, Department of Radiology, Massachusetts General Hospital, Harvard Medical School, 73 High Street, Charlestown, Massachusetts 02129, United States*

[e] *Department of Clinical Physiology, Nuclear Medicine and PET, University Hospital Copenhagen, Rigshospitalet Blegdamsvej 9, 2100 Copenhagen, Denmark*

[f] *Faculty of Health and Medical Sciences, University of Copenhagen, Denmark.*

*Corresponding author
Hanne D. Hansen, Ph.D.
Neurobiology Research Unit and Center for Integrated Molecular Brain Imaging
Copenhagen University Hospital, Rigshospitalet
Blegdamsvej 9
2100 Copenhagen, Denmark
Phone: (+45) 35 45 88 21
Email: hanne.d.hansen@nru.dk

Matthias M. Herth, Ph.D
Department for Drug Design and Pharmacology
Faculty of Health and Medical Sciences,
University of Copenhagen
Jagtvej 160
2100 Copenhagen, Denmark
Phone: (+45) 93 56 54 14
Email: matthias.herth@sund.ku.dk

Manuscript category: Article
Running title: [^{11}C]Cimbi-701 as a radiotracer for 5-HT$_7$

Abstract

Purpose: The serotonin 7 (5-HT_7) receptor is involved in a broad variety of CNS disorders. Molecular imaging of this receptor with positron emission tomography (PET) would allow studying its *in vivo* pharmacology. So far, no clinical PET radiotracer exists for this important target. Consequently, we aimed to develop such a tracer. In this study, we investigated in 3 animal species if [^{11}C]Cimbi-701 can be used for this purpose.

Procedures: Cimbi-701 was synthesized in a one-step procedure starting from SB-269970. Its selectivity profile was determined using an academic screening platform (NIMH Psychoactive Drug Screening Program). Radiolabelling of [^{11}C]Cimbi-701 was performed in an automated synthesis module and the respective *in vivo* evaluation was conducted in rats, pigs and baboons. *In vivo* specificity was investigated by selective 5-HT_7 and σ receptor blocking studies. P-glycoprotein (P-gp) efflux transporter dependency was investigated using elacridar.

Results: [^{11}C]Cimbi-701 could successfully be synthesized. Selectivity profiling revealed high affinity for the 5-HT_7 (K_i = 18 nM) and for the σ-1 (K_i = 9.2 nM) and the σ-2 (K_i = 1.6 nM) receptor. In rats, [^{11}C]Cimbi-701 acted as a strong P-gp substrate. After P-gp inhibition, rat brain uptake could selectively be blocked by 5-HT_7 and σ receptor ligands. High brain uptake of [^{11}C]Cimbi-701 was also found in the pig brain without P-gp inhibition. This uptake could selectively be blocked by 5-HT_7 and σ receptor ligands. Finally, low brain uptake in baboons was found indicating that [^{11}C]Cimbi-701 may be a P-gp substrate in baboons.

Conclusions: The low brain uptake of [^{11}C]Cimbi-701 displayed in baboons discouraged translation to humans and further investigation if a selective σ-receptor block could enable selective 5-HT_7 receptor PET imaging. Instead, we suggest exploration of this structural class, as results indicate that selective 5-HT_7 receptor imaging might be possible when non-P-gp substrates could be identified.

Introduction

The 5-hydroxytryptamine 7 (5-HT_7) receptor is the latest discovered receptor in the serotonin family.[1,2] This receptor is found in the central nervous system (CNS), the peripheral nervous system, and the periphery (e.g. gastrointestinal tract).[3] Studies using knockout mice have for example revealed an association between the 5-HT_7 receptor and a number of CNS disorders such as depression, anxiety, schizophrenia and nociception (reviewed by Matthys et al[3]). Recently, Hauser et al. also suggested a link between the receptor and alcohol and drug abuse.[4]

Positron Emission Tomography (PET) is a non-invasive imaging technique which can be used to visualize and quantify the function of a broad set of molecular targets such as enzymes and receptors *in vivo*. As such, PET is a valuable tool to study the physiology of a respective biological system and to determine its involvement in certain diseases.[5-7] PET can also be used during drug development processes and determine for example target engagement of a specific drug towards an enzymatic or receptor system.[6] This information is very valuable for determining optimal dose regimes in clinical trials. Any PET study necessitates a specific radiotracer, which is able to selectively image the target in question. This is possible by conjugating a positron-emitting nuclide (e.g. carbon-11 or fluorine-18) to a highly selective targeting molecule. Unlike drugs, radiotracers are usually applied at tracer doses (pmol-µmol) in order to avoid perturbance of the biological system under investigation.[5]

A PET radiotracer for the 5-HT_7 receptor would aid in exploring the role of this receptor in healthy and diseased brains. To our knowledge, no clinical PET tracer exists for the 5-HT_7 receptor even though several attempts have been made.[8-14] Figure 1 displays some key structures that have been used over the years. Especially derivatives of SB-269970 appear promising and have attracted attention over the years.[16,17] This is due to the high affinity and selectivity profile of SB-269970.[15]

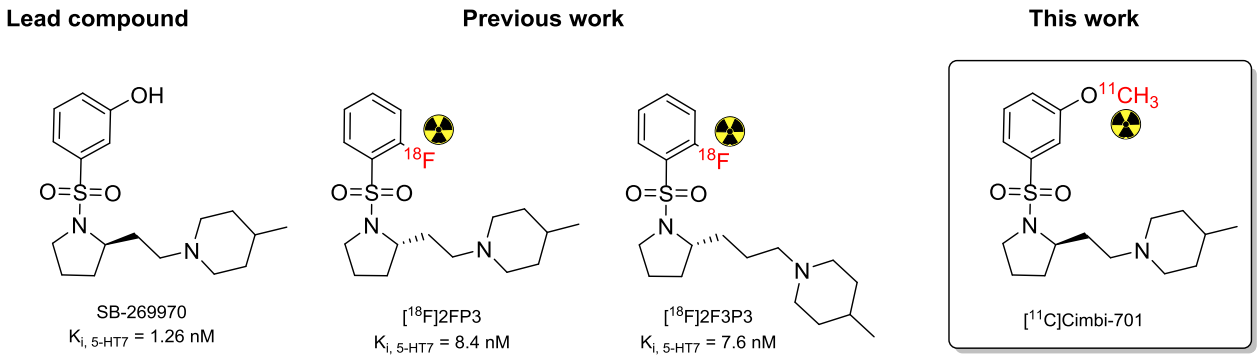

Figure 1: Schematic overview of SB-269970, examples of previously evaluated PET tracers for the 5-HT_7 receptor[15-18] and the potential PET tracer presented in this work: [^{11}C]Cimbi-701.

In this work, we continue the research in the direction. (R)-1-(2-(1-((3-methoxyphenyl)sulfonyl)pyrrolidin-2-yl)ethyl)-4-methylpiperidine (here called Cimbi-701) is a O-methylated analogue of SB-269970 (Fig 1). It was first described by Lovell et al. in 2000.[15] In the original publication, the affinity of this compound for the 5-HT_7 receptor was determined to be 10 nM. However, the selectivity profile of the compound was not reported. In here, we evaluated its *in vitro* profile, radiolabelled it and determined its potential to be used as a 5-HT_7 receptor PET radiotracer in rats, pigs and non-human primates.

Materials and methods

Reference compound synthesis

SB-269970 ● HCl (25 mg, 0.06 mmol), MeOH (6.5 µL, 0.16 mmol), PPh_3 (27 mg, 0.10 mmol) and toluene (0.8 mL) were successively added to a vial and stirred at room temperature. After a few minutes stirring, diethyl azodicarboxylate (DEAD, 70 mg, 0.15 mmol) was added dropwise and the reaction mixture was left to stir for 16 h at this temperature. The resulting crude was purified twice by column chromatography using first EtOAc–Et_3N (50:1) as eluent and thereafter EtOAc– Et_3N –MeOH (50:1:4). The product was still slightly contaminated with PPh_3 so further purification was performed using HPLC (Luna, 5 µm, C18(2) 100 Å, 150 x 4.6 mm column, Phenomenex Inc.); eluted with 0.1% TFA in MeCN–H_2O (35:65) TFA at 1.5 mL/min after 3.12 minutes). Cimbi-701 was obtained as a pale semi-solid TFA salt (5 mg, 0.010 mmol, 17%). ^{1}H NMR (400 MHz, Methanol-d_4) δ 7.57 (t, *J* = 8.0 Hz, 1H), 7.47 (ddd, *J* = 7.8, 1.7, 1.0 Hz, 1H), 7.39 (dd, *J* = 2.6, 1.7 Hz, 1H), 7.29 (ddd, *J* = 8.3, 2.6, 1.0 Hz, 1H), 3.95 – 3.36 (m, 8H), 3.33 – 2.60 (m, 4H), 2.27 – 1.22 (m, 11H), 1.07 (d, *J* = 6.5 Hz, 3H).

Radiosynthesis

[^{11}C]Methyl trifluoromethanesulfonate ([^{11}C]CH_3OTf) was produced from [^{11}C]CH_4 in an automated module in a two-step synthesis involving [^{11}C]CH_4 conversion into [^{11}C]CH_3I by iodine vapor at 720 °C and further conversion of [^{11}C]CH_3I into [^{11}C]CH_3OTf by silver triflate at 220 °C. [^{11}C]CH_3OTf was then trapped at -10 °C in 300 µL acetone solution containing (*R*)-3-[2-[2-(4-methylpiperidin-1-yl)ethyl]pyrrolidine-1-sulfonyl]phenol hydrochloride (SB-269970, 0.6 mg, 1.5 µmol) and 4 µL 2N NaOH. The reaction mixture was heated for 5 minutes at 40 °C, then diluted with 4.5 mL H_2O and injected onto a semi-preparative HPLC column (Luna 5 µm C18(2) 100 Å column, 250 x 10 mm, Phenomenex Inc.) eluted with MeCN–10 mM sodium borate

buffer (70:30) at 9 mL/min. Retention times were 350 s for [^{11}C]Cimbi-701 and 180 s for SB-269970. The [^{11}C]Cimbi-701 fraction was collected into 150 mL 0.1% ascorbic acid in sterile water, and the resulting solution was passed through a C18 Sep-Pak Plus solid-phase extraction cartridge (Waters), pre-activated with 10 mL ethanol–water mixture (1:1, v/v) before use. The cartridge was then rinsed with 3 mL of 0.1% ascorbic acid solution and eluted with 1 mL ethanol containing 0.1% H_3PO_4 into a sterile 20 mL vial. The elute was diluted with 15 mL phosphate–buffer (100 mM, pH 7). The formulated product was analysed by analytical HPLC (Luna, 5µm C18(2) 100 Å, 150 × 4.6 mm column, Phenomenex Inc.); eluted with 0.1% TFA in MeCN–H_2O (35:65) at 1.5 mL/min). In these conditions, Cimbi-701 had a retention time of 3.1 minutes and SB-269970 had a retention time of 2.2 min. The overall synthesis, purification, and formulation time were approximately 1 hour.

Experimental procedures, rats

Long-Evans female rats (200-300 g) were used in this study. The rats were housed in groups of 2-4 animals per cage in a climate controlled rodent facility with 12h/12h light cycle and provided food and water ad libitum. All experimental procedures were conducted in accordance with the FELASA guidelines for animal research and with approval from The Danish Council for Animal Ethics (license number: 2017-15-0201-01283) as well as the Department of Experimental Medicine, University of Copenhagen. On the day of the experiment rats were transported to the scanner at least 1h prior to experiment start.

The rats were anesthetized with isoflurane (3.0-3.5% isoflurane in oxygen for induction, 1.5-2.5% for maintenance) and catheters were inserted into their lateral tail veins. Then the rats were positioned prone in a custom-made 2x2 bed frame, and placed inside the field of view of the High Resolution Research Tomograph (HRRT) PET scanner (Siemens AG, Munich, Germany). Thus 4 rats could be scanned simultaneously. [^{11}C]Cimbi-701 (10-20 MBq, 0.05-0.2 nmol, and injection volumes 0.5-1 mL) was injected intravenously as a bolus through the catheter, and a 60 min dynamic PET scan was initiated at the moment of injection. After the end of the PET scan, a Tx50 transmission scan was performed with an internal source of the scanner.

The animals were scanned at baseline (no pretreatment before tracer injection) and after receiving pretreatment of the Pgp-inhibitor elacridar (5 mg/kg[19], Carbosynth, Compton, United Kingdom) with or without 5-HT_7 antagonist SB-269970 (3 mg/kg, Tocris Bioscience, Abingdon, United Kingdom), sigma and dopamine D2/3 antagonist haloperidol (1 mg/kg, Janssen-Cilag,

Birkerød, Denmark) or sigma-1 agonist SA4503 (1.5 mg/kg, Merck, Darmstadt, Germany). Pretreatment solutions, including elacridar, were injected 15-30 min before tracer injection through the intravenous catheter.

The sixty-minute list-mode PET data were reconstructed into 33 dynamic frames (6 × 10, 6 × 20, 6 × 60, 8 × 120, 7 × 300 seconds. The images consisted of 207 planes of 256 x 256 voxels of 1.22 x 1.22 x 1.22 mm. From this image each of the four rats were extracted into 4 separate images. Summed pictures of all counts in the time interval 5–60 min of the scans were made for each rat and used for co-registration to a standardized MRI-based atlas of the rat brain.[20,21] The time-activity curves (TACs) were extracted for thalamus and cerebellum volumes of interests (VOIs) for each rat. Resulting TACs were calculated as radioactive concentration (kBq/cc) over time, which were thereafter corrected for animal weight, yielding standardized uptake values (SUV).

Experimental procedures, pigs

Six female domestic pigs (crossbreed of Landrace x Yorkshire x Duroc, mean weight ± S.D., 20.7 ± 2.5 kg) were used for *in vivo* PET imaging. All animal procedures were approved by the Danish Council for Animal Ethics (journal no. 2012-15-2934-00156).

The animals were housed under standard conditions and were allowed to acclimatize for 1 week. Before scanning, anaesthesia was induced with i.m. injection of 0.13 mL/kg Zoletil veterinary mixture (10.87 mg/kg xylazine + 10.87 mg/kg ketamine + 1.74 mg/kg methadone + 1.74 mg/kg butorphanol + 10.87 mg/kg tiletamine + 10.87 mg/kg zolezepam). Hereafter, anaesthesia was maintained with constant propofol infusion (1.5 mg/kg/h i.v.; B. Braun, Melsungen, Germany). Arterial i.v. access for blood drawing was granted in the right femoral artery via a minor incision and two venous i.v. accesses for injections were granted in the left and right mammary veins. Analgesia was assured by i.v. injection of fentanyl during surgery. During anaesthesia, animals were endotracheally intubated and ventilated. Vital parameters (heart rate, body temperature, blood pressure, oxygen saturation and end tidal CO_2) were continuously monitored during the scan

[^{11}C]Cimbi-701 was given as intravenous (i.v.) bolus and the injected dose was 353 ± 140 MBq (mean ± SD, n = 11). Molar activity at time of injection was 175 ± 105 GBq/μmol (mean ± SD, n = 11) resulting in an average injected mass of 1.2 ± 0.9 μg (mean ± SD, n = 11). The pigs were scanned for 90 min in list mode. After a baseline scan, animals were given either SB-258719 (Tocris Bioscience, Abingdon, United Kingdom) or Cimbi-717 (synthesized in-house as

previously described[22]) as a continuous intravenous infusion starting 30 min prior to the injection of [^{11}C]Cimbi-701. The doses of SB-258719 were 0.2 mg/kg/h or 0.02 mg/kg/h. SB-258719 was dissolved in DMSO and diluted in saline (max 6% DMSO). The doses of Cimbi-717 were 1.0 mg/kg/h or 0.02 mg/kg/h. Cimbi-717 was dissolved in DMSO and added to a 10% beta-cyclodextrin solution (Merck, Darmstadt, Germany). In one animal, haloperidol (injection-ready, 5 mg/ml, Janssen-Cilag, Birkerød, Denmark) (0.1 mg/kg) was administered as i.v. bolus 10 min prior to the injection of the radiotracer.[17]

Description of blood sampling, determination of free fraction, radiometabolism in plasma, reconstruction of PET data and kinetic modelling are described in the Supplementary Information.

Experimental procedures, baboon

One baboon (male, 15.2 kg) was used in the study. Anaesthesia was induced with an intramuscular injection of 10 mg/kg ketamine with 0.5 mg/kg xylazine followed by reversal of xylazine with yohimbine (0.11 mg/kg). In all cases induction was also accompanied with an intramuscular injection of atropine (0.05 mg/kg). Induction of anaesthesia was performed ~100 min before the start of the PET scan. A catheter for injections was placed in the saphenous vein. During scans, anaesthesia was maintained by isoflurane (0.8–1.5%, mixed with pure oxygen) through an intubation tube without ventilation. Physiological changes (blood pressure, pulse, end-tidal CO_2, and breathing rate) were monitored continuously throughout the experiment. The procedures complied with the regulations of the Subcommittee on Research Animal Care at Massachusetts General Hospital.

One PET scan was performed with the BrainPET scanner (Siemens, Erlangen, Germany). A PET/MRI compatible eight-channel array coil customized for non-human primate brain imaging to increase image signal and quality was employed. The scan was initiated with the i.v. bolus injection of the radiotracer (195 MBq). A high-resolution anatomical scan using multiecho MPRAGE sequence (TR = 2530 ms, TE1/TE2/TE3/TE4 = 1.64/3.5/5.36/7.22 ms, TI = 1200 ms, flip angle = 7 °, and 1 mm isotropic) was acquired 30 min after scanner start. One-hundred-minute list-mode PET data were reconstructed in 26 dynamic frames (5 × 10, 6 × 20, 2 × 30, 1 × 60, 5 × 300, 8 × 300, and 7 × 600 seconds). Using the jip analysis toolkit (www.nitrc.org/projects/jip), MPRAGE data and dynamic PET data were co-registered to a baboon atlas.[23] Using PMOD 3.3 (PMOD Technologies, Zurich, Switzerland), time-activity curves for VOIs were extracted, and time-averaged SUV values were obtained.

Results

Cimbi-701 was successfully synthesized in a yield of 17% starting from SB-269970. The selectivity of Cimbi-701 was tested via the NIMH Psychoactive Drug Screening Program [24], where Cimbi-701 was tested towards 42 targets (see Supplementary Information, Table 1). Cimbi-701 had affinity for eight targets (Figure 2). In short, Cimbi-701 displayed high affinity for 5-HT_7 (18 nM), σ-1 (9.2 nM) and σ-2 (1.6 nM) receptors.

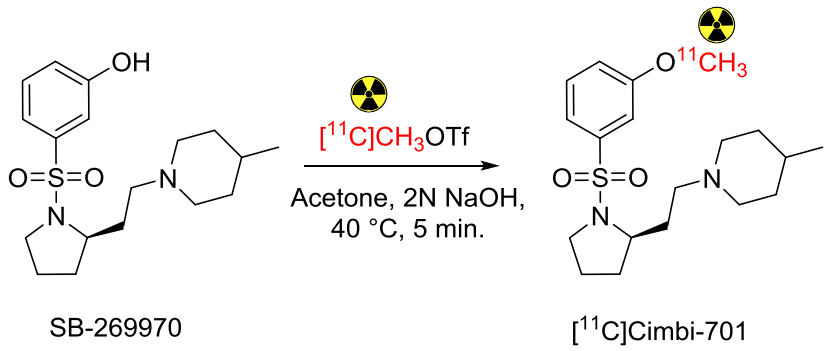

SB-269970 [11C]Cimbi-701

	5-HT_{1A}	5-ht_{5a}	5-HT_7	α_{2B}	α_{2C}	H_2	σ-1	σ-2
Cimbi-701 (K_i (nM))	633	113	18	1773	1536	6193	9.2	1.6

Figure 2. Radiolabelling of [^{11}C]Cimbi-701 (above); RCY = 10–22%, radiochemical purities above 98% and A_m of 256 ± 127 GBq/µmol (n = 13)) were obtained. Affinity (K_i) in nanomolar for Cimbi-701 (below).

Radiolabelling of [^{11}C]Cimbi-701 was successfully performed as depicted in Fig 2. A radiochemical yield (RCY) in the order of 10–22% (0.29 – 1.5 GBq were isolated) was obtained with molar activities of 256 ± 127 GBq/µmol (n = 13) and a radiochemical purity (RCP) above 98% (See supplementary Fig 1, for chromatographic information). Radiolysis was prevented with a radical scavenger (ascorbic acid).

[^{11}C]Cimbi-701 was thereafter preceded to *in vivo* imaging studies in rats, where it did not enter the brain to any major extent (Figure 3 and 4a). Standard uptake values (SUVs) increased after pretreatment with the P-gp efflux transporter inhibitor elacridar (5 mg/kg, 30 min prior to injection of the radiotracer) from 1 SUV to 3 SUV in thalamus, a 5-HT_7 receptor rich brain region. To evaluate if [^{11}C]Cimbi-701 bound specifically to 5-HT_7 receptor *in vivo*, the specific 5-HT_7 receptor antagonist SB-269970 (3 mg/kg) was administrated 15 min prior to [^{11}C]Cimbi-701 injection. This was done in combination with the specific P-gp inhibition paradigm described before. Reduced binding in thalamus (13.6%) was observed (Figure 4b). To investigate whether [^{11}C]Cimbi-701 also binds to σ receptors *in vivo*, the non-specific σ receptor antagonists

haloperidol (1 mg/kg, Figure 4c) or the specific σ-1 receptor antagonist SA4503 (1.5 mg/kg, Figure 4d) were used for blocking studies. This study was also carried using the simultaneously P-gp inhibition set-up. Pretreatment with haloperidol (1 mg/kg) led to a 21% decrease in thalamus uptake and 22.9% decrease in cerebellum uptake (Figure 4c) compared to baseline. Pretreatment with SA4503 decreased uptake in thalamus and cerebellum by 15.3% and 18.3%, respectively (Figure 4d). Calculated area-under-curve (AUC) for all TAC's are displayed as a grouped barplot (Figure 4e).

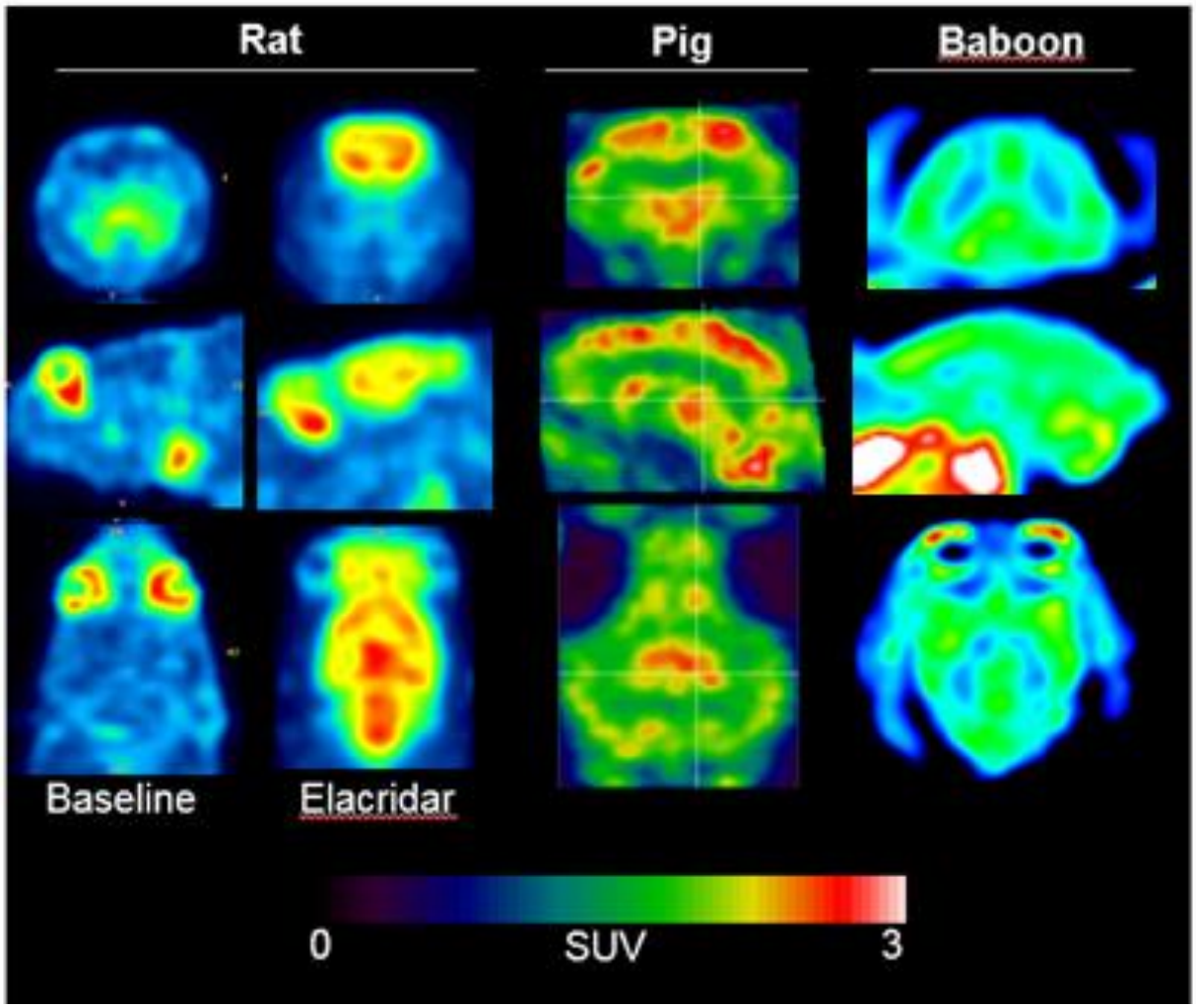

Figure 3. Summed PET images of [^{11}C]Cimbi-701 in the rat, pig and the baboon brain. For comparison, [^{11}C]Cimbi-701 in rats is shown before and after pretreatment with the P-gp efflux inhibitor elacridar (5 mg/kg).

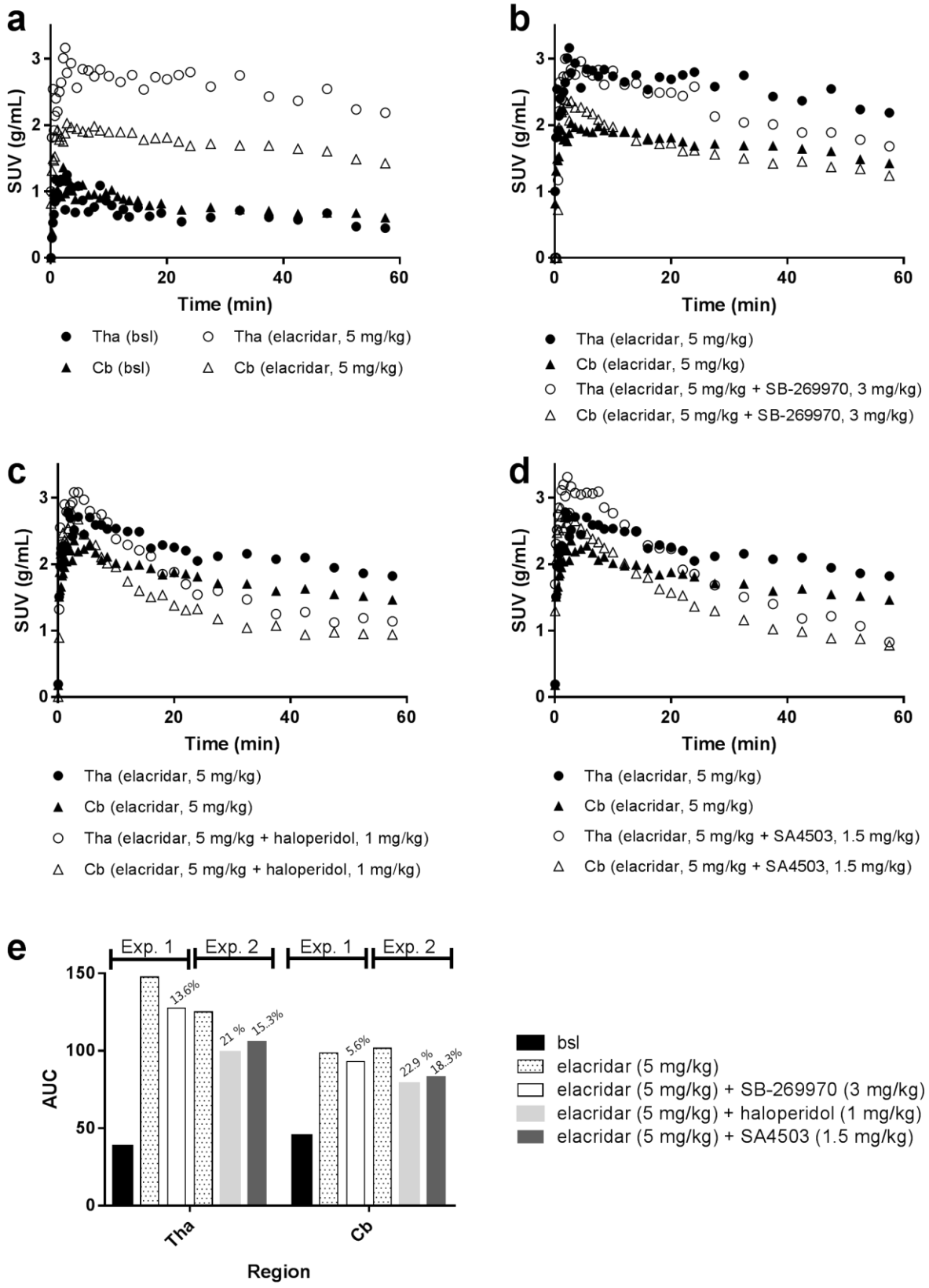

Figure 4. [^{11}C]Cimbi-701 evaluated in rats. Representative time-activity curves (TACs) of [^{11}C]Cimbi-701 in the thalamus (circles, tha) and cerebellum (triangles, Cb) in the rat brain. **a)** TACs at baseline (bsl) and after pretreatment with elacridar (5

mg/kg). **b)** Thalamus and cerebellum TACs after pretreatment with elacridar and elacridar + SB-269970 (3 mg/kg). **c)** Thalamus and cerebellum TACs after pretreatment with elacridar and elacridar + haloperidol (1 mg/kg). **d)** Thalamus and cerebellum TACs after pretreatment with elacridar and elacridar + SA4503 (1.5 mg/kg). **e)** Calculated area-under-curve (AUC) for all TACs displayed as a grouped barplot. Radiochemical purity of [^{11}C]Cimbi-701 was >98% in exp. 1 and 90% in exp. 2. Percentage reduction in AUC after blocking is shown above the bar. All TACs are normalized to injected radioactivity and animal weight resulting in the standard uptake value (SUV).

The pig brain showed a high uptake of [^{11}C]Cimbi-701 (Figure 3) with a peak SUV of 2.1. Radiotracer uptake was highest in the thalamus followed by the striatum and cortex and with the lowest uptake in the cerebellum. Furthermore, [^{11}C]Cimbi-701 kinetics were very slow with minor washout of the radiotracer during the acquisition time (Figure 5a). We investigated the specificity of the signal by pre-administration of two different 5-HT$_7$ receptor antagonists, namely SB-258719 (Figure 5b) and Cimbi-717 (Figure 5c). When SB-258719 and Cimbi-717 were administered prior to the injection of [^{11}C]Cimbi-701, the uptake of the radiotracer was dose-dependently decreased in all investigated brain regions investigated. As in rats, we investigated whether [^{11}C]Cimbi-701 binds to σ receptors. Pre-administrating of haloperidol (0.1 mg/kg) greatly reduced the uptake of [^{11}C]Cimbi-701 (Figure 5d). In contrast to rats, we investigated the radiometabolism of [^{11}C]Cimbi-701 in pigs, The radiometabolism in pig plasma revealed that the tracer was quickly metabolized with only 28% intact tracer remaining after 30 min (for more details, see Supplementary Information). The free fraction of [^{11}C]Cimbi-701 in pig plasma was 31 ± 5% (mean ± SD, n=5) at equilibrium (Supplementary Information, Figure 3).

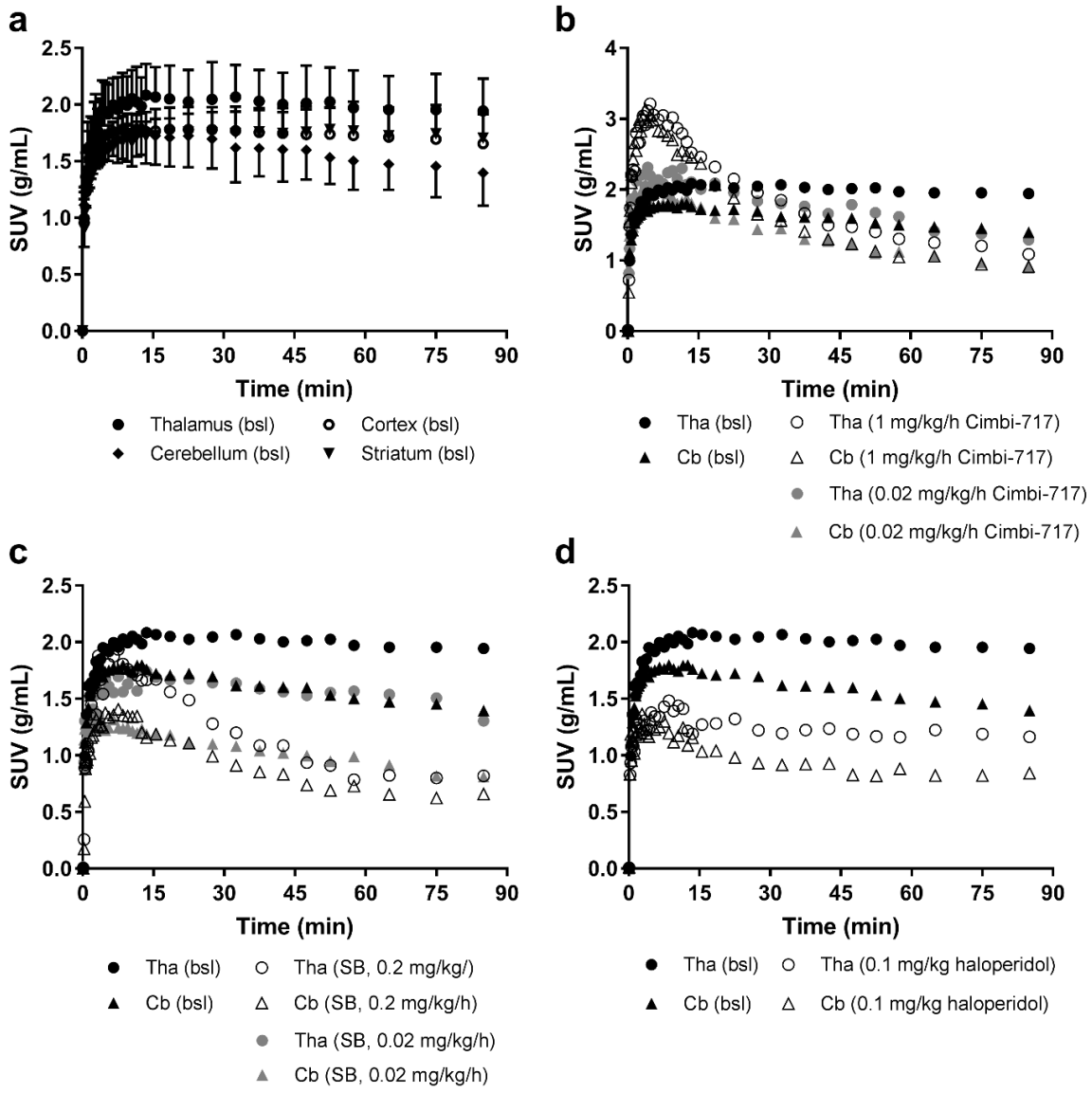

Figure 5. [^{11}C]Cimbi-701 evaluated in pigs. a) Time-activity curves (TACs) showing regional distribution of [^{11}C]Cimbi-701 at baseline (bsl, n=6). **b)** TACs for thalamus (Tha, circles) and cerebellum (Cb, triangles) at baseline (n=6, black) and after pretreatment with SB-258719: 0.2 mg/kg/h (open symbols) and 0.02 mg/kg/h (grey symbols). **c)** TACs after pretreatment with Cimbi-717: 1.0 mg/kg/h (open symbols) and 0.02 mg/kg/h (grey symbols). **d)** TACs after pretreatment with 0.1 mg/kg haloperidol (open symbols). All TACs are normalized to injected radioactivity and animal weight resulting in the standard uptake value (SUV).

Receptor binding of [^{11}C]Cimbi-701 quantified with the two-tissue compartment model generated the highest V_Ts in the thalamus (64 ± 28 mL/cm^3) and striatum (66 ± 35 mL/cm^3) and lowest in the cerebellum (23 ± 7.6 mL/cm^3), indicating good regional separation as also predicted from the TACs (Figure 5a). V_Ts were also calculated for Cimbi-717 (1.0 mg/kg/h, 0.02 mg/kg/h), haloperidol (0.1 mg/kg) and SB-258719 (0.02 mg/kg) and all values are presented in the Supplementary Information, Table 2. Occupancy plot analysis based on regional V_Ts values

(see Supplementary Information, Figure 5) revealed that pre-administration of 0.5 mg/kg/h Cimbi-717 resulted in 98% occupancy and 0.02 mg/kg/h Cimbi-717 in 90% occupancy. Pre-administration of SB-258719 (0.02 mg/kg/h) resulted in 63% occupancy. Haloperidol pre-administration resulted in a decrease in V_Ts in the cingulate cortex (46%), insula cortex (50%) and thalamus (48%). The remaining ROIs (region of intrest) had similar or slightly higher V_Ts after haloperidol treatment compared to baseline.

Lastly, [^{11}C]Cimbi-701 was evaluated in a baboon. Similar to what was already observed in rats, it was found that [^{11}C]Cimbi-701 had low brain uptake in the baboon (Figure 3), which is also evident from TACs (Figure 6). The peak SUV was 1.25 and higher uptake is observed in the cerebellum compared to the thalamus.

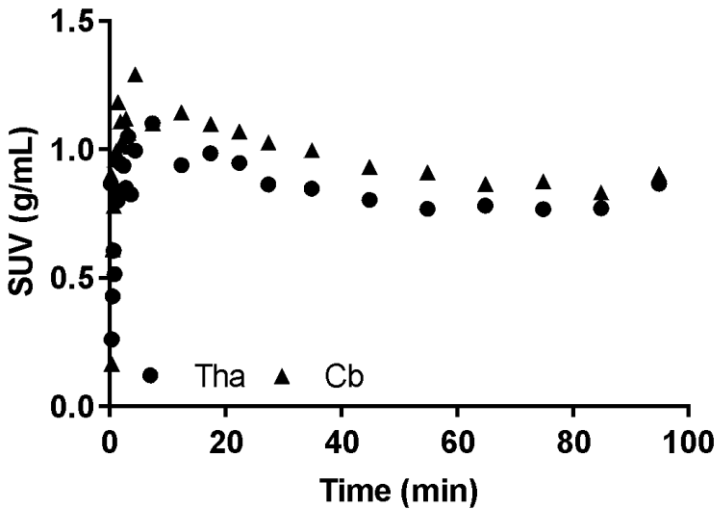

Figure 6. [^{11}C]Cimbi-701 evaluated in a non-human primate. TACs of [^{11}C]Cimbi-701 in thalamus (Tha) and cerebellum (Cb) at baseline.

Discussion

Herein, we present the synthesis, *in vitro* selectivity profile, radiosynthesis and subsequent *in vivo* evaluation of [^{11}C]Cimbi-701 in rats, pigs and baboon. Radiosynthesis of [^{11}C]Cimbi-701 was reliable, with high molar activities (256 ± 127 GBq/μmol (n = 13)) radiochemical purities above 98% and with satisfactory radiochemical yields (RCY = 10–22% d.c.) for *in vivo* evaluation. It was found that adding ascorbic acid during the formulation of the product was critical for preventing radiolysis of the radiotracer.

The receptor binding assays demonstrated low-nanomolar affinity of Cimbi-701 towards the 5-HT_7 receptor (K_i = 18 nM), which is comparable with the affinity previously published by Lovell *et al.*[14] High affinities were also observed for the σ-1 (K_i = 9.2 nM) and σ-2 (K_i = 1.6 nM)

receptors. These cross affinities may be problematic for imaging the 5-HT_7 receptors since both receptors are present in high abundance in similar regions.[22] The highest density of 5-HT_7 receptors are found in thalamus, hypothalamus, cortex, and hippocampus,[25,25] whereas the highest densities of σ receptors are found in insula and cingulate cortices and lower receptor density is found in the thalamus.[27] By comparing the receptor densities of the 5-HT_7 receptor and the σ receptors in post mortem human brain using [^{3}H]SB-269970[25] and [^{3}H]haloperidol,[28] respectively, a 5-fold higher density of σ receptors are found in the thalamus. In other brain regions, the ratio of σ-to-5-HT_7 receptors is even higher.[22]

Therefore, observed uptake of [^{11}C]Cimbi-701 in brain regions may largely represent binding to σ receptors. In this respect, we were interested in the specific *in vivo* binding component of [^{11}C]Cimbi-701 against 5-HT_7 and σ receptors, respectively. This was tested first in rats. Specific binding to 5-HT_7 receptors was investigated by pretreating the animals with SB-269970 (3 mg/kg), while simultaneously inhibiting P-gp. Inhibition of this efflux transporter was necessary since [^{11}C]Cimbi-701 is a strong P-gp substrate in rats (Figure 3). A small decrease in uptake was observed in the thalamus - both when inspecting the TACs and the calculated AUCs - indicating specific binding of [^{11}C]Cimbi-701 to the 5-HT_7 receptor *in vivo*. A very small decrease in cerebellar uptake was also observed. This corresponds to the low receptor abundance in this region.[26] Specific binding of [^{11}C]Cimbi-701 towards σ receptors was subsequently investigated. Haloperidol or SA4503 blocking studies were carried out, while inhibiting the P-gp efflux transporter with elacridar. Haloperidol was chosen since it displays high affinity for the σ-1 (K_i = 4 nM) and σ-2 receptors (K_i = 14 nM)[29] and low affinity against 5-HT_7 receptors (K_i = 380 nM).[30] As such, haloperidol should not be able to block 5-HT_7 receptor binding and any reduction in binding should be attributed to σ-binding. A pronounced decrease in uptake was observed in thalamus and in cerebellum (both σ receptor-rich regions).[28,31,32] This indicates that [^{11}C]Cimbi-701 has also a specific σ receptor binding component. In the following, we were interested if selective binding could be attributed to selective σ-1 receptor binding. SA4503 is a selective σ-1 receptor agonist (IC_{50} = 17 nM)[33] and was as such chosen as a suitable blocking agent to investigate this issue. Also, pretreatment with SA4503 greatly reduced the binding of [^{11}C]Cimbi-701 in thalamus and cerebellum. However, to the best of our knowledge, the affinity of SA4503 for the 5-HT_7 receptor is unknown and as such the decrease may also be attributed to selective 5-HT_7 receptor blocking of SA4503.

In general, the decrease in AUC after SB-269970 pre-treatment was lower in the rat thalamus compared to pre-treatment with haloperidol. SB-269970 displays no affinity towards σ receptors ($K_{i,\ \sigma\text{-}1}$ = 158 nM).[34] As such, the stronger blocking effect of haloperidol could be attributed to the higher density of σ receptors in the respective areas. In light of this, we calculated the theoretical binding ratio of the 5-HT_7- to the σ receptors ($tBR_{target/off\text{-}target}$)[35] to estimate the expected specific binding component of both receptors. A 10% decrease in signal is expected to be observed by blocking only the 5-HT_7 receptor component of [^{11}C]Cimbi-701 (see Supplementary Information for calculation and more details). We observed a 13.6% decrease in uptake after pre-treatment with SB-269970. The values are within the expected uncertainties of these calculations and give hope that indeed SB-269970 could selectively block the 5-HT_7 receptor binding of [^{11}C]Cimbi-701. This speculation is further intensified by the observation that a stronger blocking effect was observed in the thalamus (high receptor density area) compared to that in the cerebellum (low receptor density area).

Encouraged by these results, we moved forward and evaluated [^{11}C]Cimbi-701 in pigs. Contrary to rats, [^{11}C]Cimbi-701 crossed readily the blood-brain-barrier and was not a P-gp substrate in pigs. Similar behaviour has been observed for other tracers, e.g. [^{18}F]altanserin.[36] Specificity of binding was investigated by pretreating the animals with either SB-258719 (0.2 and 0.02 mg/kg, $K_{i,\ 5\text{-}HT7}$ = 3.16 nM)[37] or Cimbi-717 (1 mg/kg and 0.02 mg/kg, $K_{i,\ 5\text{-}HT7}$ = 2.6 nM).[22] Quantification of [^{11}C]Cimbi-701's uptake at baseline and after SB-258719 (0.02 mg/kg) administration resulted in 63% occupancy, which indicates that the radiotracer binds to 5-HT_7 receptors *in vivo* at least partly. Binding to σ receptors cannot be excluded as the affinity of SB-258719 for the σ receptors is unknown; hence it is not possible further elaborate on estimated expected specific binding for the experiments using this blocking agent. Occupancies after Cimbi-717 administration were very high 90–98%. However, Cimbi-717 has also affinity for the σ receptors ($K_{i,\ \sigma\text{-}1}$ = 39 nM; $K_{i,\ \sigma\text{-}2}$ = 45 nM, unpublished data) and the measured occupancy using Cimbi-717 is therefore a combination of σ and 5-HT_7 receptor blocking. As such, we decided to perform a blocking study with haloperidol to test how strong the specific binding component of σ-receptors is in pigs. Pretreatment with haloperidol resulted in a decreased brain uptake of the tracer. Approximately 50% decrease in V_T values has been observed. This confirms that [^{11}C]Cimbi-701 also binds to σ receptors in the pig brain.

In a next step, we aimed to evaluate if [^{11}C]Cimbi-701 is a promising tracer for human 5-HT_7 receptor imaging, presumable after a selective σ receptor block. In this respect, the *in vivo*

performance of [^{11}C]Cimbi-701 was evaluated in the baboon brain. Currently, baboon evaluation studies are still considered the "Gold-standard" before initiating clinical studies.[7] Similar to our results obtained in rats, uptake in the baboon brain was very low. Therefore, no further evaluation experiments were carried out. Based on our results from our rat evaluation experiments, we believe that [^{11}C]Cimbi-701 may be a P-gp substrate also in the baboon. Discrepancy in brain uptake due to differences in efflux transporter activity and expression levels have been observed in the rat, pig, monkey and human BBB.[36,38,39]

Conclusion

[^{11}C]Cimbi-701 was successfully radiolabelled in sufficient RCYs for *in vivo* evaluation in rats, pigs and baboon and species differences were observed in terms of tracer brain uptake. In rats, [^{11}C]Cimbi-701 was found to be a P-gp efflux transporter substrate whereas high brain uptake was found in pigs without P-gp inhibition. Selectivity profiling revealed that Cimbi-701 binds with high affinity to 5-HT$_7$ and the σ receptors. *In vivo* PET experiments confirmed that the radiotracer binds to both targets in the rat and pig brain. We also evaluated [^{11}C]Cimbi-701 in baboons and found a low brain uptake, which could potentially be attributed to a dependency to the P-gp efflux transporter. This result discouraged us to translate the tracer to the clinic or to investigate if a selective σ-1 and σ-2 block could enable selective 5-HT$_7$ receptor PET imaging. Alternatively, we suggest investigating the structural class of Cimbi-701 further and identify compounds with improved selectivity. Our results indicate that 5-HT$_7$ receptor selective imaging might be possible using this structural class when non-P-gp substrates could be identified.[40]

Acknowledgements

The authors wish to thank the staff of the PET and Cyclotron Unit at Rigshospitalet for expert technical assistance. The authors also wish to thank the staff at the Department of Experimental Medicine (University of Copenhagen) for preparing the animals for the experiments. Bente Dall is acknowledged for technical expertise with the HRRT scanners. The John & Birthe Meyer Foundation's financial support in acquisition of the HRRT and Cyclotron system is greatly appreciated. Receptor binding profile was generously provided by the National Institute of Mental Health's Psychoactive Drug Screening Program, Contract # HHSN-271-2018-00023-C (NIMH PDSP). The NIMH PDSP is Directed by Bryan L. Roth MD, PhD at the University of North Carolina at Chapel Hill and Project Officer Jamie Driscoll at NIMH, Bethesda MD, USA.

Conflict of interests

GMK has been an invited lecturer at Pfizer A/S, worked as a consultant and received grants from H. Lundbeck A/S and is a stockholder of Novo Nordisk/Novozymes. The remaining authors declare no conflict of interest.

References

1. Ruat M, Traiffort E, Leurs R, *et al* (**1993**) Molecular cloning, characterization, and localization of a high-affinity serotonin receptor (5-HT_7) activating cAMP formation. *Proc Natl Acad Sci* 90:8547–8551. doi: 10.1073/pnas.90.18.8547
2. Lovenberg TW, Baron BM, de Lecea L, *et al* (**1993**) A novel adenylyl cyclase-activating serotonin receptor (5-HT_7) implicated in the regulation of mammalian circadian rhythms. *Neuron* 11:449–458. doi: 10.1016/0896-6273(93)90149-L
3. Matthys A, Haegeman G, Van CK, *et al* (**2011**) Role of the 5-HT_7 Receptor in the Central Nervous System: from Current Status to Future Perspectives. *Mol Neurobiol* 43:228–253. doi: 10.1007/s12035-011-8175-3
4. Hauser SR, Hedlund PB, Roberts AJ, et al (**2015**) The 5-HT_7 receptor as a potential target for treating drug and alcohol abuse. *Front Neurosci* 8:1–9. doi: 10.3389/fnins.2014.00448
5. Miller PW, Long NJ, Vilar R, Gee AD (**2008**) Synthesis of ^{11}C, ^{18}F, ^{15}O, and ^{13}N Radiolabels for Positron Emission Tomography. *Angew Chemie Int Ed* 47:8998–9033. doi: 10.1002/anie.200800222
6. Kristensen JL, Herth MM (**2017**) *In vivo* imaging in drug discovery. Textb. Drug Des. Discov.
7. Van De Bittner GC, Ricq EL, Hooker JM (**2014**) A philosophy for CNS radiotracer design. *Acc Chem Res* 47:3127–3134. doi: 10.1021/ar500233s
8. Zhang M-R, Haradahira T, Maeda J, *et al* (**2002**) Synthesis and preliminary PET study of the 5-HT_7 receptor antagonist [^{11}C]DR4446. *J Label Compd Radiopharm* 45:857–866. doi: 10.1002/jlcr.606
9. Herth MM, Hansen HD, Ettrup A, *et al* (**2012**) Synthesis and evaluation of [^{11}C]Cimbi-806 as a potential PET ligand for 5-HT_7 receptor imaging. *Bioorg Med Chem* 20:4574–4581. doi: 10.1016/j.bmc.2012.05.005
10. Hansen HD, Herth MM, Ettrup A, *et al* (**2014**) Radiosynthesis and *In Vivo* Evaluation of Novel Radioligands for PET Imaging of Cerebral 5-HT_7 Receptors. J Nucl Med 55:640–646. doi: 10.2967/jnumed.113.128983
11. Herth MM, Andersen VL, Hansen HD, *et al* (**2015**) Evaluation of 3-Ethyl-3-

(phenylpiperazinylbutyl)oxindoles as PET Ligands for the Serotonin 5-HT_7 Receptor: Synthesis, Pharmacology, Radiolabeling, and i*n Vivo* Brain Imaging in Pigs. *J Med Chem* 58:3631–3636. doi: 10.1021/acs.jmedchem.5b00095

12. Hansen HD, Andersen VL, Lehel S, *et al* (**2015**) Labeling and preliminary *in vivo* evaluation of the 5-HT_7 receptor selective agonist [^{11}C]E-55888. *Bioorg Med Chem Lett* 25:1901–1904. doi: 10.1016/j.bmcl.2015.03.039
13. Lacivita E, Niso M, Hansen HD, *et al* (**2014**) Design, synthesis, radiolabeling and *in vivo* evaluation of potential positron emission tomography (PET) radioligands for brain imaging of the 5-HT_7 receptor. *Bioorg Med Chem* 22:1736–1750. doi: 10.1016/j.bmc.2014.01.016
14. Hansen HD, Lacivita E, Di Pilato P, *et al* (**2014**) Synthesis, radiolabeling and *in vivo* evaluation of [^{11}C](R)-1- [4-[2-(4-methoxyphenyl)phenyl]piperazin-1-yl]-3-(2-pyrazinyloxy)-2-propanol, a potential PET radioligand for the 5-HT_7 receptor. *Eur J Med Chem* 79:152–163. doi: 10.1016/j.ejmech.2014.03.066
15. Lovell PJ, Bromidge SM, Dabbs S, *et al* (**2000**) A novel, potent, and selective 5-HT_7 Antagonist: (R)-3-(2-(2-(4-Methylpiperidin-1-yl)-ethyl)pyrrolidine-1-sulfonyl)phenol (SB-269970). *J Med Chem* 43:342–345. doi: 10.1002/bit.260190912
16. Lemoine L, Andries J, Le Bars D, *et al* (**2011**) Comparison of 4 Radiolabeled Antagonists for Serotonin 5-HT_7 Receptor Neuroimaging: Toward the First PET Radiotracer. *J Nucl Med* 52:1811–1818. doi: 10.2967/jnumed.111.089185
17. Deen M, Hansen HD, Hougaard A, *et al* (**2018**) High brain serotonin levels in migraine between attacks: A 5-HT_4 receptor binding PET study. *NeuroImage Clin* 18:97–102. doi: 10.1016/j.nicl.2018.01.016
18. Colomb J, Becker G, Forcellini E, *et al* (**2014**) Synthesis and pharmacological evaluation of a new series of radiolabeled ligands for 5-HT_7 receptor PET neuroimaging. *Nucl Med Biol* 41:330–337. doi: 10.1016/j.nucmedbio.2014.01.008
19. Kallem R, P. Kulkarni C, Patel D, *et al* (**2012**) A Simplified Protocol Employing Elacridar in Rodents: A Screening Model in Drug Discovery to Assess P-gp Mediated Efflux at the Blood Brain Barrier. *Drug Metab Lett* 6:134–144. doi: 10.2174/1872312811206020134
20. Schwarz AJ, Danckaert A, Reese T, *et al* (**2006**) A stereotaxic MRI template set for the rat brain with tissue class distribution maps and co-registered anatomical atlas: Application to pharmacological MRI. *Neuroimage* 32:538–550. doi: 10.1016/j.neuroimage.2006.04.214
21. Vállez Garcia D, Casteels C, Schwarz AJ, *et al* (**2015**) A Standardized Method for the

Construction of Tracer Specific PET and SPECT Rat Brain Templates: Validation and Implementation of a Toolbox. *PLoS One* 10:e0122363. doi: 10.1371/journal.pone.0122363

22. Herth MM, Volk B, Pallagi K, *et al* (**2012**) Synthesis and *In Vitro* Evaluation of Oxindole Derivatives as Potential Radioligands for 5-HT_7 Receptor Imaging with PET. *ACS Chem Neurosci* 3:1002–1007. doi: 10.1021/cn3001137
23. Black KJ, Snyder AZ, Koller JM, *et al* (**2001**) Template Images for Nonhuman Primate Neuroimaging: 1. Baboon. *Neuroimage* 14:736–743. doi: 10.1006/nimg.2001.0752
24. Besnard J, Ruda GF, Setola V, *et al* (**2012**) Automated design of ligands to polypharmacological profiles. *Nature* 492:215–220. doi: 10.1038/nature11691
25. Varnas K, Thomas DR, Tupala E, *et al* (**2004**) Distribution of 5-HT_7 receptors in the human brain: A preliminary autoradiographic study using [^{3}H]SB-269970. *Neurosci Lett* 367:313–316. doi: 10.1016/j.neulet.2004.06.025
26. Horisawa T, Ishiyama T, Ono M, *et al* (**2013**) Binding of lurasidone, a novel antipsychotic, to rat 5-HT_7 receptor: Analysis by [^{3}H]SB-269970 autoradiography. *Prog Neuropsychopharmacol Biol Psychiatry* 40:132–137. doi: http://dx.doi.org/10.1016/j.pnpbp.2012.08.005
27. Mash DC, Zabetian CP (**1992**) Sigma receptors are associated with cortical limbic areas in the primate brain. *Synapse* 12:195–205. doi: 10.1002/syn.890120304
28. Weissman AD, Su TP, Hedreen JC, London ED (**1988**) Sigma receptors in post-mortem human brains. *J Pharmacol Exp Ther* 247:29–33.
29. Mcleod MC, Aubé J, Frankowski KJ, Frankowski KJ (**2016**) Decahydrobenzoquinolin-5-one sigma receptor ligands: Divergent development of both sigma 1 and sigma 2 receptor selective examples. *Bioorg Med Chem Lett* 26:5689–5694. doi: 10.1016/j.bmcl.2016.10.065
30. Schotte A, Janssen PFM, Gommeren W, *et al* (**1996**) Risperidone compared with new and reference antipsychotic drugs: *in vitro* and *in vivo* receptor binding. Psychopharmacology (Berl) 124:57–73. doi: 10.1007/BF02245606
31. Bouchard P, Quirion R (**1997**) [^{3}H]1,3-di(2-tolyl)guanidine and [3H](+)pentazocine binding sites in the rat brain: Autoradiographic visualization of the putative sigma1 and sigma2 receptor subtypes. *Neuroscience* 76:467–477. doi: 10.1016/S0306-4522(96)00221-7
32. James ML, Shen B, Nielsen CH, *et al* (**2014**) Evaluation of -1 Receptor Radioligand ^{18}F-

FTC-146 in Rats and Squirrel Monkeys Using PET. *J Nucl Med* 55:147–153. doi: 10.2967/jnumed.113.120261

33. Matsuno K, Nakazawa M, Okamoto K, *et al* (**1996**) Binding properties of SA4503, a novel and selective σ1 receptor agonist. *Eur J Pharmacol* 306:271–279. doi: 10.1016/0014-2999(96)00201-4
34. Ates A, Burssens P, Lorthioir O, *et al* (**2018**) 5-HT_7 Receptor Antagonists with an Unprecedented Selectivity Profile. *ChemMedChem* 13:795–802. doi: 10.1002/cmdc.201800026
35. Herth M. M, Knudsen G. M. (**2018**) PET Imaging of the 5-HT_{2A} Receptor System: A Tool to Study the Receptor's *In Vivo* Brain Function. In: Guiard BP, Di Giovanni G (eds) 5-HT_{2A} Recept. Cent. Nerv. Syst. Springer, pp 85–134
36. Syvanen S, Lindhe O, Palner M, *et al* (**2009**) Species Differences in Blood-Brain Barrier Transport of Three Positron Emission Tomography Radioligands with Emphasis on P-Glycoprotein Transport. *Drug Metab Dispos* 37:635–643. doi: 10.1124/dmd.108.024745
37. Thomas DR, Gittins SA, Collin LL, *et al* (**1998**) Functional characterisation of the human cloned 5-HT_7 receptor (long form); antagonist profile of SB-258719. *Br J Pharmacol* 124:1300–1306. doi: 10.1038/sj.bjp.0701946
38. Kubo Y, Ohtsuki S, Uchida Y, Terasaki T (**2015**) Quantitative Determination of Luminal and Abluminal Membrane Distributions of Transporters in Porcine Brain Capillaries by Plasma Membrane Fractionation and Quantitative Targeted Proteomics. *J Pharm Sci* 104:3060–3068. doi: 10.1002/jps.24398
39. Fowler JS, Ding Y-S, Logan J, *et al* (**2001**) Species differences in [^{11}C]clorgyline binding in brain. Nucl Med Biol 28:779–785. doi: 10.1016/S0969-8051(01)00245-1
40. Hansen H. D., Constantinescu C. C., Barret O, *et al* (**2018**) Evaluation of [^{18}F]2FP3 in pigs and non-human primates. *J Label Compd Radiopharm.* 1–9. doi: 10.1002/jlcr.3692

Supplementary information

Radiosynthesis and preclinical evaluation of [^{11}C]Cimbi-701 – Towards the imaging of cerebral 5-HT$_7$ receptors

Elina T. L'Estrade[a,b,c], Vladimir Shalgunov[b], Fraser Edgar[b], Martin G. Strebl-Bantillo[d], Mengfei Xiong[a,b], François Crestey[b], Ramesh Neelamegam[d], Agnete Dyssegaard[a], Szabolcs Lehel[e], Maria Erlandsson[c], Tomas Ohlsson[c], Jacob M. Hooker[d], Gitte M. Knudsen[a,f], Matthias M. Herth[b,e], Hanne D. Hansen[a]

[a] *Neurobiology Research Unit, Rigshospitalet, Blegdamsvej 9, 2100 Copenhagen, Denmark*

[b] *Department for Drug Design and Pharmacology, Faculty of Health and Medical Sciences, University of Copenhagen, Universitetesparken 2, 2100 Copenhagen, Denmark*

[c] *Radiation Physics, Nuclear Medicine Physics Unit, Skånes University Hospital, Barngatan 3, 222 42 Lund, Sweden.*

[d] *Athinoula A. Martinos Center for Biomedical Imaging, Department of Radiology, Massachusetts General Hospital, Harvard Medical School, 73 High Street, Charlestown, Massachusetts 02129, United States*

[e] *Department of Clinical Physiology, Nuclear Medicine and PET, University Hospital Copenhagen, Rigshospitalet Blegdamsvej 9, 2100 Copenhagen, Denmark*

[f] *Faculty of Health and Medical Sciences, University of Copenhagen, Denmark.*

*Corresponding authors:
Hanne D. Hansen, Ph.D.
Neurobiology Research Unit and Center for Integrated Molecular Brain Imaging
Copenhagen University Hospital, Rigshospitalet
Blegdamsvej 9
2100 Copenhagen, Denmark
Phone: (+45) 35 45 88 21
Email: hanne.d.hansen@nru.dk

Matthias M. Herth, Ph.D
Department of Drug Design and Pharmacology
Faculty of Health and Medical Sciences
University of Copenhagen
Jagtvej 160
2100 Copenhagen, Denmark
Phone: (+45) 93 56 54 14
Email: matthias.herth@sund.ku.dk

Manuscript category: Article
Running title: [^{11}C]Cimbi-701 as a radiotracer for 5-HT$_7$ and σ receptors

CONTENTS

METHODS 256
Blood sampling, pigs 256
Radiometabolism, pigs 256
Determination of free fraction, pigs 256
Reconstruction of PET data, pigs 256
Kinetic modelling, pigs 257

Results 257
Selectivity profiling: 257
Radiolabeling of [^{11}C]Cimbi-701 258
Radiometabolism in pigs 258
Plasma free fraction in pig plasma 259
[^{11}C]Cimbi-701 evaluated in pigs 259
Kinetic modelling of pig PET data 261

Theoretical binding ratio 262

Possible limitations 263

References 264

Methods

Blood sampling, pigs

During the first 30 min of the scans, radioactivity in the whole blood was continuously measured using an ABSS autosampler (Allogg Technology, Mariefred, Sweden) counting coincidences in a lead-shielded detector. Concurrently, arterial whole blood was sampled manually at times 2.5, 5, 10, 20, 30, 40, 50, 70 and 90 minutes after injection of [^{11}C]Cimbi-701. Total radioactivity in plasma (500 µL) and whole blood (500 µL) was measured in a well counter (Cobra 5003; Packard Instruments, Meriden, CT, USA), which was cross-calibrated to the HRRT scanner and autosampler. All measurements of radioactivity were decay corrected to the time of radiotracer injection.

Radiometabolism, pigs

Radiolabelled parent compound and metabolites were determined by direct injection of plasma into a radio-HPLC system (Dionex Ultimate 3000; Thermo Fisher Scientific, Hvidovre, Denmark) configured for column switching. Manually drawn arterial whole blood samples were centrifuged (1500x*g*, 7 min, 4 °C) and plasma was filtered through a syringe filter (Whatman GD/X 13 mm or 25 mm, PVDF membrane, 0.45 µm pore size; Frisenette ApS, Knebel, Denmark) prior to the analysis by HPLC as previously described.[1]

Determination of free fraction, pigs

The free fraction of [^{11}C]Cimbi-701 in pig plasma was measured using an equilibrium dialysis method as previously described[2] and calculated as the ratio between radioactivity in a buffer and plasma compartment. The free fraction at equilibrium was determined by fitting a non-linear Mikaelis-Menten fit to the data.

Reconstruction of PET data, pigs

Ninety-minute list-mode PET data were reconstructed in 38 dynamic frames (6 × 10, 6 × 20, 4 × 30, 9 × 60, 2 × 180, 8 × 300, and 3 × 600 seconds). Images consisted of 207 planes of 256 x 256 voxels of 1.22 x 1.22 x 1.22 mm. A summed picture of all counts in the 90-min scan was reconstructed for each pig and used for co-registration to a standardized MRI-based atlas of the pig brain, similar to that previously published.[3] The TACs were calculated for the following VOIs: thalamus, striatum, hippocampus, frontal cortex, temporal cortex, insula cortex, somatosensory cortex, cingulate cortex, occipital cortex, cerebellum (excluding vermis).

Radioactivity in all VOIs was calculated as the average of radioactive concentration (Bq/mL) in the left and right sides. Outcome measure in the time-activity curves (TACs) was calculated as radioactive concentration in VOI (in kBq/mL) normalized to the injected dose corrected for animal weight (in kBq/kg), yielding SUV (g/mL).

Kinetic modelling, pigs

Distribution volumes (V_Ts) for the VOIs were calculated using the two-tissue compartment model. Kinetic modelling the data was performed using PMOD 3.0 (PMOD technologies, Zürich, Switzerland). Data was modelled using the parent fraction fitted to a biexponential function. The V_T of baseline and blocked conditions was used to determine the occupancy of the administered drug (SB-258719, Cimbi-717 or haloperidol).

Results

Selectivity profiling:

Supplementary Table 1. Targets for which Cimbi-701 showed less than 50% inhibition at 10 μM.

Selectivity screening: percentage inhibition < 50 % at 10μM concentration		
5-HT_{1B}	Beta1	M1
5-HT_{1D}	Beta2	M2
5-ht1e	Beta3	M3
5-HT_{2A}	D1	M4
5-HT_{2B}	D2	M5
5-HT_{2C}	D3	DOR
5-HT_{3}	D4	KOR
5-HT_{6}	D5	MOR
Alpha_{1A}	DAT	NET
Alpha_{1B}	H1	SERT
Alpha_{1D}	H3	
Alpha_{2A}	H4	

Radiolabeling of [^{11}C]Cimbi-701

Supplementary Figure 1. A summary of the HPLC Chromatograms of the precursor, the reference compound and the final radiotracer, [^{11}C]Cimbi-701.

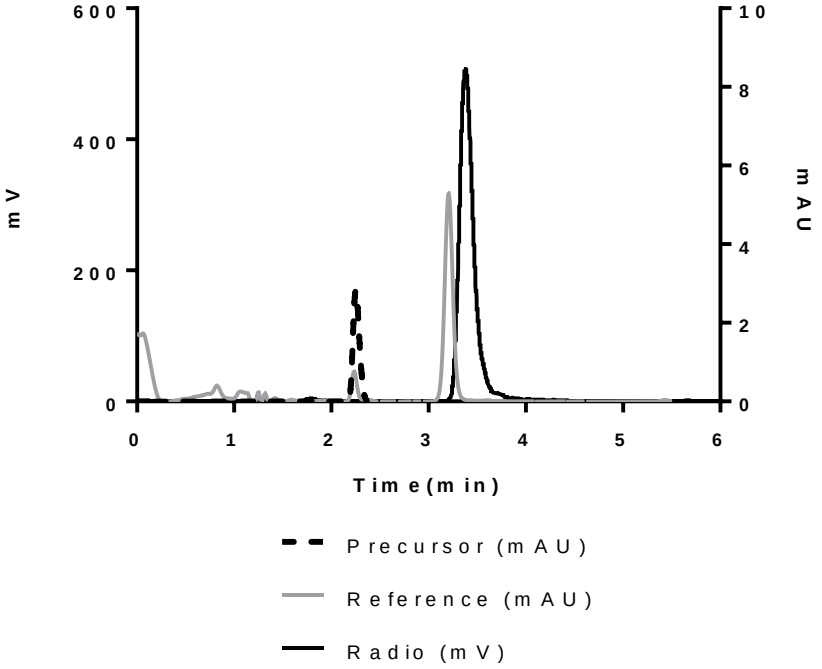

Radiometabolism in pigs

Supplementary Figure 2. Time course of the percentage of [^{11}C]Cimbi-701 measured in arterial pig plasma at baseline. Points represent mean ± SD of six pigs. Average measurements were fitted to the one-exponential non-linear regression model indicated by the line.

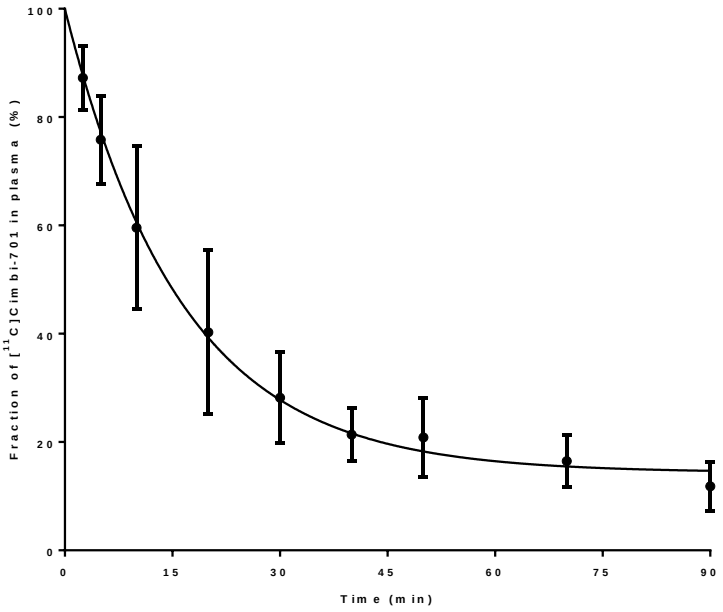

Metabolism of [^{11}C]Cimbi-701 was faster after administration of the different drugs (SB-258719, Cimbi-717 and haloperidol) except for the low dose SB-258719 (0.02 mg/kg/h). The systemic metabolism of [^{11}C]Cimbi-701 in pigs was comparable to [^{11}C]Cimbi-806, another 5-HT$_7$ receptor radiotracer evaluated in pigs,[4] with approximately 28% of the total plasma activity arising from parent compound left after 30 min. We also observed considerable variability in metabolism between animals; however, this could not be explained by differences in free fraction of the tracer (data not shown). Metabolism was slightly faster after blockade with SB-258719 (0.2 mg/kg/h), Cimbi-717 (1 mg/kg/h and 0.02 mg/kg/h) and haloperidol. This could be explained by an increased availability of the tracer to enzymatic degradation.

Plasma free fraction in pig plasma

Supplementary Figure 3. Plasma free fraction in percentage as a function of incubation time.

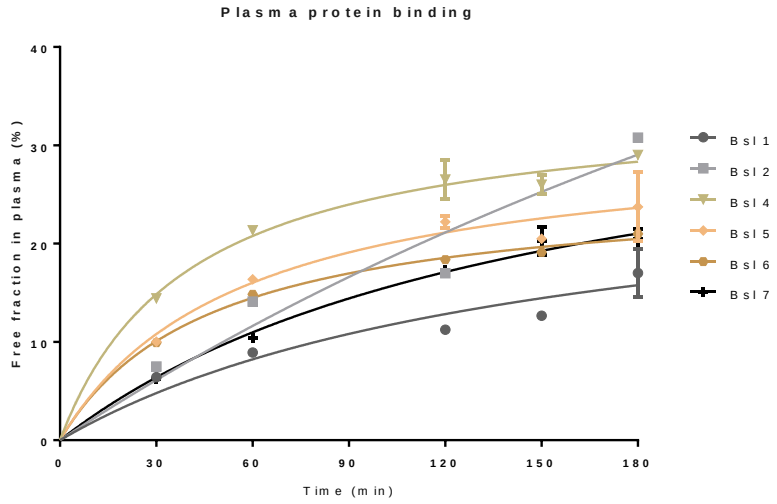

[^{11}C]Cimbi-701 evaluated in pigs

Supplementary Figure 4. Time-activity curves (TACs) showing regional distribution of [^{11}C]Cimbi-701 at baseline (bsl, n=6).

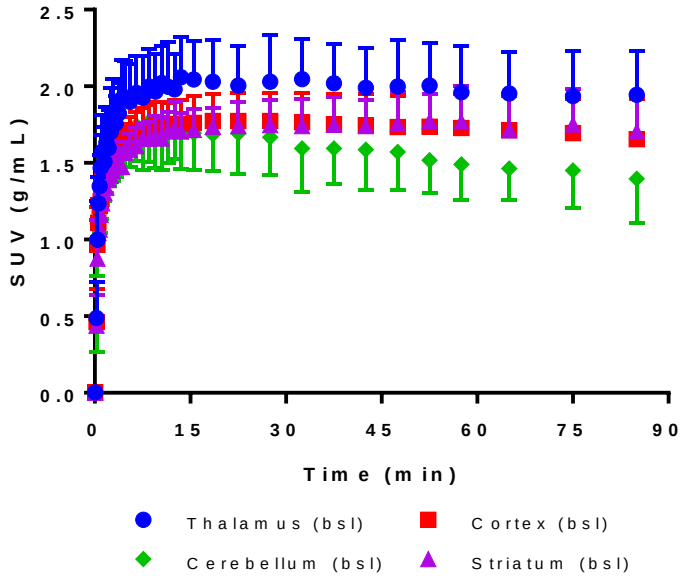
2.5
2.0
1.5
1.0
0.5
0.0
SUV (g/mL)
0
15
30
45
60
75
90
Time (min)
Thalamus (bsl)
Cortex (bsl)
Cerebellum (bsl)
Striatum (bsl)

Kinetic modelling of pig PET data

Supplementary Table 2. Distribution volumes (V_T, mL/cm^3) derived from the two-tissue compartment model. Dnf: indicates that the kinetic model could not fit the data (did not fit).

	Baseline					
ROI / Animal #	1	2	3	4	5	6
Neocortex	62.9	35.0	37.5	87.5	34.6	35.3
Thalamus	67.0	34.8	49.6	86.6	41.9	106.5
Striatum	dnf	66.1	43.1	115.5	dnf	38.9
Somatosensory cortex	55.6	33.6	40.6	98.0	41.5	38.1
Frontal cortex	54.4	32.8	42.6	79.0	30.6	33.8
Insula cortex	dnf	dnf	38.5	116.8	dnf	92.1
Occipital cortex	45.8	31.2	33.8	68.0	27.5	33.7
Temporal cortex	dnf	42.8	36.2	dnf	33.1	30.6
Cingulate cortex	47.4	42.0	31.7	119.0	26.8	66.0
Hippocampus	dnf	66.8	44.4	76.5	dnf	22.2
Cerebellum	19.2	17.5	21.1	38.2	24.4	20.3

	SB-258719		**Cimbi-717**		**Haloperidol**
	0.2 mg/kg/h	0.02 mg/kg/h	1.0 mg/kg/h	0.02 mg/kg/h	0.1 mg/kg
ROI / Animal #	2	3	4	5	6
Neocortex	dnf	23.6	11.7	13.8	39.1
Thalamus	dnf	23.8	11.3	12.9	55.8
Striatum	10.9	33.0	10.5	15.6	47.5
Somatosensory cortex	dnf	23.3	12.9	13.6	41.8
Frontal cortex	dnf	23.5	12.4	13.2	38.8
Insula cortex	dnf	27.2	13.0	15.0	45.9
Occipital cortex	dnf	23.6	9.7	14.3	36.3
Temporal cortex	dnf	25.0	11.4	14.5	36.1
Cingulate cortex	dnf	24.0	11.3	12.9	35.2
Hippocampus	5.98	20.8	dnf	13.2	25.0
Cerebellum	6.70	12.7	8.7	9.1	25.2

Unfortunately, the two-tissue compartment could not fit the data from the high-dose SB-258719 scan (0.2 mg/kg) and the occupancy could consequently not be computed.

Supplementary Figure 5. Using data shown in Supplementary Table 2, occupancy plots are computed for the administrated drugs.

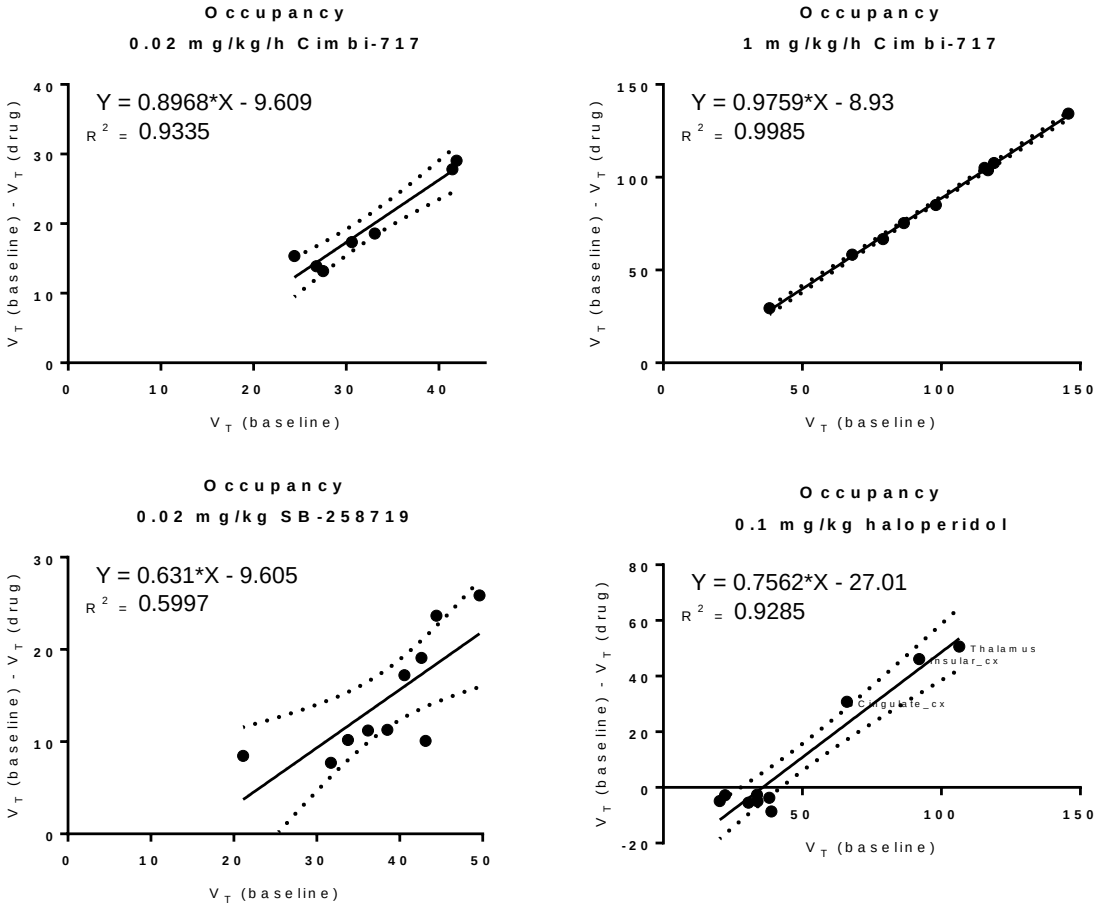

Theoretical binding ratio

Here is calculated the theoretical binding ratio of the target to another off-target ($tBR_{target/off\text{-}target}$), which is defined by the selectivity (S) of the radioligand ([^{11}C]Cimbi-701) and the ratio between the target to off-target (D) receptor availability in the brain region of interest (Eq. 1)

$$tBR_{target/off-target} = S\ x\ \ D = \left(\frac{K_{d,off-target}}{K_{d,target}}\right) x \left(\frac{B_{avail,target}}{B_{avail,off-\ target}}\right) \qquad \text{(Eq. 1)}$$

To see how much blocking effect, using SB-269970, we theoretically could expect in thalamus, taken into account the receptor availability of the 5-HT$_7$ and σ receptors, the following data was used in equation 1:

$K_{i,\ 5\text{-}HT7}$ = 18 nM

$K_{i,\ \sigma}$ = 5.4 nM

$B_{max,\ 5\text{-}HT7}$ = 47 fmol/mg tissue[7]

$B_{max,\ \sigma}$ = 70 fmol/mg tissue (estimated from the density per mg protein)[8]

An average of affinities was calculated for the σ-1 and σ-2 receptors and the B_{max}, both these facts could give possible errors in the estimation.

$$tBR_{target/off-target} = \left(\frac{5.4}{18}\right) x \left(\frac{47}{70}\right) = 0{,}2$$

So theoretically only one 1/10 of signal in thalamus will be due to binding to 5-HT_7 receptors in comparison to the σ-receptors in rats.

Possible limitations

In our setup 4 rats can be simultaneously scanned in the HRRT scanner, which allows for testing multiple tracers and/or drugs and thus provides a possibility for increased throughput screening of preclinical PET tracers. There are some limitations to the experimental setup used for this *in vivo* evaluation in rat. For example using the HRRT scanner for small animal PET might give us a lower spatial resolution and risk of partial volume effects compared to using a μPET, which can prevent precise delineation of VOIs. Both of the aforementioned limitations also make the kinetic modelling more difficult. Using reference tissue models for kinetic modelling was an option in rats as there are no 5-HT_7 receptors in the cerebellum.[7] However, since [^{11}C]Cimbi-701 binds to the σ receptors, it was found difficult to find an optimal reference region because the σ receptors are so widely distributed. The calculation of AUC of the TACs shown as grouped barplots was therefore used as pseudo-quantification method in order to present an overview of the rat data. The barplots also distinguish between experiment 1 and 2, which is due to another experimental limitation. During experiment 2, the radioactive purity of [^{11}C]Cimbi-701 was only 90%. Nevertheless, because the comparison-animal (pre-treated only with elacridar) was injected with the same tracer production, it does not alter the interpretation of the data. In experiment 2, with lower radiochemical purity, a lower ratio between the thalamus and cerebellum was observed which could indicate that the lower radiochemical purity increases the non-specific binding.

References

1. Gillings N (**2009**) A restricted access material for rapid analysis of [^{11}C]-labeled radiopharmaceuticals and their metabolites in plasma. *Nucl Med Biol* 36:961–965. doi: 10.1016/j.nucmedbio.2009.07.004
2. Kornum BR, Lind NM, Gillings N, *et al* (**2009**) Evaluation of the Novel 5-HT $_4$ Receptor PET Ligand [^{11}C]SB207145 in the Göttingen Minipig. *J Cereb Blood Flow Metab* 29:186–196. doi: 10.1038/jcbfm.2008.110
3. Villadsen J, Hansen HD, Jørgensen LM, *et al* (**2018**) Automatic delineation of brain regions on MRI and PET images from the pig. J Neurosci Methods 294:51–58. doi: 10.1016/j.jneumeth.2017.11.008
4. Herth MM, Hansen HD, Ettrup A, *et al* (**2012**) Synthesis and evaluation of [^{11}C]Cimbi-806 as a potential PET ligand for 5-HT(7) receptor imaging. *Bioorg Med Chem* 20:4574–4581. doi: 10.1016/j.bmc.2012.05.005
5. Varnas K, Thomas DR, Tupala E, *et al* (**2004**) Distribution of 5-HT$_7$ receptors in the human brain: A preliminary autoradiographic study using [^{3}H]SB-269970. *Neurosci Lett* 367:313–316. doi: 10.1016/j.neulet.2004.06.025
6. Weissman AD, Su TP, Hedreen JC, London ED (**1988**) Sigma receptors in post-mortem human brains. *J Pharmacol Exp Ther* 247:29–33.
7. Horisawa T, Ishiyama T, Ono M, *et al* (**2013**) Binding of lurasidone, a novel antipsychotic, to rat 5-HT$_7$ receptor: Analysis by [^{3}H]SB-269970 autoradiography. *Prog Neuropsychopharmacol Biol Psychiatry* 40:132–137. doi: http://dx.doi.org/10.1016/j.pnpbp.2012.08.005
8. McCann, D. J.; Weissman, A. D.; Su, T. P., Sigma-1 and Sigma-2 sites in rat brain: Comparison of regional, ontogenetic, and subcellular patterns. *Synapse* **1994,** *17* (3), 182-189.

Chapter 8

Paper VI

Synthesis, Radiolabeling, *In vitro* and *In vivo* Evaluation of [^{18}F]ENL30 – A Potential PET Radiotracer for the 5-HT$_7$ Receptor

---

Summary:

*The final paper within this thesis, **Paper VI**, is presented here in chapter 8. In this paper was [^{18}F]ENL30 developed as a fluorine-18 analogue of [^{11}C]Cimbi-701 (chapter 7, **Paper V**). Containing the radiolabelling of [^{18}F]ENL30 using [^{18}F]FETos, followed by the elucidation in vitro and in vivo.*

Authors' contribution:

Reference synthesis was made by F.G.E. The radiosynthesis and quality control were established by the author, together with F.G.E. The planning of the in vivo evaluation [^{18}F]ENL30 in rats was performed by the author. The author both produced the tracer and in collaboration performed the evaluation with M.X., S.L.B and V.S. Image analysis was done by the author. In vitro autoradiography was established and accomplished by the author and M.X. The interpretation of the results was performed by the author (with supervision from M.P). The author also formulated the outline and contributed considerably with writing of the manuscript.

Synthesis, Radiolabeling, *In vitro* and *In vivo* Evaluation of [^{18}F]ENL30 – A Potential PET Radiotracer for the 5-HT$_7$ Receptor

Elina T. L'Estrade[a,b,c], Fraser G. Edgar[b], Mengfei Xiong[a,b], Vladimir Shalgunov[b], Simone L. Baerentzen[a], Maria Erlandsson[c], Tomas G. Ohlsson[c], Mikael Palner[a,d], Gitte M. Knudsen[a,e], Matthias M. Herth[b,f]

[a] *Neurobiology Research Unit, Rigshospitalet, Blegdamsvej 9, 2100 Copenhagen, Denmark*

[b] *Department for Drug Design and Pharmacology, Faculty of Health and Medical Sciences, University of Copenhagen, Universitetesparken 2, 2100 Copenhagen, Denmark*

[c] *Radiation Physics, Nuclear Medicine Physics Unit, Skånes University Hospital, Barngatan 3, 222 42 Lund, Sweden.*

[d] *Center for Translational Neuromedicine, University of Copenhagen, Blegdamsvej 3B, 2200 Copenhagen N, Denmark*

[e] *Faculty of Health and Medical Sciences, University of Copenhagen, Denmark.*

[f] *Department of Clinical Physiology, Nuclear Medicine and PET, University Hospital Copenhagen, Rigshospitalet Blegdamsvej 9, 2100 Copenhagen, Denmark*

Keywords: PET, 5-HT$_7$ receptor, SB-269970, autoradiography, [^{18}F]FETos.

*Corresponding Author: Tel.: +45 93565414; fax: +45 35 33 60 41; e-mail: matthias.herth@sund.ku.dk

Abstract

The 5-HT$_7$ receptor (5-HT$_7$R) is involved in a broad range of physiological conditions and disorders. Currently, there is no validated clinical positron emission tomography (PET) tracer available; however we have recently developed a promising ^{11}C-labeled candidate. In this project, we aimed to further extend our efforts and develop an ^{18}F-labeled derivative, coined [^{18}F]ENL30. Fluorine-18 has several advantages over carbon-11 especially within the preclinical phase, where a long half-life usually increases evaluation through-put.

ENL30 was successfully synthesized in a low albeit sufficient overall yield. Radiolabeling succeeded with a radiochemical yield (RCY) of approximately 4.5%. Subsequent preclinical PET studies revealed that [^{18}F]ENL30 binds specifically to the 5-HT$_7$R, but suffered from affinity to σ-receptors. Additionally we identified [^{18}F]ENL30 to be a P-glycoprotein (P-gp) substrate in rats. However, we believe that [^{18}F]ENL30 may prove to be valuable in higher species which exhibit decreased P-gp dependency. If required, σ-receptor binding could, in such studies, be selectively blocked potentially allowing for selective 5-HT$_7$R imaging.

Introduction

The serotonergic system with its neurotransmitter serotonin (5-hydroxytryptamine, 5-HT) is widely spread throughout the brain and modulates a variety of psychological and behavioural functions and disorders.[1-2] In 1993, the 5-HT_7 receptor (5-HT_7R) was identified and became the most recent member to be added to the serotonin receptor subfamily.[3-5] The 5-HT_7R is a Guanidine-protein coupled receptor (GPCR), positively coupled to adenylate cyclase, with activation leading to the production of cyclic Adenosine Monophosphate (cAMP), which in turn is involved in a broad spectrum of secondary cell activation pathways.[2-5] The 5-HT_7R is abundant in the central nervous system (CNS) with the highest concentrations in thalamus, hypothalamus, hippocampus and cortex (see Supporting Information Table 1 for further details).[6-10] Preclinical studies with, e.g., 5-HT_7R knockout mice, have associated this receptor with CNS disorders such as depression, anxiety and schizophrenia.[1, 11-16] Currently, there is no clinical imaging radiotracer available to study the 5-HT_7R *in vivo*.[1, 17] Access to such a radiotracer would enable the study of the receptors physiological function and its involvement in various CNS diseases. Furthermore, since the 5-HT_7R displays the highest affinity towards serotonin of all serotonergic receptors; 5-HT_7R neuroimaging could be a valuable tool in determining changes in the concentration of 5-HT in the synaptic cleft[18]. This could significantly improve our understanding of the involvement of endogenous 5-HT in brain disorders[19] and potentially provide a path for new treatment options.

Positron Emission Tomography (PET) is a nuclear medicine molecular imaging technique that can be used to visualize and quantify receptor physiology *in vivo*.[20-22] Consequently, a PET tracer for the 5-HT_7R would allow the study of this receptor system *in vivo*, and address the aforementioned research questions. Several groups, including ours, have over the years attempted to develop a 5-HT_7R radiotracer, although so far with limited success.[9, 23-29] For example, PET tracers evaluated in pigs or cats with promising outcomes, such as [^{18}F]2FP3 or [^{11}C]Cimbi-717 (Figure 1), did not produce a specific signal in non-human primates.[10, 30] Other tracers failed at even earlier evaluation stages.[26, 28-29]

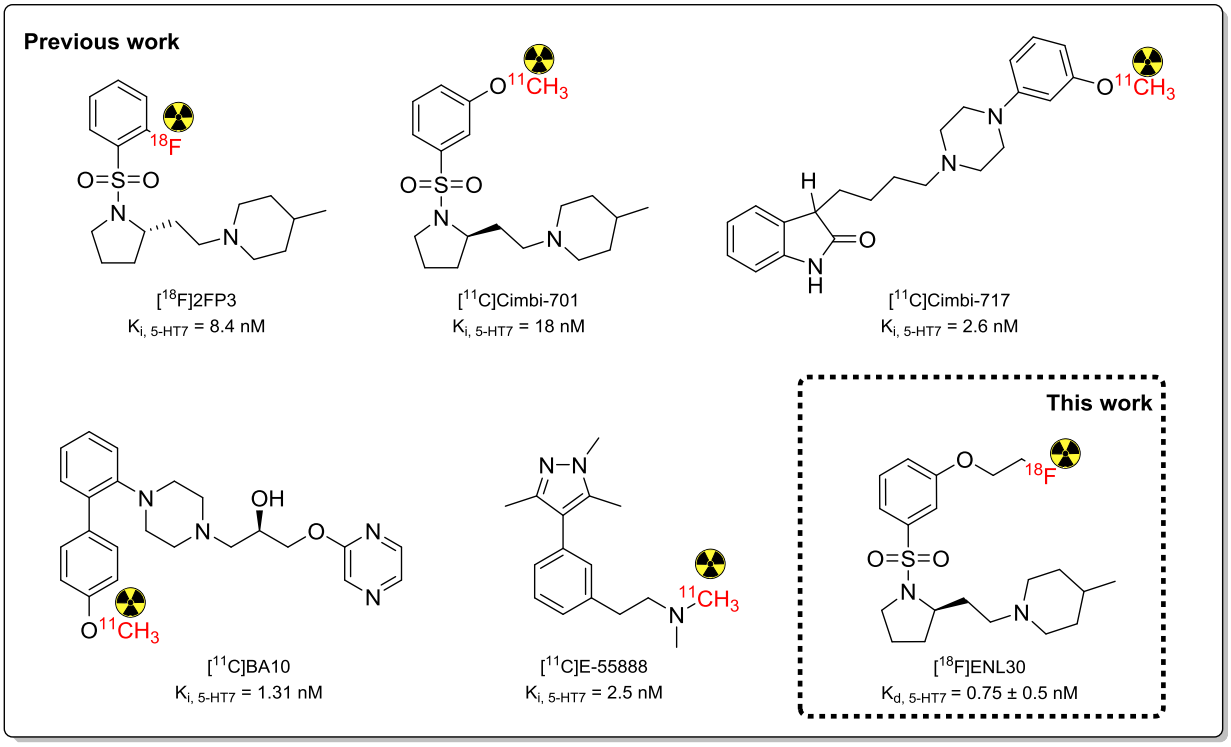

Figure 1: A Schematic overview of previously evaluated PET tracers for the 5-HT$_7$R and the structure of the new potential PET tracer presented in this work, [^{18}F]ENL30.[9-10, 25-26, 28, 31]

Our group has recently developed an O-methylated carbon-11 labelled derivative of the highly selective 5-HT$_7$R antagonist SB-269970 (Figure 1).[31] This tracer ([^{11}C]Cimbi-701) has shown promising results in pigs[30], prompting us to extend this work and develop a fluorine-18 labelled analogue. Fluorine-18 has several advantages over carbon-11 in respect to clinical translation and also preclinical work in rodents. Namely, the use of fluorine-18 can result in higher spatial resolution. Moreover, the longer half-life of fluorine-18 (109 min vs. 20.4 min) eases the use for multiple evaluation experiments with a single production .[21]

Results and discussion

A common strategy to convert a carbon-11 tracer into a fluorine-18 analogue is to exchange a methoxy functional group for a fluoroethoxy moiety. [^{18}F]MH.MZ is one of the many examples where this strategy has been successfully applied.[32-34]This attractive approach is not thought to drastically impact the pharmacological behaviour of the tracer due to similar electronic, inductive, and spatial properties of the two moities.[34] In light of that, we were inspired to apply this approach to [^{11}C]Cimbi-701 and develop a fluorine-18 labelled derivative ([^{18}F]ENL30). Reference compound **ENL30 (15)** was synthesized similar to a previously reported synthesis strategy that was applied to a phenolic analogue (Scheme 1).[31, 35-36]

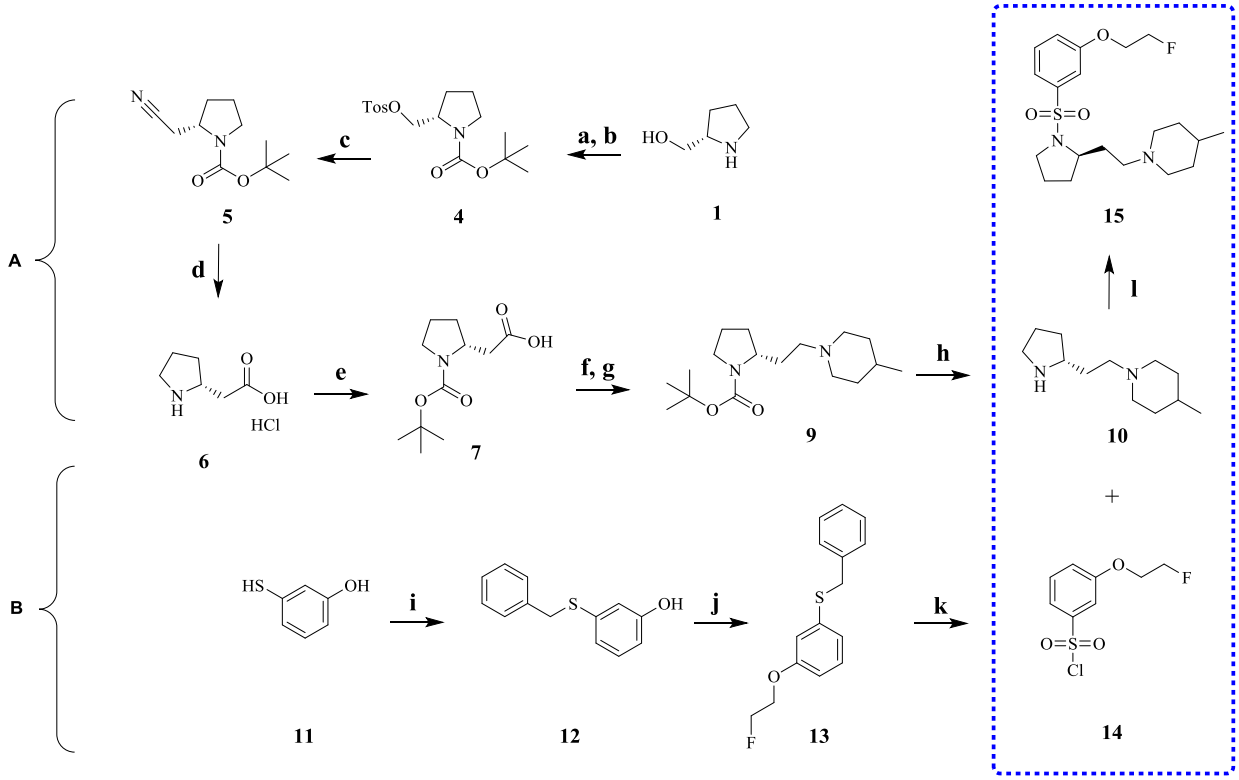

Scheme 1 – Synthetic overview of ENL30 **(15)**. **A)** The synthesis of (R)-4-methyl-1-(2-(pyrrolidin-2-yl)ethyl)piperidine **(10) B)** its sulfonyl chloride coupling partner **(14)** and the final coupling to form the sulphonamide product **15** (right). Reagents and conditions: **a)** $(Boc)_2O$, TEA, MeOH, Δ, 0.5 hr; **b**) p-TosCl, Py, DCM, 0 °C – rt, overnight; **c)** KCN, DMSO, 90 °C, 4 hr; **d)** HCl (35%), AcOH, Δ, 6 hr; **e)** $(Boc)_2O$, NaOH (2M), Acetone, 0 °C – rt, 2.5 hr; **f)** Borane-THF, THF, rt, ON; **g)** i) MsCl, Py, DCM, 0 °C – rt, 2 hr; ii) 4-methylpiperidine, ACN, rt – 50 °C, ON; **h)** TFA:DCM (1:1), rt, 0.5 hr. **i)** BnBr, NaOH, MeOH, H_2O, AcOH, ON; **j)** 1-Bromo-2-fluoroethane, NaH, DMF, 0 °C – 60 °C, 20h; **k)** 1,3-dichloro-5,5-dimethylhydantoin, ACN, AcOH, H_2O, 0 °C 5 hrs. **l)** Et_2O, NaOH, 0 °C – rt, ON.

A key intermediate for this synthesis route is (R)-4-methyl-1-(2-(pyrrolidin-2-yl)ethyl)piperidine **(10)**, which we initially tried to synthesize with a procedure described by Lovell *et al.*[31] However, the necessary intermediate tert-butyl 2-(((methylsulfonyl)oxy)methyl)pyrrolidine-1-carboxylate **(3)** and its subsequent transformation suffered from poor yields (Tables 1-2). As such, other leaving groups and reaction conditions were employed. The use of tosyl chloride and pyridine in DCM resulted in sufficient yields of the tosylate (**4**), which could then be satisfactorily transformed to the nitrile (**5**) in DMSO. This led to an optimized and satisfying yield of approximately 63% over those two steps (Tables 1-2).[31, 35-36]

Table 1 – Incorporation of a suitable leaving group.

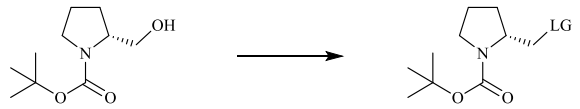

2 **3 or 4**

Leaving Group (LG)	Solvent	Base	Temperature (°C)	Time (h)	Yield (%)
OMs	THF	TEA	-78 °C – rt	2	12.6
OTos	DCM	TEA, cat. DMAP	rt	6	28.6
OTos	DCM	Pyridine	0 - rt	Overnight	76.8

Table 2 – Optimization of nitrile introduction.

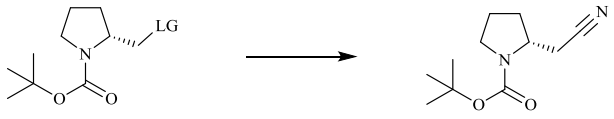

3 or 4 **5**

Leaving Group (LG)	Solvent	Temperature (°C)	Time (h)	XCN	Yield (%)
OMs	DMF	100	6	NaCN	33.4
OMs	EtOH	Reflux	Overnight	KCN	N/A
OTos	DMSO	90	4	KCN	81.9

Several catalyst mediated reaction routes have been reported to form (**10**) directly from (**5**).[31,37] But in our hands, even extensive optimization efforts did not result in any satisfying yields (see supporting information for more details). It appeared that although the initial hydrogenation did occur (nitrile to imide), the catalyst failed to eliminate the ammonia in the final step. In light of that, a previously described multi-step route was chosen to synthesis (**10**) (Scheme 1). This strategy was initially thought to be inferior since an unnecessary deprotection/protection had to be applied. However, this approach yielded in sufficient amounts of (**10**) that could be used in a subsequent coupling step with another key intermediate 3-(2-fluoroethoxy)benzenesulfonyl chloride (**14**).[31, 35-36, 38] The synthesis of **(14)** is detailed in Scheme 1**.** Notably, in the final step in the synthesis of **14,** the need for *S*-deprotection was circumvented and allowed direct oxidation of the sulfur.[39-40] In summary, the reference synthesis was completed throughout 13 steps; ending up with an overall low yield of approximately 0.2%.

In the next step, radiolabelling of [^{18}F]ENL30 (**[^{18}F]15**) was attempted applying a two-step labelling procedure starting from the commercially available precursor SB-269970 (3-[[(2R)-2-[2-(4-methyl-1-piperidinyl)ethyl]-1-pyrrolidinyl]sulfonyl]-phenol, monohydrochloride) and the

routinely produced synthon, 2-[^{18}F]fluoroethyl tosylate ([^{18}F]FETos). Using this strategy, **[^{18}F]15** could successfully be radiolabelled in a radiochemical yield (RCY) ranging between 1.2 and 15% (decay corrected, n = 8), with satisfactory molar activities (108 - 197 GBq/µmol (n = 3)) and radiochemical purities of > 98% (Scheme 2). The total synthesis time including separation and formulation took less than 180 minutes. A maximum amount of 0.9 GBq was isolated using this approach. Importantly, it was necessary to form the phenolate before starting the labelling procedure. Adding the base 40 min prior to initiating the reaction at 100 °C resulted in the highest RCY.

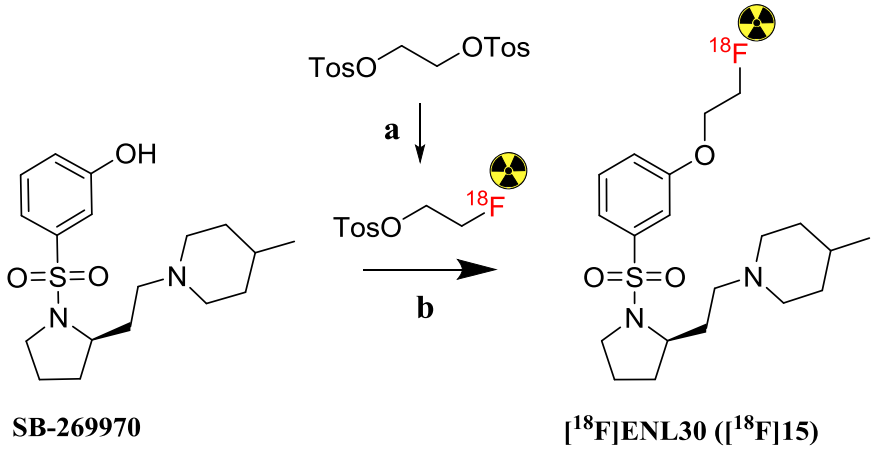

SB-269970 **[^{18}F]ENL30 ([^{18}F]15)**

Scheme 2: Radiosynthesis of [^{18}F]ENL30 (**[^{18}F]15**) **a)** [^{18}F]F$^-$, K_{222}, K_2CO_3, ACN, 80 °C, 3 min. **b)** DMF, NaOH (2N), 100 °C, 25 min.

Encouraged by these results, we performed autoradiographic studies on coronal rat brain slices, containing thalamus, a high 5-HT$_7$R density region[6-10] (Figure 2a-c). These studies were conducted to determine the affinity and selectivity of **[^{18}F]15** towards the 5-HT$_7$R. A K_d of 0.75 ± 0.5 nM (n = 9) for the 5-HT$_7$R could be determined in a saturation assay (Figure 2d). Recently close analogues of **[^{18}F]15** displayed affinity towards σ-receptors when subjected to competition assays, and so we decided to evaluate the selectivity of **[^{18}F]15** towards these receptors by performing autoradiographic blocking studies with the 5-HT$_7$R selective antagonist SB-269970 ($K_{i,\ 5\text{-}HT7}$ = 1.26 nM, $K_{i,\ 5\text{-}HT2A}$ = 32 nM and $K_{i,\ \sigma\text{-}1}$ = 158 nM)[31, 41] as well as with haloperidol as a σ-receptor blocking agent ($K_{i,\ D2}$ = 2 nM, $K_{i,\ D3}$ = 4 nM, $K_{i,\ \sigma\text{-}1}$ = 4 nM, $K_{i,\ \alpha1}$ = 12 nM, $K_{i,\ \sigma\text{-}2}$ = 14 nM, $K_{i,\ D4}$ = 15 nM, $K_{i,\ 5\text{-}HT2A}$ = 70 nM and $K_{i,\ 5\text{-}HT7}$ = 380 nM).[42-44] The results are displayed in Figure 2e. We found a dose-dependent blocking with both ligands; 13% blockage using a 50 nM solution of SB-269970 and 10.5% blockage using a 50 nM solution of haloperidol. Consequently, **[^{18}F]15** in addition to 5-HT$_7$R binding, also binds to σ-receptors.

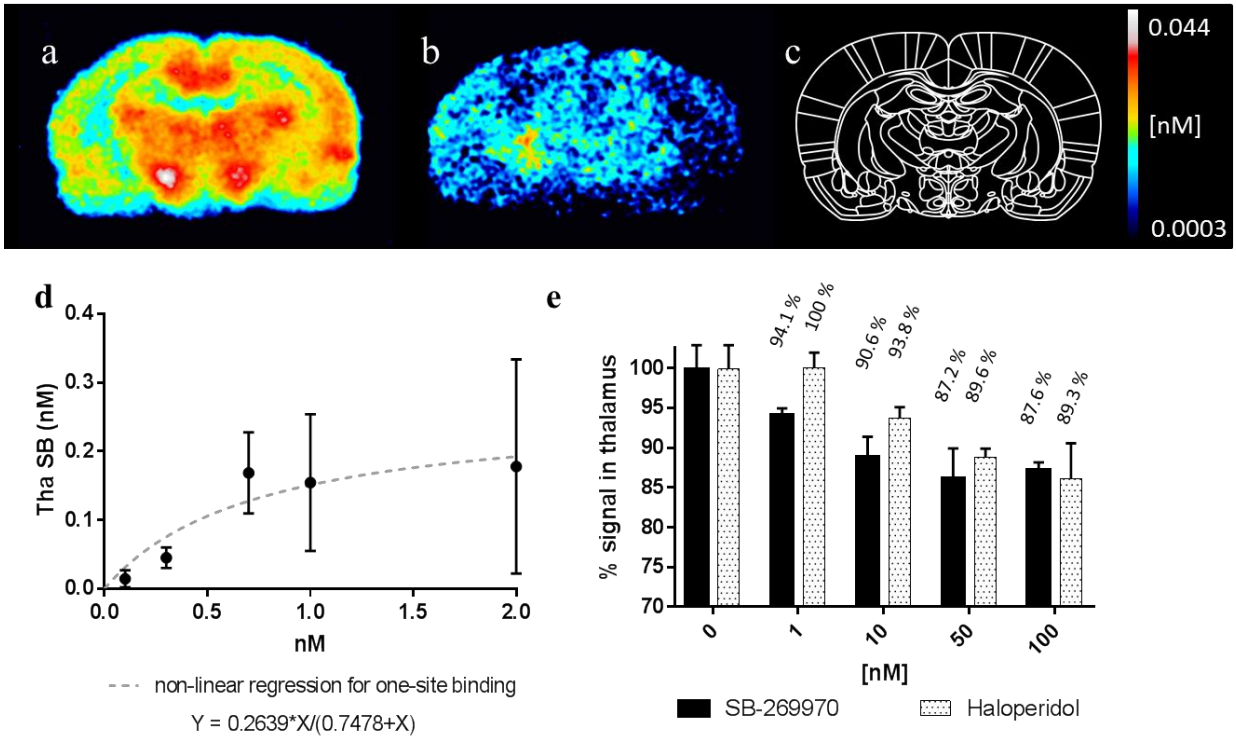

Figure 2: Results of the *in vitro* evaluation of **[^{18}F]15**. **a)-d)** Determination of K_d and B_{max} values of **[^{18}F]15** in thalamus (Tha). **a)** Coronal rat brain slice displaying the total binding of **[^{18}F]15**. **b)** Coronal rat brain slice displaying the non-specific binding of **[^{18}F]15** by blocking with SB-269970 (10 µM). **c)** The location of brain slices, around bregma -1.8. **d)** K_d and B_{max} were elucidated from one sited (specific binding) non-linear regression plotting the specific binding (SB) in nM of **[^{18}F]15** tracer concentration in nM. The data is based on 5 concentrations (0.1 nM, 0.3 nM, 0.7 nM, 1 nM, and 2 nM) and experiments were repeated 3 times (n = 9). **e)** *In vitro* autoradiography blocking study. The results are shown as a grouped barplot with the % signal in thalamus compared to 0 nM (total binding) using different concentrations (1, 10, 50 and 100 nM) of SB-269970 and haloperidol (n =3). Error bars represent standard deviation (SD).

Specific and selective PET imaging is dependent on three key factors: 1) affinity ($1/K_d$), 2) regional target density (B_{max}) compared to the density of other off-targets and 3) non-specific binding.[19, 22, 45] *In vivo* non-specific binding is usually only not determinable *in vitro*, even though more lipophilic tracers tend to have higher non-specific binding.[22, 46] Target affinity, off-target binding and B_{max} values can be determined in binding assays and have to be evaluated in respect to B_{max} over K_D and their according theoretical, observed binding ratio of the target to another off-target ($tBR_{target/off\text{-}target}$).[45] Values over 5 are considered suitable in these calculations. For **15,** these values are of concern for the $tBR_{5\text{-}HT7R/\sigma\text{-}receptors}$ even in high 5-HT_7R density areas. This is because **15** displays a specific σ-receptor binding component (Figure 2) and σ-receptors are 5-fold more prevalent than the 5-HT_7Rs in the highest binding region (thalamus).[6-9, 47] Therefore, specific σ-receptor block may be needed to enable selective 5-HT_7R imaging with **[^{18}F]15**. Keeping that in mind, we started to evaluate **[^{18}F]15** in PET experiments.

At first, *in vivo* evaluation in rats was performed at baseline conditions (Figure 3a and e-f) however unfortunately only low brain uptake was observed. Syvänen *et al*. showed in 2009 that in rodents, several well-established PET tracers are P-glycoprotein (P-gp) efflux transporter substrates. Although these tracers showed poor brain uptake by the rat brain, they have sufficient brain uptake in higher species.[48] Motivated by this, we investigated if **[^{18}F]15** is also a P-gp transporter substrate in order to potentially explain the low brain uptake. Inhibition of the P-gp efflux transporter with elacridar[49] led to increased brain uptake (Figure 3b and e-f), and thus **[^{18}F]15** was confirmed to be a P-gp efflux transporter substrate in rat.

Next, we tested if the uptake of **[^{18}F]15** in the brain after P-gp inhibition represented specific binding to the 5-HT$_7$R. Brain distribution of **[^{18}F]15** was imaged in rats that were injected with elacridar and a specific 5-HT$_7$R antagonist: the highly 5-HT$_7$R-selective SB-269970[31] or the structurally different antagonist Cimbi-717[9]. Thalamus (tha) and cerebellum (cb) were chosen as the brain regions of interest due to the high abundance of 5-HT$_7$R in thalamus and the low abundance in cerebellum.[6-9] We found that both compounds reduced the area under the time-activity curves (TACs) (SB-269970: tha = 21.6%, cb = 25.5%, Cimbi-717: tha = 38.5%, cb = 35.9%) (Figure 3c-g). The reduction in thalamus was expected since this is a high 5-HT$_7$R density region. However, the reduction in cerebellum was to a certain degree unexpected since it is a low 5-HT$_7$R density region.[6-9] Off-target binding of **[^{18}F]15** could explain this observation and since **[^{18}F]15** displayed σ-receptor affinity, we investigated if σ-receptor binding contributed to the observed PET signal. For this purpose, we imaged **[^{18}F]15** distribution in rat brain under P-gp inhibition with elacridar and sigma receptor blockade with either the subtype-unselective σ-receptor antagonist haloperidol (1 mg/kg) or the σ-1 selective antagonist SA4503 (1.5 mg/kg).[50] We saw a reduction in the area under the time-activity curves in thalamus and cerebellum both with haloperidol (Figure 3f-g, tha = 24.1% and cb = 16.2%) and with SA4503 (Figure 3g, tha = 13.5% and cb = 12.7%). Accordingly, we conclude that in rat, the observed PET signal stems from both 5-HT$_7$R and σ-receptor affinities. This could explain the larger reduction in the PET signal seen in thalamus after pretreatment with Cimbi-717 compared to SB-269970 since Cimbi-717 also displays high affinity for the σ-receptors.

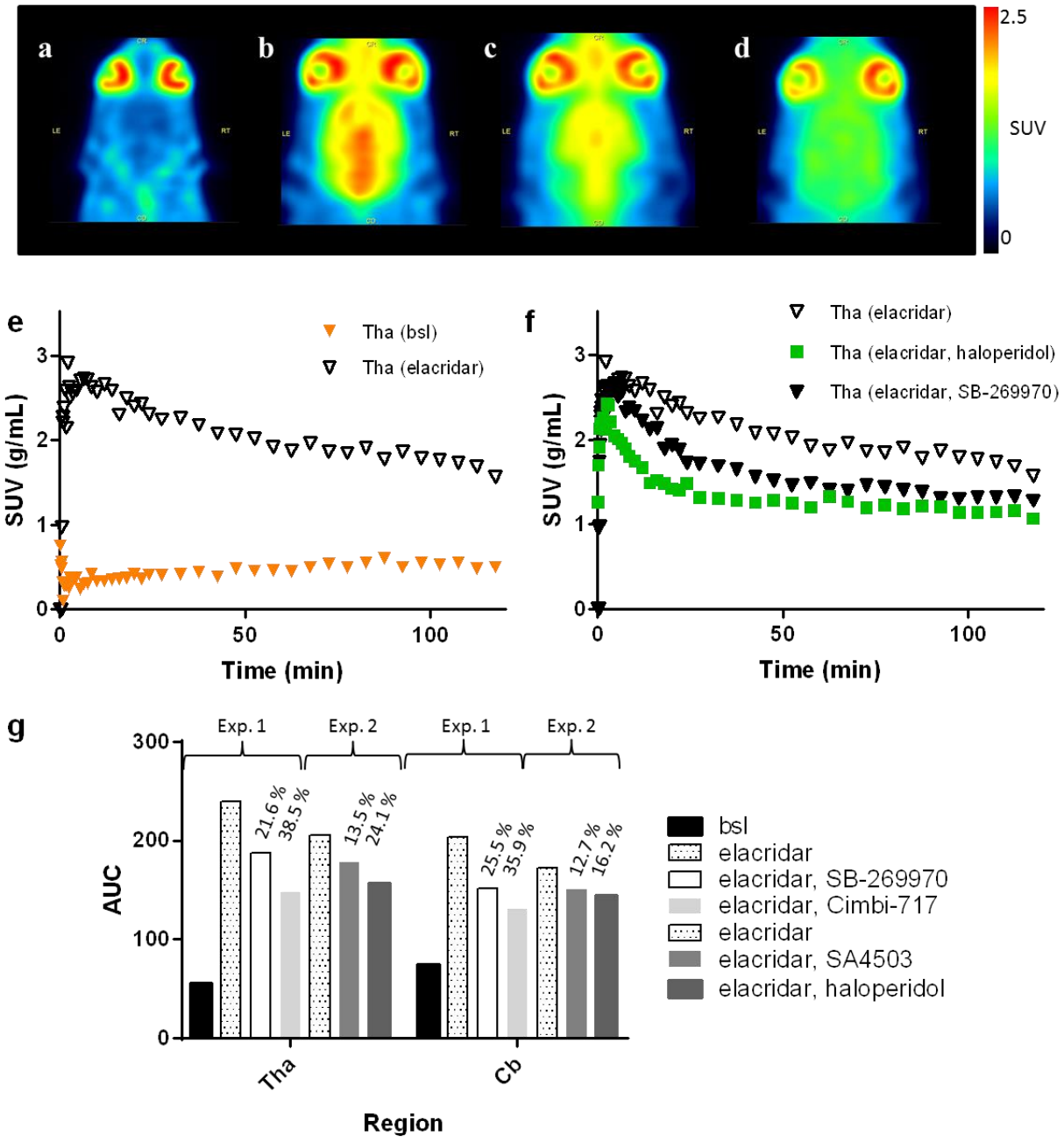

Figure 3: Results from the *in vivo* evaluation of **[^{18}F]15** in rats. Coronal PET images of **[^{18}F]15** evaluated in rats **(a-d)**, all summed images are from 5-120 min of a dynamic scan obtained in a high resolution research tomography (HRRT) scanner. **a)** Summed PET image of **[^{18}F]15** at baseline **b)** Summed PET image of **[^{18}F]15** after pretreatment with elacridar (5 mg/kg). **c)** Summed PET image of **[^{18}F]15** after pretreatment with elacridar (5 mg/kg) and SB-269970 (3 mg/kg). **d)** Summed PET image of **[^{18}F]15** after pretreatment with elacridar (5 mg/kg) and Cimbi-717 (3 mg/kg). Time-activity curves (TACs) from PET evaluation of **[^{18}F]15** in rats **(e-f). e)** Thalamus (Tha) TACs **[^{18}F]15** in baseline condition, after pretreatment with elacridar (5 mg/kg). **f)** Thalamus (Tha) TACs of **[^{18}F]15** after pretreatment with elacridar (5 mg/kg), both elacridar (5 mg/kg) and SB-269970 (3 mg/kg) and elacridar (5 mg/kg) and haloperidol (1 mg/kg) **.g)** Calculated area-under-curve (AUC) for all TACs displayed as a grouped barplot also indicating percentage AUC reduction above the blocking agent bars. All TACs are normalized to injected radioactivity and animal weight to generate the standard uptake value (SUV). Used dose for SA4503 experiments was 1.5 mg/kg.

Conclusion

[^{18}F]ENL30 (**[^{18}F]15)** was successfully synthesized using a convergent synthesis method. In rat brain slices *in vitro*, **[^{18}F]15** showed low-nanomolar affinity towards 5-HT$_7$R (K_D = 0.75 nM). *In vivo* **[^{18}F]15** displayed specific binding to 5-HT$_7$R, but also to σ-receptors. To which extent this will translate into higher species will need to be determined, but it is likely that the P-gp dependency of **[^{18}F]15** will present less of a problem.[48] Even if the *in vivo* PET-signal of **[^{18}F]15** also turns out to represent specific binding to σ-receptors in higher species, specific blocking of σ-receptors could potentially enable PET imaging of the 5-HT$_7$R system.

Experimental section

General information

Solvents and reagents were purchased from Sigma Aldrich (Merck, Darmstadt, Germany) or Thermo Fisher Scientific and used as received unless otherwise noted. The precursors for the radiosynthesis; Ethylene di(p-toluenesulfonate) (Merck, Darmstadt, Germany) and SB-269970 (Tocris Bioscience, Abingdon, United Kingdom) were commercially available.

NMR (^{1}H, ^{13}C) spectra were acquired on a 600 MHz Bruker Avance III HD or a 400 MHz Bruker Avance II at room temperature. Chemical shift (δ) are expressed in parts per million and referenced to residual solvent peak. The resonance multiplicity is abbreviated as follows or combinations thereof: s (singlet), d (doublet), t (triplet), p (quintet) and m (multiplet). The analysis of the NMR spectra was performed using the software MestReNova v12.0.0 (Mestrelab Research S.L.). Thin-layer chromatography (TLC) was run on silica plated aluminum sheets (Silica gel 60 F254) from Merck and the spots were visualized by ultraviolet light at 254 nm and the fraction of radioactivity on the TLC-plates was measured with an instant imager from Packard. Flash column chromatography was carried out manually on silica gel 60 (0.040–0.063 mm). Analytical high performance liquid chromatography (HPLC) was performed on a Dionex system consisting of a P680A pump, a UVD 170U detector and a Scansys radiodetector. The HPLC system was controlled by Chromeleon 6.8 software.

Synthesis of ENL30 **(15)**

The reference compound ENL30 ((R)-1-(2-(1-((3-(2-fluoroethoxy)phenyl)sulfonyl)pyrrolidin-2-yl)ethyl)-4-methylpiperidine) **(15)** was synthesized by a multistep reaction with the final step being the deprotection of *tert*-Butyl (R)-2-(2-(4-methylpiperidin-1-yl)ethyl)pyrrolidine-1-carboxylate **(8)** to (R)-4-methyl-1-(2-(pyrrolidin-2-yl)ethyl)piperidine (**9**) and subsequent coupling with its sulfonyl chloride coupling partner 3-(2-Fluoroethoxy)benzenesulfonyl chloride

(**13**). **(8)** was synthesized by optimization of previous protocols,[31, 35-36] see supplementary information. The synthesis of **(13)** and the final reaction step is described below.

3-(Benzylthio)phenol **(12):**

Benzyl bromide (0.52 mL, 4.4 mmol) was added to a solution of 3-mercaptophenol (0.4 mL, 3.96 mmol) and sodium hydroxide (175.9 mg, 4.4 mmol) in methanol (10 mL). The mixture was stirred overnight at room temperature, and following so was diluted with water (20 mL) and acetic acid (10 mL). The resultant mixture was then concentrated to remove organic solvents. And the resultant precipitate was collected by filtration, washed with water, to yield pure product (558.1 mg, 58.6%). ^{1}H NMR (400 MHz, Methanol-d_4) δ 7.35 – 7.20 (m, 5H), 7.09 (t, J = 7.7 Hz, 1H), 6.82 – 6.77 (m, 2H), 6.63 (ddd, J = 8.1, 2.3, 1.0 Hz, 1H), 4.14 (s, 2H). **Appendix 14.** Rf = 0.78 (7:3 Hept:EtOAc).

Benzyl(3-(2-fluoroethoxy)phenyl)sulfane **(13):**

To a solution of sodium hydride (61.89 mg, 2.58 mmol) in anhydrous DMF (10 mL) under a nitrogen atmosphere was added a solution of **12** (558.1 mg, 2.58 mmol) in anhydrous DMF (7 mL) under cooling at 0 °C. The solution was allowed to stir for 30 minutes, after which, with the solution still at 0 °C, 1-bromo-2-fluoroethane (0.2 mL, 2.58 mmol) was slowly added. The mixture was stirred for a further 20 hours at 60 °C. After such, the solvent was removed *in vacuo*. The residue was then redissolved in ethyl acetate, washed with water, and brine, dried over $MgSO_4$, and concentrated. Crude product was then purified by flash chromatography (125.4 mg, 18.6%). ^{1}H NMR (400 MHz, Methanol-d_4) δ 7.36 – 7.22 (m, 5H), 7.19 (t, J = 8.0 Hz, 1H), 6.94 (ddd, J = 7.8, 1.8, 0.9 Hz, 1H), 6.89 (dd, J = 2.5, 1.7 Hz, 1H), 6.79 (ddd, J = 8.3, 2.5, 0.9 Hz, 1H), 4.78 – 4.73 (m, 1H), 4.66 – 4.61 (m, 1H), 4.20 – 4.17 (m, 1H), 4.16 (s, 2H), 4.13 – 4.10 (m, 1H). **Appendix 15**. Rf = 0.51 (7:3 Hept:EtOAc).

3-(2-Fluoroethoxy)benzenesulfonyl chloride **(14):**

To an ice-cold solution of **13** (125.4 mg, 0.36 mmol) in a mixture of acetonitrile (3.6 mL), water (0.1 mL) and acetic acid (0.15 mL) was added 2,4-dichloro-5,5-dimethylhydontoin (141.8 mg, 0.72 mmol) portion wise. The reaction mixture was stirred at 0 °C, while monitoring the consumption of starting material by TLC. Upon consumption of starting material, the solution was concentrated to near dryness *in vacuo*. Crude product was then diluted with DCM (4.5 mL), and the solution cooled once more to 0 °C. The solution was then diluted further with an aqueous 5% $NaHCO_3$ solution. The mixture was stirred for a further 15 minutes. The lower organic layer

was then washed with an aqueous 10% brine solution, and the resultant organic layer was dried over $MgSO_4$, and concentrated *in vacuo* to give acceptably pure product (85.9 mg, 100%). ^{1}H NMR (600 MHz, Chloroform-*d*) δ 7.68 – 7.65 (m, 1H), 7.55 – 7.52 (m, 2H), 7.31 (dt, J = 8.3, 1.6 Hz, 1H), 4.85 – 4.82 (m, 1H), 4.77 – 4.74 (m, 1H), 4.35 – 4.31 (m, 1H), 4.31 – 4.27 (m, 1H). ^{13}C NMR (151 MHz, Chloroform-*d*) δ 158.87, 145.23, 130.75, 122.41, 119.68, 111.85, 81.91, 80.77. **Appendices 16-17.** Rf = 0.43 (7:3 Hept:EtOAc).

(R)-1-(2-(1-((3-(2-Fluoroethoxy)phenyl)sulfonyl)pyrrolidin-2-yl)ethyl)-4-methylpiperidine **(ENL30, 15):**

9 (4.5 mg, 15.2 μmol) was dissolved in a 1:2 solution of TFA and DCM (1.5 mL), and the resulting solution was stirred under nitrogen for 30 minutes. The organics were then removed *in vacuo*, and the residual salt dissolved in 5mL of 2M NaOH at 0 °C. To the aqueous solution was added **14** (13.7 mg, 41.9 μmol) in diethyl ether (4 mL) while still at 0 °C. The resultant biphasic solution was stirred vigorously overnight, while warming to room temperature. The reaction mixture was diluted with DCM, and acidified to pH 5. The organic layers were washed with water (2 x 5 mL), and then saturated aqueous Na_2HCO_3 (3x 5 mL). Subsequently, they were dried and concentrated under reduced pressure. The product was of sufficient purity to be used as a HPLC standard for subsequent labelling studies (6 mg, 15 μmol, 99%). ^{1}H NMR (600 MHz, Chloroform-*d*) δ 7.45 – 7.43 (m, 2H), 7.37 – 7.36 (m, 1H), 7.15 (td, J = 4.5, 2.6 Hz, 1H), 4.84 – 4.81 (m, 1H), 4.74 (dd, J = 4.7, 3.5 Hz, 1H), 4.30 (td, J = 3.5, 1.2 Hz, 1H), 4.27 – 4.24 (m, 1H), 3.73 (p, J = 6.7 Hz, 1H), 3.40 (ddd, J = 10.5, 7.2, 4.7 Hz, 1H), 3.19 (dt, J = 10.5, 7.3 Hz, 1H), 3.15 – 2.98 (m, 2H), 2.26 – 2.18 (m, 1H), 2.12 – 1.98 (m, 2H), 1.84 – 1.48 (m, 5H), 1.46 – 1.18 (m, 6H), 0.95 (d, J = 6.2 Hz, 3H). ^{13}C NMR (151 MHz, Chloroform-*d*) δ 158.90, 130.42, 128.89, 128.03, 120.44, 119.64, 113.26, 82.40, 81.26, 77.37, 67.65, 49.09, 43.96, 31.09, 29.85, 24.19, 14.27. **Appendices 18-19.** HPLC (Luna, 5μ, C-18(2) 100-A˚ column (Phenomenex Inc. 150 • 4.6 mm); 0.1% TFA in acetonitrile:water (0-100%) over 15 minutes; 2 mL/min – Rt = 6.7 min.

Radiochemistry

Production of fluoride-18

[^{18}F]Fluoride was produced via the (p,n)-reaction in a cyclotron (CTI Siemens and Scanditronix, Rigshospitalet, Denmark) by irradiating [^{18}O]H_2O with a 11 MeV proton beam.

*Radiosynthesis of [^{18}F]ENL30 (**[^{18}F]15**)*

The radiosynthesis of **[^{18}F]15** was performed in two steps on a fully automated system (Scansys Laboratorieteknik synthesis module), beginning with the production of the synthon [^{18}F]fluoroethyl tosylate ([^{18}F]FETos), which thereafter was used to [^{18}F]fluoro-alkylate the commercially available precursor SB-269970, as shown in Scheme 1.

No-carrier-added aqueous ^{18}F-fluoride from the target was collected at a non-conditioned, activated (10 mL ethanol, 20 mL water and dried with air) QMA anion-exchange cartridge (Sep-Pak Accell Plus QMA Plus Light, chloride form, Waters). A solution of 20 mg of 1,10-diaza-4,7,13,16,21,24- hexaoxabicyclo[8.8.8]hexacosane (Kryptofix-222) and 3.3 mg of K_2CO_3 in 0.65 mL of 97% aqueous methanol was used to elute the [^{18}F]fluoride off the cartridge. The elute was thereafter dried by evaporation at first 110 °C under nitrogen and then dried twice again with 1 mL acetonitrile, during the last step the temperature was lowered to 80 °C. To the dried Kryptofix®222/[^{18}F]fluoride complex, 4 mg (0.011 mmol) of the precursor Ethylene di(p-toluenesulfonate), dissolved in 1 mL MeCN was added and the mixture was further heated for 3 min.

[^{18}F]FETos was isolated using semi-preparative HPLC (Luna 5-µm C18(2) 100-Å column (Phenomenex Inc. 250 • 10 mm), H_2O/MeCN (40:60), at a flow rate of 6 mL/min). The retention times were 330 s for [^{18}F]FETos and 150 s for Ethylene di(p-toluenesulfonate). The HPLC fraction containing the [^{18}F]FETos was thereafter diluted with water (60 mL) and the product was loaded on a Sep-Pak C18 Plus Short Cartridge, Waters. The cartridge was dried with nitrogen before the [^{18}F]FETos was eluated off with 1 mL of DMSO into a vial containing; 3 mg SB-269970 (0.008 mmol) and 5 µL NaOH 2N, dissolved in 300 µL DMSO and preheated at 100 °C since start of synthesis (40 min). The reaction mixture was further heated at 100 °C for 25 min before the final isolation of **[^{18}F]15**, using semi-preparative HPLC (Luna 5-µm C18(2) 100-A˚ column (Phenomenex Inc. 250 • 10 mm), EtOH/0.1% phosphoric acid in water (25:75), at a flow rate of 3 mL/min). The final product has a retention time of 1200 s and was collected in a sterile 20 mL vial and diluted with phosphate–buffer (4 mL, 100 mM, and pH 7). The retention times of [^{18}F]FETos and SB-269970 were 300-400 and 550 s, respectively.

Determination of radiochemical purity and molar activity

The preparation of the final product was visually inspected for clarity, absence of colour and particles. Chemical and radiochemical purities were evaluated by analytical HPLC (Luna, 5µ, C-18(2) 100-A˚ column (Phenomenex Inc. 150 • 4.6 mm); 0.1% TFA in acetonitrile:water (0-

100%) over 15 minutes; 2 mL/min – retention times for [^{18}F]FETos = 7.4 min; **[^{18}F]15** = 6.7 min; SB-269970= 5 min and [^{18}F]F^- = 1-2 min). TLC analyses were also made to see the final content of [^{18}F]fluoride (SiO_2-TLC: eluent: EtOAc, R_f **[^{18}F]15**: 0.25 and R_f [^{18}F]fluoride ion: 0.0). The total synthesis time was 2.5 hours and product could be produced with molar activities between 108 - 197 GBq/µmol (n = 3) and radiochemical purities above 98%

Animals

All procedures were conducted in accordance with the FELASA guidelines for animal research and with approval from The Danish Animal Experiments Inspectorate (license number: 2017-15-0201-01283) as well as the Department of Experimental Medicine, University of Copenhagen. In both the *in vitro* and *in vivo* studies we used 200-250 gram female Long-Evans WT rats, which were housed in groups of 2-4 animals per cage in a climate controlled rodent facility with a 12h/12h light cycle. For the PET experiments, the rats were transported to the scanner at least one hour before starting the experiment and they were all fed ad libitum and had free access to water.

*In vitro **[^{18}F]15** autoradiography*

After decapitation of 3 female Long-Evans WT rats, the brains were quickly removed, rinsed in ice-cold water, and frozen using dryice. After storage at - 80 °C, the brains were cut with a cryostat (Microme HM 500 OM) and 20 µm coronal sections were collected on glass slides (Thermo Scientific^{TM} Superfrost Plus^{TM}), starting at bregma - 1.8 mm to around - 4 mm to get slices containing thalamus. The brain sections were stored at - 80 °C until the day of the experiment.

In vitro autoradiography K_d and B_{max} determination

On the day of the experiment the sections were thawed for 1-2 hours prior start and thereafter preincubated for 30 min to 60 min in assay buffer (Tris–HCl 50 mM, pH 7.4, r.t). The Sections were then incubated for 60 min at room temperate in assay buffer modified by the addition of **[^{18}F]15** to the final concentrations; 0.1 nM, 0.3 nM, 0.7 nM 1 nM and 2 nM. For every second section, SB-269970 (10 µM) was added to both the preincubation and incubation buffer to determine the non-specific binding. The incubation was thereafter terminated by washing 2 times for 5 min in ice cold assay buffer. The sections were quickly rinsed in ice cold water for 20 s and then rapidly dried under a gentle stream of air before exposure to an imaging plate (BAS-MS 2040, Fujifilm) overnight.

After obtaining the images using the BAS-1800 plate reader (Fujifilm), ImageJ v1.52i was used for image analysis and GraphPad Prism 7 for calculations and statistics. K_d and B_{max} was determined in thalamus, by calculating the specific binding (SB) by subtraction of the non-specific binding (NS) from the total binding (TB), after drawing a region of interest (ROI) containing thalamus on all brain slices (as defined in Figure 1). A calibration curve of **[^{18}F]5** solutions applied on a TLC plate and exposed together with the slices was used to recalculate the intensity into concentrations in nM. A one sited (specific binding) non-linear regression was used to acquire the K_d and B_{max} values.

In vitro autoradiography-blocking study

On the day of the experiment, the sections were thawed for 1-2 hours prior start and thereafter preincubated for 30 min to 60 min in assay buffer (Tris–HCl 50 mM, pH 7.4, r.t). The Sections were then incubated for 60 min at room temperate in assay buffer modified by the addition of **[^{18}F]15** to the final concentration of 5 nM. Either SB-269970 (1 nM, 10 nM, 50 nM or 100 nM); Haloperidol (1 nM, 10 nM, 50 nM or 100 nM, Janssen-Cilag, Birkerød, Denmark) or SA4503 (1 nM, 10 nM, 50 nM or 100 nM, Merck, Darmstadt, Germany) were added to both the preincubation and incubation buffer to determine if a dose dependent blocking effect could be seen in thalamus. The incubation was thereafter terminated by washing 2 times for 5 min in ice cold assay buffer. The sections was quickly rinsed in ice cold water for 20 s and then rapidly dried under a gentle stream of air before being exposed to an imaging plate (BAS-MS 2040, Fujifilm) for 60 min. After obtaining the images using the BAS-1800, ImageJ v1.52i was used for image analysis and GraphPad Prism 7 for the statistical calculations and presentation.

PET evaluation in rats

Anaesthesia was induced at 3-3.5% isoflurane in oxygen and maintained at 2-2.5% during scans. The PET tracers were given as intravenous (i.v) bolus injections in tail vein catheters at the start of the scan, with the injected doses being between 15-25 MBq. The rats were subsequently scanned in a high resolution research tomography (HRRT) scanner (Siemens AG, Munich, Germany), first for a 120 min dynamic PET scan followed by a point source transmission scan. The scans were performed using a homemade 2x2 rat insert which enabled the possibility of scanning 4 rats simultaneously.[51] The animals were scanned at baseline and after receiving i.v pretreatment of either elacridar[49] (5mg/kg, Carbosynth, Compton, United Kingdom) and/or either SB-269970 (3 mg/kg), Cimbi-717 (3 mg/kg, synthesized in house[9], haloperidol (1 mg/kg) or SA4503 (1.5 mg/kg) 15-30 min before tracer injection.

Reconstruction and processing of PET data

The 120 min list-mode PET data was reconstructed using the 3D ordered subset expectation maximization algorithm (3D OSEM) with attenuation and scatter correction, into 45 dynamic frames (6 × 10, 6 × 20, 6 × 60, 8 × 120 and 19 × 300 seconds) and the images consisted of 207 planes of 256 x 256 voxels of 1.22 x 1.22 x 1.22 mm. Using Pmod, an averaged picture of all frames, except the first 5 min, were reconstructed for each rat and used for co-registration to a standardized MRI-based rat brain atlas (Swartz). Volumes of interest (VOI's) containing thalamus and cerebellum were extracted from the VOI template defined for the MRI-based atlas.[52-53] Outcome measure in the time-activity curves (TACs) was calculated as radioactive concentration in VOI (kBq/cc) normalized to the injected dose and corrected for the weight of the animal yielding standardized uptake values (SUV). GraphPad Prism 7 was used for calculating the area-under-curve (AUC) for all TACs and displaying the results as a grouped barplot.

Associated content

Supporting Information contains additional experimental procedures for example HPLC chromatograms or NMR spectra.

Author information

Corresponding Author: Matthias M. Herth, University of Copenhagen, Department of Drug Design and Pharmacology, Jagtvej 160, 2100 Copenhagen, Denmark, Tel.: +45 93565414, Fax: +45 35 33 60 41, e-mail: matthias.herth@sund.ku.dk

Author Contributions

Experimental work and data evaluation were carried out by Elina T. L'Estrade, Fraser G. Edgar, Mengfei Xiong, Simone L. Baerentzen, Maria Erlandsson and Mikael Palner. Vladimir Shalgunov, Tomas G. Ohlsson, Gitte M. Knudsen and Matthias M. Herth designed the experiments, supervised the work, contributed to the research idea and were strongly involved in the evaluation of the experimental data, The manuscript was written through contributions of all authors. All authors have given approval to the final version of the manuscript.

Acknowledgement

The authors wish to thank the staff at the PET and Cyclotron unit for expert technical assistance.

References

1. Matthys, A.; Haegeman, G.; Van Craenenbroeck, K.; Vanhoenacker, P., Role of the 5-HT_7 receptor in the central nervous system: from current status to future perspectives. *Molecular Neurobiology* **2011,** *43* (3), 228-53.

2. Nichols, D. E.; Nichols, C. D., Serotonin Receptors. *Chemical Reviews* **2008,** *108* (5), 1614-1641.

3. Bard, J. A.; Zgombick, J.; Adham, N.; Vaysse, P.; Branchek, T. A.; Weinshank, R. L., Cloning of a novel human serotonin receptor (5-HT_7) positively linked to adenylate cyclase. *Journal of Biological Chemistry* **1993,** *268* (31), 23422-23426.

4. Lovenberg, T. W.; Baron, B. M.; de Lecea, L.; Miller, J. D.; Prosser, R. A.; Rea, M. A.; Foye, P. E.; Racke, M.; Slone, A. L.; Siegel, B. W., A novel adenylyl cyclase-activating serotonin receptor (5-HT_7) implicated in the regulation of mammalian circadian rhythms. *Neuron* **1993,** *11* (3), 449-458.

5. Ruat, M.; Traiffort, E.; Leurs, R.; Tardivel-Lacombe, J.; Diaz, J.; Arrang, J.-M.; Schwartz, J.-C., Molecular cloning, characterization, and localization of a high-affinity serotonin receptor (5-HT_7) activating cAMP formation. *Proceedings of the National Academy of Sciences* **1993,** *90* (18), 8547-8551.

6. Gustafson, E. L.; Durkin, M. M.; Bard, J. A.; Zgombick, J.; Branchek, T. A., A receptor autoradiographic and in situ hybridization analysis of the distribution of the 5-HT_7 receptor in rat brain. *British Journal of Pharmacology* **1996,** *117* (4), 657-66.

7. Varnäs, K.; Thomas, D. R.; Tupala, E.; Tiihonen, J.; Hall, H., Distribution of 5-HT_7 receptors in the human brain: a preliminary autoradiographic study using [^{3}H] SB-269970. *Neuroscience letters* **2004,** *367* (3), 313-316.

8. Horisawa, T.; Ishiyama, T.; Ono, M.; Ishibashi, T.; Taiji, M., Binding of lurasidone, a novel antipsychotic, to rat 5-HT_7 receptor: analysis by [^{3}H] SB-269970 autoradiography. *Progress in Neuro-Psychopharmacology and Biological Psychiatry* **2013,** *40*, 132-137.

9. Hansen, H. D.; Herth, M. M.; Ettrup, A.; Andersen, V. L.; Lehel, S.; Dyssegaard, A.; Kristensen, J. L.; Knudsen, G. M., Radiosynthesis and *in vivo* evaluation of novel radioligands for PET imaging of cerebral 5-HT_7 receptors. *Journal of Nuclear Medicine* **2014,** *55* (4), 640-6.

10. Hansen, H. D.; Constantinescu, C. C.; Barret, O.; Herth, M. M.; Magnussen, J. H.; Lehel, S.; Dyssegaard, A.; Colomb, J.; Billard, T.; Zimmer, L., Evaluation of [^{18}F] 2FP3 in pigs and non-human primates. *Journal of Labelled Compounds and Radiopharmaceuticals* **2018**.

11. Guscott, M.; Bristow, L.; Hadingham, K.; Rosahl, T.; Beer, M.; Stanton, J.; Bromidge, F.; Owens, A.; Huscroft, I.; Myers, J., Genetic knockout and pharmacological blockade studies of the 5-HT$_7$ receptor suggest therapeutic potential in depression. *Neuropharmacology* **2005,** *48* (4), 492-502.

12. Hedlund, P. B.; Huitron-Resendiz, S.; Henriksen, S. J.; Sutcliffe, J. G., 5-HT$_7$ Receptor Inhibition and Inactivation Induce Antidepressantlike Behavior and Sleep Pattern. *Biological Psychiatry* **2005,** *58* (10), 831-837.

13. Wesołowska, A.; Nikiforuk, A.; Stachowicz, K.; Tatarczyńska, E., Effect of the selective 5-HT$_7$ receptor antagonist SB 269970 in animal models of anxiety and depression. *Neuropharmacology* **2006,** *51* (3), 578-586.

14. Wesołowska, A.; Nikiforuk, A.; Stachowicz, K., Potential anxiolytic and antidepressant effects of the selective 5-HT$_7$ receptor antagonist SB 269970 after intrahippocampal administration to rats. *European journal of pharmacology* **2006,** *553* (1-3), 185-190.

15. Mnie-Filali, O.; Lambas-Señas, L.; Scarna, H.; Haddjeri, N., Therapeutic potential of 5-HT$_7$ receptors in mood disorders. *Current drug targets* **2009,** *10* (11), 1109-1117.

16. Mnie-Filali, O.; Lambás-Señas, L.; Zimmer, L.; Haddjeri, N., 5-HT$_7$ receptor antagonists as a new class of antidepressants. *Drug News Perspect* **2007,** *20* (10), 613-8.

17. Zimmer, L.; Billard, T., Molecular imaging of the serotonin 5-HT$_7$ receptors: from autoradiography to positron emission tomography. *Reviews in the Neurosciences* **2014,** *25* (3), 357-365.

18. Thomas, D. R.; Atkinson, P. J.; Hastie, P. G.; Roberts, J. C.; Middlemiss, D. N.; Price, G. W., [3H]-SB-269970 radiolabels 5-HT$_7$ receptors in rodent, pig and primate brain tissues. *Neuropharmacology* **2002,** *42* (1), 74-81.

19. Paterson, L. M.; Tyacke, R. J.; Nutt, D. J.; Knudsen, G. M., Measuring endogenous 5-HT release by emission tomography: promises and pitfalls. *Journal of Cerebral Blood Flow & Metabolism* **2010,** *30* (10), 1682-1706.

20. Kristensen, J. L.; Herth, M. M., Textbook of Drug Design and Discovery: *In vivo* imaging in drug discovery. In *Textbook of Drug Design and Discovery*, CRC Press: 2017.

21. Miller, P. W.; Long, N. J.; Vilar, R.; Gee, A. D., Synthesis of ^{11}C, ^{18}F, ^{15}O, and ^{13}N radiolabels for positron emission tomography. Angewandte Chemie International Edition *l* **2008,** *47* (47), 8998-9033.

22. Piel, M.; Vernaleken, I.; Rösch, F., Positron Emission Tomography in CNS Drug Discovery and Drug Monitoring. *Journal of Medicinal Chemistry* **2014,** *57* (22), 9232-9258.

23. Herth, M. M.; Andersen, V. L.; Hansen, H. D.; Stroth, N.; Volk, B.; Lehel, S.; Dyssegaard, A.; Ettrup, A.; Svenningsson, P.; Knudsen, G. M.; Kristensen, J. L., Evaluation of 3-Ethyl-3-(phenylpiperazinylbutyl)oxindoles as PET Ligands for the Serotonin 5-HT(7) Receptor: Synthesis, Pharmacology, Radiolabeling, and *in Vivo* Brain Imaging in Pigs. *Journal of Medicinal Chemistry* **2015,** *58* (8), 3631-6.

24. Lemoine, L.; Andries, J.; Le Bars, D.; Billard, T.; Zimmer, L., Comparison of 4 radiolabeled antagonists for serotonin 5-HT(7) receptor neuroimaging: toward the first PET radiotracer. *Journal of Nuclear Medicine* **2011,** *52* (11), 1811-8.

25. Andries, J.; Lemoine, L.; Mouchel-Blaisot, A.; Tang, S.; Verdurand, M.; Le Bars, D.; Zimmer, L.; Billard, T., Looking for a 5-HT_7 radiotracer for positron emission tomography. *Bioorganic and Medicinal Chemistry Letters* **2010,** *20* (12), 3730-3.

26. Hansen, H. D.; Andersen, V. L.; Lehel, S.; Magnussen, J. H.; Dyssegaard, A.; Stroth, N.; Kristensen, J. L.; Knudsen, G. M.; Herth, M. M., Labeling and preliminary in vivo evaluation of the 5-HT_7 receptor selective agonist [^{11}C]E-55888. *Bioorganic and Medicinal Chemistry Letters* **2015,** *25* (9), 1901-4.

27. Lacivita, E.; Niso, M.; Hansen, H. D.; Di Pilato, P.; Herth, M. M.; Lehel, S.; Ettrup, A.; Montenegro, L.; Perrone, R.; Berardi, F.; Colabufo, N. A.; Leopoldo, M.; Knudsen, G. M., Design, synthesis, radiolabeling and *in vivo* evaluation of potential positron emission tomography (PET) radioligands for brain imaging of the 5-HT_7 receptor. *Bioorganic and Medicinal Chemistry* **2014,** *22* (5), 1736-50.

28. Hansen, H. D.; Lacivita, E.; Di Pilato, P.; Herth, M. M.; Lehel, S.; Ettrup, A.; Andersen, V. L.; Dyssegaard, A.; De Giorgio, P.; Perrone, R.; Berardi, F.; Colabufo, N. A.; Niso, M.; Knudsen, G. M.; Leopoldo, M., Synthesis, radiolabeling and *in vivo* evaluation of [(11)C](R)-1-[4-[2-(4-methoxyphenyl)phenyl]piperazin-1-yl]-3-(2-pyrazinyloxy)-2-p ropanol, a potential PET radioligand for the 5-HT(7) receptor. *European Journal of Medicinal Chemistry* **2014,** *79*, 152-63.

29. Colomb, J.; Becker, G.; Forcellini, E.; Meyer, S.; Buisson, L.; Zimmer, L.; Billard, T., Synthesis and pharmacological evaluation of a new series of radiolabeled ligands for 5-HT_7 receptor PET neuroimaging. Nuclear Medicine and Biology **2014,** *41* (4), 330-7.

30. Herth, M.; Hansen, H.; Anders, E.; Lehel, S.; Kristensen, J.; Billard, T.; Zimmer, L.; Knudsen, G., Development of a novel ^{11}C-labelled SB-269970 derivative for imaging the cerebral 5-HT_7 receptors. *Journal of Nuclear Medicine* **2014,** *55* (supplement 1), 1814-1814.

31. Lovell, P. J.; Bromidge, S. M.; Dabbs, S.; Duckworth, D. M.; Forbes, I. T.; Jennings, A. J.; King, F. D.; Middlemiss, D. N.; Rahman, S. K.; Saunders, D. V.; Collin, L. L.; Hagan, J. J.; Riley, G. J.; Thomas, D. R., A novel, potent, and selective 5-HT(7) antagonist: (R)-3-(2-(2-(4-methylpiperidin-1-yl)ethyl)pyrrolidine-1-sulfonyl) phen ol (SB-269970). *Journal of Medicinal Chemistry* **2000,** *43* (3), 342-345.

32. Herth, M. M.; Debus, F.; Piel, M.; Palner, M.; Knudsen, G. M.; Luddens, H.; Rosch, F., Total synthesis and evaluation of [^{18}F]MHMZ. Bioorganic and Medicinal Chemistry Letters **2008,** *18* (4), 1515-9.

33. Van Der Born, D.; Pees, A.; Poot, A. J.; Orru, R. V.; Windhorst, A. D.; Vugts, D. J., Fluorine-18 labelled building blocks for PET tracer synthesis. *Chemical Society Reviews* **2017,** *46* (15), 4709-4773.

34. Kniess, T.; Laube, M.; Brust, P.; Steinbach, J., 2-[^{18}F] Fluoroethyl tosylate–a versatile tool for building ^{18}F-based radiotracers for positron emission tomography. *Medicinal Chemical Communications* **2015,** *6* (10), 1714-1754.

35. Cardillo, G.; Gentilucci, L.; Qasem, A. R.; Sgarzi, F.; Spampinato, S., Endomorphin-1 analogues containing β-proline are μ-opioid receptor agonists and display enhanced enzymatic hydrolysis resistance. *Journal of medicinal chemistry* **2002,** *45* (12), 2571-2578.

36. Chu, W.; Zhang, J.; Zeng, C.; Rothfuss, J.; Tu, Z.; Chu, Y.; Reichert, D. E.; Welch, M. J.; Mach, R. H., N-Benzylisatin Sulfonamide Analogues as Potent Caspase-3 Inhibitors: Synthesis, *in Vitro* Activity, and Molecular Modeling Studies. *Journal of Medicinal Chemistry* **2005,** *48* (24), 7637-7647.

37. Paryzek, Z.; Koenig, H.; Tabaczka, B., Ammonium formate/palladium on carbon: a versatile system for catalytic hydrogen transfer reductions of carbon-carbon double bonds. *Synthesis* **2003,** *2003* (13), 2023-2026.

38. Schjøth-Eskesen, C.; Jensen, H. H., Efficient Arndt–Eistert synthesis of selective 5-HT_7 receptor antagonist SB-269970. *Synthetic Communications*® **2009,** *39* (18), 3243-3253.

39. Nishiguchi, A.; Maeda, K.; Miki, S., Sulfonyl chloride formation from thiol derivatives by N-chlorosuccinimide mediated oxidation. *Synthesis* **2006,** *2006* (24), 4131-4134.

40. Veisi, H., Convenient one-pot Synthesis of sulfonamides from thiols and disulfides using 1, 3-dichloro-5, 5-dimethylhydantoin (DCH). *Bulletin of the Korean Chemical Society* **2012,** *33* (2), 383-386.

41. Ates, A.; Burssens, P.; Lorthioir, O.; Lo Brutto, P.; Dehon, G.; Keyaerts, J.; Coloretti, F.; Lallemand, B.; Verbois, V.; Gillard, M., 5-HT_7 Receptor Antagonists with an Unprecedented Selectivity Profile. *Medicinal Chemistry Communication* **2018,** *13* (8), 795-802.

42. McLeod, M. C.; Aubé, J.; Frankowski, K. J., Decahydrobenzoquinolin-5-one sigma receptor ligands: Divergent development of both sigma 1 and sigma 2 receptor selective examples. *Bioorganic & medicinal chemistry letters* **2016,** *26* (23), 5689-5694.

43. Li, P.; L Snyder, G.; E Vanover, K., Dopamine targeting drugs for the treatment of schizophrenia: past, present and future. *Current topics in medicinal chemistry* **2016,** *16* (29), 3385-3403.

44. Schotte, A.; Janssen, P.; Gommeren, W.; Luyten, W.; Van Gompel, P.; Lesage, A.; De Loore, K.; Leysen, J., Risperidone compared with new and reference antipsychotic drugs*: in vitro* and *in vivo* receptor binding. *Psychopharmacology* **1996,** *124* (1-2), 57-73.

45. Herth M. M., K. G. M., PET Imaging of the 5-HT2A Receptor System: A Tool to Study the Receptor's *In Vivo* Brain Function. 5-HT_{2A} Receptors in the Central Nervous System. In *5-HT2A Receptors in the Central Nervous System*, Guiard B., D. G. G., Ed. Humana Press, Cham: **2018**; Vol. 32, pp 85-134.

46. Kessler, R. M.; Ansari, M. S.; de Paulis, T.; Schmidt, D. E.; Clanton, J. A.; Smith, H. E.; Manning, R. G.; Gillespie, D.; Ebert, M. H., High affinity dopamine D2 receptor radioligands. 1. Regional rat brain distribution of iodinated benzamides. *Journal of Nuclear Medicine* **1991,** *32* (8), 1593-1600.

47. Weissman, A.; Su, T.-P.; Hedreen, J.; London, E., Sigma receptors in post-mortem human brains. *Journal of Pharmacology and Experimental Therapeutics* **1988,** *247* (1), 29-33.

48. Syvänen, S.; Lindhe, Ö.; Palner, M.; Kornum, B. R.; Rahman, O.; Långström, B.; Knudsen, G. M.; Hammarlund-Udenaes, M., Species differences in blood-brain barrier transport of three positron emission tomography radioligands with emphasis on P-glycoprotein transport. *Drug metabolism and disposition* **2009,** *37* (3), 635-643.

49. Kallem, R.; P Kulkarni, C.; Patel, D.; Thakur, M.; Sinz, M.; P Singh, S.; Shahe Mahammad, S.; Mandlekar, S., A simplified protocol employing elacridar in rodents: a screening

model in drug discovery to assess P-gp mediated efflux at the blood brain barrier. *Drug metabolism letters* **2012,** *6* (2), 134-144.

50. Matsuno, K.; Nakazawa, M.; Okamoto, K.; Kawashima, Y.; Mita, S., Binding properties of SA4503, a novel and selective σ1 receptor agonist. *European journal of pharmacology* **1996,** *306* (1-3), 271-279.

51. Keller, S. H.; L'Estrade, E. N.; Dall, B.; Palner, M.; Herth, M. In *Quantification accuracy of a new HRRT high throughput rat hotel using transmission-based attenuation correction: A phantom study*, Nuclear Science Symposium, Medical Imaging Conference and Room-Temperature Semiconductor Detector Workshop (NSS/MIC/RTSD), 2016, IEEE: 2016; pp 1-3.

52. Schwarz, A. J.; Danckaert, A.; Reese, T.; Gozzi, A.; Paxinos, G.; Watson, C.; Merlo-Pich, E. V.; Bifone, A., A stereotaxic MRI template set for the rat brain with tissue class distribution maps and co-registered anatomical atlas: application to pharmacological MRI. *Neuroimage* **2006,** *32* (2), 538-550.

53. Garcia, D. V.; Casteels, C.; Schwarz, A. J.; Dierckx, R. A.; Koole, M.; Doorduin, J., A standardized method for the construction of tracer specific PET and SPECT rat brain templates: validation and implementation of a toolbox. *PLoS One* **2015,** *10* (3), e0122363.

Table of Contents graphic

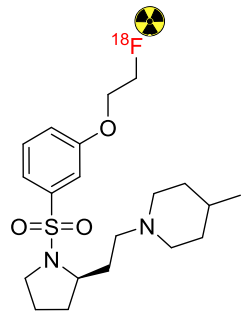

[^{18}F]ENL30 ([^{18}F]15)

Supporting Information

Synthesis, Radiolabeling, *In vitro* and *In vivo* Evaluation of [^{18}F]ENL30 – A Potential PET Radiotracer for the 5-HT$_7$ Receptor

Elina T. L'Estrade[a,b,c], Fraser G. Edgar [b], Mengfei Xiong[a,b], Vladimir Shalgunov[b], Simone L. Baerentzen[a], Maria Erlandsson[c], Tomas G. Ohlsson[c], Mikael Palner[a,d], Gitte M. Knudsen [a,e], Matthias M. Herth [b,f]

[a] *Neurobiology Research Unit, Rigshospitalet, Blegdamsvej 9, 2100 Copenhagen, Denmark*

[b] *Department for Drug Design and Pharmacology, Faculty of Health and Medical Sciences, University of Copenhagen, Universitetesparken 2, 2100 Copenhagen, Denmark*

[c] *Radiation Physics, Nuclear Medicine Physics Unit, Skånes University Hospital, Barngatan 3, 222 42 Lund, Sweden.*

[d] *Center for Translational Neuromedicine, University of Copenhagen, Blegdamsvej 3B, 2200 Copenhagen N, Denmark*

[e] *Faculty of Health and Medical Sciences, University of Copenhagen, Denmark.*

[f] *Department of Clinical Physiology, Nuclear Medicine and PET, University Hospital Copenhagen, Rigshospitalet Blegdamsvej 9, 2100 Copenhagen, Denmark*

Corresponding Author

* Tel.: +0045 93565414; fax: +0045 35 33 60 41; e-mail: matthias.herth@sund.ku.dk

CONTENTS

INTRODUCTION 289

RESULTS 290

EXPERIMENTAL SECTION 292

REFERENCES 299

APPENDICES 300

Introduction

Supporting table 1: Table summarizing the B_{max} of 5-HT_7R in different species and brain regions. Measured by autoradiography with [^{3}H]SB-269970. TE = tissue equivalent[1-4] Table originally from **Paper I**, chapter 3.

	Specific binding (fmol/mg tissue ± SE) Rat	**Specific binding (fmol/mg TE) Pig**	**Specific binding (fmol/mg TE) Non-human primate**	**Specific binding (pmol/g) Human**
Cortical regions				
Prefrontal cortex		32.7 ± 1.60		
Frontal cortex	11 ± 1	38.3 ± 2.68		
Superior frontal gyrus				2.6 ± 1.3
Inferior frontal gyrus				2.0 ± 0.67
Temporal cortex		41.0 ± 3.03	21.5 ± 4.32	2.3 ± 1.7
Cingulate cortex	12 ± 1	44.9 ± 2.60		
Occipital cortex		33.2 ± 2.40		1.2 ± 0.57
Striatum				
Putamen	4 ± 1	21.6 ± 1.64		0.97 ± 1.0
Caudate	4 ± 1	24.4 ± 2.81		0.72 ± 0.82
Thalamus	47 ± 5	45.6 ± 0.19	32.3 ± 3.61	11 ± 3.5
Thalamus (high binding subregion)		62.0 ± 5.53		
Anterior thalamus				16 ± 4.9
Paraventricular thalamic nucleus	83 ± 10			
Hypothalamus	36 ± 6	43.0 ± 6.03		5.9 ± (5.5, 6.4)
Hippocampus	14 ± 2	37.5 ± 3.35		5.7 ± 4.7
Dendate gyrus				8.7 ± 3.7
Amygdala	21 ± 2	48.3 ± 5.01		4.2 ± 1.9
Cerebellum	0	13.4 ± 2.22	14.3 ± 0.93	< 1

Results

The ammonium formate/palladium on carbon procedure was first attempted, which had been reported to be extremely versatile.[5] Unfortunately, this did not yield product, although some conversion could be seen by NMR. In an attempt to facilitate the latter, different hydrogenation possibilities have been investigated. Platinum(IV) oxide catalysed hydrogenation using hydrogen gas as well as H-Cube® hydrogenation (using different catalysts, see Supporting table 2) did not proceed. Either low yields were isolated or **(5)** did not withstand applied conditions and decomposed

Supporting table 2 – Attempted catalytic coupling.

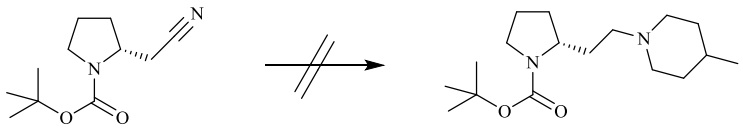

5 **6**

Catalyst	H_2 Source/Pressure	Solvent	Temperature (°C)	Time (d)	Flow rate (if applicable)
Pd/C	Ammonium formate; *in situ* generation	Anhydrous MeOH	Reflux	3	N/A
$Pt(IV)O_2$	H_2 gas; balloon pressure	Anhydrous EtOH	25	3	N/A
10% Pd/C	H-Cube®; 50 bar	EtOH	70	N/A	1 mL/min
Ra. Ni	H-Cube®; 50 bar	EtOH	70	N/A	1 mL/min
20% $Pd(OH)_2$	H-Cube®; 50 bar	EtOH	60	N/A	1 mL/min

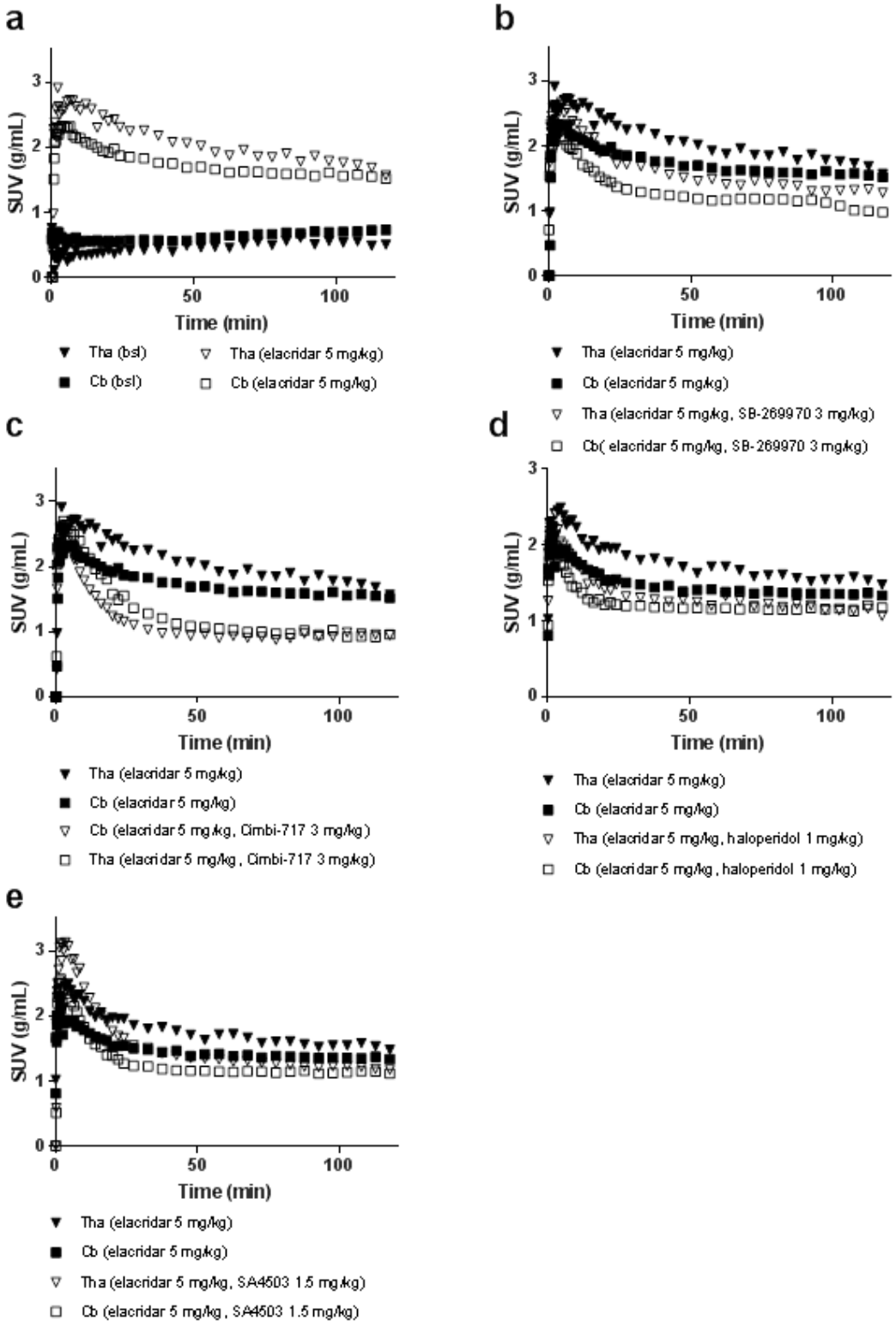

Supporting Figure 1: Time-activity curves (TACs) from PET evaluation of [^{18}F]ENL30 in rats. **a)** Thalamus (Tha, triangle symbols), and cerebellum (Cb, square symbols) TACs of [^{18}F]ENL30 in baseline condition and after pretreatment with elacridar (5 mg/kg). **b)** Tha and cb TACs of [^{18}F]ENL30 after pretreatment with elacridar (5 mg/kg) and after pretreatment with both elacridar (5 mg/kg) and SB-269970 (3 mg/kg). **c)** Tha and cb TACs of [^{18}F]ENL30 after pretreatment with elacridar (5 mg/kg) and after pretreatment with both elacridar (5 mg/kg) and Cimbi-717 (3 mg/kg). **d)** Tha and cb TACs of [^{18}F]ENL30 after pretreatment with elacridar (5 mg/kg) and after pretreatment with both elacridar (5 mg/kg) and haloperidol (1 mg/kg). **e)** Tha and

cb TACs of [^{18}F]ENL30 after pretreatment with elacridar (5 mg/kg) and after pretreatment with both elacridar (5 mg/kg) and SA4503 (1.5 mg/kg).

Experimental section

Reference synthesis

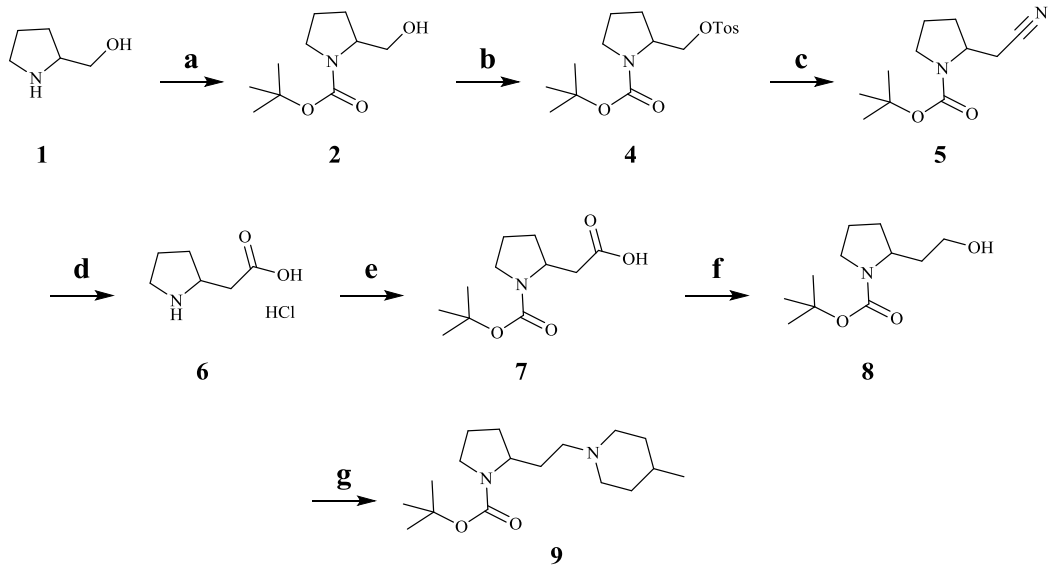

Supporting Scheme 1: Synthetic overview of the synthesis of *tert*-Butyl (R)-2-(2-(4-methylpiperidin-1-yl)ethyl)pyrrolidine-1-carboxylate **(9).** Reagents and conditions: **a)** $(Boc)_2O$, TEA, MeOH, Δ, 0.5 hr; **b)** p-TosCl, Py, DCM, 0 °C – rt, ON; **c)** KCN, DMSO, 90 °C, 4 hr; **d)** HCl (35%), AcOH, Δ, 6 hr; **e)** $(Boc)_2O$, NaOH (2M), Acetone, 0 °C – rt, 2.5 hr; **f)** Borane-THF, THF, rt, ON; **g)** i) MsCl, Py, DCM, 0 °C – rt, 2 hr; ii) 4-methylpiperidine, ACN, rt - 50 °C, ON.

tert-Butyl (R)-2-(hydroxymethyl)pyrrolidine-1-carboxylate **(2):**

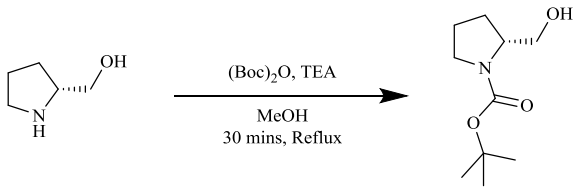

Di-*tert*-butyl dicarbonate (4.45 g, 20.4 mmol) was added to a stirred solution of *D*-Prolinol (1 mL, 10.2 mmol) in a 10% triethylamine in methanol solution (15 mL). The mixture was heated to reflux for 30 minutes, following which the mixture was concentrated under reduced pressure to give the title compound (2.05g, 100%). ^{1}H NMR (600 MHz, Chloroform-*d*) δ 4.76 – 4.68 (m, 1H), 3.96 (d, J = 6.9 Hz, 1H), 3.66 – 3.51 (m, 2H), 3.48 – 3.39 (m, 1H), 3.30 (dt, J = 10.7, 6.9 Hz, 1H), 2.00 (dq, J = 14.3, 7.3, 6.4 Hz, 1H), 1.87 – 1.73 (m, 2H), 1.46 (s, 9H). ^{13}C NMR (151 MHz, Chloroform-*d*) δ 157.11, 80.16, 67.02, 60.15, 47.49, 28.67, 28.39, 27.35**. Appendices 1-2**. Rf = 0.34 (1:1 EtOAc:Hept).

tert-Butyl (R)-2-(((methylsulfonyl)oxy)methyl)pyrrolidine-1-carboxylate **(4):**

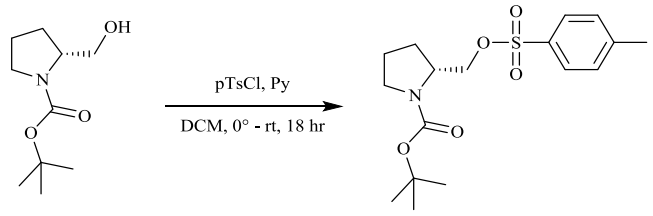

2 (2.05 g, 10.3 mmol) was dissolved in a solution of DCM (20 mL) and pyridine (15 mL), to which pTsCl (2.43 g, 12.75 mmol) was added at 0 °C. The mixture was allowed to warm to room temperature, and stir overnight. The solution was diluted with DCM (50 mL), and subsequently washed with water (2x 50 mL), and brine (2x 50 mL). The organic fractions were collected, dried with $MgSO_4$, and concentrated *in vacuo*. The crude product was purified by flash chromatography (3.07 g, 84.6%). Complex set of two rotamers. ^{1}H NMR (600 MHz, Chloroform-*d*) δ 7.77 (d, J = 8.0 Hz, 2H), 7.34 (d, J = 6.3 Hz, 2H), 4.18 – 4.04 (m, 1H), 4.00 – 3.84 (m, 1H), 3.38 – 3.20 (m, 2H), 2.44 (s, 3H), 2.00 – 1.86 (m, 3H), 1.84 – 1.75 (m, 1H), 1.38 (d, J = 21.3 Hz, 9H). ^{13}C NMR (151 MHz, Chloroform-*d*) δ 154.15, 145.00, 133.08, 130.00, 127.99, 80.04, 70.09, 55.67, 47.05, 32.01, 29.14, 28.48, 22.81, 21.74, 14.23. **Appendices 3-4.** Rf = 0.48 (1:1 EtOAc:Hept).

tert-Butyl (R)-2-(cyanomethyl)pyrrolidine-1-carboxylate **(5):**

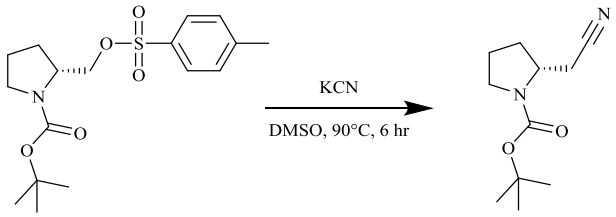

3 (3.07 g, 8.6 mmol) was dissolved in anhydrous DMSO (15 mL), to which was added KCN (1.68 g, 25.8 mmol), following which the mixture was heated to 90 °C for six hours under an inert atmosphere. The reaction was then allowed to cool to room temperature, after which ethyl acetate was added, and the organic layer was subsequently washed three times with small portions of water, followed by brine. The collected aqueous layer was then treated with potassium permanganate before disposal. The organic layers were then collected, dried, and concentrated under reduced pressure. The product was analytically pure as determined by TLC and NMR (1.49 g, 88.1%). Complex set of two rotamers. ^{1}H NMR (600 MHz, Chloroform-*d*) δ 4.00 (t, J = 8.2 Hz, 1H), 3.50 – 3.34 (m, 2H), 2.86 – 2.53 (m, 2H), 2.16 (dq, J = 15.3, 8.0 Hz, 1H), 2.06 – 1.82 (m, 3H), 1.51 – 1.44 (m, 9H). ^{13}C NMR (151 MHz, Chloroform-*d*) δ 154.46, 153.81, 117.98, 80.37, 79.94, 77.16, 53.66, 47.07, 30.37, 28.38, 23.63, 22.24. **Appendices 5-6.** Rf = 0.56 (1:1 EtOAc:Hept).

(R)-2-(Pyrrolidin-2-yl)acetic acid salt **(6):**

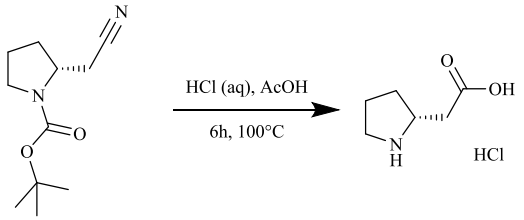

4 (1.49 g, 7.58 mmol) was dissolved in concentrated hydrochloric acid (23 mL) and acetic acid (15 mL). The subsequent solution was heated to reflux for six hours. Once cooled to room temperature the solution was washed twice with diethyl ether. The collected aqueous layers were then concentrated under reduced pressure to give the hydrochloride salt (1.2 g, 94.9%). ^{1}H NMR (400 MHz, Deuterium Oxide) δ 4.01 – 3.86 (m, 1H), 3.38 (t, J = 7.4 Hz, 2H), 2.99 (dd, J = 17.9, 4.6 Hz, 1H), 2.87 (dd, J = 17.9, 9.3 Hz, 1H), 2.31 (dtd, J = 13.2, 7.3, 4.1 Hz, 1H), 2.17 – 1.96 (m, 2H), 1.76 (dtd, J = 13.2, 9.2, 8.1 Hz, 1H). ^{13}C NMR (151 MHz, Deuterium Oxide) δ 174.04, 56.19, 45.46, 35.75, 29.56, 23.03. **Appendices 7-8.** Rf = 0 (1:1 EtOAc:Hept).

(R)-2-(1-(tert-Butoxycarbonyl)pyrrolidin-2-yl)acetic acid **(7)**

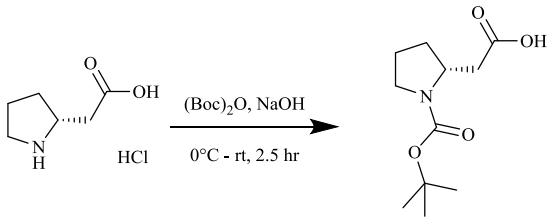

5 (1.2 g, 7.2 mmol) was dissolved in a minimal volume of water (10 mL), and the pH was subsequently adjusted to pH10 with a 2M sodium hydroxide solution at 0 °C. The solution was then diluted with acetone (12 mL), and di-*tert*-butyl dicarbonate (2.4 g, 10.9 mmol) was added while the solution remained at 0 °C. After 15minutes the solution was allowed to warm to room temperature, and the solution stirred for a further two hours. The acetone was then removed *in vacuo*, and the solution was adjusted to pH 3 with 0.5M HCl. The mixture was extracted three times with ethyl acetate; the collected organics were combined, dried over $MgSO_4$, and concentrated under reduced pressure. The product did not require purification (311.8 mg, 18.9%). Complex set of 2 rotamers: ^{1}H NMR (600 MHz, Chloroform-*d*) δ 4.20 – 4.00 (m, 1H), 3.34 (d, J = 18.4 Hz, 2H), 3.17 – 2.78 (m, 1H), 2.46 (dt, J = 17.9, 8.8 Hz, 1H), 2.14 – 2.01 (m, 1H), 1.82 (td, J = 20.7, 18.6, 10.4 Hz, 3H), 1.48 – 1.39 (m, 9H). ^{13}C NMR (151 MHz, Chloroform-*d*) δ 167.27, 154.27, 85.10, 64.64, 53.40, 46.58, 40.23, 31.15, 28.41, 27.34, 23.50, 22.73. **Appendices 9-10.**

(R)-N-Boc-2-(2-hydroxyethyl)pyrrolidine **(8)**

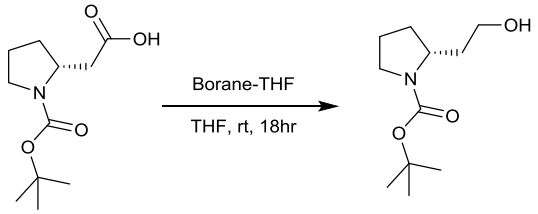

To a solution of **6** (311.8 mg, 1.36 mmol) in THF (15 mL) was added borane-THF (1M, 13 mL) under nitrogen. The solution was allowed to stir for 18 hours at room temperature. The mixture was then diluted with methanol, and concentrated under reduced pressure. To the residue was added chloroform (20 mL) the organic layer was then washed with water (20 mL), and then brine (20 mL). The organics were collected, dried over $MgSO_4$, and concentred *in vacuo* to give the title compound which did not require further purification (127.9 mg, 43.7%). Complex set of two rotamers. ^{1}H NMR (400 MHz, Chloroform-*d*) δ 4.39 (br s, 1H), 4.19 – 4.07 (m, 1H), 3.59 (dq, J = 19.6, 11.5, 8.9 Hz, 2H), 3.30 (dd, J = 6.9, 4.8 Hz, 2H), 2.03 – 1.73 (m, 3H), 1.73 – 1.52 (m, 3H), 1.45 (d, J = 2.4 Hz, 9H). **Appendix 11.** Rf = 0.34 (1:1 EtOAc:Hept).

tert-Butyl (R)-2-(2-(4-methylpiperidin-1-yl)ethyl)pyrrolidine-1-carboxylate **(9):**

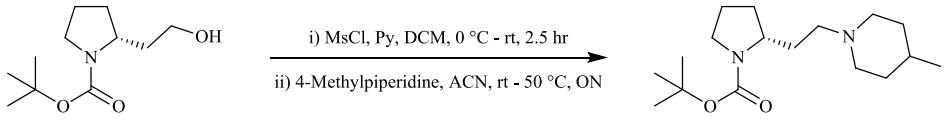

7 (127.9 mg, 0.6 mmol) was dissolved in anhydrous pyridine (3 mL), to which was added methansulfonyl chloride (70 µL, 0.9 mmol) at 0 °C under nitrogen. The solution was allowed to warm to room temperature, and stirred for a further 2 hours. The solution was then diluted with water, and extracted with DCM (3x 5 mL). The organics were collected, dried over $MgSO_4$, and concentrated to give crude mesylate. This was then dissolved in anhydrous acetonitrile (2 mL) and 4-methylpiperdine (110 µL, 0.9 mmol) was added. The mixture was stirred overnight at room temperature, and warmed then warmed to 50 °C for 90 minutes. The acetonitrile was then removed *in vacuo*, and the residue was diluted with DCM. The organic layer was washed with saturated aqueous $NaHCO_3$ and then concentrated. The crude mixture was purified by flash chromatography (petroleum ether/EtOAc/TEA 49.5:49.5:1) to give pure product of sufficient purity (11.3 mg, 6.4%). ^{1}H NMR (400 MHz, Chloroform-*d*) δ 3.75 (d, J = 9.6 Hz, 1H), 3.46 – 3.24 (m, 2H), 2.96 – 2.83 (m, 2H), 2.41 – 2.25 (m, 2H), 2.09 – 1.55 (m, 11H), 1.45 (s, 9H), 1.25 (s, 3H), 0.91 (d, J = 6.4 Hz, 3H). ^{13}C NMR (151 MHz, Chloroform-*d*) δ 154.78, 79.25, 56.35,

54.26, 53.87, 46.61, 46.38, 46.15, 34.36, 32.08, 30.87, 29.85, 28.73, 23.91, 21.99. **Appendices 12-13.** Rf = 0.5 (1:1 EtOAc:Hept).

Radiosynthesis

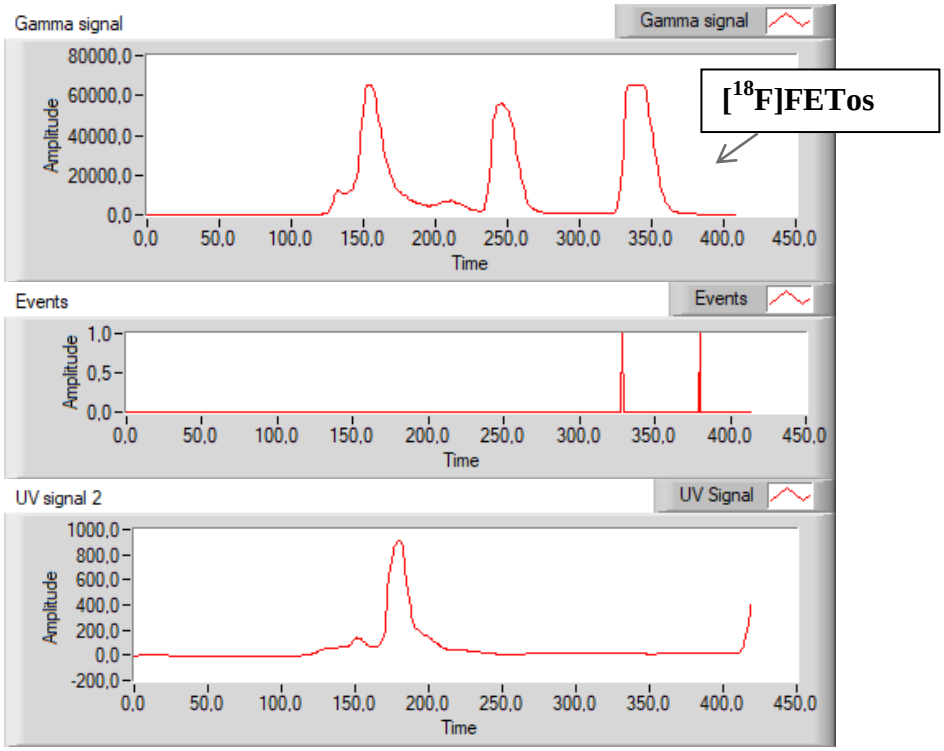

Supporting Figure 2: Semi-preparative HPLC chromatograms for isolation of [^{18}F]FETos.

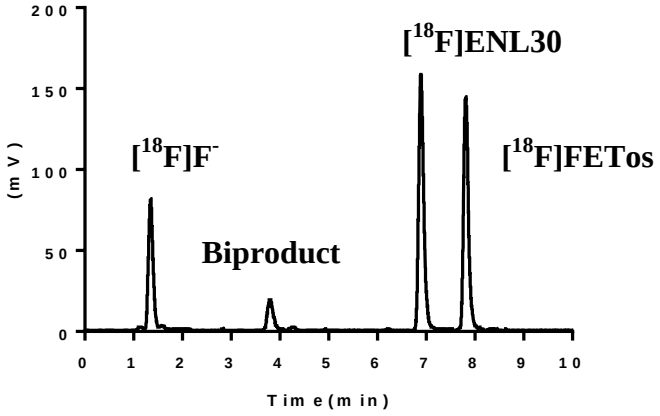

Supporting Figure 3: Analytical HPLC radio chromatogram of the crude reaction mixture.

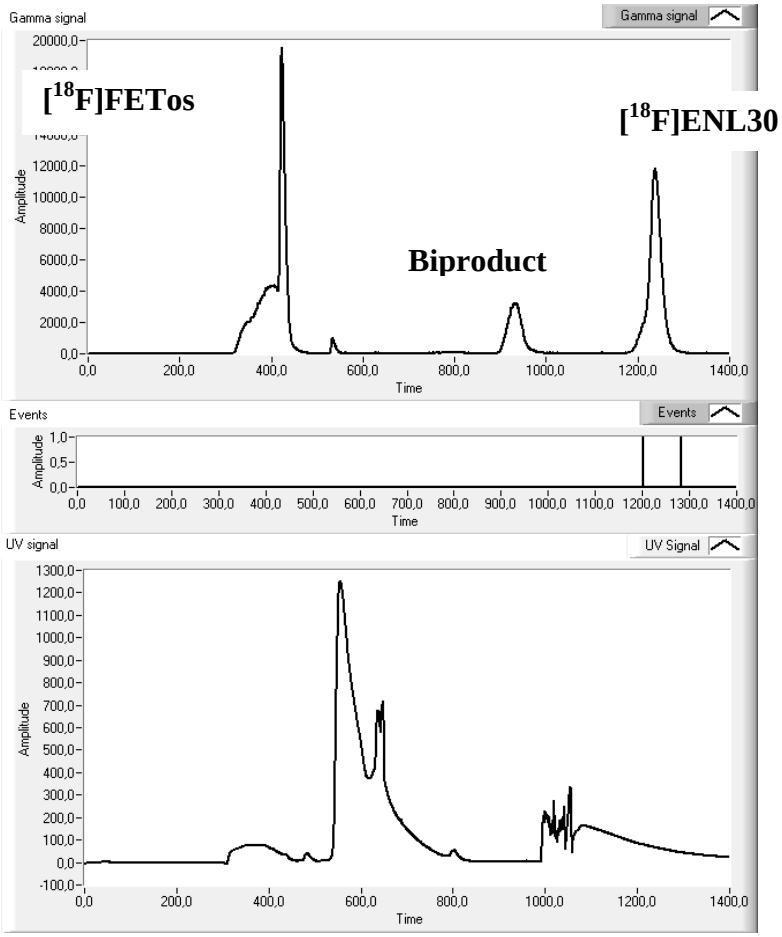

Supporting Figure 4: Semi-preparative HPLC chromatograms for isolation of final product [^{18}F]ENL30

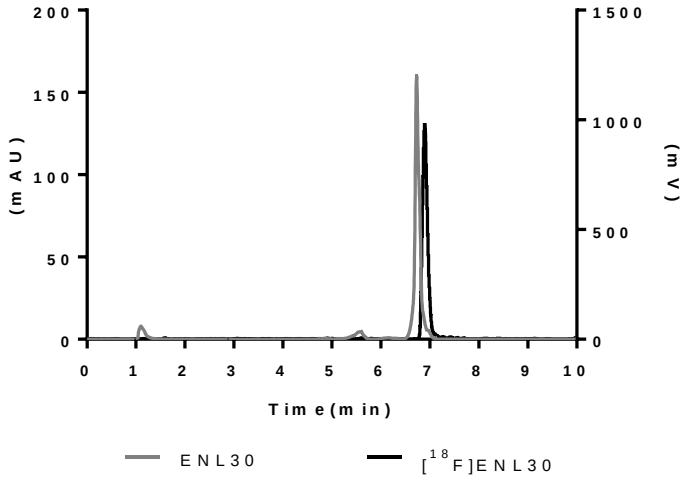

Supporting Figure 5: Analytical HPLC radio and UV chromatograms of the isolated product [^{18}F]ENL30 and reference compound ENL30

In vitro Autoradiography of ***[^{18}F]15***

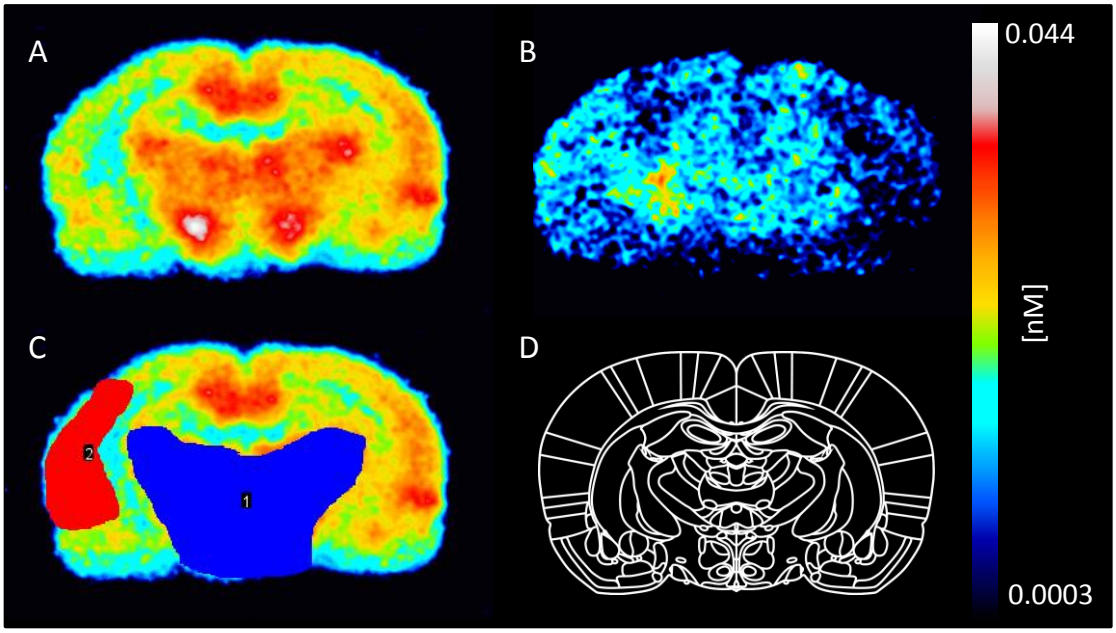

Supporting Figure 6: Results of the *in vitro* autoradiography of **[^{18}F]15**. **a)-d)** Determination of K_d and B_{max} values of **[^{18}F]15** in thalamus (Tha). **a)** Coronal rat brain slice displaying the total binding of **[^{18}F]15**. **b)** Coronal rat brain slice displaying the non-specific binding of **[^{18}F]15** by blocking with SB-269970 (10 µM).**c)** Coronal rat brain slice displaying the total binding of **[^{18}F]15** and the regions of interest, nr 1 was used and contains Tha**. d)** The location of brain slices, around bregma -1.8.

References

1. Hansen, H. D.; Herth, M. M.; Ettrup, A.; Andersen, V. L.; Lehel, S.; Dyssegaard, A.; Kristensen, J. L.; Knudsen, G. M., Radiosynthesis and *in vivo* evaluation of novel radioligands for PET imaging of cerebral 5-HT_7 receptors. *J Nucl Med* **2014,** *55* (4), 640-646.
2. Horisawa, T.; Ishiyama, T.; Ono, M.; Ishibashi, T.; Taiji, M., Binding of lurasidone, a novel antipsychotic, to rat 5-HT_7 receptor: analysis by [^{3}H] SB-269970 autoradiography. *Progress in Neuro-Psychopharmacology and Biological Psychiatry* **2013,** *40*, 132-137.
3. Varnäs, K.; Thomas, D. R.; Tupala, E.; Tiihonen, J.; Hall, H., Distribution of 5-HT_7 receptors in the human brain: a preliminary autoradiographic study using [^{3}H] SB-269970. *Neuroscience letters* **2004,** *367* (3), 313-316.
4. Hansen, H. D.; Constantinescu, C. C.; Barret, O.; Herth, M. M.; Magnussen, J. H.; Lehel, S.; Dyssegaard, A.; Colomb, J.; Billard, T.; Zimmer, L., Evaluation of [^{18}F] 2FP3 in pigs and non-human primates. *Journal of Labelled Compounds and Radiopharmaceuticals* **2018**.
5. Paryzek, Z.; Koenig, H.; Tabaczka, B., Ammonium formate/palladium on carbon: a versatile system for catalytic hydrogen transfer reductions of carbon-carbon double bonds. *Synthesis* **2003,** *2003* (13), 2023-2026.

Appendices

Appendix 1 – ^{1}H NMR of **2**

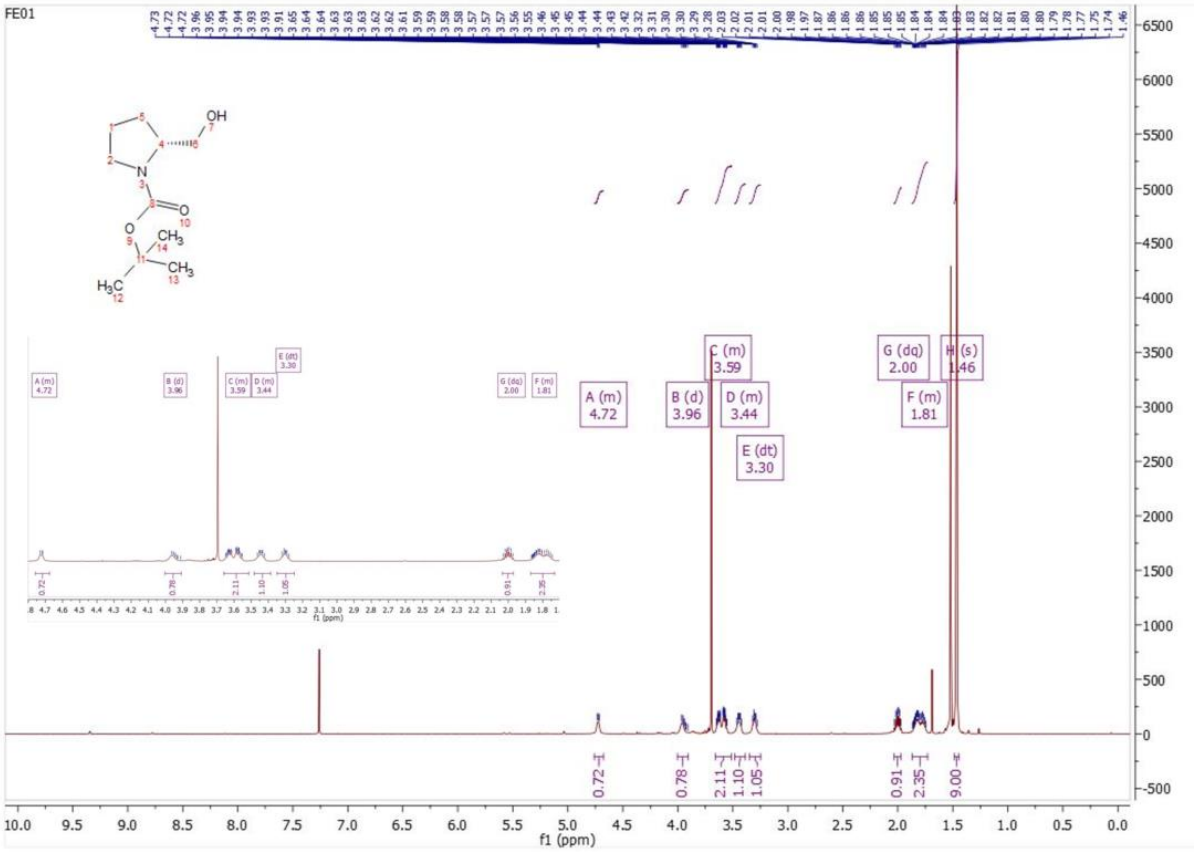

Appendix 2 – ^{13}C NMR of **2**

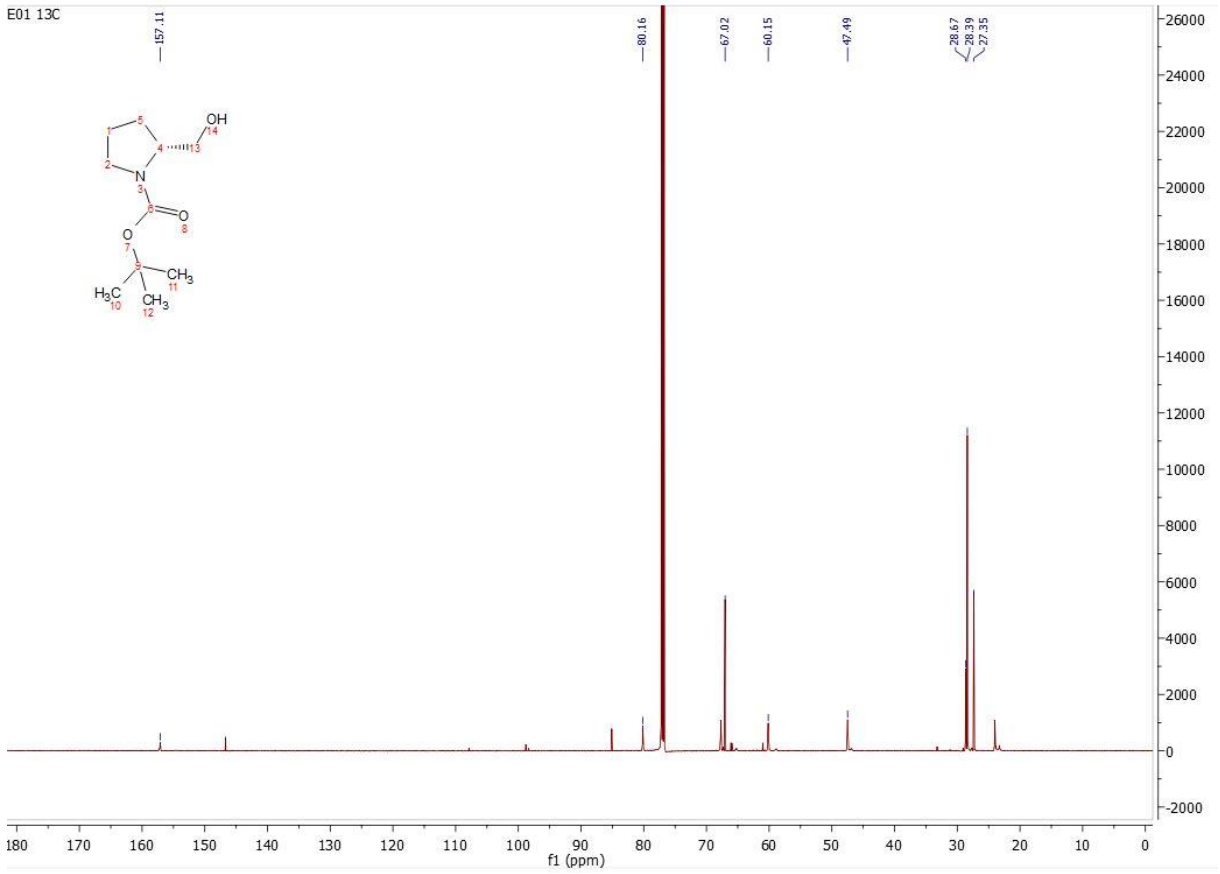

Appendix 3 – ^{1}H NMR of **4**

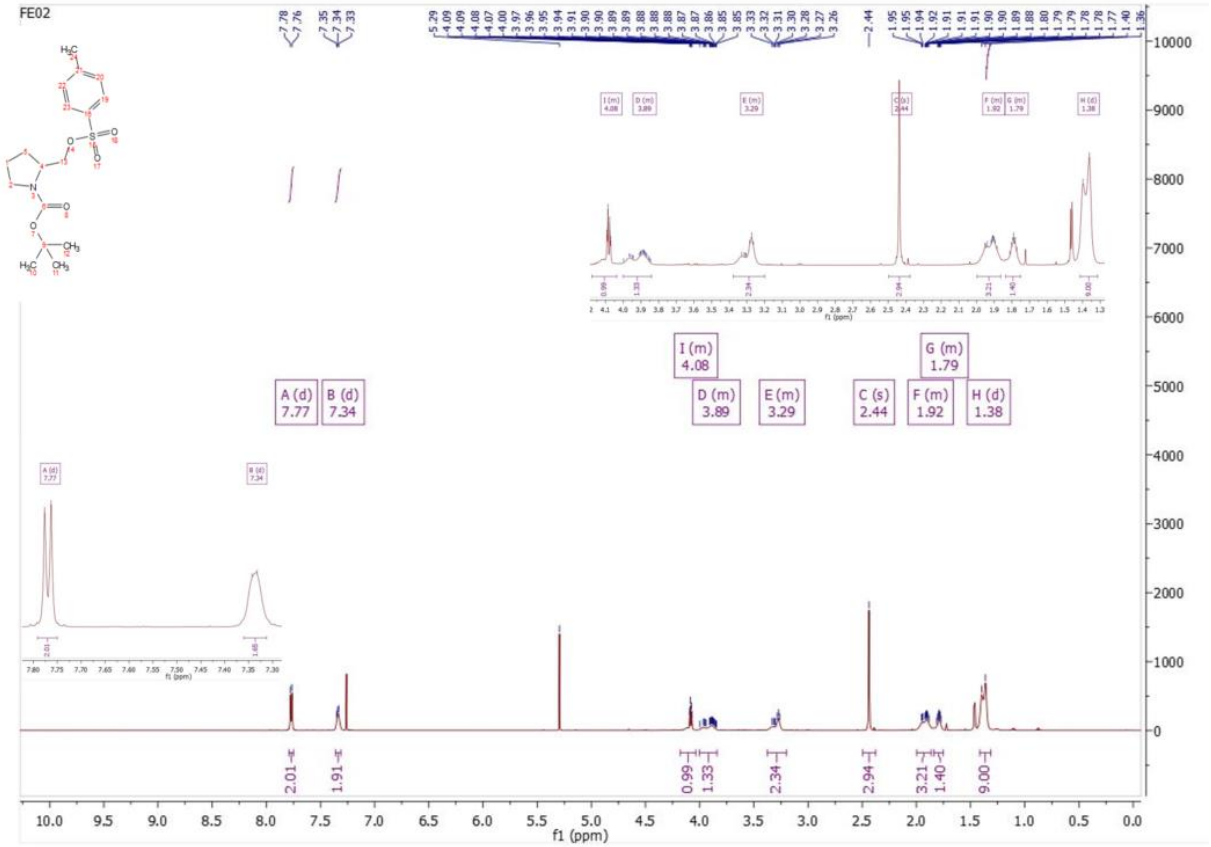

Appendix 4 – ^{13}C NMR of **4**

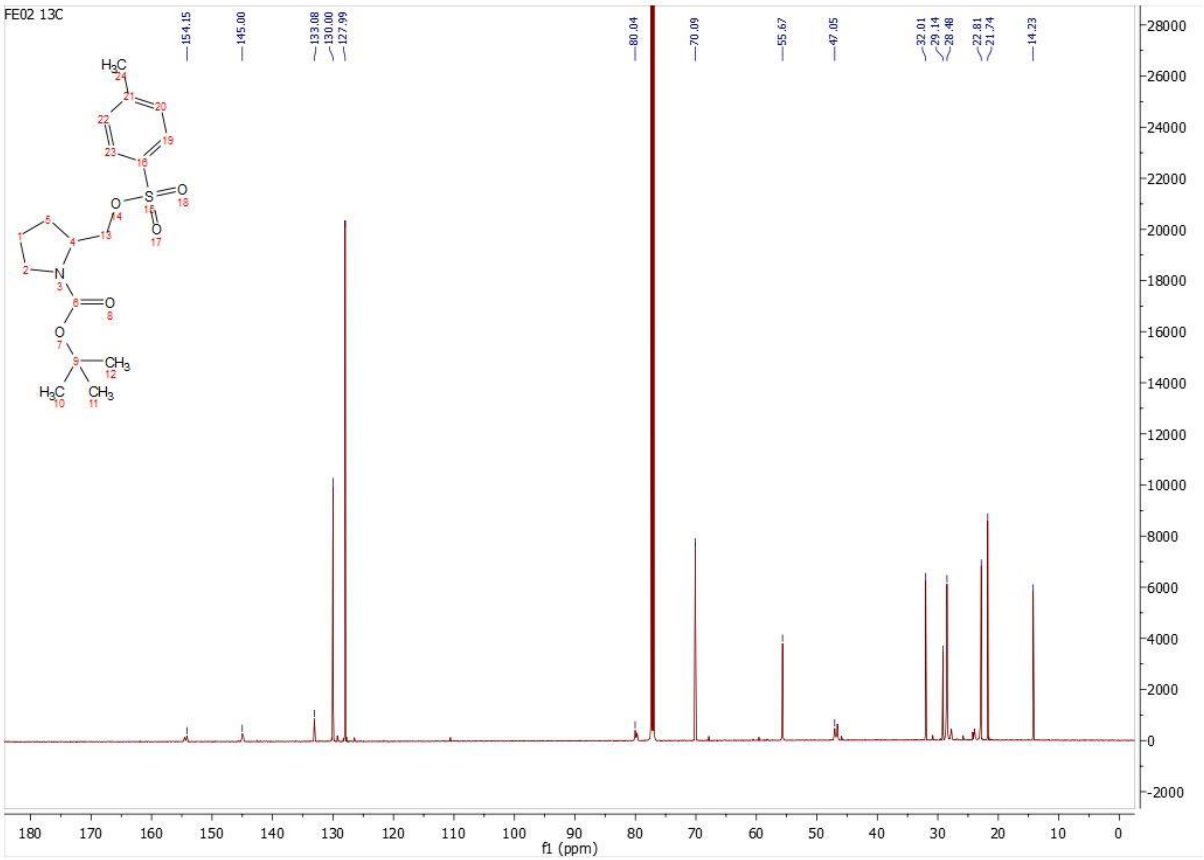

Appendix 5 – ^{1}H NMR of **5**

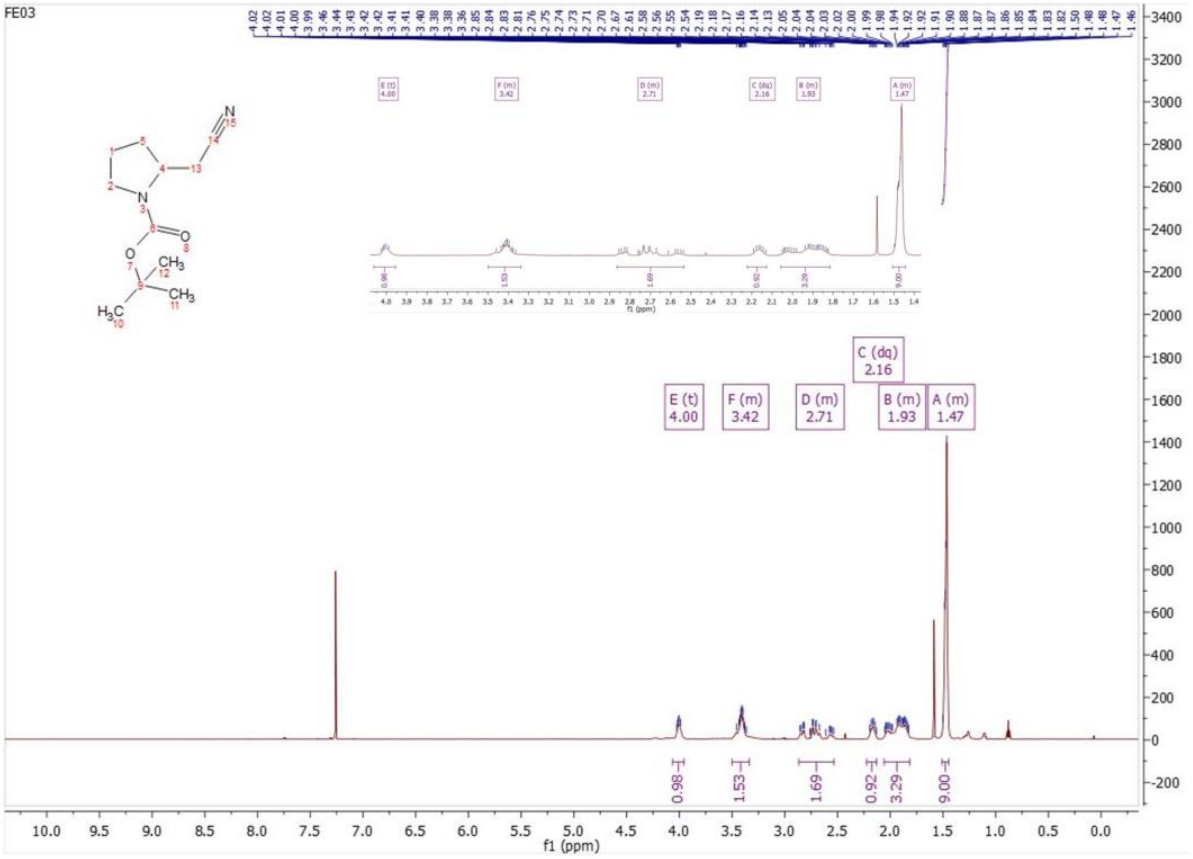

Appendix 6 – ^{13}C NMR of **5**

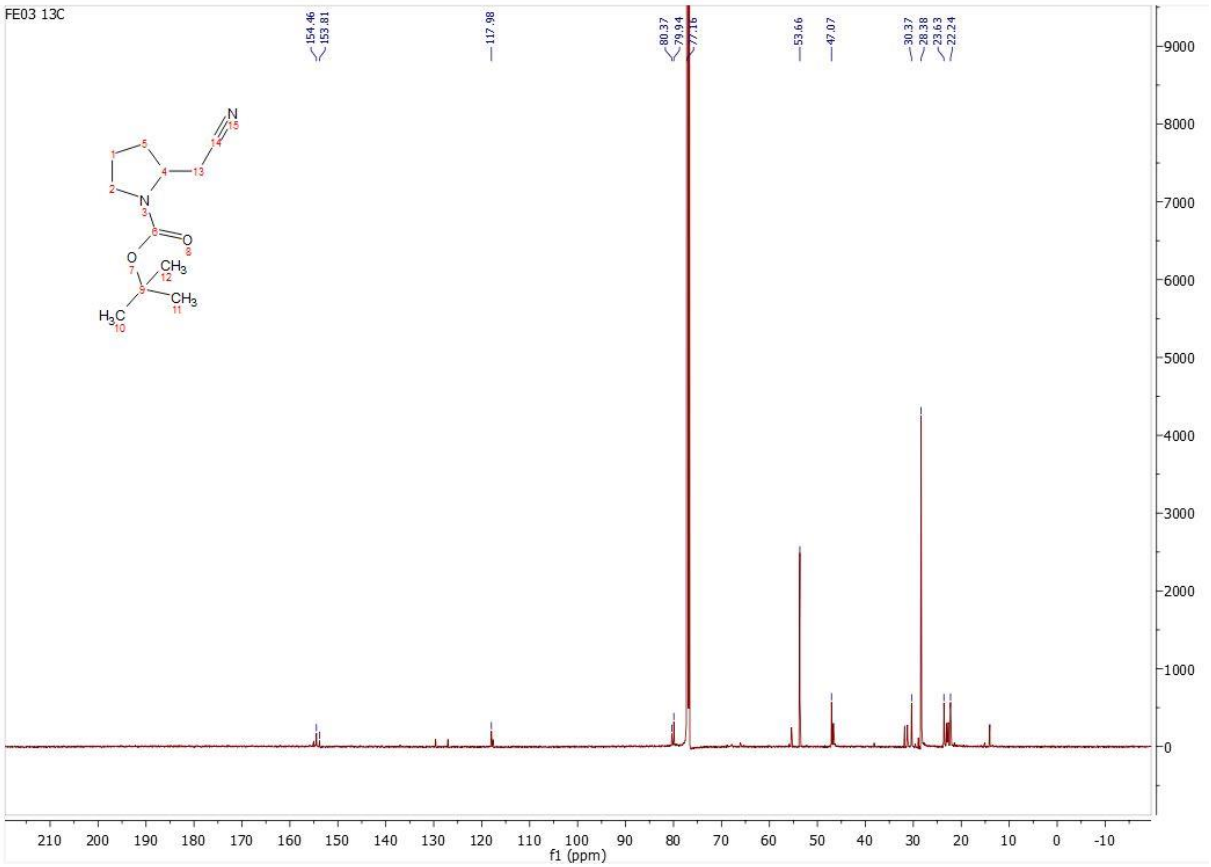

Appendix 7 – ^{1}H NMR of **6**

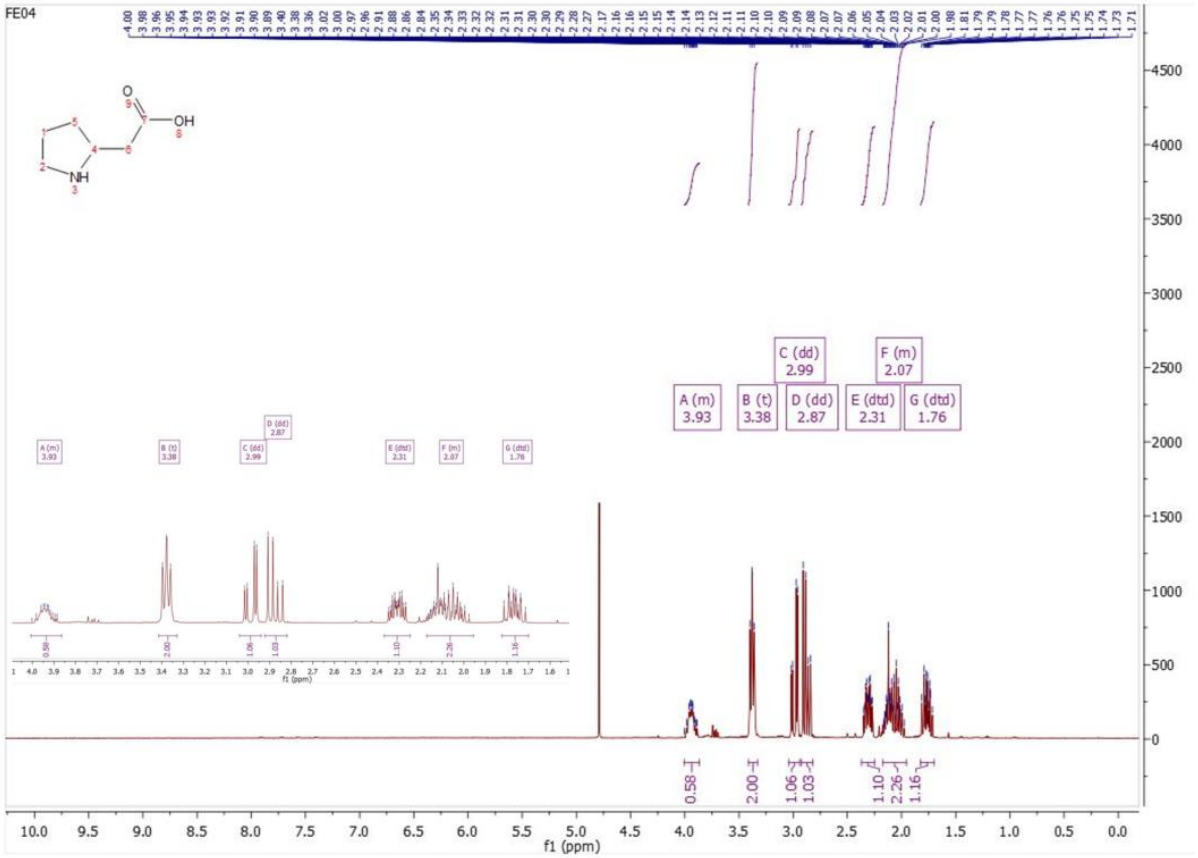

Appendix 8 – ^{13}C NMR of **6**

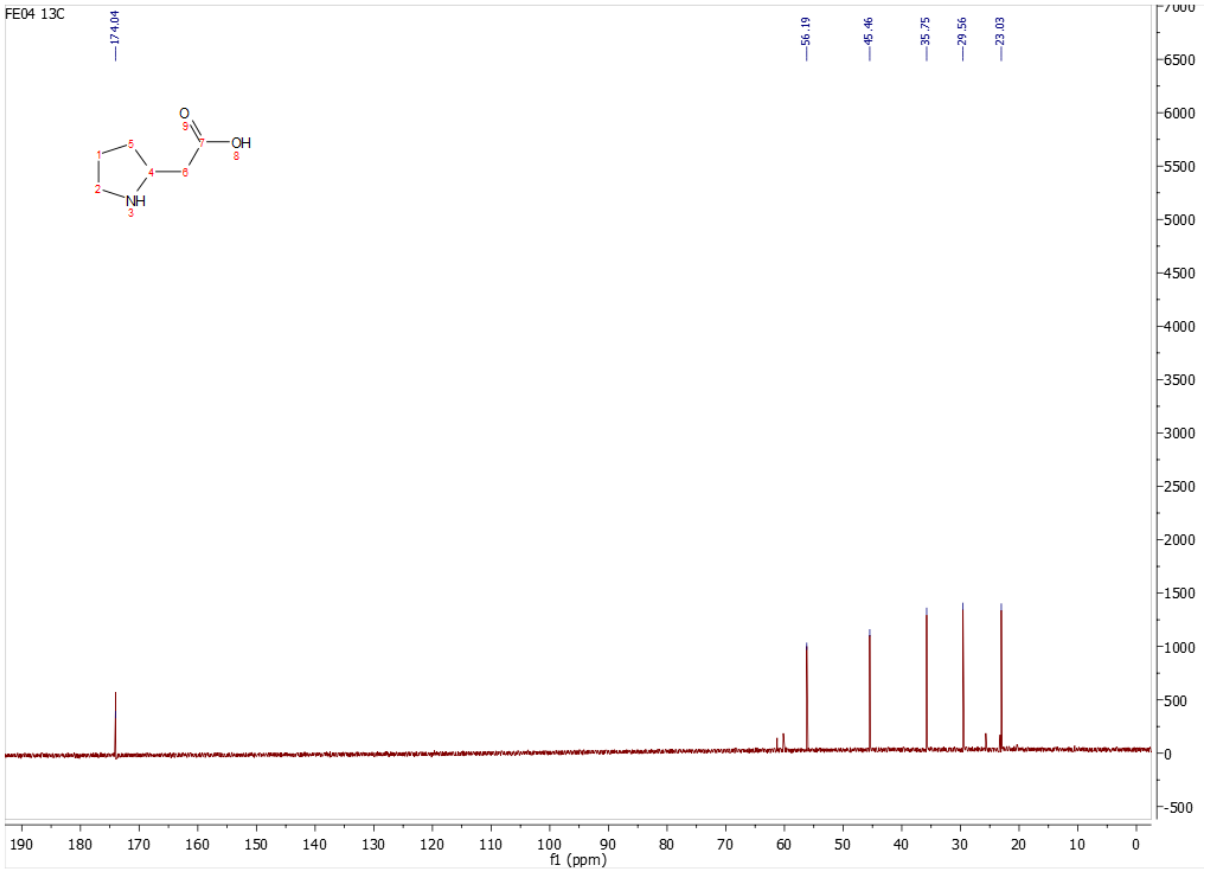

Appendix 9 – ^{1}H NMR of **7**

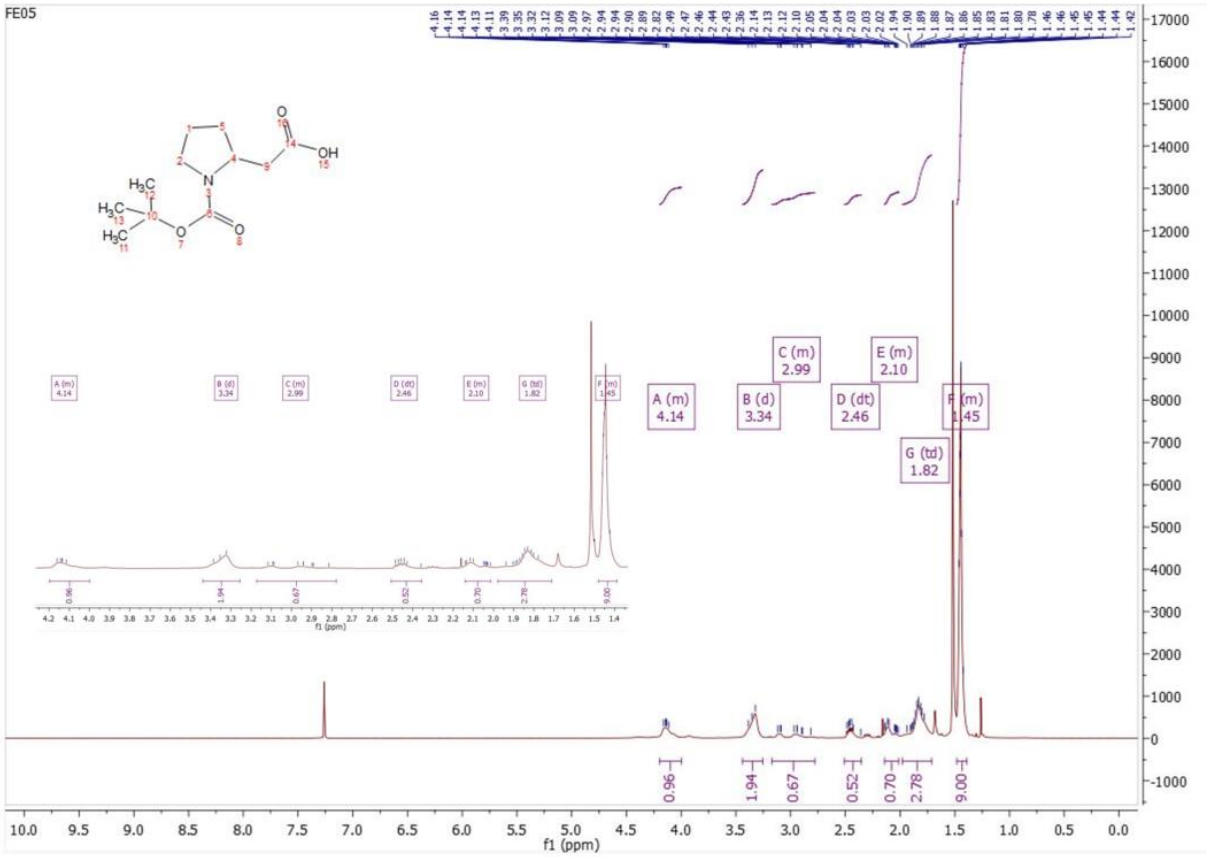

Appendix 10 – ^{13}C NMR of **7**

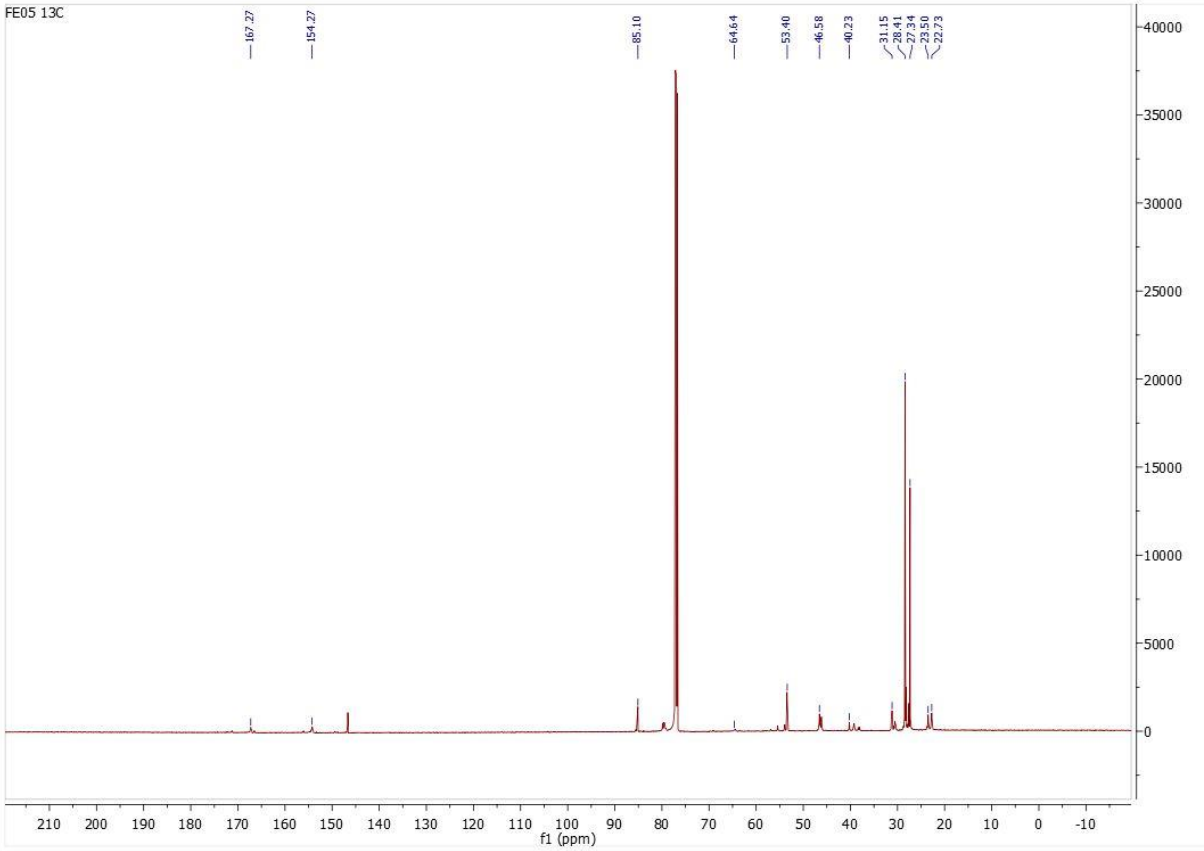

Appendix 11 – ^{1}H NMR of **8**

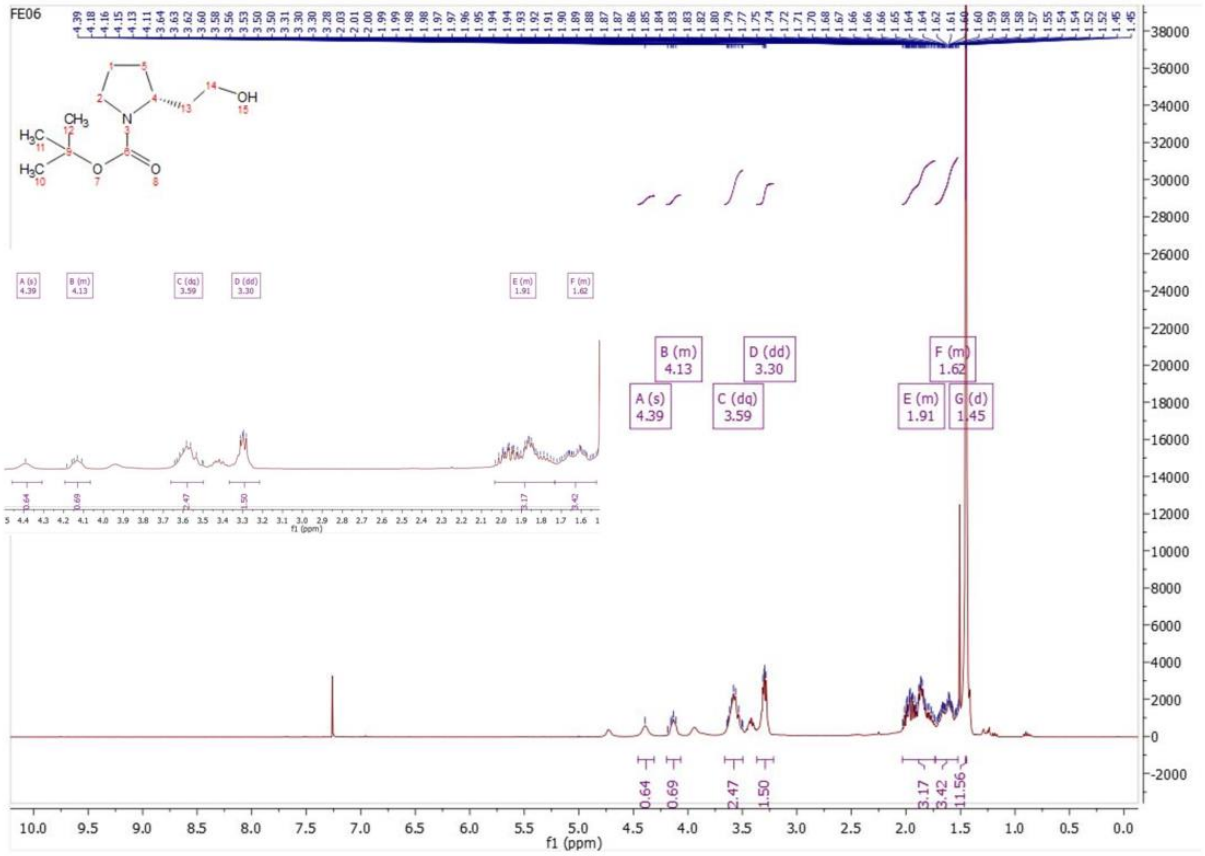

Appendix 12 – ^{1}H NMR of **9**

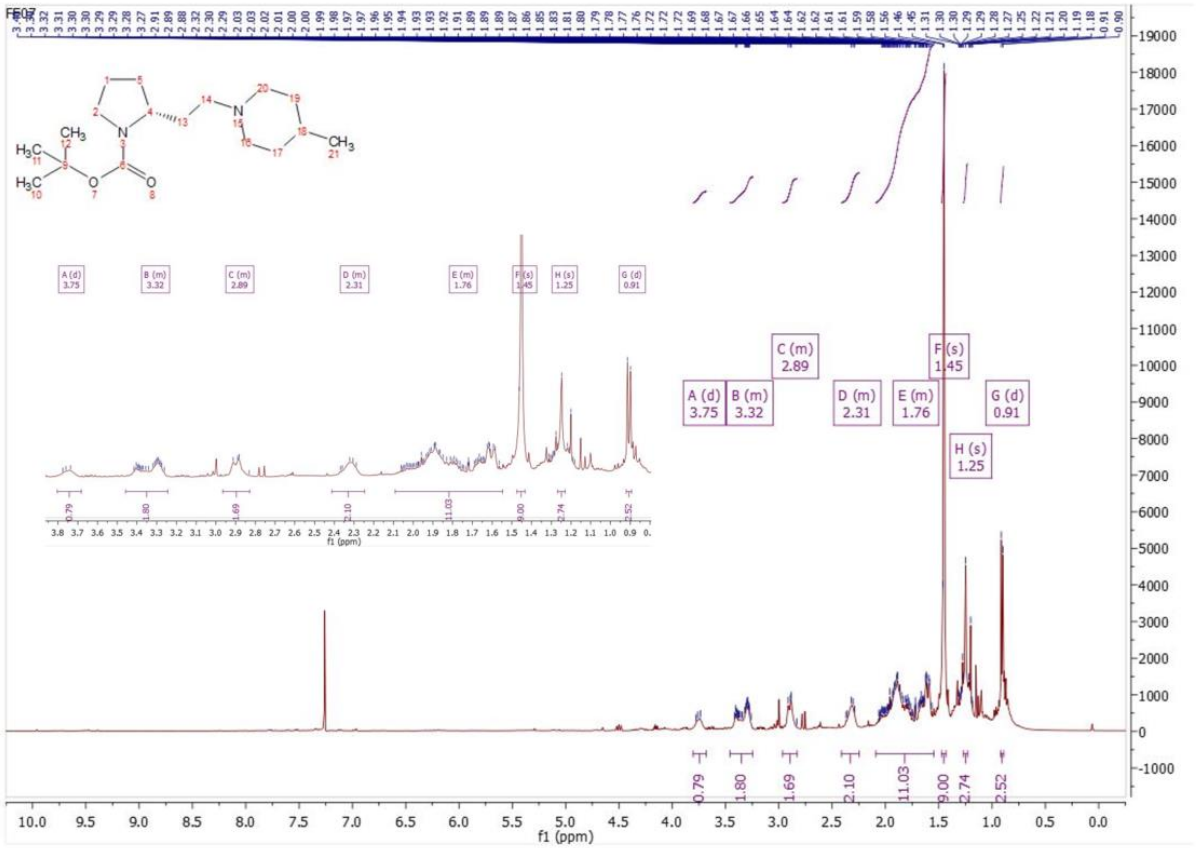

Appendix 13 – ^{13}C NMR of **9**

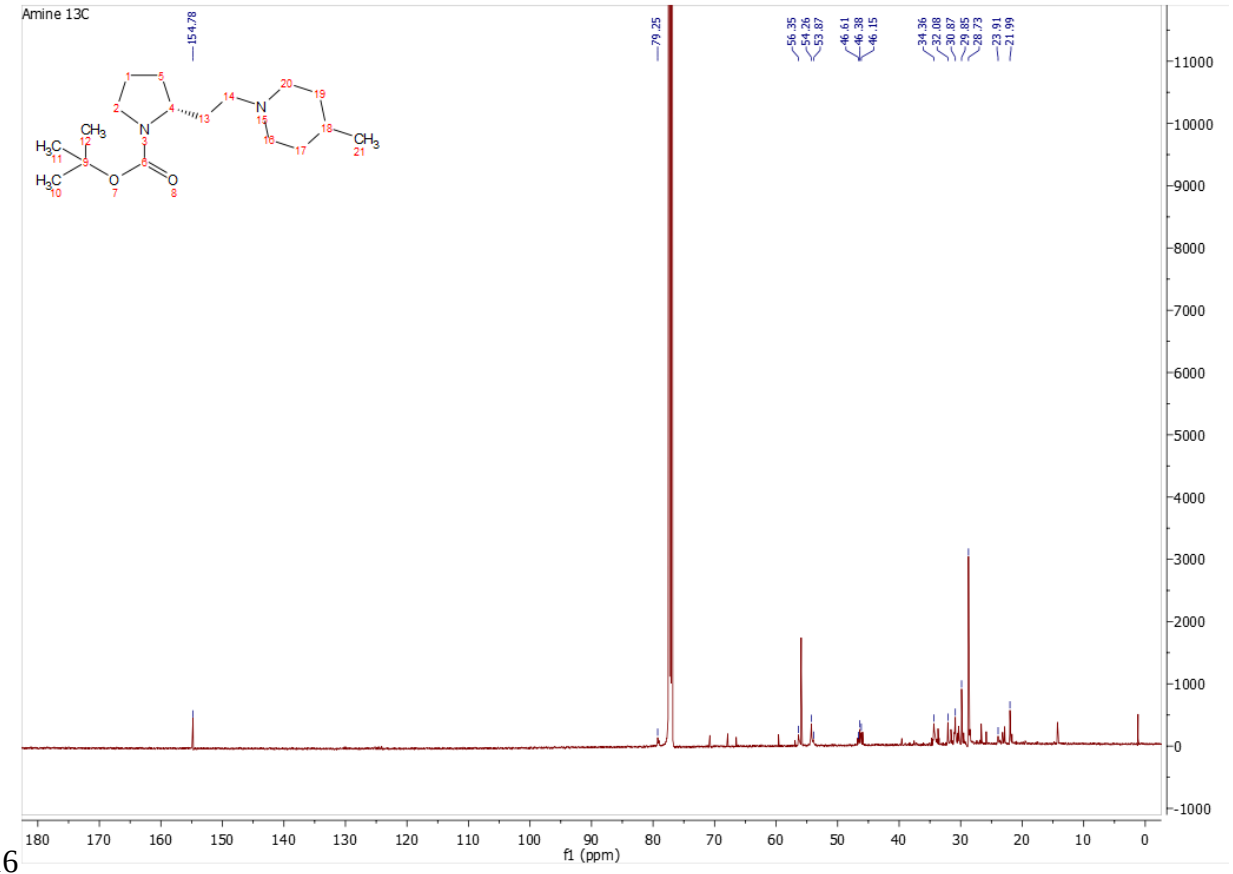

16

Appendix 14 – ^{1}H NMR of **12**

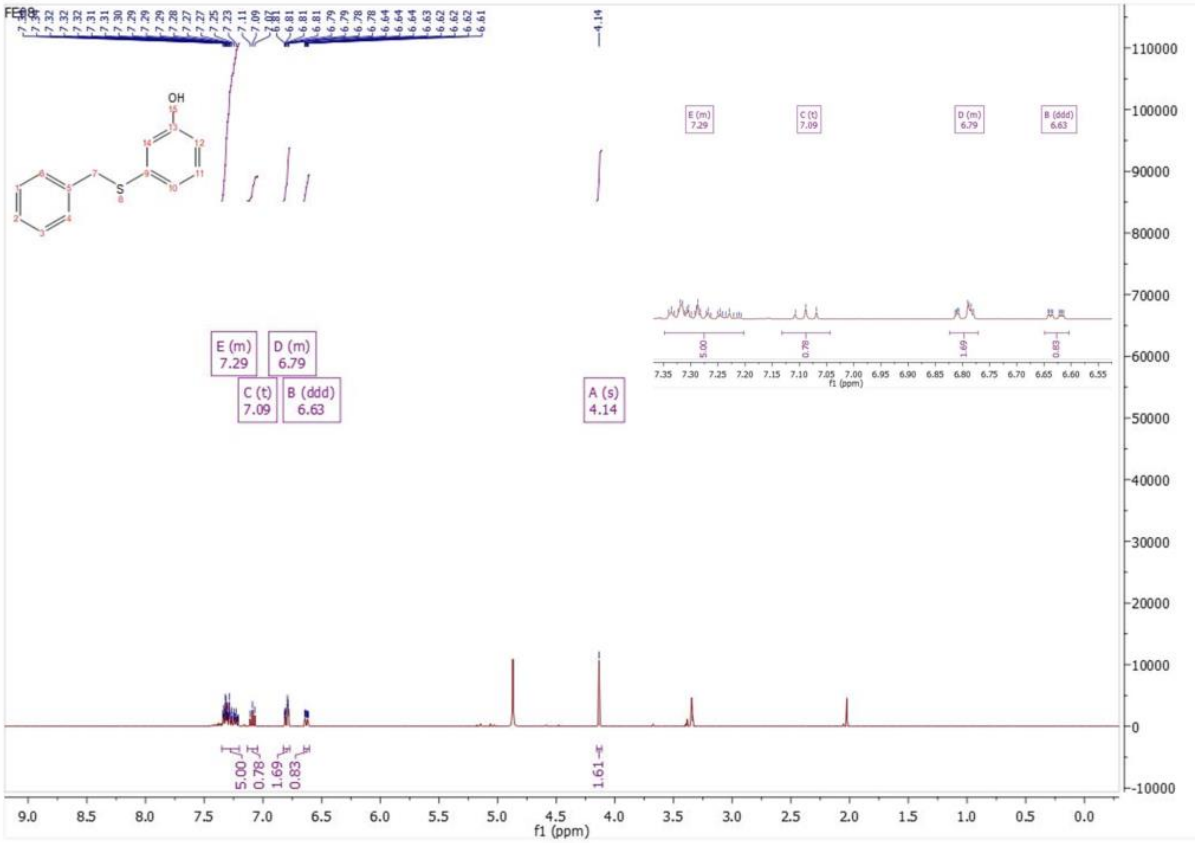

Appendix 15 – ^{1}H NMR of **13**

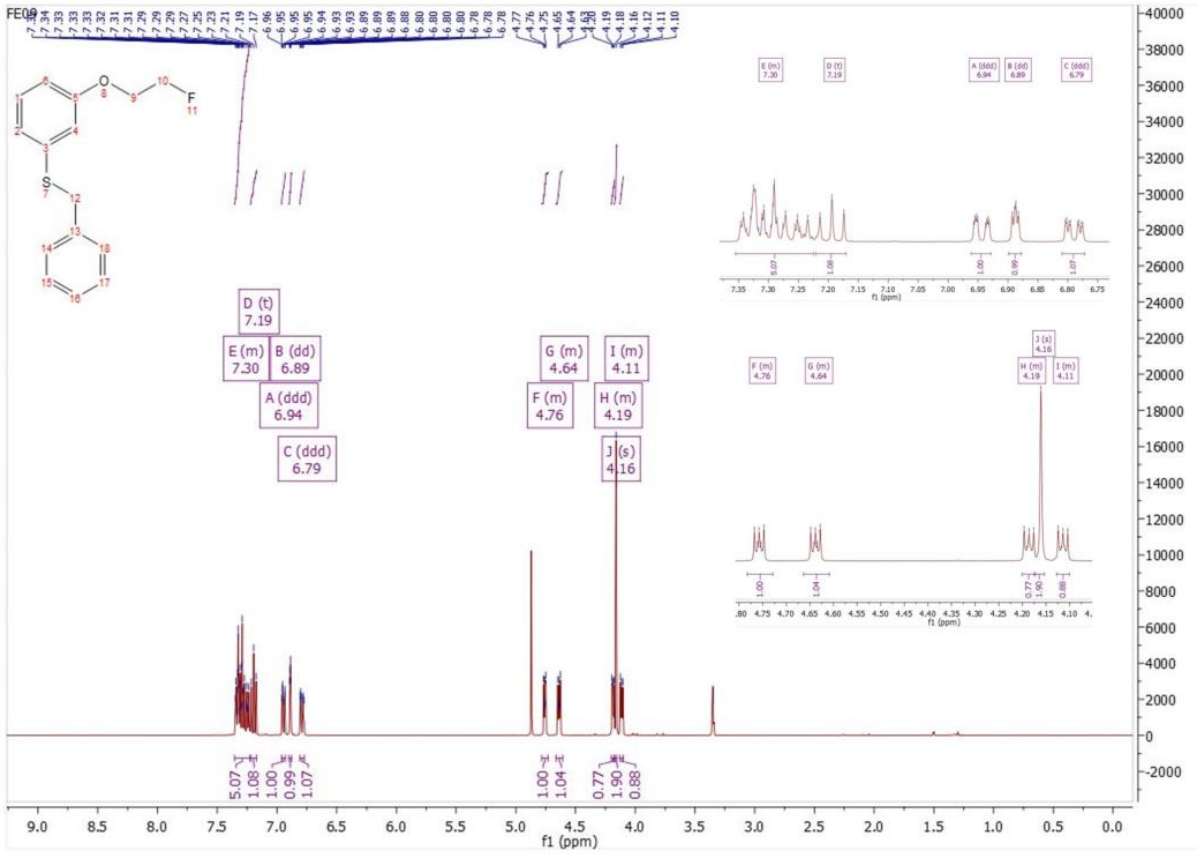

Appendix 16– ^{1}H NMR of **14**

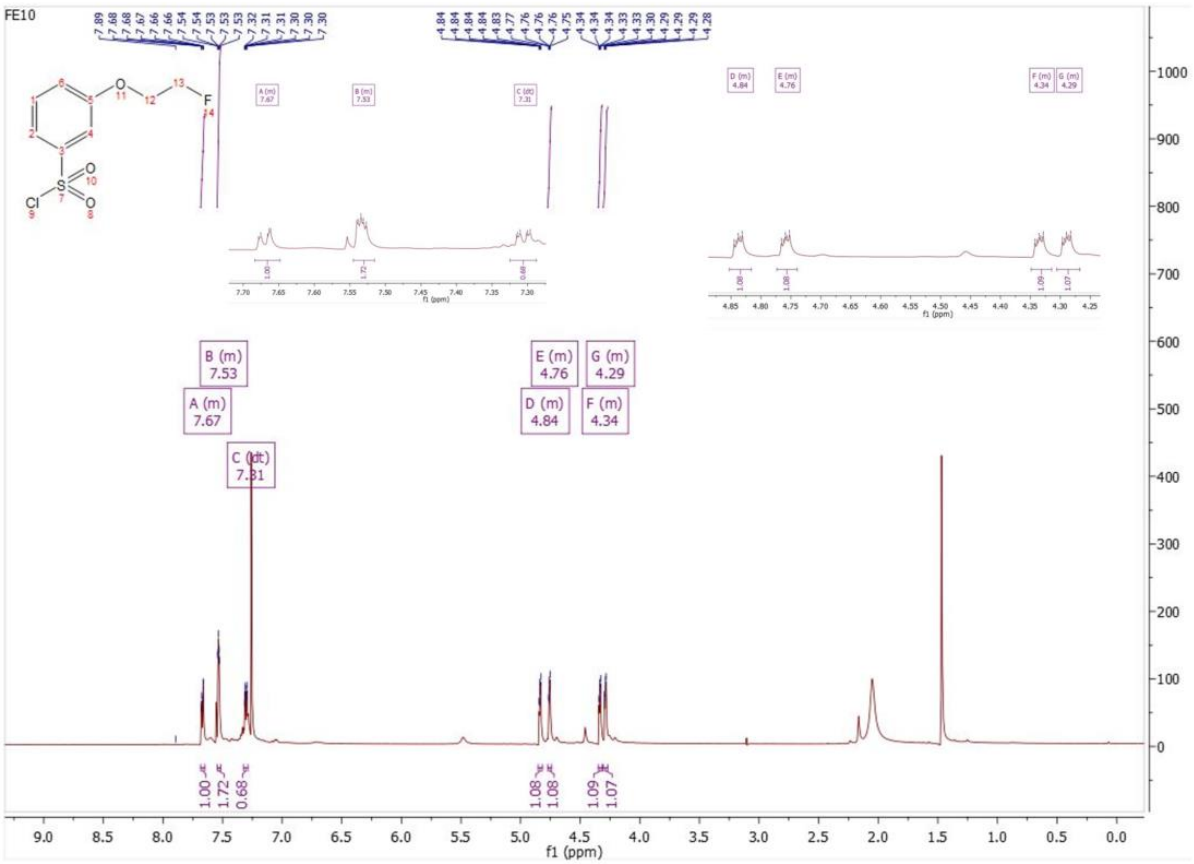

Appendix 17 – ^{13}C NMR of **14**

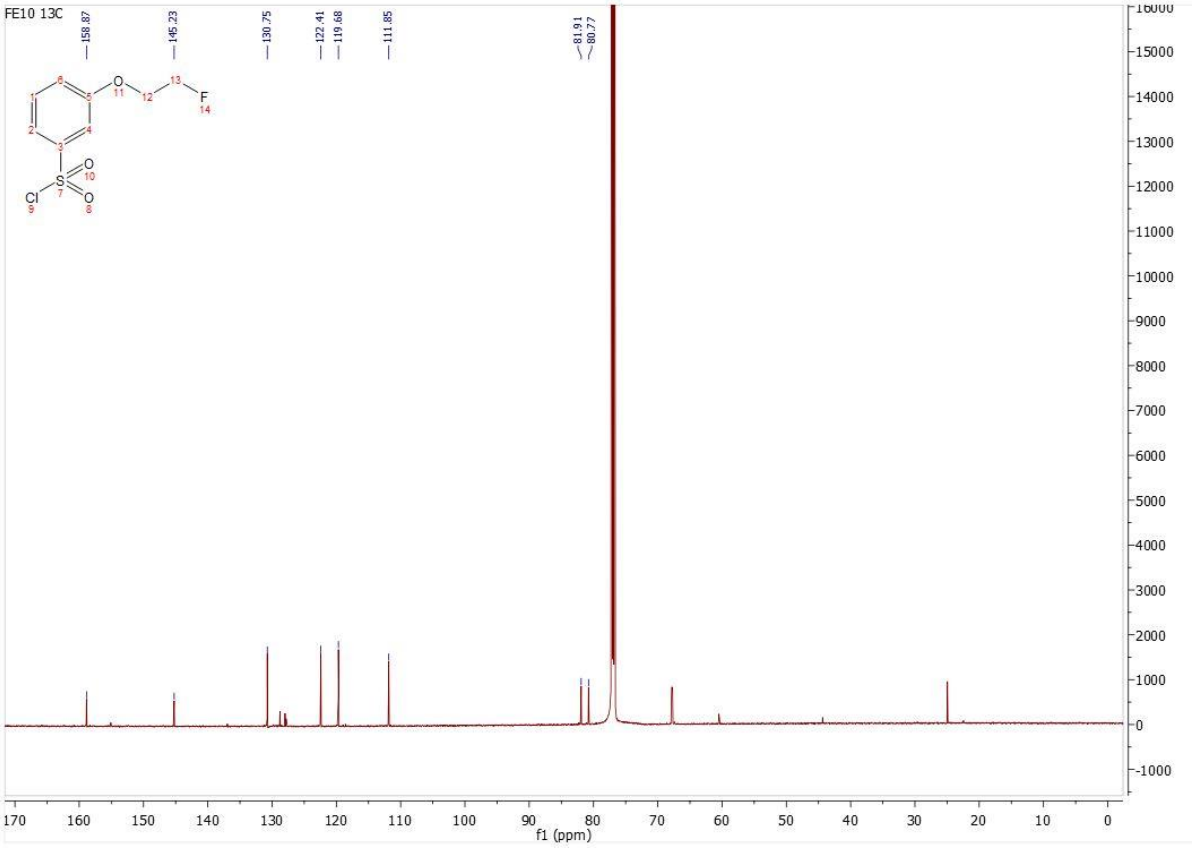

Appendix 18 – ^{1}H NMR of **ENL30 (15)**

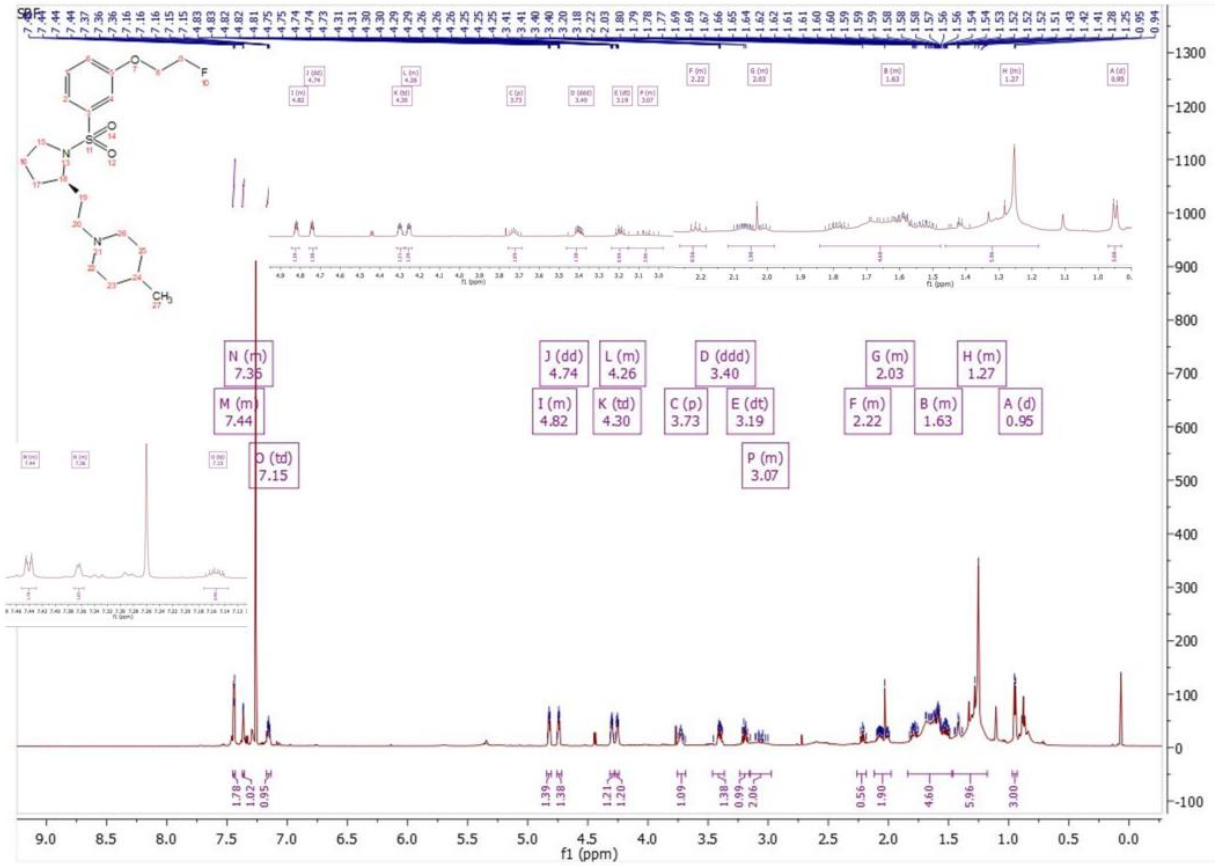

Appendix 19 – ^{13}C NMR of **ENL30 (15)**

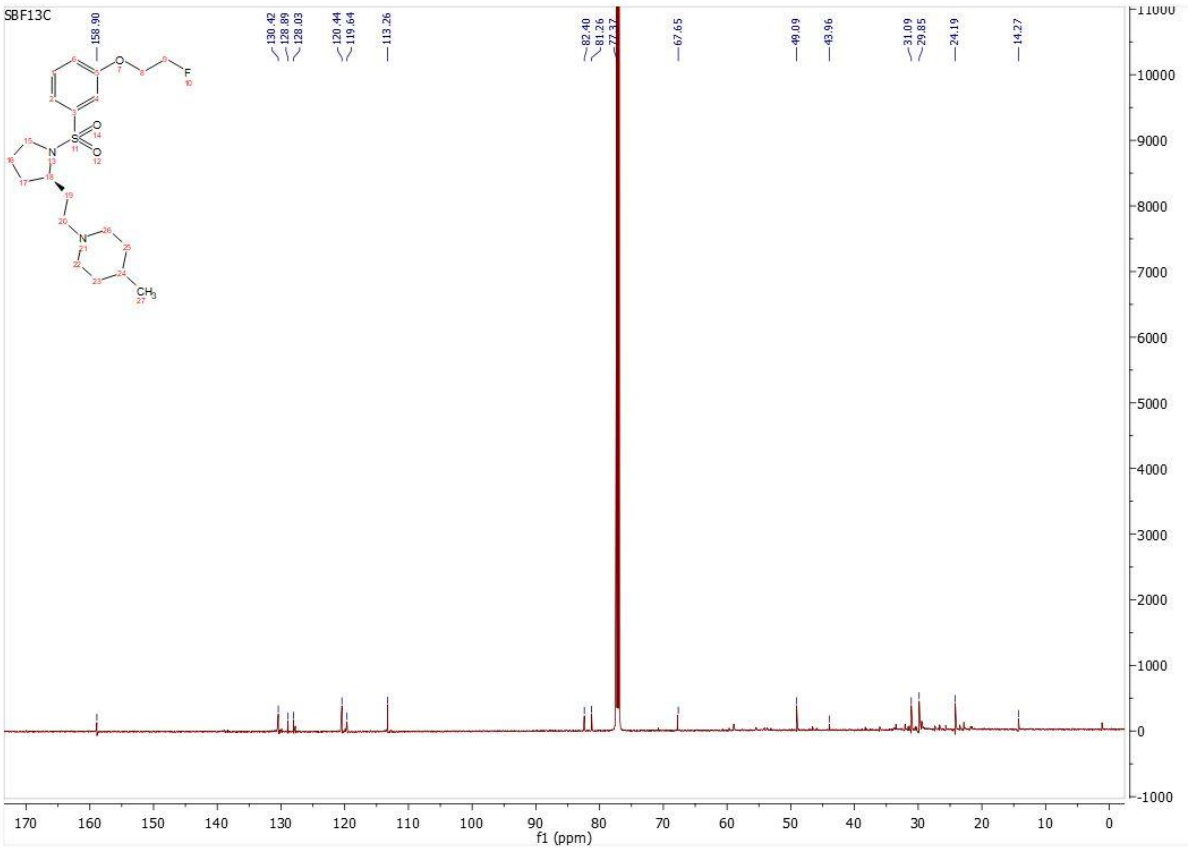

Chapter 9

Summary

Summary:

*This chapter number 9 summarizes the main results acquired in the previously presented **Papers I-VI** (chapter 3 to 8) leading up to the final conclusions and future perspectives presented in the next chapter 10.*

CHAPTER 9 - Summary

Paper I (chapter 3) is a review initially introducing the 5-HT_7 receptor (5-HT_7R). Thereafter, the main challenges and desirable characteristics necessary for developing a 5-HT_7R positron emission tomography (PET) tracer were discussed. Potential 5-HT_7R PET tracers published during the last two decades were subsequently presented and critically evaluated. Concluding remarks relating to the future development of a PET tracer for the 5-HT_7R included the need for higher affinities, perhaps in the sub-nanomolar range, lower affinities for off-targets to enable selective imaging of the receptor and a decreased P-glycoprotein (P-gp) efflux transporter dependency.

In **Paper II** (chapter 4) a newly presented structural class of 5-HT_7R agonists was chosen as the scaffold for developing a potential PET tracer.[1] [^{11}C]AGH-44 was successfully ^{11}C-labelled (Scheme 1), yielding 1.6 ± 0.1 GBq of [^{11}C]AGH-44 in a >96% radiochemical purity and in a radiochemical non-decay corrected yield of 80–90% at the end of synthesis. Typical molar activities were in the range of 637 ± 50 GBq/μmol (time of injection).

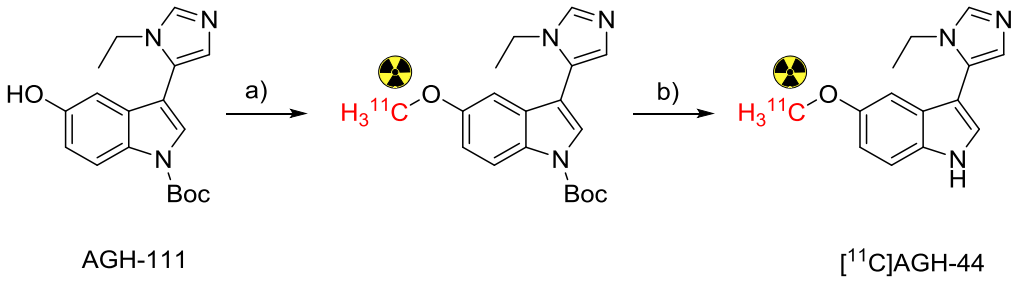

Scheme 1. Radiolabeling of [^{11}C]AGH-44. **a)** [^{11}C]CH_3OTf, Acetone, NaOH (2N), 40°C for 30 s. **b)** TFA, 80°C for 5 min. Scheme is reused from chapter 4.

We subsequently showed by PET imaging that [^{11}C]AGH-44 does not cross the blood-brain barrier (BBB) to any major extent. Inhibition of P-gp efflux transporters with elacridar (5 mg/kg)[2] did not increase brain accumulation to a satisfactory degree (Figure 1). These findings do not provide support to use the structural class of AGH-44 as a starting point for the development of a PET tracer for the 5-HT_7R.

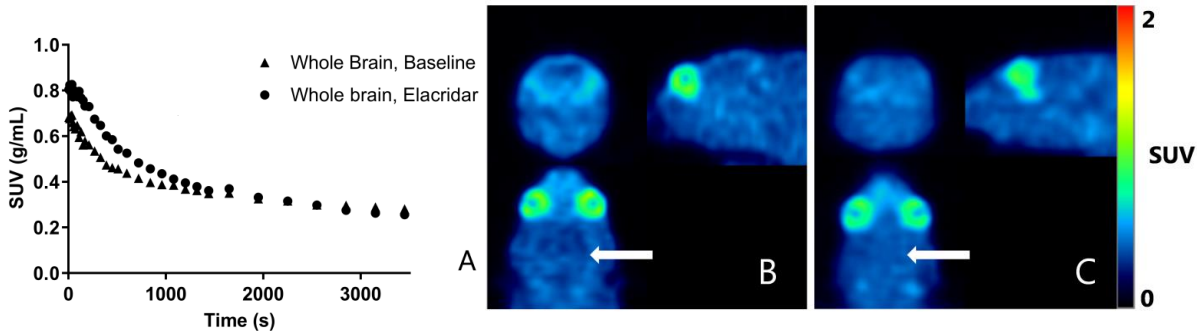

Figure 1. Results of the PET evaluation of [^{11}C]AGH-44 in rat. A) Time-activity curves for the whole rat brain with and without pretreatment with Elacridar (5 mg/kg). **B**) Coronal, sagittal (left to right up) and horizontal (down) summed PET images (baseline scan, 5–60 min) of [^{11}C]AGH-44 in the head of the rat, brain is indicated by white arrow in the horizontal image. **C**) Coronal, sagittal (left to right up) and horizontal (down) summed PET images (Elacridar (5 mg/kg) pretreatment scan, 5–60 min) of [^{11}C]AGH-44 the head of the rat, brain is indicated by white arrow in the horizontal image. **SUV**= standardized uptake value. Figure is reused from chapter 4.

The aim of the work presented in **Paper III** (chapter 5) was to extend the previously described fragment-based labelling strategy, from reductive aminations[3] to condensations of (arylpiperazinyl-butyl)oxindole analogues. The (arylpiperazinyl-butyl)oxindole scaffold was described in 2009 by Volk *et al*. as a high affinity 5-HT$_7$R antagonist.[4] The fragment-based labelling strategy enabled a faster and more efficient method to synthesize a tracer library of potentially selective ^{18}F-labelled 5-HT$_7$R PET tracers. We expanded this throughput scope, by performing dual condensations where the labelled synthon was combined with two fragments and by isolating two radiotracers during the same synthesis (Figure 2).

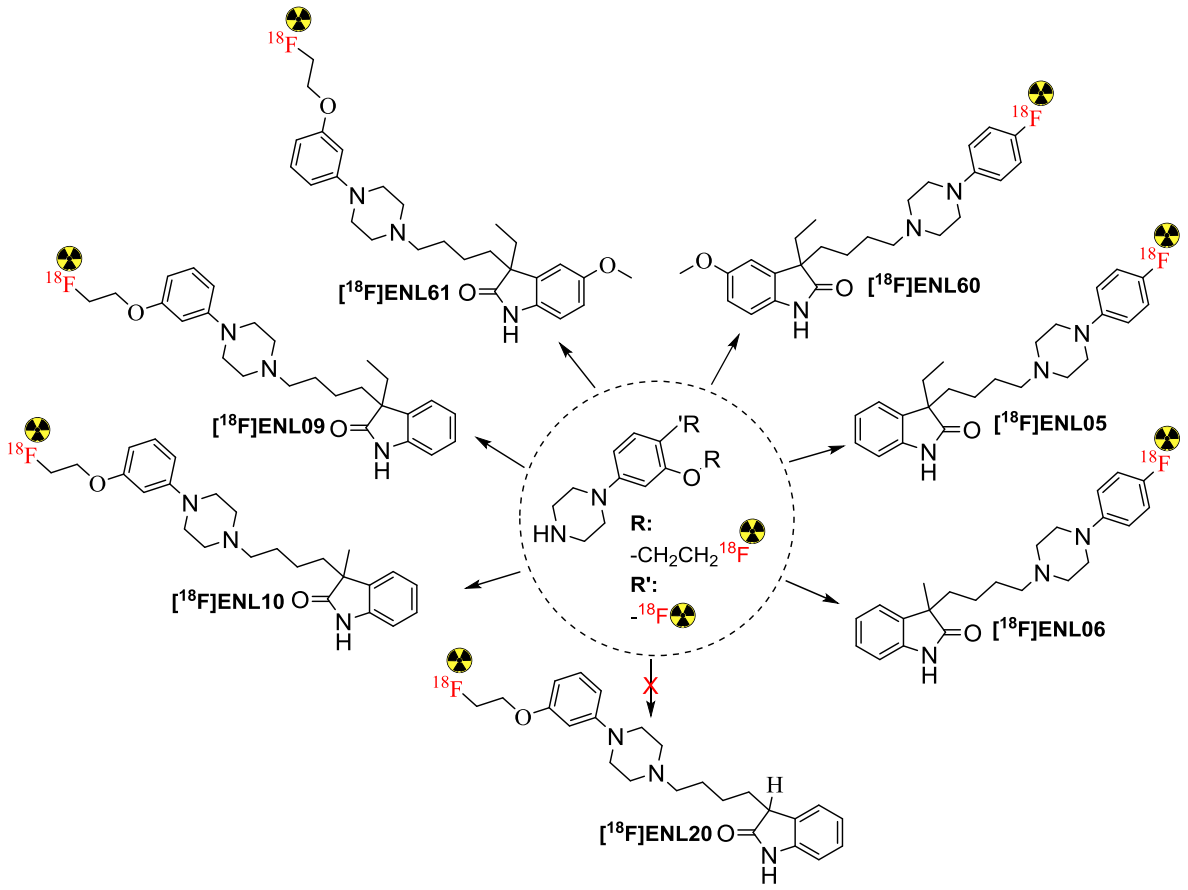

Figure 2: Potential PET tracer for the 5-HT$_7$R synthesised applying the fragment-based labelling strategy. Figure is reused from chapter 5.

In parallel to the syntheses of the 7 reference compounds, the plausibility of the fragment-based labelling strategy was investigated. This was done by ^{11}C-labelling of the synthon and then condensation with a butyloxindole building block synthesizing the previously described PET tracer [^{11}C]Cimbi-775.[5] The strategy was subsequently extended and optimized to S_N2 ^{18}F-labeling of a tosylate precursor, for which the dual-condensation was also successfully established (Figure 3). Finally, the method was used for Cu-mediated ^{18}F-fluorination of boronic pinacole ester precursors.[6] In total, 6 radiotracers were synthesized with moderate radiochemical yields (RCY) (0.2-4.7%), molar activities (1-138 GBq/µmol) and high radiochemical purity >98 %.

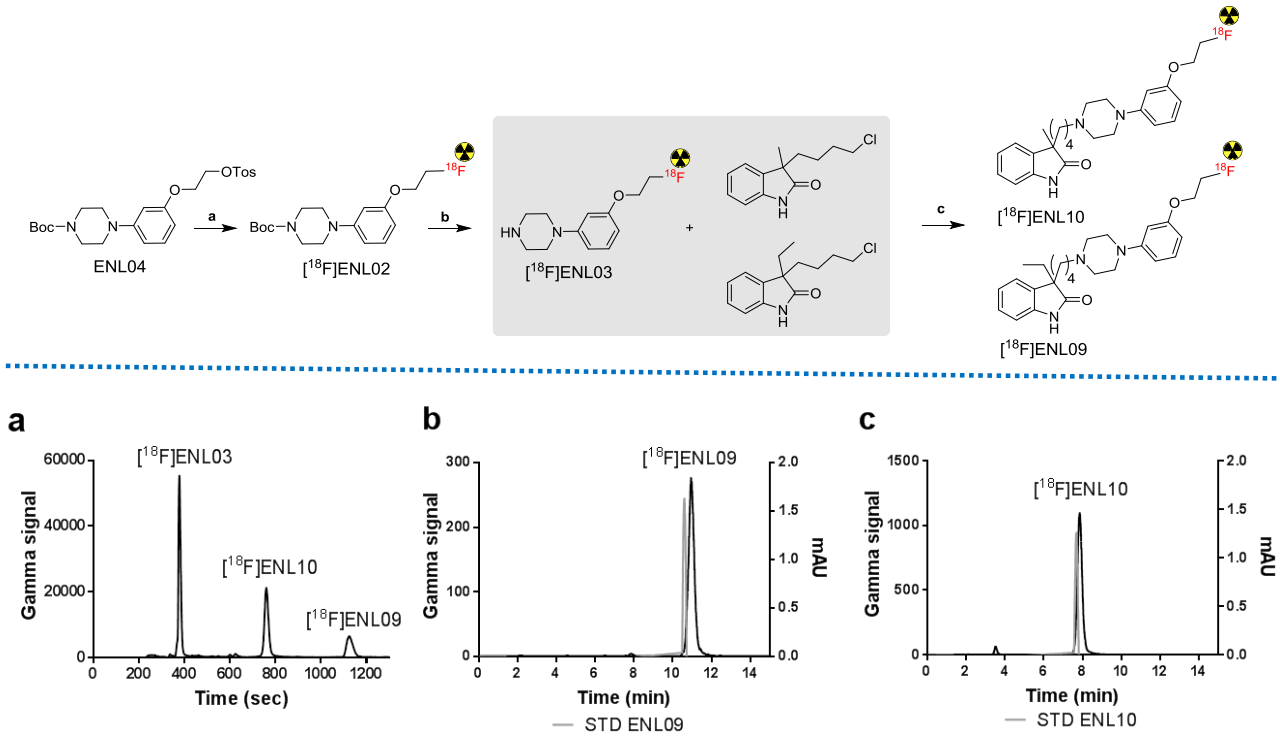

Figure 3: Radiolabelling procedure of [^{18}F]ENL09 and [^{18}F]ENL10. **Upper panel**: Radiolabelling of the synthon [^{18}F]ENL03 and subsequent condensation with two building blocks simultaneously in one-pot. a) [^{18}F]F^- , K_{222}, K_2CO_3, MeCN, 80 °C for 20 min. b) 25% TFA in MeCN at 80 °C for 10 min. c) K_2CO_3, DMSO, 170 °C for 15 min. **Lower panel**: Purification and identification control of [^{18}F]ENL09 and [^{18}F]ENL10 a) Semi-preparative HPLC of [^{18}F]ENL09 and [^{18}F]ENL10 [Luna 5 µm C18(2) 10×250 mm column, flow rate 4 mL/min, eluent: EtOH:0.1% H_3PO_4 in H_20 (30:70)] b) Analytical HPLC analysis [Luna 5 µm C18(2) 4.60×50 mm column, flow rate 1.5 mL/min, eluent: EtOH:0.1% H_3PO_4 in H_20 (30:70)] of [^{18}F]ENL09 and its respective reference ENL09 c) and [^{18}F]ENL10 and ENL10. Figure is reused from chapter 6.

In **Paper IV** (chapter 6), the synthesized library of potential 5-HT_7R PET tracers presented in **Paper III** (chapter 5) was extended to contain a total of 12 (arylpiperazinyl-butyl)oxindole analogues. After reference compound syntheses, the compounds were sent to *in vitro* affinity screening (PDSP). The revealed selectivity profiles that the most tracers displayed indeed 5-HT_7R affinity, but also overall worryingly high affinities for σ-receptors. These receptors are especially troublesome off-targets due to their high abundance in thalamus[7-8], the high density region of the 5-HT_7R.[9-12] [^{18}F]ENL09 and [^{18}F]ENL10 were identified to be the most promising candidates according to their target/off-target ratio. Consequently, both tracers were evaluated in rodents (Figure 3-5).

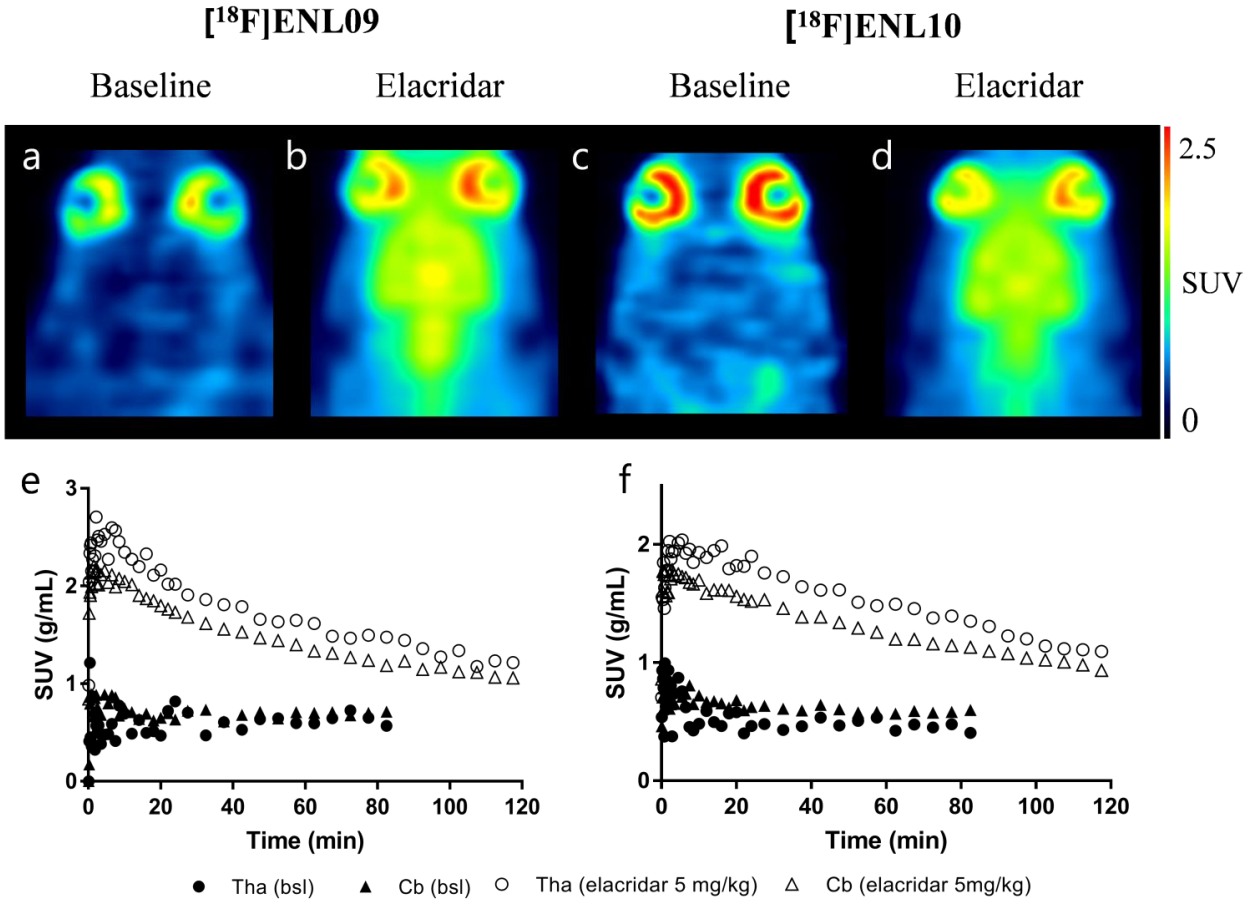

Figure 4: Coronal rat PET images of [^{18}F]ENL09 and [^{18}F]ENL10 (**a-d**) and their representative time-activity curves (TACs) (**e-f**). Summed images are created from a 2-120 min dynamic PET**. a**) Summed PET image of [^{18}F]ENL09 at baseline **b)** Summed PET image of [^{18}F]ENL09 after pretreatment with elacridar (5 mg/kg). **c**) Summed PET image of [^{18}F]ENL10 at baseline **d)** Summed PET image of [^{18}F]ENL10 after pretreatment with elacridar (5 mg/kg).**e)** Thalamus (circles, Tha) and cerebellum (triangles, Cb) TACs for [^{18}F]ENL09 at baseline and after pretreatment with elacridar (5 mg/kg). **f)** Thalamus and cerebellum TACs for [^{18}F]ENL10 at baseline and after pretreatment with elacridar (5 mg/kg). Figure is reused from chapter 6.

The evaluation revealed that both radiotracers displayed a P-gp efflux transporter dependency. This was elucidated by inhibition using elacridar[2], thereby decreasing the BBB efflux. Both PET tracers thereafter showed a brain uptake similar to the regional distribution known for the 5-HT$_7$R (Figure 4).[9-12] Howerer, only [^{18}F]ENL10 showed specific binding to the 5-HT$_7$R by a reduction of the area under the curve (AUC) for the time-activity curves (TACs) after pre-administration of SB-269970.[13] Finally, to investigate the signal contribution due to σ-receptor binding, blocking experiments using haloperidol and SA4503 were performed. The results showed low to no reduction of AUC in either of the explored brain regions for [^{18}F]ENL10, thus a major contribution of σ-receptor binding to the observed signal was excluded (Figure 5).

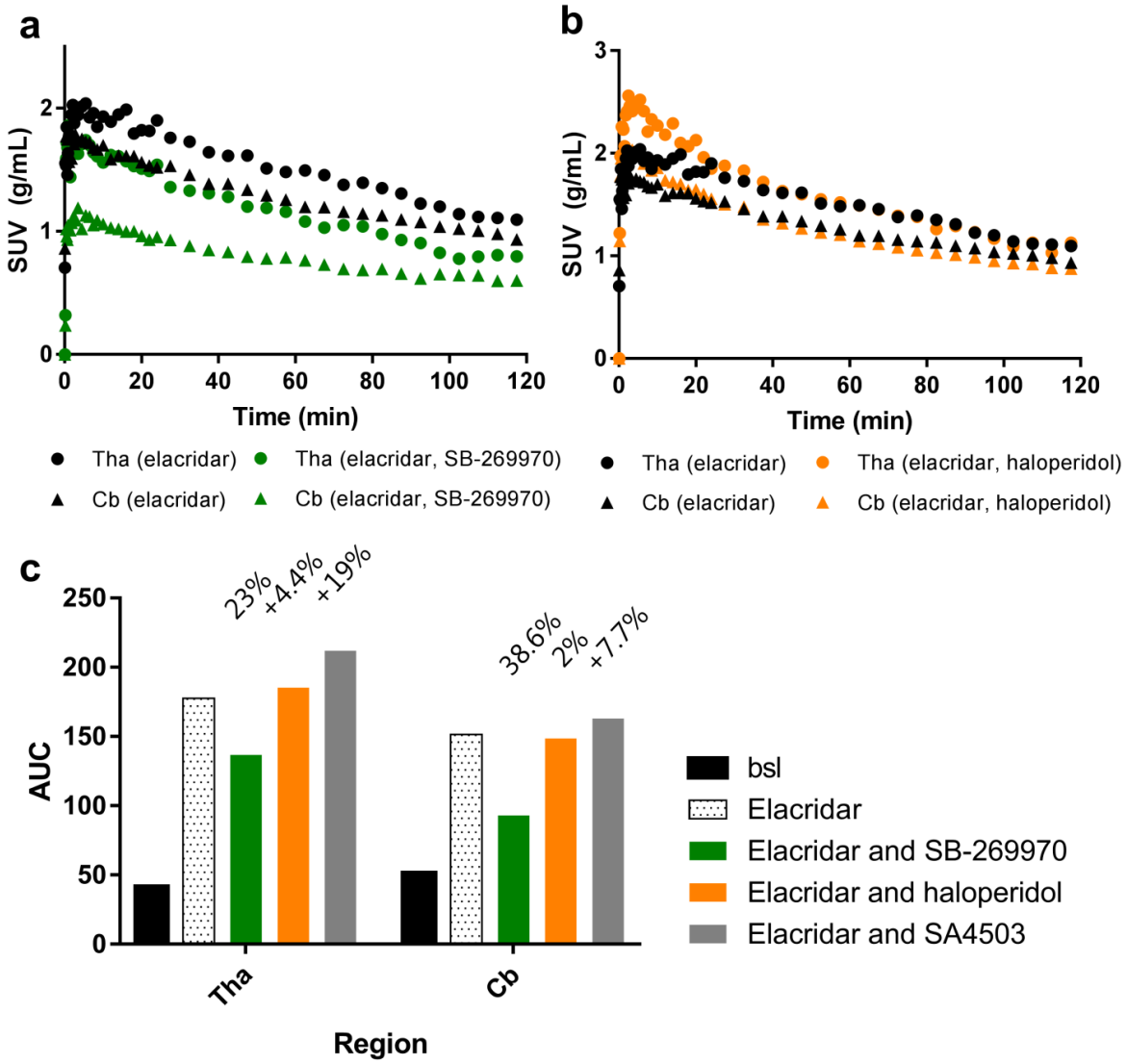

Figure 5: Representative time-activity curves (TACs) of [^{18}F]ENL10 in the thalamus (circles, Tha) and cerebellum (triangles, Cb) in the rat brain. a) Thalamus and cerebellum TACs after pretreatment with elacridar and elacridar + SB-269970 (3 mg/kg). b) Thalamus and cerebellum TACs after pretreatment with elacridar and elacridar + haloperidol (1 mg/kg). c) Calculated area-under-curve (AUC) for all TACs displayed as a grouped barplot. The reduction of AUC compared to elacridar (baseline) is displayed above the bar, the plus sign indication an increased AUC: All TACs are normalized to injected radioactivity and animal weight resulting in the standard uptake value (SUV). Pretreatment dose of SA4503 was 1.5 mg/kg. Figure is reused from chapter 6.

In **Paper V** (chapter 7) [^{11}C]Cimbi-701, an O-methylated analogue of the highly selective 5-HT$_7$R antagonist SB-269970[14] was successfully radiolabelled in sufficient RCY = 10–22%, radiochemical purities above 98% and molar activities of 256 ± 127 GBq/µmol (n = 13) for subsequent *in vivo* evaluation in rats, pigs and baboon. Further selectivity profiling revealed that Cimbi-701 binds with high affinity to the 5-HT$_7$R and the σ receptors (Figure 6).

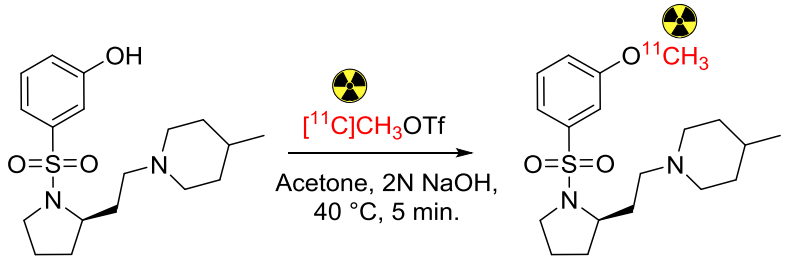

SB-269970 [11C]Cimbi-701

	5-HT$_{1A}$	5-ht$_{5a}$	5-HT$_7$	α$_{2B}$	α$_{2C}$	H$_2$	σ-1	σ-2
Cimbi-701 (nM)	633	113	18	1773	1536	6193	9.2	1.6

Figure 6: Radiolabelling of [^{11}C]Cimbi-701 (above); RCY = 10–22%, radiochemical purities above 98% and A_m of 256 ± 127 GBq/µmol (n = 13)) were obtained. Affinity (K_i) in nanomolar for Cimbi-701 (below). Figure is reused from chapter 7.

Species specific differences were observed in terms of tracer uptake into the brain. In rats, [^{11}C]Cimbi-701 was found to be a P-gp efflux transporter substrate. However, high brain uptake was found in pigs without inhibition of the P-gp efflux transporter. Low uptake was also observed in baboons, which may also be attributed to a P-gp efflux transporter dependency (Figure 7).

In agreement with the *in vitro* results, the *in vivo* PET experiments confirmed that the radiotracer binds to both targets in the brain of both rats and pigs. Even though the tracer demonstrated a limited selectivity for the 5-HT$_7$ receptor, it is believed that specific blocking of the σ receptors without affecting 5-HT$_7$ receptors could enable PET imaging of the same receptor system. Thus, due to the poor brain uptake seen in baboon, we suggest exploration of this structural class to identify non-P-gp substrates.

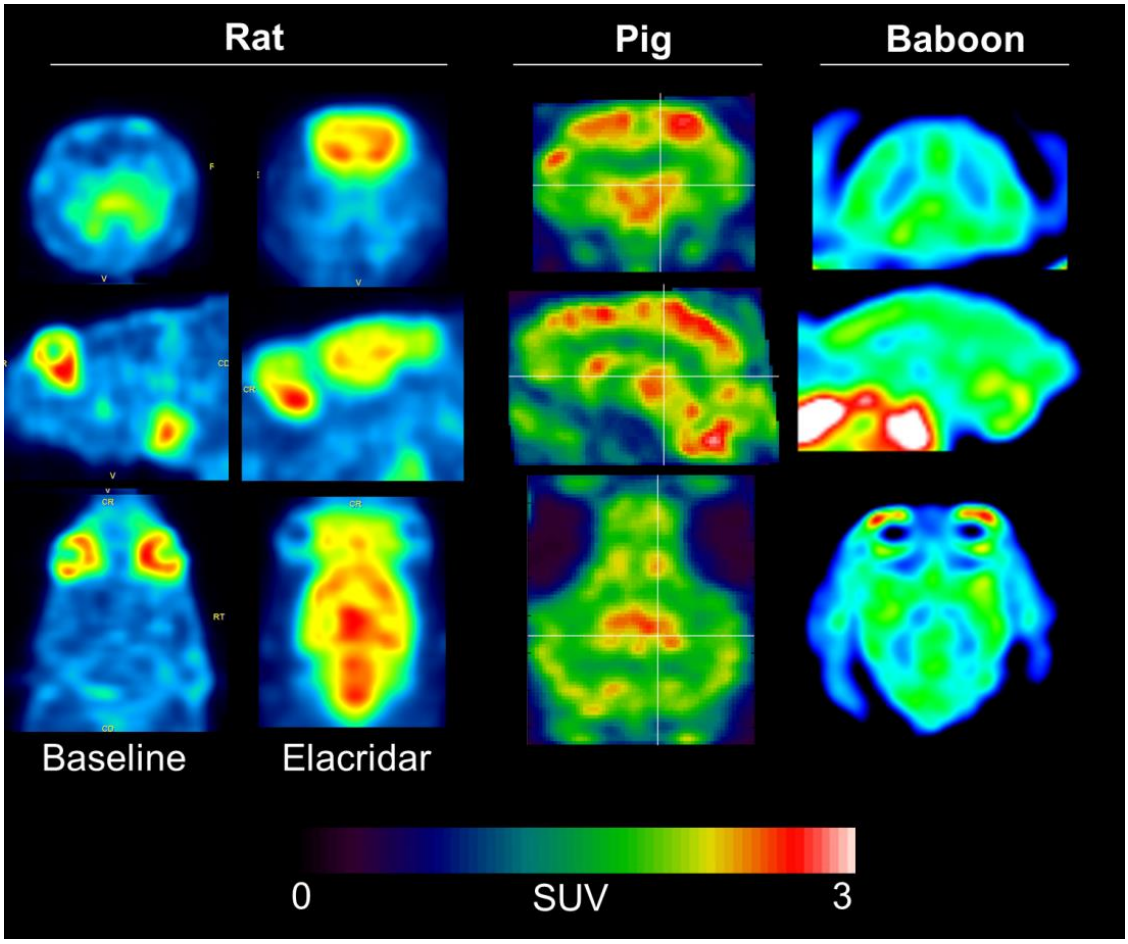

Figure 7: Summed PET images of [^{11}C]Cimbi-701 in the rat, pig and the baboon brain. For comparison, [^{11}C]Cimbi-701 in rats is shown before and after pretreatment with the P-gp efflux inhibitor elacridar (5 mg/kg). Figure is reused from chapter 7.

In parallel with the work presented in **Paper V** (chapter 7), the ^{18}F-labelled analogue [^{18}F]ENL30 was developed and presented in **Paper VI** (chapter 8). Motivated by the previously successful work, e.g. the converting of [^{11}C]MDL 100907 to [^{18}F]MH.MZ using the synthon 2-[^{18}F]fluoroethyl tosylate ([^{18}F]FETos),[15-17] the same strategy was chosen for [^{18}F]ENL30 (Scheme 2). The reference synthesis was completed through 13 steps; ending up with an overall low yield of approximately 0.2%.

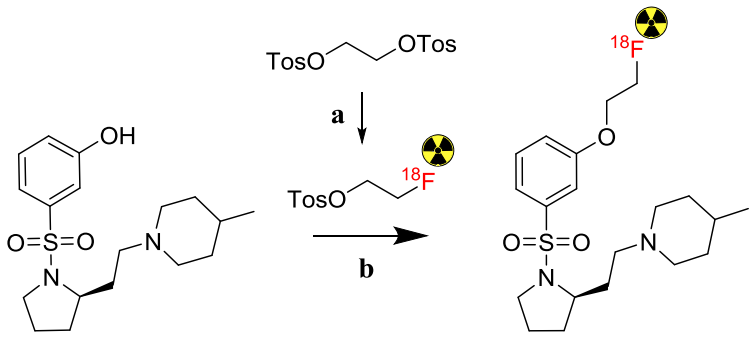

SB-269970 **[^{18}F]ENL30 ([^{18}F]15)**

Scheme 2: Radiosynthesis of [^{18}F]ENL30 **a)** [^{18}F]F^{-}, K_{222}, K_2CO_3, ACN, 80 °C, 3 min. **b)** DMF, NaOH (2N), 100 °C, 25 min. Radiochemical yields (RCY) ranging between 1.2 and 15% (decay corrected, n = 8), molar activities of 108 - 197 GBq/µmol (n = 3), and radiochemical purities > 98% were obtained. Scheme is reused from chapter 8.

Further the K_D (0.75 ± 0.5 nM) for [^{18}F]ENL30 in the thalamus was successfully determined using *in vitro* autoradiography on rat brain slices (Figure 8). The selectivity was thereafter investigated Inspired by recent data suggesting that SB-269970 has a moderate affinity for the σ-1 receptor (158 nM).[18] Moreover, this supported by the σ receptor affinity of Cimbi-701 (**Paper V**, chapter 7). Thus, blocking studies were performed both with autoradiography and PET. The following antagonists; SB-269970, Cimbi-717, haloperidol and SA4503 were used for elucidating the *in vitro* and *in vivo* selectivity profile of [^{18}F]ENL30. The affinities of the blocking agents for receptors of interest are summarized in Table 1.

Table 1: Summarizes the affinities of the blocking agents for receptors of interest.[13, 19-23]

	K_i (nM)					
	5-HT$_7$	**5-HT$_{1A}$**	**5-HT$_{2B}$**	**5-HT$_{2A}$**	**α$_1$**	**σ-1**
SB-269970	1.26			32		158
Cimbi-717	2.6	261	192	132	47	
Haloperidol	380			70	4	14
SA4503						17*

*IC_{50}

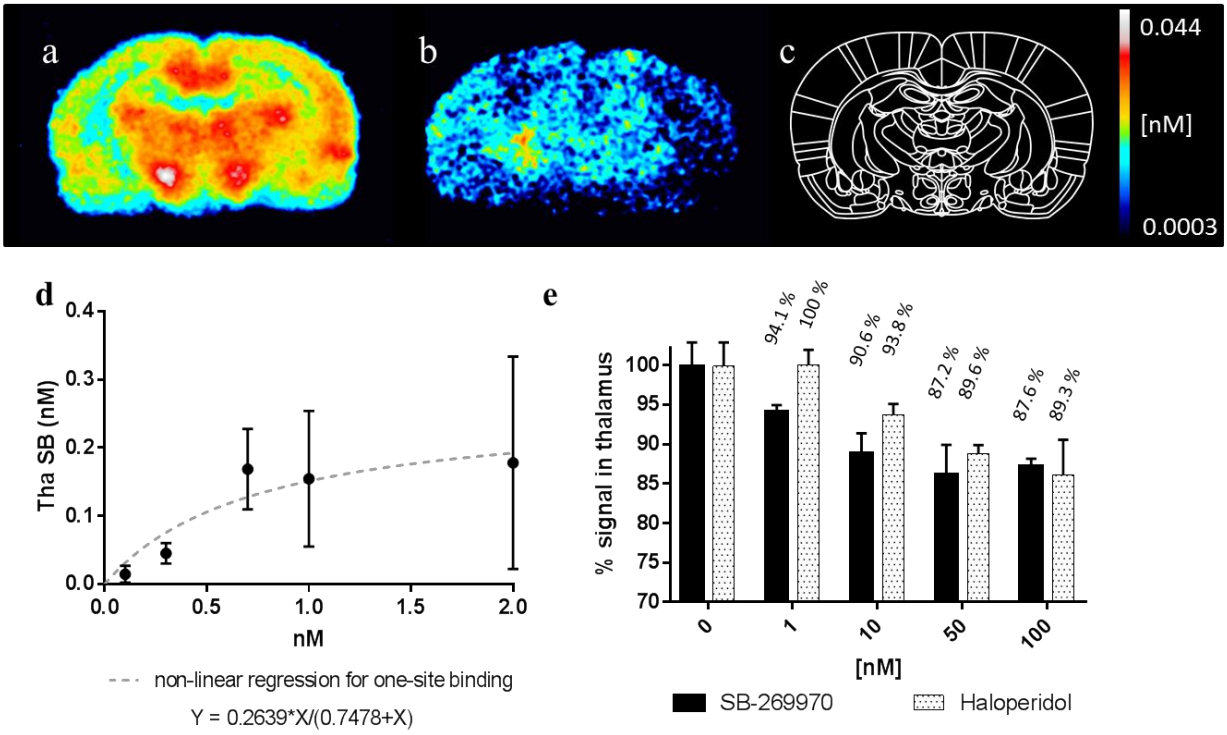

Figure 8: Results of the *in vitro* evaluation of **[^{18}F]15**. **a)-d)** Determination of K_D and B_{max} values of **[^{18}F]15** in thalamus (Tha). **a)** Coronal rat brain slice displaying the total binding of **[^{18}F]15**. **b)** Coronal rat brain slice displaying the non-specific binding of **[^{18}F]15** by blocking with SB-269970 (10 µM). **c)** The location of brain slices, around bregma -1.8. **d)** K_D and B_{max} were gained from one sited (specific binding) non-linear regression plotting the specific binding (SB) in nM of **[^{18}F]15** tracer concentration in nM. The data is based on 5 concentrations (0.1 nM, 0.3 nM, 0.7 nM 1 nM and 2 nM) and experiments were repeated 3 times (n = 9). **e)** *In vitro* autoradiography blocking study. The results are shown as a grouped barplot with the % signal in thalamus compared to 0 nM (total binding) using different concentrations (1, 10, 50 and 100 nM) of SB-269970 and haloperidol (n =3). Figure is reused from chapter 8.

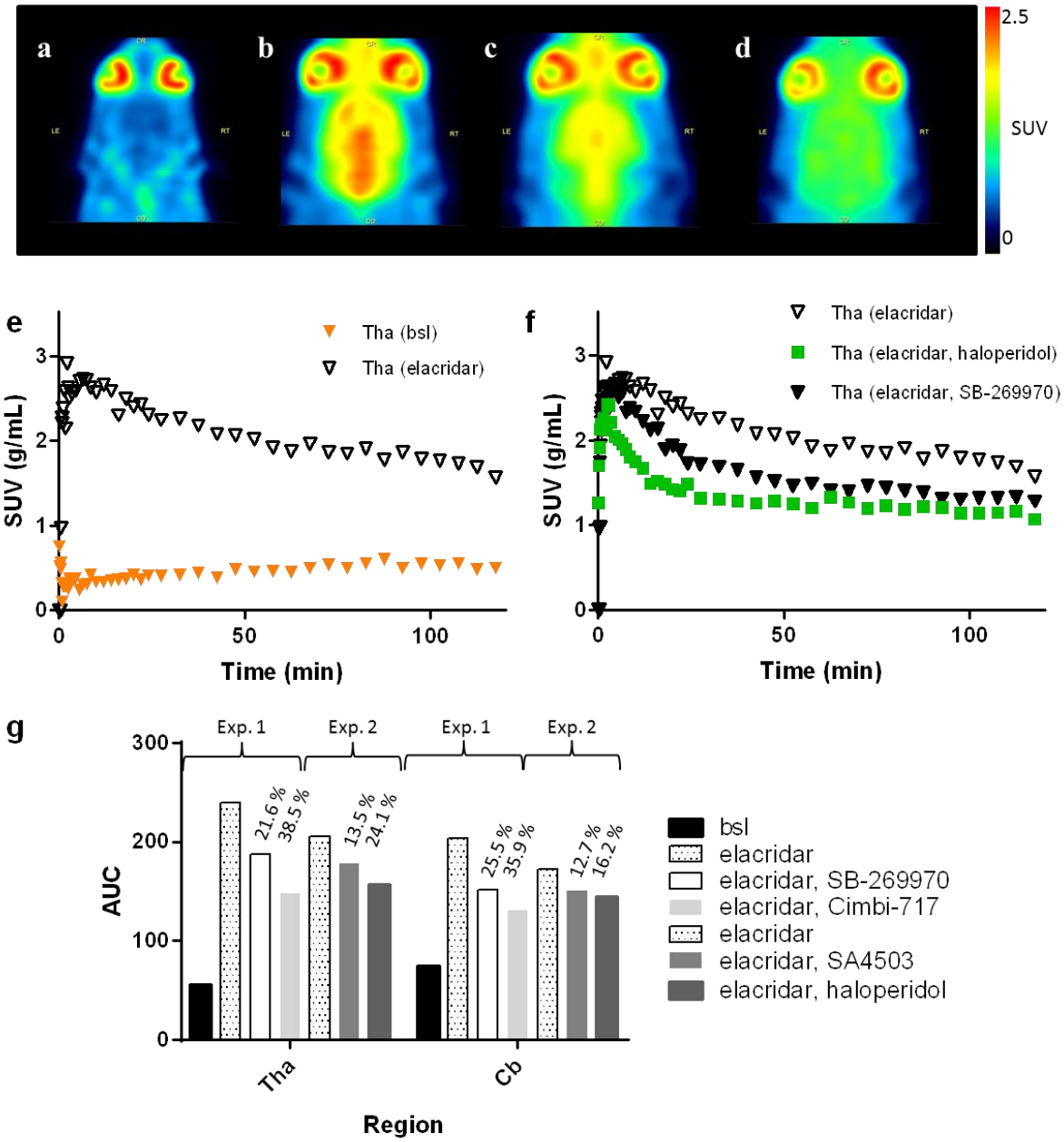

Figure 9: Results from the *in vivo* evaluation of **[^{18}F]15** in rats. Coronal PET images of **[^{18}F]15** evaluated in rats **(a-d)**, all summed images are from 5-120 min of a dynamic scan obtained in a high resolution research tomography (HRRT) scanner. **a)** Summed PET image of **[^{18}F]15** at baseline **b)** Summed PET image of **[^{18}F]15** after pretreatment with elacridar (5 mg/kg). **c)** Summed PET image of **[^{18}F]15** after pretreatment with elacridar (5 mg/kg) and SB-269970 (3 mg/kg). **d)** Summed PET image of **[^{18}F]15** after pretreatment with elacridar (5 mg/kg) and Cimbi-717 (3 mg/kg). Time-activity curves (TACs) from PET evaluation of **[^{18}F]15** in rats **(e-f). e)** Thalamus (Tha) TACs **[^{18}F]15** in baseline condition, after pretreatment with elacridar (5 mg/kg). **f)** Thalamus (Tha) TACs of **[^{18}F]15** after pretreatment with elacridar (5 mg/kg), both elacridar (5 mg/kg) and SB-269970 (3 mg/kg) and elacridar (5 mg/kg) and haloperidol (1 mg/kg) **g)** Calculated area-under-curve (AUC) for all TACs displayed as a grouped barplot also indicating percentage AUC reduction above the blocking agent bars. All TACs are normalized to injected radioactivity and animal weight to generate the standard uptake value (SUV). Figure is reused from chapter 8.

The results concluded that [^{18}F]ENL30, has a limited selectivity for the 5-HT$_7$R both *in vitro* and *in vivo* (Figure 8 and 9). But even though the tracer was found to not be selective for the target, specific blocking of the σ-receptors as off-targets without affecting 5-HT$_7$R could potentially enable PET imaging of the 5-HT$_7$R system. This would be of great value due to the lack of a validated PET tracer for the 5-HT$_7$R. But due to [^{18}F]ENL30 being a P-gp substrate in rats, we believe this should be tested in higher species, like pigs, where this problem with brain penetrance has been shown to be less pronounced.[24]

Finally, throughout this thesis the throughput of the rodent PET evaluation was greatly increased by the establishment of the 2x2 custom-made holder for the HRRT PET scanner (published in **Paper II**, chapter 4). A first version was successfully designed and built and thereafter optimized with respect to minimizing the plastic, having better space for the tails etc. Inhalation anaesthetics, isoflurane, together with suction could easily be integrated in the new version of the holder. The setup made it possible for 4 rats to be scanned simultaneously, thus multiple PET tracers or blocking regimes could be performed more time efficiently (Figure 10).

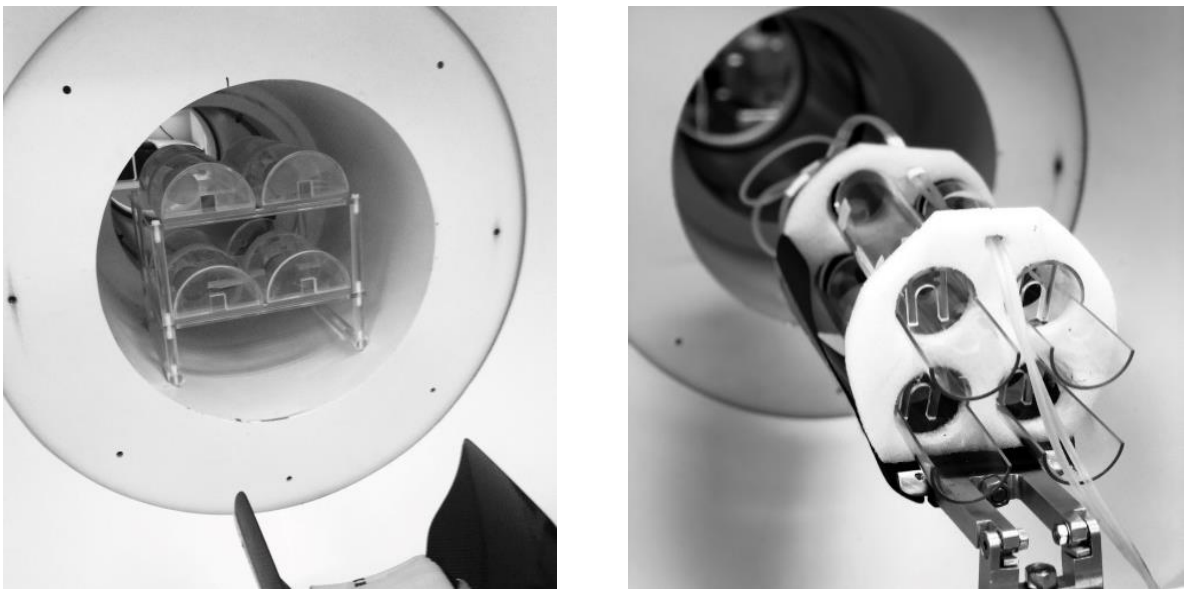

Figure 10 Images showing the first version of the custom-made 2x2 rat holder (left) for increased scanning throughput and the optimized holder with integrated isoflurane anesthetics (right). Right Figure is reused from chapter 4.

References

1. Hogendorf, A. S.; Hogendorf, A.; Kurczab, R.; Satala, G.; Lenda, T.; Walczak, M.; Latacz, G.; Handzlik, J.; Kiec-Kononowicz, K.; Wieronska, J. M.; Wozniak, M.; Cieslik, P.; Bugno, R.; Staron, J.; Bojarski, A. J., Low-basicity 5-HT_7 Receptor Agonists Synthesized Using the van Leusen Multicomponent Protocol. *Scientific Reports* **2017,** *7* (1), 1444.

2. Kallem, R.; P Kulkarni, C.; Patel, D.; Thakur, M.; Sinz, M.; P Singh, S.; Shahe Mahammad, S.; Mandlekar, S., A simplified protocol employing elacridar in rodents: a screening model in drug discovery to assess P-gp mediated efflux at the blood brain barrier. *Drug metabolism letters* **2012,** *6* (2), 134-144.

3. Herth, M. M.; Leth-Petersen, S.; Lehel, S.; Hansen, M.; Knudsen, G. M.; Gillings, N.; Madsen, J.; Kristensen, J. L., Accelerating preclinical PET-screening: reductive amination with [^{11}C] methoxybenzaldehydes. *RSC Advances* **2014,** *4* (41), 21347-21350.

4. Volk, B.; Barkóczy, J.; Hegedus, E.; Udvari, S.; Gacsályi, I.; Mezei, T.; Pallagi, K.; Kompagne, H.; Lévay, G.; Egyed, A., (Phenylpiperazinyl-butyl) oxindoles as selective 5-HT_7 receptor antagonists. *Journal of medicinal chemistry* **2008,** *51* (8), 2522-2532.

5. Herth, M. M.; Andersen, V. L.; Hansen, H. D.; Stroth, N.; Volk, B.; Lehel, S.; Dyssegaard, A.; Ettrup, A.; Svenningsson, P.; Knudsen, G. M.; Kristensen, J. L., Evaluation of 3-Ethyl-3-(phenylpiperazinylbutyl)oxindoles as PET Ligands for the Serotonin 5-HT_7Receptor: Synthesis, Pharmacology, Radiolabeling, and *in Vivo* Brain Imaging in Pigs. *Journal of medicinal chemistry* **2015,** *58* (8), 3631-6.

6. Tredwell, M.; Preshlock, S. M.; Taylor, N. J.; Gruber, S.; Huiban, M.; Passchier, J.; Mercier, J.; Génicot, C.; Gouverneur, V., A general copper-mediated nucleophilic ^{18}F fluorination of arenes. *Angewandte Chemie* **2014,** *126* (30), 7885-7889.

7. Weissman, A.; Su, T.-P.; Hedreen, J.; London, E., Sigma receptors in post-mortem human brains. *Journal of Pharmacology and Experimental Therapeutics* **1988,** *247* (1), 29-33.

8. McCann, D. J.; Weissman, A. D.; Su, T. P., Sigma-1 and Sigma-2 sites in rat brain: Comparison of regional, ontogenetic, and subcellular patterns. *Synapse* **1994,** *17* (3), 182-189.

9. Varnäs, K.; Thomas, D. R.; Tupala, E.; Tiihonen, J.; Hall, H., Distribution of 5-HT_7 receptors in the human brain: a preliminary autoradiographic study using [^{3}H] SB-269970. *Neuroscience letters* **2004,** *367* (3), 313-316.

10. Horisawa, T.; Ishiyama, T.; Ono, M.; Ishibashi, T.; Taiji, M., Binding of lurasidone, a novel antipsychotic, to rat 5-HT7 receptor: analysis by [^{3}H] SB-269970

autoradiography. *Progress in Neuro-Psychopharmacology and Biological Psychiatry* **2013,** *40*, 132-137.

11. Hansen, H. D.; Herth, M. M.; Ettrup, A.; Andersen, V. L.; Lehel, S.; Dyssegaard, A.; Kristensen, J. L.; Knudsen, G. M., Radiosynthesis and *in vivo* evaluation of novel radioligands for PET imaging of cerebral 5-HT_7 receptors. *Journal of Nuclear Medicine* **2014,** *55* (4), 640-6.

12. Hansen, H. D.; Constantinescu, C. C.; Barret, O.; Herth, M. M.; Magnussen, J. H.; Lehel, S.; Dyssegaard, A.; Colomb, J.; Billard, T.; Zimmer, L., Evaluation of [^{18}F] 2FP3 in pigs and non-human primates. *Journal of Labelled Compounds and Radiopharmaceuticals* **2018**.

13. Lovell, P. J.; Bromidge, S. M.; Dabbs, S.; Duckworth, D. M.; Forbes, I. T.; Jennings, A. J.; King, F. D.; Middlemiss, D. N.; Rahman, S. K.; Saunders, D. V., A novel, potent, and selective 5-HT_7 antagonist:(R)-3-(2-(2-(4-methylpiperidin-1-yl) ethyl) pyrrolidine-1-sulfonyl) phenol (SB-269970). *Journal of medicinal chemistry* **2000,** *43* (3), 342-345.

14. Lovell, P. J.; Bromidge, S. M.; Dabbs, S.; Duckworth, D. M.; Forbes, I. T.; Jennings, A. J.; King, F. D.; Middlemiss, D. N.; Rahman, S. K.; Saunders, D. V.; Collin, L. L.; Hagan, J. J.; Riley, G. J.; Thomas, D. R., A novel, potent, and selective 5-HT_7 antagonist: (R)-3-(2-(2-(4-methylpiperidin-1-yl)ethyl)pyrrolidine-1-sulfonyl) phen ol (SB-269970). *Journal of medicinal chemistry* **2000,** *43* (3), 342-5.

15. Herth, M. M.; Debus, F.; Piel, M.; Palner, M.; Knudsen, G. M.; Luddens, H.; Rosch, F., Total synthesis and evaluation of [^{18}F]MHMZ. *Bioorg Med Chem Lett* **2008,** *18* (4), 1515-9.

16. Van Der Born, D.; Pees, A.; Poot, A. J.; Orru, R. V.; Windhorst, A. D.; Vugts, D. J., Fluorine-18 labelled building blocks for PET tracer synthesis. *Chemical Society Reviews* **2017,** *46* (15), 4709-4773.

17. Kniess, T.; Laube, M.; Brust, P.; Steinbach, J., 2-[^{18}F] Fluoroethyl tosylate–a versatile tool for building ^{18}F-based radiotracers for positron emission tomography. *Medicinal Chemical Communication* **2015,** *6* (10), 1714-1754.

18. Ates, A.; Burssens, P.; Lorthioir, O.; Lo Brutto, P.; Dehon, G.; Keyaerts, J.; Coloretti, F.; Lallemand, B.; Verbois, V.; Gillard, M., 5-HT_7 Receptor Antagonists with an Unprecedented Selectivity Profile. *Medicinal Chemical Communication* **2018,** *13* (8), 795-802.

19. Matsuno, K.; Nakazawa, M.; Okamoto, K.; Kawashima, Y.; Mita, S., Binding properties of SA4503, a novel and selective σ1 receptor agonist. *European journal of pharmacology* **1996,** *306* (1-3), 271-279.

20. McLeod, M. C.; Aubé, J.; Frankowski, K. J., Decahydrobenzoquinolin-5-one sigma receptor ligands: Divergent development of both sigma 1 and sigma 2 receptor selective examples. *Bioorganic & medicinal chemistry letters* **2016,** *26* (23), 5689-5694.

21. Li, P.; L Snyder, G.; E Vanover, K., Dopamine targeting drugs for the treatment of schizophrenia: past, present and future. *Current topics in medicinal chemistry* **2016,** *16* (29), 3385-3403.

22. Hagan, J. J.; Price, G. W.; Jeffrey, P.; Deeks, N. J.; Stean, T.; Piper, D.; Smith, M. I.; Upton, N.; Medhurst, A. D.; Middlemiss, D. N.; Riley, G. J.; Lovell, P. J.; Bromidge, S. M.; Thomas, D. R., Characterization of SB-269970-A, a selective 5-HT_7 receptor antagonist. *British Journal of Pharmacology* **2000,** *130* (3), 539-548.

23. Herth, M. M.; Volk, B.; Pallagi, K.; Kofoed Bech, L.; Antoni, F. A.; Knudsen, G. M.; Kristensen, J. L., Synthesis and *in vitro* evaluation of oxindole derivatives as potential radioligands for 5-HT_7 receptor imaging with PET. *ACS Chemical Neuroscience* **2012,** *3* (12), 1002-1007.

24. Syvänen, S.; Lindhe, Ö.; Palner, M.; Kornum, B. R.; Rahman, O.; Långström, B.; Knudsen, G. M.; Hammarlund-Udenaes, M., Species differences in blood-brain barrier transport of three positron emission tomography radioligands with emphasis on P-glycoprotein transport. *Drug metabolism and disposition* **2009,** *37* (3), 635-643.

Chapter 10

Conclusions and future perspectives

Summary:

This chapter contains an overall conclusion of the work presented within this thesis. Following up the conclusion there is also a brief discussion on important points to bring into future work and what are the next required steps in finding a selective PET tracer for imaging of the 5-HT$_7$ receptor.

CHAPTER 10 - Conclusions and future perspectives

Detailed in this Ph.D. thesis are the extended efforts and attempts made in the pursuit of identifying a selective PET tracer for the 5-HT_7 receptor (5-HT_7R). The research was based on three different scaffolds. Fifteen PET tracer candidates were synthesized and characterized. Nine tracers were radiolabelled and only five were further selected for *in vivo* studies. In chapter 9, these efforts are summarized.

One obstacle encountered during working on this Ph.D. project was that almost all tested tracers were P-gp substrates and only *in vivo* studies could identify this. I believe it would have been a great advantage to have a blood-brain-barrier permeability assay designed for PET tracers that could be run *in vitro*. This would have greatly benefited the work in this thesis.

The development of a PET tracer is a time-demanding and labour extensive task. Coordination of medicinal chemistry, radiochemistry, radionuclide production, animal preparation, imaging and imaging processing, just to name some, are challenging and limits the speed in which new tracers can be developed. This thesis has addressed this challenge in two ways. I have extended the scope of fragment-based labelling and developed together with my colleagues a rat holder for higher through-put scanning. These are only small steps to accelerate the development process, but I hope they will help to facilitate the process. Ultimately, modelling approach or *in silico* methods would be preferred, but currently these do not exists.

In respect to 5-HT_7R PET imaging, I believe structures with higher affinity and selectivity are required to be successful. Dual or triple blocking experiments are doable, but not optimal for clinical translation. This means that further structure activity relationship studies are needed. They should be accompanied by computational modelling with the clear goal to increase affinity and selectivity from the nanomolar to picomolar range.

An additional and an interesting aspect encountered during the work presented in this PhD thesis are the species differences. I believe this is an underestimated topic within the PET tracer development process, especially for CNS targets. Future research in this direction, i.e. predicting the performance of a tracer in humans using animal models would be helpful. Finally, a possibility to determine non-specific binding in a setting prior to *in vivo* evaluation should be developed. This would have been greatly beneficial, to help discarding ligands earlier in the development process.

In conclusion, a selective 5-HT_7R tracer is still missing. However, I hope to have contributed to advancement in the field and that the knowledge created in this thesis will help to develop a 5-HT_7R PET tracer in the future.

ACKNOWLEDGEMENTS

First of all, I would like to thank my principal supervisor Matthias M. Herth for giving me the opportunity to carry out this, for me personalized Ph.D. project, which truly has suited my knowledge and anticipations to 100%. You have also throughout these 3 years inspired, motivated and encouraged me to learn and do more than I thought possible on this limited amount of time. Next would I like to thank my co-supervisors Maria Erlandsson, Gitte M. Knudsen and Tomas Ohlsson for their support and advices throughout my time as a Ph.D. student. Maria, I also want to add that I much appreciate us becoming good friends above our work relation and I am so thankful for you introducing me to hands-on work within radiochemistry.

It has been a great experience to be able to work at 4 different sites during my Ph.D., it has made it possible for me to meet and get to know so many nice and helpful people. So to all people at the Department of Clinical Physiology & PET, Farma, NRU and the Radiation Physics in Lund, I am so grateful and I wish that I could have individually thanked you all. But I would like to specifically mention some invaluable colleagues; Ida, Szabolcs, Troels, Vladimir, Daniel and Jesper at Riget and Simone, Mikael and Hanne at NRU, thank you all for helping me accomplish the work presented within this thesis. I would also like to give a special thanks to the two excellent master students that I had the pleasure to supervise; Fraser G. Edgar and Mengfei Xiong. You have both been contributing so much to this thesis and I am proud to have been a part of both of your journeys into Ph.D. positions. I am looking forward to be your colleague and follow your work going into the future. I also enjoyed co-supervising Klas in Lund and then be able to see his progress as a fellow Ph.D. student.

Finally I would like to thank the people who really made the big difference, my supportive and loving husband Ville, my family and my amazing friends. Without you I would definitely not have finalized the work within this Ph.D thesis. Jag älskar er alla, mer än allt! A special thanks to Eve who painted the front-page illustration for me and Nicole for proof-reading and helping me with the Danish abstract.

Chapter 11

Appendices

Summary:

This chapter contains further papers with work that I have been involved in during my time as a Ph.D student, but which does not fit in the scope of this thesis. Finally, co-authorship declarations, permissions for the reuse/adaption of images and the reprint of the published article are also attached in this chapter.

Classics in Neuroimaging: The serotonergic 2A receptor system - From discovery to modern molecular imaging

Elina T. L'Estrade[a,b,c], Hanne D. Hansen[a], Maria Erlandsson[c], Tomas G. Ohlsson[c], Gitte M. Knudsen[a], Matthias M. Herth[b,d]

[a]*Neurobiology Research Unit and CIMBI, Copenhagen University Hospital, Rigshospitalet, Blegdamsvej 9, 2100 Copenhagen, Denmark*

[b]*Department of Drug Design and Pharmacology, Faculty of Health and Medical Sciences, University of Copenhagen, Jagtvej 160, 2100 Copenhagen, Denmark*

[c]*Radiation Physics, Nuclear Medicine Physics Unit, Skånes University Hospital, Barngatan 3, Lund 222 42, Sweden*

[d]*Department of Clinical Physiology, Nuclear Medicine and PET, University Hospital Copenhagen, Rigshospitalet Blegdamsvej 9, 2100 Copenhagen, Denmark*

Abstract

Already in 1953, Woolley and Shaw speculated that serotonin could be involved in a range of central nervous system (CNS) disorders. Lysergic acid diethylamide (LSD) displayed an important role in this respect. It was not only used to antagonize biological effects of serotonin and to study the system itself, but also to identify serotonergic subtype receptors. The 5-HT_{2A} receptor was discovered in the 1970s and identified as the responsible receptor mediating psychedelic effects of LSD. The development of positron emission tomography (PET) allowed studying this receptor system *in vivo*. Parameters such as abundance of 5-HT_{2A} neuroreceptors or receptor occupancy can be determined using PET. As such, the development of 5-HT_{2A} receptor tracers started immediately after the introduction of PET in the mid-70s.

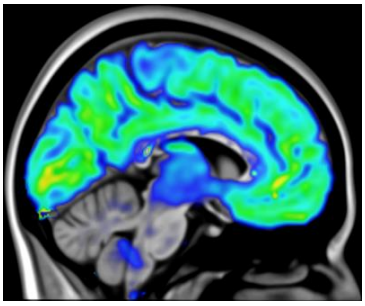

PET image of the 5-HT_{2A} receptor using [^{11}C]Cimbi-36

In this viewpoint, we provide a historical overview from the discovery of serotonin to the identification of the 5-HT_{2A} receptor subtype and the subsequent development of 5-HT_{2A} receptor subtype specific PET tracers over the last four decades. We emphasize the interplay between pharmacology, medicinal chemistry, radiochemistry and nuclear medicine that is important while developing a PET tracer. Moreover, we highlight selected examples applying 5-HT_{2A} receptor PET tracers within neurological diseases and drug occupancy studies.

Keywords: 5-HT_{2A}, PET, serotonin, [^{11}C]MDL 100907, [^{18}F]altanserin, [^{11}C]Cimbi-36, (R)-[^{18}F]MH.MZ

Manuscript

The modern era of serotonin (5-hydroxytryptamine, 5-HT) research started in the 1950s and was driven by three main major observations: 1) 5-HT can be isolated in relatively large quantities from the mammalian central nervous system (CNS) with an inhomogeneous brain distribution, 2) precursor molecules of 5-HT were identified in nervous tissues and 5-HT was only active in its free form and finally, 3) both central and peripheral actions of 5-HT could be antagonized by lysergic acid diethylamide (LSD). Especially, the latter observation provoked Woolley and Shaw in 1953 to speculate that certain mental disorders are induced by 5-HT spill-over or deficiency within distinct brain regions. They also concluded that the psychoactive effects of LSD could be due to an action on 5-HT in the brain. The pioneers of 5-HT neuropharmacology research at that time were of course thrilled by the description of the psychedelic action of LSD that was already reported by Albert Hofmann in 1943. His accident with LSD that led to his famous bike ride experiencing intense changes in perception from imagining that his next-door neighbour was a malevolent witch and going insane to enjoying fantastic exploding colour fountains is still an amusing anecdote. The structural similarity of LSD and 5-HT, the observed antagonism from LSD towards 5-HT and the psychedelic action of LSD and some metabolites of 5-HT let the mid-50s neuropharmacology researches dream to unfold the mysteries behind the human mind, mood and perception while exploring 5-HT and its connection to LSD. Following this dream, researchers could already find the first hints in the mid-50s to the mid-60s that depletion of 5-HT resulted in 'depression' and excess of 5-HT in 'excitation'. For example, resperine, a drug used for hypertension, resulted in depleted 5-HT levels and caused depression in some subjects. Analogously, iproniazid, an anti-tuberculosis drug, resulted in increased 5-HT levels in the rat brain and in behavioural excitation in some patients. It appeared that Woolley and Shaw initial speculation could have been indeed true and resulted in the 5-HT hypothesis of depression.[1]

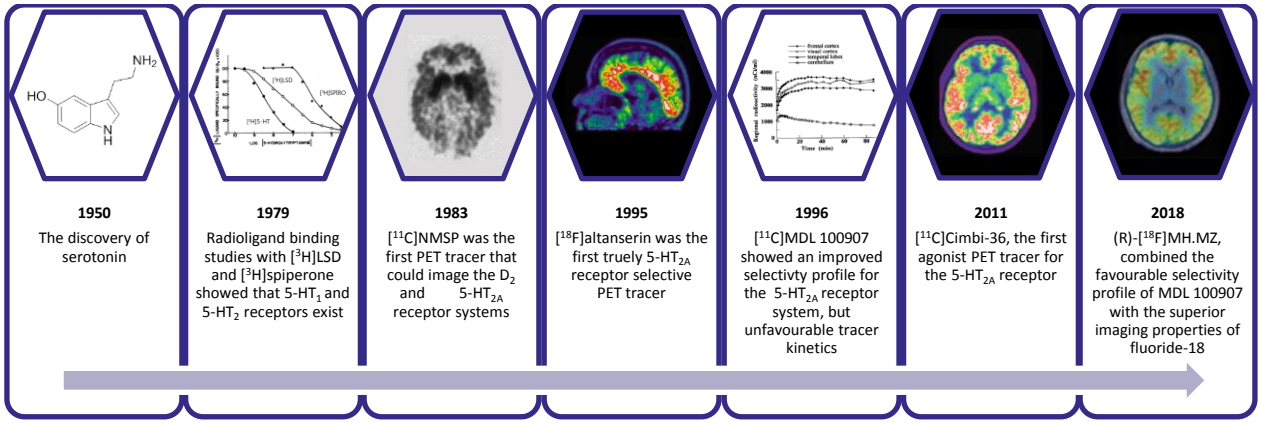

Figure 1: The evolution of 5-HT_{2A} receptor tracers[1,-5] Reprinted with permission from Peroutka, S.J., Snyder, S.H., Multiple Serotonin Receptors: Differential Binding of [^{3}H]5-Hydroxytryptamine, [^{3}H]Lysergic Acid Diethylamide and [^{3}H]Spiroperidol. *Mol Pharmacol*, **1979**, *16*(3): 687-699. Copyright [1979] [ASPET]; Reprinted with permission from Wong, D.F. *et al*., Effects of age on dopamine and serotonin receptors measured by positron tomography in the living human brain. *Science*, **1984**, *226*(4681):1393-1396. Copyright [1984] [The American Association for the Advancement of Science]; Reprinted with permission from Lundkvist, C. *et al*., [^{11}C]MDL 100907, a radioligand for selective imaging of 5-HT_{2A} receptors with positron emission tomography. *Life Sci.*, **1996**, *58*(10):187-192. Copyright [1996] [Life Sciences]; Reprinted with permission from Herth, M.M. and Knudsen, G.M., PET Imaging of the 5-HT2A Receptor System: A Tool to Study the Receptor's *In Vivo* Brain Function. Humana Press, published by Springer Nature, ISBN 978-3-319-70472-2. Copyright [2018] [Springer Nature].

However, it almost took 20 years before an *in vivo* technique that could test the 5-HT hypothesis in living subjects quantitatively became available. In 1975, Michel Ter-Pogossian, Michael E. Phelps and Edward J. Hoffman advanced the initial nuclear molecular imaging concept proposed by David E. Kuhl and developed the first Positron-Emission-Tomography (PET) scanner. The fast advancement of computer sciences made it possible to create quantifiable and time resolved images from which parameters such as receptor specificity, binding kinetics and receptor occupancy could be estimated using kinetic modelling. In parallel with the development of PET, advances in receptor physiology made it possible to distinguish between receptors subtypes that are activated by 5-HT but induce different secondary messenger responses. More precisely, Peroutka and Snyder discovered in 1979 using radioligand binding studies with [^{3}H]LSD and [^{3}H]spiperone that 5-HT_1 and 5-HT_2 receptors exist. Later it was shown that the 5-HT_2 receptor consists of three subtypes and that the 5-HT_{2A} receptor was responsible for the effects caused by LSD.[1]

Triggered by those *in vitro* findings, it took not long until the first PET tracers based on spiperone and LSD were developed and used to study the 5-HT_{2A} receptors *in vivo*. In September 1983, [^{11}C]methylspiperone ([^{11}C]NMSP) was labelled by N-alkylation of spiperone with [^{11}C]methyl iodide in a combined effort from researchers at the Johns Hopkins Medical Institute,

Baltimore, USA and the University of Uppsala, Uppsala, Sweden.[2] [^{11}C]NMSP is a dual D_2/5-HT_{2A} receptor ligand and was used in very early PET studies to visualize D_2 receptors in the striatum and to estimate changes in 5-HT_{2A} receptors in the cortex in e.g. aging and schizophrenia. As such, [^{11}C]NMSP was not very specific. In 1985, the first radioligand designed specifically to image 5-HT_{2A} receptors was developed by Lever and co-workers, again at the Johns Hopkins University School of Medicine. N1-([^{11}C]Methyl)-2-Br-LSD ([^{11}C]MBL) was first evaluated in mice and two years later in baboons and humans. Specific binding in cortex regions could be detected using a selective 5-HT_{2A} receptor antagonist in blocking experiments. However, [^{11}C]MBL still showed selective D_2 binding in high density dopaminergic regions such as the striatum. As such, the search for a 5-HT_{2A} receptor selective PET tracer continued. Ketanserin, a very selective 5-HT_{2A} receptor antagonist, developed by Janssen Pharmaceutica in 1980 was a promising candidate. The development of ketanserin as a PET tracer was carried out in parallel with the development of [^{11}C]MBL. The successful radiolabeling of ketanserin with carbon-11 was reported in January 1985 by Baron and colleagues. Unfortunately, [^{11}C]methylketanserin displayed low target-to-background ratios in the human brain and was discontinued because of that. However, the promising selectivity profile of ketanserin encouraged Janssen Pharmaceutica to continue to explore the clinical treatment potential of ketanserin derivatives. Hundreds of compounds were synthesized and tested for 5-HT_{2A} receptor selectivity. Among others, altanserin was selected for clinical trials based on its selectivity and *in vivo* pharmacology profile. This did not stay unnoticed in the PET community and the possibility to label altanserin with fluoride-18 without structural modifications of the original molecule prompted Lemaire et al. to radiolabel altanserin via nucleophilic substitution at Liege University, Liege, Belgium, in 1988. Three years later, [^{18}F]altanserin was evaluated in rodents and encouraged by these results translated into the clinic by Biver and colleagues in 1995. [^{18}F]altanserin was the first tracer that selectively bound to 5-HT_{2A} receptors in the human brain and possessed high target-to-background ratios. However, brain penetrant metabolites and a high non-specific binding component complicated the quantification of [^{18}F]altanserin. In 2003, Pinborg and colleagues from the Neurobiology Research Unit, Copenhagen, Denmark, reported a bolus-infusion experimental set up addressing these problems to a certain degree. In general, the bolus–infusion paradigm resulted in excellent test–retest reliability in large brain regions with high binding. In 1990, Hoechst Marion Roussel Ltd, Germany, developed a highly selective 5-HT_{2A} receptor antagonist with an improved selectivity profile for the potential treatment of schizophrenia. No specific binding towards other receptors than the 5-HT_{2A} receptor could be

determined. This prompted Huang and colleagues from the University of Pittsburgh School of Medicine, Pittsburgh, USA, to label MDL 100907 via O-^{11}C-methylation in 1995. Subsequent, PET studies revealed indeed selective binding, good target-to- background ratios and only minor CNS accumulation of metabolites of [^{11}C]MDL 100907. Unfortunately, [^{11}C]MDL 100907 displayed unfavourable tracer kinetics for kinetic modelling limiting its use in quantitative studies. In an attempt to address these short comings, a ^{18}F-derivative ((R)-[^{18}F]MH.MZ) was developed by Herth and colleagues in Mainz, Germany, in 2010. It showed a very similar selectivity profile as MDL 100907 and could easily be labelled using 2-[^{18}F]fluoroethyl-1-tosylate. PET imaging in mice, rats, pigs and recently in humans revealed good selectivity, but the tracer also showed slow kinetics. Kinetic modelling appeared to be more accurate compared to its ^{11}C-version, mainly due the fact that longer scan time was possible.[3,4]

The search for a PET tracer that is optimal suited to image the 5-HT$_{2A}$ system nicely shows the interplay between medicinal chemistry, pharmacology and radiochemistry that is undoubtfully required to successfully develop a PET tracer. Over the past 30 years (Figure 1), the interdisciplinary interaction between these research fields resulted in the identification of three promising structures, namely [^{18}F]altanserin, [^{11}C]MDL 100907 and (R)-[^{18}F]MH.MZ, to image the 5-HT$_{2A}$ receptor in the clinic (Scheme 1). However, the ideal combination of a PET tracer with high selectivity, non-BBB penetrating radiometabolites, high specific-to-non-specific binding and fast kinetics remains to be identified for the 5-HT$_{2A}$ receptor.[3,4]

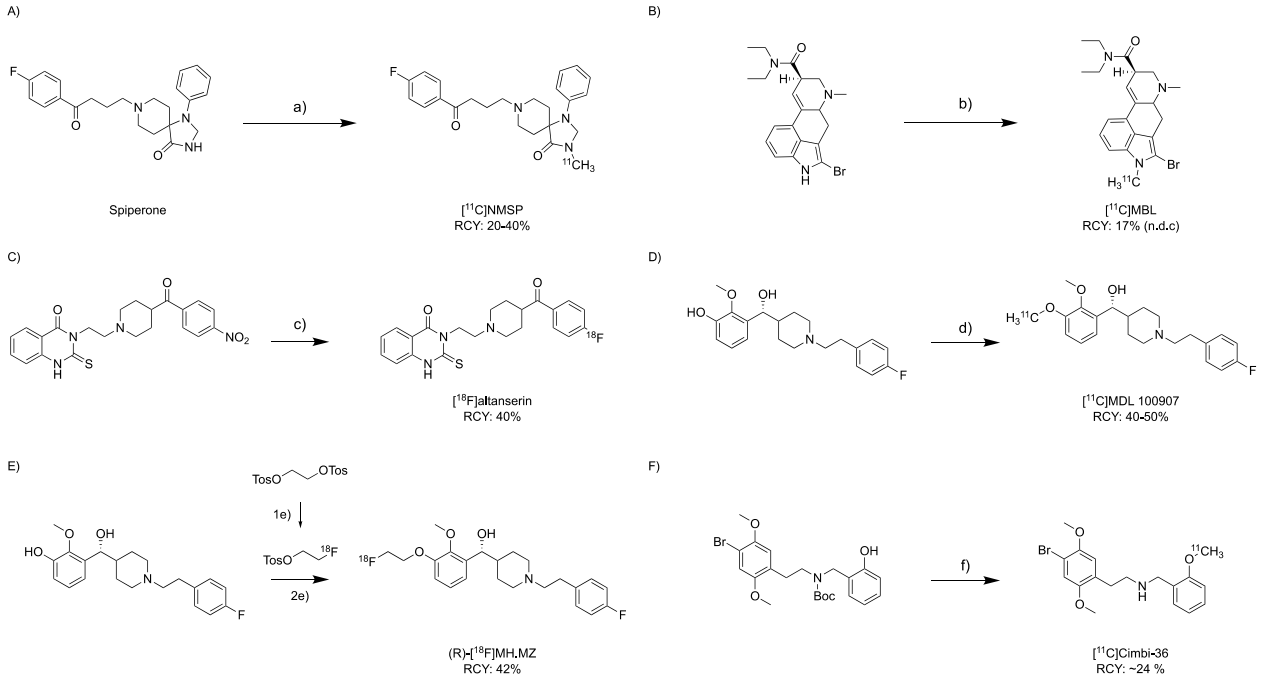

Scheme 1: Selected PET tracers of the 5-HT_{2A} receptor system. A) [^{11}C]NMSP a) 1: [^{11}C]CH_3I, DCM, TBAH (aq.), 65°C (Sonicated), 6 min. 2: Heptyl iodide, 65°C (Sonicated), 4 min. B) [^{11}C]MBL b) [^{11}C]CH_3I, DMF, TBAH (aq.), 80°C, 5 min. C) [^{18}F]altanserin c) [^{18}F]F^-, K_{222}, K_2CO_3, DMSO, MW, 5 min. D) [^{11}C]MDL 100907 d)) [^{11}C]CH_3I, Acetone, NaOH (5M), 80°C, 3 min. E) R-[^{18}F]MH.MZ 1e) [^{18}F]F^-, K_{222}, K_2CO_3, ACN, 80 °C, 3 min.; 2e) DMF, NaOH (5M) 100°C, 10 min. F) [^{11}C]Cimbi-36 1f) 1: [^{11}C]CH_3OTf, Acetone, NaOH (2N), 40°C, 30 s.; 2f: TFA,CH_3CN, 80°C, 5 min.

Over the years, many 5-HT_{2A} receptor ligand PET studies have been carried out to identify its role in for example depression, schizophrenia, obesity and Alzheimer's disease. Early studies with less optimal 5-HT_{2A} receptor tracers and using suboptimal PET study designs revealed mixed outcomes: lower or higher binding of the respective tracers have been identified which could very often not be aligned with post-mortem findings. Finally, in 2003 Meyer et al. revealed a correlation between post-mortem autoradiography and *in vivo* PET 5-HT_{2A} receptor binding in the frontal cortex. In contrast to earlier studies, Meyer and colleagues carried out their work in drug free patients.[3]

PET is increasingly used in drug development programs and discovery process of novel drug candidates. Central to the drug development is to determine the dose which will alleviate symptoms but not provoke side effects. One such example for the 5-HT_{2A} receptor is the study carried out by Nordstrom et al. in 2008 at the Karolinska Institute, Stockholm, Sweden. They tested the *in vivo* relationship between oral dose, plasma levels, and uptake of pimavanserin with the help of [^{11}C]NMSP in humans at baseline and after drug administration. Pimavanserin is a 5-HT_{2A} receptor inverse agonist developed to treat Parkinson's disease psychosis. Selective cortical 5-HT_{2A} receptor binding of [^{11}C]NMSP could be blocked in a dose-dependent manner and a single oral dose as low as 10 mg was were found to fully saturate 5-HT_{2A} receptors in the human brain. This helped ACADIA Pharmaceuticals to design the dosage that should be used in clinical trials.[3]

Recently, PET researchers became again interested to understand the relationship between 5-HT levels in the synaptic cleft and neurological disorders such as depression. Among other receptors, also the 5-HT_{2A} receptor was investigated for the possibility to determine 5-HT levels via intervention studies which change the concentration of 5-HT within the synaptic cleft. In this respect, [^{11}C]Cimbi-36, an agonistic 5-HT_{2A} receptor PET tracers, has been developed at the Center for Integrated Molecular Brain Imaging in Copenhagen in 2011. Following the ternary complex model, an agonist tracer promises to selectively map receptors in their functional and 5-HT activated state and to be more susceptible towards endogenous 5-HT. In this respect,

[^{11}C]Cimbi-36 is currently applied to determine the receptor occupancy of the hallucinogenic drug psilocybin in Copenhagen. As LSD, psilocin (the active component of psilocybin) activates 5-HT_{2A} receptors and ignites its effect via these receptors. Psilocin is presently of special interest since it can be used for the treatment of various psychiatric disorders and addiction.[3-5]

In summary, the 5-HT_{2A} receptor is of special interest for PET researchers from the very first studies conducted with PET to this day. Three promising selective antagonist PET tracers are available to study the human 5-HT_{2A} receptor system *in vivo* with PET, namely [^{18}F]altanserin, [^{11}C]MDL 100907 and (R)-[^{18}F]MH.MZ. [^{11}C]Cimbi-36 is so far the only available agonist 5-HT_{2A} receptor tracer for human PET studies.

References

1. Göthert, M. (2013) Serotonin discovery and stepwise disclosure of 5-HT receptor complexity over four decades. Part I. General background and discovery of serotonin as a basis for 5-HT receptor identification. *Pharmacological Reports*, *65*(4), 771-786.
2. Wong, D. F., Wagner, H. N., Dannals, R. F., Links, J. M., Frost, J. J., Ravert, H. T., Wilson, A.A., Rosenbaum, A.E., Gjedde, A., & Douglass, K. H. (1984) Effects of age on dopamine and serotonin receptors measured by positron tomography in the living human brain. *Science*, *226*(4681), 1393-1396.
3. Herth, M. M., & Knudsen, G. M. (2018) PET Imaging of the 5-HT 2A Receptor System: A Tool to Study the Receptor's *In Vivo* Brain Function. In *5-HT2A Receptors in the Central Nervous System* (pp. 85-134). Humana Press, published by Springer Nature, ISBN 978-3-319-70472-2
4. Herth, M. M., & Knudsen, G. M. (2015) Current radiosynthesis strategies for 5-HT2A receptor PET tracers. *Journal of Labelled Compounds and Radiopharmaceuticals*, *58*(7), 265-273.
5. Paterson, L. M., Tyacke, R. J., Nutt, D. J., & Knudsen, G. M. (2010) Measuring endogenous 5-HT release by emission tomography: promises and pitfalls. *Journal of Cerebral Blood Flow & Metabolism*, *30*(10), 1682-1706.

Synthesis and Pharmacological Evaluation of [^{11}C]4-Methoxy-N-[2-(thiophene-2-yl)imidazo[1,2-a]pyridine-3-yl]benzamide as a Brain Penetrant PET Ligand selective for the δ-Containing γ-Aminobutyric Acid Type A Receptors

Elina T. L'Estrade[a,b,c,d ‡], Hanne D. Hansen[b ‡], Christina Falk-Petersen[a], Anne Haugaard[a], Nane Griem-Krey[a], Sascha Jung[f], Hartmut Lüddens[e], Tanja Schirmeister[f], Maria Erlandsson[c], Tomas Ohlsson[c], Gitte M. Knudsen[b], Matthias M. Herth[a,b,d], Petrine Wellendorph[a], Bente Frølund[a*]

[a]*Department of Drug Design and Pharmacology, Faculty of Health and Medical Sciences, University of Copenhagen, 2100 Copenhagen, Denmark*

[b]*Neurobiology Research Unit and CIMBI, Copenhagen University Hospital, Rigshospitalet, Blegdamsvej 9, 2100 Copenhagen, Denmark*

[c]*Radiation Physics, Nuclear Medicine Physics Unit, Skånes University Hospital, Barngatan 3, Lund 222 42, Sweden*

[d]*Department of Clinical Physiology, Nuclear Medicine and PET, University Hospital Copenhagen, Rigshospitalet Blegdamsvej 9, 2100 Copenhagen, Denmark*

[e]*Department of Psychiatry and Psychotherapy, Falculty of Health and Medical Sciences, University of Medical Center Mainz, D-55131, Germany*

[f]*Institute of Pharmacy & Biochemistry, Johannes Gutenberg University Mainz, D-55128, Germany*

KEYWORDS: $GABA_A$ receptors, δ-selective compound, DS2, PET.

ABSTRACT: The $\alpha_{4/6}\beta\delta$-containing $GABA_A$ receptors are involved in a number of brain diseases. Despite the potential of a δ-selective imaging agent, no PET radioligand is currently available for *in vivo* imaging. Here, we report the characterization of DS2OMe (**1**) as a candidate radiotracer, ^{11}C-labeling and subsequent evaluation of [^{11}C]DS2OMe in a domestic pig as a PET-radioligand for visualization of the δ-containing $GABA_A$ receptors.

Introduction γ–Aminobutyric acid (GABA) is the main inhibitory neurotransmitter in the central nervous system and exerts its major physiological effect via interaction with ionotropic $GABA_A$ receptors ($GABA_ARs$). The $GABA_ARs$ are assembled from a variety of subunits (α_{1-6}, β_{1-3}, γ_{1-3}, δ, ε, θ, π, and ρ_{1-3}) forming hetero- or homo-pentameric complexes in various combinations.[1, 2] The subunit composition of $GABA_ARs$ appears to differ with subcellular localization which dictates the type of inhibition mediated.[3] The majority of $GABA_ARs$ have the general stoichiometry of 2α, 2β, and 1γ subunit.[4] However, in a subpopulation of receptors, the δ-subunit is replacing the γ-subunit. δ-subunit-containing $GABA_ARs$, e.g. $\alpha_4\beta\delta$, $\alpha_6\beta\delta$, $\alpha_1\beta_2\delta$ are primarily found in peri- or extrasynaptic locations where they mediate tonic inhibition distinct from the fast and transient synaptic inhibition.[5, 6] Aberrant tonic inhibition mediated by $\alpha_{4/6}\beta\delta$–containing receptors has been implicated in various pathophysiological conditions and related to discrete brain regions,[1] including stroke (cortex),[7] Angelman syndrome (cerebellum)[8], sleep-related disorders (thalamus)[9] and depression (hippocampus).[10] Therefore, these receptors have received a great deal of attention in the last decades as potential drug targets.[11] Consequently, development of selective tool compounds and diagnostics to further understand the pharmacology and physiological roles of these receptors will prove therapeutically important.

Among the orthosteric ligands reported, the functional δ-preferring orthosteric agonist THIP (Gaboxadol) (Figure 1) has been pursued as a novel treatment for insomnia, reaching phase III clinical development. Gaboxadol is at present in phase II clinical trials for treatment of Angelman syndrome.[12] The imidazopyridine DS2, a functionally selective $\alpha_4/_6\beta_3\delta$ positive allosteric modulator (PAM) relative to its action at $\alpha_4\beta_3\gamma_2$ and $\alpha_1\beta_3\gamma_2$ receptors, has been reported.[13, 14] However, poor brain penetration precludes the use of DS2 for *in vivo* studies.[15]

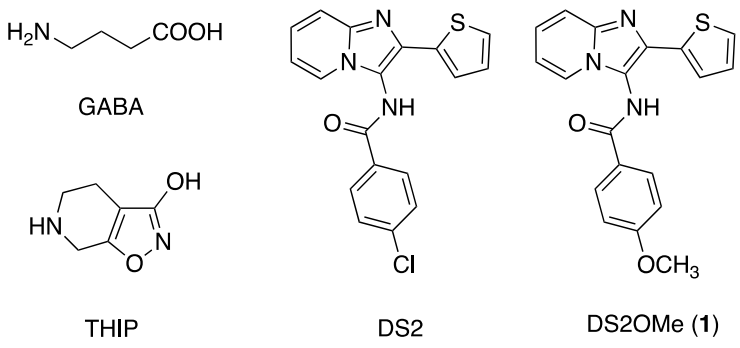

Figure 1. Chemical structures of the GABA, the orthosteric agonist THIP/Gaboxadol and the two PAMs DS2 and DS2OMe (**1**).

Recently, we reported a structure-activity study on the δ–selective imidazopyridine DS2 (Figure 1) and the corresponding 6,8-dibromo analogue DS1, and the direct modulatory effect on [^{3}H]-ethynylbicycloorthobenzoate ([^{3}H]-EBOB) binding to δ–containing $GABA_A$Rs.[16] EBOB is a potent non-competitive $GABA_A$R antagonist that binds to the picrotoxinin-binding site within the $GABA_A$R ion channel. [^{3}H]-EBOB binding is sensitive to conformational changes in the chloride channel, which can be mediated by increasing concentrations of GABA and/or affected by modulators in the presence or absence of GABA.[17-20]

Since the δ–containing $GABA_A$Rs are potentially involved in the pathogenesis and symptoms of several disorders in the central nervous system, a positron emission tomography (PET) tracer would be a valuable tool. Inspired by the structure-activity study mentioned above, we herein report the identification, radiosynthesis and *in vivo* PET studies of a low micromolar potency, selective and brain-penetrant PAM of δ–containing $GABA_A$Rs ([^{11}C]DS2OMe, [^{11}C]**1**), in pig, as a promising lead candidate for imaging the □□containing $GABA_A$Rs.

Results and Discussion Initially, a potential ^{11}C-labelling site in the core scaffold of DS2 was identified based on the reported structure-activity study and the experience obtained on the chemistry involved.[16] Since the *p*-hydroxy analog **2** (see Scheme 1) appears as an attractive precursor amenable for radiolabeling via conventional ^{11}C-methylation, the [^{11}C]-*p*-methoxy analog of DS2 ([^{11}C]**1**) was selected as candidate radiotracer.

To probe the applicability of [^{11}C]**1** as a specific radiotracer for the δ–containing $GABA_A$Rs, the selectivity profiles of **1** and DS2 were compared using a fluorescence-based FLIPR membrane potential (FMP) assay, based on transient expression of human $\alpha_{1/4/6}$ and β_2 subunits in a HEK293 Flp-In™ cell line, stably expressing the human δ–subunit, [21] or γ_2 instead of δ for comparison. To this end, the concentration of GABA corresponding to GABA EC_{20} was determined from full concentration-response curves of GABA for each of the tested receptors. The actual GABA concentrations used are given in Table 1. To investigate the importance of the α-subunit for potency, the subtypes $\alpha_1\beta_2\delta$, $\alpha_4\beta_2\delta$ and $\alpha_6\beta_2\delta$ were compared. Full concentration-response curves showed that **1** and DS2 displayed near equipotent activities (1-4 μM) at the different α-subunit-containing receptors (Table 1, Figure 2). In parallel, to confirm δ-subunit selectivity, **1** was also tested as a PAM at $\alpha_6\beta_2\gamma_{2s}$. As shown, neither DS2 nor **1** had any effect at this non-δ containing receptor subtype when tested at concentrations up to 10 μM (Table 1, Figure 2). These data summarizes **1** as a novel δ-selective DS2-analogue with low micromolar PAM activity. The cell line stably

expressing the δ-subunit has previously been used to study DS2 at $\alpha_4\beta_1\delta$ vs. binary $\alpha_4\beta_{1/3}$ receptors using both the FMP assay and whole-cell patch-clamp recordings, confirming that DS2 is δ-selective.[16]

Table 1. EC_{50} values for GABA and the modulation of GABA EC_{20} by DS2 and 1 at selected $GABA_A$ receptors

	EC_{50} (μM) (pEC_{50}±SEM, n)			EC_{20} (μM)
	1	**DS2**	**GABA**	**GABA**
$\alpha_1\beta_2\delta$	3.68 (5.43±0.055, 4)	2.97 (5.53±0.13, 3)	6.71 (5.17±0.087, 4)	1.6-2.0
$\alpha_4\beta_2\delta$	2.91 (5.54±0.069, 3)	1.41 (5.85±0.085, 3)	0.25 (6.61±0.030, 3)	0.08
$\alpha_6\beta_2\delta$	2.25 (5.65±0.0038, 3)	2.02 (5.69±0.10, 3)	0.21 (6.68±0.13, 3)	0.05
$\alpha_6\beta_2\gamma_{2s}$	No modulation (n=3)	No modulation (n=3)	0.50 (6.30±0.091, 3)	0.1-0.2

The selectivity was further explored in The National Institute of Mental Health's Psycoactive Drug Screening Program (NIMH-PDSP) (SI Table 1), where binding affinity and cross selectivity of **1** to a large panel of brain targets was assessed. **1** did not show significant affinity (K_i > 10 μM) for other tested biogenic receptors and transporters (45 in total).

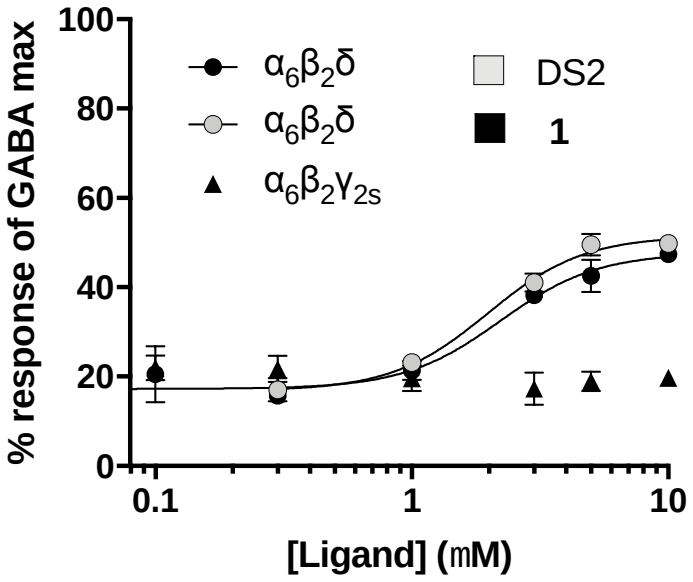

Figure 2. Concentration-response curves of the modulation of GABA EC_{20} by **1** at $\alpha_6\beta_2\delta$ and $\alpha_6\beta_2\gamma_{2s}$ receptors, and DS2 at $\alpha_6\beta_2\delta$ receptors, tested in the FMP assay. Data are shown as mean±SD of a single representative experiment performed with three technical triplicates. Two additional experiments gave similar results; data summarized in Table 1.

The high selectivity for δ–containing $GABA_A$Rs establish **1** as an interesting compound as a PET radiotracer candidate for further studying the δ–containing $GABA_A$Rs. Furthermore, since *O*-demethylation in general is a major metabolic pathway, the *O*-demethylated compound may be the major metabolite for **1**. Therefore, radiolabeling of the methoxy group, resulting in [^{11}C]**1** via

radiomethylation of the hydroxyl-analogue (**2**), was rendered the most suitable strategy to avoid/limit nonradioactive metabolite formation. This may be an advantage of the *in vivo* application of [^{11}C]**1** due to absence of other competing radioactive metabolites via *O*-demethylation pathway.

Consequently, radiolabeling of **1** was probed to obtain the corresponding [^{11}C]**1**. To obtain the hydroxylated precursor, **2**, a three-step procedure was applied, as previously reported,[16] using 2-aminopyridine and thiophene-2-carbaldehyde in a multicomponent reaction followed by amide-bond formation using 4-acetoxybenzoyl chloride. The removal of the acetoxy group was accomplished with 5M NaOH in THF at room temperature.

Scheme 1. Synthesis of [^{11}C]1

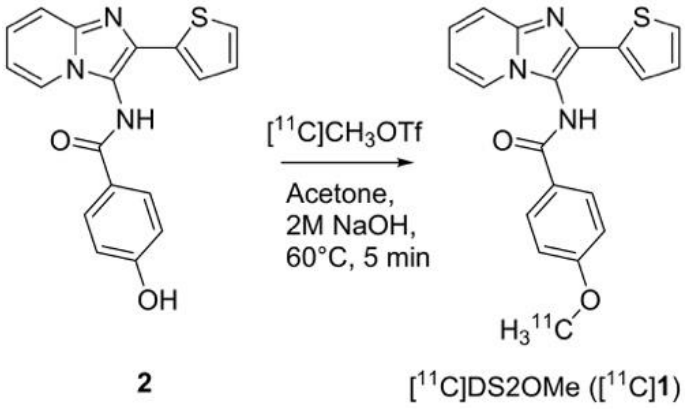

2 [^{11}C]DS2OMe ([^{11}C]**1**)

The non-radiolabelling experiment was performed by using methyl triflate and 2M NaOH in acetone for 3 min at 80 °C to enable the introduction of the *O*-methyl into **2**.

The radiolabelling of [^{11}C]DS2OMe ([^{11}C]**1**) was performed in a fully automated system. [^{11}C]CH_3OTf was dissolved in acetone containing precursor and base and reacted for 5 min at 60 ˚C. Isolation of the final radiotracer, see Scheme 1, could be achieved via semi-preparative HPLC with a total synthesis time of 37 min (SI Figure 1 and 2).

The radiolabeled compound [^{11}C]**1** was produced with a good radiochemical yield of 21 % (decay corrected), sufficient chemical and radiochemical purity of >95 %, and very high molar activities of 188-215 GBq/μmol.

Using the radiochemistry described and delineated in Scheme 1, [^{11}C]**1** was prepared for evaluation in *in vivo* PET imaging studies in a domestic pig using a high-resolution research tomography (HRRT) PET scanner. [^{11}C]**1** successfully entered the pig brain with the radioligand uptake being fairly uniform across different brain regions (Figure 3A). From the time-activity curves it is also

evident that [^{11}C]**1** has fast tracer kinetics in four different regions measured, meaning that the retention of the tracer in the brain is limited (Figure 3B).

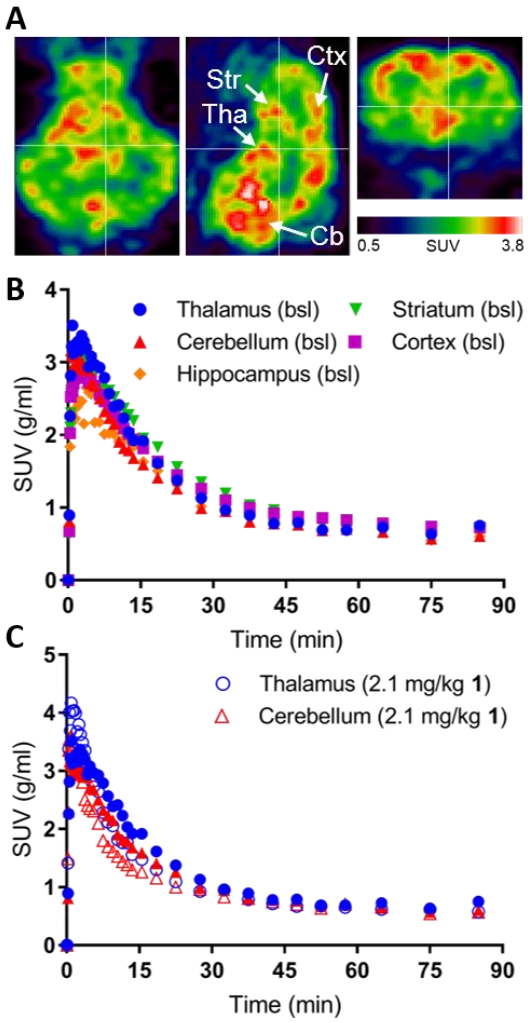

Figure 3. **A)** PET images of the pig brain in the transverse, sagittal and coronal plane (left to right). **B)** Time-activity curves of [^{11}C]**1** in the indicated regions of the pig brain. **C)** Time-activity curves of [^{11}C]**1** in thalamus and cerebellum at baseline (closed symbols) and after administration of 2.1 mg/kg unlabeled **1** (co-administrated with the tracer, open symbols). SUV: standardized uptake value. Tha: Thalamus, Str: Striatum, Ctx: Cortex, Cb: Cerebellum.

In the same animal we performed a self-block experiment, where we co-injected 2.1 mg/kg non-labelled **1** along with [^{11}C]**1**. When compared to the baseline situation, the uptake of [^{11}C]**1** was reduced in the thalamus and cerebellum, indicating specific binding of the radioligand (Figure 3C). Kinetic modelling of the baseline and self-block PET data confirmed that the binding of [^{11}C]**1** is uniform across the brain. The total distribution volume (V_T) in the baseline situation was highest in the cortex (5.6 mL/cm^3) followed by the striatum (4.5 mL/cm^3), thalamus (3.8 mL/cm^3) hippocampus (3.8 mL/cm^3) and lastly cerebellum (3.4 mL/cm^3). This is not in accordance with the

reported distribution of $\alpha_{4/6}\delta$ containing $GABA_A$Rs. After administration of unlabelled **1**, the V_Ts was decreased in all regions: V_T decreased by ~40% in the hippocampus and cortex whereas V_T decreased by ~18% in the thalamus and cerebellum (Figure 4A) indicating that there is some specific binding of [^{11}C]**1**.

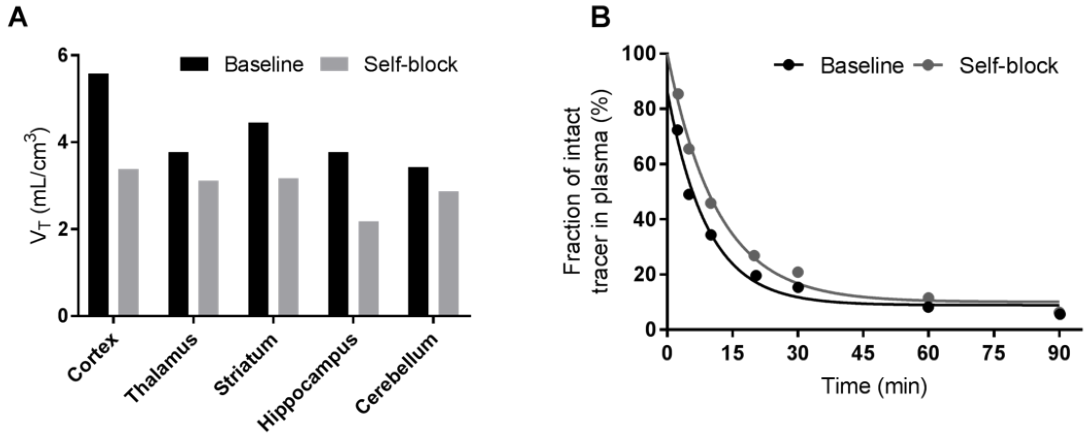

Figure 4. **A)** Regional time-activity curves of [^{11}C]**1** in four different regions. **B)** Time-activity curves of [^{11}C]**1** in the thalamus and cerebellum at baseline and after administration of 2.1 mg/kg unlabeled **1** (co-administrated with the tracer).

Radiometabolite analysis of plasma samples from the pig revealed that the metabolism of [^{11}C]**1** was fast with only 50 % of the parent compound remaining after ~5 min. If the metabolism of **1** is similarly fast in pharmacological doses, it would render this compound unsuited as a clinical drug. It is possible that the fast metabolism of [^{11}C]**1** is the reason for the observed fast tracer kinetics. After self-blockade, the radiometabolism of [^{11}C]**1** was similar to the baseline situation (Figure 4B). Only early eluting radiometabolites were detected with our radio-HPLC method suggesting that these metabolites were of a polar nature (SI Figure 3). The free fraction of [^{11}C]**1** in pig plasma was measured to 15 % using a dialysis chamber method with an incubation time of 3h. This is comparable to other radiotracers evaluated in pigs.[22, 23]

In conclusion we here show high uptake of [^{11}C]**1** into the pig brain but the uptake represents mainly non-displaceable binding and clears quickly. This is indicated by the uniform uptake across regions and only a small decrease in binding after self-blockade. By contrast to DS2,[13] [^{11}C]**1** enters the brain, which, together with its selectivity for δ–containing $GABA_A$Rs, renders it a promising lead in developing a radiotracer for the target.

EXPERIMENTAL SECTION

Radiosynthesis of [^{11}C]DS2OMe ([^{11}C]1) [^{11}C]methyl trifluoromethanesulfonate ([^{11}C]MeOTf) was produced in an automated system and trapped in 300 µL acetone solution containing the precursor 4-hydroxy-*N*-(2-(thiophen-2-yl)imidazo[1,2-a]pyridin-3-yl)benzamide (**2**, 0.1 mg, 0.3 µmol) and 5 µL 2N NaOH at RT. The reaction mixture was heated for 5 minutes at 60 °C before it was diluted in 4.3 mL 0.1% phosphoric acid and isolated using semi-preparative HPLC (C18 Onyx Semi-prep monolithic column (Phenomenex Inc. 100 · 10 mm), 70:30 100 mM phosphate–buffer:EtOH, at a flow rate of 6 mL/min). Retention times were 400 s for **[**^{11}C**]1** and 200-225 s for **2** (see SI Figure 1). The labelled product was collected into a sterile 20 mL vial containing phosphate–buffer (9 mL, 100 mM, pH 7). The final product was analysed by analytical HPLC (Luna, 5µ, C-18(2) 100-A˚ column (Phenomenex Inc. 150 4.6 mm); 60:40 0.01 M sodium borate buffer:acetonitrile; 1.5 mL/min: retention time for **1** was 4.48 minutes (see SI Figure 2). The overall synthesis, purification, and formulation time was approximately 40 min. The product [^{11}C]**1** could be produced and isolated with sufficient molar activities (188-215 GBq/µmol (n = 2)) and radiochemical purities above 95 %.

FLIPR^{TM} membrane potential (FMP) Blue Assay on GABA$_A$ receptors expressed in HEK-293 cells The FMP assay was performed on HEK-293 Flp-In^{TM} cells expressing human recombinant GABA$_A$ receptors using conditions for cell-culturing and transfection as described previously [21]. In brief, cells were plated for transfection 24 hours later with GABA$_A$ receptor plasmids with the Polyfect Transfection Reagent (Qiagen, West Sussex, UK). For expression of the δ-containing GABA$_A$ receptor subtypes, $\alpha_1\beta_2\delta$, $\alpha_4\beta_2\delta$ and $\alpha_6\beta_2\delta$, HEK-293 Flp-In cells stably expressing the GABA$_A$ δ-subunit were transfected by a 1:1 ratio of either α_1, α_4 (both pUNIV) (Addgene, Cambridge, MA, USA)[24] or α_6 (pcDNA3.1zeo), and β_2 (pcDNA3.1zeo)[25]. $\alpha_6\beta_2\gamma_{2s}$ receptors were transiently expressed in background HEK-293 Flp-In^{TM} cells[21] using a 1:1:2 ratio of α_6-, β_2- and γ_{2s}-subunits, respectively.

Transfected cells 16-24 hours post-transfection were plated into poly-D-lysine coated black clear bottom 96-well plates (BD Biosciences, Bedford, MA, USA) at a density of 50,000 cells/well and incubated for 16-20 hours. On the day of assay, media was aspirated and the cells were washed in 100 µL/well assay buffer (HBSS (Life technologies, Paisley, UK) + 20 mM HEPES pH 7.4) followed by addition of 100 µL/well of FMP blue dye (0.5 mg/mL) (Molecular Devices, Sunnyvale, CA, USA) and incubated in the dark for 30 min in CO_2 incubator at 37°C and 5 % CO_2. Ligand solutions were prepared in 5x in assay buffer, which for testing of the PAMs contained a concentration of GABA corresponding to GABA EC_{20}. The GABA EC_{20}

concentrations were determined from full GABA concentration-response curves for each subtype as described in the Results. Before reading of the plate, the ligand solutions were added to 96-well ligand plates and incubated for 15 min at 37 °C in the NOVOstar^{TM} plate reader (BMG, LABTECH GmbH, Offenburg, Germany). Fluorescence was determined by excitation of the dye at 530 nm and emission at 560 nm. The relative changes in the fluorescent signal (ΔFU) were analyzed by subtracting the baseline signal from the maximum peak/plateau signal induced by the ligands. Fluorescence signals were visually inspected and any artefacts were manually omitted from the analysis. Concentration-response curves were fitted to obtain EC_{50} values using the four-parameter concentration-response curve using GraphPad Prism 7.0 (GraphPad Software Inc., San Diego, CA, USA):

$$Response = bottom + \frac{top - bottom}{1 + 10^{((\log(EC_{50}) - [A]) \cdot n_H)}}$$

with bottom and top being the lower (e.g. the GABA EC_{20} level) and upper plateau response, respectively. [A] corresponds to the logarithmic concentration of the ligand and n_H the hill slope of the curve. The obtained EC_{50} values are based on at least 3 independent experiments with each data point performed with technical triplicates.

Animal procedures, pigs. One female domestic pig (crossbreed of Landrace x Yorkshire x Duroc, 22 kg) was used for *in vivo* PET imaging. All animal procedures were approved by the Danish Council for Animal Ethics (journal no. 2012-15-2934-00156). [^{11}C]**1** was given as intravenous (i.v.) bolus and the injected dose was 509 MBq in the baseline scan and 488 MBq in the self-block scan. Molar activity at the time of injection was 129 GBq/μmol and 113 GBq/μmol resulting in an injected mass of 1.37 μg and 1.51 μg. The pig was scanned twice for 90 min in list mode. For the second (self-block) scan, [^{11}C]**1** was co-injected with 2.14 mg/kg unlabelled **1**. **1** was dissolved in 10% beta-cyclodextrin solution (Sigma-Aldrich).

The animal was housed under standard conditions and was allowed to acclimatize for 1 week. Before scanning, anaesthesia was induced with i.m. injection of 0.13 mL/kg Zoletil veterinary mixture (10.87 mg/kg xylazine + 10.87 mg/kg ketamine + 1.74 mg/kg methadone + 1.74 mg/kg butorphanol + 10.87 mg/kg tiletamine + 10.87 mg/kg zolezepam). Hereafter, anaesthesia was maintained with constant propofol infusion (1.5 mg/kg/h intravenous (i.v.); B. Braun, Melsungen, Germany). Arterial i.v. access for blood drawing was granted in the right femoral artery via a minor incision and two venous i.v. lines for injections were granted in the left and

right mammary veins. Analgesia was assured by i.v. injection of fentanyl during surgery. During anaesthesia, animals were endotracheally intubated and ventilated. Vital parameters (heart rate, body temperature, blood pressure, blood glucose, oxygen saturation and end tidal CO_2) were continuously monitored during the scan.

Blood sampling During the first 30 min of the scans, radioactivity in the whole blood was continuously measured using an ABSS autosampler (Allogg Technology, Mariefred, Sweden) counting coincidences in a lead-shielded detector. Concurrently, arterial whole blood was sampled manually at times 2.5, 5, 10, 20, 30, 40, 50, 70 and 90 minutes after injection of [^{11}C]**1**. Total radioactivity in plasma (500 μL) and whole blood (500 μL) was measured in a well counter (Cobra 5003; Packard Instruments, Meriden, CT, USA), which was cross-calibrated to the HRRT scanner and autosampler. All measurements of radioactivity were decay corrected to the time of radioligand injection.

The free fraction of [^{11}C]**1** in pig plasma was measured using an equilibrium dialysis method as previously described[26] and calculated as the ratio between radioactivity in a buffer and plasma.

Metabolite analysis Radiolabelled parent compound and metabolites were determined by direct injection of plasma into a radio-HPLC system (Dionex Ultimate 3000; Thermo Fisher Scientific, Hvidovre, Denmark) configured for column switching. Manually drawn arterial whole blood samples were centrifuged (1500x*g*, 7 min, 4 °C), and plasma was filtered through a syringe filter (Whatman GD/X 13 mm or 25 mm, PVDF membrane, 0.45 um pore size; Frisenette ApS, Knebel, Denmark) prior to the analysis by HPLC as previously described.[27]

Reconstruction and quantification of PET data Ninety-minute list-mode PET data were reconstructed in 38 dynamic frames (6 × 10, 6 × 20, 4 × 30, 9 × 60, 2 × 180, 8 × 300, and 3 × 600 seconds). Images consisted of 207 planes of 256 x 256 voxels of 1.22 x 1.22 x 1.22 mm. A summed picture of all counts in the 90-min scan was reconstructed for the pig and used for co-registration to a multimodal pig brain atlas as described by Villadsen et all.[28] The time activity curves were calculated for the following volumes of interest (VOIs): cortex, hippocampus, thalamus, striatum, and cerebellum (excluding the vermis). Outcome measure in the time-activity curves was calculated as radioactive concentration in VOI (in kBq/mL) normalized to the injected dose corrected for animal weight (in kBq/kg), yielding standardized uptake values (g/mL). Quantification of the binding was performed in PMOD (version 3.0) with the Logan

graphical analysis, using the metabolite corrected arterial plasma concentration to calculate the total distribution volume (V_T).

ASSOCIATED CONTENT

Supporting Information

The Supporting Information is available free of charge on the ACS Publications website. Selectivity profiling in the National Institute of Mental Health's Psycoactive Drug Screening Program (Table 1), HPLC chromatograms on purification (Figure 1) and product UV HPLC (Figure 2).

AUTHOR INFORMATION

Corresponding Author

* Phone: +45 35 33 64 95. E-mail: bfr@sund.ku.dk

Author Contributions

The manuscript was written through contributions of all authors. / All authors have given approval to the final version of the manuscript. / ‡These authors contributed equally.

Funding Sources

This work was funded by The Lundbeck Foundation (grants R164-2013-15384 to A.H., R133-A12270 to P.W., R230-2016-2562 to C.B.F.-P and R90-A7722 for E.T.L.). The work was further supported by Innovation Fund Denmark (4108-0000-43).

Notes

The authors declare no competing financial interests

ACKNOWLEDGMENT

The authors would like to thank the staff at the Department of Experimental Medicine (University of Copenhagen) and the PET and cyclotron unit (Rigshospitalet) for expert technical assistance. Agnete Dyssegaard is acknowledged for conducting the HPLC analysis of plasma samples.

ABBREVIATIONS

DS2, δ-selective compound 2; GABA, γ-amino butyric acid; $GABA_AR$, γ-amino butyric acid receptor; PET, positron emission tomography; PAM, positive allosteric modulator; EBOB, ethynylbicycloorthobenzoate

References

1. Olsen, R. W.; Sieghart, W. International Union of Pharmacology. LXX. Subtypes of gamma-aminobutyric acid(A) receptors: classification on the basis of subunit composition, pharmacology, and function. Update. *Pharmacol. Rev.* **2008**, 60, 243–260.
2. Olsen, R. W.; Sieghart, W. GABA $_A$ receptors: subtypes provide diversity of function and pharmacology. *Neuropharmacol.* **2009,** 56, 141–148.
3. Sieghart, W.; Sperk, G. Subunit composition, distribution and function of GABA(A) receptor subtypes. *Curr. Top. Med. Chem.* **2002**, *2*, 795-816.
4. Whiting, P. J. GABA-A receptor subtypes in the brain: a paradigm for CNS drug discovery? *Drug Discov. Today* **2003,** I, 445–450.
5. Farrant, M.; Nusser, Z. Variations on an inhibitory theme: phasic and tonic activation of GABA(A) receptors. *Nat. Rev. Neurosci.* **2005**, *6*, 215–229.
6. Belelli, D.; Harrison, N. L.; Maguire, J.; Macdonald, R. L.; Walker, M. C.; Cope, D. W. Extrasynaptic $GABA_A$ receptors: form, pharmacology, and function. *J. Neurosci.* **2009**, *29*, 12757–12763.
7. Clarkson, A. N.; Huang, B. S.; Macisaac, S. E.; Mody, I.; Carmichael, S. T. Reducing excessive GABA-mediated tonic inhibition promotes functional recovery after stroke. *Nature* **2010**, *468*, 305–309.
8. Asahina, N.; Shiga, T.; Egawa, K.; Shiraishi, H.; Kohsaka, S.; Saitoh, S. [(11)C]flumazenil positron emission tomography analyses of brain gamma-aminobutyric acid type A receptors in Angelman syndrome. *J. Pediatr.* **2008**, *152*, 546–549, 549 e1-3.
9. Bright, D. P.; Aller, M. I.; Brickley, S. G. Synaptic release generates a tonic GABA(A) receptor-mediated conductance that modulates burst precision in thalamic relay neurons. *J. Neurosci.* **2007**, *27*, 2560–2569.
10. Holm, M. M.; Nieto-Gonzalez, J. L.; Vardya, I.; Henningsen, K.; Jayatissa, M. N.; Wiborg, O.; Jensen, K. Hippocampal GABAergic dysfunction in a rat chronic mild stress model of depression. *Hippocampus* **2011**, *21*, 422–433.
11. Brickley, S. G.; Mody, I. Extrasynaptic GABA(A) receptors: their function in the CNS and implications for disease. *Neuron* **2012**, *73*, 23–34.
12. Egawa, K.; Kitagawa, K.; Inoue, K.; Takayama, M.; Takayama, C.; Saitoh, S.; Kishino, T.; Kitagawa, M.; Fukuda, A. Decreased tonic inhibition in cerebellar granule cells causes motor dysfunction in a mouse model of Angelman syndrome. *Sci. Transl. Med.* **2012**, *4*, 163–157.

13. Jensen, M. L.; Wafford, K. A.; Brown, A. R.; Belelli, D.; Lambert, J. J.; Mirza, N. R. A study of subunit selectivity, mechanism and site of action of the delta selective compound 2 (DS2) at human recombinant and rodent native GABA(A) receptors. *Br. J. Pharmacol.* **2013**, *168*, 1118–1132.

14. Wafford, K. A.; van Niel, M. B.; Ma, Q. P.; Horridge, E.; Herd, M. B.; Peden, D. R.; Belelli, D.; Lambert, J. J. Novel compounds selectively enhance delta subunit containing $GABA_A$ receptors and increase tonic currents in thalamus. *Neuropharmacol.* **2009**, *56*, 18–19.

15. Jensen, M. L.; Wafford, K. A.; Brown, A. R.; Belelli, D.; Lambert, J. J.; Mirza, N. R. A study of subunit selectivity, mechanism and site of action of the delta selective compound 2 (DS2) at human recombinant and rodent native $GABA_A$ receptors. *Br. J. Pharmacol.* **2013**, *168*, 1118–1132.

16. Yakoub, K.; Jung, S.; Sattler, C.; Damerow, H.; Weber, J.; Kretzschmann, A.; Cankaya, A. S.; Piel, M.; Rosch, F.; Haugaard, A. S.; Frolund, B.; Schirmeister, T.; Luddens, H. Structure-Function Evaluation of Imidazopyridine Derivatives Selective for delta-Subunit-Containing gamma-Aminobutyric Acid Type A ($GABA_A$) Receptors. *J. Med. Chem.* **2018**, *61*, 1951–1968.

17. Maksay, G.; Biro, T. High affinity, heterogeneous displacement of [^{3}H]EBOB binding to cerebellar GABA A receptors by neurosteroids and GABA agonists. *Neuropharmacol.* **2005**, *49*, 431–438.

18. Maksay, G.; Korpi, E. R.; Uusi-Oukari, M. Bimodal action of furosemide on convulsant [^{3}H]EBOB binding to cerebellar and cortical GABA(A) receptors. *Neurochem. Int.* **1998**, *33*, 353–358.

19. Uusi-Oukari, M.; Maksay, G. Allosteric modulation of [^{3}H]EBOB binding to $GABA_A$ receptors by diflunisal analogues. *Neurochem. Int.* **2006**, *49*, 676–682.

20. Yagle, M. A.; Martin, M. W.; de Fiebre, C. M.; de Fiebre, N. C.; Drewe, J. A.; Dillon, G. H. [^{3}H]Ethynylbicycloorthobenzoate ([^{3}H]EBOB) binding in recombinant $GABA_A$ receptors. *Neurotoxicol.* **2003**, *24*, 817–824.

21. Falk-Petersen, C. B.; Sogaard, R.; Madsen, K. L.; Klein, A. B.; Frolund, B.; Wellendorph, P. Development of a Robust Mammalian Cell-based Assay for Studying Recombinant alpha4 beta1/3 delta $GABA_A$ Receptor Subtypes. *Basic Clin. Pharmacol. Toxicol.* **2017**, *121*, 119–129.

22. Hansen, H. D.; Ettrup, A.; Herth, M. M.; Dyssegaard, A.; Ratner, C.; Gillings, N.; Knudsen, G. M. Direct comparison of [(18) F]MH.MZ and [(18) F] altanserin for 5-HT_{2A} receptor imaging with PET. *Synapse* **2013**, *67*, 328–337.

23. Hansen, H. D.; Lacivita, E.; Di Pilato, P.; Herth, M. M.; Lehel, S.; Ettrup, A.; Andersen, V. L.; Dyssegaard, A.; De Giorgio, P.; Perrone, R.; Berardi, F.; Colabufo, N. A.; Niso, M.; Knudsen, G. M.; Leopoldo, M. Synthesis, radiolabeling and *in vivo* evaluation of [(11)C](R)-1-[4-[2-(4-methoxyphenyl)phenyl]piperazin-1-yl]-3-(2-pyrazinyloxy)-2-p ropanol, a potential PET radioligand for the 5-HT(7) receptor. *Eur. J. Med. Chem.* **2014**, *79*, 152–163.

24. Venkatachalan, S. P.; Bushman, J. D.; Mercado, J. L.; Sancar, F.; Christopherson, K. R.; Boileau, A. J. Optimized expression vector for ion channel studies in Xenopus oocytes and mammalian cells using alfalfa mosaic virus. *Pflugers Arch.* **2007**, *454*, 155–163.

25. Petersen, J. G.; Sorensen, T.; Damgaard, M.; Nielsen, B.; Jensen, A. A.; Balle, T.; Bergmann, R.; Frolund, B. Synthesis and pharmacological evaluation of 6-aminonicotinic acid analogues as novel GABA(A) receptor agonists. *Eur. J. Med. Chem.* **2014**, *84*, 404–416.

26. Kornum, B. R.; Lind, N. M.; Gillings, N.; Marner, L.; Andersen, F.; Knudsen, G. M. Evaluation of the novel 5-HT_4 receptor PET ligand [^{11}C]SB207145 in the Gottingen minipig. *J. Cereb. Blood Flow Metab.* **2009**, *29*, 186–196.

27. Gillings, N. A restricted access material for rapid analysis of [(11)C]-labeled radiopharmaceuticals and their metabolites in plasma. *Nucl. Med. Biol.* **2009**, *36*, 961–965.

28. Villadsen, J.; Hansen, H. D.; Jorgensen, L. M.; Keller, S. H.; Andersen, F. L.; Petersen, I. N.; Knudsen, G. M.; Svarer, C. Automatic delineation of brain regions on MRI and PET images from the pig. *J. Neurosci. Methods* **2018**, *294*, 51–58.

Supporting Information

Synthesis and Pharmacological Evaluation of [^{11}C]4-Methoxy-*N*-[2-(Synthesis and Pharmacological Evaluation of [^{11}C]4-Methoxy-*N*-[2-(thiophene-2-yl)imidazo[1,2-a]pyridine-3-yl]benzamide as a Brain Penetrant PET Ligand selective for the δ-Subunit-Containing γ-Aminobutyric Acid Type A Receptors

Elina T. L'Estrade,[a,b,c,d] ‡ Hanne D. Hansen,[b] ‡ Christina Falk-Petersen,[a] Anne Haugaard, [a] Nane Griem-Krey [a] Sascha Jung,[f] Hartmut Lüddens,[e] Tanja Schirmeister,[f] Maria Erlandsson,[c] Tomas Ohlsson,[c] Gitte M. Knudsen,[b] Matthias M. Herth,[a,b,d] Petrine Wellendorph,[a] Bente Frølund[a*]

[a]*Department of Drug Design and Pharmacology, Faculty of Health and Medical Sciences, University of Copenhagen, 2100 Copenhagen, Denmark*

[b]*Neurobiology Research Unit and CIMBI, Copenhagen University Hospital, Rigshospitalet, Blegdamsvej 9, 2100 Copenhagen, Denmark*

[c]*Radiation Physics, Nuclear Medicine Physics Unit, Skånes University Hospital, Barngatan 3, Lund 222 42, Sweden*

[d]*Department of Clinical Physiology, Nuclear Medicine and PET, University Hospital Copenhagen, Rigshospitalet*

Blegdamsvej 9, 2100 Copenhagen, Denmark

[e]*Department of Psychiatry and Psychotherapy, Falculty of Health and Medical Sciences, University of Medical Center Mainz, D-55131, Germany*

[f]*Institute of Pharmacy & Biochemistry, Johannes Gutenberg University Mainz, D-55128, Germany*

Corresponding Author

* Phone: +45 35 33 64 95. E-mail: bfr@sund.ku.dk

CONTENTS

Selectivity profiling: **.....363**

Radiometabolism in pigs **.....364**

Results

Selectivity profiling:

Supporting Table 1: In the table is included the targets for which DS2OMe showed less than 50% inhibition at 10 μM in the National Institute of Mental Health's Psycoactive Drug Screening Program (NIMH-PDSP).

Receptors (<50% inhibition at 10 μM)			
5-HT1A	Alpha1A	D4	M2
5-HT1B	Alpha1B	D5	M4
5-HT1D	Alpha1D	DAT	M5
5-ht1e	Alpha2A	DOR	MOR
5-HT2A	Alpha2B	H1	NET
5-HT2B	Beta1	H2	SERT
5-HT2C	Beta2	H3	Sigma 1
5-HT3	Beta3	H4	Sigma 2
5-ht5a	D1	KOR	
5-HT6	D2	M1	
5-HT7	D3	M3	

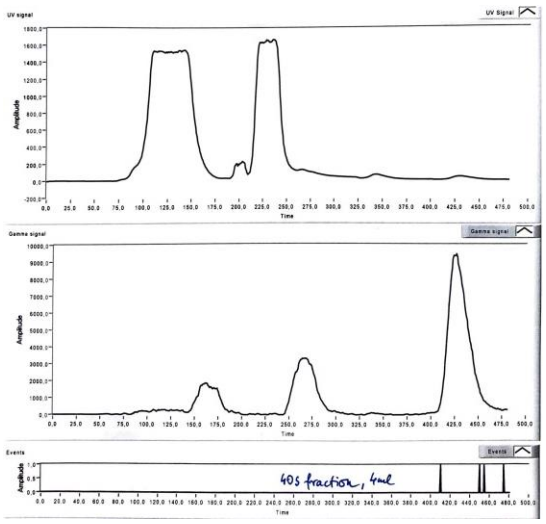

Supporting Figure 1: Semi-preparative HPLC chromatogram of radiolabeling of [^{11}C]DS2OMe ([^{11}C]**1**).

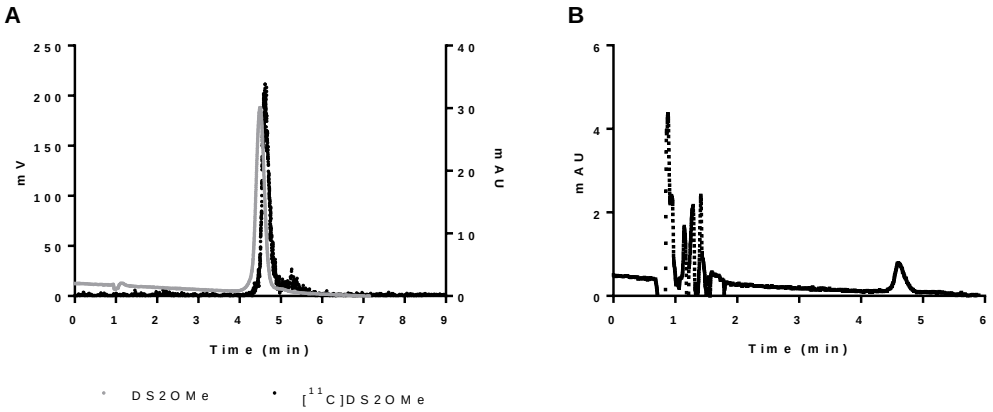

Supporting Figure 2: A) DS2OMe (**1**) (grey line) and [^{11}C]DS2OMe ([^{11}C]**1**)(black line) HPLC chromatograms. **B)** Product UV HPLC chromatogram

Radiometabolism in pigs

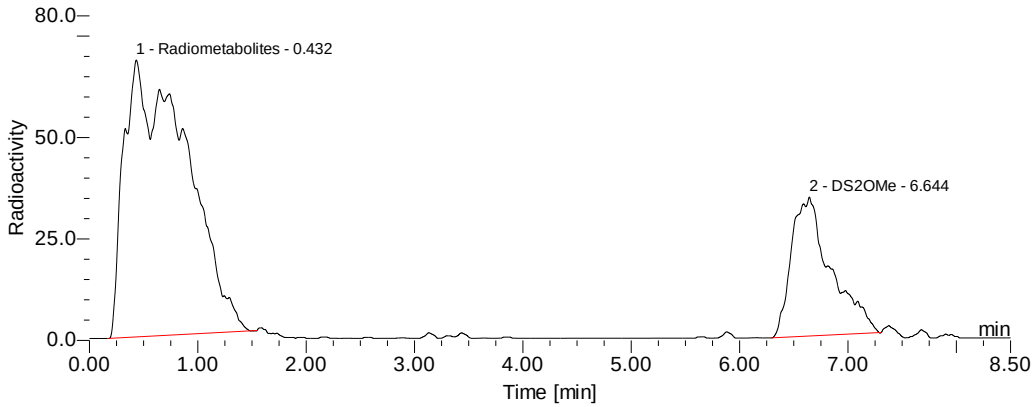

Supporting figure 3: Representative radio-chromatogram of pig plasma sample taken 20 min after injection with [^{11}C]DS2OMe.

GRADUATE SCHOOL OF HEALTH AND MEDICAL SCIENCES
UNIVERSITY OF COPENHAGEN

DECLARATION OF CO-AUTHORSHIP

Information on PhD student:	
Name of PhD student	Elina Tampio L'Estrade
E-mail	elina.nyberg@sund.ku.dk
Date of birth	20 December 1988
Work place	Department of Drug Design and Pharmacology
Principal supervisor	Assoc. Prof. Matthias M. Herth

Title of PhD thesis:
Development and Evaluation of Potential 5-HT7 Receptor PET Tracer Candidates

This declaration concerns the following article:
Towards selective PET Imaging of the 5-HT7 Receptor System: Past, Present and Future

The PhD student's contribution to the article: *(please use the scale (A,B,C) below as benchmark*)*	(A,B,C)
1. Formulation/identification of the scientific problem that from theoretical questions need to be clarified. This includes a condensation of the problem to specific scientific questions that is judged to be answerable by experiments	C
2. Planning of the experiments and methodology design, including selection of methods and method development	C
3. Involvement in the experimental work	-
4. Presentation, interpretation and discussion in a journal article format of obtained data	C

**Benchmark scale of the PhD student's contribution to the article*		
A. refers to:	*Has contributed to the co-operation*	*0-33 %*
B. refers to:	*Has contributed considerably to the co-operation*	*34-66 %*
C. refers to:	*Has predominantly executed the work independently*	*67-100 %*

Signature of the co-authors:			
Date:	**Name:**	**Title:**	**Signature:**
	Gitte M. Knudsen	Prof.	
2019-03-04	Tomas Ohlsson	Ph.D.	
2019-03-04	Maria Erlandsson	Ph.D	

GRADUATE SCHOOL OF HEALTH AND MEDICAL SCIENCES
UNIVERSITY OF COPENHAGEN

DECLARATION OF CO-AUTHORSHIP

Information on PhD student:	
Name of PhD student	Elina Tampio L'Estrade
E-mail	elina.nyberg@sund.ku.dk
Date of birth	20 December 1988
Work place	Department of Drug Design and Pharmacology
Principal supervisor	Assoc. Prof. Matthias M. Herth

Title of PhD thesis:
Development and Evaluation of Potential 5-HT7 Receptor PET Tracer Candidates

This declaration concerns the following article:
Towards selective PET Imaging of the 5-HT7 Receptor System: Past, Present and Future

The PhD student's contribution to the article: *(please use the scale (A,B,C) below as benchmark*)*	(A,B,C)
1. Formulation/identification of the scientific problem that from theoretical questions need to be clarified. This includes a condensation of the problem to specific scientific questions that is judged to be answerable by experiments	C
2. Planning of the experiments and methodology design, including selection of methods and method development	C
3. Involvement in the experimental work	-
4. Presentation, interpretation and discussion in a journal article format of obtained data	C

**Benchmark scale of the PhD student's contribution to the article*		
A. refers to:	*Has contributed to the co-operation*	*0-33 %*
B. refers to:	*Has contributed considerably to the co-operation*	*34-66 %*
C. refers to:	*Has predominantly executed the work independently*	*67-100 %*

Signature of the co-authors:			
Date:	**Name:**	**Title:**	**Signature:**
5/3-19	Gitte M. Knudsen	Prof.	
	Tomas Ohlsson	Ph.D.	
	Maria Erlandsson	Ph.D	

05.03.19	Mathias M. Herth	Assoc. Prof.	
06.03.19	Elina Tampio L'Estrade	MSc.	

Signature of the PhD student and the principal supervisor:	
Date: 06.03.19 PhD student:	Date: 5.3.19 Principal supervisor:

GRADUATE SCHOOL OF HEALTH AND MEDICAL SCIENCES
UNIVERSITY OF COPENHAGEN

DECLARATION OF CO-AUTHORSHIP

Information on PhD student:	
Name of PhD student	Elina Tampio L'Estrade
E-mail	elina.nyberg@sund.ku.dk
Date of birth	20 December 1988
Work place	Department of Drug Design and Pharmacology
Principal supervisor	Assoc. Prof. Matthias M. Herth

Title of PhD thesis:
Development and Evaluation of Potential 5-HT7 Receptor PET Tracer Candidates

This declaration concerns the following article:
Radiolabeling and in vivo evaluation of [^{11}C]AGH-44 - a potential lead structure to develop a positron emission tomography radioligand for the 5-HT$_7$ receptor

The PhD student's contribution to the article: *(please use the scale (A,B,C) below as benchmark*)*	(A,B,C)
1. Formulation/identification of the scientific problem that from theoretical questions need to be clarified. This includes a condensation of the problem to specific scientific questions that is judged to be answerable by experiments	A
2. Planning of the experiments and methodology design, including selection of methods and method development	B
3. Involvement in the experimental work	C
4. Presentation, interpretation and discussion in a journal article format of obtained data	C

**Benchmark scale of the PhD student's contribution to the article*		
A. refers to:	*Has contributed to the co-operation*	*0-33 %*
B. refers to:	*Has contributed considerably to the co-operation*	*34-66 %*
C. refers to:	*Has predominantly executed the work independently*	*67-100 %*

Signature of the co-authors:			
Date:	Name:	Title:	Signature:
05.03.19	Matthias M. Herth	Assoc. Prof.	
06.03.19	Elina Tampio L'Estrade	MSc.	

Signature of the PhD student and the principal supervisor:	
Date: 06.03.19	Date: 5.3.19
PhD student:	Principal supervisor:

GRADUATE SCHOOL OF HEALTH AND MEDICAL SCIENCES
UNIVERSITY OF COPENHAGEN

DECLARATION OF CO-AUTHORSHIP

Information on PhD student:	
Name of PhD student	Elina Tampio L'Estrade
E-mail	elina.nyberg@sund.ku.dk
Date of birth	20 December 1988
Work place	Department of Drug Design and Pharmacology
Principal supervisor	Assoc. Prof. Matthias M. Herth

Title of PhD thesis:
Development and Evaluation of Potential 5-HT7 Receptor PET Tracer Candidates

This declaration concerns the following article:
Fragment-based Labelling Using Condensation Reactions – A Possibility to Increase Throughput in Preclinical PET

The PhD student's contribution to the article: *(please use the scale (A,B,C) below as benchmark*)*	(A,B,C)
1. Formulation/identification of the scientific problem that from theoretical questions need to be clarified. This includes a condensation of the problem to specific scientific questions that is judged to be answerable by experiments	B
2. Planning of the experiments and methodology design, including selection of methods and method development	C
3. Involvement in the experimental work	C
4. Presentation, interpretation and discussion in a journal article format of obtained data	C

**Benchmark scale of the PhD student's contribution to the article*		
A. refers to:	*Has contributed to the co-operation*	*0-33 %*
B. refers to:	*Has contributed considerably to the co-operation*	*34-66 %*
C. refers to:	*Has predominantly executed the work independently*	*67-100 %*

Signature of the co-authors:			
Date:	Name:	Title:	Signature:
	Gitte M. Knudsen	Prof.	
2019-03-04	Maria Erlandssonc	Ph.D	
2019-02-27	Tomas Olsson	Ph.D.	

GRADUATE SCHOOL OF HEALTH AND MEDICAL SCIENCES
UNIVERSITY OF COPENHAGEN

DECLARATION OF CO-AUTHORSHIP

Information on PhD student:	
Name of PhD student	Elina Tampio L'Estrade
E-mail	elina.nyberg@sund.ku.dk
Date of birth	20 December 1988
Work place	Department of Drug Design and Pharmacology
Principal supervisor	Assoc. Prof. Matthias M. Herth

Title of PhD thesis:
Development and Evaluation of Potential 5-HT7 Receptor PET Tracer Candidates

This declaration concerns the following article:
Fragment-based Labelling Using Condensation Reactions – A Possibility to Increase Throughput in Preclinical PET

The PhD student's contribution to the article: *(please use the scale (A,B,C) below as benchmark*)*	(A,B,C)
1. Formulation/identification of the scientific problem that from theoretical questions need to be clarified. This includes a condensation of the problem to specific scientific questions that is judged to be answerable by experiments	B
2. Planning of the experiments and methodology design, including selection of methods and method development	C
3. Involvement in the experimental work	C
4. Presentation, interpretation and discussion in a journal article format of obtained data	C

**Benchmark scale of the PhD student's contribution to the article*		
A. refers to:	*Has contributed to the co-operation*	*0-33 %*
B. refers to:	*Has contributed considerably to the co-operation*	*34-66 %*
C. refers to:	*Has predominantly executed the work independently*	*67-100 %*

Signature of the co-authors:			
Date:	Name:	Title:	Signature:
5/3-2019	Gitte M. Knudsen	Prof.	
	Maria Erlandssonc	Ph.D	
	Tomas Olsson	Ph.D.	

	Balázs Volk	Ph.D	
27/02/19	Fraser G. Edgar	MSc.	F. Edgar
	Ida Nymann Petersen	Ph.D	
	Szabolcs Lehel	Ph.D	
05.03.19	Mathias M. Hesth	Assoc. Prof.	

Signature of the PhD student and the principal supervisor:	
Date: 06.03.19	Date: 5.3.19
PhD student:	Principal supervisor:

04.03.2019	Balázs Volk	Ph.D	
-	Eraser G. Edgar	MSc.	
26.02.2019	Ida Nymann Petersen	Ph.D	
04.03 2019	Szabolcs Lehel	Ph.D	
05.03.19	Mathias M. Herth	Assoc. Prof.	
06.03.19	Elina Tampio L'Estrade	MSc.	

Signature of the PhD student and the principal supervisor:	
Date: 06.03.19	Date: 6.3.19
PhD student:	Principal supervisor:

2

GRADUATE SCHOOL OF HEALTH AND MEDICAL SCIENCES
UNIVERSITY OF COPENHAGEN

DECLARATION OF CO-AUTHORSHIP

Information on PhD student:	
Name of PhD student	Elina Tampio L'Estrade
E-mail	elina.nyberg@sund.ku.dk
Date of birth	20 December 1988
Work place	Department of Drug Design and Pharmacology
Principal supervisor	Assoc. Prof. Matthias M. Herth

Title of PhD thesis:
Development and Evaluation of Potential 5-HT7 Receptor PET Tracer Candidates

This declaration concerns the following article:
Development and Evaluation of Two Potential 5-HT7 Receptor PET Tracers: [^{18}F]ENL09 and [^{18}F]ENL10

The PhD student's contribution to the article: *(please use the scale (A,B,C) below as benchmark*)*	(A,B,C)
1. Formulation/identification of the scientific problem that from theoretical questions need to be clarified. This includes a condensation of the problem to specific scientific questions that is judged to be answerable by experiments	B
2. Planning of the experiments and methodology design, including selection of methods and method development	C
3. Involvement in the experimental work	C
4. Presentation, interpretation and discussion in a journal article format of obtained data	C

**Benchmark scale of the PhD student's contribution to the article*		
A. refers to:	*Has contributed to the co-operation*	*0-33 %*
B. refers to:	*Has contributed considerably to the co-operation*	*34-66 %*
C. refers to:	*Has predominantly executed the work independently*	*67-100 %*

Signature of the co-authors:			
Date:	Name:	Title:	Signature:
05.03.19	Matthias M. Herth	Assoc. Prof.	
06.03.19	Elina Tampio L'Estrade	M.Sc.	

Signature of the PhD student and the principal supervisor:	
Date: 06.03.19 PhD student: Elin Tajić	Date: 5.3.19 Principal supervisor:

GRADUATE SCHOOL OF HEALTH AND MEDICAL SCIENCES
UNIVERSITY OF COPENHAGEN

DECLARATION OF CO-AUTHORSHIP

Information on PhD student:	
Name of PhD student	Elina Tampio L'Estrade
E-mail	elina.nyberg@sund.ku.dk
Date of birth	20 December 1988
Work place	Department of Drug Design and Pharmacology
Principal supervisor	Assoc. Prof. Matthias M. Herth

Title of PhD thesis:
Development and Evaluation of Potential 5-HT7 Receptor PET Tracer Candidates

This declaration concerns the following article:
Radiosynthesis and preclinical evaluation of [11C]Cimbi-701 – Towards the imaging of cerebral 5-HT7 receptors

The PhD student's contribution to the article: *(please use the scale (A,B,C) below as benchmark*)*	**(A,B,C)**
1. Formulation/identification of the scientific problem that from theoretical questions need to be clarified. This includes a condensation of the problem to specific scientific questions that is judged to be answerable by experiments	A
2. Planning of the experiments and methodology design, including selection of methods and method development	B
3. Involvement in the experimental work	B
4. Presentation, interpretation and discussion in a journal article format of obtained data	B

**Benchmark scale of the PhD student's contribution to the article*		
A. refers to:	*Has contributed to the co-operation*	*0-33 %*
B. refers to:	*Has contributed considerably to the co-operation*	*34-66 %*
C. refers to:	*Has predominantly executed the work independently*	*67-100 %*

Signature of the co-authors:			
Date:	**Name:**	**Title:**	**Signature**
2019-01-18	Hanne D. Hansen	Ph.D	Hanne D Hansen
05.03.19	Matthias M. Herth	Assoc. Prof.	
06.03.19	Elina Tampio L'Estrade	M.Sc	Elina Tampio L'Estrade

Signature of the PhD student and the principal supervisor:	
Date: 06.03.19	Date: 5.3.19
PhD student:	Principal supervisor:

GRADUATE SCHOOL OF HEALTH AND MEDICAL SCIENCES
UNIVERSITY OF COPENHAGEN

DECLARATION OF CO-AUTHORSHIP

Information on PhD student:	
Name of PhD student	Elina Tampio L'Estrade
E-mail	elina.nyberg@sund.ku.dk
Date of birth	20 December 1988
Work place	Department of Drug Design and Pharmacology
Principal supervisor	Assoc. Prof. Matthias M. Herth

Title of PhD thesis:

Development and Evaluation of Potential 5-HT7 Receptor PET Tracer Candidates

This declaration concerns the following article:

Synthesis, Radiolabeling, In vitro and In vivo Evaluation of [18F]ENL30 – A Potential PET Radiotracer for the 5-HT7 Receptor

The PhD student's contribution to the article: *(please use the scale (A,B,C) below as benchmark*)*	**(A,B,C)**
1. Formulation/identification of the scientific problem that from theoretical questions need to be clarified. This includes a condensation of the problem to specific scientific questions that is judged to be answerable by experiments	B
2. Planning of the experiments and methodology design, including selection of methods and method development	C
3. Involvement in the experimental work	C
4. Presentation, interpretation and discussion in a journal article format of obtained data	C

**Benchmark scale of the PhD student's contribution to the article*		
A. refers to:	*Has contributed to the co-operation*	*0-33 %*
B. refers to:	*Has contributed considerably to the co-operation*	*34-66 %*
C. refers to:	*Has predominantly executed the work independently*	*67-100 %*

Signature of the co-authors:

Date:	Name:	Title:	Signature:
2018-12-20	Tomas Ohlsson	PhD	
2018-12-20	Maria Erlandsson	PhD	
18/1-2019	Gitte M. Knudsen	Prof.	

2019-01-17	Vladimir Shalgunov	Ph.D	
2019.01.17	Mengfei Xiong	M.Sc	
2019-01-18	Fraser G. Edgar	M.Sc	
2019-17-01	Mikael Palner	Ph.D	
2019-01-19	Simone L. Bærentzen	M.Sc	
05.03.19	Mathlias M. Herth	Assoc. Prof.	

Signature of the PhD student and the principal supervisor:	
Date: 06.03.19 PhD student:	Date: 5.3.19 Principal supervisor:

GRADUATE SCHOOL OF HEALTH AND MEDICAL SCIENCES
UNIVERSITY OF COPENHAGEN

DECLARATION OF CO-AUTHORSHIP

Information on PhD student:	
Name of PhD student	Elina Tampio L'Estrade
E-mail	elina.nyberg@sund.ku.dk
Date of birth	20 December 1988
Work place	Department of Drug Design and Pharmacology
Principal supervisor	Assoc. Prof. Matthias M. Herth

Title of PhD thesis:
Development and Evaluation of Potential 5-HT7 Receptor PET Tracer Candidates

This declaration concerns the following article:
Classics in neuroimaging: The serotonergic 2A receptor system - from discovery to modern molecular imaging

The PhD student's contribution to the article: *(please use the scale (A,B,C) below as benchmark*)*	(A,B,C)
1. Formulation/identification of the scientific problem that from theoretical questions need to be clarified. This includes a condensation of the problem to specific scientific questions that is judged to be answerable by experiments	A
2. Planning of the experiments and methodology design, including selection of methods and method development	B
3. Involvement in the experimental work	B
4. Presentation, interpretation and discussion in a journal article format of obtained data	B

**Benchmark scale of the PhD student's contribution to the article*		
A. refers to:	*Has contributed to the co-operation*	*0-33 %*
B. refers to:	*Has contributed considerably to the co-operation*	*34-66 %*
C. refers to:	*Has predominantly executed the work independently*	*67-100 %*

Signature of the co-authors:			
Date:	Name:	Title:	Signature:
	Gitte M. Knudsen	Prof.	
2019-03-04	Tomas Ohlsson	Ph.D	
2019-03-04	Maria Erlandsson	Ph.D	

GRADUATE SCHOOL OF HEALTH AND MEDICAL SCIENCES
UNIVERSITY OF COPENHAGEN

DECLARATION OF CO-AUTHORSHIP

Information on PhD student:	
Name of PhD student	Elina Tampio L'Estrade
E-mail	elina.nyberg@sund.ku.dk
Date of birth	20 December 1988
Work place	Department of Drug Design and Pharmacology
Principal supervisor	Assoc. Prof. Matthias M. Herth

Title of PhD thesis:
Development and Evaluation of Potential 5-HT7 Receptor PET Tracer Candidates

This declaration concerns the following article:
Classics in neuroimaging: The serotonergic 2A receptor system - from discovery to modern molecular imaging

The PhD student's contribution to the article: *(please use the scale (A,B,C) below as benchmark*)*	(A,B,C)
1. Formulation/identification of the scientific problem that from theoretical questions need to be clarified. This includes a condensation of the problem to specific scientific questions that is judged to be answerable by experiments	A
2. Planning of the experiments and methodology design, including selection of methods and method development	B
3. Involvement in the experimental work	B
4. Presentation, interpretation and discussion in a journal article format of obtained data	B

**Benchmark scale of the PhD student's contribution to the article*		
A. refers to:	*Has contributed to the co-operation*	*0-33 %*
B. refers to:	*Has contributed considerably to the co-operation*	*34-66 %*
C. refers to:	*Has predominantly executed the work independently*	*67-100 %*

Signature of the co-authors:			
Date:	**Name:**	**Title:**	**Signature:**
3/5·19	Gitte M. Knudsen	Prof.	
	Tomas Ohlsson	Ph.D	
	Maria Erlandsson	Ph.D	

2019-01-18	Hanne D. Hansen	Ph.D	Hanne D Hansen

Signature of the PhD student and the principal supervisor:	
Date: PhD student:	Date: Principal supervisor:

05.03.19	Mathias M. Herth	Assoc. Prof.	M.
06.03.19	Elina Tampio L'Estrade	MSc.	Elina Tampio L'Estrade

Signature of the PhD student and the principal supervisor:	
Date: 06.03.19	Date: 5.3.19
PhD student: Elina Tampio L'Estrade	Principal supervisor: M.

2

GRADUATE SCHOOL OF HEALTH AND MEDICAL SCIENCES
UNIVERSITY OF COPENHAGEN

DECLARATION OF CO-AUTHORSHIP

Information on PhD student:	
Name of PhD student	Elina Tampio L'Estrade
E-mail	elina.nyberg@sund.ku.dk
Date of birth	20 December 1988
Work place	Department of Drug Design and Pharmacology
Principal supervisor	Assoc. Prof. Matthias M. Herth

Title of PhD thesis:
Development and Evaluation of Potential 5-HT7 Receptor PET Tracer Candidates

This declaration concerns the following article:
Synthesis and Pharmacological Evaluation of [11C]4-Methoxy-N-[2-(thiophene-2-yl)imidazo[1,2-a]pyridine-3-yl]benzamide as a Brain Penetrant PET Ligand selective for the □-Subunit-Containing □-Aminobutyric Acid Type A Receptors

The PhD student's contribution to the article: *(please use the scale (A,B,C) below as benchmark*)*	(A,B,C)
1. Formulation/identification of the scientific problem that from theoretical questions need to be clarified. This includes a condensation of the problem to specific scientific questions that is judged to be answerable by experiments	A
2. Planning of the experiments and methodology design, including selection of methods and method development	A
3. Involvement in the experimental work	B
4. Presentation, interpretation and discussion in a journal article format of obtained data	A

**Benchmark scale of the PhD student's contribution to the article*		
A. refers to:	*Has contributed to the co-operation*	*0-33 %*
B. refers to:	*Has contributed considerably to the co-operation*	*34-66 %*
C. refers to:	*Has predominantly executed the work independently*	*67-100 %*

Signature of the co-authors:			
Date:	Name:	Title:	Signature:
21-1-19	BENTE FROLUND	Proff	
09.03.19	Matthias M. Herth	Assoc. Prof.	
06.03.19	Elina Tampio L'Estrade	MSc.	

Signature of the PhD student and the principal supervisor:	
Date: 06.03.19 PhD student:	Date: 5-3.19 Principal supervisor:

ELSEVIER LICENSE
TERMS AND CONDITIONS

Dec 27, 2018

This Agreement between Elina Tampio LEstrade ("You") and Elsevier ("Elsevier") consists of your license details and the terms and conditions provided by Elsevier and Copyright Clearance Center.

License Number	4497140361756
License date	Dec 27, 2018
Licensed Content Publisher	Elsevier
Licensed Content Publication	Trends in Pharmacological Sciences
Licensed Content Title	Functional, molecular and pharmacological advances in 5-HT7 receptor research
Licensed Content Author	Peter B. Hedlund,J. Gregor Sutcliffe
Licensed Content Date	Sep 1, 2004
Licensed Content Volume	25
Licensed Content Issue	9
Licensed Content Pages	6
Start Page	481
End Page	486
Type of Use	reuse in a thesis/dissertation
Intended publisher of new work	other
Portion	figures/tables/illustrations
Number of figures/tables/illustrations	1
Format	both print and electronic
Are you the author of this Elsevier article?	No
Will you be translating?	No
Original figure numbers	Figure 1
Title of your thesis/dissertation	Development and Evaluation of Potential 5-HT7 Receptor PET Tracer Candidates
Expected completion date	Jan 2019
Estimated size (number of pages)	250
Requestor Location	Elina Tampio LEstrade Jagtvej 162 Copenhagen, Non US 2100 Denmark Attn: Elina Tampio LEstrade
Publisher Tax ID	GB 494 6272 12
Total	0.00 USD

JOHN WILEY AND SONS LICENSE TERMS AND CONDITIONS

Dec 27, 2018

This Agreement between Elina Tampio LEstrade ("You") and John Wiley and Sons ("John Wiley and Sons") consists of your license details and the terms and conditions provided by John Wiley and Sons and Copyright Clearance Center.

License Number	4497110404209
License date	Dec 27, 2018
Licensed Content Publisher	John Wiley and Sons
Licensed Content Publication	Angewandte Chemie International Edition
Licensed Content Title	Synthesis of 11C, 18F, 15O, and 13N Radiolabels for Positron Emission Tomography
Licensed Content Author	Philip W. Miller, Nicholas J. Long, Ramon Vilar, et al
Licensed Content Date	Nov 5, 2008
Licensed Content Volume	47
Licensed Content Issue	47
Licensed Content Pages	36
Type of use	Dissertation/Thesis
Requestor type	University/Academic
Format	Print and electronic
Portion	Figure/table
Number of figures/tables	1
Original Wiley figure/table number(s)	Figure 1
Will you be translating?	No
Title of your thesis / dissertation	Development and Evaluation of Potential 5-HT7 Receptor PET Tracer Candidates
Expected completion date	Jan 2019
Expected size (number of pages)	250
Requestor Location	Elina Tampio LEstrade Jagtvej 162 Copenhagen, Non US 2100 Denmark Attn: Elina Tampio LEstrade
Publisher Tax ID	EU826007151
Total	0.00 EUR

ELSEVIER LICENSE
TERMS AND CONDITIONS

Feb 25, 2019

This Agreement between Elina Tampio LEstrade ("You") and Elsevier ("Elsevier") consists of your license details and the terms and conditions provided by Elsevier and Copyright Clearance Center.

License Number	4535850188650
License date	Feb 25, 2019
Licensed Content Publisher	Elsevier
Licensed Content Publication	Progress in Neuro-Psychopharmacology and Biological Psychiatry
Licensed Content Title	Binding of lurasidone, a novel antipsychotic, to rat 5-HT7 receptor: Analysis by [3H]SB-269970 autoradiography
Licensed Content Author	Tomoko Horisawa,Takeo Ishiyama,Michiko Ono,Tadashi Ishibashi,Mutsuo Taiji
Licensed Content Date	Jan 10, 2013
Licensed Content Volume	40
Licensed Content Issue	n/a
Licensed Content Pages	6
Start Page	132
End Page	137
Type of Use	reuse in a thesis/dissertation
Portion	figures/tables/illustrations
Number of figures/tables/illustrations	1
Format	both print and electronic
Are you the author of this Elsevier article?	No
Will you be translating?	No
Original figure numbers	Figure 1
Title of your thesis/dissertation	Development and Evaluation of Potential 5-HT7 Receptor PET Tracer Candidates
Expected completion date	Jan 2019
Estimated size (number of pages)	250
Requestor Location	Elina Tampio LEstrade Jagtvej 162 Copenhagen, Non US 2100 Denmark Attn: Elina Tampio LEstrade
Publisher Tax ID	GB 494 6272 12
Total	0.00 USD

JOHN WILEY AND SONS LICENSE TERMS AND CONDITIONS

Feb 25, 2019

This Agreement between Elina Tampio LEstrade ("You") and John Wiley and Sons ("John Wiley and Sons") consists of your license details and the terms and conditions provided by John Wiley and Sons and Copyright Clearance Center.

License Number	4535850774210
License date	Feb 25, 2019
Licensed Content Publisher	John Wiley and Sons
Licensed Content Publication	Journal of Labelled Compounds and Radiopharmaceuticals
Licensed Content Title	Evaluation of [18F]2FP3 in pigs and non-human primates
Licensed Content Author	Hanne D. Hansen, Cristian C. Constantinescu, Olivier Barret, et al
Licensed Content Date	Dec 6, 2018
Licensed Content Volume	62
Licensed Content Issue	1
Licensed Content Pages	9
Type of use	Dissertation/Thesis
Requestor type	University/Academic
Format	Print and electronic
Portion	Figure/table
Number of figures/tables	1
Original Wiley figure/table number(s)	Figure 5
Will you be translating?	No
Title of your thesis / dissertation	Development and Evaluation of Potential 5-HT7 Receptor PET Tracer Candidates
Expected completion date	Jan 2019
Expected size (number of pages)	250
Requestor Location	Elina Tampio LEstrade Jagtvej 162 Copenhagen, Non US 2100 Denmark Attn: Elina Tampio LEstrade
Publisher Tax ID	EU826007151
Total	0.00 USD

ELSEVIER LICENSE
TERMS AND CONDITIONS

Feb 25, 2019

This Agreement between Elina Tampio LEstrade ("You") and Elsevier ("Elsevier") consists of your license details and the terms and conditions provided by Elsevier and Copyright Clearance Center.

License Number	4535850955743
License date	Feb 25, 2019
Licensed Content Publisher	Elsevier
Licensed Content Publication	Neuroscience Letters
Licensed Content Title	Distribution of 5-HT7 receptors in the human brain: a preliminary autoradiographic study using [3 H]SB-269970
Licensed Content Author	Katarina Varnäs,David R. Thomas,Erkki Tupala,Jari Tiihonen,Håkan Hall
Licensed Content Date	Sep 9, 2004
Licensed Content Volume	367
Licensed Content Issue	3
Licensed Content Pages	4
Start Page	313
End Page	316
Type of Use	reuse in a thesis/dissertation
Intended publisher of new work	other
Portion	figures/tables/illustrations
Number of figures/tables/illustrations	1
Format	both print and electronic
Are you the author of this Elsevier article?	No
Will you be translating?	No
Original figure numbers	Figure 1
Title of your thesis/dissertation	Development and Evaluation of Potential 5-HT7 Receptor PET Tracer Candidates
Expected completion date	Jan 2019
Estimated size (number of pages)	250
Requestor Location	Elina Tampio LEstrade Jagtvej 162 Copenhagen, Non US 2100 Denmark Attn: Elina Tampio LEstrade
Publisher Tax ID	GB 494 6272 12
Total	0.00 USD

JOHN WILEY AND SONS LICENSE TERMS AND CONDITIONS

Jan 15, 2019

This Agreement between Elina Tampio LEstrade ("You") and John Wiley and Sons ("John Wiley and Sons") consists of your license details and the terms and conditions provided by John Wiley and Sons and Copyright Clearance Center.

License Number	4510070143445
License date	Jan 15, 2019
Licensed Content Publisher	John Wiley and Sons
Licensed Content Publication	Journal of Labelled Compounds and Radiopharmaceuticals
Licensed Content Title	Synthesis and preliminary PET study of the 5-HT7 receptor antagonist [11C]DR4446
Licensed Content Author	Ming-Rong Zhang, Terushi Haradahira, Jun Maeda, et al
Licensed Content Date	Aug 5, 2002
Licensed Content Volume	45
Licensed Content Issue	10
Licensed Content Pages	10
Type of use	Dissertation/Thesis
Requestor type	University/Academic
Format	Print and electronic
Portion	Figure/table
Number of figures/tables	1
Original Wiley figure/table number(s)	Figure 2
Will you be translating?	No
Title of your thesis / dissertation	Development and Evaluation of Potential 5-HT7 Receptor PET Tracer Candidates
Expected completion date	Jan 2019
Expected size (number of pages)	250
Requestor Location	Elina Tampio LEstrade Jagtvej 162 Copenhagen, Non US 2100 Denmark Attn: Elina Tampio LEstrade
Publisher Tax ID	EU826007151
Total	0.00 USD

ELSEVIER LICENSE
TERMS AND CONDITIONS

Jan 15, 2019

This Agreement between Elina Tampio LEstrade ("You") and Elsevier ("Elsevier") consists of your license details and the terms and conditions provided by Elsevier and Copyright Clearance Center.

License Number	4510070671942
License date	Jan 15, 2019
Licensed Content Publisher	Elsevier
Licensed Content Publication	Bioorganic & Medicinal Chemistry
Licensed Content Title	Design, synthesis, radiolabeling and in vivo evaluation of potential positron emission tomography (PET) radioligands for brain imaging of the 5-HT7 receptor
Licensed Content Author	Enza Lacivita,Mauro Niso,Hanne D. Hansen,Pantaleo Di Pilato,Matthias M. Herth,Szabolcs Lehel,Anders Ettrup,Lisa Montenegro,Roberto Perrone,Francesco Berardi,Nicola A. Colabufo,Marcello Leopoldo,Gitte M. Knudsen
Licensed Content Date	Mar 1, 2014
Licensed Content Volume	22
Licensed Content Issue	5
Licensed Content Pages	15
Start Page	1736
End Page	1750
Type of Use	reuse in a thesis/dissertation
Intended publisher of new work	other
Portion	figures/tables/illustrations
Number of figures/tables/illustrations	2
Format	both print and electronic
Are you the author of this Elsevier article?	No
Will you be translating?	No
Original figure numbers	Figure 3 and Figure 4
Title of your thesis/dissertation	Development and Evaluation of Potential 5-HT7 Receptor PET Tracer Candidates
Expected completion date	Jan 2019
Estimated size (number of pages)	250
Requestor Location	Elina Tampio LEstrade Jagtvej 162 Copenhagen, Non US 2100 Denmark Attn: Elina Tampio LEstrade
Publisher Tax ID	GB 494 6272 12
Total	0.00 USD

ELSEVIER LICENSE
TERMS AND CONDITIONS

Jan 15, 2019

This Agreement between Elina Tampio LEstrade ("You") and Elsevier ("Elsevier") consists of your license details and the terms and conditions provided by Elsevier and Copyright Clearance Center.

License Number	4510061207015
License date	Jan 15, 2019
Licensed Content Publisher	Elsevier
Licensed Content Publication	Bioorganic & Medicinal Chemistry
Licensed Content Title	Synthesis and evaluation of [11C]Cimbi-806 as a potential PET ligand for 5-HT7 receptor imaging
Licensed Content Author	Matthias M. Herth,Hanne D. Hansen,Anders Ettrup,Agnete Dyssegaard,Szabolcs Lehel,Jesper Kristensen,Gitte M. Knudsen
Licensed Content Date	Jul 15, 2012
Licensed Content Volume	20
Licensed Content Issue	14
Licensed Content Pages	8
Start Page	4574
End Page	4581
Type of Use	reuse in a thesis/dissertation
Portion	figures/tables/illustrations
Number of figures/tables/illustrations	1
Format	both print and electronic
Are you the author of this Elsevier article?	No
Will you be translating?	No
Original figure numbers	Figure 2
Title of your thesis/dissertation	Development and Evaluation of Potential 5-HT7 Receptor PET Tracer Candidates
Expected completion date	Jan 2019
Estimated size (number of pages)	250
Requestor Location	Elina Tampio LEstrade Jagtvej 162 Copenhagen, Non US 2100 Denmark Attn: Elina Tampio LEstrade
Publisher Tax ID	GB 494 6272 12
Total	0.00 USD

ELSEVIER LICENSE
TERMS AND CONDITIONS

Jan 15, 2019

This Agreement between Elina Tampio LEstrade ("You") and Elsevier ("Elsevier") consists of your license details and the terms and conditions provided by Elsevier and Copyright Clearance Center.

License Number	4510070938041
License date	Jan 15, 2019
Licensed Content Publisher	Elsevier
Licensed Content Publication	Bioorganic & Medicinal Chemistry Letters
Licensed Content Title	Labeling and preliminary in vivo evaluation of the 5-HT7 receptor selective agonist [11C]E-55888
Licensed Content Author	Hanne D. Hansen,Valdemar L. Andersen,Szabolcs Lehel,Janus H. Magnussen,Agnete Dyssegaard,Nikolas Stroth,Jesper L. Kristensen,Gitte M. Knudsen,Matthias M. Herth
Licensed Content Date	1 May 2015
Licensed Content Volume	25
Licensed Content Issue	9
Licensed Content Pages	4
Start Page	1901
End Page	1904
Type of Use	reuse in a thesis/dissertation
Intended publisher of new work	other
Portion	figures/tables/illustrations
Number of figures/tables/illustrations	1
Format	both print and electronic
Are you the author of this Elsevier article?	No
Will you be translating?	No
Original figure numbers	Figure 1
Title of your thesis/dissertation	Development and Evaluation of Potential 5-HT7 Receptor PET Tracer Candidates
Expected completion date	Jan 2019
Estimated size (number of pages)	250
Requestor Location	Elina Tampio LEstrade Jagtvej 162 Copenhagen, Non US 2100 Denmark Attn: Elina Tampio LEstrade
Publisher Tax ID	GB 494 6272 12
Total	0.00 USD

JOHN WILEY AND SONS LICENSE TERMS AND CONDITIONS

Jan 15, 2019

This Agreement between Elina Tampio LEstrade ("You") and John Wiley and Sons ("John Wiley and Sons") consists of your license details and the terms and conditions provided by John Wiley and Sons and Copyright Clearance Center.

License Number	4510080573051
License date	Jan 15, 2019
Licensed Content Publisher	John Wiley and Sons
Licensed Content Publication	Journal of Labelled Compounds and Radiopharmaceuticals
Licensed Content Title	Evaluation of [18F]2FP3 in pigs and non-human primates
Licensed Content Author	Hanne D. Hansen, Cristian C. Constantinescu, Olivier Barret, et al
Licensed Content Date	Dec 6, 2018
Licensed Content Volume	0
Licensed Content Issue	0
Licensed Content Pages	9
Type of use	Dissertation/Thesis
Requestor type	University/Academic
Format	Print and electronic
Portion	Figure/table
Number of figures/tables	2
Original Wiley figure/table number(s)	Figure 2 and Figure 3
Will you be translating?	No
Title of your thesis / dissertation	Development and Evaluation of Potential 5-HT7 Receptor PET Tracer Candidates
Expected completion date	Jan 2019
Expected size (number of pages)	250
Requestor Location	Elina Tampio LEstrade Jagtvej 162 Copenhagen, Non US 2100 Denmark Attn: Elina Tampio LEstrade
Publisher Tax ID	EU826007151
Total	0.00 USD

ELSEVIER LICENSE
TERMS AND CONDITIONS

Jan 15, 2019

This Agreement between Elina Tampio LEstrade ("You") and Elsevier ("Elsevier") consists of your license details and the terms and conditions provided by Elsevier and Copyright Clearance Center.

License Number	4510101504186
License date	Jan 15, 2019
Licensed Content Publisher	Elsevier
Licensed Content Publication	Nuclear Medicine and Biology
Licensed Content Title	Synthesis and pharmacological evaluation of a new series of radiolabeled ligands for 5-HT7 receptor PET neuroimaging
Licensed Content Author	Julie Colomb,Guillaume Becker,Elsa Forcellini,Sandra Meyer,Lauriane Buisson,Luc Zimmer,Thierry Billard
Licensed Content Date	Apr 1, 2014
Licensed Content Volume	41
Licensed Content Issue	4
Licensed Content Pages	8
Start Page	330
End Page	337
Type of Use	reuse in a thesis/dissertation
Intended publisher of new work	other
Portion	figures/tables/illustrations
Number of figures/tables/illustrations	1
Format	both print and electronic
Are you the author of this Elsevier article?	No
Will you be translating?	No
Original figure numbers	Figure 5
Title of your thesis/dissertation	Development and Evaluation of Potential 5-HT7 Receptor PET Tracer Candidates
Expected completion date	Jan 2019
Estimated size (number of pages)	250
Requestor Location	Elina Tampio LEstrade Jagtvej 162 Copenhagen, Non US 2100 Denmark Attn: Elina Tampio LEstrade
Publisher Tax ID	GB 494 6272 12
Total	0.00 USD